INNOVATIVE APPROACHES IN DIAGNOSIS OF EMERGING/RE-EMERGING INFECTIOUS DISEASES

EDITED BY: Aleksandra Barac, David Ong and Mario Poljak

PUBLISHED IN: Frontiers in Microbiology and
Frontiers in Cellular and Infection Microbiology

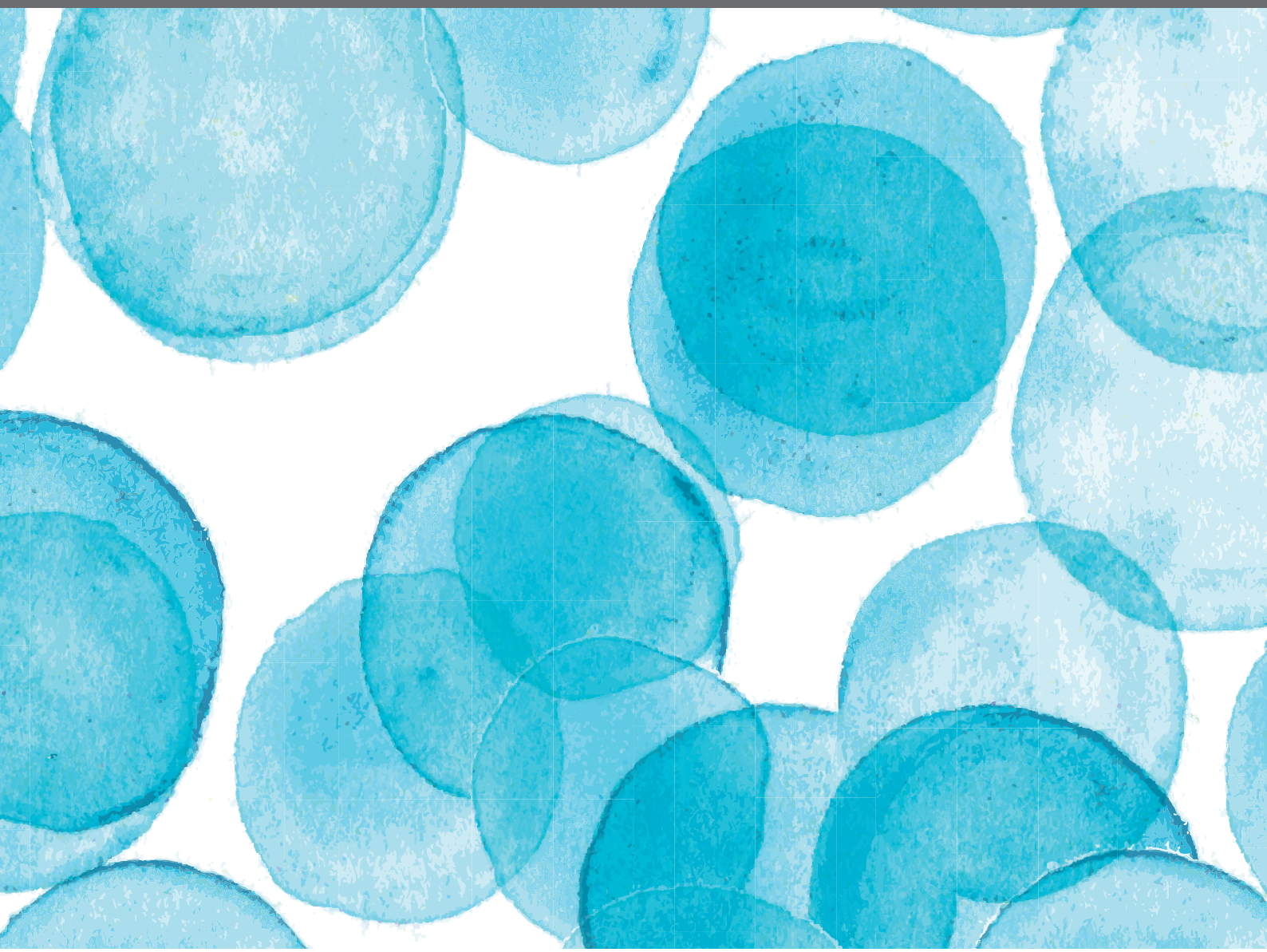

frontiers Research Topics

frontiers

ISSN 1664-8714
ISBN 978-2-88966-404-7
DOI 10.3389/978-2-88966-404-7

About Frontiers

Frontiers is more than just an open-access publisher of scholarly articles: it is a pioneering approach to the world of academia, radically improving the way scholarly research is managed. The grand vision of Frontiers is a world where all people have an equal opportunity to seek, share and generate knowledge. Frontiers provides immediate and permanent online open access to all its publications, but this alone is not enough to realize our grand goals.

Frontiers Journal Series

The Frontiers Journal Series is a multi-tier and interdisciplinary set of open-access, online journals, promising a paradigm shift from the current review, selection and dissemination processes in academic publishing. All Frontiers journals are driven by researchers for researchers; therefore, they constitute a service to the scholarly community. At the same time, the Frontiers Journal Series operates on a revolutionary invention, the tiered publishing system, initially addressing specific communities of scholars, and gradually climbing up to broader public understanding, thus serving the interests of the lay society, too.

Dedication to Quality

Each Frontiers article is a landmark of the highest quality, thanks to genuinely collaborative interactions between authors and review editors, who include some of the world's best academicians. Research must be certified by peers before entering a stream of knowledge that may eventually reach the public - and shape society; therefore, Frontiers only applies the most rigorous and unbiased reviews.
Frontiers revolutionizes research publishing by freely delivering the most outstanding research, evaluated with no bias from both the academic and social point of view. By applying the most advanced information technologies, Frontiers is catapulting scholarly publishing into a new generation.

What are Frontiers Research Topics?

Frontiers Research Topics are very popular trademarks of the Frontiers Journals Series: they are collections of at least ten articles, all centered on a particular subject. With their unique mix of varied contributions from Original Research to Review Articles, Frontiers Research Topics unify the most influential researchers, the latest key findings and historical advances in a hot research area! Find out more on how to host your own Frontiers Research Topic or contribute to one as an author by contacting the Frontiers Editorial Office: researchtopics@frontiersin.org

INNOVATIVE APPROACHES IN DIAGNOSIS OF EMERGING/RE-EMERGING INFECTIOUS DISEASES

Topic Editors:
Aleksandra Barac, University of Belgrade, Serbia
David Ong, Franciscus Gasthuis & Vlietland, Netherlands
Mario Poljak, University of Ljubljana, Slovenia

Citation: Barac, A., Ong, D., Poljak, M., eds. (2021). Innovative Approaches in Diagnosis of Emerging/re-emerging Infectious Diseases.
Lausanne: Frontiers Media SA. doi: 10.3389/978-2-88966-404-7

Table of Contents

06 ***Editorial: Innovative Approaches in Diagnosis of Emerging/Re-emerging Infectious Diseases***
Aleksandra Barac, Mario Poljak and David S. Y. Ong

09 ***A New Single Gene Differential Biomarker for* Mycobacterium tuberculosis *Complex and Non-tuberculosis Mycobacteria***
Lei Zhou, Cuidie Ma, Tongyang Xiao, Machao Li, Haican Liu, Xiuqin Zhao, Kanglin Wan and Ruibai Wang

19 ***Development of Multispecies Recombinant Nucleoprotein-Based Indirect ELISA for High-Throughput Screening of Crimean-Congo Hemorrhagic Fever Virus-Specific Antibodies***
Neha Shrivastava, Ambuj Shrivastava, Sandeep M. Ninawe, Shashi Sharma, Jyoti S. Kumar, Syed Imteyaz Alam, Amit Kanani, Sushil Kumar Sharma and Paban Kumar Dash

33 ***Development and Clinical Validation of Multiple Cross Displacement Amplification Combined With Nanoparticles-Based Biosensor for Detection of* Mycobacterium tuberculosis*: Preliminary Results***
Wei-Wei Jiao, Yi Wang, Gui-Rong Wang, Ya-Cui Wang, Jing Xiao, Lin Sun, Jie-Qiong Li, Shu-An Wen, Ting-Ting Zhang, Qi Ma, Hai-Rong Huang and A-Dong Shen

42 ***Relationship of Serum Antileishmanial Antibody With Development of Visceral Leishmaniasis, Post-kala-azar Dermal Leishmaniasis and Visceral Leishmaniasis Relapse***
Dinesh Mondal, Prakash Ghosh, Rajashree Chowdhury, Christine Halleux, Jose A. Ruiz-Postigo, Abdul Alim, Faria Hossain, Md Anik Ashfaq Khan, Rupen Nath, Malcolm S. Duthie, Axel Kroeger, Greg Matlashewski, Daniel Argaw and Piero Olliaro

54 ***Differential Culturability of* Mycobacterium tuberculosis *in Culture-Negative Sputum of Patients With Pulmonary Tuberculosis and in a Simulated Model of Dormancy***
Azger Dusthackeer, Magizhaveni Balasubramanian, Govindarajan Shanmugam, Shanmuga Priya, Christy Rosaline Nirmal, Rajadas Sam Ebenezer, Angayarkanni Balasubramanian, Rajesh Kumar Mondal, Kannan Thiruvenkadam, A. K. Hemanth Kumar, Geetha Ramachandran and Selvakumar Subbian

63 ***Clinical Features Predicting Mortality Risk in Patients With Viral Pneumonia: The MuLBSTA Score***
Lingxi Guo, Dong Wei, Xinxin Zhang, Yurong Wu, Qingyun Li, Min Zhou and Jieming Qu

73 ***Erratum: Clinical Features Predicting Mortality Risk in Patients With Viral Pneumonia: The MuLBSTA Score***
Frontiers Production Office

74 ***Immune Biomarkers for Diagnosis and Treatment Monitoring of Tuberculosis: Current Developments and Future Prospects***
Yean K. Yong, Hong Y. Tan, Alireza Saeidi, Won F. Wong, Ramachandran Vignesh, Vijayakumar Velu, Rajaraman Eri, Marie Larsson and Esaki M. Shankar

92 ***Assessment of an Antibody-in-Lymphocyte Supernatant Assay for the Etiological Diagnosis of Pneumococcal Pneumonia in Children***
Michael J. Carter, Pallavi Gurung, Claire Jones, Shristy Rajkarnikar, Rama Kandasamy, Meeru Gurung, Stephen Thorson, Madhav C. Gautam, Krishna G. Prajapati, Bibek Khadka, Anju Maharjan, Julian C. Knight, David R. Murdoch, Thomas C. Darton, Merryn Voysey, Brian Wahl, Katherine L. O'Brien, Sarah Kelly, Imran Ansari, Ganesh Shah, Nina Ekström, Merit Melin, Andrew J. Pollard, Dominic F. Kelly and Shrijana Shrestha for the PneumoNepal Study Group

108 ***Determination of Causative Human Papillomavirus Type in Tissue Specimens of Common Warts Based on Estimated Viral Loads***
Vesna Breznik, Kristina Fujs Komloš, Lea Hošnjak, Boštjan Luzar, Rajko Kavalar, Jovan Miljković and Mario Poljak

116 ***Outbreak of* Saprochaete clavata *Sepsis in Hematology Patients: Combined Use of MALDI-TOF and Sequencing Strategy to Identify and Correlate the Episodes***
Giuliana Lo Cascio, Marcello Vincenzi, Fabio Soldani, Elena De Carolis, Laura Maccacaro, Annarita Sorrentino, Gianpaolo Nadali, Simone Cesaro, Michele Sommavilla, Valentina Niero, Laura Naso, Anna Grancini, Anna Maria Azzini, Maurizio Sanguinetti, E. Tacconelli and Giuseppe Cornaglia

127 ***Rapid Detection of* Nocardia *by Next-Generation Sequencing***
Shan-Shan Weng, Han-Yue Zhang, Jing-Wen Ai, Yan Gao, Yuan-Yuan Liu, Bin Xu and Wen-Hong Zhang

132 ***Lyme Endocarditis as an Emerging Infectious Disease: A Review of the Literature***
Aleksandra Nikolić, Darko Boljević, Milovan Bojić, Stefan Veljković, Dragana Vuković, Bianca Paglietti, Jelena Micić and Salvatore Rubino

139 ***Dried Blood Spot Tests for the Diagnosis and Therapeutic Monitoring of HIV and Viral Hepatitis B and C***
Edouard Tuaillon, Dramane Kania, Amandine Pisoni, Karine Bollore, Fabien Taieb, Esther Nina Ontsira Ngoyi, Roxane Schaub, Jean-Christophe Plantier, Alain Makinson and Philippe Van de Perre

146 ***Rapid and Low-Cost Culture-Based Method for Diagnosis of Mucormycosis Using a Mouse Model***
Afsane Vaezi, Hamed Fakhim, Macit Ilkit, Leila Faeli, Mahdi Fakhar, Vahid Alinejad, Nathan P. Wiederhold and Hamid Badali

153 ***Timely Diagnosis of Histoplasmosis in Non-endemic Countries: A Laboratory Challenge***
María José Buitrago and M. Teresa Martín-Gómez

161 ***Autoinducer-2 May Be a New Biomarker for Monitoring Neonatal Necrotizing Enterocolitis***
Chun-Yan Fu, Lu-Quan Li, Ting Yang, Xiang She, Qing Ai and Zheng-Li Wang

171 ***Current and Future Point-of-Care Tests for Emerging and New Respiratory Viruses and Future Perspectives***
Philipp P. Nelson, Barbara A. Rath, Paraskevi C. Fragkou, Emmanouil Antalis, Sotirios Tsiodras and Chrysanthi Skevaki on behalf of the ESCMID Study Group for Respiratory Viruses (ESGREV)

180 ***Development of a Rapid and Sensitive Colorimetric Loop-Mediated Isothermal Amplification Assay: A Novel Technology for the Detection of* Coxiella burnetii *From Minimally Processed Clinical Samples***
Nazish Sheikh, Sanjay Kumar, Harsh Kumar Sharma, Sameer S. Bhagyawant and Duraipandian Thavaselvam

frontiers in Microbiology

EDITORIAL
published: 03 December 2020
doi: 10.3389/fmicb.2020.619498

Editorial: Innovative Approaches in Diagnosis of Emerging/Re-emerging Infectious Diseases

Aleksandra Barac[1,2]*, *Mario Poljak*[3] and *David S. Y. Ong*[4,5]

[1] Clinic for Infectious and Tropical Diseases, Clinical Center of Serbia, Belgrade, Serbia, [2] Faculty of Medicine, University of Belgrade, Belgrade, Serbia, [3] Institute of Microbiology and Immunology, Faculty of Medicine, University of Ljubljana, Ljubljana, Slovenia, [4] Department of Medical Microbiology and Infection Control, Franciscus Gasthuis & Vlietland, Rotterdam, Netherlands, [5] Department of Epidemiology, Julius Center for Health Sciences and Primary Care, University Medical Center Utrecht, Utrecht University, Utrecht, Netherlands

Keywords: infectious diseases, emerging infections, outbreak, pandemic infections, diagnosis, treatment

Editorial on the Research Topic

Innovative Approaches in Diagnosis of Emerging/Re-emerging Infectious Diseases

OPEN ACCESS

Edited by:
Axel Cloeckaert,
Institut National de Recherche pour l'agriculture, l'alimentation et l'environnement (INRAE), France

Reviewed by:
Karl Kuchler,
Medical University of Vienna, Austria

***Correspondence:**
Aleksandra Barac
aleksandrabarac85@gmail.com

Specialty section:
This article was submitted to Infectious Diseases, a section of the journal Frontiers in Microbiology

Received: *20 October 2020*
Accepted: *11 November 2020*
Published: *03 December 2020*

Citation:
Barac A, Poljak M and Ong DSY (2020) Editorial: Innovative Approaches in Diagnosis of Emerging/Re-emerging Infectious Diseases. Front. Microbiol. 11:619498. doi: 10.3389/fmicb.2020.619498

Infectious diseases can spread rapidly, causing enormous losses of health, human lives, as well as large costs to the society. Despite recent significant advances in diagnostics of infectious diseases, the frequent and affordable worldwide travel which was common before coronavirus disease 2019 (COVID-19) pandemic and increased global interdependence have added layers of complexity to recognize and timely manage several infectious diseases, including both traditional as well as emerging/re-emerging diseases (Castelli and Sulis, 2017). HIV/AIDS, multidrug-resistant tuberculosis (TB), invasive fungal infections in transplant recipients, *Clostridioides difficile* enterocolitis, malaria, measles, severe acute respiratory syndrome (SARS), Middle East respiratory syndrome (MERS), pandemic avian and H1N1 influenza, Ebola and Zika are only a few of many examples of infectious diseases which emerged in the last decades causing significant morbidity and mortality (Rechel et al., 2013). In addition, new infectious diseases with epidemic and pandemic potential emerge periodically. In extreme cases they may cause devastating pandemics such as COVID-19, whereas in other cases they result in self-limited infections or local/regional epidemics of smaller scale (Morens and Fauci, 2020). Established traditional infectious diseases may also re-emerge, for example by extending geographically or when pathogens become more transmissible, more pathogenic or resistant to standard antimicrobial therapy. Disease emergence reflects dynamic balances and imbalances, within complex globally distributed ecosystems comprising humans, animals, pathogens, and the environment. To successfully control emerging/re-emerging infectious diseases, the best strategy is to understand these variables and to halt their spread at an early stage. For this purpose, we rely on early diagnosis of disease by rapid and reliable detection of disease-causing agents. This is particularly true for newly emerging infectious disease (like SARS-CoV-2 and MERS), where we find ourselves in a race to develop and validate new diagnostic tools and approaches during an ongoing outbreak.

This Research Topic entitled "Innovative Approaches in Diagnosis of Emerging/re-emerging Infectious Diseases" includes a total of 18 manuscripts, ranging from original research to reviews within all fields of microbiology: bacteriology, virology, mycology and parasitology; all with a particular focus on diagnostics. It covers research on highly-prevalent infectious diseases such as tuberculosis and HIV, but also on emerging tropical and fungal infectious diseases.

Several new diagnostic approaches for diagnosis of TB have been studied in the last decade. This Research Topic includes four articles on TB (Zhou et al.; Jiao et al.; Dusthackeer et al.; Yong et al.). The study by Zhou et al. showed that the Ku protein is important in maintaining the genome's integrity of mycobacteria and that the ku gene was a highly specific biomarker for *Mycobacterium tuberculosis* (MTB) complex and non-tuberculosis *Mycobacteria*, which makes differentiation of *Mycobacteria* to closely related bacteria possible by a simple non-sequencing molecular method (Zhou et al.). In the study by Jiao et al. a design and evaluation of novel diagnostic assay was reported, termed multiple cross displacement amplification combined with nanoparticle-based lateral flow biosensor (MCDA), developed to simultaneously detect IS6110 and IS1081 of *Mycobacterium tuberculosis* (MTB) (Jiao et al.). Among clinically diagnosed TB patients, the sensitivity of liquid culture, Cepheid Xpert MTB/RIF and newly developed multiplex MCDA assay was 42, 50% and 88%, respectively. Among culture positive samples, the sensitivity of Xpert MTB/RIF and multiplex MCDA assay was 86 and 98%, respectively. Among culture negative samples, the sensitivity of Xpert MTB/RIF and multiplex MCDA assay was 23.2 and 81.2%, respectively. The specificity was 100% for Xpert MTB/RIF and 98.3% for multiplex MCDA. The results showed that the multiplex MCDA assay is a rapid, sensitive and easy to use tool for early diagnosis of TB (Jiao et al.). In the study of Dusthackeer et al., authors reported the presence of non-replicating bacteria in the sputum of suspected TB cases that show differential growth response to resuscitation-promoting factors (RPFs) treatment. Crude and recombinant RPF treatment improved sensitivity and reduced time to detect bacilli in the sputum samples of smear-positive/culture-negative or smear-negative/culture-negative cases. These findings have implications for improving the bacteriological diagnostic modalities currently in use for diagnosis of TB in endemic countries. New diagnostic approaches reported in this Research Topic may overcome the limitations observed with the currently available TB diagnostic tools (Acharya et al., 2020). This Research Topic also includes a review by Yong et al. on recent advances on TB biomarkers, particularly host biomarkers that have the great potential to improve diagnosis and differentiate between active and latent TB as well as on their use in disease prognosis and treatment monitoring (Yong et al.).

Another focus in this Research Topic is on novel approaches in diagnosis and treatment of emerging/reemerging tropical diseases (Shrivastava et al.; Mondal et al.; Buitrago and Martín-Gómez). Shrivastava et al. described design and evaluation of a sensitive and specific IgG indirect ELISA for high-throughput screening of Crimean-Congo hemorrhagic fever using viral multispecies recombinant nucleoprotein as an antigen. Results of Mondal et al. study (Mondal et al.) indicate that the relative quantity of serum anti-rK39 antibody is promising predictive and/or prognostic marker for visceral leishmaniasis or disease-related modalities. These could enable control programs to implement more effective measures to eliminate visceral leishmaniasis. More effective measures are also needed for histoplasmosis, which is increasingly reported in non-endemic countries as a result of recreational travels and migratory movements. Timely diagnosis is hampered by the lack of clinical awareness, and the scarcity of laboratory tools able to provide accurate results with a short turn-around time regardless of the immune status of the host and the extent of the disease. Molecular techniques are seen as a suitable alternative for this purpose in low prevalence areas and much needed efforts to standardize such assays and to define their diagnostic yield are in progress. Buitrago and Martín-Gómez reviewed current evidence behind the use of molecular tests in non-endemic areas, and as adjunctive tests for the laboratory diagnosis of histoplasmosis in high endemic areas (Buitrago and Martín-Gómez).

Two articles in this Research Topic evaluated new methods or combination of existing methods for more timely diagnosis of fungal infections (Vaezi et al.; Lo Cascio et al.). Vaezi et al. showed that the microculture assay may be useful for rapid culturing and diagnosis of mucormycosis caused by *Rhizopus arrhizus* directly in blood and tissue samples. Hence, this method may allow more timely administration of an appropriate treatment (Vaezi et al.). Despite that whole-genome sequencing is universally accepted as a reference method for identification of rare emerging pathogens, Lo Cascio et al. showed that proteomics is a promising alternative to laborious and time-consuming molecular methods for identification and evaluation of strain clonality in outbreaks of rare pathogens (Lo Cascio et al.).

Two contributions in this Research Topic reported results of studies in pediatric populations (Carter et al.; Fu et al.). Carter et al. assessed an antibody-in-lymphocyte supernatant assay for the etiological diagnosis of pneumococcal pneumonia in children (Carter et al.) and concluded that this method detected spontaneous secretion of IgG to pneumococcal protein antigens from cultured peripheral blood mononuclear cell. However, when stratified by age groups, this assay showed limited utility as a test to discriminate between pneumococcal and non-pneumococcal pneumonia in children. Fu et al. focused on autoinducer-2 (AI-2), which has a widely accepted role in bacterial intra- and interspecies communication (Fu et al.). This study found that AI-2 levels in a necrotizing enterocolitis mouse model as well as in patients correlate with intestinal flora disorder and different stages of disease. Based on these findings, AI-2 may be a new biomarker for the diagnosis and monitoring of necrotizing enterocolitis.

The possible new clinical applications of molecular methods were shown in two articles in this Research Topic (Sheikh et al.; Weng et al.). Sheikh et al. developed a colorimetric loop-mediated isothermal amplification assay (LAMP) for detection of IS1111a gene of *Coxiella burnetti* in sheep vaginal swabs (Sheikh et al.). LAMP is a more rapid and simpler method without the need for extensive sample preparation in comparison to routine PCR assay, whereas the sensitivity in Sheikh et al. study was comparable between both approaches. Moreover, LAMP could especially be attractive as point-of-care test in resource-limited settings (Ong and Poljak, 2020). Weng et al. showed that next-generation sequencing is a promising tool for rapid diagnosis of nocardiosis and could greatly reduce the turnaround time in comparison to traditional culturing methods, but current high cost and low accessibility of

next-generation sequencing still limit its utility in daily practice (Weng et al.).

Despite the great promise of newly developed breakthrough molecular methods, traditional molecular approaches remain indispensable in several clinical situations. Nikolic et al. described challenging diagnostic case of rare Lyme endocarditis diagnosed by traditional PCR. As the manifestations of Lyme endocarditis are non-specific, clinicians should test heart valve samples by PCR in case of endocarditis of unknown origin, especially in Lyme disease endemic areas (Nikolic et al.).

Innovative and practical diagnostic approaches in the field of viral infections were also evaluated in t his Research Topic (Breznik et al.; Tuaillon et al.). Breznik et al. detected human papillomaviruses (HPV) in 95% of common warts and showed that type-specific quantitative real-time PCRs could reliably assign the causative HPV type in almost 80% of cases, which provides further evidence that could be used in the selection of the most appropriate targets for future vaccines against HPV-related cutaneous tumors (Breznik et al.). Tuaillon et al. reviewed the current knowledge concerning the use of dried blood spots (DBS) for the diagnosis and therapeutic monitoring of HIV, hepatitis B and hepatitis C. DBS is a valid alternative in settings where there is no possibility for taking venous whole blood specimens or where transport of body fluids is difficult (Tuaillon et al.). Although DBS samples are suitable for testing of the presence of antibodies, antigens or nucleic acids, the lower analytical sensitivity remains one of the major limits of DBS in comparison to traditional blood samples. Therefore, the advantages of decentralized sampling and improved access to testing should be carefully outweighed against the possible limitations.

Finally, this Research Topic also includes articles on respiratory viruses, such as a review by Nelson et al. on current and future use of point-of-care tests (POCTs) for traditional and emerging respiratory viruses (Nelson et al.). During COVID-19 pandemic the use of POCTs has become more important than ever before. This review provides a description of new and innovative diagnostic techniques, ranging from biosensors to novel portable and current lab-based nucleic acid amplification methods with the potential future use in POCTs settings. In addition, Guo et al. designed an easy-to-use clinically predictive tool for assessing 90-days mortality risk of viral pneumonia. The tool can accurately stratify hospitalized patients with viral pneumonia into relevant risk categories and could provide guidance for further clinical decisions.

CONCLUSION

The original research and review articles in this Research Topic highlighted the importance and constant need for the development of novel, rapid and more accurate diagnostic tools for diagnosis of emerging/re-emerging infectious diseases. Contributions in this Research Topic described recent innovative approaches and provide hopeful prospects for improved patient care. Hopefully, this Research Topic will also stimulate further research with the ultimate goal of improving diagnosis and outcomes for patients with emerging infectious diseases, which should not be limited to the eminent threat by the current SARS-CoV-2 pandemic.

AUTHOR CONTRIBUTIONS

All authors listed have made a substantial, direct and intellectual contribution to the work, and approved it for publication.

REFERENCES

Acharya, B., Acharya, A., Gautam, S., Ghimire, S. P., Mishra, G., Parajuli, N., et al. (2020). Advances in diagnosis of tuberculosis: an update into molecular diagnosis of *Mycobacterium tuberculosis*. *Mol. Biol. Rep.* 47, 4065–4075. doi: 10.1007/s11033-020-05413-7

Castelli, F., and Sulis, G. (2017). Migration and infectious diseases. *Clin. Microbiol. Infec.* 23, 283–289. doi: 10.1016/j.cmi.2017.03.012

Morens, D. M., and Fauci, A. S. (2020). Emerging pandemic diseases: how we got to COVID-19. *Cell* 182, 1077–1092. doi: 10.1016/j.cell.2020.08.021

Ong, D. S. Y., and Poljak, M. (2020). Smartphones as mobile microbiological laboratories. *Clin. Microbiol. Infect.* 26, 421–424. doi: 10.1016/j.cmi.2019.09.026

Rechel, B., Mladovsky, P., Ingleby, D., Mackenbach, J. P., and McKee, M. (2013). Migration and health in an increasingly diverse Europe. *Lancet* 381, 1235–1245. doi: 10.1016/S0140-6736(12)62086-8

Conflict of Interest: The authors declare that the research was conducted in the absence of any commercial or financial relationships that could be construed as a potential conflict of interest.

frontiers in Microbiology

ORIGINAL RESEARCH
published: 13 August 2019
doi: 10.3389/fmicb.2019.01887

A New Single Gene Differential Biomarker for *Mycobacterium tuberculosis* Complex and Non-tuberculosis Mycobacteria

*Lei Zhou[1,2†], Cuidie Ma[1,3†], Tongyang Xiao[1], Machao Li[1], Haican Liu[1], Xiuqin Zhao[1], Kanglin Wan[1] and Ruibai Wang[1]**

[1] State Key Laboratory for Infectious Disease Prevention and Control, National Institute for Communicable Disease Control and Prevention, Chinese Center for Disease Control and Prevention, Beijing, China, [2] College of Pharmacy, Guizhou University, Guiyang, China, [3] College of Life Science and Technology, Beijing University of Chemical Technology, Beijing, China

OPEN ACCESS

Edited by:
Aleksandra Barac,
University of Belgrade, Serbia

Reviewed by:
Muge Cevik,
University of St Andrews, United Kingdom
Seyed Ehtesham Hasnain,
Jamia Hamdard University, India

***Correspondence:**
Ruibai Wang
wangruibai@icdc.cn

† These authors have contributed equally to this work

Specialty section:
This article was submitted to Infectious Diseases, a section of the journal Frontiers in Microbiology

Received: 03 May 2019
Accepted: 30 July 2019
Published: 13 August 2019

Citation:
Zhou L, Ma C, Xiao T, Li M, Liu H, Zhao X, Wan K and Wang R (2019) A New Single Gene Differential Biomarker for Mycobacterium tuberculosis Complex and Non-tuberculosis Mycobacteria. Front. Microbiol. 10:1887. doi: 10.3389/fmicb.2019.01887

Background: Tuberculosis (TB) and non-tuberculous mycobacteriosis are serious threats to health worldwide. A simple non-sequencing method is needed for rapid diagnosis, especially in less experienced hospitals, but there is no specific biomarker commonly used for all mycobacteria. The *ku* gene of the prokaryotic error-prone non-homologous end joining system (NHEJ) has the potential to be a highly specific detection biomarker for mycobacteria.

Methods: A total of 7294 mycobacterial genomes and 14 complete genomes of other families belonging to *Corynebacteriales* with *Mycobacteriaceae* were downloaded and analyzed for the existence and variation of the *ku* gene. *Mycobacterium tuberculosis* complex (MTBC) and non-tuberculosis mycobacteria (NTM)- specific primers were designed and the actual amplification and identification efficiencies were tested with 150 strains of 40 *Mycobacterium* species and 10 kinds of common respiratory pathogenic bacteria.

Results: The *ku* gene of the NHEJ system was ubiquitous in all genome sequenced *Mycobacterium* species and absent in other families of *Corynebacteriales*. On the one hand, as a single gene non-sequencing biomarker, its specific primers could effectively distinguish mycobacteria from other bacteria, MTBC from NTM, which would make the clinical detection of mycobacteria easy and have great clinical practical value. On the other hand, the sequence of *ku* gene can effectively distinguish NTM to species level with high resolution.

Conclusion: The Ku protein existed before the differentiation of *Mycobacterium* species, which was an important protein involved in maintaining of the genome's integrity and related to the special growth stage of mycobacteria. It was rare in prokaryotes. These features made it a highly special differential biomarker for *Mycobacterium*.

Keywords: *Mycobacterium*, non-homologous DNA end-joining, polymorphism, biomarker, non-tuberculosis mycobacteria, non-sequencing

INTRODUCTION

Mycobacterium is a genus of over 190 species and 13 subspecies. Apart from the causative agents, the *Mycobacterium tuberculosis* complex (MTBC) and *Mycobacterium leprae*, the other members of this genus are grouped together and termed non-tuberculosis mycobacteria (NTM). Both tuberculosis (TB) and non-tuberculous mycobacteriosis pose serious threats to health worldwide, especially with the increase of multi-drug and pan-drug-resistant strains.

Mycobacteria have completely different culture characteristics and therapeutic antibiotics from other bacteria. A preliminary discrimination of the infection as mycobacteriosis, TB or NTM, or a mixed infection of these two kinds of mycobacteria, will make the subsequent culture more directed and help improve the isolation/culture rate and appropriately administer clinical medication to reduce transmission more effectively, especially for less-experienced hospitals. This method should be simple, fast, accurate and culture-free.

Compared with the relatively easy diagnosis of tuberculosis, the diagnosis of non-tuberculosis is more dependent on culture and biochemical tests or by the exclusion that negative TB detection in smear/culture of acid-positive samples. Because of the cumbersome procedure, isolation, cultivation and identification of NTM is not actually done in many hospitals in China. The incidence and disease burden of NTM are continuously increasing in many regions, and the prevalence of NTM in aged people, human immunodeficiency virus (HIV)-infected patients and those with severely damaged immune systems is significant, even more than that of TB (Wang et al., 2014; Halstrom et al., 2015; Mortaz et al., 2018). Therefore, the rapid diagnosis of NTM is also a prominent problem. It is necessary to find a better single-gene biomarker, which can be used for both of MTBC and NTM identification.

Mycobacteria have three DNA double-strand break repair pathways, which include the NHEJ system required for the CRISPR/Cas9 system in the second step (Pitcher et al., 2006). The NHEJ system is absent in most prokaryotic cells. To date, eukaryotic NHEJ homologs have only been identified in *M. smegmatis*, *M. tuberculosis*, and *Bacillus subtilis* (*Bs*). Furthermore, prokaryotic NHEJ is a much simpler system that needs only two key proteins, Ku and ligase D (LigD) (Gong et al., 2005; Korycka-Machala et al., 2006; Shuman and Glickman, 2007; Gupta et al., 2011; Zheng et al., 2017). The Ku protein exists as a homodimer and preferentially binds to dsDNA ends (Weller et al., 2002). LigD is an adenosine triphosphate (ATP)-dependent DNA ligase that contains polymerase and nuclease domains, which facilitates the joining of long linear DNA molecules with different incompatible ends (Della et al., 2004). The rarity of the NHEJ system in bacteria hints that it may be developed into a *Mycobacterium* specific detection biomarker. Although, the NHEJ system has been confirmed existing in the *M. tuberculosis* strain H37Rv (Rv0937c and Rv0938 encoded) (Doherty et al., 2001; Weller et al., 2002), its distribution, especially the distribution of the Ku protein that could specifically stimulate LigD and suppress homologous recombination (Della et al., 2004) in other *Mycobacterium* species has not yet been elucidated. In this study, we analyzed *Mycobacterium* genome data submitted in GenBank before September 2018 to explore the existence of the *ku* gene in the *Mycobacterium* genus and determine its applicability for *Mycobacterium* identification.

MATERIALS AND METHODS

Genomic Data

We downloaded a total of 7294 genomes from 139 definite species, seven subspecies and five variants of *Mycobacterium* from the NCBI's FTP site submitted before September 2018, including 5245 genomes of *M. tuberculosis*, 1376 genomes of *M. abscessus*, 152 genomes of *M. avium*, and 70 *M. tuberculosis* variant *bovis* (**Supplementary Table 1**).

Sequence Extraction and Analysis

All the regions annotated as *ku* or *mku* and/or homologous to Rv0937c of *M. tuberculosis* were extracted from the genomes. Sequence alignments and comparisons were performed using the MEGA program version 6.0 (Tamura et al., 2013). Sequences were aligned on ClustalW using a gap opening penalty of 15 and a gap extension penalty of 6.66. Maximum likelihood trees were drawn. In each *Mycobacterium* species/variant, every *ku* sequence with even a nucleotide difference was defined as a genotype and listed in **Supplementary Table 1** with a representative sequence. The IS*6110* and *rpoB* genes were analyzed much as the *ku* gene was, and **Supplementary Table 2** lists the genotypes of the *rpoB* gene.

Primer Designed and PCR Amplification

Primers were designed using Oligo 6.0 and followed the general design principle of PCR primer. Simulated PCRs were performed using the Analyze Mix Wizard of Clone Manager Professional 9.0. The 379 *ku* genotype sequences were added as molecules in the mix.

In actual PCR amplification, the boiled DNA temples of *M. tuberculosis* H37Rv, *M. bovis* 93006 and 43 American Type Culture Collection (ATCC) NTM strains belonging to 40 species were used (**Table 1**). In addition, clinical isolates including 42 *M. tuberculosis* strains, 10 *M. abscessus* strains, 10 *M. marseillense* strains, 10 *M. avium* strains, 10 *M. kansasii* strains and 23 strains of 10 kinds of common respiratory pathogenic bacteria (**Table 1**) were also tested. PCR amplification condition was 5 min at 95°C followed by 30 cycles of 95°C 30 s, 58°C 30 s, and 72°C 1 min, with a final extension step at 72°C for 5 min. Four primer sets 16S 27f/16S907r (16SrRNA) (28), Tb11/Tb12 (*hsp65*) (Telenti et al., 1993), Myco-F/Myco-R (*rpoB*) (Adekambi and Drancourt, 2004), and 16S-1511f/23S-23r (ITS) (Harmsen et al., 2003) were used as control.

Statistical Analysis

Fourfold table Chi-square test was used to test the differences in variant rates between the *ku* and *rpoB* genes.

TABLE 1 | Strains and the amplification in the actual PCR tests.

Classification	Species	Strains	Gene targets for primers						
			Number	MTBC-ku	NTM-ku	16SrRNA	*hsp65*	*rpoB*	ITS
MTBC standard strains	*M. tuberculosis*	H37Rv	1	+	−	+	+	+	+
	M. bovis	93006	1	+	−	+	+	+	+
NTM standard strains	*M. abscessus*	95021	1	−	+	+	+	+	+
	M. aichiense	95026	1	−	+	+	+	+	+
	M. avium	25291	1	−	+	+	+	+	+
	M. bolletii	95067	1	−	+	+	+	+	+
	M. branderi	95068	1	−	+	+	+	+	+
	M. celatum	95072	1	−	+	+	+	+	+
	M. chelonae subsp. *chelonae*	93419	1	−	+	+	+	+	+
	M. diernhoferi	95149	1	−	+	+	+	+	+
	M. doricum	95078	1	−	+	+	+	+	+
	M. farcinogenes	93487	1	−	+	+	+	+	+
	M. farcinogenes	95012	1	−	+	+	+	+	+
	M. farcinogenes subsp. *senegalense*	93488	1	−	+	+	+	+	+
	M. flavescens	95030	1	−	+	+	+	+	+
	M. fluoranthenivorans	95081	1	−	+	+	+	+	+
	M. fortuitum subsp. *fortuitum*	93555	1	−	+	+	+	+	+
	M. fortuitum subsp. *fortuitum*	93556	1	−	+	+	+	+	+
	M. fortuitum subsp. *fortuitum doricum*	93407	1	−	+	+	+	+	+
	M. fortuitum subsp. *fortuitum duvalii*	93396	1	−	+	+	+	+	+
	M. frederiksbergense	95083	1	−	+	+	+	+	+
	M. gastri	95006	1	−	+	+	+	+	+
	M. gordonae	93409	1	−	+	+	+	+	+
	M. hassiacum	95085	1	−	+	+	+	+	+
	M. houstonense	95091	1	−	+	+	+	+	+
	M. kansasii	93410	1	−	+	+	+	+	+
	M. kansasii	95013	1	−	+	+	+	+	+
	M. komossense	95093	1	−	+	+	+	+	+
	M. kubicae	95094	1	−	+	+	+	+	+
	M. kumamotonense	95095	1	−	+	+	+	+	+
	M. lentiflavum	95097	1	−	+	+	+	+	+
	M. malmoense	95100	1	−	+	+	+	+	+
	M. malmoense	95148	1	−	+	+	+	+	+
	M. murale	95143	1	−	+	+	+	+	+
	M. nebraskense	95105	1	−	+	+	+	+	+
	M. neworleansense	95106	1	−	+	+	+	+	+
	M. palustre	95109	1	−	+	+	+	+	+
	M. peregrinum	95131	1	−	+	+	+	+	+
	M. saskatchewanense	95117	1	−	+	+	+	+	+
	M. senuense	95118	1	−	+	+	+	+	+
	M. smcgmatis	$Mc2^{155}$	1	−	+	+	+	+	+
	M. sphagni	95123	1	−	+	+	+	+	+
	M. terrae	95005	1	−	+	+	+	+	+
	M. vaccae	95003	1	−	+	+	+	+	+
	M. intracellulare	93519	1	−	+	+	+	+	+
	M. marseillense	95101	1	−	+	+	+	+	+
Clinical isolates	*M. tuberculosis*		42	+	−	+	+	+	+
	M. abscessus		10	−	+	+	+	+	+
	M. marseillense		10	−	+	+	+	+	+
	M. avium		10	−	+	+	+	+	+
	M. kansasii		10	−	+	+	+	+	+

(Continued)

TABLE 1 | Continued

Classification	Species	Strains	Gene targets for primers						
			Number	MTBC-ku	NTM-ku	16SrRNA	*hsp65*	*rpoB*	ITS
Common respiratory pathogenic bacteria	*Corynebacterium Diphtheria*	CMCC38105	1	–	–	+	–	–	+
	Klebsiella pneumoniae	KP3093	1	–	–	+	–	–	+
	Streptococcus pneumoniae	ATCC49619	1	–	–	+	–	–	+
	Mycoplasma pneumonia	29342	1	–	–	+	–	–	+
	Mycoplasma pneumonia	MP39505	1	–	–	+	–	–	+
	Staphylococcus aureus	CICC21601	1	–	–	+	–	–	+
	Staphylococcus aureus	CO WanI	1	–	–	+	–	–	+
	Haemophilus influenzae	M5216 Hib	1	–	–	+	–	–	+
	Neisseria meningitidis	341201	1	–	–	+	–	–	+
	Streptococcus pyogenes	CICC10373	1	–	–	+	–	–	+
	Legionella pneumophila	ATCC33152	1	–	–	+	–	–	+
	Legionella pneumophila	9797	1	–	–	+	–	–	+
	Legionella pneumophila	9134	1	–	–	+	–	–	+
	Nocardia farcinica	12	1	–	–	+	+	+	+
	Nocardia africana	75	1	–	–	+	+	+	+
	Nocardia farcinica	14	1	–	–	+	+	+	+
	Nocardia veterana	81	1	–	–	+	+	+	+
	Nocardia africana	72	1	–	–	+	+	+	+
	Nocardia nova	86	1	–	–	+	+	+	+
	Nocardia farcinica	90	1	–	–	+	+	+	+
	Nocardia veterana	84	1	–	–	+	+	+	+
	Nocardia paucivorans	79	1	–	–	+	+	+	+
	Nocardia abscessus	71	1	–	–	+	+	+	+

RESULTS

Distribution and Polymorphism of the *ku* Gene in *Mycobacterium*

The *ku* gene was found to be distributed in almost all of the 7294 *Mycobacterium* genomes with three exceptions: two incomplete genomes, *M. setense* strain 852014-10208_SCH5295773 and *M. tuberculosis* strain 0109V, without sequence analogous to the *ku* gene, and an incomplete *ku* gene in *M. tuberculosis* strain AH26_28866, with the first 290 bp in contig NZ_LKMH01000091.1 and 304–822 bp in contig NZ_LKMH01000168.1.

In *M. tuberculosis*, the *ku* gene was highly conserved. Of the 5243 *M. tuberculosis* genomes, there were 39 *ku* genotypes, of which 5149 (98.17%) genomes harbored the Rv0937c genotype, while 25 genomes were one genome with one genotype (**Supplementary Table 1**). The similarity of the *ku* gene sequence of the 39 genotypes was also very high. Only 37 sites on the 822 bp of the *ku* gene had variants, and sites 287, 449, and 451 had the highest rate of variation, at 5.13% (2/39).

In MTBC, except for *M. tuberculosis*, 116 genomes of four species (*M. africanum*, *M. bovis*, *M. caprae*, *M. microti*, and *M. pinnipedii*) and five variants (*M. canettii*, *M. decipiens*, *M. mungi*, and *M. orygis*) had 14 genotypes and 17 variant sites, among which the sequences of RN09_1148 genotypeof *M. africanum* (28/29), LH58_05105 of *M. bovis* (68/70), BBG46_05065 of *M. caprae* (2/2), MORY_05401 of *M. orygis* (1/1), MPS_4136 of *M. pinnipedii* (2/2), B8W66_10645 of *M. decipiens* (1/1) and RN08_1045 of *M. microti* (1/1) were completely identical to that of the Rv0937c genotype, as a result of which Rv0937c was the dominant genotype in the MTBC (98%, 5253/5359). On the other hand, nine *M. canettii* genomes were found to have six genotypes and two variant sites, A210G and A487G, which appeared only in all *M. canettii*, indicating obvious species specificity. In addition, from the high conservation of the *ku* gene in MTBC, we inferred that *M. tuberculosis* strain 0109V and *M. setense* strain 852014-10208_SCH5295773 might also carry the *ku* gene, and the missing of the *ku* gene was caused by the incompletion of the genomic data.

In NTM, 278 sites of the *ku* gene were conserved in all NTM genotypes, but the conservation of the *ku* gene in each species varied greatly (**Supplementary Table 1**). In some species, the *ku* gene was highly conserved and had few genotypes. For example, 91.4% (139/152) of *M. avium* were concentrated in three types (MAV_1050, IQU_02120, and O982_17680), 94.1% (16/17) of *M. immunogenum* in ABG82_05475, and 61.9% (13/21) of *M. kansasii* in MKSMC1_52900. However, most species are genotype polymorphic. There were nine genotypes among 10 genomes in *M. asiaticum* and 14 genotypes among 42 genomes

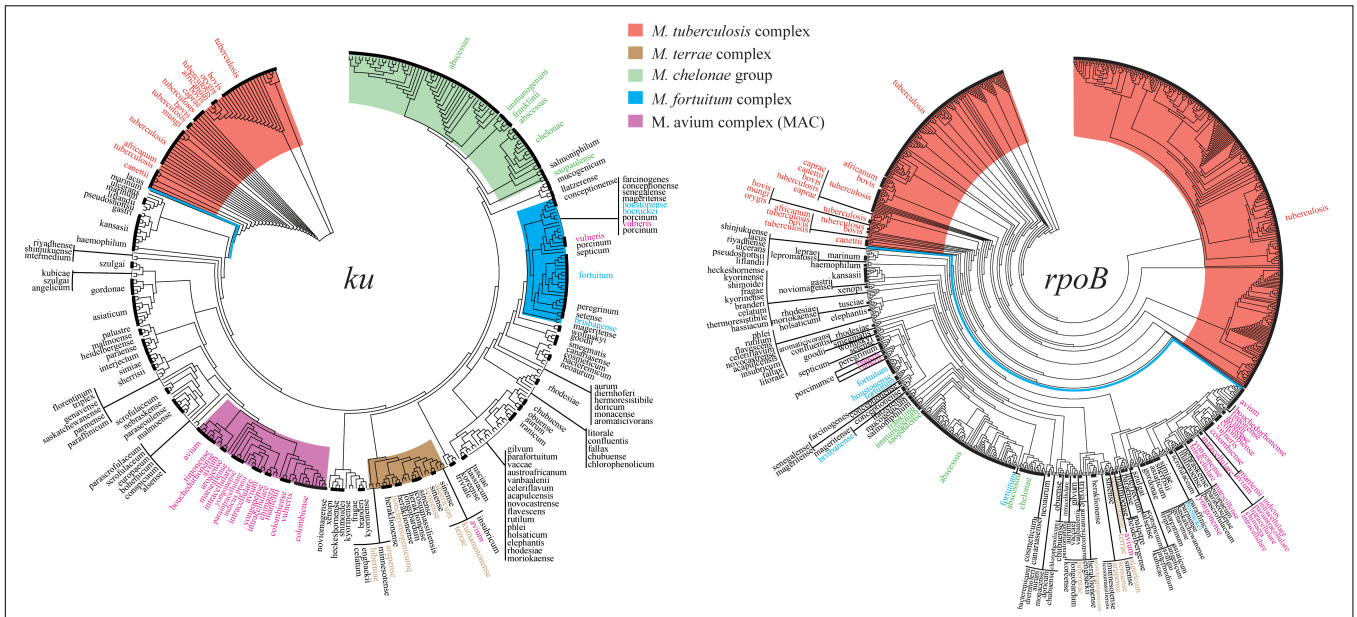

FIGURE 1 | Phylogenetic trees drawn on the basis of the *ku* and *rpoB* genes. The *Mycobacterium tuberculosis* complex (MTBC) and the four complex groups of non-tuberculous mycobacteria (NTM) are highlighted by different colors.

in *M. chelonae*. Furthermore, each genome had a genotype in some species, such as *M. heckeshornense*, *M. llatzerense*, and *M. mageritense*.

Overall, 32.4% sites (266/822) of the *ku* gene were conserved in all *Mycobacterium* genotypes, but none of the NTM genotype were 100% identical to the genotypes of MTBC, including Rv0937c. On phylogeny tree based on the *ku* gene, MTBC could be clearly separated from NTM without any exception (**Figure 1**). The *ku* genotypes in different species but having identical sequences are listed in **Table 2**. For MTBC, only *M. canettii*, *M. decipiens*, and *M. mungi* had completely special genotypes, other species of MTBC could not be separated by the *ku* gene sequence. For NTM, the genotypes of *M. avium* and *M. intracellulare*, *M. abscessus*, and *M. chelonae* only accounted for a very small proportion. Therefore, except the other 18 NTM species in **Table 2**, most of the NTMs could be identified to species level by the *ku* gene sequence.

Comparison of the *ku* Gene With the IS*6110* Element and the *rpoB* Gene

The distribution of the two most used identification loci, IS*6110* and *rpoB*, in the whole *Mycobacterium* genus had also been analyzed in this study.

The IS*6110* element has 16 completely identical copies in the *M. tuberculosis* strain H37Rv genome. There was at least one IS*6110* copy in 4450 *M. tuberculosis* genomes with identical sequence to the IS*6110* element of H37Rv. The IS*6110* element in 428 genomes were only partially identical to that of H37Rv. The IS*6110* of 306 *M. tuberculosis* genomes were located at the end of contig and were incomplete. The remaining 61 genomes, including the complete genome of *M. tuberculosis* UT205, had no sequences homologous to that of IS*6110*. In the other MTBC species/variants, the complete genomes of *M. canettii* CIPT 140070008 and 140070017 also had no sequences similar to that of IS*6110*. Therefore, even though it has been used as an important diagnostic marker to identify MTBC species (Coros et al., 2008; Guernier et al., 2017), the IS*6110* element was not common to all the MTBC strains, even *M. tuberculosis*. Tests based on it have false negatives, which is consistent with previous studies (Viana-Niero et al., 2006; Freidlin et al., 2017).

The *rpoB* gene was widely distributed in *Mycobacterium* and had a total of 861 genotypes, excluding 57 incomplete *rpoB* sequences from analysis (**Supplementary Table 2**). The *rpoB* gene had 454 variant sites in *M. tuberculosis* alone, compared to only 37 variant sites of the *ku* gene in *M. tuberculosis*. Even after standardization by gene length, the variant rate of *rpoB* gene in *M. tuberculosis* was 14.4% (454/3519 bp), which was far greater than that of the *ku* gene at 4.5% (37/822 bp) (Σ^2 = 46.872, $P < 0.01$). The *rpoB* gene could set apart the MTBC from all NTM without any exception on its phylogenetic tree, but the four complex groups of NTM could not be separated as distinctly as the tree drawn on the *ku* gene (**Figure 1**).

Scanning Similarities of the *ku* Gene in the Genomes of Other Families in *Corynebacteriales*

To confirm the results of Weller et al. (2002), we downloaded 14 whole genomic sequences of other families belonging to *Corynebacteriales* with *Mycobacteriaceae*, *Corynebacteriaceae* (CP008913.1, CP017639.1, CP026947.1, and CP026948.1), *Dietziaceae* (CP027238.1, and CP024869.1), *Gordoniaceae* (CP002907.1, NZ_CP025435.1, and CP023405.1),

TABLE 2 | *ku* genotypes in different species but with identical sequences.

	Strain numbers		Genotypes						
	Genotypes involved	**Species involved**							
MTBC	5250	5347	*M. africanum* CP010334	*M. bovis* NZ_CP009449	*M. caprae* NZ_CP016401	*M. microti* CP010333	*M. orygis* NZ_APKD01000011	*M. pinnipedii* NZ_PYQH00000000	*M. tuberculosis* NC_000962
NTM	2	9	*M. porcinum* NZ_MVIG01000003	*M. vulneris* NZ_CCBG010000002					
	2	8	*M. malmoense* NZ_MBEB01000153	*M. parascrofulaceum* NZ_GG770554					
	5	17	*M. indicuspranii* NC_018612	*M. intracellulare* NC_016948	*M. paraintracellulare* NZ_NCXN01000007	*M. yongonense* CP003347			
	2	4	*M. heckeshornense* NZ_MPJF01000011	*M. xenopi* NZ_AJFI01000095					
	4	15	*M. conceptionense* NZ_LFOD01000002	*M. mageritense* NZ_AGSZ01000485	*M. senegalense* NZ_LDCO01000015				
	10	20	*M. chimaera* NZ_CP012885	*M. intracellulare* NZ_JAON01000035					
	2	2	*M. austroafricanum* NZ_HG964452	*M. vanbaalenii* NC_008726					
	86	153	*M. avium* NC_008595	*M. bouchedurhonense* NZ_MVHL01000009					
	4	163	*M. avium* NZ_JAOD01000007	*M. intracellulare* NC_016946					
	6	1428	*M. abscessus* NZ_JMIA01000002	*M. chelonae* NZ_MAEQ01000007					

Segniliparaceae (CP001958.1), *Tsukamurellaceae* (CP001966.1), and *Nocardiaceae* (CP018082.1, CP032568.1, and CP016819.1) and blasted Rv0937c (NC_000962) with these genomes. The results showed that there was no region homologous to Rv0937c in these genomes.

Development of PCR System for Identifying of MTBC and NTM

For the rarity of the *ku* gene in bacteria and the distinct clusters of MTBC and NTM on the phylogenetic tree, we inferred that mycobacteria might be specially identified from other bacteria and MTBC from NTM only by PCR without sequencing. Afterward, the PCR system was developed.

Mycobacterium tuberculosis complex-specific primers were designed in the conservative regions that were identical in the 55 *ku* genotypes of MTBC, but different to all *ku* genotypes of NTM. Candidate primer sets with different product lengths were designed and screened. The pair with the most sufficient difference between MTBC and NTM was selected. ku-MTBC-U: GGT GGT CGA CTA CCG CGA TCT T and ku-MTBC-L: TCT TCG GGC TCG TCC AGC AAC C were located at 159–180 bp and 719–740 bp of the reference sequence of Rv0937c genotype, respectively. **Figure 2** shows that the design region of this pair of primers has a high degree of variation in NTM. Especially, the first base of the 3′ end of the upstream primer and the first, third and fourth base of the 3′ end of the downstream primer were single nucleotide polymorphic loci that completely distinguished MTBC from NTM. Simulated PCR revealed that 55 MTBC genotypes could be amplified by this primer set, but 324 NTM genotypes could not be amplified.

NZ_CP009616.seq of *M. abscessus* was used as reference of NTM for primer design. By marking the completely conserved sites in NTM on the reference sequence, it was found that the initial 1–20 bp of *ku* gene was the best region for the design of upstream primer ku-NTM-U with the most conserved sites in NTM and nine base difference to MTBC (**Figure 2**). The downstream primer Ku-NTM-L was an NTM/MTBC universal primer at 220–245 bp with eight conserved bases at the 3′ end. To improve the amplification efficiency of all NTMs, degenerate base were used. The primer set was ku-NTM-U: ATG CGT TCB ATH TGG AAR GG and ku-NTM-L: AGG CTC GCC AGR TCN TCR TCG GTG AT, and its specificity for NTM depends on the upstream primer.

In the actual PCR amplification of the 148 *Mycobacterium* and common respiratory pathogenic bacteria, all of the MTBC strains were positive for the amplification of ku-MTBC-U/L and negative for ku-NTM-U/L. The amplifications of NTM strains were opposite, and all of the 23 respiratory pathogenic bacteria were negative for both of them. The sensitivity and specificity of the two pairs of primers were 100%. Among the control primers, primers of 16SrRNA and ITS were universal and almost all of the tested strains, including the 23 respiratory pathogenic strains, were positive for them. Primers for *hsp60* and *rpoB* were specific for *Mycobacterium*. But all of the 10 *Nocardia* strains belonging to six *Nocardia* species were positive, although other

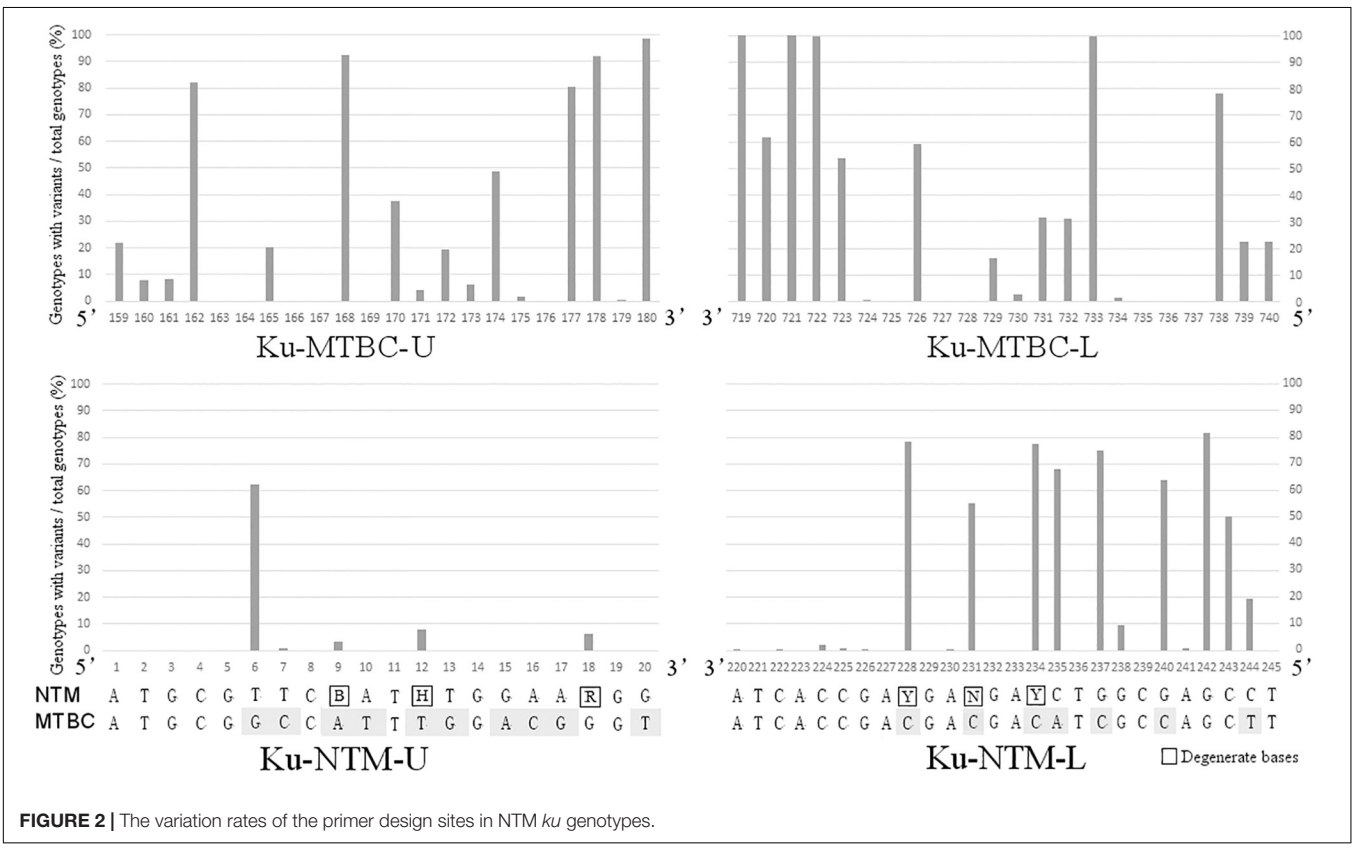

FIGURE 2 | The variation rates of the primer design sites in NTM *ku* genotypes.

respiratory pathogenic strains were negative (**Table 1**). Without sequencing, none of the four pairs of primers would be suitable for the identification of *Mycobacterium*, let alone the distinction between MTBC and NTM.

DISCUSSION

The GenBank database contains plenty of *Mycobacterium* genome data. The sensitivity and specificity of molecular detection methods can be predicted and compared before actual use. In this work, approximately 151 definite species/variants of *Mycobacterium* have been included, accounting for 79.7% of all known mycobacterial species and all submitted genomes. This work has the same coverage as the phylogenomics and comparative genomics studies of Gupta et al. (2018). Although it does not cover all the *Mycobacterium* species, it may be the most comprehensive analysis that can be done so far and includes all of the clinically common species.

The similarity between the eukaryotic and bacterial Ku proteins suggested that they were evolved from a common ancestor and very ancient process (Weller et al., 2002). The *ku* gene should be present in the *Mycobacterium* genome before the differentiation of *Mycobacterium* species. Additionally, The Ku-based NHEJ system participates in the repairing of DSBs of *Mycobacterium*, which maintains the genome integrity and is pivotal for cell survival. The *ku* gene is less likely to be lost in the evolution of *Mycobacterium*. Thus, it is reasonable that the *ku* gene is distributed and conserved in all sequenced *Mycobacterium* genomes. Moreover, the research of Weller et al. (2002) has speculated that the Ku ligase system might be related to the special growth stage of mycobacteria, especially the bacterial sporulation and the long stationary phase of life cycle. Different growth rates and culture and biochemical test characteristics are just important indicators for distinguishing *Mycobacterium* species, especially NTM. Therefore, in theory, it is not unexpected that the *ku* gene can completely distinguish MTBC from NTM and distinguish species in NTM.

Among the detection methods of *Mycobacterium*, acid-fast (AF) staining, also known as Ziehl–Neelsen stain, is currently the most widely used preliminary diagnostic method. The sensitivity of AF staining compared with culture ranges from 22 to 78%, and its limit of detection ranges from 5×10^3 to 1×10^4 bacilli/mL. However, AF staining is not specific for *Mycobacterium* detection, and *Mycobacterium* spp. cannot be distinguished from other AF bacteria, such as *Nocardia*, *Rhodococcus*, *Tsukamurella*, *Gordona*, *Dietzia*, *Legionella micdadei*, *Cryptosporidium*, *Isospora belli*, and *Cyclospora cayetanensis* and parasites such as *Sarcocystis* and *Taenia saginata*. Moreover, non-AF tuberculosis bacilli (Vilcheze and Kremer, 2017) also exist.

Thus, nucleic acid detection methods (NADMs) are becoming more and more important in the diagnosis and identification of mycobacteria (Niemann et al., 2000; Brunello et al., 2001). Loci of developed NADM include species-specific insertion sequences, such as IS*6110* for members of the *M. tuberculosis* complex (Thierry et al., 1990), IS*900* and *F57* for *M. avium* subsp. *paratuberculosis* (Slana et al., 2008), IS*901* for *M. avium* subsp. *avium* (Slana et al., 2010), IS*2404* and IS*2606* for *M. ulcerans, M. liflandii*, *M. pseudoshottsii*, and *M. shottsii* (mycolactone-producing mycobacteria) (Fyfe et al., 2007), and common shared bacterial genes, for example *16S rRNA*, *hsp65*, *rpoB* genes and the internal transcribed spacer (ITS) of broad-range sequencing approaches. Multi-genes analysis (Homolka et al., 2012; Perez-Lago et al., 2014; Gupta et al., 2018) and whole genome sequencing (Vissa et al., 2009; Fedrizzi et al., 2017; Trofimov et al., 2018) have also been used in *Mycobacterium* and because of their high resolution, they can identify mycobacteria to the species level. Methods based on sequencing and homology comparison, especially on sequences of hundreds of core genes or whole genome are more available for research purposes, and they are promising tools in the identification of new mycobacteria species, new molecules for bacterial typing and new candidate genes for multidrug resistance. But they are less practical for rapid screening of large samples and for primary hospitals without the ability of bioinformatics analysis. This is also the reason that single locus, IS*6110* and *rpoB*, are the most commonly used biomarkers. But IS*6110* cannot be applied to NTM. Although *rpoB* is used not only for identification but also for antibiotic resistance prediction, and GeneXpert assay which based on it requires little technical training and can obtained from unprocessed sputum samples in 90 min, with minimal biohazard. GeneXpert is replacing AF and endorsed by the World Health Organization (WHO) (Moure et al., 2011; Li et al., 2017), but it is also only applicable to MTBC and requires special instruments. In fact, until now, there has been no specific biomarker that is commonly used for all mycobacteria without sequencing.

The analysis in this study showed the value of the *ku* gene as a diagnostic biomarker. The *ku* gene is not a common gene of bacteria. Its rarity in prokaryotes (Weller et al., 2002), especially its absence in bacteria closely related to *Mycobacterium* (such as *Nocardia*), endows it with high specificity. Its wide distribution in all sequenced *Mycobacterium* makes it widely applicable for MTBC and NTM. Both features actualize the greatest application value of the *ku* gene, that is, they can directly distinguish mycobacteria, MTBC and NTM by PCR, and achieve the purpose of rapid clinical diagnosis. This actual application value has been confirmed by the MTBC/NTM- specific primers we designed and the testing of the standard and clinical strains. In conclusion, Ku gene is a new single-gene biomarker of *Mycobacterium* that differentiates MTBC and NTM and makes the identification of MTBC and NTM simpler and more accurate. However, it does not define the resistance of *Mycobacterium*, so it can't take into account the identification of strains and the prediction of drug resistance simultaneously as *ropB* gene does. Its application value lies in that it can be used as a single indicator for the primary screening and identification of mycobacteria, or can be combined with *rpoB* to complement its deficiencies for accurate identification of *Mycobacterium*. More sensitive detection methods based on this gene and application for the detection of different samples besides pure cultures will be explored in our further study to help the diagnosis of Tb worldwide.

DATA AVAILABILITY

All datasets generated for this study are included in the manuscript and/or the **Supplementary Files**.

AUTHOR CONTRIBUTIONS

RW conceived the project, analyzed and interpreted the data, designed the primers, and prepared the figures and manuscript. LZ, CM, and TX did the PCR testing. ML and XZ collected the strains. HL downloaded the *Mycobacterium* genomes from the GenBank database. KW revised the manuscript. All authors had full access to all the data in the study and approved the final version of the manuscript for submission.

SUPPLEMENTARY MATERIAL

The Supplementary Material for this article can be found online at: https://www.frontiersin.org/articles/10.3389/fmicb.2019.01887/full#supplementary-material

REFERENCES

Adekambi, T., and Drancourt, M. (2004). Dissection of phylogenetic relationships among 19 rapidly growing *Mycobacterium* species by 16S rRNA, hsp65, sodA, recA and rpoB gene sequencing. *Int. J. Syst. Evol. Microbiol.* 54, 2095–2105. doi: 10.1099/ijs.0.63094-0

Brunello, F., Ligozzi, M., Cristelli, E., Bonora, S., Tortoli, E., and Fontana, R. (2001). Identification of 54 mycobacterial species by PCR-restriction fragment length polymorphism analysis of the hsp65 gene. *J. Clin. Microbiol.* 39, 2799–2806. doi: 10.1128/jcm.39.8.2799-2806.2001

Coros, A., Deconno, E., and Derbyshire, K. M. (2008). IS6110, a *Mycobacterium* tuberculosis complex-specific insertion sequence, is also present in the genome of *Mycobacterium smegmatis*, suggestive of lateral gene transfer among *Mycobacterial* species. *J. Bacteriol.* 190, 3408–3410. doi: 10.1128/JB.00009-08

Della, M., Palmbos, P. L., Tseng, H. M., Tonkin, L. M., Daley, J. M., Topper, L. M., et al. (2004). *Mycobacterial* Ku and ligase proteins constitute a two-component NHEJ repair machine. *Science* 306, 683–685. doi: 10.1126/science.1099824

Doherty, A. J., Jackson, S. P., and Weller, G. R. (2001). Identification of bacterial homologues of the Ku DNA repair proteins. *FEBS Lett.* 500, 186–188. doi: 10.1016/s0014-5793(01)02589-3

Fedrizzi, T., Meehan, C. J., Grottola, A., Giacobazzi, E., Fregni Serpini, G., Tagliazucchi, S., et al. (2017). Genomic characterization of nontuberculous *Mycobacteria*. *Sci. Rep.* 7:45258. doi: 10.1038/srep45258

Freidlin, P. J., Nissan, I., Luria, A., Goldblatt, D., Schaffer, L., Kaidar-Shwartz, H., et al. (2017). Structure and variation of CRISPR and CRISPR-flanking regions in deleted-direct repeat region *Mycobacterium tuberculosis* complex strains. *BMC Genomics* 18:168. doi: 10.1186/s12864-017-3560-6

Fyfe, J. A., Lavender, C. J., Johnson, P. D., Globan, M., Sievers, A., Azuolas, J., et al. (2007). Development and application of two multiplex real-time PCR assays for the detection of *Mycobacterium ulcerans* in clinical and environmental samples. *Appl. Environ. Microbiol.* 73, 4733–4740. doi: 10.1128/aem.02971-06

Gong, C., Bongiorno, P., Martins, A., Stephanou, N. C., Zhu, H., Shuman, S., et al. (2005). Mechanism of nonhomologous end-joining in mycobacteria: a low-fidelity repair system driven by Ku, ligase D and ligase C. *Nat. Struct. Mol. Biol.* 12, 304–312. doi: 10.1038/nsmb915

Guernier, V., Diefenbach-Elstob, T., Pelowa, D., Pollard, S., Burgess, G., Mcbryde, E. S., et al. (2017). Molecular diagnosis of suspected tuberculosis from archived smear slides from the Balimo region, Papua New Guinea. *Int. J. Infect. Dis.* 67, 75–81. doi: 10.1016/j.ijid.2017.12.004

Gupta, R., Barkan, D., Redelman-Sidi, G., Shuman, S., and Glickman, M. S. (2011). Mycobacteria exploit three genetically distinct DNA double-strand break repair pathways. *Mol. Microbiol.* 79, 316–330. doi: 10.1111/j.1365-2958.2010.07463.x

Gupta, R. S., Lo, B., and Son, J. (2018). Phylogenomics and comparative genomic studies robustly support division of the genus *Mycobacterium* into an emended genus *Mycobacterium* and four novel genera. *Front. Microbiol.* 9:67. doi: 10.3389/fmicb.2018.00067

Halstrom, S., Price, P., and Thomson, R. (2015). Review: environmental *Mycobacteria* as a cause of human infection. *Int. J. Mycobacteriol.* 4, 81–91. doi: 10.1016/j.ijmyco.2015.03.002

Harmsen, D., Dostal, S., Roth, A., Niemann, S., Rothganger, J., Sammeth, M., et al. (2003). RIDOM: comprehensive and public sequence database for identification of *Mycobacterium species*. *BMC Infect. Dis.* 3:26.

Homolka, S., Projahn, M., Feuerriegel, S., Ubben, T., Diel, R., Nubel, U., et al. (2012). High resolution discrimination of clinical *Mycobacterium tuberculosis* complex strains based on single nucleotide polymorphisms. *PLoS One* 7:e39855. doi: 10.1371/journal.pone.0039855

Korycka-Machala, M., Brzostek, A., Rozalska, S., Rumijowska-Galewicz, A., Dziedzic, R., Bowater, R., et al. (2006). Distinct DNA repair pathways involving RecA and nonhomologous end joining in *Mycobacterium smegmatis*. *FEMS Microbiol. Lett.* 258, 83–91. doi: 10.1111/j.1574-6968.2006.00199.x

Li, Y., Pang, Y., Zhang, T., Xian, X., Wang, X., Yang, J., et al. (2017). Rapid diagnosis of extrapulmonary *tuberculosis* with xpert *Mycobacterium tuberculosis/rifampicin* assay. *J. Med. Microbiol.* 66, 910–914. doi: 10.1099/jmm.0.000522

Mortaz, E., Moloudizargari, M., Varahram, M., Movassaghi, M., Garssen, J., Kazempour Dizagie, M., et al. (2018). What immunological defects predispose to non-tuberculosis *Mycobacterial* infections? *Iran J. Allergy Asthma Immunol.* 17, 100–109.

Moure, R., Munoz, L., Torres, M., Santin, M., Martin, R., and Alcaide, F. (2011). Rapid detection of *Mycobacterium tuberculosis* complex and rifampin resistance in smear-negative clinical samples by use of an integrated real-time PCR method. *J. Clin. Microbiol.* 49, 1137–1139. doi: 10.1128/JCM.01831-10

Niemann, S., Harmsen, D., Rusch-Gerdes, S., and Richter, E. (2000). Differentiation of clinical *Mycobacterium tuberculosis* complex isolates by gyrB DNA sequence polymorphism analysis. *J. Clin. Microbiol.* 38, 3231–3234.

Perez-Lago, L., Navarro, Y., and Garcia-De-Viedma, D. (2014). Current knowledge and pending challenges in zoonosis caused by *Mycobacterium bovis*: a review. *Res. Vet. Sci.* 97(Suppl.), S94–S100. doi: 10.1016/j.rvsc.2013.11.008

Pitcher, R. S., Tonkin, L. M., Daley, J. M., Palmbos, P. L., Green, A. J., Velting, T. L., et al. (2006). Mycobacteriophage exploit NHEJ to facilitate genome circularization. *Mol. Cell.* 23, 743–748. doi: 10.1016/j.molcel.2006.07.009

Shuman, S., and Glickman, M. S. (2007). Bacterial DNA repair by non-homologous end joining. *Nat. Rev. Microbiol.* 5, 852–861.

Slana, I., Kaevska, M., Kralik, P., Horvathova, A., and Pavlik, I. (2010). Distribution of *Mycobacterium avium* subsp. avium and M. a. hominissuis in artificially infected pigs studied by culture and IS901 and IS1245 quantitative real time PCR. *Vet. Microbiol.* 144, 437–443. doi: 10.1016/j.vetmic.2010.02.024

Slana, I., Kralik, P., Kralova, A., and Pavlik, I. (2008). On-farm spread of *Mycobacterium avium* subsp. paratuberculosis in raw milk studied by IS900 and F57 competitive real time quantitative PCR and culture examination. *Int. J. Food Microbiol.* 128, 250–257. doi: 10.1016/j.ijfoodmicro.2008.08.013

Tamura, K., Stecher, G., Peterson, D., Filipski, A., and Kumar, S. (2013). MEGA6: Molecular Evolutionary Genetics Analysis version 6.0. *Mol. Biol. Evol.* 30, 2725–2729. doi: 10.1093/molbev/mst197

Telenti, A., Marchesi, F., Balz, M., Bally, F., Bottger, E. C., and Bodmer, T. (1993). Rapid identification of mycobacteria to the species level by polymerase chain reaction and restriction enzyme analysis. *J. Clin. Microbiol.* 31, 175–178.

Thierry, D., Cave, M. D., Eisenach, K. D., Crawford, J. T., Bates, J. H., Gicquel, B., et al. (1990). IS6110, an IS-like element of *Mycobacterium tuberculosis* complex. *Nucleic Acids Res.* 18:188.

Trofimov, V., Kicka, S., Mucaria, S., Hanna, N., Ramon-Olayo, F., Del Peral, L. V., et al. (2018). Antimycobacterial drug discovery using mycobacteria-infected amoebae identifies anti-infectives and new molecular targets. *Sci. Rep.* 8:3939. doi: 10.1038/s41598-018-22228-6

Viana-Niero, C., Rodriguez, C. A., Bigi, F., Zanini, M. S., Ferreira-Neto, J. S., Cataldi, A., et al. (2006). Identification of an IS6110 insertion site in plcD, the unique phospholipase C gene of *Mycobacterium bovis*. *J. Med. Microbiol.* 55, 451–457. doi: 10.1099/jmm.0.46364-0

Vilcheze, C., and Kremer, L. (2017). Acid-fast positive and acid-fast negative *Mycobacterium tuberculosis*: the koch paradox. *Microbiol Spectr* 5:TBTB2-TBTB0003. doi: 10.1128/microbiolspec.TBTB2-0003-2015

Vissa, V. D., Sakamuri, R. M., Li, W., and Brennan, P. J. (2009). Defining mycobacteria: shared and specific genome features for different lifestyles. *Indian J. Microbiol.* 49, 11–47. doi: 10.1007/s12088-009-0006-0

Wang, L., Zhang, H., Ruan, Y., Chin, D. P., Xia, Y., Cheng, S., et al. (2014). Tuberculosis prevalence in China, 1990-2010; a longitudinal analysis of national survey data. *Lancet* 383, 2057–2064. doi: 10.1016/S0140-6736(13)62639-2

Weller, G. R., Kysela, B., Roy, R., Tonkin, L. M., Scanlan, E., Della, M., et al. (2002). Identification of a DNA nonhomologous end-joining complex in bacteria. *Science* 297, 1686–1689. doi: 10.1126/science.1074584

Zheng, X., Li, S. Y., Zhao, G. P., and Wang, J. (2017). An efficient system for deletion of large DNA fragments in *Escherichia coli* via introduction of both Cas9 and the non-homologous end joining system from *Mycobacterium smegmatis*. *Biochem. Biophys. Res. Commun.* 485, 768–774. doi: 10.1016/j.bbrc.2017.02.129

Conflict of Interest Statement: The authors have applied for a pending Chinese patent titled "The application of the Ku protein in *Mycobacterium*," Number: 201910154948.5.

frontiers in Microbiology

ORIGINAL RESEARCH
published: 23 August 2019
doi: 10.3389/fmicb.2019.01822

Development of Multispecies Recombinant Nucleoprotein-Based Indirect ELISA for High-Throughput Screening of Crimean-Congo Hemorrhagic Fever Virus-Specific Antibodies

*Neha Shrivastava[1], Ambuj Shrivastava[1], Sandeep M. Ninawe[1], Shashi Sharma[1], Jyoti S. Kumar[1], Syed Imteyaz Alam[2], Amit Kanani[3], Sushil Kumar Sharma[1] and Paban Kumar Dash[1]**

[1] Division of Virology, Defence Research and Development Establishment, Gwalior, India, [2] Division of Biotechnology, Defence Research and Development Establishment, Gwalior, India, [3] Office of Deputy Director of Animal Husbandry, FMD Typing Scheme, Ahmedabad, India

OPEN ACCESS

Edited by:
Mario Poljak,
University of Ljubljana, Slovenia

Reviewed by:
Agustín Estrada-Peña,
University of Zaragoza, Spain
Christina Deschermeier,
Bernhard-Nocht-Institut für Tropenmedizin (BMITM), Germany
Aykut Ozkul,
Ankara University, Turkey

***Correspondence:**
Paban Kumar Dash
pabandash@drde.drdo.in

Specialty section:
This article was submitted to Infectious Diseases, a section of the journal Frontiers in Microbiology

Received: 21 May 2019
Accepted: 24 July 2019
Published: 23 August 2019

Citation:
Shrivastava N, Shrivastava A, Ninawe SM, Sharma S, Kumar JS, Alam SI, Kanani A, Sharma SK and Dash PK (2019) Development of Multispecies Recombinant Nucleoprotein-Based Indirect ELISA for High-Throughput Screening of Crimean-Congo Hemorrhagic Fever Virus-Specific Antibodies. Front. Microbiol. 10:1822. doi: 10.3389/fmicb.2019.01822

Crimean-Congo hemorrhagic fever (CCHF) is a re-emerging zoonotic viral disease prevalent in many parts of Asia, Europe, and Africa. The causative agent, Crimean-Congo hemorrhagic fever orthonairovirus (CCHFV), is transmitted through hard ticks. Tick vectors especially belonging to the *Hyalomma* species serve as the reservoir and amplifying host. The vertebrate animals including sheep, goat, and bovine act as a short-lasting bridge linking the virus and ticks. CCHFV causes fatal hemorrhagic fever in humans. Humans are usually infected with CCHFV either through the bite of infected ticks or by close contact with infected animals. Immunological assays, primarily enzyme-linked immunosorbent assay (ELISA) using whole viral antigen, are widely used for serosurveillance in animals. However, the whole virus antigen poses a high biohazard risk and can only be produced in biosafety level 4 laboratories. The present study focuses on the development and evaluation of safe, sensitive, and specific IgG indirect enzyme-linked immunosorbent assay (iELISA) using recombinant nucleoprotein (NP) of CCHF virus as an antigen. The codon-optimized NP gene sequence was synthesized, cloned, and expressed in pET28a+ vector. The recombinant NP was purified to homogeneity by affinity chromatography and characterized through Western blot and MALDI-TOF/MS analysis. The characterized protein was used to develop an indirect IgG microplate ELISA using a panel of animal sera. The in-house ELISA was comparatively evaluated vis-à-vis a commercially available ELISA kit (Vector-Best, Russia) with 76 suspected samples that revealed a concordance of 90% with a sensitivity and specificity of 79.4 and 100%, respectively. The precision analysis revealed that the assay is robust and reproducible in different sets of conditions. Further, the assay was used for serosurveillance in ruminants from different regions of India that

revealed 18% seropositivity in ruminants, indicating continued circulation of virus in the region. The findings suggest that the developed IgG iELISA employing recombinant NP is a safe and valuable tool for scalable high-throughput screening of CCHFV-specific antibodies in multiple species.

Keywords: Crimean-Congo hemorrhagic fever, antigen, protein purification, IgG, seroepidemiology, diagnosis

INTRODUCTION

Crimean Congo hemorrhagic fever orthonairovirus (CCHFV), an emerging tick-borne virus, is considered as a biothreat agent because of its potential to cause deadly hemorrhagic fever. A tick-borne virus, CCHFV belongs to the family *Nairoviridae* and genus *Orthonairovirus* (Adams et al., 2017). It is endemic in different parts of the world including Asia, Africa, and Europe with a fatality rate up to 80% (Ergönül, 2006). In humans, it causes acute hemorrhagic illness, leading to hypovolemic shock and death in extreme cases. CCHFV is primarily transmitted to humans through the bite of an infected tick. In animals, CCHF is asymptomatic and does not cause any disease but is a major threat to humans especially to those who are in close contact with infected animals particularly in farms, clinic, and abattoir (Mostafavi et al., 2017).

The genome of CCHFV is triple segmented, consisting of small (S), medium (M), and large (L) segments. Electron microscopy depicts viral particles of 90–100 nm in diameter (Zivcec et al., 2016). The open reading frame (ORF) of the S segment encodes a 482-amino-acid-long nucleocapsid protein that is highly conserved in nature and is an attractive target for development of diagnostics and vaccine (Burt et al., 1994; Carter et al., 2012; Vanhomwegen et al., 2012).

Many of the CCHF cases were reported from remote settings, where there is a lack of proper detection facility that leads to underreporting. Limited serosurveillance studies have shown high IgG positivity in livestock in different parts of endemic areas including India (Mourya et al., 2015). Ruminants play a crucial role in providing blood meal to ticks, their transportation across different territorial regions, and transmitting virus to naïve ticks and humans (Mertens et al., 2015; Spengler et al., 2016). Efforts are needed to detect the infection burden in animals using a safe, stable, and sensitive screening test that can be easily accessible in rural health care facilities.

The laboratory detection of CCHFV relies on virus isolation, RT-PCR, and serology. Virus isolation and RT-PCR are limited to biosafety level 4 (BSL-4) laboratory and highly sophisticated laboratory, respectively, having technical expertise (Al-Abri et al., 2017). Further, serological assays, viz., hemagglutination inhibition and complement fixation tests, suffer from various issues including reproducibility and sensitivity (Casals and Tignor, 1974). The currently used serological tests include immunofluorescence (IFA) and enzyme-linked immunosorbent assay (ELISA), though IFA demands specialized equipment, technique, and complexity in data interpretation, whereas ELISA can be performed in laboratory with minimum resources (Vanhomwegen et al., 2012). The widely used serological assays rely on whole virus as the antigen, primarily inactivated viral lysate, or hyper immune mouse ascitic fluid, which is used to capture antibodies (Mourya et al., 2012). Such antigen poses a high biohazard risk and their production is limited to maximum containment facilities (BSL-4), which are limited in the developing world.

The recombinant protein-based antigen is slowly replacing the viral diagnosis over the last few decades (Cuzzubbo et al., 2001; Álvarez-Rodríguez et al., 2012; Souza et al., 2012; Saxena et al., 2013). Bacterial expression systems are the preferred method of choice due to their inexpensive scale up and ease of utility (Babaeipour et al., 2010; Huang et al., 2012). The ease and reproducibility of antigen production make these antigens reliable for commercialization. Attempts were made to develop IgG ELISA for CCHF using recombinant nucleoprotein (NP) in baculovirus (Saijo et al., 2002; Samudzi et al., 2012). However, such expression systems are expensive, need to reinfect with fresh culture for each round of protein synthesis, and thus are inefficient for commercial-scale production. Recombinant NP protein was also attempted to express in prokaryotic system but protein instability was the major concern of the reported system (Liu et al., 2014). Recently, HRP-conjugated recombinant NP-based ELISA was developed for IgG detection, but the HRP-conjugated antigens are liable to lose their epitopes during conjugation and thus lack sensitivity; also, the stability of HRP-conjugated antigen is questionable until experimentally proven (Ge et al., 2017; Emmerich et al., 2018; Sas et al., 2018). Earlier, Schuster et al. (2016) reported the development of a competitive ELISA format using monoclonal antibodies against NP for serosurveillance. However, the involvement of specific monoclonal antibody and the competitive format make the process complex and costlier. The production of recombinant protein in the eukaryotic system is complex and expensive compared to the bacterial system. Keeping in view the above facts, the present study was envisaged to produce a safe and stable recombinant antigen in the prokaryotic system for the development of IgG iELISA assay. Recombinant NP was produced under native conditions in order to express its conformational epitopes to recognize all the possible antibodies. The soluble r-NP was used as a

Abbreviations: ACN, acetonitrile; AUC, area under curve; BSL 4, biosafety level 4; CCHF, Crimean-Congo hemorrhagic fever; CHCA, α-cyano-4-hydroxycinnamic acid; CID, collision-induced dissociation; DAB, 3,3'-diaminobenzidine; DTT, dithiothreitol; FMD, foot-and-mouth disease; H_2O_2, Hydrogen peroxide; HRP, horseradish peroxidase; iELISA, indirect enzyme-linked immunosorbent assay; IFA, immunofluorescence; IPTG, isopropyl-β-D-thiogalactopyranoside; MALDI/MS, matrix-assisted laser desorption ionization/mass spectrometry; NP, nucleoprotein; NPV, negative predictive value; PBS, phosphate buffer saline; PMSF, phenyl methyl sulfonyl fluoride; PPR, peste des petits ruminants; PPV, positive predictive value; RE, restriction enzyme; ROC, receiver operating characteristic; SMP, skim milk powder; TFA, trifluoroacetic acid; TIS, timed ion selector.

diagnostic intermediate for development of IgG iELISA. The assay was further evaluated with commercial system, and concordance, sensitivity, along with specificity were determined. Both intra- and inter-assay variations were also analyzed to study the precision of assay. Finally, the assay was applied for screening of animal sera from different regions in India for epidemiological serosurveillance.

MATERIALS AND METHODS

Media, Chemicals, and Solutions

Escherichia coli strain DH5α was procured from Invitrogen, United States. *E. coli* host strain BL21(DE3) for expression of plasmid was purchased from Thermo Fisher Scientific, United States. The cloning vector pUC57 (amp^r) and expression vector pET28a+ (kan^r) were purchased from Novagen, United States. Ni-NTA superflow resin was procured from Qiagen, Germany. Protease inhibiting cocktail (Sigma-Aldrich) and TB were from HiMedia. Secondary HRP conjugates (anti-sheep HRP, anti-goat HRP and anti-bovine HRP) and HRPO substrate 3,3′,5,5′-tetramethylbenzidine (TMB) were procured from Sigma-Aldrich, United States. VectoCrimea CHF IgG ELISA kit was purchased from Vector-Best, Russia.

Construction of Recombinant Plasmid

The ORF encoding NP of CCHF virus from Indian isolate ID NIV 112143 (GenBank Accession no. JN572089) was codon optimized for *E. coli* and custom synthesized from M/s Bio Basic Inc., Canada. The custom synthesized gene (1458 bp) was confirmed by nucleotide sequencing and cloned in pUC 57 cloning vector.

Sub-Cloning of Recombinant NP Gene in pET28a+ Vector

Both recombinant plasmid of NP in pUC57 cloning vector and pET28a+ expression vector were digested with *Bam*HI and *Hin*dIII restriction enzymes (RE) at 37°C for 1 h. The insert (NP) and the vector (pET28a+ expression vector) were purified using agarose gel and ligated. The ligated product was transformed into competent *E. coli* DH5α cells as per standard protocol. Transformed positive clones were selected by RE digestion and colony lysis PCR. The recombinant plasmid was isolated and further transformed into *E. coli* BL21 (DE3) cells for expression. The recombinant transformed clone was also confirmed by RE digestion, colony lysis PCR, and nucleotide sequencing.

Expression and Localization of Recombinant Protein

The logarithmic phase culture of positive colony was induced with varying concentrations of isopropyl-β-D-thiogalactopyranoside (IPTG) (0.5, 1, 1.5, and 2 mM) in Terrific broth (TB) for different time periods (1–4 h). Further, another lot was induced at 18°C for 18 h. The localization of recombinant protein was identified through sonication of cell suspension followed by centrifugation at 18,600 × *g* for 30 min at 4°C. The expression profile was studied by 10% SDS-PAGE.

Purification of Recombinant Nucleoprotein Under Native Conditions

Following induction, cells were harvested by centrifugation at 4,000 × *g* for 20 min. Harvested cells were then resuspended in lysis buffer (50 mM NaH_2PO_4, 300 mM NaCl, and 10 mM imidazole, pH 8.0) supplemented with phenylmethylsulfonylfluoride (PMSF), lysozyme, and protease inhibiting cocktail (Sigma-Aldrich, United States) and incubated at 4°C for 30 min, followed by sonication at 9 pulse on/off using microprobe at 40% frequency of sonicator (Sonics, United States) for 30 min. The sonicated culture was centrifuged at 10,000 × *g* for 20 min. The supernatant was filtered with a 0.45-μm filter and loaded on the pre-equilibrated polypropylene column containing Ni-NTA slurry for 2 h at 4°C for efficient binding. After passing the supernatant through a column, it was washed with 10 bed volumes of wash buffer (50 mM NaH_2PO_4, 300 mM NaCl, and 20 mM imidazole, pH 8.0) to remove unbound protein. Later on, the bound protein was eluted through elution buffer (50 mM NaH_2PO_4, 300 mM NaCl, and 250 mM imidazole, pH 8.0). Eluted protein was concentrated using an Amicon Ultra centrifugal filter device with a 30-kDa MWCO membrane. Purified protein was dialyzed overnight against dialysis buffer (50 mM NaH_2PO_4 and 300 mM NaCl). Protein was analyzed on 10% SDS-PAGE followed by staining with Coomassie Brilliant Blue. The concentration of purified protein was estimated by bicinchoninic acid assay (Thermo Fisher Scientific, United States) and stored at −80°C with 5% glycerol to enhance the stability of recombinant NP.

Characterization of r-NP Through Western Blot Analysis

Characterization of r-CCHF-NP was carried out using commercial rabbit polyclonal antibody against NP of CCHFV (Abcam, United States) and anti-His antibody (Sigma-Aldrich, United States) with Western blot. The purified r-NP protein was resolved on 10% SDS and transferred to nitrocellulose membrane. Membranes were blocked with 2% SMP for 2 h, followed by washing with 1 × PBS. Then, the membranes were incubated with 1:500 dilution of commercial polyclonal antibody and 1:1,000 dilution of anti-His antibody diluted in 1% SMP overnight, respectively. After washing thrice with 0.1% PBST, membranes were incubated with their respective HRP conjugate (anti-rabbit and anti-mice HRP conjugate). The conjugates were diluted in 1% Skim milk powder (1:1000) for 2 h followed by washing with 0.1% PBST. The membrane was finally developed using 3,3-diaminobenzidine (DAB) as substrate and H_2O_2.

In-Gel Protein Digestion

Gel pieces were excised from the SDS-PAGE and destained by three washes of 50% ACN/50 mM NH_4HCO_3 for 30 min each at room temperature. The protein was subjected to reduction with 10 mM DTT followed by an alkylation with 50 mM iodoacetamide. Gel pieces were dried after treatment with ACN and 100 ng of trypsin in 50 mM NH_4HCO_3 was added to the gel pieces. Tryptic digestion was carried out overnight at 37°C and the peptides were extracted with 60% ACN and 0.1% TFA. The

peptides were vacuum dried and resuspended in 0.5% TFA before the MALDI-MS/MS analysis.

MALDI-TOF-TOF Analysis of Recombinant Nucleoprotein of CCHF

The recombinant NP of CCHF was identified by Applied Biosystems 4800 plus MALDI TOF/TOF Analyzer (AB Sciex, United States) using the tryptic digest of the protein. The digested peptides were spotted onto the target plate following mixing with 1:1 volume of CHCA matrix solution (10 mg/ml). MS mass spectrum was recorded in the reflector positive mode using a laser with accelerated voltage of 2 kV (200 Hz repetition rate with a wavelength of 355 nm). A default calibration was applied for 13 calibration points on 384-well MALDI plate, using a six-component peptide standard in a mass range of 905–3,660 Da. The MS/MS mass spectra were acquired by the data-dependent acquisition method by collision-induced dissociation (CID) at 1 kV voltage. MS/MS fragment ions were generated for 20 strongest precursors selected between the m/Z range of 850–4,000 Da and filtered with a signal-to-noise (S/N) ratio >20 from one MS scan. The precursor ions were selected for fragmentation by a timed ion selector (TIS), using air as collision gas at 1 kV energy and a recharge pressure threshold of 1.5e-006. MS and MS/MS spectra were accumulated for at least 1,200 and 1,600 laser shots, respectively. Peak list was generated using the 4000 Series Explorer Software v. 3.5 (Applied Biosystems) wherein the MS/MS peaks were selected on the basis of a S/N ratio greater than 10. The data thus obtained were explored employing Protein Pilot version 4.0 (Applied Biosystems) and MASCOT 2.0 search engine (Matrix Science, London, United Kingdom). Finally, the peak list was searched against all entries at the non-redundant protein sequence database of NCBI with 16,338,050 sequences using the following search parameters: mass tolerance of 50 ppm for precursor ion and ± 0.6 Da for fragment ion with $+1$ charge state, trypsin digestion with one missed cleavage, and variable modifications of oxidation of methionine and carbamidomethylation of cysteine.

Recombinant Nucleoprotein-Based IgG ELISA

Recombinant CCHF NP protein was tested for its antigenicity in terms of recognition by anti-CCHFV antibody in bovine, sheep, and goat serum samples. For standardization of indirect IgG ELISA, each well of a 96-well maxisorp microtiter plate (Nunc, Denmark) was coated with 300 ng of recombinant CCHF r-NP protein in carbonate–bicarbonate buffer (pH-9.6). Following overnight incubation, the plate was washed thrice with PBST (PBS containing 0.05% Tween 20) and blocked with 5% SMP overnight at 4°C. Test sera were heat inactivated at 56°C for 30 min prior to dilution (1:1,000) in 1% SMP in 0.1% PBS-T. The diluted sera were added to each well and incubated at 37°C for 60 min. The plate was washed with wash buffer (0.1% PBST) five times and then incubated with 1:10,000 dilution of respective HRP-conjugated antibody (Sigma-Aldrich, United States) in 0.05% PBST at 37°C for 60 min. This was followed by washing five times with wash buffer and the reaction was developed by adding 100 μl of TMB (Sigma-Aldrich, United States). Following incubation at room temperature for 10 min, the reaction was stopped using 100 μl of 1N HCl as stop solution and the absorbance was recorded at 450 nm using an ELISA plate reader (BioTek, United States). Thirty negative control sera from healthy animals were included for the standardization of IgG iELISA. All these parameters including coating, dilution of serum and conjugate, washing, and incubation were optimized by taking into account the S/N ratio.

Comparative Evaluation of In-House ELISA With Commercial ELISA Kit

A panel of 76 animal samples from the CCHF-affected region of Gujarat, India, were tested in parallel with in-house iELISA and commercial VectoCrimea CHF IgG ELISA kit (Vector-Best, Russia). The protocol standardized above was used for in-house iELISA, whereas that recommended by M/s Vector-Best was followed during performance of VectoCrimea IgG ELISA kit, with optimization of animal conjugates through checkerboard titration.

Data Analysis

Data were analyzed with SigmaStat 4.0 software by applying confidence of interval at 95%. Vector-Best ELISA was considered as reference test in this study. The cutoff value of in-house iELISA was determined employing receiver operating characteristic (ROC) curve and area under the curve (AUC) analysis. The ROC curve of in-house and VectoCrimea was eventually compared (Hewson et al., 2004) to determine the sensitivity, specificity, positive predictive value (PPV), and negative predictive value (NPV) of the in-house iELISA. The correlation and percent agreement between the two assays were calculated using Spearman correlation coefficient. The inter-rater agreement of two assays was measured using Cohen's kappa coefficient.

Assay Reproducibility

Robustness of the assay is a crucial parameter for validation of assay, which is defined as the ability of a method to remain unaffected by small variation (Chan et al., 2013). Intra-assay variation (i.e., variation of replicates in one experiment), inter-assay variation (i.e., variation between experiments performed on different days by same operator), and inter-operator variation (i.e., variation between experiments performed by different operators) were performed to study the validation and reproducibility of the assay in different sets of conditions. Intra-assay was performed to monitor the variation in replicates within an assay. Each of six samples (three positive and three negative) were tested in five replicates within an assay, and intra-assay coefficient of variation (standard deviation/average $\times$ 100) was calculated. Kruskal–Wallis and repeated measures (RM) one-way ANOVA were calculated for intra-assay. The test was then performed using these calibrators in duplicate on eight different days for inter-assay variation. A total of 16 replicates were tested using the in-house IgG iELISA. The inter-operator assay variation was performed at different laboratories with different operators

using the panel of calibrators of low, medium, and high IgG positive samples along with IgG negative sera samples. The values thus obtained were statistically analyzed with Kruskal–Wallis, one-way ANOVA, and percent coefficient of variation for comparing two or more groups.

Serosurveillance for CCHF in Animal Species

In-house IgG iELISA was then applied to screen a total of 640 animal samples including sheep (n = 198), goat (n = 249), and bovine (n = 193), collected from different Indian states such as Gujarat, Jammu and Kashmir, and Rajasthan.

RESULTS

Cloning, Expression, and Solubility Optimization of CCHF NP Gene

The synthetic gene (1,458 bp) coding for CCHF NP cloned in pUC57 vector was used to release the insert using *Bam*HI and *Hin*dIII RE (**Figure 1A**). The insert was gel purified revealing a size of 1458 bp (**Figure 1B**). The insert was cloned into pET28a+ expression vector at *Bam*HI and *Hin*dIII sites and transformed in *E. coli* BL21 (DE3) cells. The presence of insert was confirmed through RE analysis, which revealed the release of a 1,458-bp insert (**Figure 1C**). The expression of NP from

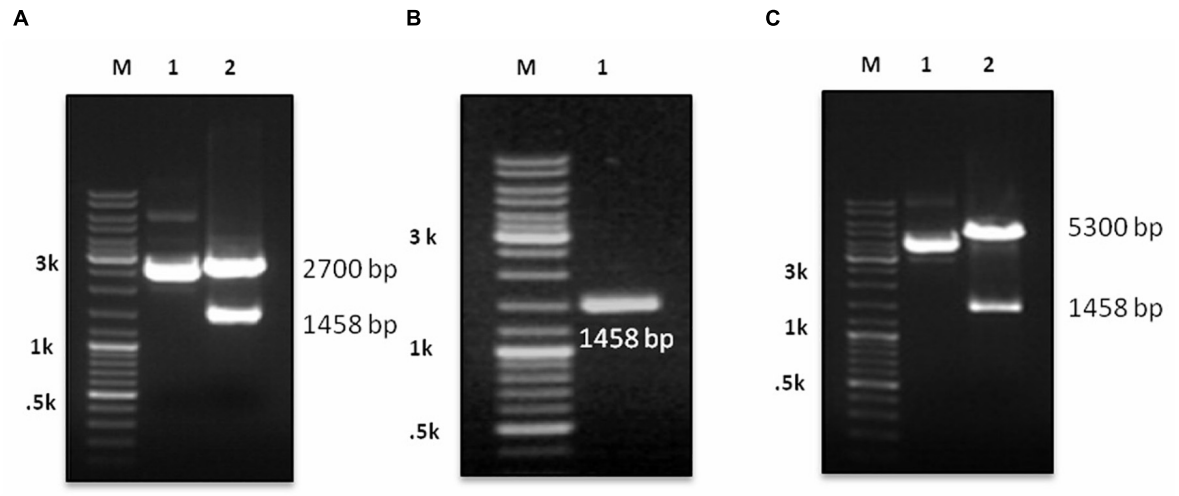

FIGURE 1 | (A) M: DNA Marker (GeneRuler DNA Ladder, Cat. # SM0333, Thermo Fisher Scientific), lane 1: undigested pUC 57 with cloned gene, lane 2: digestion of recombinant plasmid with *Bam*HI and *Hin*dIII revealing release of insert. **(B)** M: DNA Marker; lane 1: LMP purified gene insert (1458 bp). **(C)** M: DNA Marker; lane 1: ligated gene insert (1458 bp) with pET28a+ expression vector, lane 2: confirmation of ligation through RE digestion of recombinant plasmid with *Bam*HI and *Hin*dIII, revealing fragment 5300 bp of vector and 1458 bp of gene insert.

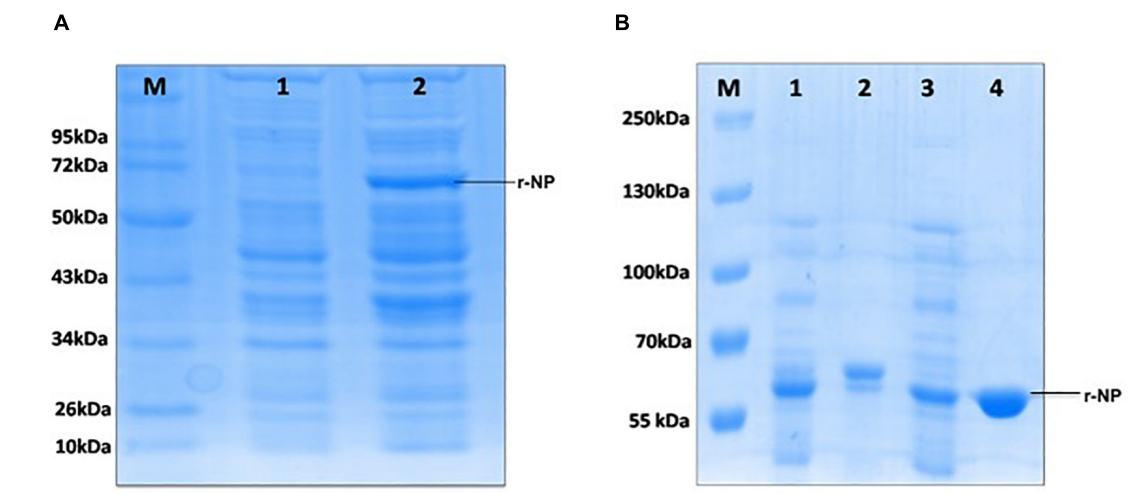

FIGURE 2 | (A) M: Protein molecular weight marker (Cat. # SM0661, Fermentas); lane 1: uninduced BL21 (pET28a+), lane 2: induced BL21 (pET28a+) with 1 mM IPTG. **(B)** M: Protein molecular weight marker (Cat. #26619, Thermo Fisher Scientific); lane 1: induced bacterial lysate in insoluble form, lane 2: purified protein from insoluble lysate (under denaturing condition), lane 3: induced bacterial lysate in soluble form, lane 4: purified protein from soluble lysate (under native condition).

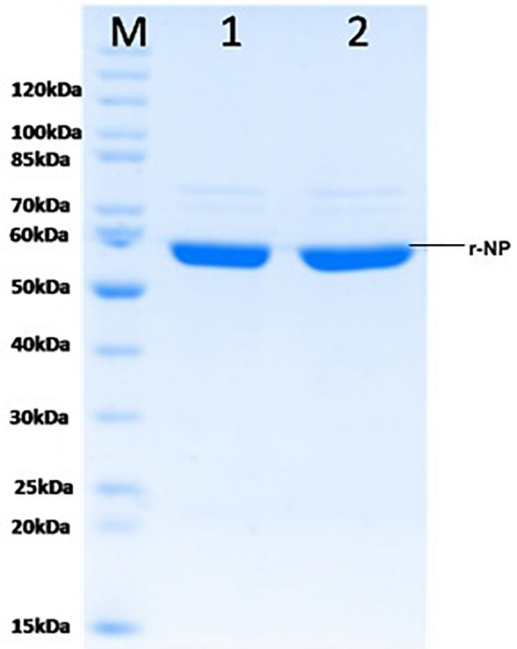

FIGURE 3 | SDS-PAGE analysis of purified r-NP protein. M: Protein molecular weight marker (Cat. # SM0661, Fermentas); lanes 1 and 2, purified recombinant nucleoprotein expressed in BL21 (DE3) cells (56 kDa) using Ni-NTA affinity chromatography.

positive clone was analyzed in SDS-PAGE. A clear band of 56 kDa was observed in induced culture compared to uninduced cells (**Figure 2A**). Optimization of induction profile with varying IPTG concentration led to an optimum IPTG concentration of 1 mM (**Supplementary Figure S1A**). SDS-PAGE analysis revealed that the fraction of r-NP was found in insoluble form as inclusion bodies in post-induced culture up to 4 h at 37°C. To shift the expression to soluble form, conditions were further optimized by lowering the temperature of post-induction (from 36 to 18°C) (**Figure 2B** and **Supplementary Figure S1B**). After optimization, transformed BL21 (DE3) cells were grown in TB broth supplemented with 1% glycerol (Vagenende et al., 2009) and 50 μg/ml kanamycin. The expression of mid-log phase culture was induced by IPTG and grown post-induction at 18°C overnight that revealed expression of r-NP of 56 kDa size in soluble form.

Purification of Recombinant CCHF Nucleoprotein

To maintain the conformational epitopes of recombinant NP, the purification process was carried out employing native conditions. The protein was mixed with Ni-NTA slurry and finally eluted with 250 mM imidazole. The gel analysis revealed a 56-kDa recombinant NP, as a single intense band (**Figure 3**). The quantity of purified r-NP was 8 mg/L of shake flask culture. The protein r-NP was stored at -80°C to enhance the stability of r-NP in terms of its aggregation and thus functionality.

Characterization of Recombinant CCHF Nucleoprotein

Recombinant purified NP was characterized using Western blot and MALDI-TOF/MS analysis. In Western blot and chemiluminescent analysis, recombinant NP from both soluble and insoluble fractions was probed with commercial rabbit anti CCHF NP polyclonal antibody and mouse anti-His antibody that showed reactivity at 56-kDa protein band, representing the immunological activity of recombinant NP protein (**Figures 4A–C**). The recombinant NP was identified

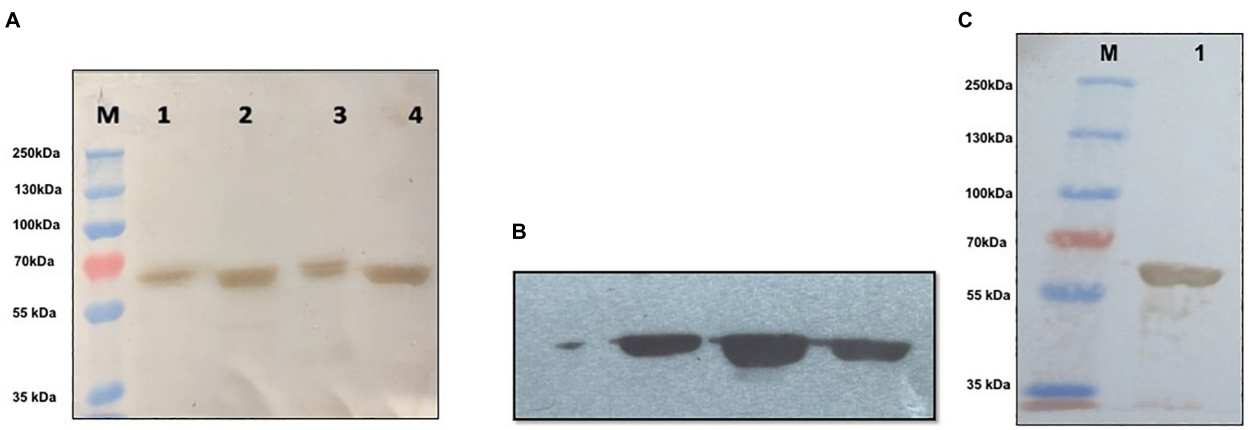

FIGURE 4 | Western blot and chemiluminescent analysis of purified recombinant nucleoprotein (rNP). **(A)** Characterization of purified nucleoprotein of CCHFV. M: Prestained marker (ColorBurst™ Electrophoresis Marker, Cat # C1992, Sigma-Aldrich), lane 1: induced bacterial lysate generated in denaturing condition, lane 2: Purified rNP in insoluble condition, lane 3: induced bacterial lysate generated in soluble condition, lane 4: purified rNP in soluble condition showing immunological reactivity with commercial polyclonal antibody raised in rabbit against CCHFV (Abcam, United States) at 56 kDa. **(B)** Chemiluminescent analysis showing reaction of rNP from three different lots with commercial antibody against CCHFV (Abcam, United States). **(C)** M: Prestained marker (PageRuler™ Plus Prestained Protein Ladder, Cat # 26619, Thermo Fisher Scientific); lane 1: specific binding between rNP and mouse monoclonal anti-His antibody (Sigma-Aldrich, United States).

TABLE 1 | Identification of recombinant nucleoprotein of CCHFV by MS/MS analysis of tryptic peptides using MALDI-TOF-TOF.

Peptides	Observed *m/Z* (Da)	Mr Experimental	Position	Ion score	RMS Error (ppm)
LYELFADDSFQQNR	1,745.8160	1,744.8056	359–372	117	2
KLYELFADDSFQQNR	1,873.9119	1,872.9006	358–372	107	2
AQGAQIDTAFSSYYWLYK	2,112.0076	2,111.0000	299–316	119	2
AGVTPETFPTVSQFLFELGK	2,168.1318	2,167.1201	317–336	98	2
GNGLVDTFTNSYSFCESVPNLDR	2,592.1702	2,591.1599	23–45	133	2
TGFNIQDMDIVASEHLLHQSLVGK	2,668.3560	2,667.3327	439–462	70	2

The protein was identified as nucleoprotein from CCHF virus [gi|15788941] with a MASCOT score of 637 and a sequence coverage of 20% on MS/MS data.

by MS/MS analysis of tryptic peptides using MALDI-TOF-TOF. The peak list was searched against the complete non-redundant protein sequence database of NCBI with 16,338,050 sequence entries. The protein was identified as a NP from CCHF virus [gi|15788941] with a MASCOT score of 637 and a sequence coverage of 20% on MS/MS data (**Table 1**).

Standardization of Indirect IgG ELISA

Crimean-Congo hemorrhagic fever iELISA was standardized with well-characterized antigen, conjugate, and a panel of positive and negative animal sera obtained from Gujarat and Madhya Pradesh. No cross-reactivity was observed with FMD and PPR positive and apparently healthy animal sera. The cutoff of IgG iELISA was set as thrice the average OD value of negative control sera.

Comparative Evaluation and Statistical Analysis

A panel of 76 suspected samples from different animals (sheep, goat, and bovine) were tested in parallel using in-house iELISA assay and commercial VectoCrimea IgG ELISA kit. The comparative evaluation of both the assays is shown in **Table 2**.

The cutoff was further determined using the ROC curve analysis of in-house iELISA assay and commercial VectoCrimea IgG ELISA assay. The different cutoff was compared in respect to sensitivity and specificity of iELISA. The OD value of 0.414 was recommended as cutoff based on the 95% confidence interval (92.22 to 100%) of in-house assay. The cutoff OD value of 0.4 for the commercial VectoCrimea kit was calculated as per manufacturer instructions. At this threshold value, sensitivity, specificity, PPV, and NPV were calculated. The area under curve (AUC) within ROC showed a value of 0.856 with a Youden's index (*J*) of 0.933, reflecting a virtuous accuracy of in-house iELISA (**Figure 5**). The difference between the ROC curves of in-house and Vector-Best was 0.166, with lowest significance level (p = 0.0008) (**Figure 6A**). The comparative evaluation of both the assays indicated a concordance of 90.7%. The sensitivity and specificity of the assay were found to be 79.4 and 100%, while the PPV and NPV of the assay were 100 and 85.7%, respectively (**Table 3** and **Figure 6B**). Rho factor generated through Spearman correlation coefficient using SigmaStat 4.0 was 0.78, whereas the Cohen's kappa coefficient was found to be 0.748, depicting the strong correlation between the in-house and commercial assays (**Figure 7**).

TABLE 2 | Comparative evaluation of the in-house CCHF r-NP IgG ELISA with commercially available kit (Vector-Best, Novosibirsk, Russia) revealing true positive, false positive, true negative, and false negative.

In-house CCHF iELISA	Vector-Best Indirect ELISA		
	Positive	Negative	Total
Positive	27	0	27
Negative	07	42	49
Total	34	42	76

True positive = 27, true negative = 42, false positive = 0, false negative = 7.

Assay Reproducibility

A panel of calibrators with low, medium, and high IgG positive samples along with negative sera samples were

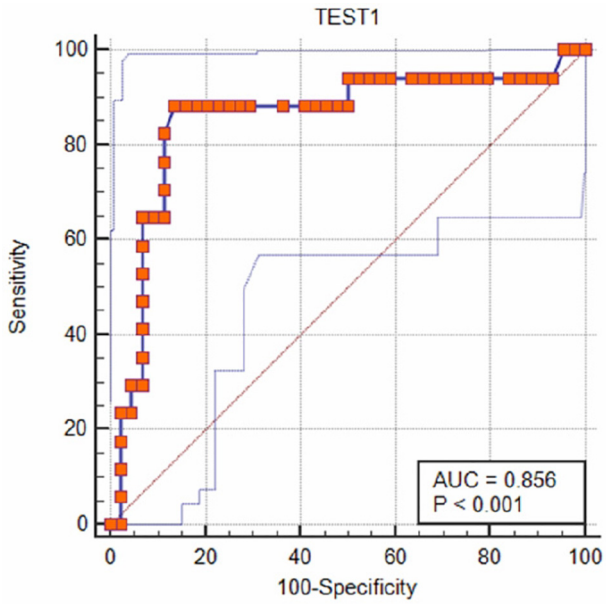

FIGURE 5 | Receiver operating characteristic (ROC) analysis. ROC curve of in-house iELISA was generated with 52 negative sera and 24 positive sera. The area under ROC (AUC) was 0.856 (95% confidence interval). Youden's index (*J*) for the optimal cutoff was 0.933. Orange dotted blue line represents ROC at 95% confidence interval.

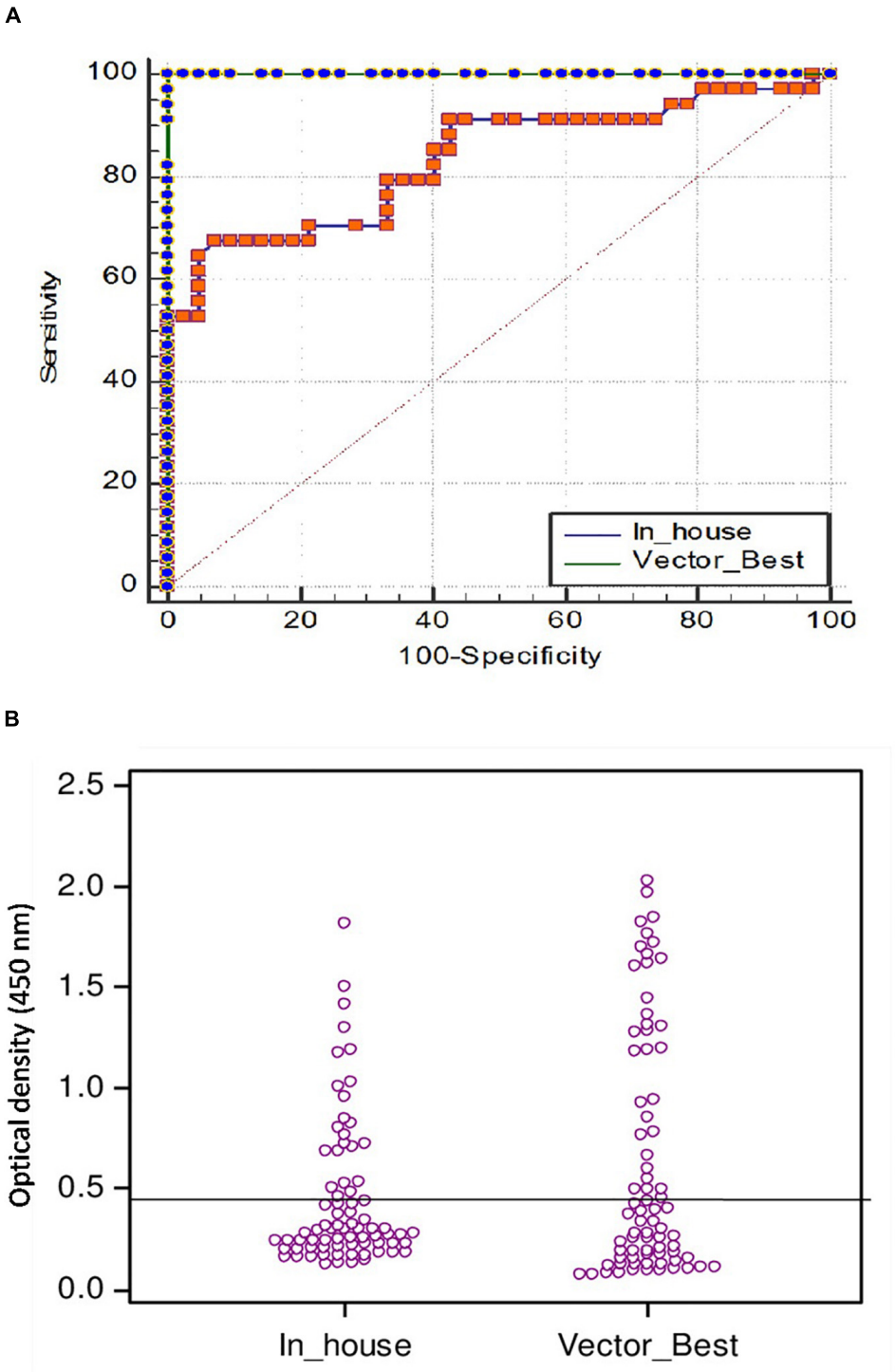

FIGURE 6 | (A) Comparison of ROC curves of VectoCrimea IgG ELISA and in-house IgG ELISA using SigmaStat 4.0 with a panel of 76 positive and negative samples. Vector-Best [blue dotted green line; area under the curve (AUC) = 1.00], In-house (Orange dotted blue line; AUC = 0.856). The red dotted line represents the reference diagonal line of non-discrimination and is plotted from point 0,0 to point 1,1. The difference between two curves was 0.166 with a significance value of $p = 0.0008$. **(B)** Threshold of in-house iELISA was determined in comparison to VectoCrimea ELISA assay, estimated as 0.414 at 79.4% sensitivity and 100% specificity.

TABLE 3 | Statistical analysis of comparative evaluation of the CCHF r-NP IgG ELISA with commercially available kit (Vector-Best, Novosibirsk, Russia).

Accordance (%)	Sensitivity (%)	Specificity (%)	PPV (%)	NPV (%)
90.7%	79.4%	100%	100%	85.7%

True Positive (a) = 27; True Negative (d) = 42; False positive (c) = 00; False negative (b) = 07; Accordance = a + d/a + b + c + d; Sensitivity = a/a + b; Specificity = d/c + d; Positive predictive value = a/a + c; Negative predictive value = d/b + d.

used to study the intra-assay, inter-assay and inter-operator variation analysis. Intra-assay CV was estimated to be 6.4%, depicting the lower level of dispersion around the mean (**Figure 8A**). Kruskal–Wallis value for intra-assay variation was found to be 0.993, and RM one-way ANOVA *p* value for intra-assay was found to be 0.342, stating no significant difference within the replicates. Kruskal–Wallis value and one-way ANOVA significance was found to be 0.997 and 1.0 for inter-assay variation, respectively, which shows that there is no statistical difference when test was performed in different days (**Figure 8B**). Percent coefficient of variation for inter-assay was found to be 8.2%.

In the inter-operator assay, the Kruskal–Wallis significance value was 0.835 and one-way ANOVA significance value was 0.983 (**Figure 8C**). Percent coefficient of variation for inter-operator assay was found to be 14%, which should lie within 15% for inter assay variations. The overall performance of assay is shown in **Table 4**.

Serosurveillance for CCHF in Animal Species

The CCHF iELISA test was applied to screen a total of 640 samples from different domestic ruminants. The result revealed a seropositivity of 17.67% ($n = 35$), 24% ($n = 60$), and 12% ($n = 23$) in sheep, goat, and bovine, respectively. The region (state) and species-wise seropositivity is provided in **Table 5**.

DISCUSSION

Crimean-Congo hemorrhagic fever virus is considered as the one of the most emerging tick-borne viral diseases with recurrent sporadic human cases in various countries of the world. CCHF virus circulates in multiple vertebrate hosts in nature but humans are the dead end host. Hard ticks are the principal vector and infected ticks serve as the lifelong reservoir of the virus. The virus is maintained through transovarial and transstadial transmission. Multiple wild and domestic animals including sheep, goat, and bovine are exposed to the virus through the bite of an infected tick. These ruminants remain asymptomatic, but develop a short viremia followed by seroconversion. CCHFV is maintained through a silent tick–vertebrate–tick enzootic cycle (Spengler et al., 2016). Humans in close contact of these animals or their products are at high risk of acquiring infection. Delayed confirmation of CCHF infection is associated with a risk of nosocomial infection leading to outbreak situations (Aradaib et al., 2010).

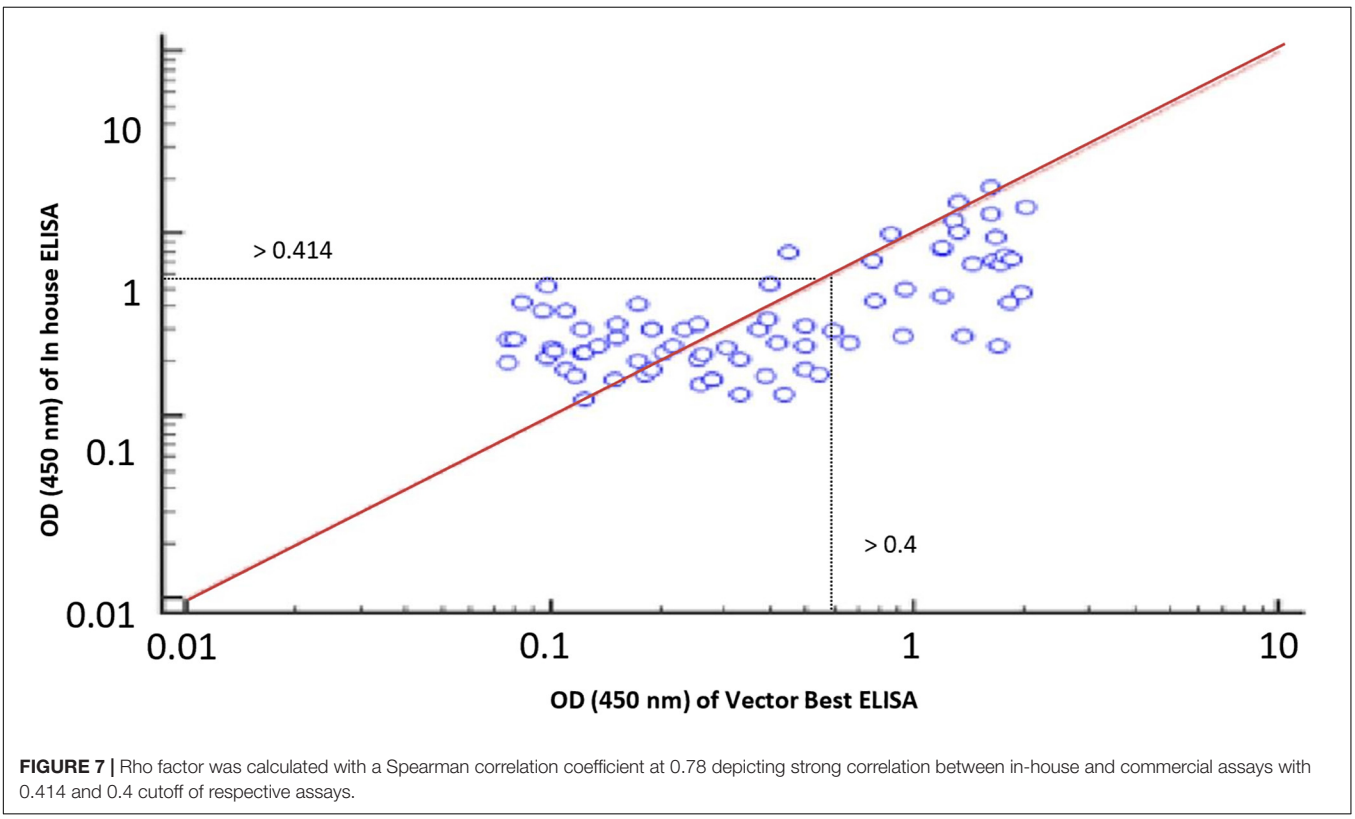

FIGURE 7 | Rho factor was calculated with a Spearman correlation coefficient at 0.78 depicting strong correlation between in-house and commercial assays with 0.414 and 0.4 cutoff of respective assays.

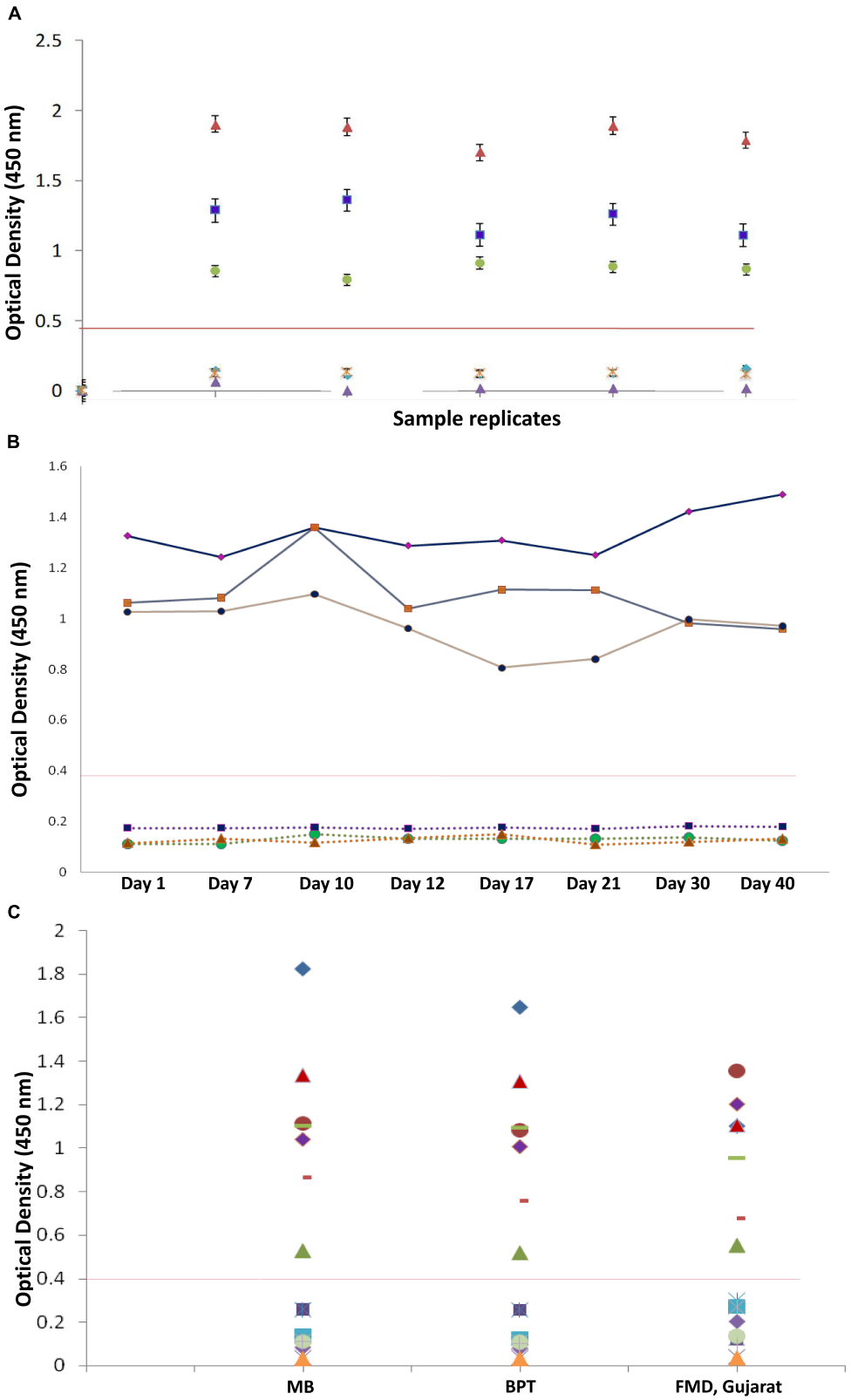

FIGURE 8 | Reproducibility of in-house indirect IgG ELISA. **(A)** Intra-assay variation (variation of replicates in one experiment) of IgG iELISA was performed with a panel of one from each low, medium, and high positive sample and three negative samples and five replicates within a plate. **(B)** Inter-assay-variation (variation

(Continued)

FIGURE 8 | Continued
between experiments) performed on eight different days (days 1, 7, 10, 12, 17, 21, 30, and 40) in duplicates by the same operator. **(C)** Inter-operator variation (variation between experiments performed by different operators) and assay precision were conducted at different institutional laboratories and at FMD Centre, Gujarat, with a panel of seven positive and nine negative samples with different operators. Data interpretation was performed with Kruskal–Wallis and one-way ANOVA.

In spite of widespread circulation, there is a lack of safe and effective surveillance system in various developing countries (Al-Abri et al., 2017). ELISA is a preferred method for serosurveillance of various diseases in animals. In order to minimize the disease burden in the form of mortality and morbidity, rapid and high-throughput screening is paramount. Availability of a field-based detection system is critical for early and efficient management of CCHF, which is often reported from rural settings. Currently available ELISA systems utilize inactivated virus or suckling mouse brain antigen that poses high biohazard risk. With the advent of recombinant DNA technology, various ELISA systems based on recombinant proteins are developed that provides a safe alternative to infectious viral antigen. In the present study, NP was targeted as a diagnostic intermediate, as it is one of the most important and conserved structural protein of CCHFV. The NP of CCHFV reveals more than 95% conservancy across different genotypes (Hewson et al., 2004; Hawman and Feldmann, 2018). This high conservancy enables applicability of NP from a specific genotype for other genotypes in serodiagnosis testing (Saijo et al., 2002; Emmerich et al., 2018). The NP is also the predominantly expressed antigen after infection and is thus a good candidate for detection of viral antibodies (Schmaljohn and Nichol, 2007).

Though NP has been earlier expressed in several expression systems including baculovirus and prokaryote, its expensive production and instability limit its application for serodiagnosis (Tang et al., 2003; Saijo et al., 2005; Dowall et al., 2012). Therefore, in this study, we have developed a safe, stable, and soluble recombinant NP-based indirect IgG ELISA for serosurveillance. As r-NP does not need any posttranslational modification, a bacterial system was preferred. The recombinant NP was expressed with 6 × histidine tag in *E. coli* BL21 and was purified under native conditions using Ni-NTA affinity chromatography. Since rNP was found in insoluble form when induced at 37°C, the expression was shifted to soluble form by lowering the post-induction temperature to 18°C. This led to the expression of rNP in soluble form, which maintained the conformational integrity of the epitopes. The maintenance of native condition of rNP is crucial as that will enable recognition of antibodies against both linear and conformational epitopes. The high degree of purity (∼95%) and yield (8 mg/L) achieved through shake flask culture in this study shows the potential of the process for commercial exploitation. Further, the immunoreactivity of purified rNP was confirmed using both anti-CCHFV antibody and anti-His antibody in Western blot. The authenticity of expressed rNP was also confirmed through MALDI/TOF-MS. In-house ELISA was optimized through checkerboard titration of antigen, serum, and conjugate with a panel of known positive and negative sera. The cutoff was decided through ROC analysis. Currently, there is no validated commercial serodiagnostic kit available for use in animals. The commercial, Vector-Best kit, which is intended and widely used for human, was adapted in the current study for comparative evaluation of in-house assay as reported earlier (Schuster et al., 2016; Papa et al., 2018; Sas et al., 2018). Further, comparative evaluation of in-house assay and commercial kit was performed, which revealed 90% correlation. The result indicated a diagnostic sensitivity of 79.4% and a diagnostic specificity of 100%, thus minimizing the false-positive result that is crucial in serosurveillance. The stability and performance of in-house assay were also studied with intra-assay, inter-assay, and inter-operator assay variations. In all the validation tests, assay was found to be stable and robust in different sets of conditions such as different days, laboratories, and operators with no statistically

TABLE 4 | Overall performance of developed in-house IgG iELISA.

Parameters	In-house IgG ELISA
True positive	27
True negative	42
False positive	00
False negative	07
Sensitivity	79.4%
Specificity	100%
Accordance	90%
AUC	0.856
Youden's index *J*	0.933
Kruskal–Wallis significance value of intra-assay	0.992
One-way ANOVA significance value of intra-assay	0.342
Percent coefficient of variation of intra-assay	6.2%
Kruskal–Wallis significance value of inter-assay	0.997
One-way ANOVA significance value of inter-assay	1.000
Percent coefficient of variation of inter-assay	8.2%
Kruskal–Wallis significance value of inter-operator assay	0.835
One-way ANOVA significance value of inter-operator assay	0.983
Percent coefficient of variation of inter-operator assay	14%

TABLE 5 | State and species-wise serosurveillance for CCHF in India.

State	Species of ruminants	No. of sample tested	No. of sample positive	Percent positivity
Gujarat (*n* = 468)	Sheep	158	30	18.98
	Goat	189	51	26.98
	Bovine	121	20	16.52
Jammu and Kashmir (*n* = 72)	Bovine	72	3	4.16
Rajasthan (*n* = 100)	Sheep	4 0	5	12.50
	Goat	60	9	15.00
Total		640	118	18.43

significant difference, indicating the robustness and potential utility of in-house iELISA for large-scale applications.

Serosurveillance remains one of the important factors in tracing the circulation of virus in new areas and assists in prevention of infections from animals to human (Bente et al., 2013). This becomes important particularly when there is noprophylaxis and treatment is only supportive for CCHFV. The serosurveillance was carried out using 640 sera from three different ruminant species belonging to three different geographical regions of India. It revealed a seropositivity of 18%, thereby indicating endemicity of CCHFV in India. The relatively higher seropositivity in Gujarat samples is due to the fact that this region is a hotspot for CCHF in India as regular outbreaks have been reported since 2011 (Mourya et al., 2012). The Gujarat samples used in this study were collected from areas reporting human outbreaks with Asia-II lineage (Yadav et al., 2014). The lowest seropositivity in Jammu and Kashmir may be linked to the isolated high-altitude Himalayan region. Interestingly, the successful detection of antibody in Rajasthan samples, where a different lineage (Asia-I) is circulating, clearly demonstrates the utility of in-house iELISA for different lineages (Singh et al., 2016; Yadav et al., 2016). The successful demonstration of the single assay for detection of anti CCHFV antibodies in different animals makes this format amenable for commercial multispecies application. However, this format needs to be further evaluated with a larger sample size from different animals and human.

CONCLUSION

The present study led to the development of a process for expression and purification of immunogenic recombinant NP of CCHFV in native conformation. Further, the soluble rNP was explored for the development of a safe, stable, and scalable indirect ELISA that can be used in primary health care facilities to trace the circulation of virus in both human and animals. This assay can also be explored and converted into an on-site point of care testing (POCT) device that eases the diagnosis and surveillance program in resource-limited settings. Further directed and regular serosurveillance programs need to be undertaken in combating the emerging threats of CCHF virus in developing world.

DATA AVAILABILITY

All datasets generated for this study are included in the manuscript/**Supplementary Files**.

AUTHOR CONTRIBUTIONS

PD conceived the idea. NS performed all the experiments. AS and SN contributed to statistical analysis. JK and SS contributed to sample analysis. SA performed and analyzed MALDI-TOF-TOF. SKS and AK collected and provided suspected animal samples. NS and PD wrote the manuscript. AS and SS critically revised the manuscript. All authors read and approved the final manuscript.

FUNDING

The authors thank Defence Research and Development Organisation (DRDO), Ministry of Defence, Government of India for providing necessary financial support for this study.

ACKNOWLEDGMENTS

We are thankful to Dr. D. K. Dubey, Director, DRDE, Gwalior, for his keen interest, constant support, and provision of necessary facilities for this study. This manuscript is assigned DRDE accession no. DRDE/VIRO/17/2019. We would like to thank Director, DIHAR, Leh for providing animal serum samples. We are also thankful to Dr. Subodh Kumar, Head, Microbiology Division and Dr. A. K. Goel, Head, BioProcess Technology Division, DRDE, for their help in inter-assay analysis. NS would also like to thank Department of Science and Technology, Government of India for providing INSPIRE fellowship.

SUPPLEMENTARY MATERIAL

The Supplementary Material for this article can be found online at: https://www.frontiersin.org/articles/10.3389/fmicb.2019.01822/full#supplementary-material

FIGURE S1 | (A) Induction of *E. coli* BL21 cells at different IPTG concentrations. M: protein molecular weight marker; lane 1: uninduced BL21 culture, lane 2: induction was given at 0.5 mM IPTG, lane 3: induced at 1.0 mM IPTG, lane 4: induced at 1.5 mM IPTG, lane 5: induced at 2.0 mM IPTG, lane 6: induced at 2.5 mM IPTG. **(B)** Induction of BL21 cells at different temperature and time. M: protein molecular weight marker; lane 1: induced BL21 cells for 1 h at 37°C (protein in inclusion bodies), lane 2: induced BL21 cells for 2 h at 37°C (protein in inclusion bodies), lane 3: induced BL21 cells for 3 h at 37°C (protein in inclusion bodies), lane 4: induced BL21 cells for 4 h at 37°C (protein in inclusion bodies), lane 5: induced BL21 cells for 18 h at 18°C (protein in soluble form).

REFERENCES

Adams, M. J., Lefkowitz, E. J., King, A. M. Q., Harrach, B., Harrison, R. L., Knowles, N. J., et al. (2017). Changes to taxonomy and the international code of virus classification and nomenclature ratified by the international committee on taxonomy of viruses. *Arch. Virol.* 162, 2505–2538. doi: 10.1007/s00705-017-3358-5

Al-Abri, S. S., Abaidani, I. A., Fazlalipour, M., Mostafavi, E., Leblebicioglu, H., and Pshenichnaya, N. (2017). Current status of crimean-congo haemorrhagic fever in the world health organization eastern mediterranean region: issues, challenges, and future directions. *Int. J. Infect. Dis.* 58, 82–89. doi: 10.1016/j.ijid.2017.02.018

Álvarez-Rodríguez, L. M., Ramos-Ligonio, A., Rosales-Encina, J. L., Martínez-Cázares, M. T., Parissi-Crivelli, A., and López-Monteon, A. (2012). Expression,

purification, and evaluation of diagnostic potential and immunogenicity of a recombinant NS3 protein from all serotypes of dengue virus. *J. Trop. Med.* 2012:956875. doi: 10.1155/2012/956875

Aradaib, I. E., Erickson, B. R., Mustafa, M. E., Khristova, M. L., Saeed, N. S., Elageb, R. M., et al. (2010). Nosocomial outbreak of crimean-congo hemorrhagic fever. *Sudan. Emerg. Infect. Dis.* 16:837. doi: 10.3201/eid1605.091815

Babaeipour, V., Shojaosadati, S. A., Khalilzadeh, R., Maghsoudi, N., and Farnoud, A. M. (2010). Enhancement of human γ-interferon production in recombinant E. coli using batch cultivation. *Appl. Biotechnol. Biochem.* 160, 2366–2376. doi: 10.1007/s12010-009-8718-5

Bente, D. A., Forrester, N. L., Watts, D. M., McAuley, A. J., Whitehouse, C. A., and Bray, M. (2013). Crimean-congo hemorrhagic fever: history, epidemiology, pathogenesis, clinical syndrome and genetic diversity. *Antiviral Res.* 100, 159–189. doi: 10.1016/j.antiviral.2013.07.006

Burt, F. J., Leman, P. A., Abbott, J. C., and Swanepoel, R. (1994). Serodiagnosis of crimean-congo haemorrhagic fever. *Epidemiol. Infect.* 113, 551–562. doi: 10.1017/s0950268800068576

Carter, S. D., Surtees, R., Walter, C. T., Ariza, A., Bergeron, É, Nichol, S. T., et al. (2012). Structure, function, and evolution of the crimean-congo hemorrhagic fever virus nucleocapsid protein. *J. Virol.* 86, 10914–10923.

Casals, J., and Tignor, G. H. (1974). Neutralization and hemagglutination-inhibition tests with crimean hemorrhagic fever-Congo virus. *Proc. Soc. Exp. Biol. Med.* 145, 960–966. doi: 10.3181/00379727-145-37933

Chan, W. T., Verma, C. S., Lane, D. P., and Gan, S. K. (2013). A comparison and optimization of methods and factors affecting the transformation of *Escherichia coli*. *Biosci. Rep.* 33:e00086. doi: 10.1042/BSR20130098

Cuzzubbo, A. J., Endy, T. P., Nisalak, A., Kalayanarooj, S., Vaughn, D. W., Ogata, S. A., et al. (2001). Use of recombinant envelope proteins for serological diagnosis of dengue virus infection in an immunochromatographic assay. *Clin. Vaccine Immunol.* 8, 1150–1155. doi: 10.1128/cdli.8.6.1150-1155.2001

Dowall, S. D., Richards, K. S., Graham, V. A., Chamberlain, J., and Hewson, R. (2012). Development of an indirect ELISA method for the parallel measurement of IgG and IgM antibodies against crimean-congo haemorrhagic fever (CCHF) virus using recombinant nucleoprotein as antigen. *J. Virol. Methods* 179, 335–341. doi: 10.1016/j.jviromet.2011.11.020

Emmerich, P., Mika, A., von Possel, R., Rackow, A., Liu, Y., Schmitz, H., et al. (2018). Sensitive and specific detection of crimean-congo hemorrhagic fever virus (CCHFV)—Specific IgM and IgG antibodies in human sera using recombinant CCHFV nucleoprotein as antigen in μ-capture and IgG immune complex (IC) ELISA tests. *PLoS Negl. Trop. Dis.* 12:e0006366. doi: 10.1371/journal.pntd.0006366.

Ergönül, Ö (2006). Crimean-congo haemorrhagic fever. *Lancet Infect. Dis.* 6, 203–214. doi: 10.1016/s1473-3099(06)70435-2

Ge, M., Li, R. C., Qu, T., Gong, W., and Yu, X. L. (2017). Construction of an HRP-streptavidin bound antigen and its application in an ELISA for porcine circovirus 2 antibodies. *AMB Express* 7:177. doi: 10.1186/s13568-017-0473-3

Hawman, D. W., and Feldmann, H. (2018). Recent advances in understanding crimean–congo hemorrhagic fever virus. *F1000Res.* 7:1715. doi: 10.12688/f1000research.16189.1

Hewson, R., Chamberlain, J., Mioulet, V., Lloyd, G., Jamil, B., Hasan, R., et al. (2004). Crimean-congo haemorrhagic fever virus: sequence analysis of the small RNA segments from a collection of viruses worldwide. *Virus Res.* 102, 185–189. doi: 10.1016/j.virusres.2003.12.035

Huang, C. J., Lin, H., and Yang, X. (2012). Industrial production of recombinant therapeutics in *Escherichia coli* and its recent advancements. *Ind. Microbiol. Biotechnol.* 39, 383–399. doi: 10.1007/s10295-011-1082-9

Liu, D., Li, Y., Zhao, J., Deng, F., Duan, X., Kou, C., et al. (2014). Fine epitope mapping of the central immunodominant region of nucleoprotein from crimean-congo hemorrhagic fever virus (CCHFV). *PLoS One* 9:e108419. doi: 10.1371/journal.pone.0108419

Mertens, M., Vatansever, Z., Mrenoshki, S., Krstevski, K., Stefanovska, J., Djadjovski, I., et al. (2015). Circulation of crimean-congo hemorrhagic fever virus in the former yugoslav republic of macedonia revealed by screening of cattle sera using a novel enzyme-linked immunosorbent assay. *PLoS Negl. Trop. Dis.* 9:e0003519. doi: 10.1371/journal.pntd.0003519

Mostafavi, E., Pourhossein, B., Esmaeili, S., Bagheri Amiri, F., Khakifirouz, S., Shah-Hosseini, N., et al. (2017). Seroepidemiology and risk factors of crimean-congo hemorrhagic fever among butchers and slaughterhouse workers in southeastern Iran. *Int. J. Infect. Dis* 64, 85–89. doi: 10.1016/j.ijid.2017.09.008

Mourya, D. T., Yadav, P. D., Shete, A. M., Gurav, Y. K., Raut, C. G., Jadi, R. S., et al. (2012). Detection, isolation and confirmation of crimean-congo hemorrhagic fever virus in human, ticks and animals in ahmadabad, india, 2010-2011. *PLoS Negl. Trop. Dis.* 6:e1653. doi: 10.1371/journal.pntd.0001653

Mourya, D. T., Yadav, P. D., Shete, A. M., Sathe, P. S., Sarkale, P. C., Pattnaik, B., et al. (2015). Cross-sectional serosurvey of crimean-congo hemorrhagic fever virus igg in livestock, india, 2013–2014. *Emerg. Infect. Dis.* 21, 1837–1839. doi: 10.3201/eid2110.141961

Papa, A., Papadopoulou, E., Tsioka, K., Kontana, A., Pappa, S., Melidou, A., et al. (2018). Isolation and whole-genome sequencing of a crimean-congo hemorrhagic fever virus strain. *Greece. Ticks Tick Borne Dis.* 9, 788–791. doi: 10.1016/j.ttbdis.2018.02.024

Saijo, M., Qing, T., Niikura, M., Maeda, A., Ikegami, T., Prehaud, C., et al. (2002). Recombinant nucleoprotein based enzyme linked immunosorbent assay for detection of immunoglobulin G to crimean–congo hemorrhagic fever virus. *J. Clin. Microbiol.* 40, 1587–1591. doi: 10.1128/jcm.40.5.1587-1591.2002

Saijo, M., Tang, Q., Shimayi, B., Han, L., Zhang, Y., Asiguma, M., et al. (2005). Antigen-capture enzyme-linked immunosorbent assay for the diagnosis of crimean-congo hemorrhagic fever using a novel monoclonal antibody. *J. Med. Virol.* 77, 83–88. doi: 10.1002/jmv.20417

Samudzi, R. R., Leman, P. A., Paweska, J. T., Swanepoel, R., and Burt, F. J. (2012). Bacterial expression of crimean-congo hemorrhagic fever virus nucleoprotein and its evaluation as a diagnostic reagent in an indirect ELISA. *J. Virol. Methods* 179, 70–76. doi: 10.1016/j.jviromet.2011.09.023

Sas, M. A., Comtet, L., Donnet, F., Mertens, M., Vatansever, Z., Tordo, N., et al. (2018). A novel double-antigen sandwich ELISA for the species-independent detection of crimean-congo hemorrhagic fever virus-specific antibodies. *Antiviral Res.* 151, 24–26. doi: 10.1016/j.antiviral.2018.01.006

Saxena, D., Parida, M., Rao, P. V. L., and Kumar, J. S. (2013). Cloning and expression of an envelope gene of west nile virus and evaluation of the protein for use in an IgM ELISA. *Diagn. Microbiol. Infect. Dis.* 75, 396–401. doi: 10.1016/j.diagmicrobio.2012.12.007

Schmaljohn, C. S., and Nichol, S. T. (2007). *'Bunyaviridae"', in Fields Virology*. Philadelphia: Lippincott Williams & Wilkins, 1741–1789.

Schuster, I., Mertens, M., Köllner, B., Korytáø, T., Keller, M., Hammerschmidt, B., et al. (2016). A competitive ELISA for species-independent detection of crimean-congo hemorrhagic fever virus specific antibodies. *Antiviral Res.* 134, 161–166. doi: 10.1016/j.antiviral.2016.09.004

Singh, P., Chhabra, M., Sharma, P., Jaiswal, R., Singh, G., Mittal, V., et al. (2016). Molecular epidemiology of crimean-congo haemorrhagic fever virus in India. *Epidemiol. Infect.* 144, 3422–3425. doi: 10.1017/s0950268816001886

Souza, I. I., Melo, E. S., Ramos, C. A., Farias, T. A., Osório, A. L., Jorge, K. S., et al. (2012). Screening of recombinant proteins as antigens in indirect ELISA for diagnosis of bovine tuberculosis. *Springer plus* 1:77. doi: 10.1186/2193-1801-1-77

Spengler, J. R., Estrada-Peña, A., Garrison, A. R., Schmaljohn, C., Spiropoulou, C. F., and Bergeron, É (2016). A chronological review of experimental infection studies of the role of wild animals and livestock in the maintenance and transmission of crimean-congo hemorrhagic fever virus. *Antiviral Res.* 135, 31–47. doi: 10.1016/j.antiviral.2016.09.013

Tang, Q., Saijo, M., Zhang, Y., Asiguma, M., Tianshu, D., Han, L., et al. (2003). A patient with crimean-congo hemorrhagic fever serologically diagnosed by recombinant nucleoprotein-based antibody detection systems. *Clin. Vaccine Immunol.* 10, 489–491. doi: 10.1128/cdli.10.3.489-491.2003

Vagenende, V., Yap, M. G. S., and Trout, B. L. (2009). Mechanisms of protein stabilization and prevention of protein aggregation by glycerol. *Biochemistry* 48, 11084–11096. doi: 10.1021/bi900649t

Vanhomwegen, J., Alves, M. J., Županc, T. A., Bino, S., Chinikar, S., Karlberg, H., et al. (2012). Diagnostic assays for crimean-congo hemorrhagic fever. *Emerg. Infect. Dis.* 18, 1958–1965. doi: 10.3201/eid1812.120710

Yadav, P., Patil, D. Y., Shete, A. M., Kokate, P., Goyal, P., Jadhav, S., et al. (2016). Nosocomial infection of CCHF among health care workers in rajasthan. india. *BMC Infect. Dis.* 16:624. doi: 10.1186/s12879-016-1971-7

Yadav, P., Raut, C., Patil, D., Majumdar, T. D., and Mourya, D. T. (2014). Crimean-congo hemorrhagic fever: current scenario in india. *Proc. Natl. A. Sci. India Sec B Biol. Sci.* 84, 9–18. doi: 10.1007/s40011-013-0197-3

Zivcec, M., Scholte, F., Spiropoulou, C., Spengler, J., and Bergeron, É. (2016). Molecular insights into crimean-congo hemorrhagic fever virus. *Viruses* 8:106. doi: 10.3390/v8040106

Conflict of Interest Statement: The authors declare that the research was conducted in the absence of any commercial or financial relationships that could be construed as a potential conflict of interest.

frontiers in Microbiology

METHODS
published: 13 September 2019
doi: 10.3389/fmicb.2019.02135

Development and Clinical Validation of Multiple Cross Displacement Amplification Combined With Nanoparticles-Based Biosensor for Detection of *Mycobacterium tuberculosis*: Preliminary Results

Wei-Wei Jiao[1], Yi Wang[1], Gui-Rong Wang[2], Ya-Cui Wang[1], Jing Xiao[1], Lin Sun[1], Jie-Qiong Li[1], Shu-An Wen[2], Ting-Ting Zhang[2], Qi Ma[1], Hai-Rong Huang[2] and A-Dong Shen[1]**

[1] Key Laboratory of Major Diseases in Children, Ministry of Education, National Key Discipline of Pediatrics (Capital Medical University), National Clinical Research Center for Respiratory Diseases, Beijing Key Laboratory of Pediatric Respiratory Infection Disease, Beijing Pediatric Research Institute, Beijing Children's Hospital, Capital Medical University, National Center for Children's Health, Beijing, China, [2] National Tuberculosis Clinical Laboratory, Beijing Key Laboratory for Drug Resistance Tuberculosis Research, Beijing Tuberculosis and Thoracic Tumor Research Institute, Beijing Chest Hospital, Capital Medical University, Beijing, China

Tuberculosis is still a major threat to global public health. Here, a novel diagnosis assay, termed as multiple cross displacement amplification combined with nanoparticle-based lateral flow biosensor (MCDA-LFB), was developed to simultaneously detect IS*6110* and IS*1081* of *Mycobacterium tuberculosis* (MTB) in DNA extracted from reference strain H37Rv and clinical samples. The amplification can be finished within 30 min at a fixed temperature (67°C), thus the whole procedure, including rapid template preparation (15 min), isothermal reaction (30 min) and result reporting (2 min), can be completed within 50 min. The limit of detection of multiplex MCDA assay was 10 fg per reaction. By using the multiplex MCDA protocol, cross-reaction with non-mycobacteria and non-tuberculous mycobacteria (NTM) strains was not observed. Among clinically diagnosed TB patients, the sensitivity of liquid culture, Xpert MTB/RIF and multiplex MCDA assay was 42.0% (50/119), 49.6% (59/119), and 88.2% (105/119), respectively. Among culture positive samples, the sensitivity of Xpert MTB/RIF and multiplex MCDA assay was 86.0% (43/50) and 98.0% (49/50), respectively. Among culture negative samples, the sensitivity of Xpert MTB/RIF and multiplex MCDA assay was 23.2% (16/69) and 81.2% (56/69), respectively. The specificity was 100% (60/60) for Xpert MTB/RIF and 98.3% (59/60) for multiplex MCDA. Therefore, the multiplex MCDA assay for MTB detection is rapid, sensitive and easy to use and may be a promising test for early diagnosis of TB.

Keywords: *Mycobacterium tuberculosis*, multiple cross displacement amplification, lateral flow biosensor, MCDA-LFB, limit of detection

OPEN ACCESS

Edited by:
Aleksandra Barac,
University of Belgrade, Serbia

Reviewed by:
Amit Singh,
All India Institute of Medical Sciences, India
Anand Kumar Maurya,
All India Institute of Medical Sciences Bhopal, India

***Correspondence:**
A-Dong Shen
shenad18@126.com
Hai-Rong Huang
huanghairong@tb123.org

Specialty section:
This article was submitted to Infectious Diseases, a section of the journal Frontiers in Microbiology

Received: *10 June 2019*
Accepted: *30 August 2019*
Published: *13 September 2019*

Citation:
Jiao W-W, Wang Y, Wang G-R, Wang Y-C, Xiao J, Sun L, Li J-Q, Wen S-A, Zhang T-T, Ma Q, Huang H-R and Shen A-D (2019) Development and Clinical Validation of Multiple Cross Displacement Amplification Combined With Nanoparticles-Based Biosensor for Detection of Mycobacterium tuberculosis: Preliminary Results. Front. Microbiol. 10:2135. doi: 10.3389/fmicb.2019.02135

INTRODUCTION

Tuberculosis, caused by *Mycobacterium tuberculosis* (MTB), is still a major threat to global public health, with an estimated 10 million new cases and 1.3 million deaths in 2017 (World-Health-Organizaion, 2018). Therefore, rapid and accurate detection of the causative agent is a key factor highly associated with prognosis and treatment cost.

Conventional MTB detection methods, including sputum smear microscopy and mycobacterial culture, remain the major tools in the TB endemic countries. The former lacks sensitivity. The latter has been used as the gold standard of TB diagnosis for many decades but it is a time-consuming, laborious and technically demanding technique. In particular, bacterial culture cannot meet the requirement for rapid diagnosis in clinical settings.

In recent years, many molecular techniques have been devised for rapidly detecting MTB directly from clinical samples. Xpert MTB/RIF and loop-mediated isothermal amplification (LAMP) are recommended by the WHO as rapid molecular methods for MTB detection (World-Health-Organizaion, 2011, 2016). Xpert MTB/RIF provides a convenient and sensitive way to detect MTB (Boehme et al., 2010). However, the high device and consumable costs impede its usage in peripheral laboratories. TB-LAMP relies on a relatively simple device, and the results are based on turbidity visualized with unaided eyes or under ultraviolet light (Ou et al., 2014; Bojang et al., 2016). However, a visualization of the TB-LAMP products by color change with the naked eye is somewhat subjective; therefore, ambiguous results may occur when the concentration of MTB templates is very low.

To address the shortcomings posed by Xpert MTB/RIF and TB-LAMP, we developed a novel molecular assay based on the before-mentioned multiple cross displacement amplification (MCDA) (Wang et al., 2015). MCDA assay achieves rapid and effective amplification of nucleic acid sequences under isothermal conditions within ∼20–40 min (Wang et al., 2018a). MCDA displays extremely high specificity for target sequence amplification, as it comprises ten primers designed for each target, including two displacement primers (F1 and F2), two cross primers (CP1 and CP2), and six amplification primers (C1, D1, R1, C2, D2, and R2). More recently, nanoparticle-based lateral flow biosensors (LFBs) have been devised and applied for simply, rapidly, visually, and objectively indicating the MCDA results (Wang et al., 2018b,c).

In this study, we firstly report a MCDA combined with the LFB (MCDA-LFB) method for simple, visible and reliable detection of MTB using two target genes (IS*6110* and IS*1081*) and validate its potential clinical application using clinical samples from patients.

METHODS

Experiment Design

Two sets of MCDA primers, including the IS*6110*-MCDA primer set and IS*1081*-MCDA primer set, were designed based on the MTB conserved sequences, IS*6110* and IS*1081*, respectively. The details of primers used in this study were shown in **Figure 1** and **Table 1**. All the primers were synthesized by TianyiHuiyuan Biotechnology Co. Ltd. (Beijing, China). The glass bead-based kits (CapitalBio Co.) were used to extract DNA from bacteria and clinical samples. Isothermal amplification kits and visual detection reagent (VDR) were obtained from BeiJing-HaiTaiZhengYuan Technology Co., Ltd. (Beijing, China).

MCDA Reactions

The singlex MCDA reaction system for IS*6110* or IS*1081* was performed in the 25-μl mixture containing 12.5 μl of 2X supplied buffer, 0.4 μM each of F1 and F2; 0.8 μM each of C1*, C2, R1, R2, D1# and D2; 1.6 μM each of CP1 and CP2; 1 μl of VDR; 1 μl (8 U) of *Bst*2.0 DNA polymerase; and DNA template (1 μl for cultured strains, 5 μl for clinical samples).

The multiplex MCDA was also performed in a 25-μl mixture containing 12.5 μl 2 X of the supplied buffer; 0.2 μM each of IS*6110*-F1, IS*6110*-F2, IS*1081*-F1 and IS*1081*-F2; 0.4 μM each of IS*6110*-C1*, IS*6110*-C2, IS*6110*-R1, IS*6110*-R2, IS*6110*-D1#, IS*6110*-D2, IS*1081*-C1*, IS*1081*-C2, IS*1081*-R1, IS*1081*-R2,

TABLE 1 | The sequences of primers used in this study.

Assay	Primers	Sequence (5′–3′)	Target gene
MTB-MCDA	6110-F1	CGCGGTCAGCACGATT	IS*6110*
	6110-F2	GACGCGGTCTTTAAAATCG	IS*6110*
	6110-CP1	TCTCCGCGCAGCCAACACGGAG TGGGCAGCGAT	IS*6110*
	6110-CP2	CCGGGACCACGACCGAAGACGCA ATTCGGCGTTGTC	IS*6110*
	6110-C2	CCGGGACCACGACCGAAGA	IS*6110*
	6110-D2	GCTGAGCTGAAGCGCTT	IS*6110*
	6110-R1	GCACCCACTTACGCAC	IS*6110*
	6110-R2	AGGCGCAGGTCGATGC	IS*6110*
	1081-F1	TGGCGACCTGCTACCT	IS*1081*
	1081-F2	TGTGCACCCCGACGAC	IS*1081*
	1081-CP1	GGAAAGCTTTGTCACACCAAGTG TGCTGGGAGTATCCACTCG	IS*1081*
	1081-CP2	CTCGATGCCGGCCCGTATTCG CGCACCTTGAGC	IS*1081*
	1081-C2	CTCGATGCCGGCCCGTAT	IS*1081*
	1081-D2	CGCCGACGCCCTGGT	IS*1081*
	1081-R1	ATCGACACTTGCGACTT	IS*1081*
	1081-R2	ATGGCCAAAGAGCTCGA	IS*1081*
Primers labeled	6110-C1*	5′-FITC-TCTCCGCGCAGCCAACA-3′	IS*6110*
	6110-D1#	5′-biotin-AAGTAGACGGGCGACCT-3′	IS*6110*
	1081-C1*	5′-FITC-GGAAAGCTTTGTCACACCAAGTGT-3′	IS*1081*
	1081-D1#	5′-biotin-GACCAGGCGCTCCATC-3′	IS*1081*

FITC, fluorescein isothiocyanate.

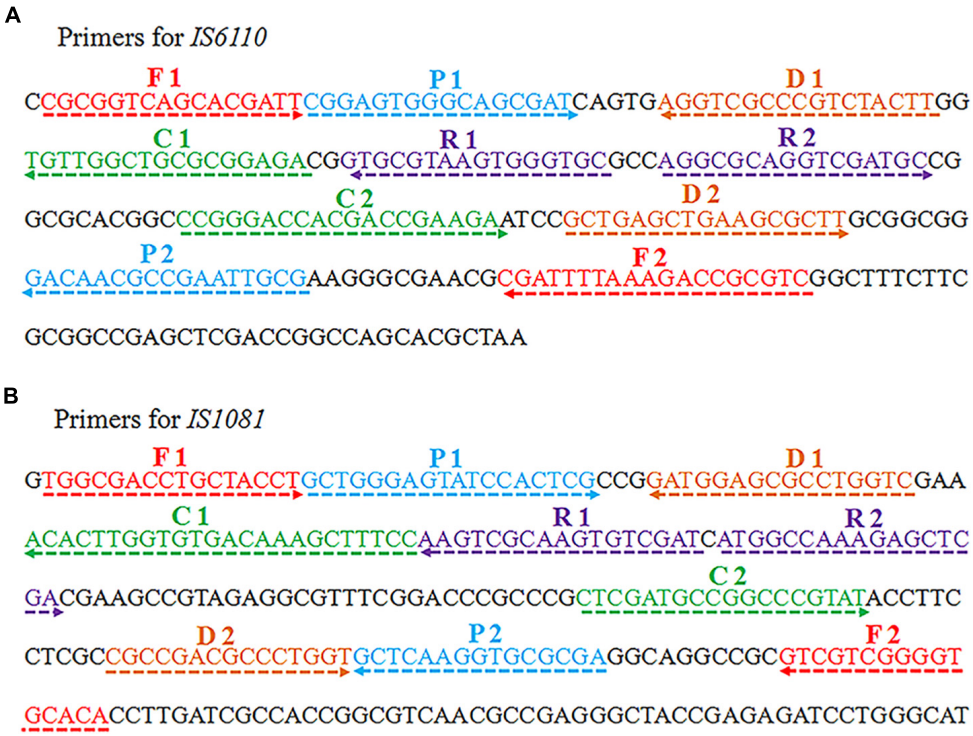

FIGURE 1 | Schematic view of sequences and location of MCDA primers. The nucleotide sequences of the sense strand of IS*6110* **(A)** and IS*1081* **(B)** are shown. The locations of primers are marked with different colors. Right and left arrows indicate the sense and complementary sequences.

IS*1081*-D1# and IS*1081*-D2; 0.8 μM each of IS*6110*-CP1, IS*6110*-CP2, IS*1081*-CP1 and IS*1081*-CP2; 1 μl of VDR, 1 μl (8 U) of *Bst*2.0 DNA polymerase; and DNA template (1 μl for isolated strains, 5 μl for clinical samples).

The VDR, real-time turbidity (LA-320C) and LFB platform were used to demonstrate and confirm the MCDA products. The LFB platform was prepared according to the previous studies (Wang et al., 2017). In brief, Dye (Crimson red) streptavidin-coated polymer nanoparticles (SA-DNPs, Fishers, IN, United States) were gathered in the conjugate pad, and anti-FITC and biotin-BSA were affixed at the test line (TL) and control line (CL), respectively. The MCDA products (0.5 μl) and running buffer (70 μl) were added into the immersion pad. Through the capillary flow, the MCDA products and SA-DNPs were transferred to TL and CL. As a result, FITC/MCDA/SA-DNPs complexes and non-complexed SA-DNPs were indicated by crimson red lines at the TL and CL, respectively. The colorimetric bands were easily visible within 2 min.

In this report, the amplification temperatures of the two sets of MCDA primers (target for IS*6110* and IS*1081*) were optimized from 61°C to 68°C at 1°C intervals. The DNA template of H37Rv (1 ng) was used as positive control, and *Mycobacterium abscessus* DNA (1 ng) and distilled water (DW) were used as negative control and blank control, respectively. The reactions were analyzed by real-time turbidity detection.

Sensitivity of MCDA Assays

The DNA template of the reference strain H37Rv was quantified using Nanodrop ND-1000 at A260/280 and then serially diluted to 10 ng, 1 ng, 100 pg, 10 pg, 1 pg, 100 fg, 10 fg, and 1 fg per microliter. A volume of 1 μl of each dilution was added into the MCDA reaction. The limits of detection (LOD) of singlex (IS*6110*-MCDA and IS*1081*-MCDA) and multiplex MCDA reactions were determined as the last positive dilution.

Then, the duration of reaction time for multiplex MCDA was optimized. Four different amplification times, including 10 min, 20 min, 30 min, and 40 min, were compared under the optimal reaction conditions, and the results were confirmed using LFB.

Specificity of Multiplex MCDA Assay

To verify the specificity of multiplex MCDA assay, a total of 52 genomic DNA samples (at least 1 ng/μl) from different bacterial strains were examined, including 1 MTB reference strain H37Rv, 1 BCG strain, 20 MTB strains isolated from clinical patients, 21 non-mycobacteria strains and 9 non-tuberculous mycobacteria (NTM) strains (**Table 2**). The multiplex MCDA results were confirmed using LFB.

Validation of the Feasibility of Multiplex MCDA Assay Using Clinical Samples

The optimized multiplex MCDA assay was directly evaluated using clinical samples in parallel with Xpert MTB/RIF and/or

TABLE 2 | Genomic DNA used to determine the specificity of MCDA.

Bacteria	Strain no. (source of strains)[a]	No. of strains	MCDA result[b]
M. tuberculosis	H37Rv	1	P
	BCG	1	P
	Isolated strains (BCH)	20	P
Klebsiella pneumoniae	Isolated strains (BCH)	1	N
Streptococcus pneumonia	Isolated strains (BCH)	1	N
Pseudomonas aeruginosa	Isolated strains (BCH)	1	N
Listeria monocytogenes	Isolated strains (BCH)	1	N
Staphylococcus epidermidis	Isolated strains (BCH)	1	N
Staphylococcus aureus	Isolated strains (BCH)	1	N
Bacillus cereus	Isolated strains (BCH)	1	N
Enterobacter sakazakii	Isolated strains (BCH)	1	N
Campylobacter jejuni	Isolated strains (BCH)	1	N
Escherichia coli	Isolated strains (BCH)	1	N
Aeromonas hydrophila	Isolated strains (BCH)	1	N
Pseudomonas Shigella	Isolated strains (BCH)	1	N
Salmonella	Isolated strains (BCH)	1	N
Shigella flexneri	Isolated strains (BCH)	1	N
Shigella boydii	Isolated strains (BCH)	1	N
Shigella dysenteriae	Isolated strains (BCH)	1	N
Shigella sonnei	Isolated strains (BCH)	1	N
Vibrio parahaemolyticus	Isolated strains (BCH)	1	N
Vibrio vulnificus	Isolated strains (BCH)	1	N
Enterococcus faecium	Isolated strains (BCH)	1	N
Enterococcus faecalis	Isolated strains (BCH)	1	N
M. fortuitum	Isolated strain (BCH-NTCL)	1	N
M. abscessus	Isolated strain (BCH-NTCL)	1	N
M. avium	Isolated strain (BCH-NTCL)	1	N
M. intracellulare	Isolated strain (BCH-NTCL)	1	N
M. malmoense	Isolated strain (BCH-NTCL)	1	N
M. kansasii	Isolated strain (BCH-NTCL)	1	N
M. gordonae	Isolated strain (BCH-NTCL)	1	N
M. chelonei	Isolated strain (BCH-NTCL)	1	N
M. flavescens	Isolated strain (BCH-NTCL)	1	N

[a]*BCH, Beijing Children's Hospital; BCH-NTCL, National Tuberculosis Clinical Laboratory, Beijing Chest Hospital.* [b]*P, positive; N, negative. Only genomic DNA templates from MTBC could be detected by MCDA assay, indicating the extremely high specificity of the method.*

culture. All the participants included in this study signed informed consent (the guardian signed it on his/her behalf if the child was younger than 15 years old). This study was reviewed and approved by the Ethics committee of Beijing Children's Hospital, Capital Medical University (No. 2015-45) and Beijing Chest Hospital, Capital Medical University (No. 2014-36-1).

Two groups of patients were enrolled. The first group included adult patients with pulmonary tuberculosis (PTB) from January 2, 2019 to January 17, 2019. The second group included pediatric patients with excluded TB (diagnosed as pneumonia with confirmed etiological evidence of infection with virus, mycoplasma or bacteria) from January 1, 2019 to February 22, 2019. All the patients were categorized into three groups according to the Chinese Pulmonary Diagnosis Criteria WS288-2017 (National-Health-and-Family-Planning-commission-of-the-People's-Republic-of-China, 2017): (i) definite case: a biological specimen positive by smear microscopy, or culture, or molecular methods, or histopathological change; (ii) clinically diagnosed case: radiographic evidence consistent with TB, and at least one of the following: symptoms of TB, positive tuberculin skin test or interferon-γ release assay results, histopathological or bronchoscopic examination consistent with TB; (iii) non-TB: alternative diagnosis established and clinical resolution made without anti-TB treatment.

For the enrolled patients, about 3 ml of clinical samples were collected. Liquid culture using Bactec 960 (BD Microbiology Systems, Sparks, MD, United States) and Xpert MTB/RIF assay (Cepheid, Sunnyvale, CA, United States) was performed according to the manufacturers' instructions. The remaining samples (1 ml) were digested with equal volume of 4% NaOH. The genomic DNA was extracted using glass bead-based kits (CapitalBio Co.). A total of 100 μl of DNA solution was obtained and 5 μl was used for the multiplex MCDA assay. Reference strain H37Rv and DW were used as positive and negative controls, respectively.

RESULTS

Amplification Temperature Optimization

The reaction temperature is an important factor for the MCDA technique, which affects the amplification efficiency and reaction speed of target assay. According to our result (**Figure 2**), the optimum reaction temperature ranged from 64 to 68°C for the IS*6110*-MCDA assay, and from 66 to 68°C for the IS*1081*-MCDA assay. The faster amplifications were observed at an assay temperature of 67°C for both assays, thus this reaction temperature was used for performing the rest of IS*6110*-MCDA, IS*1081*-MCDA and multiplex MCDA reactions described in this report.

Sensitivity of MCDA Assays

As shown in **Figure 3**, the LOD of IS*6110*-MCDA, IS*1081*-MCDA and multiplex MCDA assays is 10 fg, 100 fg, and 10 fg per reaction, respectively. By LFB, two crimson lines (TL and CL) simultaneously appear on the biosensor for positive MCDA reactions, and only a crimson band (CL) appears on the biosensor for negative reactions (**Figures 3A–C**; upper row). By VDR, light green in the positive reaction tube was observed, while negative reaction was colorless (**Figures 3A–C**; bottom row). In particular, the analysis sensitivity obtained from LFB detection is in conformity with VDR analysis (**Figure 3**).

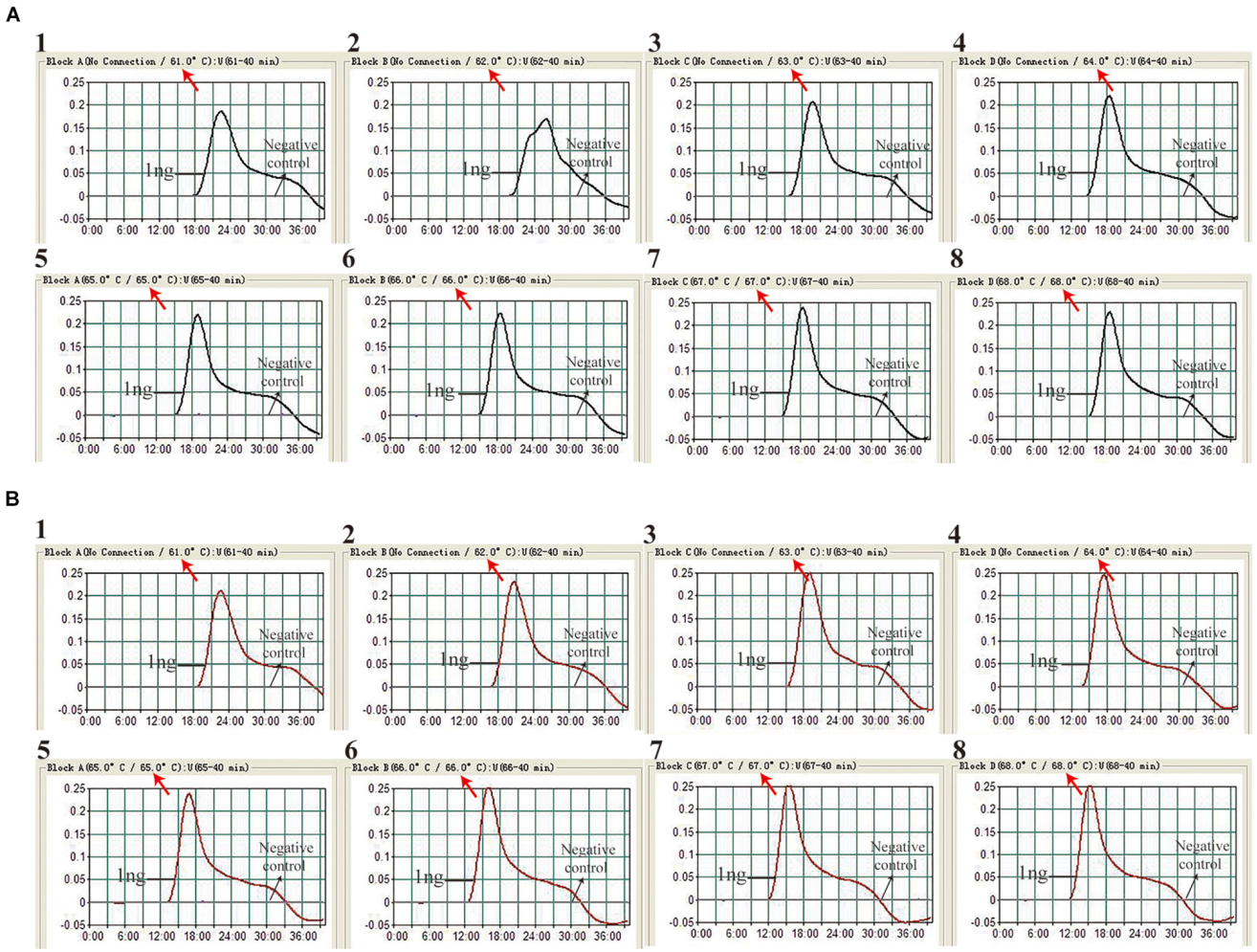

FIGURE 2 | Optimization of amplification temperature for MCDA primer sets. The MCDA assays for MTB detection were monitored by real-time measurement of turbidity. The threshold value was 0.1, thus turbidity of >0.1 was regarded to be positive. Eight kinetic graphs (1–8) were obtained at different temperatures (61 –68°C at 1°C intervals), with 1 ng H37Rv template per reaction for IS*6110* primer set **(A)** and IS*1081* primer set **(B)**, respectively.

Optimized Reaction Time for Multiplex MCDA Assay

The target template at the LOD level (10 fg) can be detected when multiplex MCDA lasted 30 min (**Figure 4C**). Hence, 30 min was determined as the optimal amplification time for multiplex MCDA assay. As a result, the whole procedure, including rapid DNA extraction (15 min), MCDA reaction (30 min), and result indicating (2 min), could be completed within 50 min.

Specificity of Multiplex MCDA Assay

Multiplex MCDA assay specifically detected all MTBC strains (such as H37Rv, BCG and MTB clinical strains), while non-MTBC bacterial pathogens were not detected. By biosensor, two crimson red lines (TL and CL) simultaneously appeared at detection zones of biosensor, suggesting the positive results for MTBC pathogens (**Figure 5**, biosensor 1-8). Only one CL appeared at the detection regions of biosensor, reporting the negative results for non-MTBC strains and blank control (DW) (**Figure 5**, biosensor 9-39). Our results confirm that the multiplex MCDA assay established here has a high specificity (100%) and is able to successfully differentiate MTBC from other bacteria and NTM strains.

Application of Multiplex MCDA Assay in Clinical Samples

According to WS288-2017, total 119 PTB patients (50 were culture positive) and 60 non-TB patients were enrolled in this study. In the TB group, males accounted for 72.3% (86/119), and the mean age was 46.57 years old. The specimen type included 93 sputum, 18 bronchial lavage fluid, and 8 pleural fluid samples. In the non-TB group, 33 (55%) were males and the average age was 5.15 years old. The samples included 57 sputum and 3 pleural fluid samples. These non-TB patients were diagnosed as having pneumonia with confirmed pathogen (19 with bacterial infection,

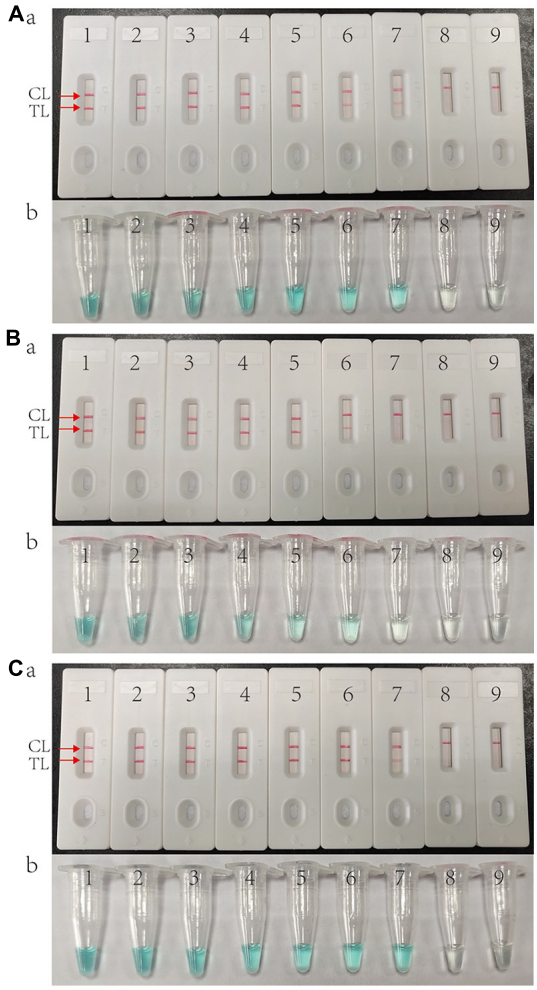

FIGURE 3 | Sensitivity of MCDA assay using serially diluted genomic template of H37Rv. **(A)** IS*6110* MCDA assay; **(B)** IS*1081* MCDA assay; **(C)** Multiplex MCDA assay for both IS*6110* and IS*1081*. Biosensors **(Aa, Ba, Ca)**/tubes **(Ab, Bb, Cb)** 1–9 represented the DNA templates of H37Rv 10 ng, 1 ng, 100 pg, 10 pg, 1 pg, 100 fg, 10 fg, 1 fg per reaction and blank control (DW).

2 with viral infection, 27 with *Mycoplasma pneumonia* infection, and 12 with mixed infection).

Among all the enrolled PTB patients, the sensitivity of liquid culture, Xpert MTB/RIF and multiplex MCDA assay was 42.0% (50/119), 49.6% (59/119) and 88.2% (105/119), respectively (**Table 3**). TB patients were further subdivided into culture-positive group and culture-negative group. Among culture-positive samples, the sensitivity of Xpert MTB/RIF and multiplex MCDA assay was 86.0% (43/50) and 98.0% (49/50), respectively. Among those samples with negative culture results, the sensitivity of Xpert MTB/RIF and multiplex MCDA assay was 23.2% (16/69) and 81.2% (56/69), respectively, indicating that multiplex MCDA assay can further improve the detection rate of culture-negative specimens. The specificity was 100% (60/60) for Xpert MTB/RIF and 98.3% (59/60) for multiplex MDCA when testing the samples from non-TB patients.

DISCUSSION

In this study, we firstly established a multiplex MCDA-LFB method for simple, rapid, sensitive and reliable detection of MTB. A simple instrument (such as a heater or water-bath) is sufficient for maintaining a fixed temperature (67°C), and the whole procedure can be finished in 50 min. The LOD of the multiplex MCDA-LFB method was 10 fg per reaction with pure cultures, and 100% specificity was acquired using cultured bacteria. Most importantly, when the multiplex MCDA-LFB was used to detect clinical samples, it showed 88.2% sensitivity and 98.3% specificity.

Choosing an appropriate target is important for the high sensitivity and specificity of the diagnostic assay. IS*6110* and IS*1081* are multi-copy insertion sequences that are specific for MTBC. In the genome of reference strain H37Rv, IS*6110* and IS*1081* copy numbers are 16 and 6, respectively, which makes them useful as diagnostic markers. However, the copy number of IS*6110* is low (even only one copy) or absent in a certain proportion of MTB strains of Southeast Asia (Yuen et al., 1993; Fomukong et al., 1994; Cronin et al., 2001). Another insertion sequence IS*1081* (five to six copies in MTBC strains) was examined as a subsidiary marker (van Soolingen et al., 1992; Yang et al., 1994). The combined detection of IS*1081* can increase the positive rate for such strains. This is the reason that the new generation of Xpert assay, Xpert MTB/RIF ultra, also integrated IS*1081* (Chakravorty et al., 2017; Dorman et al., 2018). In this study, for each target gene, 10 primers were designed that bind to different regions and ensure high specificity. Two sets of primers were labeled in the same way (C1-FITC labeled, D1-biotin labeled). In this case, the amplification products can be detected simultaneously by the anti-FITC on the LFB strip, which not only guarantees the sensitivity but also reduces total cost.

The real-time turbidity analysis and visual agent detection are usually used to indicate the isothermal amplification results. However, the former requires a complex, expensive and precise apparatus, and the later usually produces ambiguous results when the concentration of target sequences is very low (Wang et al., 2018b). In this study, LFB platform was used to analyze the MCDA products. It is rapid (the results can be seen in 2 min), simple (does not need complex equipment) and sensitive (LOD is 10 fg), which is suitable for clinical use and field detection.

To verify the value of multiplex MCDA for clinical application, clinical samples from 179 patients were evaluated and compared with the WHO-recommended method of Xpert MTB/RIF and liquid culture using Bactec MGIT960. According to our assay, the sensitivity was the lowest for liquid culture (42.0%), followed by Xpert MTB/RIF (49.6%) and multiplex MCDA (88.2%) among 119 clinically diagnosed TB patients. We further divided the samples into culture-positive group (50 patients) and culture-negative group (69 patients). Among culture-positive specimens, both Xpert MTB/RIF and multiplex MCDA assay had good sensitivity (86.0% and 98.0%,

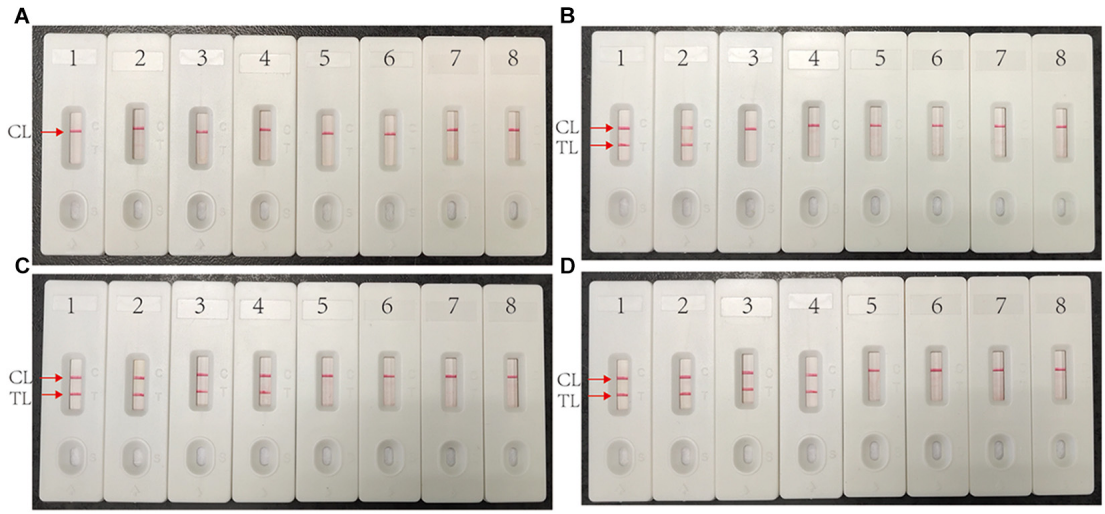

FIGURE 4 | Optimized reaction time for multiplex MCDA assay. Four different duration times (**A**, 10 min; **B**, 20 min; **C**, 30 min; **D**, 40 min) were determined at optimal amplification temperature (67°C). Biosensors 1, 2, 3, 4, 5, and 6 represent genomic DNA template of H37Rv 10 pg, 1 pg, 100 fg, 10 fg, 1 fg, 100 ag. Biosensors 7 and 8 represent negative control (genomic DNA from *M. abscessus* 1 ng) and blank control (DW).

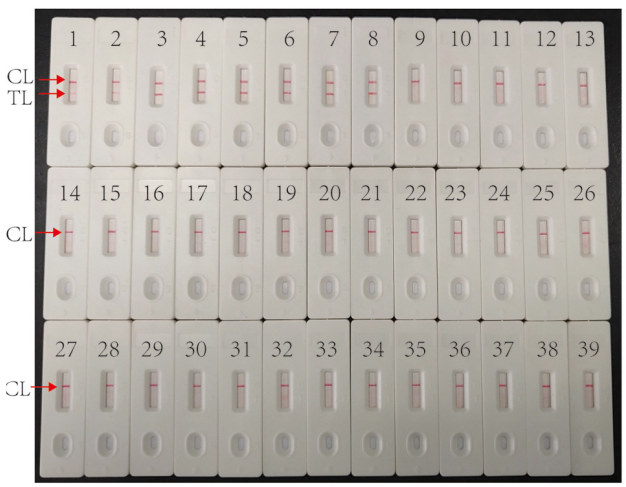

FIGURE 5 | Specificity of multiplex MCDA assay using DNA templates from different bacteria. Biosensor 1 represents reference strain H37Rv. Biosensors 2–7 represent cultured MTB strains from clinical patients. Biosensor 8 represents BCG strain. Biosensors 9–29 represent 21 different non-mycobacteria bacteria (details shown in **Table 2**). Biosensors 30–38 represent nine different NTM strains (details shown in **Table 2**). Biosensor 39 represents blank control (DW).

TABLE 3 | Comparison of different methods for MTB detection in clinical TB patients.

	Sensitivity, % (n[a]/N)		Specificity, % (n/N)
	Culture positive (*N* = 50)	Culture negative (*N* = 69)	
Xpert MTB/RIF	86.0% (43/50)	23.2% (16/69)	100% (60/60)
MTB-MCDA	98.0% (49/50)	81.2% (56/69)	98.3% (59/60)

[a]*n number of samples with positive results using a specific method.*

respectively). The performance of Xpert MTB/RIF showed similar sensitivity with that reported in a recent systematic review (85%) (Horne et al., 2019), indicating that there is no deviation in the selection and detection of specimens. While among the culture-negative samples, the positive rates of Xpert MTB/RIF and multiplex MCDA assay were 23.2% and 81.2%, respectively. Thus, the multiplex MCDA greatly improved the detection rate in culture-negative patients. As a consequence, more TB patients will be early diagnosed using multiplex MCDA assay, and then reduce the transmission possibility.

A concern of this multiplex MCDA assay is the reliability of its positive outcomes, especially for the samples with culture-negative outcomes (Wang et al., 2015). Although we could not clarify those extra positive results of MCDA in this study, the specificity of 98.3% (59/60) could confirm its reliability to some extent. However, since the yield of isothermal amplification is very large, contamination will be a big challenge during application (Wang et al., 2015). Aerosol droplets that contain a high concentration of MCDA products could lead to false positive results in subsequent experiments. Accordingly, special measures should be taken to avoid contamination and false positive outcome.

CONCLUSION

A multiplex MCDA-LFB assay targeting both IS*6110* and IS*1081* for MTB detection was successfully developed and validated using pure cultures and clinical samples. It is a rapid and

simple diagnostic method with high sensitivity and specificity for *M. tuberculosis* detection. Further prospective study will be needed to evaluate its ability for early TB diagnosis in specific groups, such as children and HIV-infected patients.

DATA AVAILABILITY

The raw data supporting the conclusions of this manuscript will be made available by the authors, without undue reservation, to any qualified researcher.

ETHICS STATEMENT

The studies involving human participants were reviewed and approved by Ethics committee of the Beijing Children's Hospital, Capital Medical University and Beijing Chest Hospital, Capital Medical University. Written informed consent to participate in this study was provided by the participants' legal guardian/next of kin.

AUTHOR CONTRIBUTIONS

W-WJ conceived and designed the experiments. W-WJ, YW, Y-CW, JX, LS, J-QL, S-AW, T-TZ, and QM performed the experiments. W-WJ, H-RH, and A-DS contributed to the reagents and materials. W-WJ, H-RH, and A-DS analyzed the data. W-WJ and YW performed the software. W-WJ, YW, H-RH, and A-DS wrote the manuscript. All authors have contributed and approved the final version of the manuscript.

FUNDING

This study was supported by the Beijing Young Talents Project (2016000021223ZK38), Beijing Health System High-level Health Technology Talents Training Plan (2015-3-081), Beijing Municipal Administration of Hospitals' Ascent Plan (DFL20181602), and Beijing Municipal Administration of Hospitals Clinical Medicine Development of Special Funding Support (ZYLX201809).

REFERENCES

Boehme, C. C., Nabeta, P., Hillemann, D., Nicol, M. P., Shenai, S., Krapp, F., et al. (2010). Rapid molecular detection of Tuberculosis and rifampin resistance. *N. Engl. J. Med.* 363, 1005–1015. doi: 10.1056/NEJMoa0907847

Bojang, A. L., Mendy, F. S., Tientcheu, L. D., Otu, J., Antonio, M., Kampmann, B., et al. (2016). Comparison of TB-LAMP, GeneXpert MTB/RIF and culture for diagnosis of pulmonary tuberculosis in The Gambia. *J. Infect.* 72, 332–337. doi: 10.1016/j.jinf.2015.11.011

Chakravorty, S., Simmons, A. M., Rowneki, M., Parmar, H., Cao, Y., Ryan, J., et al. (2017). The new xpert MTB/RIF ultra: improving detection of mycobacterium tuberculosis and resistance to rifampin in an assay suitable for point-of-care testing. *mBio* 8, e812–e817. doi: 10.1128/mBio.00812-17

Cronin, W. A., Golub, J. E., Magder, L. S., Baruch, N. G., Lathan, M. J., Mukasa, L. N., et al. (2001). Epidemiologic usefulness of spoligotyping for secondary typing of *Mycobacterium tuberculosis* isolates with low copy numbers of IS6110. *J. Clin. Microbiol.* 39, 3709–3711. doi: 10.1128/JCM.39.10.3709-3711.2001

Dorman, S. E., Schumacher, S. G., Alland, D., Nabeta, P., Armstrong, D. T., King, B., et al. (2018). Xpert MTB/RIF Ultra for detection of *Mycobacterium tuberculosis* and rifampicin resistance: a prospective multicentre diagnostic accuracy study. *Lancet Infect. Dis.* 18, 76–84. doi: 10.1016/S1473-3099(17)30691-6

Fomukong, N. G., Tang, T. H., al-Maamary, S., Ibrahim, W. A., Ramayah, S., Yates, M., et al. (1994). Insertion sequence typing of *Mycobacterium tuberculosis*: characterization of a widespread subtype with a single copy of IS6110. *Tuber. Lung Dis.* 75, 435–440. doi: 10.1016/0962-8479(94)90117-1

Horne, D. J., Kohli, M., Zifodya, J. S., Schiller, I., Dendukuri, N., Tollefson, D., et al. (2019). Xpert MTB/RIF and Xpert MTB/RIF Ultra for pulmonary tuberculosis and rifampicin resistance in adults. *Cochrane Database Syst. Rev.* 6:CD009593. doi: 10.1002/14651858.CD009593.pub4

National-Health-and-Family-Planning-commission-of-the-People's-Republic-of-China (2017). *Diagnosis for Pulmonary tuberculosis (WS288-2017)*. Beijing: National Health and Family Planning Commission.

Ou, X., Li, Q., Xia, H., Pang, Y., Wang, S., Zhao, B., et al. (2014). Diagnostic accuracy of the PURE-LAMP test for pulmonary tuberculosis at the county-level laboratory in China. *PLoS One* 9:e94544. doi: 10.1371/journal.pone.0094544

van Soolingen, D., Hermans, P. W., de Haas, P. E., and van Embden, J. D. (1992). Insertion element IS1081-associated restriction fragment length polymorphisms in *Mycobacterium tuberculosis* complex species: a reliable tool for recognizing *Mycobacterium bovis* BCG. *J. Clin. Microbiol.* 30, 1772–1777.

Wang, Y., Deng, J. P., Liu, D. X., Wang, Y., Xu, J. G., and Ye, C. Y. (2018a). Nanoparticles-based lateral flow biosensor coupled with multiple cross displacement amplification Plus for simultaneous detection of nucleic acid and prevention of carryover contamination. *Sens. Actuators BChem.* 255, 3332–3343. doi: 10.1016/j.snb.2017.09.160

Wang, Y., Li, H., Wang, Y., Xu, H., Xu, J., and Ye, C. (2018b). Antarctic thermolabile uracil-DNA-glycosylase-supplemented multiple cross displacement amplification using a label-based nanoparticle lateral flow biosensor for the simultaneous detection of nucleic acid sequences and elimination of carryover contamination. *Nano Res.* 11, 2632–2647. doi: 10.1007/s12274-017-1893-z

Wang, Y., Yan, W., Fu, S., Hu, S., Wang, Y., Xu, J., et al. (2018c). Multiple cross displacement amplification coupled with nanoparticles-based lateral flow biosensor for detection of *Staphylococcus aureus* and identification of methicillin-resistant *S. aureus*. *Front. Microbiol.* 9:907. doi: 10.3389/fmicb.2018.00907

Wang, Y., Wang, Y., Ma, A. J., Li, D. X., Luo, L. J., Liu, D. X., et al. (2015). Rapid and sensitive isothermal detection of nucleic-acid sequence by multiple cross displacement amplification. *Sci. Rep.* 5:11902. doi: 10.1038/srep11902

Wang, Y., Wang, Y., Zhang, L., Xu, J. G., and Ye, C. Y. (2017). Visual and multiplex detection of nucleic acid sequence by multiple cross displacement amplification coupled with gold nanoparticle-based lateral flow biosensor. *Sens. Actuators B Chem.* 241, 1283–1293. doi: 10.1016/j.snb.2016.10.001

World-Health-Organizaion (2011). *Policy Statement: Automated Real-Time Nucleic Acid Amplification Technology for Rapid and Simultaneous Detection of Tuberculosis and Rifampicin Resistance: Xpert MTB/RIF System*. Geneva: World Health Organization.

World-Health-Organizaion (2016). *The Use of Loop-Mediated Isothermal Amplification (TB-LAMP) for the Diagnosis of Pulmonary Tuberculosis: Policy Guidance*. Geneva: World Health Organization.

World-Health-Organizaion (2018). *Global Tuberculosis Report 2018*. Geneva: World Health Organization.

Yang, Z. H., de Haas, P. E., van Soolingen, D., van Embden, J. D., and Andersen, A. B. (1994). Restriction fragment length polymorphism *Mycobacterium tuberculosis* strains isolated from Greenland during 1992: evidence of tuberculosis transmission between Greenland and Denmark. *J. Clin. Microbiol.* 32, 3018–3025.

Yuen, L. K., Ross, B. C., Jackson, K. M., and Dwyer, B. (1993). Characterization of *Mycobacterium tuberculosis* strains from vietnamese patients by Southern blot hybridization. *J. Clin. Microbiol.* 31, 1615–1618.

Conflict of Interest Statement: The authors declare that the research was conducted in the absence of any commercial or financial relationships that could be construed as a potential conflict of interest.

frontiers in Microbiology

ORIGINAL RESEARCH
published: 09 October 2019
doi: 10.3389/fmicb.2019.02268

Relationship of Serum Antileishmanial Antibody With Development of Visceral Leishmaniasis, Post-kala-azar Dermal Leishmaniasis and Visceral Leishmaniasis Relapse

Dinesh Mondal[1], Prakash Ghosh[1], Rajashree Chowdhury[1], Christine Halleux[2], Jose A. Ruiz-Postigo[3], Abdul Alim[1], Faria Hossain[1], Md Anik Ashfaq Khan[1], Rupen Nath[1], Malcolm S. Duthie[4], Axel Kroeger[5], Greg Matlashewski[6], Daniel Argaw[3] and Piero Olliaro[2,7]*

[1] Emerging Infections and Parasitology Laboratory, International Centre for Diarrhoeal Disease Research, Dhaka, Bangladesh, [2] UNICEF/UNDP/World Bank/WHO Special Programme for Research and Training in Tropical Diseases (TDR), World Health Organization, Geneva, Switzerland, [3] Department of Neglected Tropical Diseases, World Health Organization, Geneva, Switzerland, [4] Infectious Disease Research Institute, Seattle, WA, United States, [5] Centre for Medicine and Society, University Medical Center Freiburg, Freiburg im Breisgau, Germany, [6] Department of Microbiology and Immunology, McGill University, Montreal, QC, Canada, [7] Centre for Tropical Medicine and Global Health, Nuffield Department of Medicine, University of Oxford, Oxford, United Kingdom

OPEN ACCESS

Edited by:
Aleksandra Barac, University of Belgrade, Serbia

Reviewed by:
Debanjan Mukhopadhyay, University of California, Davis, United States
Shibabrata Mukherjee, Cincinnati Children's Research Foundation, United States

***Correspondence:**
Dinesh Mondal
din63d@icddrb.org

Specialty section:
This article was submitted to Infectious Diseases, a section of the journal Frontiers in Microbiology

Received: *27 June 2019*
Accepted: *18 September 2019*
Published: *09 October 2019*

Citation:
Mondal D, Ghosh P, Chowdhury R, Halleux C, Ruiz-Postigo JA, Alim A, Hossain F, Khan MAA, Nath R, Duthie MS, Kroeger A, Matlashewski G, Argaw D and Olliaro P (2019) Relationship of Serum Antileishmanial Antibody With Development of Visceral Leishmaniasis, Post-kala-azar Dermal Leishmaniasis and Visceral Leishmaniasis Relapse. Front. Microbiol. 10:2268. doi: 10.3389/fmicb.2019.02268

Introduction: To sustain the achievement of kala-azar elimination program (KEP), early detection and treatment of the visceral leishmaniasis (VL) cases and associated modalities such as treatment failure (TF), relapse VL (RVL), and Post-kala-azar dermal leishmaniasis (PKDL) is the cornerstone. A predictive biomarker for VL development and related complications could also play a crucial role in curtailing disease incidence and transmission. Investigations to find a biomarker with prospective capabilities are, however, scarce. Using samples and known clinical outcomes generated within two previous longitudinal cohort studies, we aimed to determine if fluctuations in serum anti-rK39 antibody levels could provide such predictive value.

Materials and Methods: Serum samples collected at four different time points (Baseline, 12, 18, and 24 months) from 16 patients who had developed VL within the monitoring period and 15 of their asymptomatic healthy controls counterparts were investigated. To investigate potential prediction of VL related complications, serum samples of 32 PKDL, 10 RVL, 07 TF, and 38 cured VL from a single dose AmBisome trial were analyzed. Of this second panel, all patients were monitored for 5 years and sera were collected at four time points (Baseline then 1, 6, and 12 months after treatment). The level of anti-rK39 antibodies in archived samples was measured by a semi-quantitative ELISA.

Results: The mean antibody level was significantly higher in VL patients compared to their asymptomatic healthy counterparts at each time point. Likewise, we observed a

trend toward elevations in antibody levels for PKDL, RVL, TF relative to the reducing levels observed in cured VL. Receiver operating characteristic (ROC) analysis found a promising predictive power of rK39 antibody levels to reveal progression from asymptomatic *Leishmania donovani* infection stage to VL, defined as 87.5% sensitive and 95% specific. Following treatment, rk39 antibody notably showed 100% sensitivity and 95% specificity in predicting TF.

Conclusion: Our data indicate that the relative quantity of serum anti-rK39 antibody has promise within either a predictive or prognostic algorithm for VL and VL-related modalities. These could enable VL control programs to implement more effective measures to eliminate the disease. Further research is, however, imperative to standardize the rK39 antibody ELISA between sites prior to broader use.

Keywords: visceral leishmaniasis (VL), treatment failure (TF), relapse VL (RVL), Post-kala-azar dermal leishmaniasis (PKDL), rK39 antibody, ELISA, predictive biomarker

INTRODUCTION

Visceral leishmaniasis (VL) is one of the twenty neglected tropical infectious diseases (NTDs) listed by the World Health Organization (WHO). On the Indian sub-continent, where VL is known also as kala-azar, it is caused by *Leishmania donovani* (LD) transmitted during the blood meals of female *Phlebotomus argentipes* sand flies (Chappuis et al., 2007). The first reported outbreak of VL was in 1824 in the Jessore of British Bengal and killed 75,000 people within 3 years (Bern and Chowdhury, 2006). Since then, periodic epidemics of VL have been common on the Indian sub-continent. Besides, 90% of VL cases occur in mainly six countries including Bangladesh, India, Nepal, Ethiopia, Sudan, and Brazil (Chappuis et al., 2007).

For VL case management, control and elimination, critical remaining questions are which individuals are at risk of becoming diseased and who can transmit the infection. A person may have several outcomes after being infected by *L. donovani*. Approximately 90% of infected individuals do not develop VL symptoms but rather remain asymptomatic (dos Santos et al., 2016), while about 10% go on to develop clinically overt disease with fever, enlarged spleen, anemia or pancytopenia (VL patient) (unpublished data). While VL is almost invariably fatal if left untreated, timely and proper treatment with current therapies is mostly effective, with only 2–3% of cases failing to respond to initial treatment (treatment failure, TF) (Mondal et al., 2014). A recent cohort study from Bangladesh established that 3–7% of initially cured VL patients may develop VL again, and this is collectively defined as VL relapse (VLR) (Mondal et al., 2019). In Bangladesh, 10–20% of cured VL patients may develop Post-kala-azar dermal leishmaniasis (PKDL), a dermatological sequela of VL, usually within 3 years following treatment (Mondal et al., 2019). The skin lesions of PKDL can be macular, papular, nodular, and polymorphic (Zijlstra et al., 2003; Mukhopadhyay et al., 2014). In Bangladesh approximately 10% of asymptomatic may also develop PKDL without having had clinical VL (Rahman et al., 2010).

While VL patients are generally believed to be the engine of *L. donovani* transmission, we have demonstrated that VL, VLR, and PKDL cases can all transmit LD to sand flies (Addy and Nandy, 1992; Molina et al., 2017; Mondal et al., 2018). The transmission potential of a VL and PKDL case through a single sand fly bite is nearly 80 and 65%, respectively (Mondal et al., 2018). In reality, however, this theoretical potential may be altered by factors such as frequency of exposure to bites and healthcare seeking behaviors. Being symptomatic pushes VL cases to seek medical care actively, though often they experience delays of several months' times before receiving proper treatment, a period during which they continue to be a source of infection (Mondal et al., 2009). Conversely, PKDL cases usually do not seek medical care until they are stigmatized by their skin lesions and they therefore can remain a source of transmission for years (Basher et al., 2015). Theoretically, asymptomatic infections could also be transmitters of the infection, especially in the pre-patent period, but this has not yet been formally documented.

Under the aegis of the WHO, the Governments of Bangladesh, India, and Nepal committed to reduce and maintain the incidence of VL less than 1 per 10,000 people at the upazila (sub-district), block and district level respectively, to eliminate VL as a public health problem (World Health and Organization, 2005). While the kala-azar elimination program (KEP) has achieved remarkable successes in reducing VL incidence throughout the Indian subcontinent, it will not be possible to sustain elimination unless sources of new infections are detected and managed early. Much research has been conducted in an effort to detect *L. donovani* infection and VL-associated complications (Chappuis et al., 2007). As a means to provide early detection of relapsing VL, Mollet et al. (2018) conducted a case-control study and reported a significant difference in rK39 IgG1 level between cured and relapse VL (RVL) cases. A cohort study, however, has not yet been conducted to validate the findings Moreover, very few prospective cohort studies have been conducted to enable the prediction of VL and VL-associated modalities such as TF, RVL, and PKDL (Gasim et al., 2000; Hasker et al., 2014; Chapman et al., 2015; Chakravarty et al., 2019). Therefore, evaluation of new or available biomarkers that can potentially predict VL and

its associated modalities are still required. Such studies, and the biomarkers they may reveal, could have a crucial role in facilitating control strategies in consolidation and maintenance phases of the KEP.

To address the current gaps in prognosis of VL and VL-associated modalities we investigated the dynamics of anti-rK39 antibodies by longitudinal comparative assessment in asymptomatic and emergent VL patients to determine if altered levels can predict those most likely to develop VL. Among a second serum panel, we evaluated if quantitative measurement of anti-rK39 antibodies could reveal VL cases at risk for development of PKDL, TF or relapse.

MATERIALS AND METHODS

Study Design and Site

The study was a laboratory-based evaluation and was carried out in International Centre For Diarrhoeal Disease Research, Bangladesh (ICDDR,B), Dhaka, Bangladesh from November 2015 to November 2017 using archive samples, patients' metadata and informed voluntary consent from adult patients and guardian of minor patients of previous studies.

Study Population, Sampling Method, and Sample Size

Asymptomatic Subjects Included in This Study

The asymptomatic cohort included 200 individuals from a trial involving micronutrient intervention and de-worming to prevent the development of symptomatic VL (trial registration number NCT01069198). These were apparently healthy asymptomatic individuals living in a VL-endemic village, without VL or PKDL symptoms but positive on the rK39-antibody detection rapid test. Children aged less than 2 years, adults aged more than 60 years, pregnant women and persons with signs and symptoms of any chronic disease were not enrolled, nor were non-consenting individuals. The study ended on October 30, 2012 and 196 of 200 completed (98%) the 2-year follow-up. Serum samples were analyzed at baseline, 12, 18, and 24 months from the 16 subjects who developed symptomatic VL and were treated following national guidelines in the public hospital in Trishal, Mymensingh, as well as those of 15 asymptomatic controls (rK39-positive, asymptomatic subjects without subsequent VL) (**Figure 1**).

VL Patients Included in This Study

The study included serum samples from VL patients (before and after treatment) of a previous study (PR-11001 and amendment SDA–Trial registration number ACTRN12612000367842). This study was originally a single-arm clinical trial for VL patients who were treated with 10 mg/kg body weight single-dose liposomal Amphotericin B (LAmB). The study started in February 2012 and was completed in August 2013, but was subsequently amended to allow for a 5-years follow-up of the cohort (VL cohort), which was completed in 2016. A VL patient was defined according to the National Kala-azar Elimination Guideline as a person living in the kala-azar endemic area with fever lasting for more than 2 weeks, splenomegaly and a positive rK39 rapid test (Ahmed et al., 2014). The study enrolled 300 VL patients with the following entry criteria and 296 patients completed study per protocol.

Inclusion criteria

Both sexes, age $\geq$5 years, history of fever for more than 2 weeks, splenomegaly, positive rK39 rapid test, hemoglobin $\geq$5 g/dl, written informed consent from the patient, or parent or guardian if under 18 years old.

Exclusion criteria

History of intercurrent or presence of clinical signs/symptoms of concurrent diseases/conditions (e.g., chronic alcohol consumption or drug addiction, renal, hepatic, cardiovascular or CNS disease; diabetes mellitus, dehydration, other infectious diseases or major psychiatric diseases) only if the intercurrent conditions were not under control before starting LAmB treatment; any condition which, according to the investigator, might prevent the patient from completing the study therapy and subsequent follow-up; history of allergy or hypersensitivity to Amphotericin B; previous treatment for VL within 2 months of enrollment into the study; prior TF with Amphotericin B; PKDL; pregnancy.

Seven and 289 of 296 had respectively TF and final cure by day 180 since treatment. Ten and 32 of the 289 cured cases went on to develop respectively VLR and PKDL during the 5-year follow-up. Two hundred forty seven of 289 did not have TF/VLR/PKDL during 5-year follow-up (**Figure 1**). The definitions of TF, VLR, and PKDL were:

Treatment failure (TF): A treated VL patient who had no clinical improvement at 30 days after treatment, or had an initial improvement at 30 days followed by recurrence of sign and symptom of VL and had LD bodies in spleen aspirates within day 180 after treatment.

VL relapse (VLR): A VL patient who is cured at the 180-day visit who had reappearance of symptoms and LD bodies in spleen aspirates during subsequent follow-up.

Post-kala-azar Dermal Leishmaniasis (PKDL): A cured VL patient at day 180 with no relapse and with skin lesions (macular, popular, nodular or polymorphic), positive on the rK39 rapid test, negative for fungal infection by microscopic examination and negative for leprosy using skin sensation test and with skin specimen positive for LD bodies by microscopy and/or positive for LD DNA by qPCR.

Randomly selected 38 of 247 cured patients served as control (VL control) in this study. TF and VLR were treated with multiple-dose LAmB (a total dose of 15 mg/kg body weight divided into three, 5 mg/kg applications given) every other day. PKDL cases were treated following national guideline (Ahmed et al., 2014).

Laboratory Methods

For asymptomatic individuals included in this study, rK39 rapid test and rK39 ELISA were performed on serum samples corresponding to baseline, month 12, month 18, and month 24. For former VL patients, rK39 rapid test and rK39 ELISA were performed on serum samples corresponding to baseline, day 30, day 180, and day 365.

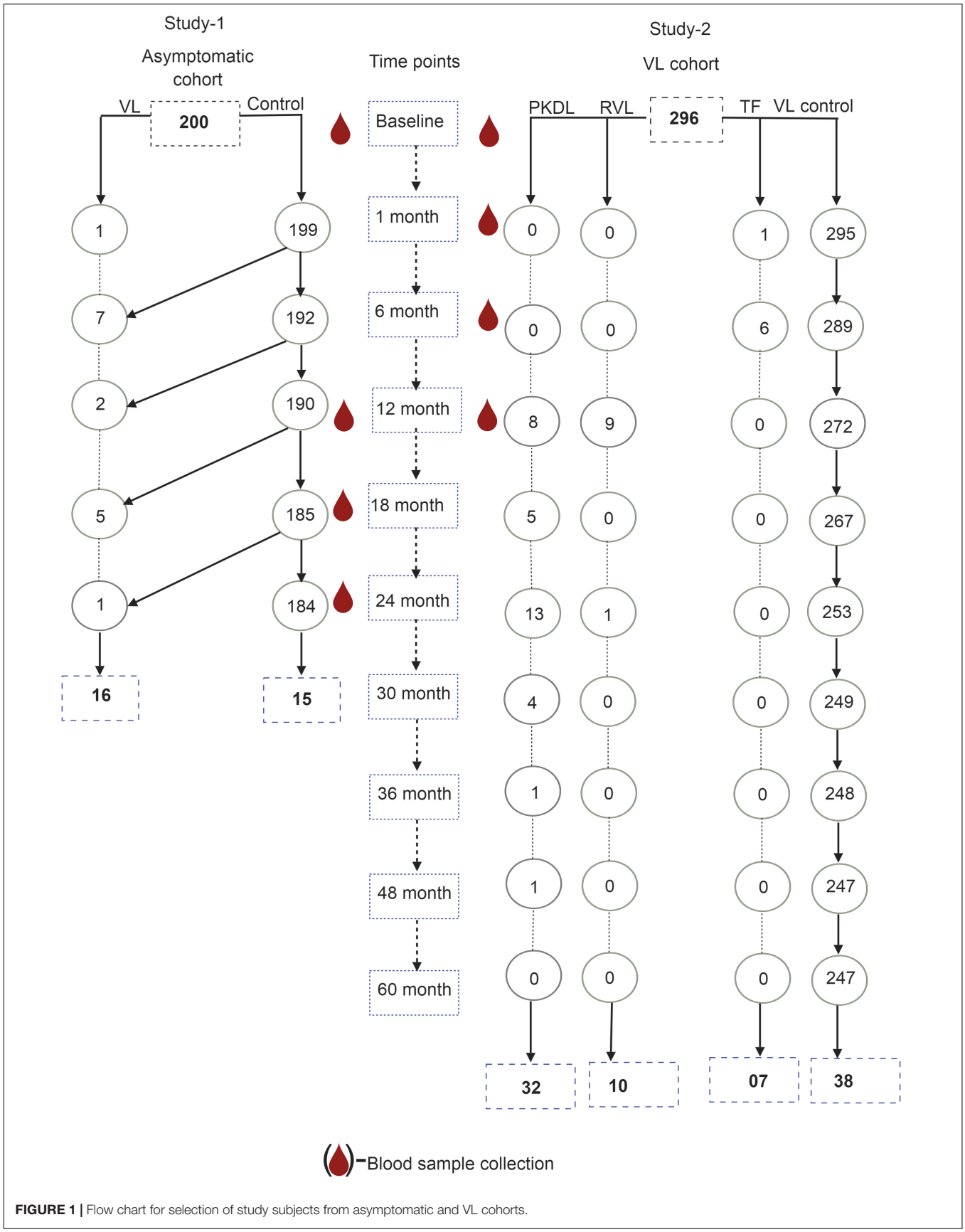

FIGURE 1 | Flow chart for selection of study subjects from asymptomatic and VL cohorts.

Rapid Diagnostic Test

The rK39 rapid diagnostic test (RDT) was performed using serum by Kala-azar detect Rapid test (InBios, Seattle, WA, United States) following the manufacture's instruction.

Semi-Quantitative ELISA

A semi-quantitative rK39 ELISA was performed with improvisation to quantify antibody levels in serum as previously described (Vaish et al., 2012; Ghosh et al., 2016). In brief, flat bottom 96-well microtiter plates (Greiner-Bioone) were coated with 25 ng/well of rK39 antigen in PBS (pH 7.4) and incubated overnight at 4°C. On the following day, plates were washed three times with wash buffer (PBS containing 0.05% Tween 20, pH 7.4) and then blocked with blocking buffer (PBS containing 1% BS, pH 7.4) for 3 h at 37°C. Following 5 times wash with wash buffer, 50 μl of 1:400 diluted serum sample was added to the respective wells and incubated for 1 h at 37°C. After incubation, the plates were washed five times with wash buffer and peroxidase-conjugated rabbit anti-human IgG (Jackson Immune-Research, United States) (1:5000 times dilution in DF) was added to each well and incubated for 1 h at 37°C. After washing five times, 100 μl of TMB substrate (Sigma, United States) was added in each well then the plate was placed in the dark for 20 min. The optical density (OD) was measured at 450 nm in a micro-plate reader. A standard curve was constructed for each plate with serially diluted positive pooled serum and antibody levels were estimated from the standard curve. Pooled serum was serially diluted two times to get a range from 16,000 to 4,096,000 for preparing the standard curve. The antibody level was expressed as arbitrary unit (AU) for each dilution. 1000 AU was assigned to the OD value of the pooled serum corresponding to 16,000 times dilution. Antibody level in experimental serum samples was determined from the standard curve.

Data Management and Statistical Analysis

After computing lab data from laboratory reporting forms, descriptive and inferential statistics were carried out. Comparisons between means were done by a parametric and non-parametric method when applicable. Proportions between groups were compared by Chi-square test. The receiver operating characteristic curve (ROC) approach was used to find the cutoff for prediction of asymptomatic at risk for VL and VL patients at risk for an unfavorable outcome. A two-tailed p-value of ≤ 0.05 was considered as significant. Data analysis was performed with SPSS version 20.

Quality Assurance

Serum samples were archived at −20°C immediately after separation from blood and at −80°C for long time archives. Pooled serum samples from confirmed VL patients were aliquoted in multiple tubes to avoid repetitive fridge-thaw cycles during ELISA. Each sample was run in triplicate to measure the appropriate arbitrary titer of antibody.

Research Ethics

This research was approved by the ICDDR,B, ethics committee (Dhaka, Bangladesh) and the WHO Ethics Review Committee. All study participants or their guardians of previous studies provided written informed consent for use of their collected samples for subsequent studies on VL research.

RESULTS

Population Characteristics and Risks for VL, TF, VLR, and PKDL

Of the 200 asymptomatic rK39 antibody-positive subjects who completed the 2-year follow-up, 16 (8.2%) went on to develop symptomatic VL of which 10 (5.1%) developed disease within the first year of follow-up. Of the 296 patients treated for VL who completed the 3-year follow-up, 7 (2.4%) failed treatment by 6 months, and 10 (3.4%) and 32 (10.8%), respectively relapsed or developed PKDL between month 6 and 5 years post-treatment (**Table 1**).

The study population included 16 VL conversions from 200 asymptomatic cases and 15 asymptomatic cases as the counterpart of VL patients who did not convert to VL and 7, 10, 32 and 38 VL patients, respectively with TF, VLR, PKDL, and VL controls with favorable treatment outcome. Asymptomatic subjects with and without subsequent VL did not differ statistically significantly regarding their sex, body mass index and blood hemoglobin levels at enrollment (**Table 1**). The TF, VLR, PKDL, and VL control also did not differ significantly regarding their sex, age, and body mass index. However, the blood hemoglobin of TF patients was statistically significantly lower than VL controls (**Table 1**).

The risk for development of VL within next 24 months after being diagnosed as asymptomatic by the rK39 RDT was 8.2% (**Table 2**). The risks for TF, VLR and PKDL among VL patients within 5 years post-treatment with single-dose LAmB was respectively 2.4, 3.4, and 10.8% (**Table 2**).

Dynamic of rK39 Antibody Titer in Asymptomatic *L. donovani*-Infected Individuals

The mean rK39 antibody titers as determined by ELISA from asymptomatic cases who developed VL were significantly higher than those from asymptomatic cases who did not develop VL throughout the 2-year follow-up (**Figure 2**). The serum titers of rK39 antibodies were inversely related to hemoglobin level ($r = -0.182$, $p = 0.043$) while they did not vary with sex, age, and BMI. The ROC curve shows a cutoff of rK39 antibody titer of 802,497 AUs predicts asymptomatic infection progression to VL within the next 24 months with a sensitivity of 87.5% and specificity of 95% (**Figure 3**).

We determined the relation between the rK39 RDT result and the rK39 antibody ELISA along with the longevity of the rK39 RDT-positive results. The planned number of rK39 RDT and ELISA evaluations in 31 asymptomatic at 4 time points was 124, of which 116 tests were completed (94%).

TABLE 1 | Population characteristics of asymptomatic participants with rK39-positive and VL patients.

Cohort	Subject type (*n*)	Sex % female (*n*)	Age in years (95% CI)	Body mass index (95% CI)	Hemoglobin g/dl (95% CI)
Asymptomatic	with subsequent VL (16)	44 (7)	14.78 (8.13–21.44)	15.70 (14.34–17.05)	12.53 (11.26–13.80)
	without subsequent VL (15)	47 (7)	15.94 (14.34–17.05)	15.94 (14.40–17.47)	12.80 (11.57–14.11)
	p-value between groups	0.56	0.90	0.80	0.71
VL patients	Treatment failure (7)	14.3 (1)	114.9 (5.0–224.7)	13.6 (11.9–15.3)	7.8# (6.5–9.1)
	VL relapse (10)	50.0 (5)	169.2 (74.1–264.3)	14.1 (11.6–16.5)	10.1 (8.8–11.4)
	Post-kala-azar Dermal Leishmaniasis (32)	37.5 (12)	247.1 (184.3–309.9)	15.3 (14.2–16.3)	9.3 (8.7–10.0)
	VL control (38)	34.2 (13)	231.5 (175.9–287.1)	15.2 (14.4–16.0)	10.1# (9.5–10.6)
	p-value between groups	0.49	0.21	0.16	0.82

#*p = 0.008.*

TABLE 2 | Risks for VL, TF, VLR, and PKDL.

Condition	Denoted by	Probability by month *x*	*n* with condition	*N* evaluable	Risk %	95% CI
Infected asymptomatic	A					
Develop clinical VL	V	P (V¦A)24	16	196	8.2	4.3–12
Do not develop VL	∼V	P (∼V¦A)24	180	196	91.8	88–95.7
VL case treated	Vt					
Fail treatment	F	P (F¦Vt)60	7	296	2.4	0.6–4.1
Relapse post-treatment	R	P (R¦Vt)60	10	296	3.4	1.3–5.4
Develop PKDL	D	P (D¦Vt)60	32	296	10.8	7.3–14.3
Definitive cure	∼V	P (∼V¦Vt)60	247	296	83.4	79.2–87.7

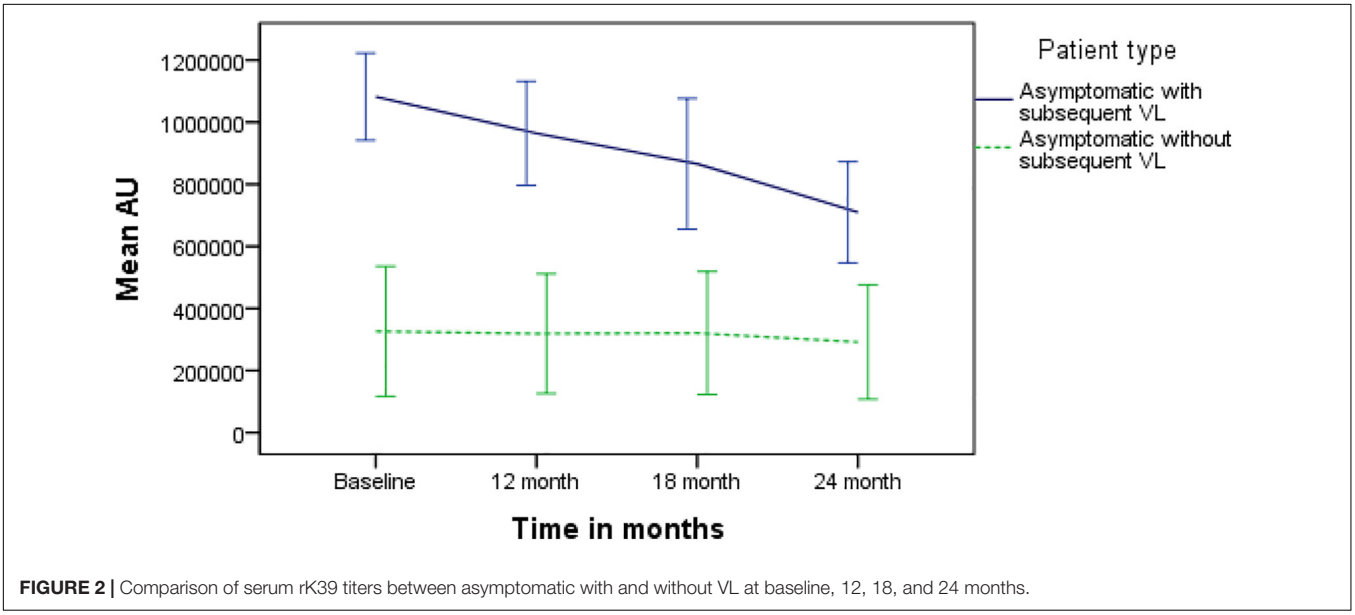

FIGURE 2 | Comparison of serum rK39 titers between asymptomatic with and without VL at baseline, 12, 18, and 24 months.

The average (95% CI) arbitrary rK39 antibody titer for RDT negative (n = 20) and RDT positive test (n = 96) was respectively 308,986 (95% CI, 1,25,406–4,92,565) and 670,560 (5,78,173–7,62,948), p-value = 0.002. All asymptomatic cases had a positive rK39 RDT at baseline as per enrollment criteria. Five of 16 (33%) asymptomatic *L. donovani*-infected individuals that developed VL had a negative rK39 RDT after treatment, however, at 24 months all but one was positive. About 60% (9/15) asymptomatic cases that did not develop VL had negative rK39 RDT at some point during follow-up,

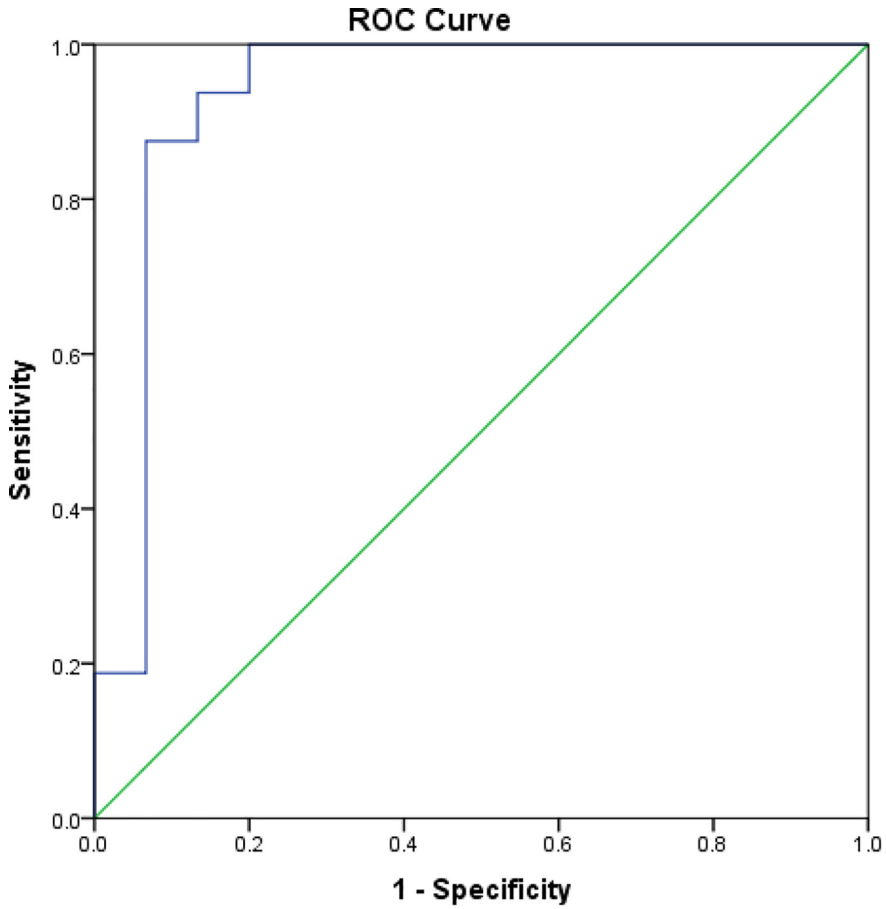

FIGURE 3 | Receiver operating characteristic curve for cutoff of rK39 AB titer for prediction of asymptomatic at risk for VL within subsequent 24 months.

but at 24 months only 20% (3/15) had a negative rK39 RDT result (**Table 2**).

Trend of rK39 Antibody Titer in VL Patients

Comparisons of rK39 antibody titers between TF, VLR, PKDL, and VL control are given in **Table 3**. The TF group had the lowest titers compared to all other groups at all-time points except at day 365 when it did not differ from control. This indicates that the rK39 antibody titer at day 30 could potentially predict TF. An arbitrary titer of rK39 antibodies ≤626,195 at baseline before treatment predicted TF in this group with a sensitivity and specificity of 100 and 95%, respectively (**Figure 4**).

The dynamic of rK39 antibody titers of TF, VLR, PKDL and VL control was different (**Figure 5**). The rK39 antibody titer of VL controls was not statistically different from the titer of VLR and PKDL at baseline, day 30 and 180 after treatment (**Table 3** and **Figure 5**). At day 365, however, the mean titer of the VL controls was significantly lower than that of PKDL and VLR indicating that the rK39 antibody titer at 1 year could be used to identify cured VL cases at risk for PKDL/VLR (**Table 3** and **Figure 5**). ROC analysis showed that on day 365 an rK39 antibody titer of ≥1,400,000 predicts development of PKDL with

TABLE 3 | Comparison of mean serum rK39AB titer (95% CI) different groups at different time points.

Time	TF (*N* = 7) (95% CI)	VLR (*N* = 10) (95% CI)	PKDL (*N* = 32) (95% CI)	VL control (*N* = 38) (95% CI)
Baseline	399,461[@] (306,173–492,749)	878,968[#] (666,143–1,091,794)	1,558,044 (1,497,948–1,618,139)	1,456,777 (1,323,891–1,589,664)
Day 30	294,483[@] (154,558–434,408)	1,103,701[&] (879,257–1,328,145)	1,516,932 (1,433,444–1,600,421)	1,400,044 (1,250,620–1,549,467)
Day 180	426,072[@] (319,139–533,006)	1,256,668 (858,581–1,654,754)	1,299,201 (1,129,658–1,468,745)	1,039,447 (853,583–1,225,312)
Day 365	619,544[@@] (224,207–1,014,880)	1,516,307 (1,370,435–1,662,180)	1,370,186** (1,205,538–1,534,834)	935,618 (777,604–1,093,632)

*[@]p < 0.01 compared to all other groups; [#]p < 0.001 compared to PKDL and Control; [&]p < 0.001 compared to PKDL; [@@]p = 0.001 compared to VLR & PKDL; **p = 0.001 compared to control.*

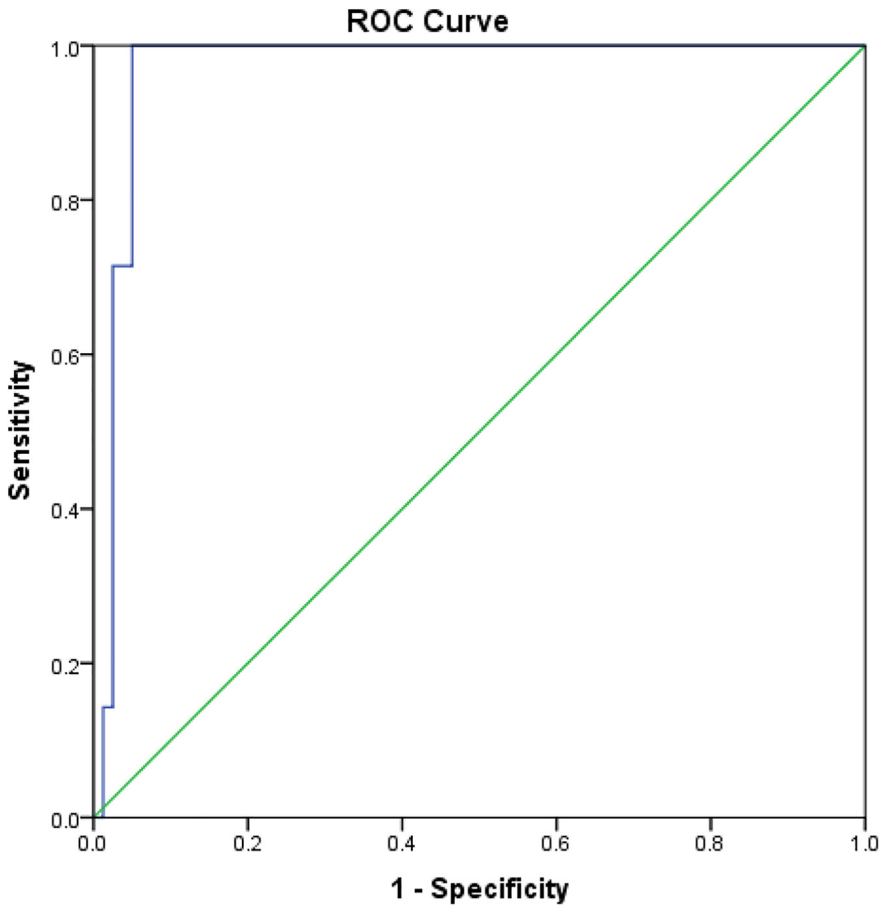

FIGURE 4 | Receiver operating characteristic for prediction of VL patients with subsequent treatment failure.

a sensitivity of 70% and specificity of 85% (**Figure 6**). A rK39 antibody titer ≥1,518,584 predicts VLR with a sensitivity and specificity of 60 and 87%, and a titer of ≥1,455,535 predicts PKDL/VLR with a sensitivity and specificity of 67 and 86%, respectively. Regarding the rK39 RDT, all patients remained positive at day 180, while at day 365, 57% (4/7), 100% (10/10), 94% (30/32), and 84% (32/38), respectively with TF, VLR, PKDL, and VL control were still positive by rK39 RDT.

DISCUSSION

There are several important observations made in this study. High levels of serum antibodies to rK39 could help predict which asymptomatic individuals will progress to VL. Determining antibody levels to rK39 could also predict TFs and relapse in treated VL patients. Interestingly, low serum antibody titers to rK39 were found to be associated with TF. Our study also revealed that the majority of VL patients remained positive by the rK39 RDT for a long time after successful treatment, whereas this was variable in case of asymptomatic *L. donovani* infections. The study also quantifies risks of subjects being potential sources of transmission: about 8% of asymptomatic infections progressed to symptomatic VL, and when treated about 17% of these, either did not respond, relapsed or developed PKDL.

There are several published cohort studies that have assessed risk factors for asymptomatic *L. donovani* infection progressing to VL and long-term risk of treated VL patients for PKDL and relapse (Gasim et al., 2000; Hasker et al., 2014; Chakravarty et al., 2019). A recent study from India found that higher titers in direct agglutination test (DAT) and rK39 evaluations were associated with higher odds for progression to VL (Hasker et al., 2014; Chakravarty et al., 2019). This study corroborates previous findings of a strong association between high rK39 antibody titers and subsequent progression to disease from an asymptomatic state (Hasker et al., 2014; Chakravarty et al., 2019). Furthermore, this study substantiates the previous findings on the prognostic value of rK39 antibody toward development of RVL and/or PKDL following the treatment for VL (Singh et al., 1995, 2002; Houghton et al., 1998; Kumar et al., 2001). This is however, the first study to explore the predictive value of rK39 antibody titers for developing PKDL and VLR after successful VL treatment, and the first to provide evidence of lower rK39 antibody titers associated with VL TF.

Achieving the KEP target of less than 1 VL case per 10,000 inhabitants at the upazila level in Bangladesh may

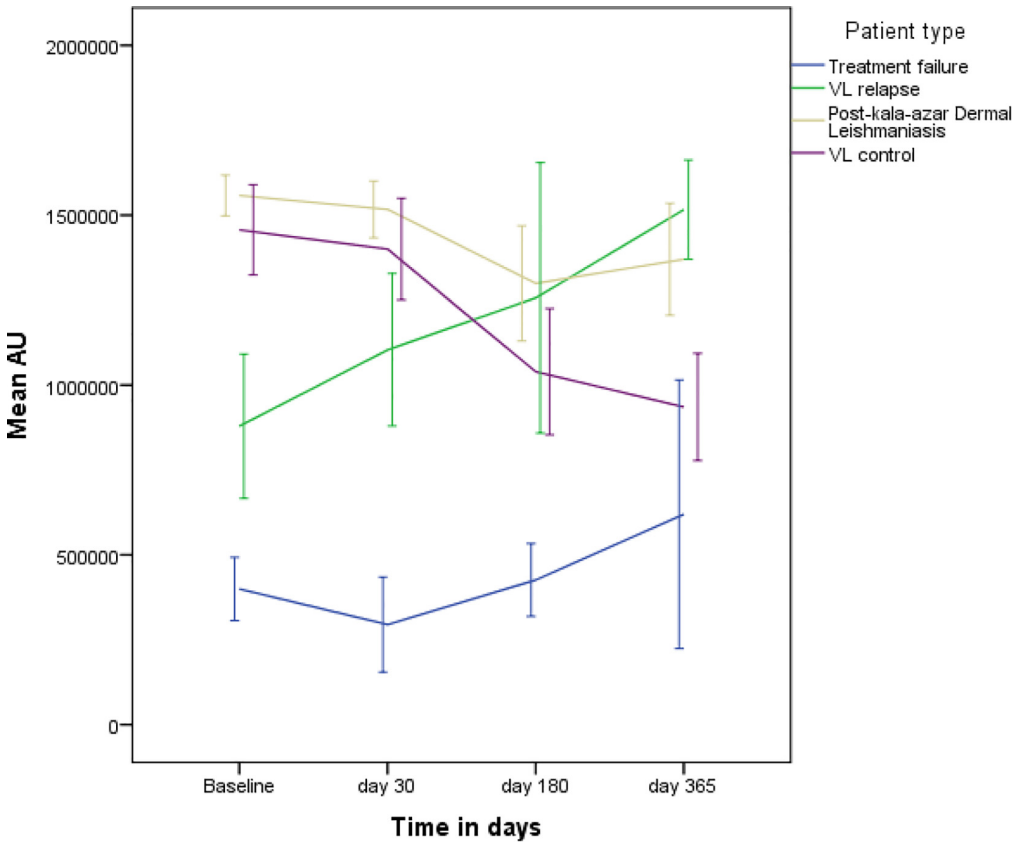

FIGURE 5 | Dynamics of serum rK39AB titer of TF, VLR, PKDL, and VL controls.

not be enough to ensure long-term sustainability. Evidence collected through this and other studies highlights the risks of continuing transmission and potential resurgence of the disease. Unfortunately, we do not have the right intervention tools to aim for zero transmission. Key to this is the ability to identify early LD-infected individuals who can potentially transmit, including asymptomatic cases likely to develop symptomatic VL, PKDL, and VL treatment relapses. Although there is no treatment regimen for asymptomatic infections, the high antibody titer could serve as a biomarker for periodic follow-up of such latent cases. Mathematical models show that early diagnosis of VL is important to eliminate the disease in line with the WHO recommendations for prompt effective treatment to curtail transmission and improve treatment outcome (WHO, 2010; Medley et al., 2015; Welay et al., 2017; Le Rutte et al., 2018). An individual's poor prognosis is sometimes linked to other variables such as age or low platelet count (Braga et al., 2013). Our study findings could provide valuable direction to adapt such mathematical models to explore the importance of early diagnosis of PKDL and VLR as well in restricting parasite transmission. Noteworthy, we recently showed that PKDL and VLR cases are potential reservoirs for transmission of infection (Mondal et al., 2018). A second generation rK39 rapid test based on validated cutoff titer(s) to identify progression to VL and early detection of VLR and PKDL now appears to be required.

Our findings regarding VL patients at risk for TF are interesting since our data suggest that a low rK39 antibody titer was associated with TF. This could imply a weakened immune response in these patients to the infection due to immune-suppression from a high parasite burden or malnutrition of the host. Though we did not find significant differences between groups regarding their body mass index, the TF group had statistically significantly lower hemoglobin levels compared to VL cured controls indicating a potential micronutrient deficiency. Anti-leishmanial drugs including liposomal amphotericin B have immunostimulatory effects in addition to parasiticidal effects that is dose-dependent (Murray, 2001). Immunosuppression in the TF group could explain why these VL patients failed to respond to a standard single dose of 10 mg/kg, but they did response to a total dose of 15 mg/kg AmBisome divided into three treatments. Additional studies are required to confirm immune-suppression and TF.

The present study has some limitations. One is the small sample size in each group. Nevertheless, it provides very useful information for a new window of opportunity for early detection of TFs, relapses and PKDL based on quantitative measurement of rK39 antibody levels. Furthermore, we used only a serological biomarker, which is dependent on many factors including individual's immune response, nutrition and genetic factors. Detecting the presence of the parasite including nucleic acids,

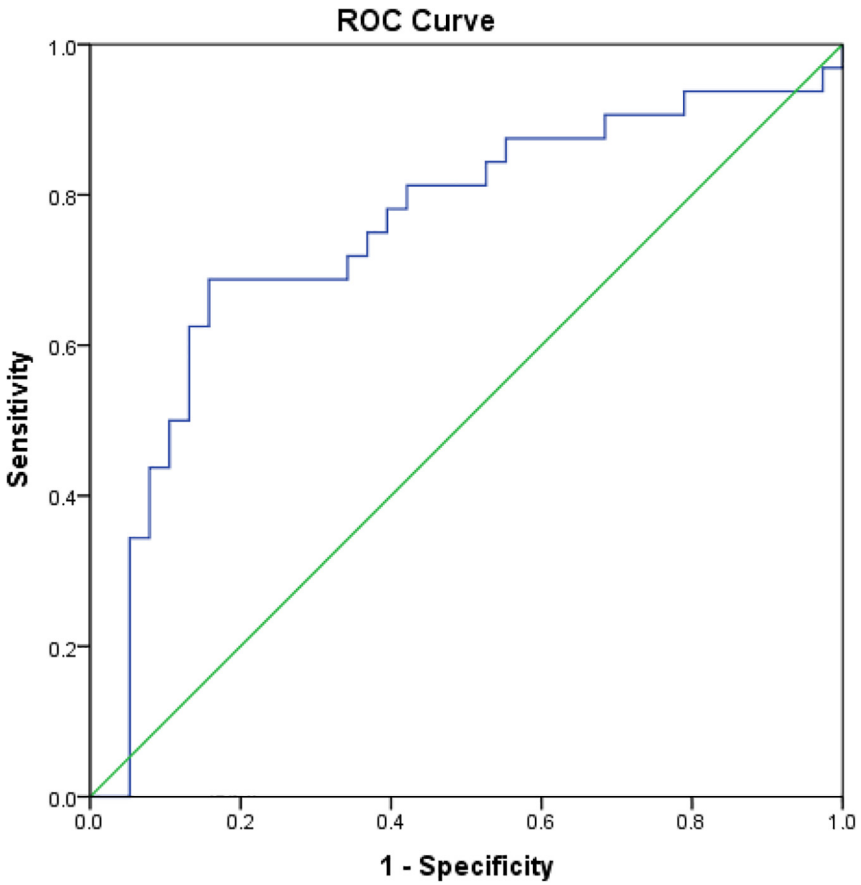

FIGURE 6 | Receiver operating characteristic curve for cutoff of rK39 AB titer at 365 day since treatment for prediction of cured VL at risk for PKDL within subsequent 24 months.

metabolites and antigens may also represent bona-fide predictors of infection/disease outcome. However, such signature particles from LD parasite are yet to be validated, some of them even for diagnostic purposes. In our previous study we demonstrated the applicability of qPCR as a mean for both detection and quantification of parasite DNA to allow treatment monitoring of VL and PKDL patients (Hossain et al., 2017). Recently, Moulik et al. (2017) reported that parasite kDNA could be used as the promising bio-marker for the prognosis of PKDL patients. Full investigation of parasite kinetics (parasite load) through longitudinal studies is still required to validate this strategy before large scale application.

Another issue is the case definition of "asymptomatic cases" for which there is no clear consensus. Different methods exist to determine *Leishmania* infection status including *Leishmania* specific antibody, antigen, nucleic acid detection or markers of cellular immunity in combination with a clinical assessment of symptoms. According to previous studies, asymptomatically infected persons could be defined as those with no clinical signs or symptoms of VL but are positive in at least one marker of infection including the Leishmanin Skin Test (LST), DAT, rK39 antibody ELISA, IFAT or qualitative/quantitative PCR to detect *Leishmania* DNA (Chakravarty et al., 2019). Most previous studies, including this study, have used the rK39 antibody ELISA/RDT as the biomarker because it has been widely validated as a diagnostic test. Finally, we performed a semi-quantitative ELISA for measuring antibody titer, while a quantitative ELISA could bolster the study findings.

CONCLUSION

Quantification of rK39 antibody serum levels could represent an important biomarker for predicting which asymptomatic cases will progress to VL and further could help to predict VL treatment failure, relapse and evolution to PKDL. Validation studies are required through a larger prospective field study. More research involving parasite-specific biomarkers is required to develop better diagnostic and prognostic tools for VL, and facilitate completion of the VL elimination agenda.

DATA AVAILABILITY STATEMENT

The datasets generated for this study are available on request to the corresponding author.

ETHICS STATEMENT

The studies involving human participants were reviewed and approved by IRB ICDDR,B. Written informed consent was obtained from the participants and for minors, consent was obtained from the parents or legal guardians.

AUTHOR CONTRIBUTIONS

DM, PG, CH, PO, JR-P, MD, GM, AK, and DA conceived and designed the study. PG, RC, FH, MK, AA, and RN performed the experiments and maintained the data source. DM, AA, PG, and PO performed the statistical analysis. DM, CH, JR-P, MD, AK, GM, DA, and PO drafted the manuscript. All authors read and approved the final version of the manuscript.

FUNDING

We are grateful to the Bill & Melinda Gates Foundation (GCE round 2) and TDR & WHO/NTD for financial support for respectively study 1 and study 2. We highly appreciate financial support from the TDR for this study. The publication fee was supported by Bill & Melinda Gates Foundation (BMGF).

ACKNOWLEDGMENTS

We are thankful to our study participants and all members of the Parasitology laboratory, ICDDR,B. We highly appreciate the unrestricted support from the ICDDR,B and its core donors.

REFERENCES

Addy, M., and Nandy, A. (1992). Ten years of kala-azar in west Bengal, Part I. Did post-kala-azar dermal *Leishmaniasis* initiate the outbreak in 24-Parganas? *Bull. World Health Organ.* 70, 341–346.

Ahmed, B. N., Nabi, S. G., Rahman, M., Selim, S., Bashar, A., Rashid, M. M., et al. (2014). Kala-azar (visceral *Leishmaniasis*) elimination in Bangladesh: successes and challenges. *Curr. Infect. Dis. Rep.* 1, 163–169. doi: 10.1007/s40475-014-0027-6

Basher, A., Nath, P., Nabi, S. G., Selim, S., Rahman, M. F., Sutradhar, S. R., et al. (2015). A study on health seeking behaviors of patients of post-kala-azar dermal *Leishmaniasis*. *Biomed. Res. Int.* 2015:314543. doi: 10.1155/2015/31454

Bern, C., and Chowdhury, R. (2006). The epidemiology of visceral *Leishmaniasis* in Bangladesh: prospects for improved control. *Indian J. Med. Res.* 123, 275–288.

Braga, A. S., Toledo Junior, A. C., and Rabello, A. (2013). Factors of poor prognosis of visceral *Leishmaniasis* among children under 12 years of age. a retrospective monocentric study in Belo Horizonte, state of Minas Gerais, Brazil, 2001-2005. *Rev. Soc. Bras. Med. Trop.* 46, 55–59. doi: 10.1590/0037-868216432013

Chakravarty, J., Hasker, E., Kansal, S., Singh, O. P., Malaviya, P., Singh, A. K., et al. (2019). Determinants for progression from asymptomatic infection to symptomatic visceral *Leishmaniasis*: a cohort study. *PLoS Negl. Trop. Dis.* 13:e0007216. doi: 10.1371/journal.pntd.0007216

Chapman, L. A., Dyson, L., Courtenay, O., Chowdhury, R., Bern, C., Medley, G. F., et al. (2015). Quantification of the natural history of visceral *Leishmaniasis* and consequences for control. *Parasit. Vectors* 8:521. doi: 10.1186/s13071-015-1136-3

Chappuis, F., Sundar, S., Hailu, A., Ghalib, H., Rijal, S., Peeling, R. W., et al. (2007). Visceral *Leishmaniasis*: what are the needs for diagnosis, treatment and control? *Nat. Rev. Microbiol.* 5, 873–882. doi: 10.1038/nrmicro1748

dos Santos, P. L., de Oliveira, F. A., Santos, M. L., Cunha, L. C., Lino, M. T., de Oliveira, M. F., et al. (2016). The severity of visceral *Leishmaniasis* correlates with elevated levels of serum IL-6, IL-27 and sCD14. *PLoS Negl. Trop. Dis.* 10:e0004375. doi: 10.1371/journal.pntd.0004375

Gasim, S., Elhassan, A. M., Kharazmi, A., Khalil, E. A., Ismail, A., and Theander, T. G. (2000). The development of post-kala-azar dermal *Leishmaniasis* (PKDL) is associated with acquisition of Leishmania reactivity by peripheral blood mononuclear cells (PBMC). *Clin. Exp. Immunol.* 119, 523–529. doi: 10.1046/j.1365-2249.2000.01163.x

Ghosh, P., Bhaskar, K. R., Hossain, F., Khan, M. A., Vallur, A. C., Duthie, M. S., et al. (2016). Evaluation of diagnostic performance of rK28 ELISA using urine for diagnosis of visceral *Leishmaniasis*. *Parasit. Vectors* 9:383. doi: 10.1186/s13071-016-1667-2

Hasker, E., Malaviya, P., Gidwani, K., Picado, A., Ostyn, B., Kansal, S., et al. (2014). Strong association between serological status and probability of progression to clinical visceral *Leishmaniasis* in prospective cohort studies in India and Nepal. *PLoS Negl. Trop. Dis.* 8:e2657. doi: 10.1371/journal.pntd.0002657

Hossain, F., Ghosh, P., Khan, M. A., Duthie, M. S., Vallur, A. C., Picone, A., et al. (2017). Real-time PCR in detection and quantitation of *Leishmania* donovani for the diagnosis of visceral *Leishmaniasis* patients and the monitoring of their response to treatment. *PloS one* 12:e0185606. doi: 10.1371/journal.pone.0185606

Houghton, R. L., Petrescu, M., Benson, D. R., Skeiky, Y. A., Scalone, A., Badaró, R., et al. (1998). A cloned antigen (recombinant K39) of *Leishmania* chagasi diagnostic for visceral *Leishmaniasis* in human immunodeficiency virus type 1 patients and a prognostic indicator for monitoring patients undergoing drug therapy. *J. Infect. Dis.* 177, 1339–1344. doi: 10.1086/515289

Kumar, R., Pai, K., Pathak, K., and Sundar, S. (2001). Enzyme-linked immunosorbent assay for recombinant K39 antigen in diagnosis and prognosis of Indian visceral *Leishmaniasis*. *Clin. Diagn. Lab. Immunol.* 8, 1220–1224. doi: 10.1128/cdli.8.6.1220-1224.2001

Le Rutte, E. A., Chapman, L. A., Coffeng, L. E., Ruiz-Postigo, J. A., Olliaro, P. L., Adams, E. R., et al. (2018). Policy recommendations from transmission modeling for the elimination of visceral *Leishmaniasis* in the Indian subcontinent. *Clin. Infect. Dis.* 66(Suppl._4), S301–S308. doi: 10.1016/j.epidem.2017.01.002

Medley, G. F., Hollingsworth, T. D., Olliaro, P. L., and Adams, E. R. (2015). Health-seeking behaviour, diagnostics and transmission dynamics in the control of visceral *Leishmaniasis* in the Indian subcontinent. *Nature* 528, S102–S108. doi: 10.1038/nature16042

Molina, R., Ghosh, D., Carrillo, E., Monnerat, S., Bern, C., Mondal, D., et al. (2017). Infectivity of post-kala-azar dermal *Leishmaniasis* patients to sand flies: revisiting a proof of concept in the context of the kala-azar elimination program in the Indian subcontinent. *Clin Infect. Dis.* 65, 150–153. doi: 10.1093/cid/cix245

Mollet, G., Bremer Hinckel, B. C., Bhattacharyya, T., Marlais, T., Singh, O. P., Mertens, P., et al. (2018). Detection of IgG1 against rK39 improves monitoring of treatment outcome in visceral *Leishmaniasis*. *Clin. Infect. Dis.* 69, 1130–1135. doi: 10.1093/cid/ciy1062

Mondal, D., Alvar, J., Hasnain, M. G., Hossain, M. S., Ghosh, D., Huda, M. M., et al. (2014). Efficacy and safety of single-dose liposomal amphotericin B for visceral *Leishmaniasis* in a rural public hospital in Bangladesh: a feasibility study. *Lancet Glob. Health.* 2, e51–e57. doi: 10.1016/S2214-109X(13)70118-9

Mondal, D., Bern, C., Ghosh, D., Rashid, M., Molina, R., Chowdhury, R., et al. (2018). Quantifying the infectiousness of post-kala-azar dermal *Leishmaniasis* towards sandflies. *Clin Infect. Dis.* 69, 251–258. doi: 10.1093/cid/ciy891

Mondal, D., Kumar, A., Sharma, A., Ahmed, M. M., Hasnain, M. G., Alim, A., et al. (2019). Relationship between treatment regimens for visceral *Leishmaniasis* and development of postkala-azar dermal *Leishmaniasis* and visceral *Leishmaniasis* relapse: a cohort study from Bangladesh. *PLoS.Negl. Trop. Dis* 13:e0007653. doi: 10.1371/journal.pntd.0007653

Mondal, D., Singh, S. P., Kumar, N., Joshi, A., Sundar, S., Das, P., et al. (2009). Visceral *Leishmaniasis* elimination programme in India, Bangladesh, and Nepal: reshaping the case finding/case management strategy. *PLoS Negl. Trop. Dis.* 3:e355. doi: 10.1371/journal.pntd.0000355

Moulik, S., Chaudhuri, S. J., Sardar, B., Ghosh, M., Saha, B., Das, N. K., et al. (2017). Monitoring of parasite kinetics in Indian post–kala-azar dermal *Leishmaniasis*. *Clinl. Infect. Dis.* 66, 404–410. doi: 10.1093/cid/cix808

Mukhopadhyay, D., Dalton, J. E., Kaye, P. M., and Chatterjee, M. (2014). Post kala-azar dermal *Leishmaniasis*: an unresolved mystery. *Trends parasitol.*. 30, 65–74. doi: 10.1016/j.pt.2013.12.004

Murray, H. W. (2001). Clinical and experimental advances in treatment of visceral *Leishmaniasis*. *Antimicrob. Agents Chemother.* 45, 2185–2197. doi: 10.1128/AAC.45.8.2185-2197.2001

Rahman, K. M., Islam, S., Rahman, M. W., Kenah, E., Galive, C. M., Zahid, M. M., et al. (2010). Increasing incidence of post-kala-azar dermal *Leishmaniasis* in a population-based study in Bangladesh. *Clinl. Infect. Dis.* 50, 73–76. doi: 10.1086/648727

Singh, S., Gilman-Sachs, A., Chang, K. P., and Reed, S. G. (1995). Diagnostic and prognostic value of K39 recombinant antigen in Indian *Leishmaniasis*. *J. Parasitol.* 81, 1000–1003.

Singh, S., Kumari, V., and Singh, N. (2002). Predicting kala-azar disease manifestations in asymptomatic patients with latent *Leishmania* donovani infection by detection of antibody against recombinant K39 antigen. *Clin. Diagn. Lab. Immunol.* 9, 568–572. doi: 10.1128/cdli.9.3.568-572.2002

Vaish, M., Sharma, S., Chakravarty, J., and Sundar, S. (2012). Evaluation of two novel rapid rKE16 antigen-based tests for diagnosis of visceral *Leishmaniasis* in India. *J. Clinl. Microbiol.* 50, 3091–3092. doi: 10.1128/JCM.00475-12

Welay, G. M., Alene, K. A., and Dachew, B. A. (2017). Visceral *Leishmaniasis* treatment outcome and its determinants in northwest Ethiopia. *Epidemiol. Health* 39, e2017001. doi: 10.4178/epih.e2017001

WHO (2010). *Cot Leishmaniases: Report of a Meeting of the WHO Expert Committee on the Control of Leishmaniases*. WHO Technical Report Series No. 949. Geneva: WHO.

World Health and Organization (2005). *Regional Strategic Framework for Elimination of Kala-Azar from the South-East Asia region (2005–2015)*. New Delhi: WHO Regional Office for South-East Asia.

Zijlstra, E. E., Musa, A. M., Khalil, E. A., El Hassan, I. M., and El-Hassan, A. M. (2003). Post-kala-azar dermal *Leishmaniasis*. *Lancet. Infect. Dis.* 3, 87–98. doi: 10.1016/S1473-3099(03)00517-6

Disclaimer: The authors alone are responsible for the views expressed in this article and they do not necessarily represent the views, decisions or policies of the institutions with which they are affiliated.

Conflict of Interest: The authors declare that the research was conducted in the absence of any commercial or financial relationships that could be construed as a potential conflict of interest.

frontiers in Microbiology

ORIGINAL RESEARCH
published: 23 October 2019
doi: 10.3389/fmicb.2019.02381

Differential Culturability of *Mycobacterium tuberculosis* in Culture-Negative Sputum of Patients With Pulmonary Tuberculosis and in a Simulated Model of Dormancy

Azger Dusthackeer[1], Magizhaveni Balasubramanian[1], Govindarajan Shanmugam[1], Shanmuga Priya[2], Christy Rosaline Nirmal[1], Rajadas Sam Ebenezer[1], Angayarkanni Balasubramanian[1], Rajesh Kumar Mondal[1], Kannan Thiruvenkadam[1], A. K. Hemanth Kumar[1], Geetha Ramachandran[1] and Selvakumar Subbian[3]**

[1] National Institute for Research in Tuberculosis, Chennai, India, [2] National Institute of Epidemiology, Chennai, India, [3] Public Health Research Institute, New Jersey Medical School, Rutgers University, Newark, NJ, United States

Tuberculosis (TB) remains a leading killer among infectious diseases of humans worldwide. Delayed diagnosis is a crucial problem in global TB control programs. Bacteriological methods currently used to diagnose TB in endemic countries take up to 8 weeks, which poses a significant delay in starting antibiotic therapy. The presence of a heterogeneous population of *Mycobacterium tuberculosis*, the causative agent of TB, is among the reasons for delayed diagnosis by bacteriological methods. Previously, it has been shown that mycobacterial resuscitation-promoting factors (RPFs), a family of proteins secreted by actively growing bacteria into the media, are capable of activating the growth of dormant bacteria, thus enhancing the detection of bacilli in the sputum of confirmed TB cases. However, the variability in bacterial resuscitation by RPF in the sputum of suspected pulmonary TB cases that showed differential smear and/or culture positivity during diagnosis has not been fully explored. Here, we report the presence of non-replicating bacteria in the sputum of suspected TB cases that show differential growth response to RPF treatment. Using crude and recombinant RPF treatment, we show improved sensitivity and reduced time to detect bacilli in the sputum samples of smear-positive/culture-negative or smear-negative/culture-negative cases. We also report the phenotypic heterogeneity in the RPF responsiveness among Mtb strains using an *in vitro* dormancy model. Our findings have implications for improving the bacteriological diagnostic modalities currently used to diagnose TB in endemic countries.

Keywords: tuberculosis, bacteriological diagnosis, resuscitation, *Mycobacteirum tuberculosis*, clinical isolate organism, sputum samples, dormancy

OPEN ACCESS

Edited by:
Aleksandra Barac,
University of Belgrade, Serbia

Reviewed by:
Jann-Yuan Wang,
National Taiwan University Hospital, Taiwan
Willy Ssengooba,
Makerere University, Uganda
Margarita Shleeva,
A N Bach Institute of Biochemistry (RAS), Russia

****Correspondence:***
Azger Dusthackeer
azgar_007@hotmail.com;
azger@nirt.res.in
Selvakumar Subbian
subbiase@njms.rutgers.edu

Specialty section:
This article was submitted to Infectious Diseases, a section of the journal Frontiers in Microbiology

Received: *19 August 2019*
Accepted: *01 October 2019*
Published: *23 October 2019*

Citation:
Dusthackeer A, Balasubramanian M, Shanmugam G, Priya S, Nirmal CR, Sam Ebenezer R, Balasubramanian A, Mondal RK, Thiruvenkadam K, Hemanth Kumar AK, Ramachandran G and Subbian S (2019) Differential Culturability of Mycobacterium tuberculosis in Culture-Negative Sputum of Patients With Pulmonary Tuberculosis and in a Simulated Model of Dormancy. Front. Microbiol. 10:2381. doi: 10.3389/fmicb.2019.02381

INTRODUCTION

Tuberculosis (TB) caused by *Mycobacterium tuberculosis* (Mtb) is a leading killer among infectious diseases that accounts for 1.5 million deaths and about 10 million new cases worldwide in 2017. Nearly 1.7 billion (23%) of the global population have been estimated to harbor asymptomatic latent Mtb infection (LTBI)[1]. One of the key characteristics that make Mtb a successful intracellular pathogen is its ability to survive amid various stresses, including hypoxia, reactive oxygen, and nitrogen species (ROS and RNS) and nutrition starvation that prevails in the infected host (Voskuil et al., 2011). Besides, Mtb can establish a non-replicating dormancy state and persist in host tissues for prolonged periods without causing symptomatic disease (Gomez and McKinney, 2004; Gengenbacher and Kaufmann, 2012). Importantly, individuals with LTBI, harboring quiescent Mtb population, can resume active bacterial growth to develop symptomatic TB if/when the host immunity wanes (Magombedze et al., 2013; Peddireddy et al., 2017). However, the host and bacterial factors responsible for reactivation of dormant Mtb upon immune-suppressing host conditions are not fully understood.

The efficiency of the standard multidrug antibiotic regimen currently used for TB treatment is closely linked with the nature of Mtb in the infected host. Clinical and experimental studies have demonstrated the presence of various Mtb phenotypes to co-exist in the same sample than it was previously thought (Mukamolova et al., 2010; Ayrapetyan et al., 2015). While actively replicating bacilli are killed rapidly and effectively by first-line drugs such as isoniazid, the dormant form of Mtb is seldom eliminated by the current antibiotic regimen (Deb et al., 2009). The presence of dormant bacilli that are resilient to killing by antibiotics is one of the reasons for the prolonged duration (minimum of 6 months) of current treatment (Zhang, 2004). The ability of dormant Mtb to persist in a non-replicating state that is phenotypically tolerant to drugs is also a significant impediment in the diagnosis and treatment of LTBI cases; at present, there are no growth-based tests available to measure the burden of dormant bacilli in clinical samples (Cardona and Ruiz-Manzano, 2004). Although the presence of dormant, non-replicating bacteria has been shown in the sputum of patients with active pulmonary TB that showed positive culture results, these bacillary populations do not grow well on standard agar media used for diagnosis. Moreover, little is known about the physiology and phenotypic nature of Mtb persisting during LTBI *in vivo*.

Resuscitation-promoting factors (RPFs), a group of five proteins (Rpf A–E) secreted by actively replicating virulent Mtb into the culture media, have been demonstrated to reactive at growth of dormant bacteria *in vitro* and in the sputum of patients with TB (Gupta and Srivastava, 2012). Although sputum has traditionally been thought to contain exclusively actively replicating Mtb, bacterial transcript analyses disprove this notion (Garton et al., 2008). For example, Mukamolova et al. (2010) have shown that smear-positive sputum samples from TB patients are dominated by the presence of Mtb that is mostly non-cultivable by conventional, standard bacteriological methods used in diagnostic settings. Recently, Kana et al. have shown the presence of differentially cultivable tubercle bacilli (DCTB) in the sputum of culture-positive pulmonary TB patients. These samples had bacteria that showed heterogeneity in their response to treatment with RPF-containing culture filtrate (Chengalroyen et al., 2016).

Moreover, the RPF dependency of Mtb was lost after the bacteria were isolated from the patient sputum. Interestingly, during TB chemotherapy, the proportion of RPF-dependent Mtb increased relative to the actively growing bacterial population that form colonies on standard growth media (Mukamolova et al., 2010). Thus, change in the number of non-cultivable Mtb during and at the end of chemotherapy depends on the ability of this population to become dormant (Nathan and Barry, 2015). These findings suggest that the sensitivity of existing culture-based techniques to detect Mtb in pulmonary samples can be considerably improved with RPF treatment. However, the ability of RPF-containing media to resuscitate Mtb in the sputum samples of suspected TB cases that are smear-positive and culture-negative or smear and culture-negative status remains unclear. This insufficiency in current bacteriological tools to efficiently diagnose cases with subclinical and incipient forms of TB has a high impact on global TB elimination goals, since they pose additional challenges on diagnosis and treatment, compared to smear- and/or culture-positive cases (Garcia-Basteiro et al., 2019).

Previously, using a diagnostic luciferase reporter phage assay that can detect non-replicating bacilli in patient sputum, we have identified 30 additional positives samples, which failed to grow on standard Lowenstein–Jensen (LJ) agar medium (Dusthackeer et al., 2012). The presence of viable bacilli in these samples was confirmed by reverse transcriptase-PCR for the *Mtb* 16S rRNA gene, indicating that either the improved sensitivity of the assay to detect actively growing bacilli or its ability to detect non-replicating persistor bacilli ultimately increased the diagnostic potential of culture-based assays. In this study, we provide more evidence for the presence of non-replicating persistors in the sputum specimen of suspected TB cases that showed negative result in the conventional microbiological diagnosis. Using RPF-containing culture filtrates of Mtb to treat sputum samples of suspected TB cases, we have improved the sensitivity and rapidity of standard culture-based diagnosis. We also report the phenotypic heterogeneity in RPF-responsive Mtb *in vitro* using Wayne's dormancy model.

MATERIALS AND METHODS

Clinical Specimen and Ethics Statement

Previous studies have evaluated the presence of RPF-dependent Mtb in smear and/or culture-positive sputum samples from active TB patients (Mukamolova et al., 2010; Chengalroyen et al., 2016). In our study, we wanted to investigate the

[1]https://www.who.int/tb/publications/factsheets/en/

presence of RPF-dependent Mtb in suspected TB cases from local patients in TB-endemic South Indian region (Chennai; coordinates: 13.04°N 80.17°E). The sputum samples from these patients varied in their microbiologic diagnosis (i.e., smear-positive/culture-negative, smear-negative/culture-negative, and smear-positive/culture-positive). A total of 421 sputum specimens, collected from consecutive adult patients (two samples per patient, see below) suspected of TB were used in this study. Of these, 251 were smear- and culture-negative, 17 were smear-negative but culture-positive, 55 were smear- and culture-positive, and 98 were smear-positive but culture-negative (**Supplementary Figure S1**). Sputum samples were collected at the baseline (minimum of 5 ml, before the start of treatment) from suspected TB patients. These patients were newly diagnosed of suspected TB and were about to start their standard antibiotic therapy. All sputum samples were collected in a routine clinical setting at the National Institute for Research on Tuberculosis. Expectorated sputum samples were collected using standardized procedures and processed in a microbiology laboratory under sterile conditions. No follow-up sputum samples were collected from these patients.

From each patient, two sputum samples were collected; one collected at home and the other collected at the clinic. Both samples were separately processed by modified Petroff's method, as mentioned in the manuscript. There was no discrepancy in the results, such as smear positivity rating or culture results obtained between these two sputum samples for any of the patients. We used the sputum collected in the clinic for consistency in collection and processing methodology between patients. The sterility of the collection container and proper collection of samples were ensured by medical personnel. The sputum samples were stored at −80°C until further processing. Sputum samples were processed by modified Petroff's method, and smear positivity was assessed by sputum microscopy using auramine phenol staining (Verma et al., 2013; Datta et al., 2019). The total sample size was estimated at 5% level of the significance at 80% power with the design effect of two. Also, the 10% error rate was added to compensate for the follow-up/estimation error. Informed consent was obtained from the patients, and the Institutional Ethical Committee of the National Institute for Research on Tuberculosis, a body of Indian Council of Medical Research approved the sample collection and downstream application procedures.

Bacterial Strains

Strains of *M. tuberculosis* (H37Rv, H37Ra, Erdman, DRBL2, MTB01, MTB02), *Mycobacterium smegmatis*, and *Escherichia coli* DH5α were grown and maintained as per standard procedures in LJ slants, Middlebrook 7H9 broth, and Middlebrook 7H11 agar media supplemented with oleic acid dextrose and catalase enrichment (OADC) (BD Biosciences) and glycerol or in Luria-Bertani (LB) media (for *E. coli*)[2]. In all the experiments, bacterial cultures at the mid-log phase (OD_{600} = 0.6) were used unless stated otherwise.

[2]http://www.nirt.res.in/pdf/bact/SOP.pdf

Preparation of Crude RPF Containing Media

Crude RPF-containing culture filtrate from bacterial cultures was prepared as described previously (Kana et al., 2008). Briefly, wild type and laboratory strains of *M. tuberculosis* and *M. smegmatis* were grown in Middlebrook 7H9 media supplemented with OADC and *E. coli* were grown in LB media to an OD_{600} = 0.4. Bacterial cultures were centrifuged at 12,000 × *g* for 20 min at 10°C, and the supernatant was filtered through a 0.2-μm membrane filter and immediately diluted with an equal volume of 7H9 broth. The bacterial cultures were treated with RPF protein at a 1:10 ratio. The culture was plated on Middlebrook 7H11 agar media. At 7 days post-treatment, the colony-forming units (CFU) were enumerated.

Effect of RPF on Culture Sensitivity

The impact of RPF in increasing the sensitivity of Mtb detection and the presence of non-replicating persistors was tested on the sputum samples of suspected TB patients. A total of 268 samples, including smear/culture-negative (n = 251) and smear-negative/culture-positive (n = 17) sputum samples, were used to determine the presence of resuscitable Mtb (RCs). Bacterial growth induction was confirmed by both the increase in the optical density (OD_{600}) of broth culture and growth of RC on Middlebrook 7H11 agar plates. The results for each sample were compared to their corresponding diagnostic smear and/or culture status from the clinic.

One set of processed sputum sediment of 0.9 ml from smear-positive, culture-negative patients was treated with 0.1 ml of RPF for the resuscitation of Mtb and inoculated onto LJ slants, incubated at 37°C, and observed at 7-day intervals for the appearance of Mtb colonies for 8 weeks. Control samples were treated with sterile 7H9 broth, plated on LJ slants, and kept at similar growth conditions as above. For liquid culture, the minimum probable number (MPN) assay was used as described previously (Chengalroyen et al., 2016). Briefly, smear-negative and culture-negative sputum specimens were treated with crude RPF at 1:9 ratio and incubated at 37°C for 4 weeks. Another aliquot of the same sample was treated with sterile 7H9 broth as a control. Bacterial growth was measured by an increase in OD_{600} at every 24 h using a spectrophotometer. The possibility of contamination of the cultures was screened by spotting 5 μl of the culture onto Brain Heart Infusion agar plates. The presence of non-replicating persistors and their sensitivity to antibiotics were determined by comparing the number of bacterial CFU between RPF-treated and untreated samples.

Effect of RPF on Time to Detect (TTD) Mtb in Clinical Samples

To test whether RPF can reduce the TTD Mtb, we analyzed 55 smear- and culture-positive sputum specimens. The sputum-smear gradation of smear-positive/culture-positive samples used to evaluate TTD Mtb is presented in **Supplementary Table S1**. Each sputum sample was divided into two aliquots and treated with either crude RPF or sterile 7H9 broth, respectively, and plated on 7H11 agar media as described above. The plates were

observed periodically for 8 weeks for bacterial growth, and the difference in the time taken for the appearance of Mtb colonies was recorded in each case.

Comparative Assessment of Resuscitation Potential of Crude and Recombinant RPF

Recombinant RPF (rRPF) protein from Mtb that was heterologously expressed using an *E. coli* system was a kind gift from Tom H. Ottenhoff of Leiden University Medical Center, Netherlands (Commandeur et al., 2011). The rRPF contains RPF-A (Rv0867c) and RPF-D (Rv2389c) proteins. Details about the cloning and characterization of the rRPF proteins have been published previously (Commandeur et al., 2011). These two RPFs (out of five) were selected since they showed the highest recognition by TB patient samples in a cross-sectional cohort study (Commandeur et al., 2011). The rRPF was transported under cold-chain conditions and stored at −20°C till further use. The efficiency of rRPF (10 pmol) in resuscitating dormant bacteria was compared with crude RPF extracted directly from the *Mtb* cultures. A total of 98 smear-positive, culture-negative samples were split into three aliquots, and each was treated with sterile 7H9 broth (control) or crude RPF or rRPF, respectively. Treated samples were inoculated onto LJ slants, incubated at 37°C, and observed till 8 weeks for Mtb colonies. The number of Mtb colonies and yield of positivity were noted and compared between the groups.

Effect of RPF on Mtb Dormancy *in vitro*

The potential of RPF in resuscitating Mtb from dormancy to metabolically active form was tested using an *in vitro* anaerobic culture system developed by Wayne and Hayes (1996). In brief, two clinical Mtb isolates, MTB01 and MTB02, were inoculated at a final OD_{600} = 0.1 into 7H9 broth supplemented with OADC and glycerol in an airtight container and incubated at 37°C with very gentle stirring. As reported previously, at 45 days post-inoculation, a hypoxic, non-replicating persistent stage (NRP) was achieved under these conditions, as indicated by discoloration of methylene blue indicator (**Supplementary Figure S2**; Wayne and Hayes, 1996). At this state, Mtb adapts to a dormant phenotype. This state of metabolically inactive dormant condition was also confirmed by spotting the bacterial culture onto 7H11 agar media supplemented with OADC and glycerol. The quiescent bacterial cultures were treated with either sterile 7H9 broth (control) or crude RPF extracted from pathogenic Mtb (H37Rv, Erdmann), non-pathogenic mycobacteria (H37Ra, *M. smegmatis*), or *E. coli* DH5α as mentioned above. The culture exposed to RPF or control broth was serially diluted and spotted onto 7H11 agar plates, incubated at 37°C, and observed regularly for up to 8 weeks for the appearance of Mtb colonies.

Statistical Analysis

Statistical significance for pairwise comparisons was performed using paired Student's *t* test, and multiple comparisons were calculated by one-way ANOVA using GraphPad Prism. *P* value < 0.05 was considered statistically significant.

RESULTS

Crude RPF Increases the Sensitivity of Liquid Culture

In the agar plating method, among the crude RPF-treated samples, 20 out of 268 (7.5%) yielded bacterial CFU and were positive for RCs. These samples were previously classified as negative by conventional smear/culture-based diagnostic methods. Among these 20 samples that showed positive CFU with RPF, treatment with sterile 7H9 broth (placebo) resulted in Mtb CFU, and positive RCs for only five samples (25%) (**Figure 1A**). Thus, the treatment of smear/culture-negative sputum with crude RPF can improve case detection by about 75%. In addition, about 2% of smear/culture-negative sputum spontaneously reverts to bacterial growth, as shown in samples treated with placebo broth. Overall, crude RPF treatment resulted in nearly a four-fold higher number of positive case detection among smear/culture-negative sputum samples.

In the MPN assay that is based on bacterial growth in liquid media, a significant (P = 0.036) increase in the number of positive samples was noted between crude RPF-treated and placebo broth-treated samples (86 vs. 77 out of total 268 samples) (**Figure 1B**). We performed a linear regression analysis to determine the correlation significance between samples treated with RPF and 7H9 broth. As shown in **Figure 1C**, bacterial growth in samples treated with RPF was significantly high, compared to the same samples treated with 7H9 media (P = 0.0163), which clearly shows that RPF significantly induces bacterial growth (**Figure 1C**). The standard deviation from the average is low for RPF-treated, compared to 7H9-treated samples, which indicates the consistency of RPF in resuscitating Mtb in the sample. The culture positivity in both liquid and solid media was further confirmed by acid-fast staining, and microscopy.

Crude RPF Treatment Significantly Reduces the TTD Mtb in Clinical Specimens

The possibility of reducing the TTD Mtb in clinical specimens by using crude RPF treatment was tested in 55 smear- and culture-positive sputum samples. The average time taken for positive Mtb detection was 6.1 days for RPF-treated samples, compared to an average of about 9 days for the 7H9 broth (placebo)-treated samples ($P \leq 0.001$) (**Figure 2**). Therefore, treatment with crude RPF significantly reduced the TTD Mtb in the specimen as indicated by the appearance of colonies at least 3 days earlier than the placebo (7H9 media)-treated samples (**Supplementary Figure S3**).

Crude RPF Is More Potent Than rRPF in Reactivating Mtb Growth

Among 98 smear-positive/culture-negative samples tested, treatment with crude RPF yielded positivity in 24 specimens (24.5%), while 6 samples (6.1%) showed positive results for Mtb when treated with placebo broth and 13 samples (13.2%) showed positivity for Mtb after treatment with rRPF. Four out of the six

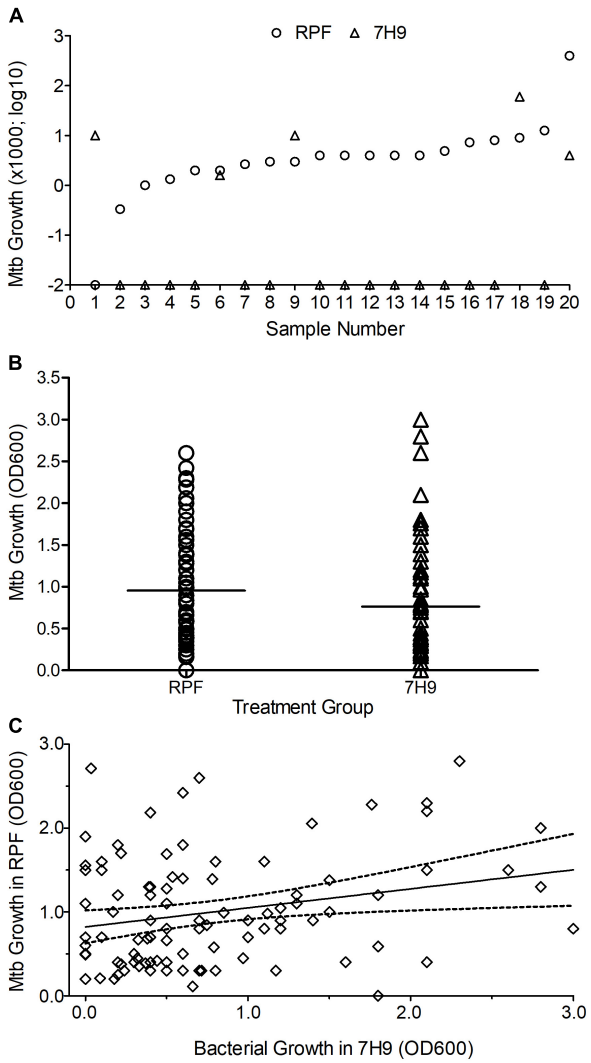

FIGURE 1 | Effect of crude RPF on Mtb growth. **(A)** Bacterial CFU obtained from sputum samples treated with crude RPF or placebo (7H9). The difference in CFU between RPF (23.9 CFU ± 19.8) and 7H9 (4.3 ± 3.0) is not statistically significant as determined by paired Student's *t* test ($P = 0.34$). **(B)** Bacterial growth in the sputum samples treated with crude RPF or placebo (7H9) as determined by OD_{600}. The difference in OD_{600} between RPF (0.96 ± 0.06) and 7H9 (0.76 ± 0.08) is statistically significant as determined by paired Student's *t* test ($P = 0.036$). **(C)** Linear regression analysis for the correlation significance of Mtb growth in crude RPF versus 7H9 broth. Treatment with RPF significantly improved bacterial recovery ($P = 0.016$).

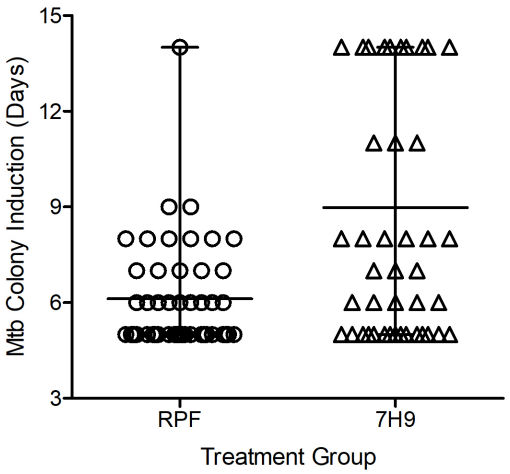

FIGURE 2 | Effect of crude RPF on time to detect (TTD) Mtb from sputum samples of smear-positive and culture-positive TB cases. The TTD analysis shows a significant reduction in time when samples are treated with crude RPF, compared to placebo (7H9) as analyzed by paired Student's *t* test ($P < 0.001$).

positives noticed in placebo-treated samples showed a higher culture yield when treated with crude RPF or rRPF. Most of the positives obtained by crude RPF treatment were reported negative by placebo broth treatment. Among the tested samples, the Mtb culture yield in crude RPF and rRPF treatment showed 4 $\log_{10}$ and 2 $\log_{10}$ higher positivity rates, respectively, compared to placebo broth treatment. Out of 13 positive cultures observed with rRPF treatment, seven yielded RCs only in the presence of rRPF and not with either crude RPF or placebo broth treatment. Similarly, 18 samples yielded positive RCs only in the presence of crude RPF, while two samples were positive exclusively for placebo broth treatment (**Figure 3**). These data suggest a higher positivity rate for samples treated with crude RPF, which is more effective in improving the sensitivity of Mtb detection in a clinical specimen, compared to treatment with recombinant RPF. However, some of the tested samples reactivated Mtb only in the presence of rRPF, while few other samples treated with placebo spontaneously revived Mtb growth. These observations suggest the complexity of Mtb growth stimulation during treatment with RPF, which remains to be determined.

Effect of RPF From Different Bacterial Strains on Dormant Mtb

Crude RPF obtained from the cultures of different virulent Mtb strains, including H37Rv, DRBL2 (a clinical isolate of W-Beijing lineage), 1338 (a clinical strain of East African Indian lineage), Erdman, and avirulent mycobacteria such as H37Ra, *M. smegmatis*, as well as *E. coli* were tested for their potency to reactivate clinical Mtb strains (MTB01 and MTB02) grown *in vitro* to dormancy by oxygen depletion. Clinical Mtb isolates MTB01 and MTB02 were grown to dormancy and treated with the crude RPF obtained from various bacterial species (**Figure 4**). Results show heterogeneity in response between MTB01 and MTB02 in their ability to resuscitate from dormancy upon treatment with crude RPF (**Figures 4A,B**). The latter strain showed a robust response than the former, as measured by the number of cultivatable bacterial CFU. A clear difference in the number of reactivated dormant Mtb was noted with crude RPF from various bacterial cultures compared to 7H9 control broth (**Figure 4**). While crude RPF from *E. coli* failed to show any resuscitation of the tested Mtb strains, the crude RPF from mycobacteria, including H37Ra, H37Rv, W-Beijing, *M. smegmatis*, and Erdmann strains showed

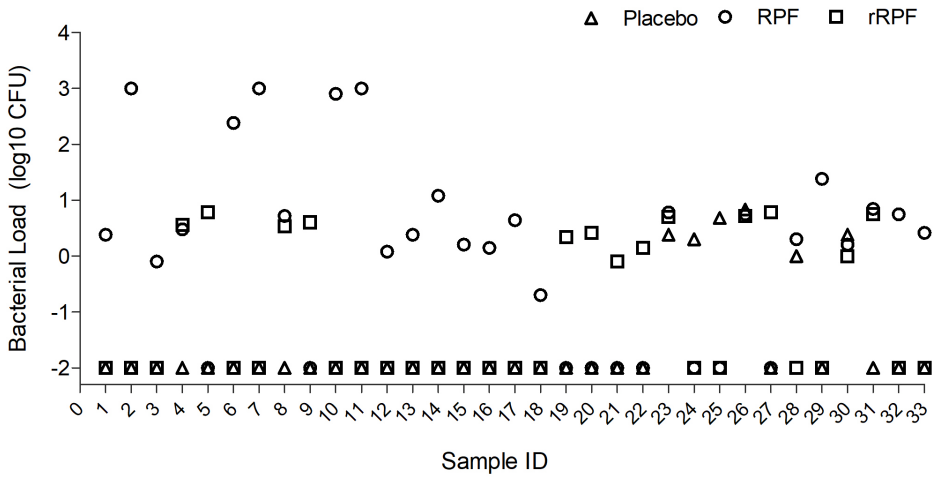

FIGURE 3 | Effect of crude RPF and recombinant RPF proteins on Mtb growth. Sputum samples from 33 smear-negative/culture-negative TB patients were treated with placebo (H9) or crude RPF or recombinant RPF protein (rRPF). Treated samples were plated on 7H11 agar to enumerate bacterial CFU. The difference in bacterial CFU was statistically significant between H9 and RPF ($P = 0.03$), H9 and rRPF ($P = 0.049$), and RPF and rRPF ($P = 0.032$) as analyzed by one-way ANOVA with the *post hoc* test.

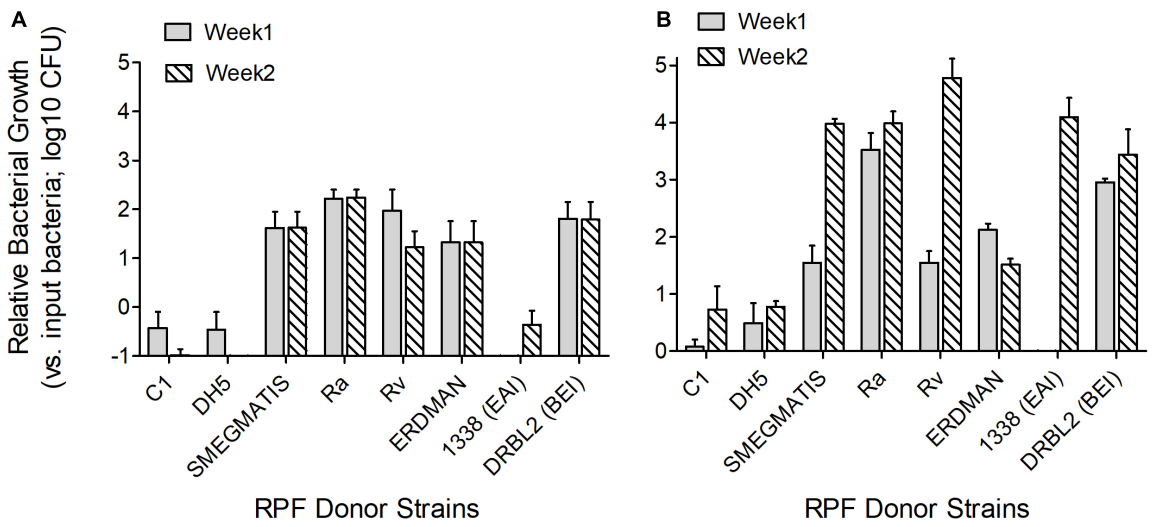

FIGURE 4 | Effect of crude RPF isolated from different bacterial strains in resuscitating dormant clinical Mtb isolates. Clinical Mtb isolates MTB01 **(A)** and MTB02 **(B)** were grown to dormancy in an *in vitro* hypoxia model and treated with crude RPF isolated from *E. coli* (DH5a), *M. smegmatis* mc^2155, Mtb H37Ra, Mtb H37Ra, Mtb 1338-EAI, Mtb DRBL2-BEI, and Mtb Erdmann strains or placebo (7H9 broth; C1). Treated Mtb culture was plated on 7H11 agar media to enumerate bacterial CFU. The data in **A** and **B**, except C1 and DH5, are significant; $P < 0.05$.

significant resuscitation of more number of bacilli, leading to an increased number of Mtb CFU from the sample. Thus, it appears that different mycobacterial strains/species, irrespective of their virulence potential, are capable of resuscitating dormant Mtb *in vitro*.

DISCUSSION

Tuberculosis is a disease of global importance. About 90% of Mtb-infected individuals are asymptomatic (latent) and harbor the bacteria in a dormant form. These cases have a 5–10% lifetime risk for reactivation to symptomatic TB (Gomez and McKinney, 2004; Gengenbacher and Kaufmann, 2012). Although both host- and bacteria-derived factors are implicated in the establishment of latency, the mechanisms underlying reactivation of dormant Mtb *in vivo* and the conversion of latent infection to active TB remains poorly understood (Kana and Mizrahi, 2010). RPFs, a family of muralytic enzymes, secreted by actively growing mycobacteria, are among such factors that are found to reactivate/resuscitate growth of dormant bacilli, which grow poorly or do not grow at all in conventional growth

media that supports growth of actively replicating bacteria (Mukamolova et al., 1998, 2002; Kana and Mizrahi, 2010). Sputum specimens of patients with active TB are reported to harbor a heterogeneous population of metabolically different classes of Mtb, ranging from fully replicating to non-replicating persisters (Garton et al., 2008). In clinical specimens of patients with active pulmonary TB, the presence of Mtb population with quiescent metabolic stages was revealed upon treatment of the specimen with RPF-containing media (Mukamolova et al., 2010; Chengalroyen et al., 2016). Further, CF treatment of smear-positive sputum specimens from TB patients increased the number of bacterial CFU counts, compared to no-CF treated samples. Moreover, the resuscitating potential was lost when CF from the Mtb strain mutant for RPF genes was used to treat the sputum samples.

Similarly, biological samples, other than sputum, from patients with extrapulmonary TB were shown to contain differentially culturable Mtb by their ability to grow only in the presence of RPF-containing culture filtrate (Mukamolova et al., 2010; O'Connor et al., 2015). These results highlight the essentiality of functional RPF for the resuscitation of Mtb in clinical samples (Mukamolova et al., 2010; Chengalroyen et al., 2016).

In the present study, we have tested sputum specimens from patients with clinical features suspected for pulmonary TB; these specimens were mostly negative for Mtb in smear and culture tests, two key bacteriological diagnostic methods widely used in endemic countries. We used RPF-containing culture filtrate (CF) from actively growing mycobacteria or recombinant RPF to treat sputum specimens. Results clearly show improved detection of viable but non-culturable (VBNC) Mtb, based on growth in liquid media (measured by OD_{600}) and growth of viable bacilli (viable cells – VC) on conventional agar media as described previously (Dusthackeer et al., 2012). In the current study, we were able to detect Mtb in about 75% more of several smear/culture-negative samples from patients who completed anti-TB therapy; these samples were declared negative by conventional microbiological diagnoses, such as smear microscopy and culture (unpublished results). Thus, our results suggest that even after successful completion of antibiotic treatment for TB, residual Mtb can persist without forming colonies on conventional microbiologic media. This leads not only to the underestimation of bacteriological cure rates among treated patients, but the persisting bacilli can cause reactivation of disease and contribute to the generation of drug resistance. Our findings are consistent with a study by Chengalroyen et al. that reports about 19% of sputum samples from TB patients with or without HIV co-infection to be dependent on culture filtrate (CF) (Chengalroyen et al., 2016). Another study tested the effect of RPF on sputum samples from TB patients before antibiotic treatment. Results of that study show that about 95% of bacteria were able to grow only in the presence of RPF-containing CF (Mukamolova et al., 2010), suggesting that the presence of RPF-dependent Mtb is frequent in a clinical specimen.

Our finding that a fraction of the NRP population of Mtb in clinical specimen responds to RPF treatment has clinical implications. Thus, in this study about 25% of the patients, whose specimen revealed the presence of RPF-dependent NRPs, either relapsed to active disease or met with treatment failure, including two patients who died of treatment-associated complications (unpublished results). Importantly, these two patients completed the full course of antibiotic treatment and showed negative-culture conversion, which was indicative of a good clinical prognosis. However, in the sputum samples of these patients, the presence of the RPF-dependent NRP bacterial population was evident from our assays. Therefore, we predict that the presence of such RPF-dependent NRP is responsible for disease relapse in these patients. Taken together, the presence of resuscitable/viable Mtb even after successful completion of treatment provides a piece of crucial evidence for extending the current treatment duration and for testing the drug susceptibility pattern of infecting Mtb.

In our studies, the differential growth of Mtb in a clinical specimen was more prominent in the presence of crude RPF than treatment with a cocktail of purified, recombinant RPF. Previous reports show that both recombinant RPF and the culture filtrate supernatant of young cultures of *M. tuberculosis* were able to produce increased growth of viable cells among the cells maintained in the stationary phase of growth (Shleeva et al., 2002; Wu et al., 2008; Huang et al., 2014). These studies also show reduced TTD Mtb when recombinant RPFs were added individually to mycobacteria growth indicator tube (MGIT)-inoculated cultures and from sputum specimens. In addition, Mukamolova et al. (2010) reported the potential of the recombinant RPF proteins to induce the growth of Mtb maintained in the stationary phase of growth in a genus-specific manner, irrespective of the species of *Mycobacterium* [*M. luteus*, *M. smegmatis*, and *M. bovis* (BCG)]. These studies suggest that RPFs do not mimic the role of just being a growth supplement or nutrient; instead, these proteins play a vital mechanistic role as a growth stimulant, based on the requirement of picomolar level concentration in the medium to reactivate bacterial growth. Moreover, Turapov et al. concluded that the potential of both recombinant RPF and the culture filtrate supernatant are equivocal; although reports from other groups contradicted this observation (Mukamolova et al., 2010; Chengalroyen et al., 2016). Using the CF of quintuple Mtb mutant for RPF (rpfA–D), Chengalroyen et al. (2016) showed resuscitation of non-replicating Mtb, suggesting that RPF can be dispensable to a certain extent in resuscitating dormant Mtb. This could be due to the presence of other Mtb-derived factors, including mucopeptides and lipids, in the crude RPF.

In this study, we have not evaluated the effect of RPF on the diagnostic potential of MGIT. However, we have used the same components of MGIT assay in our culture conditions (i.e., using 7H9 media base supplemented with OADC and antibiotics). Therefore, our observations could be relatable and extended to MGIT conditions. Nonetheless, this claim warrants further evaluation with actual experiments to test the beneficial effect of RPF on MGIT assays, which will be the focus of our future research.

CONCLUSION

In conclusion, we demonstrate the presence of viable Mtb in the clinical specimen of patients with pulmonary TB who had negative results in conventional microbiological tests. We show that crude RPF, as well as recombinant RPF proteins, are capable of resuscitating dormant Mtb and improve the bacillary load as well as reduce the duration to detect Mtb in a clinical specimen. The mechanistic basis for the heterogeneity among Mtb in their response to RPF needs further investigation. Our findings have clinical implications since the treatment of patient sputum samples with RPFs has the potential to improve the current microbiological diagnosis of TB.

DATA AVAILABILITY STATEMENT

All datasets generated for this study are included in the manuscript/**Supplementary Files**. The raw data is available upon request to AD.

ETHICS STATEMENT

The studies involving human participants were reviewed and approved by Institutional Ethical Committee of the National Institute for Research on Tuberculosis, a body of Indian Council of Medical Research. The patients/participants provided their written informed consent to participate in this study.

AUTHOR CONTRIBUTIONS

AD and SS conceived the concept, designed the experimental studies, wrote and edited the manuscript. AD, MB, GS, SP, and AB performed the experiments. SS, KT, AD, CN, RS, RM, and KT analyzed the data. AH and GR assisted with sample procurement and documentation. All authors read and agreed to publish.

FUNDING

This work was funded by the National Institute for Research in Tuberculosis, Chennai, India.

ACKNOWLEDGMENTS

The authors sincerely acknowledge Prof. Bavesh Kana, DST/NRF Centre of Excellence for Biomedical TB Research, University of the Witwatersrand, Johannesburg, South Africa, for technical advice on obtaining RPF-containing supernatant from Mtb cultures, and Dr. Tom Ottenhoff, Leiden University Medical Center, Netherlands, for providing the purified recombinant RPF. The authors would like to thank the patients involved in this study.

SUPPLEMENTARY MATERIAL

The Supplementary Material for this article can be found online at: https://www.frontiersin.org/articles/10.3389/fmicb.2019.02381/full#supplementary-material

FIGURE S1 | Flow chart showing the type and number of samples used for different assays in this study.

FIGURE S2 | Establishment of non-replicating persistence stage of Mtb. Actively growing Mtb culture was sub-cultured into fresh media containing methylene blue, an indicator dye for oxygen tension **(A)** that de-colorizes as the culture becomes hypoxic **(B)**. Representative vials are shown either immediately after Mtb inoculation (blue color; **A**) and after the establishment of hypoxia (no color; **B**).

FIGURE S3 | Colony formation by Mtb treated with crude RPF or placebo. Dormant cultures of wild type Mtb H37Rv (a laboratory strain) and representative clinical isolates (2474 and 2572) were treated with crude RPF or 7H9 broth for day 3 days **(A)** or 45 days **(B)** and serial dilutions were plated on 7H11 agar media for colonies to appear. Visible colonies were noted on day-7 post-inoculation for samples treated with RPF **(A)**. Prominent colony formation was observed on day-21 post-inoculation for samples treated with control 7H9 broth **(B)**.

TABLE S1 | Smear gradation of samples used in this study.

REFERENCES

Ayrapetyan, M., Williams, T. C., Baxter, R., and Oliver, J. D. (2015). Viable but nonculturable and persister cells coexist stochastically and are induced by human serum. *Infect. Immun.* 83, 4194–4203. doi: 10.1128/IAI.00404-15

Cardona, P. J., and Ruiz-Manzano, J. (2004). On the nature of *Mycobacterium tuberculosis*-latent bacilli. *Eur. Respir. J.* 24, 1044–1051. doi: 10.1183/09031936.04.00072604

Chengalroyen, M. D., Beukes, G. M., Gordhan, B. G., Streicher, E. M., Churchyard, G., and Hafner, R. (2016). Detection and quantification of differentially culturable tubercle bacteria in sputum from patients with tuberculosis. *Am. J. Respir. Crit. Care Med.* 194, 1532–1540. doi: 10.1164/rccm.201604-0769oc

Commandeur, S., van Meijgaarden, K. E., Lin, M. Y., Franken, K. L., Friggen, A. H., and Drijfhout, J. W. (2011). Ottenhoff, Identification of human T-cell responses to *Mycobacterium tuberculosis* resuscitation-promoting factors in long-term latently infected individuals. *Clin. Vaccine Immunol.* 18, 676–683. doi: 10.1128/CVI.00492-10

Datta, S., Alvarado, K., Gilman, R. H., Valencia, T., Aparicio, C., Ramos, E. S., et al. (2019). Optimising fluorescein diacetate sputum smear microscopy for assessing patients with pulmonary tuberculosis. *PLoS One* 14:e0214131. doi: 10.1371/journal.pone.0214131

Deb, C., Lee, C. M., Dubey, V. S., Daniel, J., Abomoelak, B., Sirakova, T. D., et al. (2009). A novel in vitro multiple-stress dormancy model for *Mycobacterium tuberculosis* generates a lipid-loaded, drug-tolerant, dormant pathogen. *PLoS One* 4:e6077. doi: 10.1371/journal.pone.0006077

Dusthackeer, V. N., Balaji, S., Gomathi, N. S., Selvakumar, N., and Kumar, V. (2012). Diagnostic luciferase reporter phage assay for active and non-replicating persistors to detect tubercle bacilli from sputum samples. *Clin. Microbiol. Infect* 18, 492–496. doi: 10.1111/j.1469-0691.2011.03592.x

Garcia-Basteiro, A. L., Jenkins, H. E., and Rangaka, M. (2019). The burden of latent multidrug-resistant tuberculosis. *Lancet Infect. Dis.* 19, 802–803. doi: 10.1016/s1473-3099(19)30271-3

Garton, N. J., Waddell, S. J., Sherratt, A. L., Lee, S. M., Smith, R. J., and Senner, C. (2008). Cytological and transcript analyses reveal fat and lazy persister-like bacilli in tuberculous sputum. *PLoS Med.* 5:e75. doi: 10.1371/journal.pmed.0050075

Gengenbacher, M., and Kaufmann, S. H. (2012). *Mycobacterium tuberculosis*: success through dormancy. *FEMS Microbiol. Rev.* 36, 514–532. doi: 10.1111/j.1574-6976.2012.00331.x

Gomez, J. E., and McKinney, J. D. (2004). M *tuberculosis* persistence, latency, and drug tolerance. *Tuberculosis* 84, 29–44. doi: 10.1016/j.tube.2003.08.003

Gupta, R. K., and Srivastava, R. (2012). Resuscitation promoting factors: a family of microbial proteins in survival and resuscitation of dormant mycobacteria. *Indian J. Microbiol.* 52, 114–121. doi: 10.1007/s12088-011-0202-6

Huang, W., Qi, Y., Diao, Y., Yang, F., Zha, X., Ren, C., et al. (2014). Use of resuscitation-promoting factor proteins improves the sensitivity of culture-based tuberculosis testing in special samples. *Am. J. Respir. Crit. Care Med.* 189, 612–614. doi: 10.1164/rccm.201310-1899le

Kana, B. D., Gordhan, B. G., Downing, K. J., Sung, N., Vostroktunova, G., and Machowski, E. E. (2008). The resuscitation-promoting factors of *Mycobacterium tuberculosis* are required for virulence and resuscitation from dormancy but are collectively dispensable for growth in vitro. *Mol. Microbiol.* 67, 672–684. doi: 10.1111/j.1365-2958.2007.06078.x

Kana, B. D., and Mizrahi, V. (2010). Resuscitation-promoting factors as lytic enzymes for bacterial growth and signaling. *FEMS Immunol. Med. Microbiol.* 58, 39–50. doi: 10.1111/j.1574-695x.2009.00606.x

Magombedze, G., Dowdy, D., and Mulder, N. (2013). Latent tuberculosis: models, computational efforts, and the pathogen's regulatory mechanisms during dormancy. *Front. Bioeng. Biotechnol.* 1:4. doi: 10.3389/fbioe.2013.00004

Mukamolova, G. V., Kaprelyants, A. S., Young, D. I., Young, M., and Kell, D. B. (1998). A bacterial cytokine. *Proc. Natl. Acad. Sci. U.S.A.* 95, 8916–8921.

Mukamolova, G. V., Turapov, O., Malkin, J., Woltmann, G., and Barer, M. R. (2010). Resuscitation-promoting factors reveal an occult population of tubercle Bacilli in Sputum. *Am. J. Respir. Crit. Care Med.* 181, 174–180. doi: 10.1164/rccm.200905-0661OC

Mukamolova, G. V., Turapov, O. A., Young, D. I., Kaprelyants, A. S., Kell, D. B., and Young, M. (2002). A family of autocrine growth factors in *Mycobacterium tuberculosis*. *Mol. Microbiol.* 46, 623–635. doi: 10.1046/j.1365-2958.2002.03184.x

Nathan, C., and Barry, C. E. III (2015). TB drug development: immunology at the table. *Immunol. Rev.* 264, 308–318. doi: 10.1111/imr.12275

O'Connor, B. D., Woltmann, G., Patel, H., Turapov, O., Haldar, P., and Mukamolova, G. V. (2015). Can resuscitation-promoting factors be used to improve culture rates of extra-pulmonary tuberculosis? *Int. J. Tuberc. Lung Dis.* 19, 1556–1557. doi: 10.5588/ijtld.15.0682

Peddireddy, V., Doddam, S. N., and Ahmed, N. (2017). Mycobacterial dormancy systems and host responses in tuberculosis. *Front. Immunol.* 8:84. doi: 10.3389/fimmu.2017.00084

Shleeva, M. O., Bagramyan, K., Telkov, M. V., Mukamolova, G. V., Young, M., Kell, D. B., et al. (2002). Formation and resuscitation of "non-culturable" cells of Rhodococcus rhodochrous and *Mycobacterium tuberculosis* in prolonged stationary phase. *Microbiology* 148, 1581–1591. doi: 10.1099/00221287-148-5-1581

Verma, S., Dhole, T. N., Kumar, M., and Kashyap, S. (2013). Novel approach for improving the sensitivity of microscopic detection of acid-fast bacilli (AFB) by use of the ReaSLR method. *J. Clin. Microbiol.* 51, 3597–3601. doi: 10.1128/JCM.01570-13

Voskuil, M. I., Bartek, I. L., Visconti, K., and Schoolnik, G. K. (2011). The response of *Mycobacterium tuberculosis* to reactive oxygen and nitrogen species. *Front. Microbiol.* 2:105. doi: 10.3389/fmicb.2011.00105

Wayne, L. G., and Hayes, L. G. (1996). An *in vitro* model for sequential study of shift-down of *Mycobacterium tuberculosis* through two stages of nonreplicating persistence. *Infect. Immun.* 64, 2062–2069.

Wu, X., Yang, Y., Han, Y., Zhang, J., Liang, Y., Li, H., et al. (2008). Effect of recombinant Rv1009 protein on promoting the growth of *Mycobacterium tuberculosis*. *J. Appl. Microbiol.* 105, 1121–1127. doi: 10.1111/j.1365-2672.2008.03850.x

Zhang, Y. (2004). Persistent and dormant tubercle bacilli and latent tuberculosis. *Front. Biosci.* 9:1136–1156. doi: 10.2741/1291

Conflict of Interest: The authors declare that the research was conducted in the absence of any commercial or financial relationships that could be construed as a potential conflict of interest.

frontiers in Microbiology

ORIGINAL RESEARCH
published: 03 December 2019
doi: 10.3389/fmicb.2019.02752

Clinical Features Predicting Mortality Risk in Patients With Viral Pneumonia: The MuLBSTA Score

Lingxi Guo[1,2], Dong Wei[3,4], Xinxin Zhang[3,4,5], Yurong Wu[6], Qingyun Li[1,2], Min Zhou[1,2] and Jieming Qu[1,2]**

[1] Department of Respiratory and Critical Care Medicine, Ruijin Hospital, Shanghai Jiao Tong University School of Medicine, Shanghai, China, [2] Institute of Respiratory Diseases, Shanghai Jiao Tong University School of Medicine, Shanghai, China, [3] Research Laboratory of Clinical Virology, Ruijin Hospital, Shanghai Jiao Tong University School of Medicine, Shanghai, China, [4] Department of Infectious Diseases, Institute of Infectious and Respiratory Diseases, Ruijin Hospital, Shanghai Jiao Tong University School of Medicine, Shanghai, China, [5] Clinical Research Center, Ruijin Hospital North, Shanghai Jiao Tong University School of Medicine, Shanghai, China, [6] Department of Respiratory Medicine, The Third People's Hospital of Zhengzhou, Henan, China

Objective: The aim of this study was to further clarify clinical characteristics and predict mortality risk among patients with viral pneumonia.

Methods: A total of 528 patients with viral pneumonia at RuiJin hospital in Shanghai from May 2015 to May 2019 were recruited. Multiplex real-time RT-PCR was used to detect respiratory viruses. Demographic information, comorbidities, routine laboratory examinations, immunological indexes, etiological detections, radiological images and treatment were collected on admission.

Results: 76 (14.4%) patients died within 90 days in hospital. A predictive MuLBSTA score was calculated on the basis of a multivariate logistic regression model in order to predict mortality with a weighted score that included multilobular infiltrates (OR = 5.20, 95% CI 1.41–12.52, $p = 0.010$; 5 points), lymphocyte $\leq 0.8*10^9$/L (OR = 4.53, 95% CI 2.55–8.05, $p < 0.001$; 4 points), bacterial coinfection (OR = 3.71, 95% CI 2.11–6.51, $p < 0.001$; 4 points), acute-smoker (OR = 3.19, 95% CI 1.34–6.26, $p = 0.001$; 3 points), quit-smoker (OR = 2.18, 95% CI 0.99–4.82, $p = 0.054$; 2 points), hypertension (OR = 2.39, 95% CI 1.55–4.26, $p = 0.003$; 2 points) and age ≥60 years (OR = 2.14, 95% CI 1.04–4.39, $p = 0.038$; 2 points). 12 points was used as a cut-off value for mortality risk stratification. This model showed sensitivity of 0.776, specificity of 0.778 and a better predictive ability than CURB-65 (AUROC = 0.773 vs. 0.717, $p < 0.001$).

Conclusion: Here, we designed an easy-to-use clinically predictive tool for assessing 90-day mortality risk of viral pneumonia. It can accurately stratify hospitalized patients with viral pneumonia into relevant risk categories and could provide guidance to make further clinical decisions.

Keywords: virus pneumonia, predicting mortality, bacterial coinfection, predictive score model, clinical feature

Abbreviations: AdV, adenovirus; ARDS, acute respiratory distress syndrome; AUROC, area under ROC curve; CAP, community acquired pneumonia; CoV, coronavirus; CURB-65, confusion, urea, blood pressure, respiratory rate, age ≥65 year; ECMO, extracorporeal membrane oxygenation; EV, enterovirus; FluA, influenza A; FluB, influenza B; HMPV, human metapneumovirus; HRV, human rhinovirus; ICU, intensive care unit; IL, interleukin; MuLBSTA Score, multilobular infiltration, hypo-lymphocytosis, bacterial coinfection, smoking history, hyper-tension and age; NRI, net reclassification improvement; PIV, parainfluenza; ROC, receiver operator characteristic; RSVA, respiratory syncytial virus A; RSVB, respiratory syncytial virus B; RT-PCR, reverse-transcription polymerase chain reaction; TNF-α, tumor necrosis factor-α.

OPEN ACCESS

Edited by:
David Ong,
Sint Franciscus Gasthuis, Netherlands

Reviewed by:
Christina Tsigalou,
Democritus University of Thrace, Greece
Cornelis H. Van Werkhoven,
University Medical Center Utrecht, Netherlands

****Correspondence:***
Min Zhou
doctor_zhou_99@163.com
Jieming Qu
jmqu0906@163.com

Specialty section:
This article was submitted to Infectious Diseases, a section of the journal Frontiers in Microbiology

Received: *06 June 2019*
Accepted: *12 November 2019*
Published: *03 December 2019*

Citation:
Guo L, Wei D, Zhang X, Wu Y, Li Q, Zhou M and Qu J (2019) Clinical Features Predicting Mortality Risk in Patients With Viral Pneumonia: The MuLBSTA Score. Front. Microbiol. 10:2752. doi: 10.3389/fmicb.2019.02752

STATEMENT

Viral infections could present with severe pneumonia, acute respiratory distress syndrome or are complicated by bacterial super-infections in many patients. Influenza and other respiratory viruses are common reasons of acute pneumonia which can result in significant morbidity or mortality in the setting of high-risk factors such as extremes of age, pregnancy, obesity or chronic pre-existing conditions. Cytokines and chemokines, on the other hand, are regarded as possible hallmarks of severe disease and many of them reach high serum levels in the setting of severe infection. Although a variety of clinical prediction rules for pneumonia such as CRB-65 and CURB-65 are widely used in the assessment of community acquired pneumonia, no standard rule for the calculation of viral pneumonia severity scores has been established to our knowledge. Here, we designed a easy-to-use clinically predictive score for assessing mortality risk of viral pneumonia. This model showed better predictive ability with a c-index of 0.811, sensitivity of 0.776 and specificity of 0.778. A cut-off value of 12 points could be used for mortality risk stratification.

BACKGROUND

Viral infections, in spite of their common manifestations as mild illnesses, present with severe pneumonia, acute respiratory distress syndrome (ARDS) or bacterial coinfections in many patients (Shorr et al., 2017). In recent years, the dissemination of PCR has increased the ability to detect respiratory viruses in both upper and lower-respiratory tract samples (Das et al., 2015). Influenza and other respiratory viruses are common reasons of acute respiratory infection. Patients predisposed to bacterial infections have greater morbidity and mortality levels (Hanada et al., 2018).

During natural infection, both the adaptive and innate immune responses play important roles in controlling respiratory virus infection (Nussing et al., 2018). Adaptive T and B cells maintain immunological memory and provide protection against subsequent virus infections. Cytokines and chemokines, on the other hand, are regarded as possible hallmarks of severe disease and many of them reach high serum levels in the setting of severe infections (La Gruta et al., 2007). Such variables also could guide clinical decision making as well as infectious disease management.

Although a variety of clinical prediction rules for pneumonia such as CRB-65 and CURB-65 are widely used in the assessment of community acquired pneumonia (CAP) (Viasus et al., 2016; Uranga et al., 2018), most remain not applicable in the setting of viral infection. Other reported risk factors for influenza pneumonia such as PO2/FiO2, lymphocyte count, and antigen-specific T cells are likewise useful in predicting mortality and deciding on appropriate management (Viasus et al., 2011; Shi et al., 2017). To our knowledge, no standard rule for the calculation of viral pneumonia severity scores has been established.

Here, we aimed to further elucidate the potential risk factors and attempt to predict the probability of mortality among patients infected with respiratory viruses.

MATERIALS AND METHODS

Study Design and Population

A retrospective single-center observational study was conducted from May 2015 to May 2019 in RuiJin Hospital, Shanghai, China. The study was approved by Ruijin Hospital Ethics Committee and written informed consent was obtained from all patients involved before enrolment.

We retrospectively studied all hospitalized patients with positive result of multiplex real-time reverse-transcription polymerase chain reaction (RT-PCR, TIB respiratory kit, ROCHE, Switzerland) aiming to detect respiratory viruses. The time period of this study was selected because of the introduction of the viral test panel. Patients who were diagnosed pneumonia according to the 2009 Infectious Diseases Society of American (IDSA)/American Thoracic Society (ATS) guidelines (Charles et al., 2009) were enrolled in this study. Patients were excluded if: 1) age <18 years; 2) had a clear alternative final diagnosis as lung cancer or other non-pneumonia illness; 3) long hospitalization >3 months before death.

767 hospitalized patients had initial positive RT-PCR results and 562 of them were enrolled with pneumonia. A total of 34 cases were excluded: final diagnosis of non-pneumonia illness (n = 31), children or adolescent patient (n = 3). 528 pneumonia patients with positive viral detection were finally included in this analysis (**Figure 1**).

Data Collection

Infections due to influenza A (FluA), adenovirus (AdV), bocavirus, human rhinovirus (HRV), influenza B (FluB), parainfluenza (PIV), coronavirus (CoV), respiratory syncytial virus A (RSVA), respiratory syncytial virus B (RSVB), enterovirus (EV) and human metapneumovirus (HMPV) were confirmed using RT-PCR via nasal wash products. Data were collected on admission including demographic information, comorbidities, routine laboratory examinations, chest radiography or CT scanning, immunological and etiological detections. We used positive bacterial culture of blood and sputum samples as the criteria for bacterial growth. The use of antiviral therapy and steroids was recorded, including the drug, start date, duration and dosage. Patients were evaluated as deemed clinically appropriate at any time when pneumonia was suspected. CURB-65 score of each patient was calculated (Barlow et al., 2007). Length of stay and outcome state of each patient were recorded. Those improved patients with hospital stay <90 days were followed up by a phone call to determine survival status if they were not seen in the outpatient clinic. Finally, the outcome of mortality was defined as overall mortality within 90 days.

Statistical Methods

Viral pneumonia patients were classified into two groups: survival group and 90-day death group. Univariate analysis was

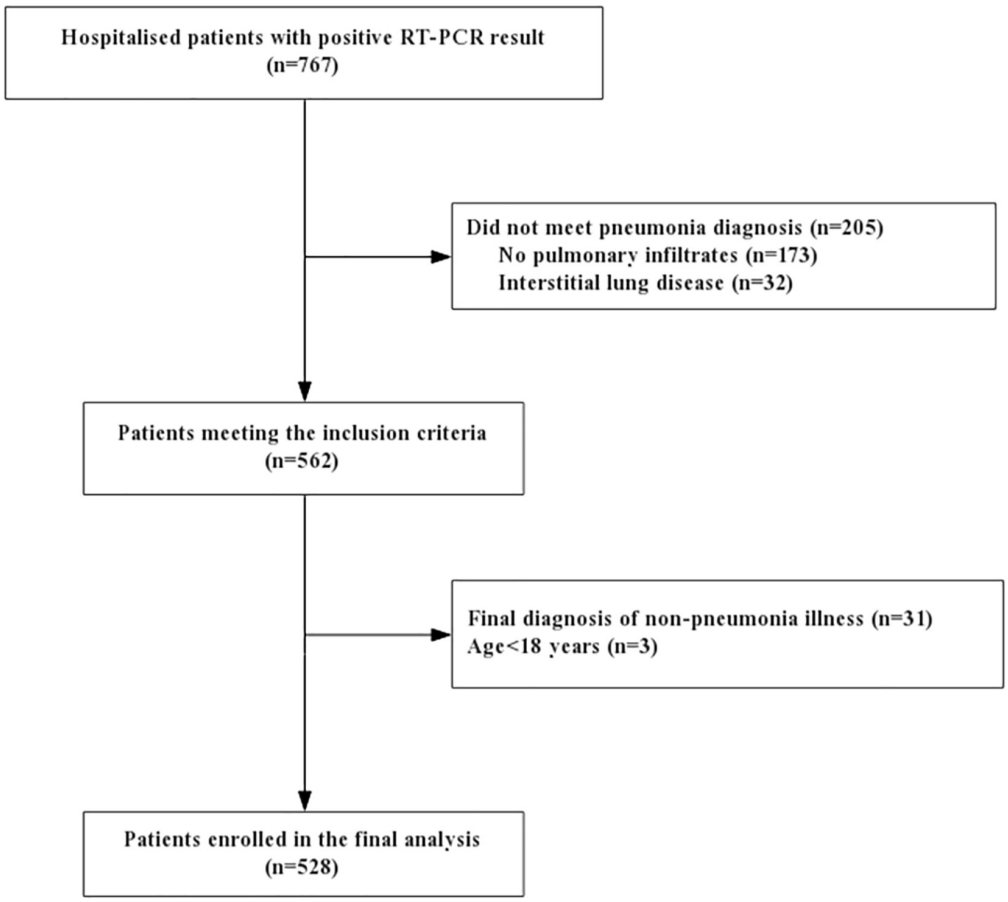

FIGURE 1 | Study flowchart. RT-PCR: reverse-transcription polymerase chain reaction.

initially used to compare risk factors for mortality separately among patients with viral pneumonia. Proportions or means with SD were used to characterize the patient sample. Continuous variables were compared using *t*-tests or one-way ANOVA while $\chi 2$ or Fisher exact tests were used for categorical dependent data analysis, as appropriate.

The percentages of missing values of variables in our cohort were lower than 50%. We imputed missing data of the covariates by using multiple imputations (Sterne et al., 2009). Conclusions of univariate logistic regression analyses with or without imputed data were unchanged. Continuous variables were categorized and retained for multivariate testing. Cut-off points were identified following Youden's index of receiver operator characteristic (ROC) curve or a clinically relevant cut-off. Variables with $p < 0.10$ were regarded as potential risk factors and included in multivariate regression analysis against overall mortality reduced by a backward elimination procedure (conditional likelihood ratio test and elimination if $p \geq 0.05$).

Data of 528 patients was partitioned randomly into two complementary subsets: the training set of 423 (80%) was used to establish the model; the testing set of 105 (20%) was used to validate the analysis. For pragmatic reasons, scores for each predictors were assigned as integer values relative to the regression coefficient. Cut-off points were identified following Youden's index of ROC. Survival analysis was performed using univariate approach with Kaplan-Meier analysis between low-risk and high-risk group according to the cut-off value.

Performance of the score was assessed by measuring the area under ROC curve (AUROC) while sensitivity and specificity were calculated. Internal validation was assessed by AUROC of 2000 bootstrapped samples. The cross-validation was assessed by calculating AUROC of the testing set. ROC curve and net reclassification improvement (NRI) (Leening et al., 2014) analyses were used to assess the improvement in risk predicting capacity compared with CURB-65. Statistical analysis was performed using SPSS version 22.0 and R 3.5.0. All tests were two-sided and a *p*-value <0.05 was considered significant.

RESULTS

Patients Characteristics

Baseline characteristics of complete cases and different groups are described in **Table 1**. The mean age of viral pneumonia patients was 63.56 (SD 19.08) years and 61.2% were male.

TABLE 1 | Population description and comparison between survivors and those who died in 90-days after admission.

	Total population, *n* = 528	Survivors, *n* = 452	Died, *n* = 76	*p*-value※
Socio-demographic details				
Age (years)	63.56 ± 19.08	63.23 ± 19.58	65.47 ± 15.82	0.344
≥60#	371 (70.3)	308 (68.1)	63 (82.9)	**0.009**
Male#	323 (61.2)	270 (59.7)	53 (69.7)	0.092
Smoking#				**<0.001**
Acute-smoker	111 (21)	83 (18.4)	28 (36.8)	
Quit-smoker	57 (10.8)	47 (10.4)	10 (13.2)	
Non-smoker	360 (68.2)	322 (71.2)	38 (50)	
Occupation#				**0.052**
Unemployed	39 (7.4)	37 (8.2)	2 (2.6)	
Retired	366 (69.3)	304 (67.3)	62 (81.6)	
Inservice	112 (21.3)	100 (22.2)	12 (15.8)	
Student	11 (2.1)	11 (2.4)	0	
BMI#	23.44 ± 4.34	23.61 ± 4.32	22.47 ± 4.39	**0.036**
Comorbidity				
Hypertension#	263 (49.8)	218 (48.2)	45 (59.2)	**0.076**
Diabetes	135 (25.6)	116 (25.7)	19 (25)	0.902
Asthma	28 (5.3)	25 (5.6)	3 (3.9)	0.564
COPD	76 (14.4)	66 (14.7)	10 (13.2)	0.729
Heart failure	39 (7.4)	31 (6.9)	8 (10.5)	0.263
Coronary heart disease	85 (16.1)	74 (16.4)	11 (14.5)	0.666
Liver disease	46 (8.7)	41 (9.1)	5 (6.6)	0.470
Renal disease	95 (18)	83 (18.4)	12 (15.8)	0.112
Cancer	72 (13.6)	58 (12.8)	14 (18.4)	0.189
Clinical features§				
Cough	406 (76.9)	343 (75.9)	63 (82.9)	0.180
Expectoration	392 (74.2)	345 (76.3)	47 (61.8)	**0.008**
Wheeze	188 (35.6)	141 (31.2)	47 (61.8)	**<0.001**
Fever ≥ 38°C	321 (60.8)	271 (60)	50 (65.8)	0.335
Lymphocyte#	1.187 ± 0.762	1.237 ± 0.766	0.884 ± 0.664	**<0.001**
PaO2/FiO2#	274.93 ± 114.37	292.74 ± 109.34	209.36 ± 109.22	**<0.001**
Bacteria (+)*#	141 (26.7)	45 (59.2)	96 (21.2)	**<0.001**
Multi-viral infection	35 (6.7)	30 (6.7)	5 (6.6)	0.977
Fungi#	25 (4.8)	12 (2.7)	13 (17.1)	**<0.001**
Tuberculosis	11 (2.1)	1 (1.3)	10 (2.2)	0.938
Multi-lobular# infiltration	383 (72.5)	72 (94.7)	311 (68.8)	**<0.001**
Early antiviral therapy	166 (31.6)	140 (31.1)	26 (34.2)	0.591
Corticosteroid therapy#	198 (37.6)	139 (30.9)	59 (77.6)	**<0.001**
Ventilation				**<0.001**
Non-invasive	75 (14.2)	54 (11.9)	21 (27.6)	
Traumatic	47 (8.9)	18 (4)	29 (38.2)	
ICU	144 (27.3)	95 (21)	49 (64.5)	**<0.001**
Length of hospital stay	20.72 ± 20.35	20.04 ± 19.73	24.79 ± 23.45	**0.037**
Hospitalization cost	55644.36 ± 93022.15	43601.47 ± 81814.74	127267.8 ± 120328.9	**<0.001**

*Continuous parameters presented as mean ± SD, categorical data as n (%). *Patients with positive sputum or sanguine culture of bacteria were included. §All clinical symptoms were collected on admission. ※P-value represented the comparison between survival group and death group. #Variables cited in the table above were the candidates which were tested univariably. The bolded values are p-values < 0.05, which represent significant differences between survival group and death group. BMI, body mass index; COPD, chronic obstructive pulmonary disease; ICU, intensive care unit.*

Approximately a third of patients had smoking history (31.8%, among them 10.8% had quit smoking before infection). A total of 360 (68.4%) patients had comorbidities, with hypertension the most commonly observed (49.8%), followed by diabetes, renal disease, coronary heart disease and chronic obstructive pulmonary disease (COPD). Overall, 141 patients (26.7%) had bacterial coinfection, 25 (4.8%) had fungi infection and 11 (2.1%) had tuberculosis. As for treatment, 166 patients (31.6%) received oseltamivir the first 48 h on admission. 144 patients (27.3%) were admitted to intensive care unit (ICU).

TABLE 2 | Comparison of T-lymphocyte subtypes, humoral immunity and cytokines between bacterial co-infection group and pneumonia severity group.

	Survival group	Overall death	*p*	Non-bacteria	Co-bacteria	*p*
T lymphocytes						
CD3 + (%)	68.62 ± 12.63	61.29 ± 17.67	**<0.001**	68.57 ± 13.06	64.60 ± 15.27	**0.020**
CD4 + (%)	40.03 ± 11.19	34.14 ± 14.16	**0.001**	39.67 ± 11.56	37.54 ± 12.70	0.149
CD8 + (%)	26.01 ± 10.74	24.07 ± 15.54	0.271	26.04 ± 11.80	24.85 ± 11.43	0.409
CD3 absolute count	975.35 ± 662.75	530.34 ± 426.76	**<0.001**	1002.81 ± 644.67	666.09 ± 602.81	**<0.001**
CD4 absolute count	466.40 ± 333.71	256.41 ± 191.23	**<0.001**	468.47 ± 318.11	344.52 ± 320.07	**0.008**
CD8 absolute count	328.07 ± 208.02	223.37 ± 231.10	**0.006**	339.19 ± 208.94	245.02 ± 216.68	**0.003**
CD4 + /CD8 + Ratio	1.88 ± 1.09	1.99 ± 1.38	0.536	1.89 ± 1.09	1.91 ± 1.25	0.940
Cytokine						
IL-1	5.69 ± 2.59	7.25 ± 8.34	0.092	6.19 ± 5.41	5.95 ± 3.73	0.763
IL-2R	1290.12 ± 1145.35	1899.69 ± 1323.24	**0.009**	1194.46 ± 1031.01	1732.77 ± 1353.35	**0.008**
IL-6	32.83 ± 74.75	136.22 ± 215.29	**<0.001**	24.74 ± 45.68	95.94 ± 178.97	**0.001**
IL-8	120.51 ± 291.26	207.67 ± 310.19	0.131	115.26 ± 185.37	173.91 ± 392.94	0.239
IL-10	11.12 ± 12.14	16.58 ± 15.72	**0.033**	9.70 ± 10.39	15.81 ± 15.51	**0.005**
TNF-α	15.59 ± 14.53	14.97 ± 10.77	0.828	15.06 ± 14.65	15.85 ± 12.62	0.749

The bolded values are p-values < 0.05, which represent significant differences between subgroups.

The mean length of hospital stay in viral pneumonia patients was 20.72 (SD 20.25) days and hospital cost was 55644.36 (SD 93022.15) yuan.

In total, 76 (14.4%) died during hospital stay. Significant differences between survivors and non-survivors were shown in **Table 1**. The median length of stay was 24.79 (SD 23.44) days. There were no statistically significant differences in the early use of antiviral therapy and amount of virus infection between patients survived or dead.

Immune Responses Among Pneumonia Subgroups

Immune examinations between survival and dead patients are described in **Table 2** Lower serum levels of T-lymphocyte subtypes were noted in death group ($p < 0.01$). Moreover, patients from death group were found to possess lower serum levels of T-lymphocyte subtypes ($p < 0.01$) and elevated levels of the cytokines IL-2R ($p = 0.009$), IL-6 ($p < 0.001$) and IL-10 ($p = 0.033$).

We further analyzed these same immunological indices in patient subgroups with or without bacterial infections. Lower levels of $CD3^+$ ($p < 0.001$), $CD4^+$ ($p = 0.008$) and $CD8^+$ ($p = 0.003$) T-lymphocyte counts were found in the group suffering bacterial infections. As for interleukins, elevated levels of the cytokines IL-2R ($p = 0.008$), IL-6 ($p = 0.001$) and IL-10 ($p = 0.005$) were also found in bacterial group. There were no statistically significant differences in $CD4^+/CD8^+$, IL-1, IL-8 and TNF-α in both comparisons.

Distribution and Severe Outcome of Bacterial Co-infection

26.7% hospitalized patients had bacterial coinfection. *Acinetobacter baumannii* was the most commonly isolated pathogen (42.6%, 60/141) followed by *Klebsiella pneumoniae* (35.5%, 50/141), *Stenotrophomonas maltophilia* (18.4%, 26/141), *Staphylococcus aureus* (12.1%, 17/141), *Escherichia coli* (12.1%, 17/141), *Pseudomonas aeruginosa* (10.6%, 15/141), *Haemophilus influenzae* and *Staphylococcus haemolyticus* (**Figure 2**).

We compared the CURB-65 score, severity and prognoses among patients with or without bacterial co-infection (**Table 3**). Patients with bacterial infections revealed striking differences in CURB-65 scores, use of either non-invasive or invasive ventilation, ICU admission rate, length of hospitalization and treatment cost as compared with those who simply suffered viral infections.

Risk Factors of Mortality

Multiple imputation of missing data was performed for: serum interleukins (28.9% missing); PaO2/FiO2 (25.3% missing); T lymphocyte subsets levels (27.4% missing); body mass index (BMI) and lymphocyte count (all < 1% missing).

According to the methods and analyses above, the following categorical variables were entered in a backward stepwise logistic regression analysis: male; age ≥60 years; smoking history; hypertension; lymphocyte $\leq 0.8*10^9$/L; PO2/FiO2 ≤ 260; IL-6 ≥ 13pg/ml; IL-2R ≥ 1000pg/ml; positive sputum or sanguine culture for bacteria; fungi infection; multilobular infiltration (**Table 4**).

In order to develop a simple and useful clinical predicting tool, relative weights were assigned according to the regression coefficient of each categorical variable (β). **Figure 3** shows coefficient, odd ratio (OR), 95% CI and calculation of the Multilobular infiltration, hypo-Lymphocytosis, Bacterial coinfection, Smoking history, hyper-Tension and Age (MuLBSTA) Score. AUROC of the training set was 0.821 (95% CI 0.764 to 0.878), and AUROC of the testing set was 0.800 (95% CI 0.683–0.916). For the total 528 patients, AUROC was 0.811 (95% CI 0.76–0.863). Sensitivity, specificity and corresponding risk of death of MuLBSTA are shown in **Table 5**. Patients were divided in to high-risk and low-risk groups considering the cut-off value of 12. The Kaplan-Meier survival curves for high-risk and low-risk groups are shown in **Figure 4**.

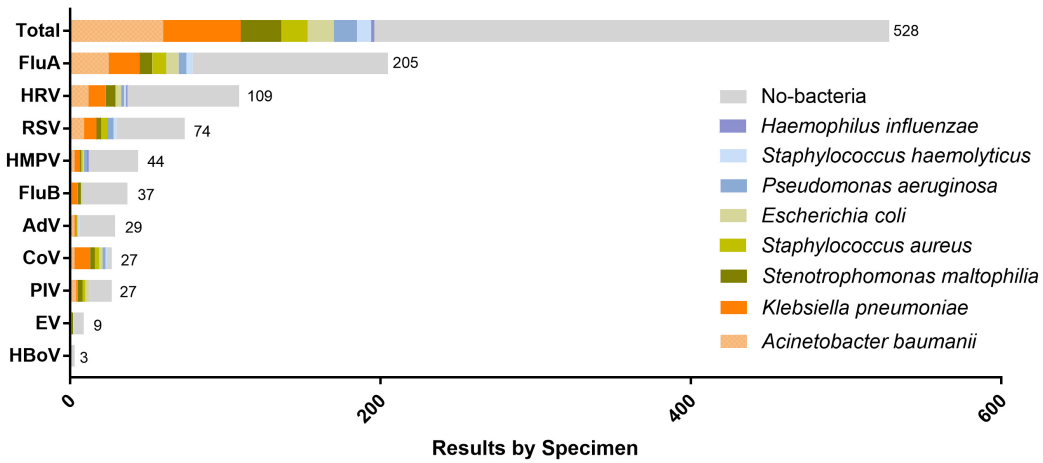

FIGURE 2 | Distribution of respiratory virus and proportion of bacterial infection detected by sputum or blood culture for each virus. The number of patients infected by each virus is presented on the right side of the corresponding horizontal axis.

TABLE 3 | Comparison of the severity and prognosis between individuals of virus infected pneumonia with or without bacteria co-infection.

	Non-bacteria, *n* = 387	Co-bacteria, *n* = 141	*p*
CURB-65 score			<0.001
0–1	269 (69.6)	53 (37.6)	
2	87 (22.5)	47 (33.8)	
≥3	31 (8)	41 (29)	
Ventilation			<0.001
Non-invasive	46 (11.9)	31 (22)	
Traumatic	9 (2.3)	38 (27)	
ICU	62 (15.9)	82 (59)	<0.001
Length of stay	15.35 ± 12.38	34.53 ± 28.08	<0.001
Hospitalization cost	29290.51 ± 33255.59	119230.31 ± 119727.77	<0.001

Continuous parameters presented as mean ± SD, categorical data as n (%).

TABLE 4 | Univariate analysis associated with mortality of virus-infected pneumonia patients.

Clinical feature	Univariate analysis	
	Odds Ratio (95% CI)	*p*-value
Male	1.553 (0.920–2.624)	0.096
Age ≥ 60	2.266 (1.208–4.250)	0.011
Smoking		0.001
Acute-smoker	2.136 (1.111–4.109)	
Quit-smoker	1.043 (0.829–2.056)	
Non-smoker	1.0	
Hypertension	1.558 (0.951–2.552)	0.072
Lymphocyte ≤ 0.8	5.365 (3.156–9.122)	<0.001
PO2/FiO2 ≤ 260	4.835 (2.557–9.144)	<0.001
IL-6 ≥ 13	3.367 (1.757–6.454)	<0.001
IL-2R ≥ 1000	2.522 (1.315–4.838)	0.005
Bacterial infection	5.383 (3.233–8.963)	<0.001
Fungi infection	7.566 (3.306–17.314)	<0.001
Multilobe infiltrate	6.580 (2.354–18.397)	<0.001

In comparison, the nomogram of the full regression model in original form is shown in **Supplemental Figure 1**. Compared with the MuLBSTA score, there was no difference between the AUROC for the original regression model (0.811 vs. 0.847, $p = 0.19$).

In our cohort, MuLBSTA was a significantly stronger predictor of overall mortality than CURB-65 (AUROC = 0.811 vs. 0.734, $p = 0.018$, $n = 528$) (**Figure 5**). The average AUROC of bootstrapped ($n = 2000$) MuLBSTA model and CURB-65 score were 0.806 and 0.728 separately. NRI of MuLBSTA was also improved than CURB-65 (NRI 0.0578, 95% CI 0.0016–0.0865, $p = 0.04$). As CURB-65 was commonly used to predict 30-day mortality, we also assessed the use of MuLBSTA score in 30-day mortality which tended to be a stronger predictor than CURB-65 (AUROC = 0.773 vs. 0.717, $p < 0.001$, $n = 528$).

DISCUSSION

In patients hospitalized with viral pneumonia, a simple prognostic tool was made for overall mortality which is useful for prediction several days after admission upon obtaining culture results. This score predicts prognoses with greater accuracy than CURB-65.

Pneumonia is a global cause of death with high short-term and long-term mortality. Though short-term mortality rates are high in this acute disease, long-term mortality within 90 days, 1 year and 5 years are also noteworthy in previous studies (Mortensen et al., 2003; Uranga et al., 2018). Nowadays, the survival time for patients with severe lung failure with the progress of radiological image, new drugs and supporting techniques like extracorporeal membrane oxygenation (ECMO) (Pappalardo et al., 2013). A prospective research on viral pneumonia showed a higher 90-day mortality rate than overall mortality as length of hospital stay was between 7 to 14 days (Zhou et al., 2019). During hospitalization, 76 patients in our

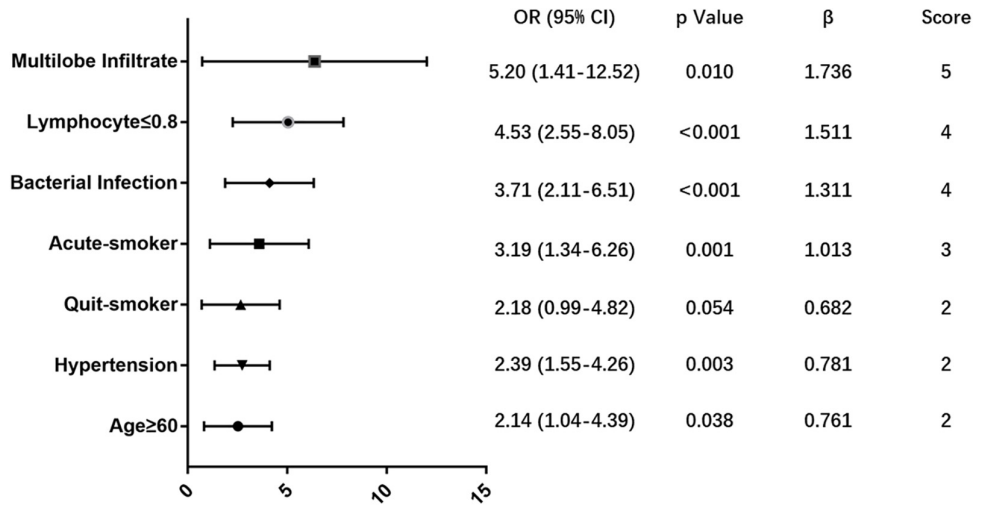

FIGURE 3 | Multivariate analysis associated with mortality of virus-infected pneumonia patients.

TABLE 5 | MuLBSTA score and overall mortality risk.

Total score	*n*	Overall death	Estimate of risk (%)	Sensitivity	Specificity
0	21	0	0.473	1	0
2	17	0	0.872	1	0.105
3	11	0	1.182	1	0.135
4	25	4	1.601	0.966	0.198
5	23	0	2.165	0.966	0.261
6	11	1	2.921	0.948	0.289
7	41	1	3.930	0.931	0.399
8	20	1	5.271	0.914	0.451
9	60	2	7.033	0.879	0.612
10	14	0	9.329	0.879	0.651
11	41	5	12.274	0.793	0.749
12	**11**	**1**	**15.985**	**0.776**	**0.778**
13	50	14	20.555	0.534	0.876
14	17	9	26.027	0.379	0.898
15	19	3	32.363	0.328	0.942
16	5	1	39.419	0.310	0.953
17	20	9	46.945	0.155	0.983
18	6	3	54.613	0.103	0.991
19	4	2	62.068	0.069	0.997
20	5	4	68.994	0	1
21	0	0	NA	NA	NA
22	0	0	NA	NA	NA

MuLBSTA, multilobular infiltration, hypo-lymphocytosis, bacterial coinfection, smoking history, hyper-tension and age. The bolded values represent the cut-off value of MuLBSTA score and the corresponding estimate of viral pneumonia risk, sensitivity and specificity.

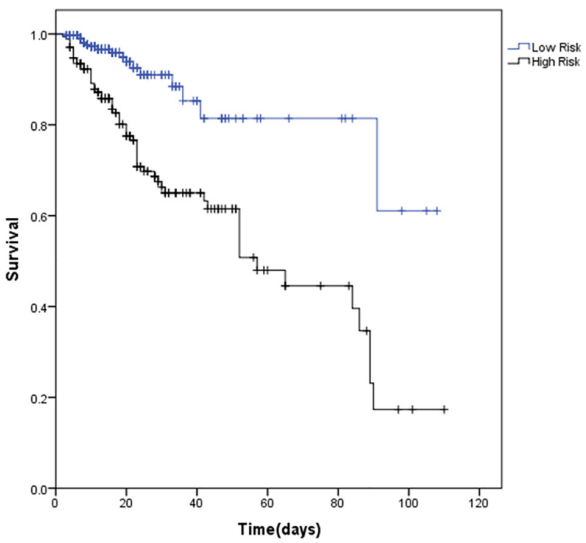

FIGURE 4 | Survival of viral pneumonia patients by different levels of MuLBSTA score ($p < 0.001$). For inhospital mortality: MuLBSTA 0–11 = Low risk; ≥12 = High risk.

study died between 4 and 89 days of hospital stay, among them 18 (23.7%) lived longer than 30 days, which makes 90-day mortality worthy of attention.

As immune deficiency is a close relative of mortality, evaluating immune condition could be conductive to monitor patient's general condition and estimate prognosis. In our study, all T-lymphocyte subtypes were reduced in death group reflecting the deficiency of adaptive immune response. Prior research on viral infection indicated that adaptive T cells provide broader and more lasting cross-reactive cellular immunity with less limitations of strain-specific restriction, especially $CD8^+$ T cells (Bender et al., 1992). Besides, the higher level of proinflammatory cytokines had been documented to attribute to severe disease and lung damage (Das et al., 2015). Accordingly, IL-2R and IL-6, which appeared to significantly correlate with illness severity by complementing $CD8^+$ T cell function (Nussing et al., 2018), presented with significantly higher serum levels in death group. IL-2R and IL-6 were also found related to mortality

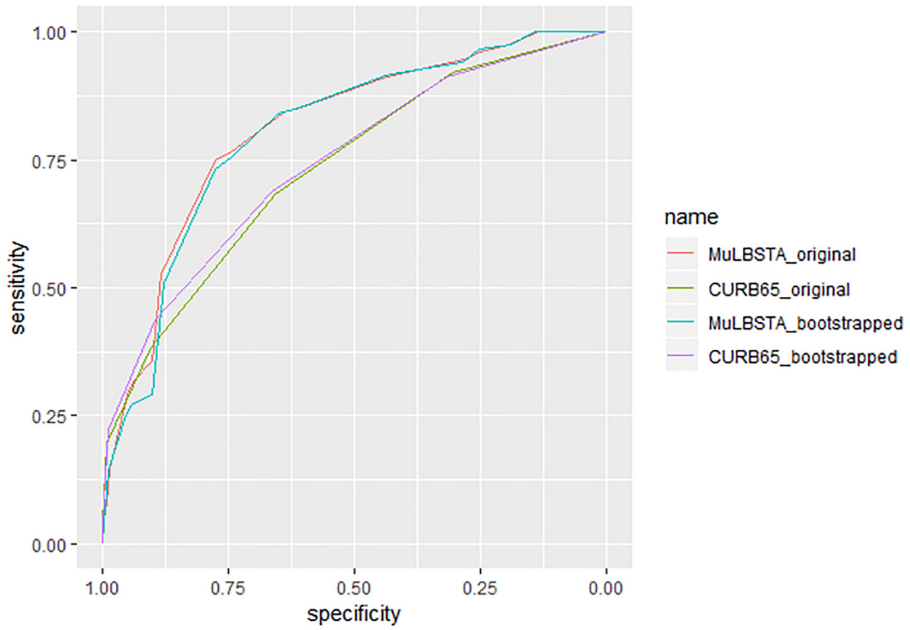

FIGURE 5 | Characteristic curves for prediction of patients with viral pneumonia (n = 528). C-index of MuLBSTA score and CURB-65 score are 0.811 and 0.735 separately. The bootstrapped (n = 2000) c-index of MuLBSTA and CURB-65 are 0.803 and 0.743.

in univariate regression. Meanwhile, IL-10 secreted along with adoptive transfer of Th2 $CD4^+$ T cell clones, but it was associated with delayed viral clearance and failed to cause protective effect (La Gruta et al., 2007). Although the test of interleukin is not yet widely available, we suggest that patients could be stratified by IL-2R and IL-6 regarding mortality risk.

Bacterial coinfection in the setting of viral pneumonia is known as another major cause of mortality. *Acinetobacter baumannii* is one of the most commonly encountered pathogens both in prior studies and in our investigation (Gao et al., 2013). We further compared patients with or without bacterial infection. Bacterial co-infection not only manifested with worsened outcomes but also prolonged hospital stay and significantly increased the cost of hospital care. Bacterial infection is an independent predictor without other driving forces.

Viral pneumonia further deteriorates when bacterial infection occurs spontaneously. This process is considered to be associated with the dysregulation of T-cell, antigen-specific T cell and plasma cytokine levels (Li and Cao, 2017). Levels of inflammatory cytokines, such as IL-6 and IL-18, were found to be higher in patients suffering bacterial and influenza virus co-infections than in patients infected by a sole pathogen (Li et al., 2012). As such, the remarkably increased IL-6 in patients co-infected with bacteria demonstrated its predictive potential once again.

Despite intense efforts, the development of antiviral therapy to prevent or treat respiratory virus infections is under limitation. Influenza antivirals as oseltamivir or zanamivir were commonly used on the basis of international recommendations (Jefferson et al., 2014). However, oral oseltamivir has a relatively strict time window and several secondary effects like nausea and renal syndromes, and it's hard to use for unconscious patients (Lee et al., 2017). There is no effective listed antiviral or vaccine approved for the prevention or treatment of non-influenza viruses (Heylen et al., 2017). In our study, oseltamivir was commonly used as antiviral therapy; while acyclovir, ganciclovir or foscarnet were used for cytomegalovirus or herpes simplex virus. Nevertheless, early antiviral treatment did not prevent progression to pneumonia consistent with earlier studies (Elizaga et al., 2001; Chemaly et al., 2012). The confused choice of respiratory virus therapy makes it urgent to predict mortality more accurately.

To date, a variety of studies concerning respiratory viruses were found to demonstrate risk factors by multivariate regression. Consistent with previous report, PO2/FiO2 $\leq$ 250 in combination with lymphopenia (peripheral blood lymphocyte count $<0.8*10^{9}/L$) were reported to be simple and reliable predictors of influenza (Shi et al., 2017). Multilobular infection was also noted in our study, which was also a remarkable factor in prior report (Jennings et al., 2008). In our study, PO2/FiO2 was also statistically significant mortality predictors according to univariate analysis, while the cut-off was adjusted to 260. Moreover, younger age, chronic comorbid conditions, morbid obesity, high-dose steroid use, hematopoietic stem cell therapy, lower levels of $CD4^+$T specific cells and a lack of early antiviral therapy were also regarded as independent risk factors for severe disease, according to prior reports (Viasus et al., 2011; Chemaly et al., 2012; Li and Cao, 2017). However, none of these were significant in our study.

The 2009 IDSA/ATS guidelines had recommended CURB-65 (confusion, urea, respiratory rate, blood pressure, age $\geq$65 year) as one of CAP severity score (Charles et al., 2009). However,

it had a low mortality rate among patients categorized as low risk (Mandell et al., 2007). Several studies argued that increasing age had worse predicting ability due to the fact that influenza A virus had been reported to occur in younger individuals (Riquelme et al., 2011; Bjarnason et al., 2012). Meanwhile, the relative mortality rate of virus infectious diseases in the elderly are reported more than twice those of the young (Pawelec et al., 2002). Early study suggested that a high $CD8^+$ T cell count and low NK activity correlated significantly with survival of infectious diseases in the elderly (Ogata et al., 2001), suggesting that aging could lead to increasing immunity deficiency and mortality. In our population of 528 hospitalized viral pneumonia patients, age $\geq$60 years was statistically associated with mortality while the weight coefficient was relatively small. It is not reasonable to completely deny the importance of age, but appropriate weight adjustment may enhance the predictive capacity of the model.

All parameters identified in the MuLBSTA score are easy to get clinically and all examinations are recommended to be done on admission of hospitalization. ROC and NRI analysis suggests that our new score has better predictive capacity in comparison with CURB-65. Moreover, the MuLBSTA score shows promise for the risk stratification of patients hospitalized with viral pneumonia. the death rates for each grade (**Table 5**) suggest the following risk categories: MuLBSTA 0-11 ('low-risk', mortality = 5.07%); MuLBSTA 12–22 ('high-risk', mortality = 33.92%). A higher MuLBSTA score might be used as a good predictor of prognosis.

Some limitations of this study should also be acknowledged. The retrospective single-center design leads to missing data and unavoidable biases in identifying and recruiting participants. The sample size was relatively small in order to build up a predicting score. Despite these limitations, the study was designed to reflect the 'real life' clinical situation. Clinical information was meticulously gathered using standard protocols by admitted medical team. This score might assist clinicians in making appropriate decisions and optimizing the use of hospital resources.

CONCLUSION

We found that the MuLBSTA score, based on six parameters routinely available in hospital, has a strong predictive ability for 90-day mortality. It can accurately stratify hospitalized patients with viral pneumonia into relevant risk categories and could provide guidance to make further clinical decisions.

DATA AVAILABILITY STATEMENT

The datasets analyzed for this study can be found in the Figshare. Link: https://figshare.com/articles/dataset_for_the_MuLBSTA_score_xlsx/10333475.

ETHICS STATEMENT

This study was approved by the Coordinating Ethics Committee of Ruijin Hospital Affiliated to Shanghai Jiao Tong University School of Medicine (No. 2017-205). Written informed consents were obtained from all patients involved before enrolment. In our study, patients from 18 to 96 years old were included. The consent obtained from the participants was both informed and written.

AUTHOR CONTRIBUTIONS

MZ and XZ conceived or designed the work. LG, DW, and YW collected the data. LG, DW, and QL analyzed and interpreted the data. LG, DW, QL, and JQ drafted the manuscript. All authors critically revised the manuscript and approved the final version of the manuscript to be published.

FUNDING

This work was supported by National Key R&D Program of China (Grant Nos. 2017YFC1309700 and 2017YFC1309701), by the National Natural Science Foundation of China (Grant No. 81570029), and by Shanghai Key Discipline for Respiratory Diseases (Grant No. 2017ZZ02014). This work was also funded in part by a grant from Innovative research team of high-level local universities in Shanghai, and by Institute of Respiratory Disease, School of Medicine, Shanghai Jiao Tong University.

SUPPLEMENTARY MATERIAL

The Supplementary Material for this article can be found online at: https://www.frontiersin.org/articles/10.3389/fmicb.2019.02752/full#supplementary-material

REFERENCES

Barlow, G., Nathwani, D., and Davey, P. (2007). The CURB65 pneumonia severity score outperforms generic sepsis and early warning scores in predicting mortality in community-acquired pneumonia. *Thorax* 62, 253–259. doi: 10.1136/thx.2006.067371

Bender, B. S., Croghan, T., Zhang, L., and Small, P. A. Jr. (1992). Transgenic mice lacking class I major histocompatibility complex-restricted T cells have delayed viral clearance and increased mortality after influenza virus challenge. *J. Exp. Med.* 175, 1143–1145. doi: 10.1084/jem.175.4.1143

Bjarnason, A., Thorleifsdottir, G., Löve, A., Gudnason, J. F., Asgeirsson, H., Hallgrimsson, K. L., et al. (2012). Severity of influenza A 2009 (H1N1) pneumonia is underestimated by routine prediction rules. Results from a prospective, population-based study. *PloS One* 7:e46816. doi: 10.1371/journal.pone.0046816

Charles, P. G., Davis, J. S., and Grayson, M. L. (2009). Rocket science and the Infectious Diseases Society of America/American Thoracic Society (IDSA/ATS) guidelines for severe community-acquired pneumonia. *Clin. Infect. Dis.* 48:1796. doi: 10.1086/599227

Chemaly, R. F., Hanmod, S. S., Rathod, D. B., Ghantoji, S. S., Jiang, Y., Doshi, A., et al. (2012). The characteristics and outcomes of parainfluenza virus infections in 200 patients with leukemia or recipients of hematopoietic stem cell transplantation. *Blood* 119, 2738–2745. doi: 10.1182/blood-2011-08-371112

Das, D., Le Floch, H., Houhou, N., Epelboin, L., Hausfater, P., Khalil, A., et al. (2015). Viruses detected by systematic multiplex polymerase chain reaction in adults with suspected community-acquired pneumonia attending emergency departments in France. *Clin. Microbiol. Infect.* 21, e1–e8. doi: 10.1016/j.cmi.2015.02.014

Elizaga, J., Olavarria, E., Apperley, J., Goldman, J., and Ward, K. (2001). Parainfluenza virus 3 infection after stem cell transplant: relevance to outcome of rapid diagnosis and ribavirin treatment. *Clin. Infect. Dis.* 32, 413–418. doi: 10.1086/318498

Gao, H. N., Lu, H. Z., Cao, B., Du, B., Shang, H., Gan, J. H., et al. (2013). Clinical findings in 111 cases of influenza a (H7N9) virus infection. *N. Engl. J. Med.* 368, 2277–2285. doi: 10.1056/NEJMoa1305584

Hanada, S., Pirzadeh, M., Carver, K. Y., and Deng, J. C. (2018). Respiratory Viral Infection-Induced Microbiome Alterations and Secondary Bacterial Pneumonia. *Front. Immunol.* 9:2640. doi: 10.3389/fimmu.2018.02640

Heylen, E., Neyts, J., and Jochmans, D. (2017). Drug candidates and model systems in respiratory syncytial virus antiviral drug discovery. *Biochem. Pharmacol.* 127, 1–12. doi: 10.1016/j.bcp.2016.09.014

Jefferson, T., Jones, M., Doshi, P., Spencer, E. A., Onakpoya, I., and Heneghan, C. J. (2014). Oseltamivir for influenza in adults and children: systematic review of clinical study reports and summary of regulatory comments. *BMJ Apr.* 9:348. doi: 10.1136/bmj.g2545

Jennings, L. C., Anderson, T. P., Beynon, K. A., Chua, A., Laing, R. T., Werno, A. M., et al. (2008). Incidence and characteristics of viral community-acquired pneumonia in adults. *Thorax* 63, 42–48. doi: 10.1136/thx.2006.075077

La Gruta, N. L., Kedzierska, K., Stambas, J., and Doherty, P. C. (2007). A question of self-preservation: immunopathology in influenza virus infection. *Immunol. Cell Biol.* 85, 85–92. doi: 10.1038/sj.icb.7100026

Lee, J., Park, J. H., Jwa, H., and Kim, Y. H. (2017). Comparison of Efficacy of Intravenous Peramivir and Oral Oseltamivir for the Treatment of Influenza: Systematic Review and Meta-Analysis. *Yonsei Med. J.* 58, 778–785. doi: 10.3349/ymj.2017.58.4.778

Leening, M. J., Vedder, M. M., Witteman, J. C., Pencina, M. J., and Steyerberg, E. W. (2014). Net reclassification improvement: computation, interpretation, and controversies: a literature review and clinician's guide. *Ann. Intern. Med.* 160, 122–131. doi: 10.7326/M13-1522

Li, H., and Cao, B. (2017). Pandemic and Avian Influenza A Viruses in Humans: Epidemiology, Virology, Clinical Characteristics, and Treatment Strategy. *Clin. Chest Med.* 38, 59–70. doi: 10.1016/j.ccm.2016.11.005

Li, W., Moltedo, B., and Moran, T. M. (2012). Type I interferon induction during influenza virus infection increases susceptibility to secondary Streptococcus pneumoniae infection by negative regulation of gammadelta T cells. *J. Virol.* 86, 12304–12312. doi: 10.1128/JVI.01269-12

Mandell, L. A., Wunderink, R. G., Anzueto, A., Bartlett, J. G., Campbell, G. D., Dean, N. C., et al. (2007). Infectious Diseases Society of America/American Thoracic Society consensus Guidelines on the Management of Community–Acquired Pneumonia in Adults. *Clin. Infect. Dis.* 44(Suppl. 2), S27–S72. doi: 10.1086/511159

Mortensen, E. M., Kapoor, W. N., Chang, C. C., and Fine, M. J. (2003). Assessment of mortality after long-term follow-up of patients with community-acquired pneumonia. *Clin. Infect. Dis.* 37, 1617–1624. doi: 10.1086/379712

Nussing, S., Sant, S., Koutsakos, M., Subbarao, K., Nguyen, T. H. O., and Kedzierska, K. (2018). Innate and adaptive T cells in influenza disease. *Front. Med.* 12, 34–47. doi: doi: 10.1007/s11684-017-0606-8

Ogata, K., An, E., Shioi, Y., Nakamura, K., Luo, S., Yokose, N., et al. (2001). Association between natural killer cell activity and infection in immunologically normal elderly people. *Clin. Exp. Immunol.* 124, 392–397. doi: 10.1046/j.1365-2249.2001.01571.x

Pappalardo, F., Pieri, M., Greco, T., Patroniti, N., Pesenti, A., Arcadipane, A., et al. (2013). Predicting mortality risk in patients undergoing venovenous ECMO for ARDS due to influenza A (H1N1) pneumonia: the ECMOnet score. *Intensive Care Med.* 39, 275–281. doi: 10.1007/s00134-012-2747-1

Pawelec, G., Barnett, Y., Forsey, R., Frasca, D., Globerson, A., McLeod, J., et al. (2002). T cells and aging, January 2002 update. *Front. Biosci.* 7, d1056–d1183. doi: 10.2741/a831

Riquelme, R., Jimenez, P., Videla, A. J., Lopez, H., Chalmers, J., Singanayagam, A., et al. (2011). Predicting mortality in hospitalized patients with 2009 H1N1 influenza pneumonia. *Int. J. Tuberc. Lung. Dis.* 15, 542–546. doi: 10.5588/ijtld.10.0539

Shi, S. J., Li, H., Liu, M., Liu, Y. M., Zhou, F., Liu, B., et al. (2017). Mortality prediction to hospitalized patients with influenza pneumonia: PO2 /FiO2 combined lymphocyte count is the answer. *Clin. Respir. J.* 11, 352–360. doi: 10.1111/crj.12346

Shorr, A. F., Zilberberg, M. D., Micek, S. T., and Kollef, M. H. (2017). Viruses are prevalent in non-ventilated hospital-acquired pneumonia. *Respir. Med.* 122, 76–80. doi: 10.1016/j.rmed.2016.11.023

Sterne, J. A., White, I. R., Carlin, J. B., Spratt, M., Royston, P., Kenward, M. G., et al. (2009). Multiple imputation for missing data in epidemiological and clinical research: potential and pitfalls. *BMJ* 29:b2393. doi: 10.1136/bmj.b2393

Uranga, A., Quintana, J. M., Aguirre, U., Artaraz, A., Diez, R., Pascual, S., et al. (2018). Predicting 1-year mortality after hospitalization for community-acquired pneumonia. *PloS One* 13:e0192750. doi: 10.1371/journal.pone.0192750

Viasus, D., Del Rio-Pertuz, G., Simonetti, A. F., Garcia-Vidal, C., Acosta-Reyes, J., Garavito, A., et al. (2016). Biomarkers for predicting short-term mortality in community-acquired pneumonia: a systematic review and meta-analysis. *J. Infect.* 72, 273–282. doi: 10.1016/j.jinf.2016.01.002

Viasus, D., Pano-Pardo, J. R., Pachon, J., Campins, A., López-Medrano, F., Villoslada, A., et al. (2011). Factors associated with severe disease in hospitalized adults with pandemic (H1N1) 2009 in Spain. *Clin. Microbiol. Infect.* 17, 738–746. doi: 10.1111/j.1469-0691.2010.03362.x

Zhou, F., Wang, Y., Liu, Y., Liu, X., Gu, L., Zhang, X., et al. (2019). Disease severity and clinical outcomes of community-acquired pneumonia caused by non-influenza respiratory viruses in adults: a multicentre prospective registry study from the CAP-China Network. *Eur. Respir. J.* 54:1802406. doi: 10.1183/13993003.02406-2018

Conflict of Interest: The authors declare that the research was conducted in the absence of any commercial or financial relationships that could be construed as a potential conflict of interest.

frontiers in Microbiology

ERRATUM
published: 09 June 2020
doi: 10.3389/fmicb.2020.01304

Erratum: Clinical Features Predicting Mortality Risk in Patients With Viral Pneumonia: The MuLBSTA Score

*Frontiers Production Office**

Frontiers Media SA, Lausanne, Switzerland

Keywords: virus pneumonia, predicting mortality, bacterial coinfection, predictive score model, clinical feature

OPEN ACCESS

Approved by:
Frontiers Editorial Office, Frontiers Media SA, Switzerland

***Correspondence:**
Frontiers Production Office
production.office@frontiersin.org

Specialty section:
This article was submitted to Infectious Diseases, a section of the journal Frontiers in Microbiology

Received: *20 May 2020*
Accepted: *22 May 2020*
Published: *09 June 2020*

Citation:
Frontiers Production Office (2020) Erratum: Clinical Features Predicting Mortality Risk in Patients With Viral Pneumonia: The MuLBSTA Score. Front. Microbiol. 11:1304. doi: 10.3389/fmicb.2020.01304

An Erratum on

Clinical Features Predicting Mortality Risk in Patients With Viral Pneumonia: The MuLBSTA Score
by Guo, L., Wei, D., Zhang, X., Wu, Y., Li, Q., Zhou, M, et al. (2019). Front. Microbiol. 10:2752. doi: 10.3389/fmicb.2019.02752

Due to a production error, the author "Jieming Qu" (jmqu0906@163.com) was not included in the Correspondence section. The publisher apologizes for this mistake.

The original article has been updated.

frontiers in Microbiology

REVIEW
published: 18 December 2019
doi: 10.3389/fmicb.2019.02789

Immune Biomarkers for Diagnosis and Treatment Monitoring of Tuberculosis: Current Developments and Future Prospects

*Yean K. Yong[1], Hong Y. Tan[1,2], Alireza Saeidi[3], Won F. Wong[4], Ramachandran Vignesh[1], Vijayakumar Velu[5], Rajaraman Eri[6], Marie Larsson[7] and Esaki M. Shankar[8]**

[1] Laboratory Center, Xiamen University Malaysia, Sepang, Malaysia, [2] Department of Traditional Chinese Medicine, Xiamen University Malaysia, Sepang, Malaysia, [3] Department of Pediatrics, Emory Vaccine Center, Atlanta, GA, United States, [4] Department of Medical Microbiology, Faculty of Medicine, University of Malaya, Kuala Lumpur, Malaysia, [5] Department of Microbiology and Immunology, Emory Vaccine Center, Atlanta, GA, United States, [6] School of Health Sciences, College of Health and Medicine, University of Tasmania, Launceston, TAS, Australia, [7] Division of Molecular Virology, Department of Clinical and Experimental Medicine, Linkoping University, Linkoping, Sweden, [8] Division of Infection Biology and Medical Microbiology, Department of Life Sciences, Central University of Tamil Nadu (CUTN), Thiruvarur, India

OPEN ACCESS

Edited by:
Aleksandra Barac, University of Belgrade, Serbia

Reviewed by:
Joel Fleury Djoba Siawaya, Centre Hospitalier Universitaire Mère-enfant Fondation Jeanne EBORI, Gabon
Matthieu Perreau, Lausanne University Hospital (CHUV), Switzerland
Cecilia Lindestam Arlehamn, La Jolla Institute for Immunology (LJI), United States

***Correspondence:**
Esaki M. Shankar
shankarem@cutn.ac.in

Specialty section:
This article was submitted to Infectious Diseases, a section of the journal Frontiers in Microbiology

Received: *06 June 2019*
Accepted: *18 November 2019*
Published: *18 December 2019*

Citation:
Yong YK, Tan HY, Saeidi A, Wong WF, Vignesh R, Velu V, Eri R, Larsson M and Shankar EM (2019) Immune Biomarkers for Diagnosis and Treatment Monitoring of Tuberculosis: Current Developments and Future Prospects. Front. Microbiol. 10:2789. doi: 10.3389/fmicb.2019.02789

Tuberculosis (TB) treatment monitoring is paramount to clinical decision-making and the host biomarkers appears to play a significant role. The currently available diagnostic technology for TB detection is inadequate. Although GeneXpert detects total DNA present in the sample regardless live or dead bacilli present in clinical samples, all the commercial tests available thus far have low sensitivity. Humoral responses against *Mycobacterium tuberculosis* (Mtb) antigens are generally low, which precludes the use of serological tests for TB diagnosis, prognosis, and treatment monitoring. Mtb-specific $CD4^+$ T cells correlate with Mtb antigen/bacilli burden and hence might serve as good biomarkers for monitoring treatment progress. Omics-based techniques are capable of providing a more holistic picture for disease mechanisms and are more accurate in predicting TB disease outcomes. The current review aims to discuss some of the recent advances on TB biomarkers, particularly host biomarkers that have the potential to diagnose and differentiate active TB and LTBI as well as their use in disease prognosis and treatment monitoring.

Keywords: biomarkers, diagnostics, treatment monitoring, tuberculosis, HIV

INTRODUCTION

Tuberculosis (TB) represents a major public health problem worldwide, and is transmitted via inhalation of aerosolized droplets carrying *Mycobacterium tuberculosis* (Mtb). It is estimated that approximately one-third (∼2 billion) of the global population is living with latent TB (LTBI) (World Health Organization [WHO], 2002), of which ∼10% likely progress to develop active TB within 2 years after initial exposure to the tubercle bacilli (Corbett et al., 2003). The risk of reactivation of latent TB is remarkably high among individuals infected with the human immunodeficiency virus (HIV) as well as in individuals on long-term immunosuppressive treatment with TNF-α inhibitors (Selwyn et al., 1989; Getahun et al., 2010; Day et al., 2018; Amelio et al., 2019). According to the latest

WHO Global TB Report, Mtb has led to 10 million cases of TB in 2017, and is also one of the top 10 causes of mortality with ∼1.6 million (1.3 and 0.3 million in HIV-negative and HIV-positive individuals, respectively) deaths in 2017, which translates to ∼4000 deaths each day (Tiberi et al., 2018; World Health Organization [WHO], 2018). Although universal Bacillus Calmette-Guérin (BCG) is administered in many countries, the vaccine is only effective against disseminated TB in children, and it's efficacy in adults largely remains controversial (Colditz et al., 1994; Zwerling et al., 2011; Amelio et al., 2017).

Tuberculosis treatment monitoring is paramount to clinical decision-making and the host biomarkers appears to play a significant role. Patients diagnosed with TB are generally put under a four drugs regimen (isoniazid, rifampicin, pyrazinamide, and ethambutol) for 2 months, known as the intensive phase; followed by 4 months maintenance phase with isoniazid and rifampicin. In spite of 6-long-months of anti-TB therapy, some patients however, will experience recurrence of infection and have an increased risk of M/XDR-TB. This 6-month duration may lead to prohibitive delay for clinical management. Exposure of Mtb to suboptimal drug concentrations risks robust bacterial replication and dissemination, increased rates of transmission and development of drug resistance. WHO reported an estimated 558,000 cases of rifampicin-resistant TB in 2017, of which 82% are infected with MDR-TB (World Health Organization [WHO], 2018). This has caused significant complications to the patients as they are to be treated with second-line drugs for an even longer duration (18–24 months) (World Health Organization [WHO], 2016), despite that their survival rate was merely <50% (World Health Organization [WHO], 2017). Hence, biomarkers that indicate an efficacious treatment at the early therapeutic phase as well as at the end of treatment, which predicts relapse could enormously improve clinical prognosis.

In order to achieve global control of TB disease, development of an effective novel vaccine (Zwerling et al., 2011) and novel drugs with shortened treatment duration (Abu-Raddad et al., 2009; Argun et al., 2016; Tiberi et al., 2018), as well as simpler and more accurate diagnostic tests (Walzl et al., 2011, 2018; Goletti et al., 2016, 2018) are of upmost importance. Hence, there is a pressing need to develop a low cost, minimal-invasive, non-sputum-based, highly sensitive and specific TB diagnostic test that uses easily accessible biological specimens such as blood and urine (Strimbu and Tavel, 2010; Nalejska et al., 2014; World Health Organization [WHO], 2014; Ballman, 2015; Buschmann et al., 2016; Goletti et al., 2016, 2018). Biomarkers can generally be divided into: (i) Mtb components, (ii) antibody responses to Mtb antigens, (iii) cellular immune responses to Mtb antigens, and (iv) unbiased "omics" approach (i.e., transcriptomics, proteomics and metabolomics). Here, we discussed some of the recent advances on TB biomarkers, particularly host biomarkers that have the potential to diagnose and differentiate active TB and LTBI as well as their use in disease prognosis and treatment monitoring. References for this review were identified through searches of PubMed for articles published from January 2005 to December 2018, by use of the terms "Mtb," "LTBI," "diagnosis," "biomarkers," "prognosis," "monitoring," "transcriptomics," and "proteomics." Articles resulting from these searches and relevant references cited in those articles were reviewed. Articles published in English alone were included.

PROSPECTS OF DETECTION OF BIOMARKERS ASSOCIATED WITH Mtb

Recent Advances in the Detection of Mtb by Conventional Methods

It is widely accepted that the currently available diagnostic technology for TB detection is simply inadequate (Wallis et al., 2010). The most widely used diagnostic test to date is the microscopic detection of acid-fast bacilli (AFB) in sputum, which suffers from poor sensitivity ranging from 34–80% (Davies and Pai, 2008). This is because the AFB test requires at least 10,000 bacilli/ml of sputum to produce a positive result. If the concentration of bacilli falls below the cut-off, the chance to produce an AFB positive result is merely <10% (World Health Organization [WHO], 2004; Moro et al., 2010; Desikan, 2013). Sputum culture is relatively more sensitive than sputum AFB test but has a turnaround time of a few weeks. Furthermore, culture of Mtb requires Biosafety Level 3 facilities (World Health Organization [WHO], 2007), which are seldom available across TB endemic areas.

The recently developed PCR-based technique to amplify Mtb gene namely GeneXpert MTB/RIF represents a major breakthrough in TB diagnostics. The test is not only easy to operate, requiring less training for laboratory personnel, but is also capable of "killing two birds with one stone" by detecting Mtb and rifampicin-resistance simultaneously within 2 h (Zeka et al., 2011; Kwak et al., 2013), thereby significantly improving the rates of detection of Mtb. However, its use is only limited to active pulmonary TB (PTB), and not LTBI. Besides, all the sputum-based diagnostic methods have their own intrinsic limitations in that they are seldom useful in the detection of extra-pulmonary TB (EPTB) disease. Hence, the diagnosis of EPTB is reliant on sampling of site-specific tissues as well as other biological fluids such as pleural fluid and cerebral spinal fluid (CSF) which often involve invasive procedures (Goletti et al., 2016). This could be a real problem as the incidence of EPTB in some developing countries ranges from 13% to as high as 37% (Arora and Chopra, 2007; Gomes et al., 2014; Gaifer, 2017), and sampling often involves invasive procedures. Therefore, the use of host biomarkers that reflect the pathological process or host immune responses to active TB, EPTB, and LTBI could be a better choice.

Developments in the Detection of Mtb DNA

From the pathogen perspective, detection of Mtb product such as Mtb DNA has been widely used as a diagnostic tool. GeneXpert has been shown to detect Mtb in a wide variety of clinical specimens including blood, urine, and CSF with better sensitivity and specificity as compared to Mtb culture (Cannas et al., 2008; da Cruz et al., 2011; Maynard-Smith et al., 2014; Theron et al., 2014). Sputum culture conversion either using solid and liquid media at the 2nd month post-initiation of TB therapy has long

been used to monitor the efficacy of TB treatment, although this method usually take weeks (World Health Organization [WHO], 2013). GeneXpert MTB/RIF offers rapid detection in this regard and has shown good sensitivity (97%) and correlation time to culture positivity, but suffers from poor specificity ranging from 49 to 72% (Marlowe et al., 2011; Friedrich et al., 2013). This is in part due to GeneXpert, which is a PCR-based technique that detects total DNA present in the sample regardless live or dead bacilli present in clinical samples. Nonetheless, others have shown that patients who are positive for Mtb in blood are at an increased risk for death (Feasey et al., 2013). By using digital PCR (dPCR), a theoretically ten-fold more sensitive technique than real-time quantitative PCR, Li et al. developed a MTB detection test based on the MTB insertional sequence IS6110. This novel assay has been shown to have ∼twofold higher sensitivity than GeneXpert MTB/RIF assay in detecting MTB among probable and possible TB meningitis patients (Li et al., 2019).

Prospects of Detecting Miscellaneous Components of Mtb

Other Mtb components such as the 17.5 kDa Mtb cell wall lipoarabinomannan (LAM) has also been used to detect the presence of Mtb in urine. However, all the commercial tests available thus far have low sensitivity. In a meta-analysis, Minion et al. (2011) showed that the sensitivity of urine LAM test in seven studies is highly variable ranging from 13 to 93%. Hamasur et al. (2015) had further improved the assay by concentrating the LAM antigen present in urine up to 5–100 times using immunoprecipitation method. This action has enhanced the sensitivity of the urine LAM assay, but only restricted to HIV-TB co-infected patients. The sensitivity of the assay among HIV-negative TB patients remains very low (Hamasur et al., 2015). Several possible reasons might explain the higher sensitivity of LAM assay in HIV patients; (i) there might be a higher Mtb load among HIV patients since they are immunodeficient (Boehme et al., 2005; Shah et al., 2010); or (ii) there might have been HIV-associated nephropathy among these patients that increases the glomerular permeability resulting in higher levels of LAM in urine (Doublier et al., 2007; Peter et al., 2010). Nonetheless, the assay has been used to monitor anti-TB therapy responses (Drain et al., 2015) and has also been shown to predict the onset of TB-associated immune reconstitution inflammatory syndrome (TB-IRIS) (Conesa-Botella et al., 2011) and death (Gupta-Wright et al., 2016) among TB-HIV co-infected patients.

Another Mtb secretory protein, the 30–35 kDa antigen 85 complex (Ag85A, Ag85B, and Ag85c) (Kashyap et al., 2005, 2007), early secretory antigen target-6 (ESAT-6), culture filtrate protein-10 (CFP-10) (Kalra et al., 2010; Feng et al., 2011; Shen et al., 2011; Zhang et al., 2015) and MPT64 (Kumar et al., 2011; Martin et al., 2011; Arora et al., 2015) have also been evaluated for their suitability as diagnostic reagents. The Ag85 complex is present in the sputum of patients with PTB (Kashyap et al., 2007) as well as in the CSF of patients with TB meningitis (Kashyap et al., 2005); but the sensitivity is inconsistent in various studies (Bentley-Hibbert et al., 1999; Kashyap et al., 2007). Other secretory proteins such as ESAT-6, CFP-10, and MPT64 are facing a similar problem. In one study, Turbawaty et al. attempted to detect the presence of all the three antigens in urine using a cocktail of polyclonal antibodies against all the three antigens. The authors showed that this strategy increased the sensitivity to 90%, although the specificity remained poor at <30% (Turbawaty et al., 2017).

PROSPECTS WITH DETECTION OF HOST IMMUNE BIOMARKERS IN Mtb INFECTION

Host Antibody Responses to Mtb Antigens

Infection and immunity are the two sides of the same coin. When an individual is infected with Mtb, the pathogen will inevitably activate the immune response of the host leading to changes in host biomarkers. Pathogen-specific antibodies are the commonly used host biomarkers for pathogen diagnostics as they are simple to perform, inexpensive and are feasible for point-of-care. Many of the available serological tests employ either the lateral-flow or the ELISA format. A number of Mtb antigen-specific antibodies against PPD, antigen 60, ESAT-6, CFP-10, lipid-derived antigens and heat shock protein have been studied extensively (Verma and Jain, 2007). Of note, several Mtb antigens such as ESAT-6 and CFP-10 are not present in the genome of BCG strain, and hence detection of an immune response specific to these antigens can distinguish between and Mtb infection from vaccination responses (Andersen et al., 2000; Arend et al., 2000). Unfortunately, these assays so far have displayed poor sensitivity (ranges from 14% – 85%) and specificity (53–98.7%) (Steingart et al., 2007, 2009, 2011; Achkar and Ziegenbalg, 2012; Lagrange et al., 2014).

More recently, several highly antigenic MTB antigens have been developed for diagnostics with improved sensitivity and specificity than the classical ESAT-6- and CFP-10-based assays such as RV0310c-E and RV1255c-E. Receiver operating characteristic (ROC) analyses have shown that serum IgG against both RV0310c-E and RV1255c-E antigens has better sensitivity and specificity (AUC = 0.8 and 0.808, respectively) in diagnosing MTB compared to ESAT-6 and CFP-10 (AUC = 0.665 and 0.623, respectively) (Luo et al., 2017). Lopez-Ramos et al. (2018) showed that the antibodies against MTB antigen P12037 has a sensitivity and specificity of 92% and 91%, respectively in diagnosing active TB when used in concert with sCD14. Other researchers have found that antibody to MTB antigens such as proline-proline-glutamic acid protein 17 (PPE17) (Abraham et al., 2018) and mycobacterial DNA binding protein (MDP-1) (Maekura et al., 2019) can differentiate between patients with LTBI and active TB. Maekura et al. (2019) further showed that MDBP-1 may also be a good monitoring tool as persistently elevated IgG against MDBP-1 post anti-TB therapy could be associated with relapse after completion of treatment. Nonetheless, studies have also found that antibody responses against Mtb antigens are generally low among children (Achkar and Ziegenbalg, 2012) therefore, the use

of serological tests for TB diagnosis, prognosis, and treatment monitoring can only be effectively used among adult patients.

One interesting study by Lu et al. on "resister," a group of individuals highly exposed to MTB but who tested negative by T-cell based interferon gamma releasing assay (IGRA) and tuberculin skin test (TST), as well as did not develop LTBI has shed some light on TB pathogenesis. The authors found that the "resister" possessing MTB-specific IgM and class switched IgG; however, displayed reduced CD4-mediated IFN-γ responses toward ESAT-6, CFP-10, Ag85A, and Ag85B. Lu et al. (2019) also showed that the IgG of "resister" has higher avidity to MTB antigens compared to LTBI and healthy controls and further analysis also showed that the "resister" had significantly higher levels of IgG1 compared to other IgG subclasses. This suggests that the level of IgG1 could potentially be a prognosis biomarker, and holds the key to development of novel MTB therapeutics.

Host Cytokine Responses to Mtb Antigens – Beyond Interferon-γ

Unlike antibody responses, the cellular immune responses against Mtb-specific antigens have shown better consistency. In the past, the TST has been widely used to diagnose active TB and LTBI. However, due to cross-reactivity, the test cannot differentiate between Mtb and other non-tuberculous mycobacterial infections as well as BCG vaccination. Besides, the TST also suffers from poor sensitivity among immunocompromised patients (Nahid et al., 2006; Frahm et al., 2011). Since the last decade, the T-cell based IGRA has emerged as the most popular tool in TB diagnostics (Ferrara et al., 2009). IGRA measure IFN-γ production after *ex vivo* stimulation of whole blood with Mtb-specific antigens such as ESAT-6 and CFP-10 (Lalvani et al., 2001b; Mori et al., 2004). There are two formats of IGRA assay, the ELISA-based QuantiFERON TB Gold assay (Mori et al., 2004) and the ELISPOT-based T-SPOT assay (Lalvani et al., 2001a). The T-SPOT assay has a higher sensitivity compared to QuantiFERON TB Gold assay in detecting active TB (91 and 80.2%, respectively) (Bae et al., 2016). In general, IGRA is sensitive and more specific than TST (Pai et al., 2008). Although IGRA is less affected by the HIV-status as compared to TST (Mendelson, 2007; Rangaka et al., 2007), the assay appears to perform poorly in children with advanced HIV infection (Hormi et al., 2018); however, IGRA performed using peripheral blood mononucleocytes (PBMC) isolated from specific sites of TB disease such as pleural fluid, bronchioalveolar lavage (BAL) and CSF has been found to be highly sensitive and specific (Losi et al., 2007; Thomas et al., 2008).

Some studies suggested that IGRA response is stronger in active TB than LTBI, and hence, allows the differentiation of the two forms of TB disease (Janssens, 2007). However, other studies suggested that IGRA may not be suitable for the diagnosis of active TB and LTBI in high TB-burden regions (Sharma et al., 2017). This may be attributed to the nature of the antigen used in the IGRA, i.e., ESAT-6 and CFP-10 as they are secretory proteins of MTB especially during active infection. One study by Arroyo et al. (2018) showed that the use of latency-related antigens, i.e., dormancy survival regulon (DosR) and resuscitation promoting factor (Rpf) in IGRA could be better. The DosR peptide RV2029c and the Rpf peptide RV2389c have shown to differentiate LTBI from active PTB with a sensitivity of 90 and 85%, respectively (Arroyo et al., 2018).

Given the sensitivity and specificity of IGRA, the assay has also been suggested for use as a treatment monitoring tool (Ribeiro et al., 2009; Bocchino et al., 2010; Chee et al., 2010). Several studies have shown that patients who are IGRA negative on completion of anti-TB therapy experienced complete clinical and microbiological recovery (Goletti et al., 2008; Kabeer et al., 2011; Helmy et al., 2012). Another cohort by Kaneko et al. (2015) showed that patients who were IGRA positive at the end of treatment developed TB reactivation; whilst those who were IGRA negative did not develop TB reactivation for 2 years of follow-up.

One advantage of IGRA as an *ex vivo* stimulation assay is that the same assay tubes can be re-used to study other biomarkers either by multiplex cytokine bead array or by flow cytometry to obtain "biosignature" that may differentiate between different stage of TB disease (Chegou et al., 2009). One biomarker at the downstream of IFN-γ, i.e., IP-10 has shown to be of good use as a biomarker. Elevation of plasma level of IP-10 in un-stimulated tubes has been associated with active TB (Azzurri et al., 2005; Whittaker et al., 2008; Lighter et al., 2009; Novel et al., 2013; Petrone et al., 2015). IP-10 not only is as sensitive as IFN-γ (Kabeer et al., 2011) in blood but also offer several additional advantages. For instance, detection of IP-10 in the urine of children (Petrone et al., 2015) and adults (Darrah et al., 2007) with active TB makes sample collection easier. Further, unlike IFN-γ, IP-10 is less affected by HIV status; making it a robust biomarker to be used in *ex vivo* stimulation assays (Ruhwald et al., 2008; Goletti et al., 2010a,b; Kabeer et al., 2011).

Several studies have been conducted using multiplex cytokine bead array on plasma with or without *ex vivo* stimulation to differentiate active TB and LTBI. These studies employ a combination of 5–15 biomarkers in their analysis whose sensitivity ranges from 82.3 to 96.7% (Mihret et al., 2013; Won et al., 2017; La Manna et al., 2018). Despite the combination of biomarkers used by different studies, IFN-γ and IP-10 are the most common biomarkers used in these studies. Besides, other studies have shown that the ratio of IFN-γ and IL-10 (Sai Priya et al., 2010), ratio of IL-2 and IFN-γ (Wu et al., 2017), IL-8, IP-10, MIP-1α, sIL-2Rα, vascular endothelial growth factor (VEGF), MCP-3 (Yao et al., 2017; Hoel et al., 2019) as well as soluble markers to TLR-4 pathway such i.e., sCD14, MD-2, and LPS (Feruglio et al., 2013) can distinguish between active TB and LTBI and can also correlate with treatment success. By screening 38 cytokines, Luo et al. (2019) found that by using a combination of three cytokines, i.e., eotaxin, CCL22 and MCP-1, they were able to discriminate LTBI from active TB with a sensitivity and specificity of 87.8 and 91.8%, respectively (AUC = 0.94). Other plasma markers that associated with treatment success (measured as time to sputum conversion) include IL-6, MCP-1 (Djoba Siawaya et al., 2009), VEGF (Riou et al., 2012), hemeoxygenase-1 (HO-1), matrix metalloproteinases (MMP) (Andrade et al., 2013), serum amyloid, proteasome activation

complex subunit-1, IL-11 receptor antagonist, and 2-antiplasmin (Nahid et al., 2014). However, further studies are required to evaluate and validate these markers.

Host Cellular Immune Responses to Mtb Antigens

Flow cytometry is a powerful technique used to analyze the characteristics of individual cells within heterogeneous populations. In principle, following Mtb antigen exposure, $CD4^+$ and $CD8^+$ T cells undergo several stages of differentiation from naïve T-cells (T_N) progressing to central memory (T_{CM}), effector memory (T_{EM}) and finally to terminally differentiated T cells (T_{EMRA}) (Harari et al., 2011; Rovina et al., 2013); and the more antigenic exposure (in quantity, antigenicity, and duration) of T cells the more advance the cellular differentiation. Based on this principle, several efforts have been made to characterize the functional signature of T cells (i.e., the combination of subsets and their cytokine production) that associated with stages of TB disease. CD69 is a co-stimulatory receptor and an early activation marker (Borrego et al., 1999; Yong et al., 2017) and increased levels of $CD4^+CD69^+IFN\text{-}\gamma^+$ T cells is associated with early active TB or recent TB infection (Nikolova et al., 2013). Similarly, the frequency of CD137, a co-stimulatory molecule responsible to sustain effective activation, proliferation and survival of T-cells has also been shown to be associated with active TB (Yan et al., 2017).

A study done by Millington et al. (2007) reported that the polyfunctional $CD4^+$ $IFN\text{-}\gamma^+IL\text{-}2^+TNF\text{-}\alpha^+$ T cells are predominantly seen in patients with active TB as compared to $CD4^+IL\text{-}2^+IFN\text{-}\gamma^+$ T cells and $CD4^+IFN\text{-}\gamma^+$ only in LTBI. More detail studies found that the non-active form of TB response including LTBI or BCG vaccination and treated TB are associated with predominant $CD4^+IFN\text{-}\gamma^+IL\text{-}2^+$ T_{EM} and $CD4^+IL\text{-}2^+$ T_{CM}; whilst active TB is associated with predominantly $CD4^+IFN\text{-}\gamma^+$ T_{EMRA} cells (Sutherland et al., 2009; Caccamo et al., 2010; Casey et al., 2010; Sester et al., 2011). By using CD38, an immune activation marker and CD27, a maturation marker, Ahmed et al. (2018) showed that active TB was associated with increased frequency of CD38 + $CD27^{low}$; whilst LTBI was associated with CD38-$CD27^{high}$. Another study showed that LTBI is associated mostly with polyfunctional $CD4^+$ T cells expressing IFN-γ, IL-2, and TNF-α and in combination; whilst active TB is predominated with $CD4^+$ T cells expressing only TNF-α, and not IFN-γ as measured by IGRA (Harari et al., 2011). CD27, a member of TNF-α receptor superfamily was found to be useful in differentiating active TB and LTBI. Streitz et al. (2007) showed that active TB patients had significantly higher $CD4^+CD27^+$ T cells as compared to BCG vaccinees and patients with LTBI had an intermediate level of $CD4^+CD27^+$ T-cells. Other studies found that CD27 (Adekambi et al., 2012; Nikitina et al., 2012; Petruccioli et al., 2013, 2015; Portevin et al., 2014) and Mtb-specific $CD4^+$ T cells (Adekambi et al., 2012; Nikolova et al., 2013) correlate with Mtb antigen/bacilli burden and hence might serve as good biomarkers for monitoring treatment progress. Other subpopulations of T cells such as IL-10 + Th17 T cells were found to be significantly higher among LTBI; whilst IFN-γ + Th17 was significantly higher in active TB when stimulated with DosR (Rakshit et al., 2017). Besides T-cells, dendritic cells, especially the percentage of BDCA3 + mDC and CD123 + pDCs were significantly reduced in patients with active TB; while the same subtypes were found to be significantly activated among patients with LTBI (Parlato et al., 2018).

Several other surface markers including the immune activation marker CD38 and HLA-DR, the proliferation marker Ki-67 (Adekambi et al., 2012) as well as the percentage of myeloid-derived suppressor cells (MDSCs) (El Daker et al., 2015) have also been suggested as biomarkers to monitor treatment efficacy. The expression of immune activation markers such as CD38 and HLA-DR on T cells was significantly reduced by week 9 after initiation of the anti-TB therapy. The slope of decline in the expression of these markers was correlated with the time of stable culture conversion (Ahmed et al., 2018). Study also showed that individuals had a substantial amount of T_{EM} at the sixth month of anti-TB therapy suggesting that persistence of live Mtb may lead to relapse; while individuals who retained only T_{CM} may hint complete clearance of Mtb (Goletti et al., 2006; Butera et al., 2009; Millington et al., 2010; Wang et al., 2010; Pollock et al., 2013; Chiacchio et al., 2014; Petruccioli et al., 2015). Similarly, follow up on the anti-TB treatment showed that patients who had significant reduction in TB load showed a shift from $CD4^+IFN\text{-}\gamma^+$ T_{EMRA} cells to $CD4^+IFN\text{-}\gamma^+IL\text{-}2^+$ T_{EM} (Caccamo et al., 2010). In a longitudinal prospective study on active TB on anti-TB therapy, Ferrian et al. studied the association between Tregs and treatment efficacy. By using cut-off point at day 71 after initiation of anti-TB therapy, the authors classified the patients into two groups: (i) those who achieved stable sputum culture conversion faster than day 71 as rapid responders, and (ii) those achieved stable sputum culture conversion later than day 71 as slow responders. The authors found that the frequencies of Treg was significantly higher in slow responders and could predict time to stable culture conversion with the sensitivity of 81% and specificity of 85% (AUC = 0.87).

PROSPECTS OF BIOMARKERS BY UNBIASED "OMICS" APPROACH

Omics approach, i.e., genomic, transcriptomic, proteomic and metabolomics is a high throughput method that allows thousands of biomarkers of multi-dimension, to be unbiasedly acquired in one step (Kell and Oliver, 2004). While genomics provide an overview of genetic instruction provide by DNA, transcriptomics would investigate the gene expression patterns, proteomics the dynamic of protein products, and metabolomics the interactions and understanding of the entire metabolism of an individual in a disease setting. These "omics" approaches have been used not only in TB diagnosis, monitoring treatment efficacy, predicting treatment outcomes, but also used to improve understanding the pathogenesis of TB disease.

One genomic study has investigated SP110, a gene encoded for IFN-induced nuclear protein in a large cohort of patients including 301 active TB, 68 LTBI and 278 healthy controls. From the 5 index SNPs, i.e., rs7580900, r7580912, rd9061, rs11556887, and rs2241525, the study identified that rs9061 was significantly associated with increased susceptibility to LTBI (Chang et al., 2018). Further investigations indicated that individuals bearing this SNP had decreased levels of plasma TNF-α (Leu et al., 2018).

One transcriptomic study identified a profile of 393-transcripts signatures in whole-blood characterizing active TB; and 86-transcript signature that distinguishes TB from other infections. Through modular and pathway enrichment analysis the study revealed that active TB was predominated with neutrophil-driven interferon-inducible genes, consisting of both IFN-γ and type I IFN-αβ signaling (Berry et al., 2010). These findings have been further validated by several independent cohorts (Lesho et al., 2011; Maertzdorf et al., 2011a,b; Ottenhoff et al., 2012; Bloom et al., 2013; Kaforou et al., 2013; Walter et al., 2015) and the profile of transcript signatures decreased after the initiation of treatment (Ottenhoff, 2009; Bloom et al., 2013; Cliff et al., 2016). Moreover, Anderson et al. (2014) also showed that the transcription profile was able to distinguish between active TB and LTBI.

The cytotoxic cell gene transcripts may also be used for end treatment assessment to predict TB relapse (Joosten et al., 2012; Cliff et al., 2016). Maertzdorf et al. (2011b) found that the high-affinity IgG Fc receptor IB (FcγRIB) along with other four different transcripts are differentially expressed among between active TB and LTBI. Other transcripts such as lactotransferrin, CD64 (also known as FcγR1A) also can discriminate active TB from LTBI (Sutherland et al., 2014). Another study by Lee et al. (2016) found that genes related to innate immune responses are highly expressed among patients with active TB; whilst genes related to apoptosis and natural killer (NK) cell activation are predominantly expressed in patients with LTBI. RAS and RAB interactor 3 (RIN3) also could discriminate between active TB, LTBI, and recurrent infection (Mistry et al., 2007).

In the pass, the transcriptomic studies have mainly studied the profiling of mRNA expression, but more recently, there has been a growing interest on the non-coding region of mRNA. Although these non-coding RNA does not encode for any protein, they do possess certain regulatory functions and hence may be altered by different stages of TB disease. By comparing the micro RNA (miRNA) profile of children infected with TB, adult patients with active PTB, active EPTB, TB/HIV co-infection as well as LTBI, Miotto et al. (2013) managed to identify a set of 15 miRNA signature that was common for TB infection with a sensitivity and specificity of 82 and 77%, respectively. Another study by Fu et al. has looked into the circular RNA (circRNA) and their association with TB disease. circRNA is a recently discovered, endogenous, covalently closed without free 3′- and 5′-end non-coding RNA. Being a covalently closed circular RNA, it is highly resistant to RNase degradation and hence are abundant and long-lasting in cells. The authors found that there were 171 deregulated circRNA in TB infection where circRNA_103017, circRNA_059914, circRNA_101128 were most profoundly elevated whilst circRNA_062400 was decreased. This circRNA signature could potentially be a useful marker for TB (Fu et al., 2019). Chakrabarty et al. (2019) also identified several miRNA including 2 from human, i.e., hsa-miR-146a-5p and hsa-miR-125b-5p and one miRNA from MTB, i.e., MTB-miR5 that increased among patients with active TB. miRNA has also been used to differentiate LTBI from active TB. By studying 250 miRNAs, Lyu et al. (2019) also identified the patterns where the hsa-let-7e-5p, hsa-let-7d-5p, hsa-miR-450a-5p, and has-miR-140-5p were differentially expressed among patients with LTBI; whilst hsa-miR-1246, hsa-miR-2110, hsa-miR-370-3p, hsa-miR-28-3p, hsa-miR-193b-5p were associated differentially expressed among patients with active TB.

Besides, by using proteomic microarray method, Hai et al. screened 4262 MTB antigens and found that IgG toward 152 Mtb antigens were differentially elevated among patients with active TB when compared to patients with LTBI. Further analysis showed that RV2031c, RV1408 and RV2421c were able to discriminate between active TB and LTBI (Cao et al., 2018). By studying 1011 host serum biomarkers, Liu et al. found that 153 protein were significantly elevated among patients with severe TB. These included α-1-acid glycoprotein 2 (ORM2), IL-36α, s100 calcium-binding protein (S100-A9), and superoxide dismutase (SOD) (Liu et al., 2018). Aiming to improve understanding on TB progression, Duffy et al. investigated a cohort of household contacts of TB index cases HHCs and non-human primate challenge model. By combining both blood transcriptomic, serum metabolomics and pathway analysis, the authors identified a novel immunemetabolic signature involving cortisol, tryptophan, glutathione and tRNA acylation that associated with the progression of latent to active TB (Duffy et al., 2019).

Summary of each biomarkers and their applications are given in **Table 1**.

FUTURE DEVELOPMENTS AND CONCLUSION

As omics approach is capable to provide a more holistic picture for the disease mechanisms and hence more accurate in predicting disease outcomes (Clarke et al., 2008; Heidecker et al., 2008; Gesthalter et al., 2015; Jong et al., 2016; Kohonen et al., 2017; Lowe et al., 2017). Based on the omics profile, new hypotheses will be generated for further examination. There have already been a few successful cases in the search for TB biomarkers (Weiner et al., 2012; Kaforou et al., 2013; Goletti et al., 2016; Maertzdorf et al., 2014, 2016; Weiner and Kaufmann, 2017) and the number of study is still increasing. It is also worthwhile to point out that Mtb-specific immune responses are probably not homogenous in human populations and might be influenced by HIV-1 co-infection, heredity and several other exogenous environmental factors [183–185]. State-of-the-art data mining tools including supervised and unsupervised learning as

TABLE 1 | Biomarkers for diagnosis, prognosis, and monitoring of MTB infection.

	Biomarker	Specimen					Application					Remark
		Sputum	Body fluids	CSF	Blood/ serum/ plasma	PBMC	Mtb diagnosis	Distinguish active TB vs. LTBI	Monitoring	Predict relapse /worsen/ progress	Predict treatment success	
Microbiology technique	AFB staining	•	•	•	•		•		•			– Rapid, convenient and inexpensive test – Non-specific, must accompanied with confirmation tests – Limited sensitivity; required at least 5000 AFB/mL to be detected – High false negative rate
	Mtb culture	•	•	•	•		•		•			– Long turnaround time (3–8 weeks) – Required biosafety level three facilities to handle Mtb culture
Detection of Mtb components	Mtb DNA detection (GeneEpert)	•	•	•	•		•			•		– Rapid, diagnosis, and detection of drug resistant Mtb – Low sensitivity (49–72%) – Patient positive with Mtb in blood assoc. with increased risk of death
	Mtb antigens • LAM		•						•	•		– Low sensitivity (13–93%) – Use to monitor anti-TB response in TB-HIV – co-infected patients – Predict TB-IRIS and death among TB-HIV co-infected patients
	Mtb antigens • Ag 85 complex, ESAT-6, CFP-10, MPT64	•	•	•	•							– Sensitivity is in consistent Poor specificity
	Digital PCR (dPCR)				•		•					– Supreme sensitivity then conventional qPCR – Twofold higher sensitivity than GeneXpert in detecting MTB among probable/possible TB meningitis – The study uses CSF, but can be apply for sputum, serum/plasma and other body fluid

(Continued)

TABLE 1 | Continued

	Biomarker	Specimen					Application					Remark
		Sputum	Body fluids	CSF	Blood/ serum/ plasma	PBMC	Mtb diagnosis	Distinguish active TB vs. LTBI	Monitoring	Predict relapse /worsen/ progress	Predict treatment success	
Host antibodies responses against ex-vivo stimulation of Mtb Ags	PPD, Ag60, ESAT-6, CFP-10	•			•							– Poor sensitivity (14–85%); poor specificity (53–98%) – Antibody response usually very low among children
	RV0310c-E RV1255c-E				•		•					– Better sensitivity than ESAT-6 and CFP-10
	P12037				•		•					– Sensitivity = 92%, specificity = 91%
	PPE17 MDP-1				•		•	•	•			– More antigenic antigen than ESAt-6 and CFP-10
	RV2031c, RV1408, RV2421c				•		•	•				– IgG against these three Ags were initial identified by screening done by proteomics
Host cytokines responses against ex-vivo stimulation of MTB Ags	Tuberculin skin test (TST)	–	–	–	–	–	•	•	•			– Poor sensitivity among HIV/immunocompromised patients
	Ag: ESAT-6, CFP-10 IFN-γ (IGRA)				•	•	•			•	•	– T-SPOT sensitivity (91.2%); QuantiFERON sensitivity (80.2%) – More specific than TST – Less affected by HIV-status compared to TST – Predict TB-reactivation within 2 years – Associated with complete clinical and microbiological recovery
	Ag: ESAT-6, CFP-10 IP-10				•		•	•				– High IP-10 in unstimulated tube associated with active TB – Less affected by HIV status

(Continued)

TABLE 1 | Continued

	Biomarker	Specimen					Application					Remark
		Sputum	Body fluids	CSF	Blood/ serum/ plasma	PBMC	Mtb diagnosis	Distinguish active TB vs. LTBI	Monitoring	Predict relapse /worsen/ progress	Predict treatment success	
	Ag: ESAT-6, CFP-10 sCD14, MD-2, LPS				•		•	•			•	– Distinguish between active-TB and LTBI – Levels correlated with treatment success
	Ag: ESAT-6, CFP-10 IL-8, MIP-1a, sIL-2Ra, VEGF, MCP-3				•		•	•				
	Ag: ESAT-6, CFP-10 IL-6, MCP-1, VEGF, HO-1, MMP, IL-11R antagonist, 2-antiplasmin				•						•	
Host cytokines responses against ex-vivo stimulation of MTB Ags	**Ag:** ESAT-6, CFP-10 ratio of IL-2/IFN-γ				•		•	•				
	Ag: ESAT-6, CFP-10 eotaxin, CCL22, MCP-1				•		•	•				– When used in combination, the sensitivity = 87.8% and specificity = 91.8%
	Ag: DosR, RV2029c, Rpf, RV2389c IFN-γ (IGRA)				•	•	•	•				– Both DosR and Rpf are antigen expressed during latent infection – When used in combination, the sensitivity = 90% and specificity = 85%
Host cellular immune responses against ex-vivo stimulation of Mtb antigens	CD4 + CD69 + IFN-γ+					•	•	•				– Associate with early or recent Tb-infection
	CD4 + IFN-γ + IL-2 + T_{EM}					•	•	•				– Associated with LTBI

(Continued)

TABLE 1 | Continued

Biomarker	Specimen					Application					Remark
	Sputum	Body fluids	CSF	Blood/ serum/ plasma	PBMC	Mtb diagnosis	Distinguish active TB vs. LTBI	Monitoring	Predict relapse /worsen/ progress	Predict treatment success	
CD4 + IL-2 + T_{CM}					•	•	•				– Associated with LTBI
CD4 + IFN-γ + T_{EMRA}					•	•	•			•	– Associated with active TB-infection
											– Shift of functional signature from CD4 + IFN-γ + T_{EMRA} to CD4 + IFN-γ + IL-2 + T_{EM} after completion of ATT indicate successful treatment
CD4 + IFN-γ + IL-2 + TNF-α+					•	•	•			•	– Associated with active TB-infection
CD4 + IFN-γ + IL-2+					•	•	•			•	– Associated with active LTBI
CD4 + IFN-γ+					•	•	•			•	– Associated with active LTBI
											– Shift of functional signature from CD4 + IFN-γ + TNF-α + to CD4 + IFN-γ + IL-2 + or CD4 + IFN-γ + after completion of ATT indicate successful treatment
T_{EM} T_{CM}					•				•	•	– High T_{EM} at sixth months of ATT assoc. with TB reactivation
											– High T_{CM} at sixth months of ATT assoc. with complete clearance of TB
CD4 + CD27+					•	•	•				– Differentiate between active TB and LTBI
											– High CD4 + CD27 + associated with active TB
											– Intermediate CD4 + CD27+ associated with LTBI
CD137 + T-cells				•	•						– Is a member of TNF receptor superfamily
											Associated with active TB
IL-10 + Th17				•	•		•				– Associated with LTBI, when stimulated with DosR

(Continued)

TABLE 1 | Continued

	Biomarker	Specimen					Application				Remark
		Sputum	Body fluids	CSF	Blood/ serum/ plasma	PBMC	Mtb diagnosis	Distinguish active TB vs. LTBI	Monitoring	Predict relapse /worsen/ progress	Predict treatment success	
	IFN-γ + Th17				•	•		•				– Associated with active TB, when stimulated with DosR
	%BDCA3 + mDC				•	•		•				– Reduction in% indicated active TB infection
	%CD123 + pDC MFI BDCA3 + mDC MFI CD123 + pDC				•	•		•				– Increase activation markers in these subsets indicated LTBI
	CD38, HLA-DR								•	•	•	– Used for monitoring of time to culture conversion after initiation of anti-TB therapy – Slope of reduction in CD38 and HLA-DR correlated with time to culture conversion
	Treg								•	•	•	– Low% of Treg found among rapid responder – Percentage of Treg inversely correlated with time to culture conversion
Genomics, transcriptomic, proteomics, and metabolomics	• Neutrophil derived IFN-γ, IFN-α and β					•	•	•				– Further validations required
	• FcγR1B					•	•	•				– Further validations required
	• Lacto transferrin CD64, RIN3					•	•	•				– Further validations required
	circRNA _103017, _059914, _101128, _062400				•	•		•				– Covalently closed circular RNA, highly resistant to RNase, hence presence in abundance in cytoplasm – Increase in these three circRNAs is associated with LTBI – Decreased in this circRNA is associated with active TB infection
	host miRNA _hsa-miR-146a-5p				•		•	•				– Increase in these miRNA is associated with active TB infection

(Continued)

TABLE 1 | Continued

Biomarker	Specimen					Application					Remark
	Sputum	Body fluids	CSF	Blood/ serum/ plasma	PBMC	Mtb diagnosis	Distinguish active TB vs. LTBI	Monitoring	Predict relapse /worsen/ progress	Predict treatment success	
_hsa-miR-125b-5p											
MTB miRNA											
_MTB-miR5				•		•	•				
Host miRNA				•		•	•				– Elevation of these miRNA were associated with LTBI
_hsa-let-7e-5p											
_hsa-let-7d-5p											
_hsa-miR-450a-5p											
_hsa-miR-140-5p											
Host miRNA				•		•	•				– Elevation of these miRNA were
_hsa-miR-1246											
_ hsa-miR-2110 = hsa-miR-370-3p											– associated with active TB infection
_ hsa-miR-28-3p											
_ hsa-miR-193b-5p											
Host proteomics ORM2, IL-36α, S1000-A9, SOD				•					•	•	– Elevation of these plasma markers were associated with severe TB infection
Host metabolomics • Cortisol, tryptophan, glutathione, tRNA acylation				•					•		– Predict progression from LTBI to active TB (applicable to host hold contact of TB infected individual)
Host genomics • SNP of SP110 gene (rs9061)					•				•		– SP100 gene encoding for IFN induced nuclear protein – Individual bearing this SNP was associated lower plasma level of TNF and increase susceptibility to LTBI

well as new algorithms must be designed to handle such big data. Further, since the number of variables in omics studies is usually way larger than the sample size, the statistical power for detecting a few suitable biomarkers will inevitably decrease profoundly. Given that high investment is required for omics studies, which obviously may be impractical for developing countries, the well-validated omics markers should be applied for simple and rapid point-of-care tests.

AUTHOR CONTRIBUTIONS

YY and ES wrote the first draft of the manuscript. HT, AS, WW, RV, RE, VV, and ML contributed to the writing of the manuscript. YY, HT, AS, WW, VV, ML, and ES agreed with the manuscript's results and conclusion. All authors have read and confirmed that they meet, ICMJE criteria for authorship.

FUNDING

This work was supported by a grant from Xiamen University Malaysia Research Funding (XMUMRF), XMUMRF/2018-C2/ILAB/0001. ML was supported by the Swedish Research Council, the Swedish Physicians against AIDS Research Foundation; VINNMER for Vinnova, Linköping University Hospital Research Fund, ALF Grants Region Östergötland, FORSS. The funders had no role in study design, data collection and analysis, decision to publish, or preparation of the manuscript.

REFERENCES

Abraham, P. R., Devalraju, K. P., Jha, V., Valluri, V. L., Mukhopadhyay, S. (2018). PPE17 (Rv1168c) protein of *Mycobacterium tuberculosis* detects individuals with latent TB infection. *PLoS One* 13:e0207787. doi: 10.1371/journal.pone.0207787

Abu-Raddad, L. J., Sabatelli, L., Achterberg, J. T., Sugimoto, J. D., Longini, I. M. Jr., and Dye, C., et al. (2009). Epidemiological benefits of more-effective tuberculosis vaccines, drugs, and diagnostics. *Proc. Natl. Acad. Sci. U.S.A.* 106, 13980–13985.

Achkar, and J. M., Ziegenbalg, A. (2012). Antibody responses to mycobacterial antigens in children with tuberculosis: challenges and potential diagnostic value. *Clin. Vacc. Immunol.* 19, 1898–1906.

Adekambi, T., Ibegbu, C. C., Kalokhe, A. S., Yu, T., Ray, S. M., Rengarajan, J. (2012). Distinct effector memory CD4+ T cell signatures in latent *Mycobacterium tuberculosis* infection, BCG vaccination and clinically resolved tuberculosis. *PLoS One* 7:e36046. doi: 10.1371/journal.pone.0036046

Ahmed, M. I. M., Ntinginya, N. E., Kibiki, G., Mtafya, B. A., Semvua, H., Mpagama, S., et al. (2018). Phenotypic changes on *Mycobacterium tuberculosis*-specific CD4 T cells as surrogate markers for tuberculosis treatment efficacy. *Front. Immunol.* 9:2247. doi: 10.3389/fimmu.2018.02247

Amelio, P., Portevin, D., Hella, J., Reither, K., Kamwela, L., Lweno, O., et al. (2019). HIV infection functionally impairs *Mycobacterium tuberculosis*-specific CD4 and CD8 T-cell responses. *J. Virol.* 93:e01728-18.

Amelio, P., Portevin, D., Reither, K., Mhimbira, F., Mpina, M., Tumbo, A., et al. (2017). Mixed Th1 and Th2 *Mycobacterium tuberculosis*-specific CD4 T cell responses in patients with active pulmonary tuberculosis from Tanzania. *PLoS Negl. Trop. Dis.* 11:e0005817. doi: 10.1371/journal.pntd.0005817

Andersen, P., Munk, M. E., Pollock, J. M., Doherty, T. M. (2000). Specific immune-based diagnosis of tuberculosis. *Lancet* 356, 1099–1104.

Anderson, S. T., Kaforou, M., Brent, A. J., Wright, V. J., Banwell, C. M., Chagaluka, G., et al. (2014). Diagnosis of childhood tuberculosis and host RNA expression in Africa. *N. Engl. J. Med.* 370, 1712–1723.

Andrade, B. B., Pavan Kumar, N., Mayer-Barber, K. D., Barber, D. L., Sridhar, R., Rekha, V. V., et al. (2013). Plasma heme oxygenase-1 levels distinguish latent or successfully treated human tuberculosis from active disease. *PLoS One* 8:e62618. doi: 10.1371/journal.pone.0062618

Arend, S. M., Andersen, P., van Meijgaarden, K. E., Skjot, R. L., Subronto, Y. W., van Dissel, J. T., et al. (2000). Detection of active tuberculosis infection by T cell responses to early-secreted antigenic target 6-kDa protein and culture filtrate protein 10. *J. Infect. Dis.* 181, 1850–1854.

Argun, M., Uzum, K., Sonmez, M. F., Ozyurt, A., Derya, K., Cilenk, K. T., et al. (2016). Cardioprotective effect of metformin against doxorubicin cardiotoxicity in rats. *Anat. J. Cardiol.* 16, 234–241.

Arora, J., Kumar, G., Verma, A. K., Bhalla, M., Sarin, R., Myneedu, V. P. (2015). Utility of MPT64 antigen detection for rapid confirmation of *Mycobacterium tuberculosis* complex. *J. Glob. Infect. Dis.* 7, 66–69.

Arora, V. K., and Chopra, K. K. (2007). Extra pulmonary tuberculosis. *Indian J. Tuberculosis* 54, 165–167.

Arroyo, L., Marin, D., Franken, K., Ottenhoff, T. H. M., and Barrera, L. F. (2018). Potential of DosR and Rpf antigens from *Mycobacterium tuberculosis* to discriminate between latent and active tuberculosis in a tuberculosis endemic population of Medellin Colombia. *BMC Infect. Dis.* 18:26. doi: 10.1186/s12879-017-2929-0

Azzurri, A., Sow, O. Y., Amedei, A., Bah, B., Diallo, S., Peri, G., et al. (2005). IFN-gamma-inducible protein 10 and pentraxin 3 plasma levels are tools for monitoring inflammation and disease activity in *Mycobacterium tuberculosis* infection. *Microbes Infect.* 7, 1–8.

Bae, W., Park, K. U., Song, E. Y., Kim, S. J., Lee, Y. J., Park, J. S., et al. (2016). Comparison of the sensitivity of QuantiFERON-TB gold in-tube and T-SPOT.TB according to patient age. *PLoS One* 11:e0156917. doi: 10.1371/journal.pone.0156917

Ballman, K. V. (2015). Biomarker: predictive or prognostic? *J. Clin. Oncol.* 33, 3968–3971.

Bentley-Hibbert, S. I., Quan, X., Newman, T., Huygen, K., and Godfrey, H. P. (1999). Pathophysiology of antigen 85 in patients with active tuberculosis: antigen 85 circulates as complexes with fibronectin and immunoglobulin G. *Infect. Immun.* 67, 581–588.

Berry, M. P., Graham, C. M., McNab, F. W., Xu, Z., Bloch, S. A., Oni, T., et al. (2010). An interferon-inducible neutrophil-driven blood transcriptional signature in human tuberculosis. *Nature.* 466, 973–977.

Bloom, C. I., Graham, C. M., Berry, M. P., Rozakeas, F., Redford, P. S., Wang, Y., et al. (2013). Transcriptional blood signatures distinguish pulmonary tuberculosis, pulmonary sarcoidosis, pneumonias and lung cancers. *PLoS One* 8:e70630. doi: 10.1371/journal.pone.0070630

Bocchino, M., Chairadonna, P., Matarese, A., Bruzzese, D., Salvatores, M., Tronci, M., et al. (2010). Limited usefulness of QuantiFERON-TB Gold In-Tube for monitoring anti-tuberculosis therapy. *Respir. Med.* 104, 1551-6.

Boehme, C., Molokova, E., Minja, F., Geis, S., Loscher, T., Maboko, L., et al. (2005). Detection of mycobacterial lipoarabinomannan with an antigen-capture ELISA in unprocessed urine of Tanzanian patients with suspected tuberculosis. *Trans. R. Soc. Trop. Med. Hyg.* 99, 893–900.

Borrego, F., Robertson, M. J., Ritz, J., Pena, J., Solana, R. (1999). CD69 is a stimulatory receptor for natural killer cell and its cytotoxic effect is blocked by CD94 inhibitory receptor. *Immunology* 97, 159–165.

Buschmann, D., Haberberger, A., Kirchner, B., Spornraft, M., Riedmaier, I., Schelling, G. et al. (2016). Toward reliable biomarker signatures in the age of liquid biopsies - how to standardize the small RNA-Seq workflow. *Nucleic acids Res.* 44, 5995–6018.

Butera, O., Chiacchio, T., Carrara, S., Casetti, R., Vanini, V., Meraviglia, S. et al. (2009). New tools for detecting latent tuberculosis infection: evaluation of RD1-specific long-term response. *BMC Infect. Dis.* 9:182. doi: 10.1186/1471-2334-9-182

Caccamo, N., Guggino, G., Joosten, S. A., Gelsomino, G., Di Carlo, P., Titone, L. et al. (2010). Multifunctional CD4(+) T cells correlate with active Mycobacterium tuberculosis infection. *Eur. J. Immunol.* 40, 2211–2220.

Cannas, A., Goletti, D., Girardi, E., Chiacchio, T., Calvo, L., Cuzzi, G. et al. (2008). *Mycobacterium tuberculosis* DNA detection in soluble fraction of urine from pulmonary tuberculosis patients. *Int. J. Tuberculosis Lung Dis.* 12, 146–151.

Cao, S. H., Chen, Y. Q., Sun, Y., Liu, Y., Zheng, S. H., Zhang, Z. G. et al. (2018). Screening of serum biomarkers for distinguishing between latent and active tuberculosis using proteome microarray. *Biomed. Environ. Sci.* 31, 515–526.

Casey, R., Blumenkrantz, D., Millington, K., Montamat-Sicotte, D., Kon, O. M., Wickremasinghe, M. et al. (2010). Enumeration of functional T-cell subsets by fluorescence-immunospot defines signatures of pathogen burden in tuberculosis. *PLoS One* 5:e15619. doi: 10.1371/journal.pone.0015619

Chakrabarty, S., Kumar, A., Raviprasad, K., Mallya, S., Satyamoorthy, K., Chawla, K. (2019). Host and MTB genome encoded miRNA markers for diagnosis of tuberculosis. *Tuberculosis* 116, 37–43.

Chang, S. Y., Chen, M. L., Lee, M. R. ., Liang, Y. C., Lu, T. P., Wang, J. Y. et al. (2018). SP110 polymorphisms are genetic markers for vulnerability to latent and active tuberculosis infection in Taiwan. *Dis. Mark.* 2018:4687380.

Chee, C. B., KhinMar, K. W., Gan, S. H., Barkham, T. M., Koh, C. K., Shen, L. et al. (2010). Tuberculosis treatment effect on T-cell interferon-gamma responses to *Mycobacterium tuberculosis*-specific antigens. *Eur. Respir. J.* 36, 355–361.

Chegou, NN., Black, GF., Kidd, M., van Helden, PD., Walzl, G. (2009). Host markers in QuantiFERON supernatants differentiate active TB from latent TB infection: preliminary report. *BMC Pulmon. Med.* 9:21. doi: 10.1186/1471-2466-9-21

Chiacchio, T., Petruccioli, E., Vanini, V., Cuzzi, G., Pinnetti, C., Sampaolesi, A. et al. (2014). Polyfunctional T-cells and effector memory phenotype are associated with active TB in HIV-infected patients. *J. Infect.* 69, 533–545.

Clarke, R., Ressom, H. W., Wang, A., Xuan, J., Liu, M. C., Gehan, E. A. et al. (2008). The properties of high-dimensional data spaces: implications for exploring gene and protein expression data. *Nat. Rev. Cancer* 8, 37–49.

Cliff, J. M., Cho, J. E., Lee, J. S., Ronacher, K., King, E. C., van Helden, P. et al. (2016). Excessive cytolytic responses predict tuberculosis relapse after apparently successful treatment. *J. Infect. Dis.* 213, 485–495. doi: 10.1093/infdis/jiv447

Colditz, G. A., Brewer, T. F., Berkey, C. S., Wilson, M. E., Burdick, E., Fineberg, H. V. et al. (1994). Efficacy of BCG vaccine in the prevention of tuberculosis. Meta-analysis of the published literature. *JAMA* 271, 698–702. doi: 10.1001/jama.271.9.698

Conesa-Botella, A., Loembe, M. M., Manabe, Y. C., Worodria, W., Mazakpwe, D., Luzinda, K. et al. (2011). Urinary lipoarabinomannan as predictor for the tuberculosis immune reconstitution inflammatory syndrome. *J. Acq. Immune Defic. Syndromes* 58, 463–468. doi: 10.1097/qai.0b013e31823801de

Corbett, E. L., Watt, C. J., Walker, N., Maher, D., Williams, B. G., Raviglione, M. C. et al. (2003). The growing burden of tuberculosis: global trends and interactions with the HIV epidemic. *Arch. Intern. Med.* 163, 1009–1021.

da Cruz, H. L., de Albuquerque Montenegro, R., de Araujo Lima, J. F., da Rocha Poroca, D., da Costa Lima, J. F., Maria Lapa Montenegro, L. et al. (2011). Evaluation of a nested-PCR for mycobacterium tuberculosis detection in blood and urine samples. *Braz. J. Microbiol.* 42, 321–329. doi: 10.1590/s1517-83822011000100041

Darrah, PA., Patel, DT., De Luca, PM., Lindsay, RW., Davey, DF., Flynn, BJ. et al. (2007). Multifunctional TH1 cells define a correlate of vaccine-mediated protection against Leishmania major. *Nat. Med.* 13, 843–850. doi: 10.1038/nm1592

Davies, and P. D., Pai, M. (2008). The diagnosis and misdiagnosis of tuberculosis. *Int. J. Tuberculosis Lung Dis.* 12, 1226–1234.

Day, C. L., Abrahams, D. A., Bunjun, R., Stone, L., de Kock, M., Walzl, G. et al. (2018). PD-1 expression on *Mycobacterium tuberculosis*-specific CD4 T cells is associated with bacterial load in human tuberculosis. *Front. Immunol.* 9:1995. doi: 10.3389/fimmu.2018.01995

Desikan, P. (2013). Sputum smear microscopy in tuberculosis: is it still relevant? *Indian J. Med. Res.* 137, 442–444.

Djoba Siawaya, J. F., Beyers, N., van Helden, P., Walzl, G. (2009). Differential cytokine secretion and early treatment response in patients with pulmonary tuberculosis. *Clin. Exp. Immunol.* 156, 69–77. doi: 10.1111/j.1365-2249.2009.03875.x

Doublier, S., Zennaro, C., Spatola, T., Lupia, E., Bottelli, A., Deregibus, M. C. et al. (2007). HIV-1 Tat reduces nephrin in human podocytes: a potential mechanism for enhanced glomerular permeability in HIV-associated nephropathy. *Aids* 21, 423–432. doi: 10.1097/qad.0b013e328012c522

Drain, P. K., Gounder, L., Grobler, A., Sahid, F., Bassett, I. V., Moosa, M. Y. (2015). Urine lipoarabinomannan to monitor antituberculosis therapy response and predict mortality in an HIV-endemic region: a prospective cohort study. *BMJ Open* 5:e006833. doi: 10.1136/bmjopen-2014-006833

Duffy, F. J., Weiner, J., III., Hansen, S., Tabb, D. L., Suliman, S., Thompson, E. et al. (2019). Immunometabolic signatures predict risk of progression to active tuberculosis and disease outcome. *Front. Immunol.* 10:527. doi: 10.3389/fimmu.2019.00527

El Daker, S., Sacchi, A., Tempestilli, M., Carducci, C., Goletti, D., Vanini, V. et al. (2015). Granulocytic myeloid derived suppressor cells expansion during active pulmonary tuberculosis is associated with high nitric oxide plasma level. *PLoS One* 10:e0123772. doi: 10.1371/journal.pone.0123772

Feasey, N. A., Banada, P. P., Howson, W., Sloan, D. J., Mdolo, A., Boehme, C. et al. (2013). Evaluation of Xpert MTB/RIF for detection of tuberculosis from blood samples of HIV-infected adults confirms *Mycobacterium tuberculosis* bacteremia as an indicator of poor prognosis. *J. Clin. Microbiol.* 51, 2311–2316. doi: 10.1128/jcm.00330-13

Feng, T. T., Shou, C. M., Shen, L., Qian, Y., Wu, Z. G., Fan, J. et al. (2011). Novel monoclonal antibodies to ESAT-6 and CFP-10 antigens for ELISA-based diagnosis of pleural tuberculosis. *Int. J. Tuberculosis Lung Disease* 15, 804–810. doi: 10.5588/ijtld.10.0393

Ferrara, G., Losi, M., Fabbri, L. M., Migliori, G. B., Richeldi, L., Casali, L. (2009). Exploring the immune response against *Mycobacterium tuberculosis* for a better diagnosis of the infection. *Arch. Immunol. Ther. Exp.* 57, 425–433. doi: 10.1007/s00005-009-0050-9

Feruglio, S. L., Troseid, M., Damas, J. K., Kvale, D., Dyrhol-Riise, A. M. (2013). Soluble markers of the Toll-like receptor 4 pathway differentiate between active and latent tuberculosis and are associated with treatment responses. *PLoS One* 8:e69896. doi: 10.1371/journal.pone.0069896

Frahm, M., Goswami, N. D., Owzar, K., Hecker, E., Mosher, A., Cadogan, E. et al. (2011). Discriminating between latent and active tuberculosis with multiple biomarker responses. *Tuberculosis* 91, 250–256. doi: 10.1016/j.tube.2011.02.006

Friedrich, S. O., Rachow, A., Saathoff, E., Singh, K., Mangu, C. D., Dawson, R. et al. (2013). Assessment of the sensitivity and specificity of Xpert MTB/RIF assay as an early sputum biomarker of response to tuberculosis treatment. *Lancet Respir. Med.* 1, 462–470. doi: 10.1016/s2213-2600(13)70119-x

Fu, Y., Wang, J., Qiao, J., Yi, Z. (2019). Signature of circular RNAs in peripheral blood mononuclear cells from patients with active tuberculosis. *J. Cell. Mol. Med.* 23, 1917–1925. doi: 10.1111/jcmm.14093

Gaifer, Z. (2017). Epidemiology of extrapulmonary and disseminated tuberculosis in a tertiary care center in Oman. *Int. J. Mycobacteriol.* 6, 162–166.

Gesthalter, Y. B., Vick, J., Steiling, K., Spira, A. (2015). Translating the transcriptome into tools for the early detection and prevention of lung cancer. *Thorax* 70, 476–481. doi: 10.1136/thoraxjnl-2014-206605

Getahun, H., Gunneberg, C., Granich, R., Nunn, P. (2010). HIV infection-associated tuberculosis: the epidemiology and the response. *Clin. Infect. Dis.* 50(Suppl 3), S201–S207.

Goletti, D., Butera, O., Bizzoni, F., Casetti, R., Girardi, E., Poccia, F. (2006). Region of difference 1 antigen-specific CD4+ memory T cells correlate with a favorable outcome of tuberculosis. *J. Infect. Dis.* 194, 984–992. doi: 10.1086/507427

Goletti, D., Carrara, S., Mayanja-Kizza, H., Baseke, J., Mugerwa, M. A., Girardi, E. et al. (2008). Response to *M. tuberculosis* selected RD1 peptides in Ugandan HIV-infected patients with smear positive pulmonary tuberculosis: a pilot study. *BMC Infect. Dis.* 8:11. doi: 10.1186/1471-2334-8-11

Goletti, D., Lee, M. R., Wang, J. Y., Walter, N., Ottenhoff, T. H. M. (2018). Update on tuberculosis biomarkers: from correlates of risk, to correlates of active disease and of cure from disease. *Respirology* 23, 455–466. doi: 10.1111/resp.13272

Goletti, D., Petruccioli, E., Joosten, S. A., Ottenhoff, T. H. (2016). Tuberculosis biomarkers: from diagnosis to protection. *Infect. Dis. Rep.* 8:6568.

Goletti, D., Raja, A., Ahamed Kabeer, B. S., Rodrigues, C., Sodha, A., Butera, O. et al. (2010a). IFN-gamma, but not IP-10, MCP-2 or IL-2 response to RD1 selected peptides associates to active tuberculosis. *J. Infect.* 61, 133–143. doi: 10.1016/j.jinf.2010.05.002

Goletti, D., Raja, A., Syed Ahamed Kabeer, B., Rodrigues, C., Sodha, A., Carrara, S. et al. (2010b). Is IP-10 an accurate marker for detecting *M. tuberculosis*-specific response in HIV-infected persons? *PLoS One* 5:e12577. doi: 10.1371/journal.pone.0012577

Gomes, T., Reis-Santos, B., Bertolde, A., Johnson, J. L., Riley, L. W., Maciel, E. L. (2014). Epidemiology of extrapulmonary tuberculosis in Brazil: a hierarchical model. *BMC Infect. Dis.* 14:9. doi: 10.1186/1471-2334-14-9

Gupta-Wright, A., Peters, J. A., Flach, C., Lawn, S. D. (2016). Detection of lipoarabinomannan (LAM) in urine is an independent predictor of mortality risk in patients receiving treatment for HIV-associated tuberculosis in sub-Saharan Africa: a systematic review and meta-analysis. *BMC Med.* 14:53. doi: 10.1186/s12916-016-0603-9

Hamasur, B., Bruchfeld, J., van Helden, P., Kallenius, G., Svenson, S. (2015). A sensitive urinary lipoarabinomannan test for tuberculosis. *PLoS One* 10:e0123457. doi: 10.1371/journal.pone.0123457

Harari, A., Rozot, V., Bellutti Enders, F., Perreau, M., Stalder, J. M., Nicod, L. P. et al. (2011). Dominant TNF-alpha+ *Mycobacterium tuberculosis*-specific CD4+ T cell responses discriminate between latent infection and active disease. *Nat. Med.* 17, 372–376. doi: 10.1038/nm.2299

Heidecker, B., Kasper, E. K., Wittstein, I. S., Champion, H. C., Breton, E., Russell, S. D. et al. (2008). Transcriptomic biomarkers for individual risk assessment in new-onset heart failure. *Circulation* 118, 238–246. doi: 10.1161/circulationaha.107.756544

Helmy, N., Abdel, SL., Kamela, M. M., Ashoura, W., and El Kattan, E. (2012). Role of Quantiferon TB gold assays in monitoring the efficacy of antituberculosis therapy. *Egypt. J. Chest Dis. Tuberculosis* 61, 329–336. doi: 10.1016/j.ejcdt.2012.09.011

Hoel, I. M., Jorstad, M. D., Marijani, M., Ruhwald, M., Mustafa, T., Dyrhol-Riise, A. M. (2019). IP-10 dried blood spots assay monitoring treatment efficacy in extrapulmonary tuberculosis in a low-resource setting. *Sci. Rep.* 9:3871.

Hormi, M., Guerin-El Khourouj, V., Pommelet, V., Jeljeli, M., Pedron, B., Diana, J. S., et al. (2018). Performance of the QuantiFERON-TB gold assay among HIV-infected children with active tuberculosis in France. *Pediatr. Infect. Dis. J.* 37, 339–344. doi: 10.1097/inf.0000000000001774

Janssens, J. P. (2007). Interferon-gamma release assay tests to rule out active tuberculosis. *Eur. Respir. J.* 30, 183–184; author reply 4–5.

Jong, V. L., Ahout, I. M., van den Ham, H. J., Jans, J., Zaaraoui-Boutahar, F., Zomer, A., et al. (2016). Transcriptome assists prognosis of disease severity in respiratory syncytial virus infected infants. *Sci. Rep.* 6:36603.

Joosten, S. A., Goeman, J. J., Sutherland, J. S., Opmeer, L., de Boer, K. G., Jacobsen, M., et al. (2012). Identification of biomarkers for tuberculosis disease using a novel dual-color RT-MLPA assay. *Genes Immun.* 13, 71–82.

Kabeer, B. S., Raja, A., Raman, B., Thangaraj, S., Leportier, M., Ippolito, G., et al. (2011). IP-10 response to RD1 antigens might be a useful biomarker for monitoring tuberculosis therapy. *BMC Infect. Dis.* 11:135. doi: 10.1186/1471-2334-11-135

Kaforou, M., Wright, V. J., Oni, T., French, N., Anderson, S. T., Bangani, N., et al. (2013). Detection of tuberculosis in HIV-infected and -uninfected African adults using whole blood RNA expression signatures: a case-control study. *PLoS Med.* 10:e1001538. doi: 10.1371/journal.pmed.1001538

Kalra, M., Khuller, G. K., Grover, A., Behera, D., Wanchu, A., Verma, I. (2010). Utility of a combination of RD1 and RD2 antigens as a diagnostic marker for tuberculosis. *Diagn. Microbiol. Infect. Dis.* 66, 153–161. doi: 10.1016/j.diagmicrobio.2009.09.005

Kaneko, Y., Nakayama, K., Kinoshita, A., Kurita, Y., Odashima, K., Saito, Z., et al. (2015). Relation between recurrence of tuberculosis and transitional changes in IFN-gamma release assays. *Am. J. Respir. Crit. Care Med.* 191, 480–483. doi: 10.1164/rccm.201409-1590le

Kashyap, R. S., Dobos, K. M., Belisle, J. T., Purohit, H. J., Chandak, N. H., Taori, G. M., et al. (2005). Demonstration of components of antigen 85 complex in cerebrospinal fluid of tuberculous meningitis patients. *Clin. Diagn. Lab. Immunol.* 12, 752–758. doi: 10.1128/cdli.12.6.752-758.2005

Kashyap, R. S., Rajan, A. N., Ramteke, S. S., Agrawal, V. S., Kelkar, S. S., Purohit, H. J., et al. (2007). Diagnosis of tuberculosis in an Indian population by an indirect ELISA protocol based on detection of Antigen 85 complex: a prospective cohort study. *BMC Infect. Dis.* 7:74. doi: 10.1186/1471-2334-7-74

Kell, D. B., and Oliver, S. G. (2004). Here is the evidence, now what is the hypothesis? The complementary roles of inductive and hypothesis-driven science in the post-genomic era. *BioEssays* 26, 99–105. doi: 10.1002/bies.10385

Kohonen, P., Parkkinen, J. A., Willighagen, E. L., Ceder, R., Wennerberg, K., Kaski, S., et al. (2017). A transcriptomics data-driven gene space accurately predicts liver cytopathology and drug-induced liver injury. *Nat. Commun.* 8:15932.

Kumar, V. G., Urs, T. A., Ranganath, R. R. (2011). MPT 64 antigen detection for rapid confirmation of *M.tuberculosis* isolates. *BMC Res. Notes* 4:79. doi: 10.1186/1756-0500-4-79

Kwak, N., Choi, S. M., Lee, J., Park, Y. S., Lee, C. H., Lee, S. M., et al. (2013). Diagnostic accuracy and turnaround time of the Xpert MTB/RIF assay in routine clinical practice. *PLoS One* 8:e77456. doi: 10.1371/journal.pone.0077456

La Manna, M. P., Orlando, V., Li Donni, P., Sireci, G., Di Carlo, P., Cascio, A., et al. (2018). Identification of plasma biomarkers for discrimination between tuberculosis infection/disease and pulmonary non tuberculosis disease. *PLoS One* 13:e0192664. doi: 10.1371/journal.pone.0192664

Lagrange, P. H., Thangaraj, S. K., Dayal, R., Deshpande, A., Ganguly, N. K., Girardi, E., et al. (2014). A toolbox for tuberculosis (TB) diagnosis: an Indian multi-centric study (2006-2008); evaluation of serological assays based on PGL-Tb1 and ESAT-6/CFP10 antigens for TB diagnosis. *PLoS One* 9:e96367. doi: 10.1371/journal.pone.0096367

Lalvani, A., Nagvenkar, P., Udwadia, Z., Pathan, A. A., Wilkinson, K. A., Shastri, J. S., et al. (2001a). Enumeration of T cells specific for RD1-encoded antigens suggests a high prevalence of latent *Mycobacterium tuberculosis* infection in healthy urban Indians. *J. Infect. Dis.* 183, 469–477. doi: 10.1086/318081

Lalvani, A., Pathan, A. A., Durkan, H., Wilkinson, K. A., Whelan, A., Deeks, J. J., et al. (2001b). Enhanced contact tracing and spatial tracking of *Mycobacterium tuberculosis* infection by enumeration of antigen-specific T cells. *Lancet* 357, 2017–2021. doi: 10.1016/s0140-6736(00)05115-1

Lee, S. W., Wu, L. S., Huang, G. M., Huang, K. Y., Lee, T. Y., Weng, J. T. (2016). Gene expression profiling identifies candidate biomarkers for active and latent tuberculosis. *BMC Bioinform.* 17(Suppl 1):3. doi: 10.1186/s12859-015-0848-x

Lesho, E., Forestiero, F. J., Hirata, M. H., Hirata, R. D., Cecon, L., Melo, F. F., et al. (2011). Transcriptional responses of host peripheral blood cells to tuberculosis infection. *Tuberculosis* 91, 390–399. doi: 10.1016/j.tube.2011.07.002

Leu, J. S., Chang, S. Y., Mu, C. Y., Chen, M. L., Yan, B.S. (2018). Functional domains of SP110 that modulate its transcriptional regulatory function and cellular translocation. *J. Biomed. Sci.* 25:34.

Li, Z., Pan, L., Lyu, L., Li, J., Jia, H., Du, B., et al. (2019). Diagnostic accuracy of droplet digital PCR analysis of cerebrospinal fluid for tuberculous meningitis in adult patients. *Clin. Microbiol. Infect.* doi: 10.1016/j.cmi.2019.07.015 [Epub ahead of print].

Lighter, J., Rigaud, M., Huie, M., Peng, C. H., Pollack, H. (2009). Chemokine IP-10: an adjunct marker for latent tuberculosis infection in children. *Int. J. Tuberculosis Lung Dis.* 13, 731–736.

Liu, Q., Pan, L., Han, F., Luo, B., Jia, H., Xing, A., et al. (2018). Proteomic profiling for plasma biomarkers of tuberculosis progression. *Mol. Med. Rep.* 18, 1551–1559.

Lopez-Ramos, J. E., Macias-Segura, N., Cuevas-Cordoba, B., Araujo-Garcia, Z., Bastian, Y., Castaneda-Delgado, J. E., et al. (2018). Improvement in the diagnosis of tuberculosis combining *Mycobacterium tuberculosis* immunodominant peptides and serum host biomarkers. *Arch. Med. Res.* 49, 147.e1-53 e1.

Losi, M., Bossink, A., Codecasa, L., Jafari, C., Ernst, M., Thijsen, S., et al. (2007). Use of a T-cell interferon-gamma release assay for the diagnosis of tuberculous pleurisy. *Eur. Respir. J.* 30, 1173–1179. doi: 10.1183/09031936.00067307

Lowe, R., Shirley, N., Bleackley, M., Dolan, S., Shafee, T. (2017). Transcriptomics technologies. *PLoS Comput. Biol.* 13:e1005457. doi: 10.1371/journal.pcbi.1005457

Lu, L. L., Smith, M. T., Yu, K. K. Q., Luedemann, C., Suscovich, T. J., Grace, P. S., et al. (2019). IFN-gamma-independent immune markers of *Mycobacterium tuberculosis* exposure. *Nat. Med.* 25, 977–987.

Luo, J., Zhang, M., Yan, B., Li, F., Guan, S., Chang, K., et al. (2019). Diagnostic performance of plasma cytokine biosignature combination and MCP-1 as

individual biomarkers for differentiating stages *Mycobacterium tuberculosis* infection. *J. Infection.* 78, 281–291. doi: 10.1016/j.jinf.2018.10.017

Luo, L., Zhu, L., Yue, J., Liu, J., Liu, G., Zhang, X., et al. (2017). Antigens Rv0310c and Rv1255c are promising novel biomarkers for the diagnosis of *Mycobacterium tuberculosis* infection. *Emerg. Microbes Infect.* 6:e64.

Lyu, L., Zhang, X., Li, C., Yang, T., Wang, J., Pan, L., et al. (2019). Small RNA profiles of serum exosomes derived from individuals with latent and active tuberculosis. *Front. Microbiol.* 10:1174. doi: 10.3389/fmicb.2019.01174

Maekura, R., Kitada, S., Osada-Oka, M., Tateishi, Y., Ozeki, Y., Fujicawa, T., et al. (2019). Serum antibody profiles in individuals with latent *Mycobacterium tuberculosis* infection. *Microbiol. Immunol.* 63, 130–138. doi: 10.1111/1348-0421.12674

Maertzdorf, J., Kaufmann, S. H., Weiner, J., III (2014). Toward a unified biosignature for tuberculosis. *Cold Spring Harbor Perspect. Med.* 5:a018531.

Maertzdorf, J., McEwen, G., Weiner, J., III, Tian, S., Lader, E., Schriek, U., et al. (2016). Concise gene signature for point-of-care classification of tuberculosis. *EMBO Mol. Med.* 8, 86–95. doi: 10.15252/emmm.201505790

Maertzdorf, J., Ota, M., Repsilber, D., Mollenkopf, H. J., Weiner, J., Hill, P. C., et al. (2011a). Functional correlations of pathogenesis-driven gene expression signatures in tuberculosis. *PLoS One* 6:e26938. doi: 10.1371/journal.pone.0026938

Maertzdorf, J., Repsilber, D., Parida, S. K., Stanley, K., Roberts, T., Black, G., et al. (2011b). Human gene expression profiles of susceptibility and resistance in tuberculosis. *Genes Immun.* 12, 15–22. doi: 10.1038/gene.2010.51

Marlowe, E. M., Novak-Weekley, S. M., Cumpio, J., Sharp, S. E., Momeny, M. A., Babst, A., et al. (2011). Evaluation of the cepheid xpert MTB/RIF assay for direct detection of *Mycobacterium tuberculosis* complex in respiratory specimens. *J. Clin. Microbiol.* 49, 1621–1623. doi: 10.1128/jcm.02214-10

Martin, A., Bombeeck, D., Mulders, W., Fissette, K., De Rijk, P., Palomino, J. C. (2011). Evaluation of the TB Ag MPT64 Rapid test for the identification of *Mycobacterium tuberculosis* complex. *Int. J. Tubercu. Lung Dis.* 15, 703–705.

Maynard-Smith, L., Larke, N., Peters, J. A., Lawn, S. D. (2014). Diagnostic accuracy of the Xpert MTB/RIF assay for extrapulmonary and pulmonary tuberculosis when testing non-respiratory samples: a systematic review. *BMC Infect. Dis.* 14:709. doi: 10.1186/s12879-014-0709-7

Mendelson, M. (2007). Diagnosing tuberculosis in HIV-infected patients: challenges and future prospects. *Br. Med. Bull.* 81-82, 149–165. doi: 10.1093/bmb/ldm009

Mihret, A., Bekele, Y., Bobosha, K., Kidd, M., Aseffa, A., Howe, R., et al. (2013). Plasma cytokines and chemokines differentiate between active disease and non-active tuberculosis infection. *J. Infect.* 66, 357–365. doi: 10.1016/j.jinf.2012.11.005

Millington, K. A., Gooding, S., Hinks, T. S., Reynolds, D. J., Lalvani, A. (2010). *Mycobacterium tuberculosis*-specific cellular immune profiles suggest bacillary persistence decades after spontaneous cure in untreated tuberculosis. *J. Infect. Dis.* 202, 1685–1689. doi: 10.1086/656772

Millington, K. A., Innes, J. A., Hackforth, S., Hinks, T. S., Deeks, J. J., Dosanjh, D. P., et al. (2007). Dynamic relationship between IFN-gamma and IL-2 profile of *Mycobacterium tuberculosis*-specific T cells and antigen load. *J. Immunol.* 178, 5217–5226. doi: 10.4049/jimmunol.178.8.5217

Minion, J, Leung, E, Talbot, E, Dheda, K, Pai, M, Menzies, D. (2011). Diagnosing tuberculosis with urine lipoarabinomannan: systematic review and meta-analysis. *Eur. Respir. J.* 38, 1398–1405. doi: 10.1183/09031936.00025711

Miotto, P., Mwangoka, G., Valente, I. C., Norbis, L., Sotgiu, G., Bosu, R., et al. (2013). miRNA signatures in sera of patients with active pulmonary tuberculosis. *PLoS One* 8:e80149. doi: 10.1371/journal.pone.0080149

Mistry, R., Cliff, J. M., Clayton, C. L., Beyers, N., Mohamed, Y. S., Wilson, P. A., et al. (2007). Gene-expression patterns in whole blood identify subjects at risk for recurrent tuberculosis. *J. Infect. Dis.* 195, 357–365. doi: 10.1086/510397

Mori, T., Sakatani, M., Yamagishi, F., Takashima, T., Kawabe, Y., Nagao, K., et al. (2004). Specific detection of tuberculosis infection: an interferon-gamma-based assay using new antigens. *Am. J. Respir. Crit. Care Med.* 170, 59–64. doi: 10.1164/rccm.200402-179oc

Moro, M. L., Nascetti, S., Morsillo, F., Morandi, M., Italian TB-SORV Project Working Group, (2010). Laboratory procedures for the diagnosis of tuberculosis: a survey in ten Italian Regions. *Annali dell'Istituto superiore di sanita.* 46, 178–184.

Nahid, P., Bliven-Sizemore, E., Jarlsberg, L. G., De Groote, M. A., Johnson, J. L., Muzanyi, G., et al. (2014). Aptamer-based proteomic signature of intensive phase treatment response in pulmonary tuberculosis. *Tuberculosis* 94, 187–196. doi: 10.1016/j.tube.2014.01.006

Nahid, P., Pai, M., Hopewell, P. C. (2006). Advances in the diagnosis and treatment of tuberculosis. *Proc. Am. Thoracic Soc.* 3, 103–110.

Nalejska, E., Maczynska, E., Lewandowska, M. A. (2014). Prognostic and predictive biomarkers: tools in personalized oncology. *Mol. Diagn. Ther.* 18, 273–284. doi: 10.1007/s40291-013-0077-9

Nikitina, I. Y., Kondratuk, N. A., Kosmiadi, G. A., Amansahedov, R. B., Vasilyeva, I. A., Ganusov, V. V., et al. (2012). Mtb-specific CD27low CD4 T cells as markers of lung tissue destruction during pulmonary tuberculosis in humans. *PLoS One* 7:e43733. doi: 10.1371/journal.pone.0043733

Nikolova, M., Markova, R., Drenska, R., Muhtarova, M., Todorova, Y., Dimitrov, V., et al. (2013). Antigen-specific CD4- and CD8-positive signatures in different phases of *Mycobacterium tuberculosis* infection. *Diagn. Microbiol. Infect. Dis.* 75, 277–281. doi: 10.1016/j.diagmicrobio.2012.11.023

Novel, N. C., Lani, T., Elisabetta, W., Anna, M. M., Anneke, C. H., Gerhard, W., et al. (2013). Utility of host markers detected in quantiferon supernatants for the diagnosis of tuberculosis in children in a high-burden setting. *PLoS One* 8:e64226. doi: 10.1371/journal.pone.0064226

Ottenhoff, T. H. (2009). Overcoming the global crisis: "yes, we can", but also for TB. ? *Eur. J. Immunol.* 39, 2014–2020. doi: 10.1002/eji.200939518

Ottenhoff, T. H., Ellner, J. J., Kaufmann, S. H. (2012). Ten challenges for TB biomarkers. *Tuberculosis* 92(Suppl 1), S17–S20.

Pai, M., Zwerling, A., Menzies, D. (2008). Systematic review: T-cell-based assays for the diagnosis of latent tuberculosis infection: an update. *Ann. Int. Med.* 149, 177–184.

Parlato, S., Chiacchio, T., Salerno, D., Petrone, L., Castiello, L., Romagnoli, G., et al. (2018). Impaired IFN-alpha-mediated signal in dendritic cells differentiates active from latent tuberculosis. *PLoS One* 13:e0189477. doi: 10.1371/journal.pone.0189477

Peter, J., Green, C., Hoelscher, M., Mwaba, P., Zumla, A., Dheda, K. (2010). Urine for the diagnosis of tuberculosis: current approaches, clinical applicability, and new developments. *Curr. Opin. Pulm. Med.* 16, 262–270. doi: 10.1097/mcp.0b013e328337f23a

Petrone, L., Cannas, A., Aloi, F., Nsubuga, M., Sserumkuma, J., Nazziwa, R. A., et al. (2015). Blood or urine IP-10 cannot discriminate between active tuberculosis and respiratory diseases different from tuberculosis in children. *BioMed Res. Int.* 2015, 589471.

Petruccioli, E., Petrone, L., Vanini, V., Cuzzi, G., Navarra, A., Gualano, G., et al. (2015). Assessment of CD27 expression as a tool for active and latent tuberculosis diagnosis. *J. Infect.* 71, 526–533. doi: 10.1016/j.jinf.2015.07.009

Petruccioli, E., Petrone, L., Vanini, V., Sampaolesi, A., Gualano, G., Girardi, E., et al. (2013). IFNgamma/TNFalpha specific-cells and effector memory phenotype associate with active tuberculosis. *J. Infect.* 66, 475–486. doi: 10.1016/j.jinf.2013.02.004

Pollock, K. M., Whitworth, H. S., Montamat-Sicotte, D. J., Grass, L., Cooke, G. S., Kapembwa, M. S., et al. (2013). T-cell immunophenotyping distinguishes active from latent tuberculosis. *J. Infect. Dis.* 208, 952–968. doi: 10.1093/infdis/jit265

Portevin, D., Moukambi, F., Clowes, P., Bauer, A., Chachage, M., Ntinginya, N. E., et al. (2014). Assessment of the novel T-cell activation marker-tuberculosis assay for diagnosis of active tuberculosis in children: a prospective proof-of-concept study. *Lancet Infect. Dis.* 14, 931–938. doi: 10.1016/s1473-3099(14)70884-9

Rakshit, S., Adiga, V., Nayak, S., Sahoo, P. N., Sharma, P. K., van Meijgaarden, K. E., et al. (2017). Circulating *Mycobacterium tuberculosis* DosR latency antigen-specific, polyfunctional, regulatory IL10(+) Th17 CD4 T-cells differentiate latent from active tuberculosis. *Sci. Rep.* 7:11948.

Rangaka, M. X., Wilkinson, K. A., Seldon, R., Van Cutsem, G., Meintjes, G. A., Morroni, C., et al. (2007). Effect of HIV-1 infection on T-Cell-based and skin test detection of tuberculosis infection. *Am. J. Respir. Crit. Care Med.* 175, 514–520. doi: 10.1164/rccm.200610-1439oc

Ribeiro, S., Dooley, K., Hackman, J., Loredo, C., Efron, A., Chaisson, R. E., et al. (2009). T-SPOT.TB responses during treatment of pulmonary tuberculosis. *BMC Infect. Dis.* 9:23. doi: 10.1186/1471-2334-9-23

Riou, C., Perez Peixoto, B., Roberts, L., Ronacher, K., Walzl, G., Manca, C., et al. (2012). Effect of standard tuberculosis treatment on plasma cytokine levels in patients with active pulmonary tuberculosis. *PLoS One* 7:e36886. doi: 10.1371/journal.pone.0036886

Rovina, N., Panagiotou, M., Pontikis, K., Kyriakopoulou, M., Koulouris, N. G., Koutsoukou, A. (2013). Immune response to mycobacterial infection: lessons from flow cytometry. *Clin. Dev. Immunol.* 2013, 464039.

Ruhwald, M., Petersen, J., Kofoed, K., Nakaoka, H., Cuevas, L. E., Lawson, L., et al. (2008). Improving T-cell assays for the diagnosis of latent TB infection: potential of a diagnostic test based on IP-10. *PLoS One* 3:e2858. doi: 10.1371/journal.pone.0002858

Sai Priya, V. H., Latha, G. S., Hasnain, S. E., Murthy, K. J., Valluri, V. L. (2010). Enhanced T cell responsiveness to *Mycobacterium bovis* BCG r32-kDa Ag correlates with successful anti-tuberculosis treatment in humans. *Cytokine* 52, 190–193. doi: 10.1016/j.cyto.2010.07.001

Selwyn, P. A., Hartel, D., Lewis, V. A., Schoenbaum, E. E., Vermund, S. H., Klein, R. S., et al. (1989). A prospective study of the risk of tuberculosis among intravenous drug users with human immunodeficiency virus infection. *N. Eng. J. Med.* 320, 545–550. doi: 10.1056/nejm198903023200901

Sester, U., Fousse, M., Dirks, J., Mack, U., Prasse, A., Singh, M., et al. (2011). Whole-blood flow-cytometric analysis of antigen-specific CD4 T-cell cytokine profiles distinguishes active tuberculosis from non-active states. *PLoS One* 6:e17813. doi: 10.1371/journal.pone.0017813

Shah, M., Martinson, N. A., Chaisson, R. E., Martin, D. J., Variava, E., Dorman, S. E. (2010). Quantitative analysis of a urine-based assay for detection of lipoarabinomannan in patients with tuberculosis. *J. Clin. Microbiol.* 48, 2972–2974. doi: 10.1128/jcm.00363-10

Sharma, S. K., Vashishtha, R., Chauhan, L. S., Sreenivas, V., Seth, D. (2017). Comparison of TST and IGRA in diagnosis of latent tuberculosis infection in a high TB-burden setting. *PLoS One* 12:e0169539. doi: 10.1371/journal.pone.0169539

Shen, G. H., Chiou, C. S., Hu, S. T., Wu, K. M., Chen, J. H. (2011). Rapid identification of the *Mycobacterium tuberculosis* complex by combining the ESAT-6/CFP-10 immunochromatographic assay and smear morphology. *J. Clin. Microbiol.* 49, 902–907. doi: 10.1128/jcm.00592-10

Steingart, K. R., Dendukuri, N., Henry, M., Schiller, I., Nahid, P., Hopewell, P. C., et al. (2009). Performance of purified antigens for serodiagnosis of pulmonary tuberculosis: a meta-analysis. *Clin. Vaccine Immunol.* 16, 260–276. doi: 10.1128/cvi.00355-08

Steingart, K. R., Flores, L. L., Dendukuri, N., Schiller, I., Laal, S., Ramsay, A., et al. (2011). Commercial serological tests for the diagnosis of active pulmonary and extrapulmonary tuberculosis: an updated systematic review and meta-analysis. *PLoS Med.* 8:e1001062. doi: 10.1371/journal.pmed.1001062

Steingart, K. R., Henry, M., Laal, S., Hopewell, P. C., Ramsay, A., Menzies, D., et al. (2007). Commercial serological antibody detection tests for the diagnosis of pulmonary tuberculosis: a systematic review. *PLoS Med.* 4:e202. doi: 10.1371/journal.pmed.0040202

Streitz, M., Tesfa, L., Yildirim, V., Yahyazadeh, A., Ulrichs, T., Lenkei, R., et al. (2007). Loss of receptor on tuberculin-reactive T-cells marks active pulmonary tuberculosis. *PLoS One.* 2:e735. doi: 10.1371/journal.pone.0000735

Strimbu, K., and Tavel, J. A. (2010). What are biomarkers? *Curr. Opin. HIV AIDS* 5, 463–466.

Sutherland, J. S., Adetifa, I. M., Hill, P. C., Adegbola, R. A., Ota, M. O. (2009). Pattern and diversity of cytokine production differentiates between *Mycobacterium tuberculosis* infection and disease. *Eur. J. Immunol.* 39, 723–729. doi: 10.1002/eji.200838693

Sutherland, J. S., Loxton, A. G., Haks, M. C., Kassa, D., Ambrose, L., Lee, J. S., et al. (2014). Differential gene expression of activating Fcgamma receptor classifies active tuberculosis regardless of human immunodeficiency virus status or ethnicity. *Clin. Microbiol. Infect.* 20:O230–O238.

Theron, G., Peter, J., Calligaro, G., Meldau, R., Hanrahan, C., Khalfey, H., et al. (2014). Determinants of PCR performance (Xpert MTB/RIF), including bacterial load and inhibition, for TB diagnosis using specimens from different body compartments. *Sci. Rep.* 4:5658.

Thomas, M. M., Hinks, T. S., Raghuraman, S., Ramalingam, N., Ernst, M., Nau, R., et al. (2008). Rapid diagnosis of *Mycobacterium tuberculosis* meningitis by enumeration of cerebrospinal fluid antigen-specific T-cells. *Int. J. Tuberc. Lung Dis.* 12, 651–657.

Tiberi, S., du Plessis, N., Walzl, G., Vjecha, M. J., Rao, M., Ntoumi, F., et al. (2018). Tuberculosis: progress and advances in development of new drugs, treatment regimens, and host-directed therapies. *Lancet Infect. Dis.* 18:e183–e98.

Turbawaty, D. K., Sugianli, A. K., Soeroto, A. Y., Setiabudiawan, B., and Parwati, I. (2017). Comparison of the performance of urinary *Mycobacterium tuberculosis* antigens cocktail (ESAT6, CFP10, and MPT64) with culture and microscopy in pulmonary tuberculosis patients. *Int. J. Microbiol.* 2017:3259329.

Verma, R. K., and Jain, A. (2007). Antibodies to mycobacterial antigens for diagnosis of tuberculosis. *FEMS Immunol. Med. Microbiol.* 51, 453–461.

Wallis, R. S., Pai, M., Menzies, D., Doherty, T. M., Walzl, G., Perkins, M. D, et al. (2010). Biomarkers and diagnostics for tuberculosis: progress, needs, and translation into practice. *Lancet* 375, 1920–1937. doi: 10.1016/s0140-6736(10)60359-5

Walter, N. D., Dolganov, G. M., Garcia, B. J., Worodria, W., Andama, A., Musisi, E., et al. (2015). Transcriptional adaptation of drug-tolerant *Mycobacterium tuberculosis* during treatment of human tuberculosis. *J. Infect. Dis.* 212, 990–998.

Walzl, G., McNerney, R., du Plessis, N., Bates, M., McHugh, T. D., Chegou, N. N., et al. (2018). Tuberculosis: advances and challenges in development of new diagnostics and biomarkers. *Lancet Infect. Dis.* 18, e199–e210. doi: 10.1016/s1473-3099(18)30111-7

Walzl, G., Ronacher, K., Hanekom, W., Scriba, T. J., and Zumla, A. (2011). Immunological biomarkers of tuberculosis. *Nat. Rev. Immunol.* 11, 343–354. doi: 10.1038/nri2960

Wang, X., Cao, Z., Jiang, J., Niu, H., Dong, M., Tong, A., et al. (2010). Association of mycobacterial antigen-specific CD4(+) memory T cell subsets with outcome of pulmonary tuberculosis. *J. Infect.* 60, 133–139. doi: 10.1016/j.jinf.2009.10.048

Weiner, J. III., Parida, S. K., Maertzdorf, J., Black, G. F., Repsilber, D., Telaar, A., et al. (2012). Biomarkers of inflammation, immunosuppression and stress with active disease are revealed by metabolomic profiling of tuberculosis patients. *PLoS One* 7:e40221. doi: 10.1371/journal.pone.0040221

Weiner, J., and Kaufmann, S. H. (2017). High-throughput and computational approaches for diagnostic and prognostic host tuberculosis biomarkers. *Int. J. Infect. Dis.* 56, 258–262. doi: 10.1016/j.ijid.2016.10.017

Whittaker, E., Gordon, A., and Kampmann, B. (2008). Is IP-10 a better biomarker for active and latent tuberculosis in children than IFNgamma? *PLoS One* 3:e3901. doi: 10.1371/journal.pone.0003901

Won, E. J., Choi, J. H., Cho, Y. N., Jin, H. M., Kee, H. J., Park, Y. W, et al. (2017). Biomarkers for discrimination between latent tuberculosis infection and active tuberculosis disease. *J. Infect.* 74, 281–293. doi: 10.1016/j.jinf.2016.11.010

World Health Organization [WHO], (2002). *WHO Report Global Tuberculosis Control: Surveillence, Planning, Financing*. Geneva: WHO.

World Health Organization [WHO], (2004). *Toman's Tuberculosis. Case Detection, Treatment, and Monitoring*. Geneva: WHO

World Health Organization [WHO], (2007). *The Use of Liquid Medium for Culture and DST*. Geneva: WHO.

World Health Organization [WHO], (2013). *Systemetic Screening for Active Tuberculosis: Principle and Recommendation*. Geneva: WHO.

World Health Organization [WHO], (2014). *Meeting Report. High-Priority Target Product profiles for New Tuberculosis Diagnostics: Report of a Consensus Meeting*. Geneva: WHO.

World Health Organization [WHO], (2016). *WHO Treatment Guidelines for Drugresistant Tuberculosis*. Geneva: WHO.

World Health Organization [WHO], (2017). *Global Tuberculosis Report 2017*. Geneva: WHO

World Health Organization [WHO], (2018). *Global Tuberculosis Report 2018*. Geneva: WHO

Wu, J., Wang, S., Lu, C., Shao, L., Gao, Y., Zhou, Z., et al. (2017). Multiple cytokine responses in discriminating between active tuberculosis and latent tuberculosis infection. *Tuberculosis* 102, 68–75. doi: 10.1016/j.tube.2016.06.001

Yan, Z. H., Zheng, X. F., Yi, L., Wang, J., Wang, X. J., Wei, P. J., et al. (2017). CD137 is a useful marker for identifying CD4(+) T Cell responses to

Mycobacterium tuberculosis. *Scand. J. Immunol.* 85, 372–380. doi: 10.1111/sji.12541

Yao, X., Liu, Y., Liu, Y., Liu, W., Ye, Z., Zheng, C., et al. (2017). Multiplex analysis of plasma cytokines/chemokines showing different immune responses in active TB patients, latent TB infection and healthy participants. *Tuberculosis* 107, 88–94. doi: 10.1016/j.tube.2017.07.013

Yong, Y. K., Tan, H. Y., Saeidi, A., Rosmawati, M., Atiya, N., Ansari, A. W., et al. (2017). Decrease of CD69 levels on TCR Valpha7.2(+)CD4(+) innate-like lymphocytes is associated with impaired cytotoxic functions in chronic hepatitis B virus-infected patients. *Innate Immun.* 23, 459–467. doi: 10.1177/1753425917714854

Zeka, A. N., Tasbakan, S., and Cavusoglu, C. (2011). Evaluation of the GeneXpert MTB/RIF assay for rapid diagnosis of tuberculosis and detection of rifampin resistance in pulmonary and extrapulmonary specimens. *J. Clin. Microbiol.* 49, 4138–4141. doi: 10.1128/jcm.05434-11

Zhang, C., Song, X., Zhao, Y., Zhang, H., Zhao, S., Mao, F., et al. (2015). *Mycobacterium tuberculosis* secreted proteins as potential biomarkers for the diagnosis of active tuberculosis and latent tuberculosis infection. *J. Clin. Lab. Anal.* 29, 375–382. doi: 10.1002/jcla.21782

Zwerling, A., Behr, M. A., Verma, A., Brewer, T. F., Menzies, D., and Pai, M. (2011). The BCG World Atlas: a database of global BCG vaccination policies and practices. *PLoS Med.* 8:e1001012. doi: 10.1371/journal.pmed.1001012

Conflict of Interest: The authors declare that the research was conducted in the absence of any commercial or financial relationships that could be construed as a potential conflict of interest.

frontiers in Cellular and Infection Microbiology

ORIGINAL RESEARCH
published: 17 January 2020
doi: 10.3389/fcimb.2019.00459

Assessment of an Antibody-in-Lymphocyte Supernatant Assay for the Etiological Diagnosis of Pneumococcal Pneumonia in Children

Michael J. Carter[1,2,3,4,5†], Pallavi Gurung[3†], Claire Jones[1,2], Shristy Rajkarnikar[3], Rama Kandasamy[1,2], Meeru Gurung[3], Stephen Thorson[3], Madhav C. Gautam[3], Krishna G. Prajapati[3], Bibek Khadka[3], Anju Maharjan[3], Julian C. Knight[5], David R. Murdoch[6], Thomas C. Darton[1,2,7], Merryn Voysey[1,2], Brian Wahl[8], Katherine L. O'Brien[8], Sarah Kelly[1,2], Imran Ansari[3], Ganesh Shah[3], Nina Ekström[9], Merit Melin[9], Andrew J. Pollard[1,2], Dominic F. Kelly[1,2‡] and Shrijana Shrestha[3‡] for the PneumoNepal Study Group*

[1] Oxford Vaccine Group, Department of Paediatrics, University of Oxford, Oxford, United Kingdom, [2] NIHR Oxford Biomedical Research Centre, Oxford, United Kingdom, [3] Patan Academy of Health Sciences, Kathmandu, Nepal, [4] School of Life Course Sciences, King's College London, London, United Kingdom, [5] Wellcome Centre for Human Genetics, University of Oxford, Oxford, United Kingdom, [6] Department of Pathology, University of Otago, Christchurch, Christchurch, New Zealand, [7] Department of Infection, Immunity and Cardiovascular Disease, University of Sheffield Medical School, Sheffield, United Kingdom, [8] International Vaccine Access Center, Department of International Health, Johns Hopkins Bloomberg School of Public Health, Baltimore, MD, United States, [9] Expert Microbiology Unit, National Institute for Health and Welfare (THL), Helsinki, Finland

New diagnostic tests for the etiology of childhood pneumonia are needed. We evaluated the antibody-in-lymphocyte supernatant (ALS) assay to detect immunoglobulin (Ig) G secretion from *ex vivo* peripheral blood mononuclear cell (PBMC) culture, as a potential diagnostic test for pneumococcal pneumonia. We enrolled 348 children with pneumonia admitted to Patan Hospital, Kathmandu, Nepal between December 2015 and September 2016. PBMCs sampled from participants were incubated for 48 h before harvesting of cell culture supernatant (ALS). We used a fluorescence-based multiplexed immunoassay to measure the concentration of IgG in ALS against five conserved pneumococcal protein antigens. Of children with pneumonia, 68 had a confirmed etiological diagnosis: 12 children had pneumococcal pneumonia (defined as blood or pleural fluid culture-confirmed; or plasma CRP concentration ≥60 mg/l and nasopharyngeal carriage of serotype 1 pneumococci), and 56 children had non-pneumococcal pneumonia. Children with non-pneumococcal pneumonia had either a bacterial pathogen isolated from blood (six children); or C-reactive protein <60 mg/l, absence of radiographic consolidation and detection of a pathogenic virus by multiplex PCR (respiratory syncytial virus, influenza viruses, or parainfluenza viruses; 23 children). Concentrations of ALS IgG to all five pneumococcal proteins were significantly higher in children with pneumococcal pneumonia than in children with non-pneumococcal pneumonia. The concentration of IgG in ALS to the best-performing antigen discriminated between children with pneumococcal and non-pneumococcal pneumonia with a sensitivity of 1.0 (95% CI

OPEN ACCESS

Edited by:
Max Maurin, Université Grenoble Alpes, France

Reviewed by:
Clark Donald Russell, University of Edinburgh, United Kingdom
David Ong, Sint Franciscus Gasthuis, Netherlands

***Correspondence:**
Michael J. Carter
michael.carter@kcl.ac.uk

[†] *These authors share first authorship*

[‡] *These authors share senior authorship*

Specialty section:
This article was submitted to Clinical Microbiology, a section of the journal Frontiers in Cellular and Infection Microbiology

Received: *13 June 2019*
Accepted: *16 December 2019*
Published: *17 January 2020*

Citation:
Carter MJ, Gurung P, Jones C, Rajkarnikar S, Kandasamy R, Gurung M, Thorson S, Gautam MC, Prajapati KG, Khadka B, Maharjan A, Knight JC, Murdoch DR, Darton TC, Voysey M, Wahl B, O'Brien KL, Kelly S, Ansari I, Shah G, Ekström N, Melin M, Pollard AJ, Kelly DF and Shrestha S (2020) Assessment of an Antibody-in-Lymphocyte Supernatant Assay for the Etiological Diagnosis of Pneumococcal Pneumonia in Children. Front. Cell. Infect. Microbiol. 9:459. doi: 10.3389/fcimb.2019.00459

0.73–1.0), specificity of 0.66 (95% CI 0.52–0.78) and area under the receiver-operating characteristic curve (AUROCC) 0.85 (95% CI 0.75–0.94). Children with pneumococcal pneumonia were older than children with non-pneumococcal pneumonia (median 5.6 and 2.0 years, respectively, $p < 0.001$). When the analysis was limited to children ≥2 years of age, assay of IgG ALS to pneumococcal proteins was unable to discriminate between children with pneumococcal pneumonia and non-pneumococcal pneumonia (AUROCC 0.67, 95% CI 0.47–0.88). This method detected spontaneous secretion of IgG to pneumococcal protein antigens from cultured PBMCs. However, when stratified by age group, assay of IgG in ALS to pneumococcal proteins showed limited utility as a test to discriminate between pneumococcal and non-pneumococcal pneumonia in children.

Keywords: pneumococcus (*Streptococcus pneumoniae*), pneumonia, antibodies, diagnostic test (MeSH), lymphocytes

INTRODUCTION

Pneumonia is the leading cause of childhood mortality after the neonatal period, yet the pathogen-specific etiology of childhood pneumonia remains poorly defined (Liu et al., 2016; Feikin et al., 2017b). Using data from randomized controlled vaccine trials, vaccine-probe studies help reveal the pathogen-specific burden of disease by estimating the difference in disease between vaccinated and unvaccinated individuals (Feikin et al., 2014). Results from these studies estimate that approximately one third of children with pneumonia and radiographic consolidation have pneumococcal pneumonia in settings prior to the introduction of vaccines that prevent etiology-specific pneumonia, regardless of geography (O'Brien et al., 2009; Wahl et al., 2018). However, microbiological data to support this prevalence estimate are lacking. Accurate diagnostic tests for the etiology of pneumonia are needed to assess the etiology of pneumonia in changing epidemiological contexts, notably following vaccine implementation (Feikin et al., 2017b).

Direct aspiration of infected (lung) tissue is rarely used due to perceived safety concerns (Ideh et al., 2011; Howie et al., 2014), while culture of broncho-alveolar lavage samples is only possible on samples from children requiring mechanical ventilation. Culture of bacteria from blood is therefore the most widely used test for bacterial pneumonia in children admitted to hospital. However, estimates of yield from "true positive" bacterial pneumonia cases are <20% (Cutts et al., 2005), depending on prior antibiotic exposure, sample volume and culture technique (Driscoll et al., 2017). In the recent Pneumonia Etiology Research for Child Health (PERCH) case-control study, quantitative (q)PCR of *lytA* to determine whole blood pneumococcal load (Deloria Knoll et al., 2017), and density of nasopharyngeal (NP) colonization with *S. pneumonia* (Baggett et al., 2017), demonstrated only moderate ability to discriminate between pneumococcal pneumonia and age-matched community children.

An alternative approach to the diagnosis of pneumococcal pneumonia is to assess the immune response to the pathogen. Unfortunately, serological assays have limited specificity in the acute phase, or require convalescent samples to discriminate from past infections (Tuerlinckx et al., 2013; Andrade et al., 2016). We hypothesized that we could combine the etiological specificity of serological assays to a time-specific population of B cells (plasmablasts), that circulate during active infection (Carter et al., 2017), using the antibody-in-lymphocyte supernatant (ALS) assay.

The ALS assay was originally developed to assess vaccine-induced serological responses, and has since been developed for the diagnosis of enteric fever and tuberculosis (Chang and Sack, 2001; Sheikh et al., 2009; Darton et al., 2017b; Sariko et al., 2017). This assay is based upon testing the secretions of lymphocytes that are incubated *in vitro* following sampling from an unwell patient (without *ex vivo* stimulation). Following incubation, harvested supernatant can be tested for pathogen-specific antibodies using standard serological techniques.

We assessed the diagnostic performance of the ALS assay for the diagnosis of pneumococcal infection in a prospective study of childhood pneumonia in Nepal, a low income country in South Asia with a high burden of childhood pneumonia (Ministry of Health Population (MOHP) et al., 2012). We used five pneumococcal proteins as target antigens (choline binding protein A, CbpA; protein for cell wall separation of group B streptococci, PcsB; pneumococcal histidine triad D, PhtD; pneumolysin, Ply; serine threonine kinase protein C, StkpC). These antigens are thought to be expressed by all pathogenic pneumococci, are specific to pneumococci or closely related species, and have been used to assess the serological response to pneumococcal pneumonia (Andrade et al., 2014, 2016; Borges et al., 2016).

MATERIALS AND METHODS

Ethics Statement

This prospective study was carried out in accordance with the protocol and the International Conference on Harmonization Good Clinical Practice standard. Literate parents/legal guardians all gave informed written consent prior to enrolment. Non-literate parents/legal guardians gave verbal and thumbprint consent in the presence of a literate (non-hospital/research

staff) witness who could attest to the explanation of the patient information leaflet and the agreement of the signatory. The study protocol was approved by the Nepal Health Research Council (286/2014) and the Oxford Tropical Research Ethics Committee (09/15).

Study Site and Population

Patan Hospital is in the Lalitpur sub-Metropolitan district of Nepal, contiguous with the city of Kathmandu. It is one of the largest hospitals in the country, and one of few with inpatient pediatric and pediatric critical care facilities. During the study period, the primary infant vaccination schedule included diphtheria-tetanus-pertussis, bacille-Calmette-Guérin, hepatitis B, *Haemophilus influenzae* type b (from 2009), oral and inactivated poliovirus and measles, rubella and Japanese encephalitis antigens, with 83% coverage for all antigens in 2011 in the Central Development Region of Nepal (including Lalitpur) [Ministry of Health Population (MOHP) et al., 2012]. Ten-valent pneumococcal conjugate vaccination (10-valent PCV) was introduced to the infant immunization schedule in Lalitpur in August 2015 at 6 and 10 weeks, and 9 months of age. There was a limited PCV catch-up campaign among infants.

Enrolment and Sampling

Children were enrolled for this study between 22nd December 2015 and 30th September 2016. Children were eligible for enrolment if ≥60 days of age and <15 years of age and being admitted to Patan Hospital with a clinical diagnosis of pneumonia. A small number of patients were diagnosed with pneumonia, enrolled, and then discharged directly before admission; their data are included here (**Figure 1**). The diagnosis of pneumonia was made by admitting pediatricians, reviewed by a consultant (attending) pediatrician, and was typically prior to results from radiographs or blood tests becoming available. Children who did not have a clinical diagnosis of pneumonia were excluded from the study. A digitalized radiograph was obtained on all children on study enrolment. All radiographs were independently interpreted using standardized WHO criteria (Liu et al., 2016) as endpoint consolidation, other infiltrate, or no consolidation/effusion/infiltrate by two specific readers (a pediatrician, and a radiologist). A second specific radiologist arbitrated upon all discordant results, and 10% of other radiographs. Radiographic findings were not used to exclude children from the study. Child healthy controls were enrolled from a vaccine clinic at 10 months of age, and all controls had been vaccinated with three doses of 10-valent PCV (most recent dose received ≥28 days prior to sampling).

Enrolled cases and controls all had 2 ml of blood sampled into heparinized and sterile centrifuge tubes for this study by peripheral venepuncture within 48 h of admission. In addition all enrolled children had full blood count, plasma (for storage) and inoculation of blood into Bactec Peds Plus culture bottles (Becton Dickinson, BD; USA) for automated incubation (Bactec, BD), subculture and identification of isolated organisms. Heparinized blood was immediately taken to the Microbiology Laboratory and processed within 4 h of sampling as described below. C-reactive protein (CRP) concentrations were measured following shipment of plasma to Oxford at Oxford University Hospitals NHS Foundation Trust.

A single flocked swab (Thermo Fisher Scientific, UK) was used to sample the nasopharynx, and a digital chest radiograph was taken, at admission. The NP swab was immediately and aseptically placed into skim-milk-tryptone-glucose-glycerin media and transported to the on-site Microbiology Laboratory, cultured for pneumococci, and subjected to Quellung serotyping. NP swabs in STGG media were subsequently stored at −80°C before transport to the UK on dry ice and further storage at −80°C. All chest radiographs underwent blinded review for radiographic endpoint consolidation by two clinicians (a pediatrician and a radiologist) according to World Health Organization criteria (Cherian et al., 2005), with quality control and discordant readings arbitrated upon by a second radiologist.

PCR Methods

NP swabs were defrosted and DNA was extracted from 200 μl STGG media using the QIAGEN DNeasy 96 kit (QIAGEN, UK) using a modified protocol. Extracted DNA was subsequently transported to Micropathology Ltd (Warwick, UK) where samples (40 μl extracted DNA) were analyzed using the NxTAG Luminex Respiratory Pathogen Panel (Luminex Corp, USA) (Tang et al., 2016) according to manufacturer's instructions for: influenza A, influenza A H1, influenza A H3, influenza B, RSV A, RSV B, parainfluenza 1–4, coronaviruses 229E/NL63/OC43/HKU1, human metapneumovirus, rhinovirus/enterovirus, adenovirus, human bocavirus, *Chlamydophila pneumoniae*, *Legionella pneumophila*, and *Mycoplasma pneumoniae*. Results were reported as positive or negative for each pathogen. We considered RSV (any group), influenza virus (any serotype) or any of the parainfluenza viruses 1–4 as pathogenic, since these were highly associated with case status in the PERCH study, and were prevalent (≥5 cases for each virus) in our cohort.

Antibody-in-Lymphocyte Supernatant Assay

Samples of fresh, heparinized, whole blood were separated by centrifugation over Ficoll media with a density of 1.077 g/ml (Histopaque 1077, Sigma-Aldrich, USA) at 400 g for 20 min with minimal acceleration and deceleration. This yielded plasma, peripheral blood mononuclear cells (PBMCs) and a sediment of red cells and polymorphonuclear cells. The PBMC layer was manually aspirated and washed by resuspension and centrifugation twice into RPMI culture media plus penicillin (500 U/l), streptomycin (0.25 mg/l), and L-glutamine (10 mmol/L; all Sigma-Aldrich; "R0 medium"). Following manual counting and calculation of the total number of PBMCs, the cells were resuspended into R0 medium plus 10% fetal bovine serum (heat-inactivated and sterile-filtered, Sigma-Aldrich; "R10 medium"), and incubated in a sterile cell culture plate (Greiner, Germany) at 37°C and 5% CO_2 for 48 h. Following incubation the cell suspension was separated by centrifugation with the resulting supernatant (ALS) preserved with 40X protease inhibitors (25 μl per ml of ALS) and stored immediately at −80°C before shipping to Oxford and Helsinki on dry ice for further analyses.

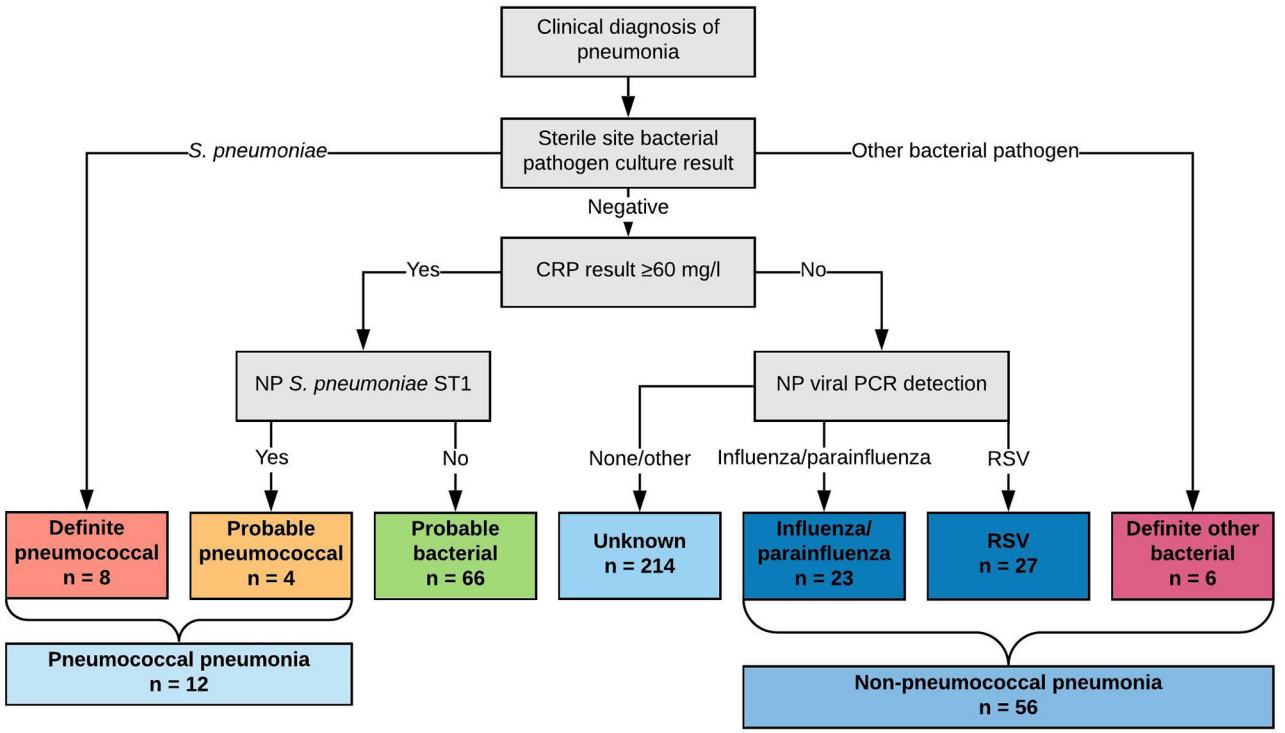

FIGURE 1 | Classification of children by likely etiology of pneumonia into comparator groups (*definite pneumococcal*, *probable pneumococcal*, *probable bacterial*, *unknown*, *influenza/parainfluenza virus*, *RSV*, and *definite other bacterial*) and by diagnosis of "*pneumococcal pneumonia*" and "*non-pneumococcal pneumonia*".

A fluorescent multiplexed bead-based immunoassay (FMIA) to detect IgG ALS to five pneumococcal proteins (CbpA, PcsB, PhtD, Ply, and StkpC) was used for this study as previously described (Andrade et al., 2014, 2016). In brief, samples of ALS were diluted to 1/25 in phosphate buffered saline containing 10% fetal bovine serum, with the FMIA performed as a 5-plex assay with 1,200 beads per region per well. IgG in ALS were detected using RPE-conjugated goat anti-human IgG (Jackson Immunoresearch, USA). Pneumococcal reference standard serum 007sp (NIBSC, UK) was used as the reference with an arbitrary assigned concentration of 100 units/ml for each anti-pneumococcal antibody.

Classification of Childhood Pneumonia Etiology by Comparator Group

We classified children by comparator groups based on likely etiology of pneumonia (where these comparator groups are used in the text, they are italicized for clarity.) This classification scheme is described in **Figure 1**. Specifically, we classified children into comparator groups as *definite pneumococcal pneumonia* (*S. pneumoniae* cultured from blood or pleural fluid), *probable pneumococcal pneumonia* (CRP concentration ≥60 mg/l and NP carriage of serotype 1 pneumococci), *probable bacterial pneumonia* (CRP concentration ≥60 mg/l only), *unknown pneumonia* (CRP concentration <60 mg/l only), *influenza/parainfluenza viral pneumonia* (CRP <60 mg/l and influenza/parainfluenza viruses detected by qPCR from NP specimen), *RSV pneumonia* (CRP <60 mg/l and RSV detected by qPCR from NP specimen), and *definite other bacterial pneumonia* (other bacterial pathogen cultured from blood or pleural fluid). These were ordered by hypothesized probability of pneumococcal infection from *definite pneumococcal pneumonia* to *definite other bacterial pneumonia* (left to right, **Figure 1**).

To assess the utility of acute IgG ALS to pneumococcal proteins to identify pneumococcal pneumonia we compounded *definite pneumococcal pneumonia* and *probable pneumococcal pneumonia* into a single category (*pneumococcal pneumonia*); and we combined *influenza/parainfluenza virus pneumonia*, *RSV pneumonia* and *definite other bacterial pneumonia* into a single category (*non-pneumococcal pneumonia*).

The classification scheme was modified from similar schemes for the development of novel diagnostic tests to discriminate between bacterial and viral infection (Herberg et al., 2016; Kaforou et al., 2017). Recent data have estimated a threshold to discriminate between bacterial and viral pneumonia at a CRP concentration of ∼50–60 mg/l in children in South Asia and in low and middle-income countries in the PERCH study (Lubell et al., 2015; Higdon et al., 2017b). We chose NP carriage of pneumococcal serotype 1 (by culture) as a predictor of pneumococcal infection. The association of NP carriage of serotype 1 pneumococci in cases compared with controls, has been previously established in unvaccinated populations (Scott et al., 1996). NP carriage of serotype 1 was also associated with cases in comparison with controls

in 938 children with pneumonia at Patan Hospital between 2014 and 2015 (prior to 10-valent PCV introduction) and 3,202 age-stratified control (non-pneumonia) children (odds ratio for case status of 5.0, 95% confidence interval, CI, 1.7–14.0; **Figure S1**). This was supported by unpublished data from childhood invasive pneumococcal disease at Patan Hospital from 2005 to 2016, where 58/124 (47%) isolated pneumococci were of serotype 1. Similar findings have been reported from other epidemiological settings (Scott et al., 1996; Johnson et al., 2010). We chose NP carriage (as detected by PCR) of influenza or parainfluenza virus, and RSV to represent viral pneumonia since carriage of these viruses was associated with radiographically-confirmed pneumonia in the PERCH study (Feikin et al., 2017a).

While we used NP carriage of serotype 1 pneumococci as a predictor of *pneumococcal pneumonia*, we also subsequently investigated for an association of NP carriage of pneumococci with increased IgG ALS to pneumococcal proteins. To avoid confounding with undetected pneumococcal infection, we limited this analysis to children with *non-pneumococcal pneumonia* (i.e., *definite other bacterial pneumonia*, *influenza/parainfluenza pneumonia* or *RSV pneumonia*).

Statistical Methods

Continuous variables were compared using Student's *t*-test, following appropriate transformation (log transformation of age distribution; and taking the reciprocal of ALS concentrations to pneumococcal protein for the comparison of ALS concentrations to pneumococcal proteins between *probable bacterial pneumonia* and *unknown pneumonia*). Assay signals that were undetectable were assigned a value below the threshold of detection. Fisher exact tests, Wilcoxon rank sum tests, and χ^2 test were used as indicated. Kruskal-Wallis tests were used to assess for confounding of acute IgG ALS to pneumococcal proteins with age, and length of illness. Formal statistical testing for an interaction between age (grouped, due to a non-normal distribution) and acute IgG ALS to pneumococcal proteins stratified by comparator group was not possible due to small numbers and tied ALS values. Analyses were pre-specified, with the exception of a *post-hoc* analysis of the effects of age on IgG ALS to pneumococcal proteins. We used best subsets regression analysis to investigate optimal combinations of pneumococcal protein antigens for IgG ALS to discriminate between children with *pneumococcal pneumonia* and *non-pneumococcal pneumonia* and assessed for multiple co-linearity.

RESULTS

Characteristics of the Cohort

One thousand nine hundred four children were admitted to Patan Hospital during the study period. Of admitted children, 356 (19%) children had a clinician diagnosis of pneumonia, as had an additional 37 children who were diagnosed with pneumonia, but not admitted, totaling 393 children. 369 children were enrolled to the study, with data on ALS to pneumococcal proteins available on 348 of these children (**Figure 2**). Of 348 children, 122 (35%) had endpoint consolidation/effusions on chest radiograph, 32 (9%) had infiltrates, 178 had neither consolidation/effusions or infiltrates, 2 (<1%) were uninterpretable and 14 (4%) children did not have a chest radiograph. Of 304 children <5 years of age, 217 (71%) met the WHO criteria for pneumonia (fast breathing or chest indrawing) and 87 (29%) did not. In addition, 48 healthy infants (controls) aged 10 months of age were enrolled, on whom ALS was analyzed on a random subset of 20 infants. All healthy infant controls had received three doses of 10-valent PCV, with the most recent dose ≥28 days prior to enrolment to this study. The clinical characteristics of children with pneumonia are described in **Table 1** by comparator group (and **Table S1** by other classifications).

We classified eight children as *definite pneumococcal*, four children as *probable pneumococcal* (totaling 12 as *pneumococcal pneumonia*), 66 children as *probable bacterial*, 214 children as *unknown*, 23 children as *parainfluenza/influenza virus*, 27 children as *RSV*, and six children as *definite other bacterial pneumonia.* This totaled 56 children as *non-pneumococcal pneumonia.*

On comparison of children with *pneumococcal pneumonia* vs. children with *non-pneumococcal pneumonia*, there were significant differences in age (median 6.3 years, interquartile range 4.2–8.3 and 0.8 years, IQR 0.5–2.2, *t*-test following log transformation of age distribution, $p < 0.001$), sex (females 8 and 46%, Fisher exact test, $p = 0.02$), length of illness (3 days, IQR 2–3.3 and 4.5 days, IQR 3–7, Wilcoxon rank sum test, $p < 0.001$), and proportion with radiographic endpoint consolidation (92 and 23%, χ^2 test, $p < 0.001$). The youngest child with *pneumococcal pneumonia* was 3.8 years of age.

Diagnostic Accuracy of IgG ALS to Pneumococcal Proteins

IgG ALS to pneumococcal proteins was detected and quantifiable in 348 acute samples from children with pneumonia.

Acute IgG ALS was higher in children with *pneumococcal pneumonia* than children with all other pneumonia (including possible cases of undiagnosed pneumococcal pneumonia within the comparator groups *probable bacterial pneumonia*, *unknown*, *influenza/parainfluenza pneumonia*, *RSV pneumonia*, *definite other bacterial pneumonia*) for 4/5 pneumococcal proteins (**Figure 3**). Assay of acute IgG ALS to pneumococcal proteins discriminated between pneumococcal pneumonia and all other pneumonia with good accuracy for CbpA, PcsB and PhtD, but not Ply or StkpC: AUROC curve was 0.81 (95% CI 0.73–0.89) for CbpA, 0.77 (95% CI 0.65, 0.89) for PcsB, 0.78 (95% CI 0.67–0.89) for PhtD, 0.59 (95% CI 0.42–0.76) for Ply, and 0.66 (95% CI 0.50–0.81) for StkpC.

Acute IgG ALS was higher in children with *pneumococcal pneumonia* than with *non-pneumococcal pneumonia* for all five pneumococcal proteins (**Figure 4**). Acute IgG ALS to pneumococcal proteins discriminated between *pneumococcal pneumonia* and *non-pneumococcal pneumonia* in children enrolled to the study with good sensitivity and specificity, with AUROC curve ranging from 0.60 (95% CI 0.42–0.79) for Ply,

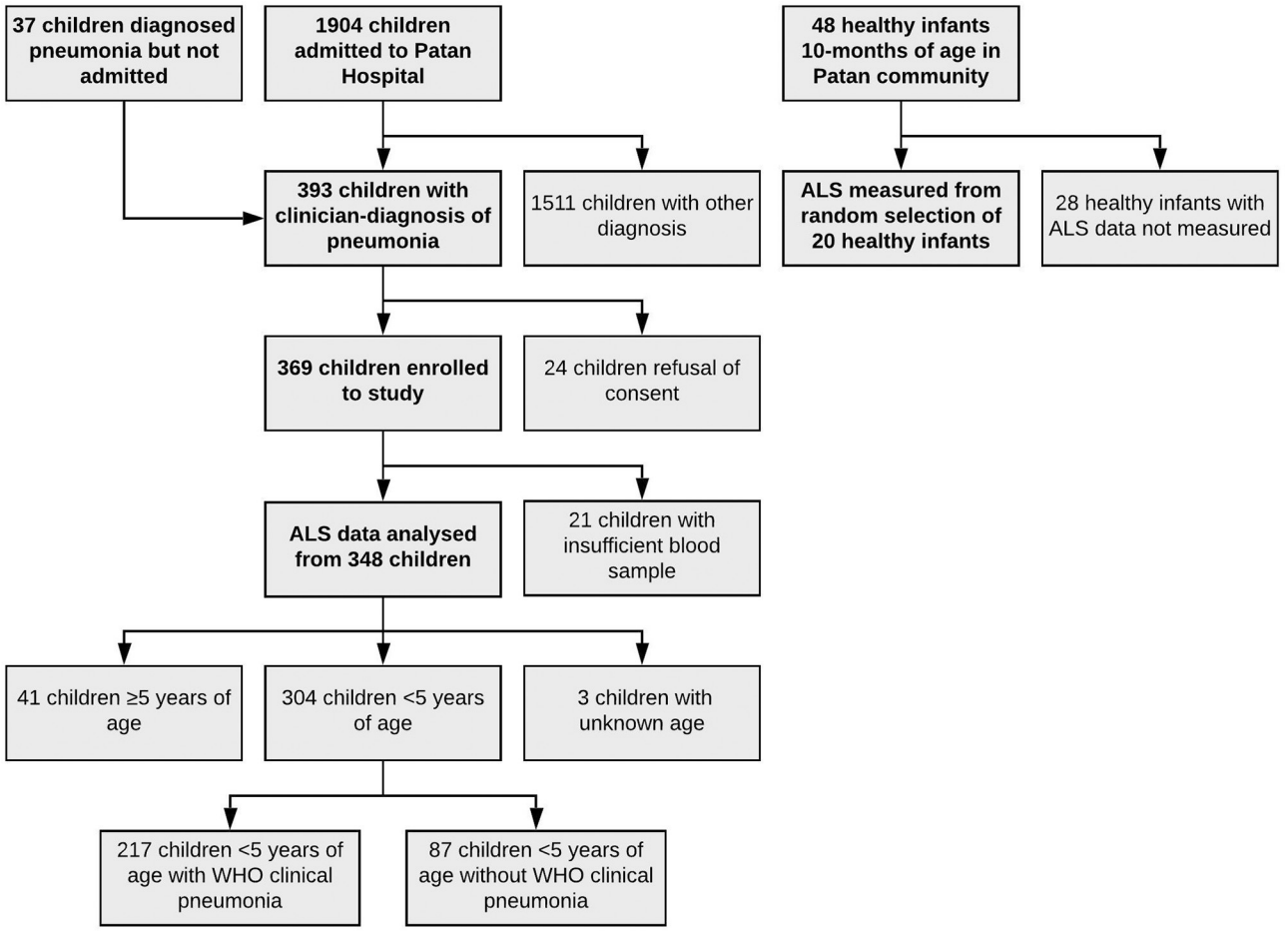

FIGURE 2 | Flow diagram of enrolment to the study.

to 0.85 (95% CI 0.75–0.94) for CbpA, using thresholds derived from the Youden Index (**Table 2**). There was a high degree of co-linearity between acute IgG ALS to all five pneumococcal proteins measured with *pneumococcal pneumonia* (and *non-pneumococcal pneumonia*) in best subsets logistic regression analysis.

Discriminating between *pneumococcal pneumonia* patients and healthy controls, acute IgG ALS had an AUROC curve ranging from 0.68 for Ply (95% CI 0.49–0.87) to 0.98 for CbpA (95% CI 0.94–1.0; **Figure S2**, **Table S2**).

Among children with *pneumococcal pneumonia*, there was no significant increase in acute IgG ALS to any of the pneumococcal proteins measured with increasing length of illness (simple linear regression, $p > 0.5$ for all five proteins; **Figure S3**). There were too few female cases with *pneumococcal pneumonia* to investigate sex differences.

Among children with *non-pneumococcal pneumonia*, there was no significant difference in acute IgG ALS to pneumococcal proteins between children with viral pneumonia (influenza/parainfluenza, RSV) or definite other bacterial pneumonia (CbpA, $p = 0.06$; PcsB, $p = 0.50$; PhtD, $p = 0.28$; Ply, $p = 0.92$; StkpC, 0.93).

Children with *probable bacterial pneumonia* had higher concentrations of acute IgG ALS to CbpA, PcsB, PhtD, Ply, and StkpC than children with *unknown pneumonia* (Wilcoxon rank sum test, $p < 0.001$ for all). The proportion of children with acute IgG ALS concentrations greater than the threshold derived from ROC curve analysis differed significantly for CbpA (71% of *probable bacterial pneumonia* and 32% of *unknown pneumonia*, χ^2 test, $p < 0.001$), PcsB (55 and 35%, $p = 0.007$), PhtD (45 and 25%, $p = 0.002$), but did not differ for Ply and StkpC (threshold lines not applicable to **Figure 5**).

Sensitivity Analyses: Age Distribution

Pneumococcal pneumonia was only diagnosed in children ≥2 years of age. We therefore undertook a *post-hoc* analysis of acute IgG to pneumococcal proteins in children ≥2 years of age for the etiological diagnosis of pneumonia. Children ≥2 years of age known to have a qualitatively different humoral immune response to pneumococcal polysaccharide antigens, although not pneumococcal protein antigens, in comparison with young infants (Clutterbuck et al., 2007; Borges et al., 2016; Ramos-Sevillano et al., 2019). The clinical characteristics of children ≥2

TABLE 1 | Clinical characteristics of children of all ages with pneumonia enrolled to the study, by comparator group.

Clinical characteristic	*Pneumococcal pneumonia*				*Non-pneumococcal pneumonia*			
	Definite pneumococcal pneumonia	*Probable pneumococcal pneumonia*	*Probable bacterial pneumonia*	*Unknown*	*Influenza/para-influenza pneumonia*	*RSV pneumonia*	*Definite other bacterial pneumonia*	*p*
n	8	4	66	214	23	27	6[a]	
Age (years; median, IQR)	5.6 (4.2–8.1)	7.5 (5.8–8.3)	2.7 (1.7–5.1)	1.1 (0.6–2.0)	1.1 (0.7–2.5)	0.6 (0.3–1.5)	2.0 (0.7–7.4)	<0.001[b]
2–11 months	0	0	10 (15%)	93 (44%)	11 (48%)	19 (70%)	3 (50%)	
12–23 months	0	0	11 (17%)	64 (30%)	4 (17%)	3 (11%)	0	
24–59 months	3 (38%)	1 (25%)	27 (42%)	42 (20%)	7 (30%)	5 (19%)	1 (17%)	
≥5–14 years	5 (63%)	3 (75%)	17 (26%)	13 (6%)	1 (4%)	0	2 (33%)	
Female sex	1 (13%)	0	27 (41%)	86 (40%)	9 (39%)	15 (56%)	2 (33%)	0.27[c]
Length of illness (days; median, IQR)	2.5 (2–3)	3.5 (2.8–4.3)	4 (3–6)	3 (3–5.8)	5 (3–6.5)	4 (3–6.5)	6 (4.5–6.8)	0.32[b]
Prior antibiotic use	6 (75%)	2 (50%)	30 (45%)	94 (44%)	13 (56%)	11 (41%)	6 (100%)	0.25[c]
NP pneumococcal carriage	2 (25%)	4 (100%)	25 (38%)	59 (28%)	8 (35%)	4 (15%)	1 (17%)	0.02[c]
NP pneumococcal carriage (serotype 1)	1 (12.5%)	4 (100%)	0	1 (0.5%)	0	0	0	–
Endpoint consolidation	8 (100%)	3 (75%)	47 (71%)	51 (24%)	6 (26%)	4 (15%)	3 (50%)	–
CRP concentration (mg/l; median, IQR)	142 (56–183)	133 (97–171)	115 (82–183)	9.7 (2.7–22)	12.4 (5.6–19)	7.0 (1.5–23)	52 (14–113)	–
CRP concentration ≥60 mg/l	5 (63%)	4 (100%)	66 (100%)	0	0	0	3 (50%)	–
NP RSV carriage	0	0	3 (4.9%)	0	1 (4.3%)	27 (100%)	0	–
NP other viral carriage	0	0	4 (6.6%)	0	23 (100%)	0	0	–

[a] *Three Staphylococcus aureus, one each of Neisseria meningitidis, Pseudomonas spp., and Escherichia coli.*

[b] *Kruskal-Wallis test.*

[c] *Fisher exact test (simulated p-values). P-values were not calculated for variables that were entered into the classification scheme in* ***Figure 1****. Values are expressed as the percentage of n for each column (excepting continuous variables).*

years of age with *pneumococcal pneumonia* or *non-pneumococcal pneumonia* from the cohort are described in **Table 3**.

Restricting the analysis to children ≥2 years of age reduced the ability to discriminate between *pneumococcal pneumonia* (12 children) and *non-pneumococcal pneumonia* (16 children) for all pneumococcal proteins to non-significance in this smaller number of samples (Wilcoxon rank sum tests; CbpA, $p = 0.12$; PcsB, $p = 0.10$; PhtD, $p = 0.17$; Ply, $p = 0.13$; StkpC, $p = 0.26$; **Figure 6** and **Table 4**). A visual examination of data points did not suggest that children with *definite other bacterial pneumonia* had different acute IgG ALS to pneumococcal proteins than other children with *non-pneumococcal pneumonia* (red crosses and black crosses, **Figure 6**).

Effects of Nasopharyngeal Carriage of Pneumococci

Among all children enrolled, those with NP carriage of pneumococci had higher acute IgG ALS than those without NP carriage of pneumococci (Wilcoxon rank sum tests, $p < 0.001$ for all five pneumococcal proteins). Among children with *non-pneumococcal pneumonia* (i.e., not "confounded" by *definite pneumococcal* or *probable pneumococcal* or *probable bacterial* or *unknown pneumonia*), those with NP carriage of pneumococci had higher acute IgG ALS to all five pneumococcal proteins than those without NP carriage (Wilcoxon rank sum tests; CbpA, $p < 0.001$; PcsB, $p < 0.001$; PhtD, $p < 0.001$; Ply, $p < 0.001$; StkpC, $p < 0.001$; **Figure 7**). Among children ≥2 years of age with *non-pneumococcal pneumonia*, there were no significant differences in acute IgG ALS to any pneumococcal protein detected between those with ($n = 19$) and without ($n = 49$) NP carriage of pneumococci (Wilcoxon rank sum tests, $p > 0.5$ for all comparisons, **Figure S4**). Stratification of this age group to those who had not received antibiotics prior to NP sampling did not significantly affect these results.

Final Analysis

We used acute IgG ALS to PcsB as the most parsimonious approach to investigate acute IgG to pneumococcal proteins in children ≥2 years of age across the cohort. The number of children (proportion) that had acute IgG ALS greater than, or equal to, the optimum threshold to discriminate between *pneumococcal pneumonia* and *non-pneumococcal pneumonia* was: *definite pneumococcal pneumonia* 5/8 (0.63), *probable pneumococcal pneumonia* 4/4 (1.0), *probable bacterial pneumonia* 20/44 (0.45), *unknown pneumonia* 23/55 (0.42), *influenza/parainfluenza pneumonia* 3/8 (0.38), *RSV pneumonia* 1/5 (0.2), *definite other bacterial pneumonia* 2/3 (0.67; **Figure 8**).

DISCUSSION

The development of novel diagnostic tests for the etiology of pneumonia is partly driven by the need to assess the impact of vaccination strategies on the total, and pathogen-specific burden of pneumonia in diverse settings. We have chosen to focus our

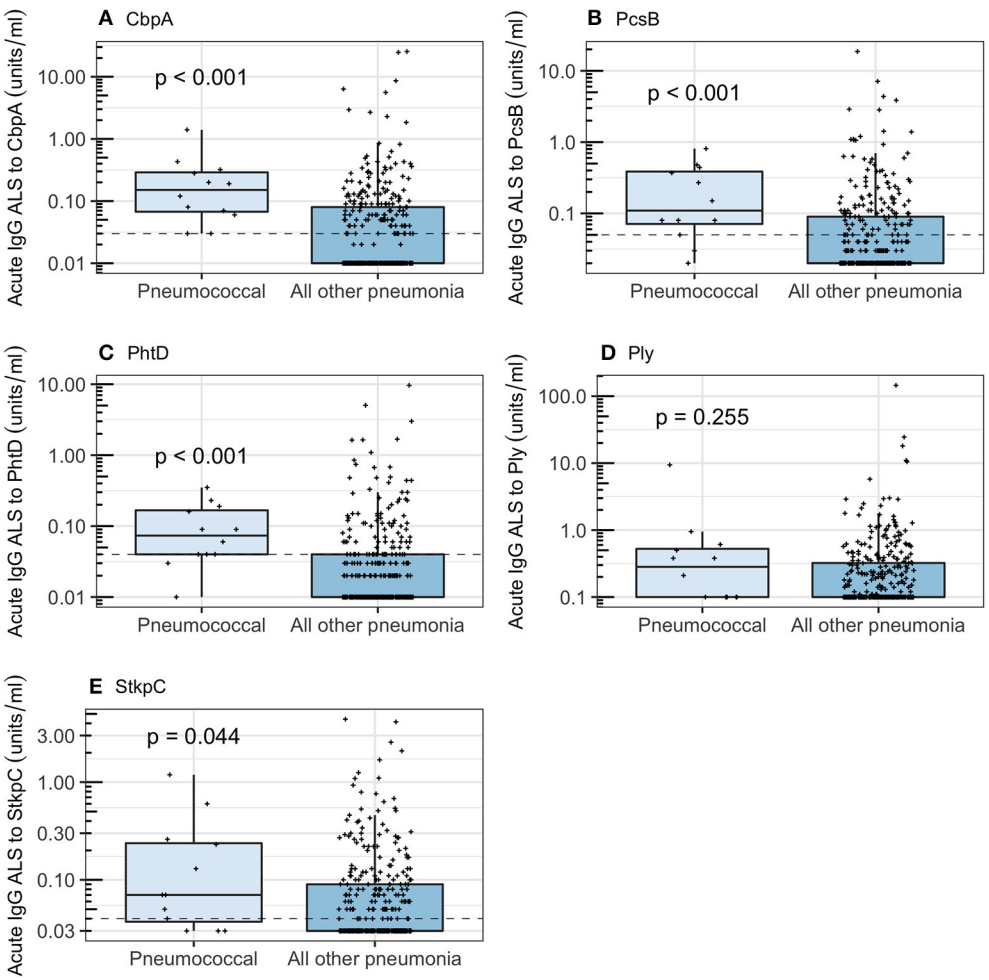

FIGURE 3 | Acute IgG ALS to pneumococcal proteins by children with *pneumococcal pneumonia* and all other pneumonia in children enrolled into the study. Dashed horizontal lines represent thresholds derived from the Youden Index, *p*-values were derived from the Wilcoxon rank sum test. For all box and whisker plots: the solid line represents the median value, lower hinge 25th centile, upper hinge 75th centile, and whiskers represent 1.5 times the interquartile range. All data points have also been plotted. **(A)** Choline binding protein A (CbpA); **(B)** protein for cell wall separation of group B streptococci (PcsB); **(C)** pneumococcal histidine triad D (PhtD); **(D)** pneumolysin (Ply); **(E)** serine threonine kinase protein C (StkpC).

work on pneumococcal pneumonia, during the introduction of 10-valent PCV to the infant immunization schedule in Nepal.

Currently available diagnostic tests for pneumonia etiology lack sensitivity or specificity in children. Culture of pneumococci from blood or pleural fluid from children with pneumonia is presumed to be highly specific for pneumococcal pneumonia but lacks sensitivity (O'Brien et al., 2009; Wu et al., 2016). Theoretically, sampling infected tissue (the lung) might improve sensitivity. A review of studies using lung biopsy followed by culture for the diagnosis of pneumonia etiology identified an increase in yield of bacterial pathogens from 14 to 47% of children tested (Ideh et al., 2011). However, lung biopsy requires peripheral radiographic consolidation, and was therefore not possible in approximately three quarters of patients with clinically severe pneumonia in a recent prospective cohort (Howie et al., 2014). This, in addition to safety concerns, has prevented lung biopsy for diagnostic sampling from becoming a widespread technique (Ideh et al., 2011). Interpretation of samples from the nasopharynx of children is limited by poor specificity, with many pathogens detected at similar prevalence in children with pneumonia and in community controls (Higdon et al., 2017a). Culture or molecular detection of pathogens from of broncho-alveolar lavage samples is only possible on samples from children receiving mechanical ventilation.

We hypothesized that analysis of the immune response to pneumococci may be useful as a diagnostic approach to pneumonia etiology in children. We evaluated a new diagnostic strategy, assay of ALS, based on quantification of antibodies against pneumococcal proteins that are spontaneously secreted by transiently circulating lymphocytes from children with pneumonia. We were able to detect, and quantify, IgG ALS to five specific pneumococcal proteins (CbpA, PcsB, PhtD, Ply, and StkpC) from children with pneumonia using a multiplexed immunoassay (FMIA). Concentrations of ALS IgG to these antigens were significantly higher in supernatants from PBMCs obtained from children with *pneumococcal pneumonia* than

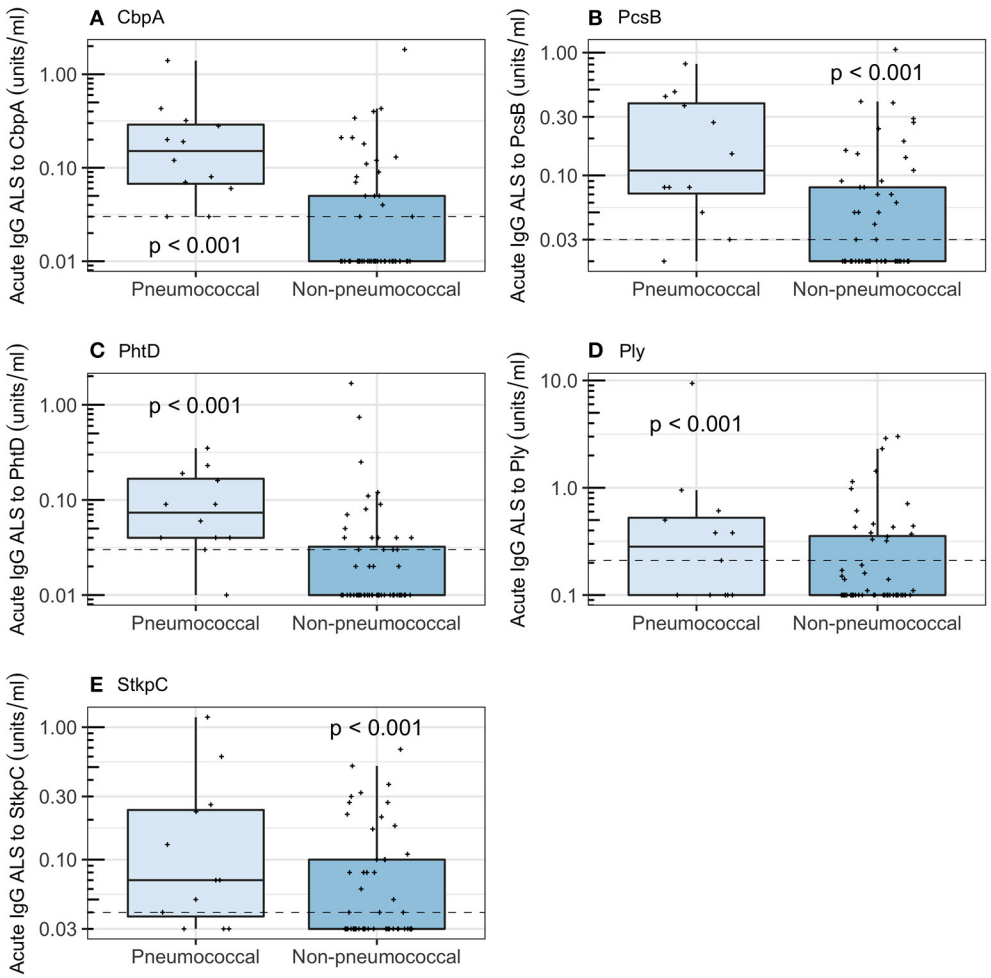

FIGURE 4 | Acute IgG ALS to pneumococcal proteins by children with *pneumococcal pneumonia* and *non-pneumococcal pneumonia* in all children enrolled into the study. Dashed horizontal lines represent thresholds derived from the Youden Index, *p*-values were derived from the Wilcoxon rank sum test. **(A)** Choline binding protein A (CbpA); **(B)** protein for cell wall separation of group B streptococci (PcsB); **(C)** pneumococcal histidine triad D (PhtD); **(D)** pneumolysin (Ply); **(E)** serine threonine kinase protein C (StkpC).

TABLE 2 | Diagnostic accuracy, using thresholds derived from the Youden Index, for acute IgG ALS to pneumococcal proteins to discriminate between *pneumococcal pneumonia* and *non-pneumococcal pneumonia* in children with pneumonia in Nepal (all age groups).

Pneumococcal pneumonia* and *non-pneumococcal pneumonia					
	CbpA	**PcsB**	**PhtD**	**Ply**	**StkpC**
Cut-off value	0.03	0.03	0.03	0.21	0.04
Sensitivity	1.0 (0.73–1.0)	0.92 (0.62–1.0)	0.92 (0.62–1.0)	0.58 (0.28–0.85)	0.75 (0.43–0.95)
Specificity	0.66 (0.52–0.78)	0.57 (0.43–0.70)	0.68 (0.54–0.80)	0.70 (0.56–0.81)	0.57 (0.43–0.70)
AUROCC	0.85 (0.75–0.94)	0.79 (0.65–0.92)	0.82 (0.70–0.95)	0.60 (0.42–0.79)	0.66 (0.50–0.83)

AUROCC, area under the receiver-operating characteristic curve.

from children with *non-pneumococcal pneumonia*. For children of all ages, acute IgG ALS to the best-performing antigen (CbpA) appeared highly sensitive, and moderately specific, with an AUROC curve of 0.85, for the discrimination of *pneumococcal pneumonia* from *non-pneumococcal pneumonia*. This is considerably higher than previously reported approaches, including quantification of pneumococcal DNA in blood, or in NP specimens by qPCR (Baggett et al., 2017; Deloria Knoll et al., 2017), to discriminate between children with microbiologically confirmed pneumococcal pneumonia and non-pneumococcal pneumonia, or between pneumococcal pneumonia and healthy controls.

Despite this reasonable performance, we observed a statistically significant association between acute IgG ALS and age, independent of diagnostic comparator group. The limited overlap in ages between children with *pneumococcal*

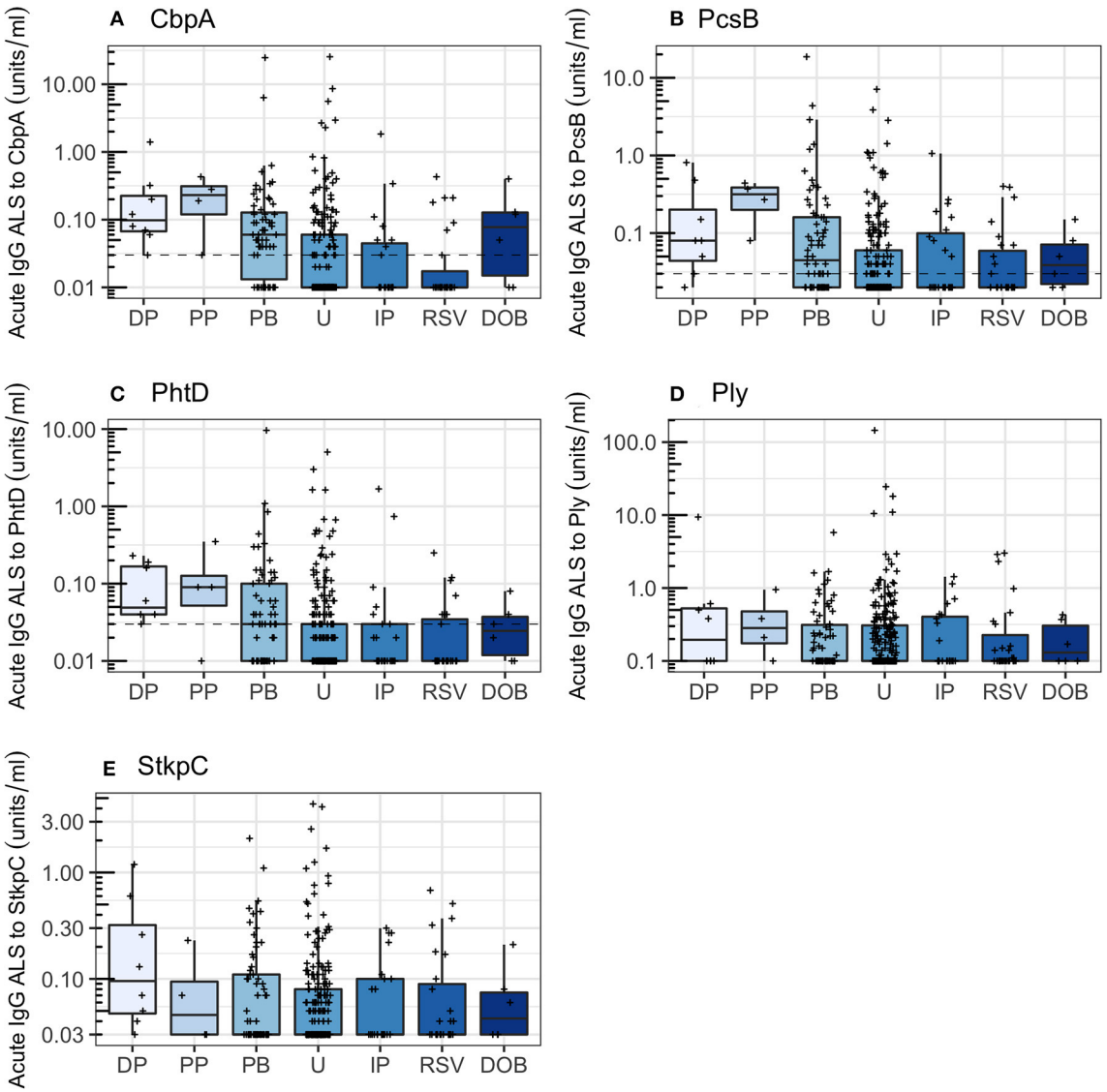

FIGURE 5 | Acute IgG ALS to pneumococcal proteins by comparator group in all children enrolled into the study. Dotted horizontal lines represent thresholds derived from the Youden Index. DP, *definite pneumococcal*; PP, *probable pneumococcal*; PB, *probable bacterial*; U, *unknown*; IP *influenza/parainfluenza virus*; RSV, *respiratory syncytial virus*; DOB, *definite other bacterial pneumonia*. Dashed horizontal lines represent thresholds derived from the Youden Index. **(A)** Choline binding protein A (CbpA); **(B)** protein for cell wall separation of group B streptococci (PcsB); **(C)** pneumococcal histidine triad D (PhtD); **(D)** pneumolysin (Ply); **(E)** serine threonine kinase protein C (StkpC).

pneumonia and *non-pneumococcal pneumonia* made adjustment for this important confounding variable infeasible. The age distribution of children with *pneumococcal pneumonia* in this study was consistent with unpublished data from long-term surveillance of childhood invasive pneumococcal disease at Patan Hospital, but is in contrast to other sites in South Asia where 50% or more of confirmed pneumococcal pneumonia is detected in infants (Baqui et al., 2007; Arifeen et al., 2009; Saha et al., 2015; Manoharan et al., 2017).

We therefore undertook *post-hoc* analysis in children ≥2 years of age. In this age group, ALS assay to the best-performing antigen (PcsB) was unable to discriminate between children with *pneumococcal pneumonia* and *non-pneumococcal pneumonia* with an AUROC curve of 0.69 (with wide confidence intervals in these data). Our experience suggests that this is insufficiently sensitive or specific for clinical use. Assay of acute IgG ALS may be informative for the etiological diagnosis of childhood pneumonia in epidemiological studies, but future studies will need careful accounting for age between comparator groups.

We also described the effect of NP carriage of pneumococci on acute IgG ALS in children with *non-pneumococcal pneumonia*. Previous work has shown specific IgG and IgA responses can be induced through stimulation of *ex vivo* child adenoidal mononuclear cells with pneumococcal protein antigens. These ALS responses were found to be positively associated with age and serum antibody concentrations, and were higher from cells

TABLE 3 | Acute IgG ALS to pneumococcal proteins by children with *pneumococcal pneumonia* and *non-pneumococcal* pneumonia in children ≥2 years of age enrolled in the study.

Clinical characteristic	*Pneumococcal pneumonia*	*Non-pneumococcal pneumonia*	*p*
n	12	16	
Age (years; median, IQR)	6.3 (4.2–8.3)	3.2 (2.3–4.3)	<0.001[a]
24–59 months	4 (33%)	13 (81%)	–
≥5–14 years	8 (67%)	3 (19%)	–
Female sex	1 (8%)	11 (69%)	0.002[b]
Length of illness (days; median, range)	3 (2–3.3)	5.5 (3–7)	<0.001[c]
Prior antibiotic use	8 (67%)	9 (56%)	0.70[b]
NP pneumococcal carriage	6 (50%)	11 (69%)	0.54[c]
NP pneumococcal carriage (serotype 1)	5 (42%)	0	–
Invasive pneumococcal disease	8 (67%)	0	–
Other invasive bacterial disease[d]	0	3 (19%)	–
Endpoint consolidation	11 (92%)	7 (44%)	–
CRP (mg/l; median, IQR)	133 (63–183)	21 (14–50)	0.02[c]
CRP concentration ≥60 mg/l	9 (75%)	3 (19%)	–
NP RSV carriage	0	11 (31%)	–
NP other viral carriage	0	8 (50%)	–

Values are expressed as a percentage for each column. p represents tests between the two groups.
[a] *t-test following reciprocal transformation of age distribution for non-pneumococcal pneumonia.*
[b] *Fisher exact test.*
[c] *Wilcoxon rank sum test; χ^2 test.*
[d] *Two Staphylococcus aureus, one Pseudomonas spp.*

from adenoids colonized by pneumococci (Zhang et al., 2002, 2006). Our data suggest that NP carriage of pneumococci in pneumonia—without apparent pneumococcal disease (Palkola et al., 2012, 2016)—also induces IgG secretion from antibody-secreting cells, thus confounding the utility of an ALS-based diagnostic approach.

Strengths of this study include the unselected cohort, and the breadth of clinical and microbiological data used to classify the likely etiology of pneumonia by comparator group. In April and May 2015 central Nepal (including the Kathmandu valley) experienced earthquakes that led to the deaths of ∼8,000 people in the central region of Nepal, and large population movements (Hall et al., 2017). In addition, a severe fuel shortage and increased construction from September 2015 to February 2016 may have contributed to severe pollution in the Kathmandu Valley through the increased burning of biofuels (Budhathoki and Gelband, 2016). Both earthquakes and increased pollution may have affected pneumococcal pneumonia incidence at Patan Hospital during the study period.

Despite the lack of additional selection, our cohort was enriched for invasive pneumococcal disease (IPD) in comparison to similar cohorts within South Asia. Our cohort included 8 children bacteremic for the pneumococcus from 369 children (2.2%). In comparison, separate studies of pneumonia in rural Bangladesh [7 cases of IPD from 840 children, 0.8% (Baqui et al., 2007)], severe febrile illness [25 cases of IPD from 6,925 children, 0.4% (Arifeen et al., 2009)], and 220 cases of IPD from a meta-analysis of 26,258 blood cultures from children (0.1%) across south-east Asia between 1990 and 2010 (Deen et al., 2012), were identified. The recently published PERCH study isolated the pneumococcus in 19 cases from 4,232 children (0.4%) with pneumonia (O'Brien et al., 2019). Our cohort had a similar prevalence of IPD as among rural Gambian or rural Kenyan children with pneumonia [2.5% (Cutts et al., 2005) and 1.7%, respectively (Berkley et al., 2005)] prior to introduction of PCV.

Any test for pneumonia etiology should identify children in whom there is pneumococcal infection, but no bacteremia. For this reason, and to increase the number of children available for comparator standards, we defined four children with pneumonia, high CRP and NP carriage of serotype 1 as *pneumococcal pneumonia* (**Figure 1**). All of these children also had consolidation on chest radiograph. We chose NP carriage of serotype 1 due to its high odds ratio for carriage in pneumonia vs. community controls (**Figure S1**) in our unpublished data from Kathmandu, and in published data from Israel (Greenberg et al., 2011), the UK, and South America (Scott et al., 1996). Of 128 children with IPD admitted to Patan Hospital between 2005 and 2016, 58 (45%) had serotype 1 pneumococci identified. We therefore believe that class of children with NP carriage of serotype 1 and high CRP as pneumococcal pneumonia has biological relevance, and internal and external validity.

We focused our analysis on comparisons between children with *pneumococcal pneumonia* and *non-pneumococcal pneumonia*, rather than on discriminating between children with *pneumococcal pneumonia* and age-matched community controls. This substantially reduced the measured diagnostic accuracy of acute IgG ALS to pneumococcal proteins that we present in the main text (in this study: optimum antigen AUROC curve 0.98 for *pneumococcal pneumonia* and healthy controls; 0.84 for *pneumococcal pneumonia* and *non-pneumococcal pneumonia* in all ages; 0.69 for *pneumococcal pneumonia* and *non-pneumococcal pneumonia* in children ≥2 years of age). However, testing acute IgG ALS to pneumococcal proteins for the diagnosis of pneumococcal pneumonia, in the context of an unselected cohort of pneumonia patients (as presented here), rather than in healthy controls gives a meaningful representation of accuracy in the context in which the test would be potentially implemented.

Assay of ALS for the etiological diagnosis of pneumonia might be optimized to yield more accurate diagnostic information. Reviews of B cell responses to vaccination (Mitchell et al., 2014) and to infection (Carter et al., 2017) suggest that the optimum time for sampling transiently circulating plasmablasts from peripheral blood is 7–10 days following the onset of illness. There are difficulties defining length of illness in children with pneumonia. Nevertheless, the median length of illness prior to blood sampling in our study was 4 days. A delay in sampling until 7 days of illness may improve test

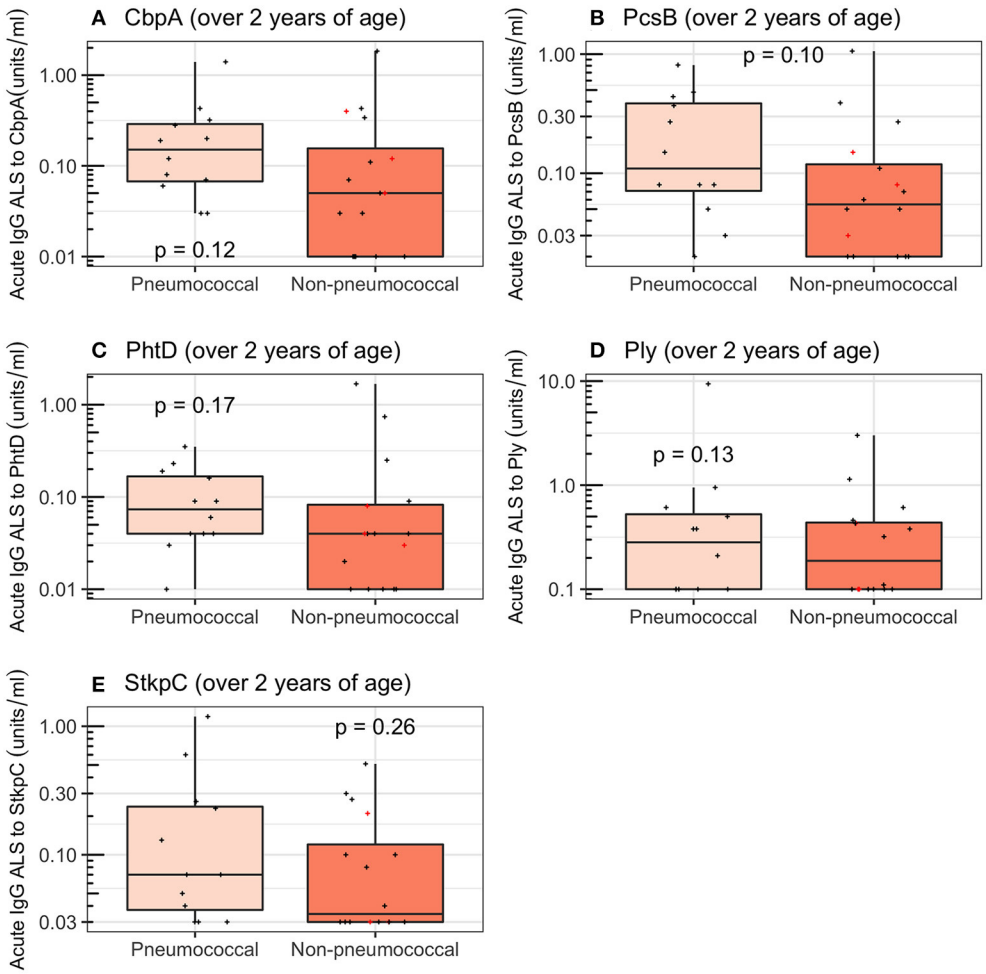

FIGURE 6 | Acute IgG ALS to pneumococcal proteins in children with *pneumococcal pneumonia* and *non-pneumococcal pneumonia* ≥2 years of age enrolled into the study. Red crosses represent children with definite other bacterial pneumonia (two children with *Staphylococcus aureus*, and one child with *Pseudomonas* spp. isolated from blood). Dashed horizontal lines represent thresholds derived from the Youden Index, *p*-values were derived from the Wilcoxon rank sum test. **(A)** Choline binding protein A (CbpA); **(B)** protein for cell wall separation of group B streptococci (PcsB); **(C)** pneumococcal histidine triad D (PhtD); **(D)** pneumolysin (Ply); **(E)** serine threonine kinase protein C (StkpC).

specificity. An additional method to improve specificity of the ALS assay would be to sort recently activated plasmablasts for incubation using flow cytometry. However, separation, washing, and incubation of PBMCs to generate and store ALS requires reagents (Ficoll-paque) and equipment (centrifuges, incubators with CO_2, and −80°C freezers) that are not readily available in routine microbiology laboratories. The use of flow cytometry would limit the potential availability of this test further. Finally, although we described a high degree of co-linearity in acute IgG ALS to the pneumococcal proteins measured, a larger array of pneumococcal antigens might be considered to optimize ALS cognate antigens using variable selection methods (Zou and Hastie, 2005; Darton et al., 2017a). Quantification of ALS to pneumococcal capsular polysaccharides may also enable serotype-specific measure of pneumococcal pneumonia burden to inform vaccination strategies (Tuerlinckx et al., 2013).

A major limitation of any study of pneumonia etiology is the lack of a "gold standard." Blood culture is presumed to be specific, but insensitive, for bacterial pneumonia—a "silver standard" (Wu et al., 2016). We used a series of comparator groups ("standards") against which to test the ALS assay. In this cohort, the low prevalence and different age distribution of confirmed pneumococcal pneumonia cases, in comparison to other pneumonia cases, limited our measures of the diagnostic accuracy of ALS between comparator groups. Assay of ALS was also confounded by the association of acute IgG ALS with NP carriage of pneumococci. Diagnostic accuracy of ALS assay may be better in studies of pneumonia of other etiology (notably RSV pneumonia), where reasonably accurate diagnostic tests already exist with a high positive and negative predictive value for disease, as a point of comparison.

Despite the high prevalence of pneumococcal pneumonia in the cohort relative to other studies (Baqui et al., 2007; Arifeen et al., 2009; Deen et al., 2012; O'Brien et al., 2019), the majority of children in the study (81%) were designated as *probable*

TABLE 4 | Diagnostic accuracy, using thresholds derived from the Youden Index, for acute IgG ALS to pneumococcal proteins to discriminate between *pneumococcal pneumonia* and *non-pneumococcal pneumonia* in children ≥2 years of age with pneumonia in Nepal.

	***Pneumococcal pneumonia* and *non-pneumococcal pneumonia* in children ≥2 years of age**				
	CbpA	**PcsB**	**PhtD**	**Ply**	**StkpC**
Cut-off value	0.06	0.08	0.03	0.50	0.04
Sensitivity	0.83 (0.52–0.98)	0.75 (0.43–0.95)	0.92 (0.61–1.00)	0.33 (0.10–0.65)	0.75 (0.43–0.95)
Specificity	0.56 (0.30–0.80)	0.63 (0.35–0.85)	0.38 (0.15–0.65)	0.81 (0.54–0.96)	0.50 (0.25–0.75)
AUROCC	0.67 (0.47–0.88)	0.69 (0.48–0.89)	0.65 (0.44–0.86)	0.53 (0.31–0.74)	0.61 (0.40–0.82)

AUROCC, area under the receiver-operating characteristic curve.

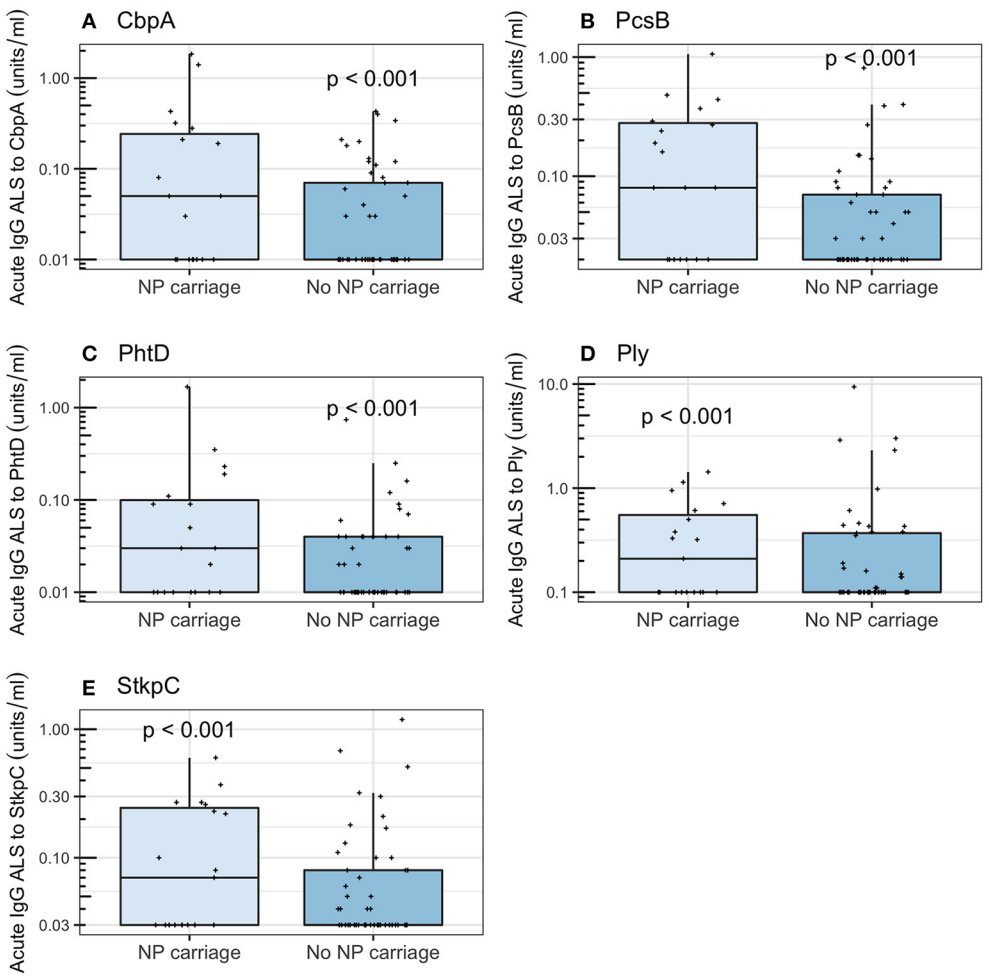

FIGURE 7 | Acute IgG ALS to pneumococcal proteins in children with *non-pneumococcal pneumonia* and NP carriage of pneumococci and without NP carriage of pneumococci enrolled into the study (all age groups). *P*-values were derived from the Wilcoxon rank sum test. **(A)** Choline binding protein A (CbpA); **(B)** protein for cell wall separation of group B streptococci (PcsB); **(C)** pneumococcal histidine triad D (PhtD); **(D)** pneumolysin (Ply); **(E)** serine threonine kinase protein C (StkpC).

bacterial pneumonia or *unknown pneumonia*. In a cohort that were largely unvaccinated with PCV, only 8 children had invasive pneumococcal disease, with a further 4 children with *probable pneumococcal pneumonia*. Many comparisons were therefore underpowered. Although this limits the ability to fully assess assay of IgG ALS for the diagnosis of pneumococcal pneumonia, at a minimum, a clinically useful test should be "positive" in cases of IPD (the silver standard). Our data show that this was not the case, with low IgG ALS assay in 3 of 8 children with pneumococcal bacteremia (**Figure 8**).

In summary, we detected spontaneously secreted antibodies to pneumococcal proteins from PBMCs isolated from a

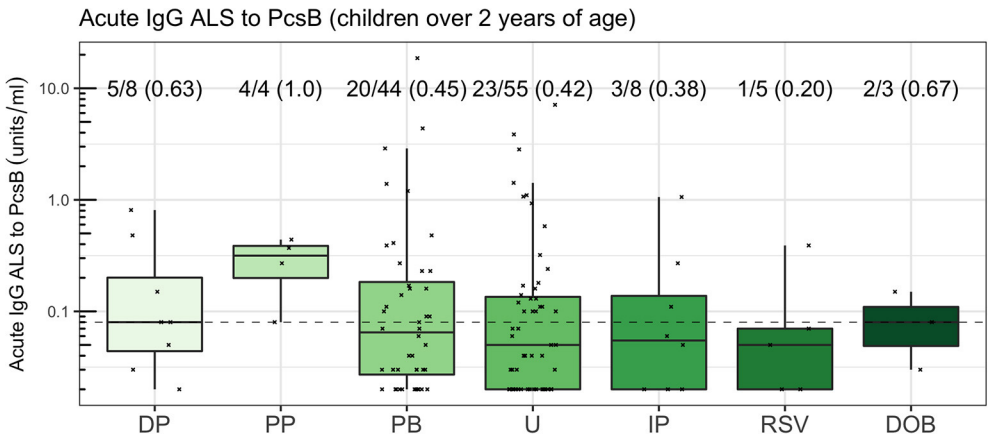

FIGURE 8 | Acute IgG ALS to PcsB by comparator group in children ≥2 years of age. The dotted horizontal line represents a threshold of 0.08 units/ml, the threshold derived from the Youden Index. The proportion of children with acute IgG ALS to PcsB concentration greater than, or equal to, the threshold derived from ROC curve analysis to discriminate *pneumococcal pneumonia* from *non-pneumococcal pneumonia* is annotated.

proportion of children with pneumonia in Nepal using the ALS assay. Concentrations of IgG ALS to the pneumococcal proteins CbpA, PcsB and PhtD were higher in children with *pneumococcal pneumonia* than *non-pneumococcal pneumonia*, with good ability to discriminate between groups. However, these results were confounded by different age distributions of children with *pneumococcal pneumonia* and *non-pneumococcal pneumonia*. Assay of ALS to pneumococcal proteins did not discriminate between these groups when stratified by ≥2 years of age. Our data suggest that assay of IgG ALS to pneumococcal proteins is not sufficiently accurate as a diagnostic test for clinical utility. Alternative new diagnostic tests for the cause of childhood pneumonia should be sought.

DATA AVAILABILITY STATEMENT

The datasets generated for this study are available on request to the corresponding author.

ETHICS STATEMENT

The studies involving human participants were reviewed and approved by Nepal Health Research Council and the Oxford Tropical Research Ethics Committee. Written informed consent to participate in this study was provided by the participants' legal guardian/next of kin.

AUTHOR CONTRIBUTIONS

MC, CJ, DM, AP, DK, and SS designed the study and analysis. MC, PG, SR, MG, ST, SK, IA, GS, MCG, KP, BK, and AM performed the studies and collected sample material. MC, PG, SR, RK, NE, and MM performed the assays. MC, JK, MV, KO'B, BW, AP, and DK performed the analyses. MC, DK, and AP wrote the manuscript to which all authors had significant input. MC, DK, JK, and AP acquired the funding directly for this study. This study was also supported by the PneumoNepal Study Group.

FUNDING

This project was funded by the Wellcome Trust (Research Training Fellowship to MC, grant number 104439/Z/14/Z); Gavi, the Vaccine Alliance; and the European Union's Horizon 2020 research and innovation programme under grant agreement number 668303.

ADDITIONAL PNEUMONEPAL STUDY GROUP MEMBERS

Kate Park, Matthew Smedley, Puja Amatya, Ruby Basi, Jennifer Moïsi, Maria Deloria Knoll, Brad Gessner.

ACKNOWLEDGMENTS

We thank all of the children, and their parents, who participated in this study; and the clinical teams at Patan Hospital who gave unstinting help. PhtD was kindly supplied by Sanofi Pasteur (Sanofi Pasteur S.A., Marcy L'Etoile, France), StkpC and PcsB by Dr. Andreas Meinke (Valneva, Vienna, Austria), and Ply and CbpA by Dr. Elaine Tuomanen (St. Jude Children's Research Hospital, Memphis, TN, USA). We thank Leena Saarinen and Camilla Virta for technical assistance, and Dr. Dafne Andrade and Dr. Igor Borges who set up and validated the FMIA for antibodies to pneumococcal proteins (all at THL). Dr. Timothy James (Biochemistry Laboratory, Oxford University Hospital NHS Foundation Trust, UK) kindly supported the measurement of CRP concentrations. Dr. Colin Fink and team (Micropathology Ltd, Warwick, UK), Prof. Mike Levin and team (Imperial College, London, UK), and the PERFORM

consortium (https://www.perform2020.org/) supported PCR identification of NP viruses. We also thank reviewers for helpful comments.

SUPPLEMENTARY MATERIAL

The Supplementary Material for this article can be found online at: https://www.frontiersin.org/articles/10.3389/fcimb.2019.00459/full#supplementary-material

Figure S1 | Odds ratios for nasopharyngeal carriage of pneumococcal serotypes contained within 13-valent PCV and non-typeable (NT) pneumococci in pneumonia and community control children, adjusted for age and sex, prior to introduction of the vaccine into the Kathmandu valley. Error bars show 95% confidence intervals.

Figure S2 | Acute IgG ALS to pneumococcal proteins by children with pneumococcal pneumonia and healthy infant controls. Dashed horizontal lines represent represent thresholds derived from the Youden Index, *p*-values were derived from the Wilcoxon rank sum test. For all box and whisker plots: the solid line represents the median value, lower hinge 25th centile, upper hinge 75th centile, and whiskers represent 1.5 times the interquartile range. All data points have also been plotted.

Figure S3 | Linear regression analysis of length of illness with acute IgG ALS to pneumococcal proteins (grey colouring represents 95% confidence intervals about the regression line; p-value > 0.5 for all proteins).

Figure S4 | Acute IgG ALS to pneumococcal proteins in children with non-pneumococcal pneumonia by nasopharyngeal carriage of pneumococci.

REFERENCES

Andrade, D. C., Borges, I. C., Ivaska, L., Peltola, V., Meinke, A., Barral, A., et al. (2016). Serological diagnosis of pneumococcal infection in children with pneumonia using protein antigens: a study of cut-offs with positive and negative controls. *J. Immunol. Methods* 433, 31–37. doi: 10.1016/j.jim.2016.02.021

Andrade, D. C., Borges, I. C., Laitinen, H., Ekström, N., Adrian, P. V., Meinke, A., et al. (2014). A fluorescent multiplexed bead-based immunoassay (FMIA) for quantitation of IgG against *Streptococcus pneumoniae*, *Haemophilus influenzae* and *Moraxella catarrhalis* protein antigens. *J. Immunol. Methods* 405, 130–143. doi: 10.1016/j.jim.2014.02.002

Arifeen, S. E., Saha, S. K., Rahman, S., Rahman, K. M., Rahman, S. M., Bari, S., et al. (2009). Invasive pneumococcal disease among children in rural Bangladesh: results from a population-based surveillance. *Clin. Infect. Dis.* 48, S103–S113. doi: 10.1086/596543

Baggett, H. C., Watson, N. L., Deloria Knoll, M., Brooks, W. A., Feikin, D. R., Hammitt, L. L., et al. (2017). Density of upper respiratory colonization with *Streptococcus pneumoniae* and its role in the diagnosis of pneumococcal pneumonia among children aged <5 years in the PERCH study. *Clin. Infect. Dis.* 64, S317–S327. doi: 10.1093/cid/cix100

Baqui, A. H., Rahman, M., Zaman, K., El Arifeen, S., Chowdhury, H. R., Begum, N., et al. (2007). A population-based study of hospital admission incidence rate and bacterial aetiology of acute lower respiratory infections in children aged less than five years in Bangladesh. *J. Health Popul. Nutr.* 25, 179–188. Available online at: https://www.ncbi.nlm.nih.gov/pmc/articles/PMC2754000/

Berkley, J. A., Lowe, B. S., Mwangi, I., Williams, T., Bauni, E., Mwarumba, S., et al. (2005). Bacteremia among children admitted to a rural hospital in Kenya. *N. Engl. J. Med.* 352, 39–47. doi: 10.1056/NEJMoa040275

Borges, I. C., Andrade, D. C., Cardoso, M. R., Toppari, J., Vähä-Mäkilä, M., Ilonen, J., et al. (2016). Natural development of antibodies against *Streptococcus pneumoniae*, *Haemophilus influenzae*, and *Moraxella catarrhalis* protein antigens during the first 13 years of life. *Clin. Vaccine Immunol.* 23, 878–883. doi: 10.1128/CVI.00341-16

Budhathoki, S. S., and Gelband, H. (2016). Manmade earthquake: the hidden health effects of a blockade-induced fuel crisis in Nepal. *BMJ Glob. Health* 1:e000116. doi: 10.1136/bmjgh-2016-000116

Carter, M. J., Mitchell, R. M., Meyer Sauteur, P. M., Kelly, D. F., and Trück, J. (2017). The antibody-secreting cell response to infection: kinetics and clinical applications. *Front. Immunol.* 8:630. doi: 10.3389/fimmu.2017.00630

Chang, H. S., and Sack, D. A. (2001). Development of a novel *in vitro* assay (ALS assay) for evaluation of vaccine-induced antibody secretion from circulating mucosal lymphocytes. *Clin. Diagn. Lab. Immunol.* 8, 482–488. doi: 10.1128/CDLI.8.3.482-488.2001

Cherian, T., Mulholland, E. K., Carlin, J. B., Ostensen, H., Amin, R., de Campo, M., et al. (2005). Standardized interpretation of paediatric chest radiographs for the diagnosis of pneumonia in epidemiological studies. *Bull WHO* 83, 353–359. Available online at: https://www.ncbi.nlm.nih.gov/pmc/articles/PMC2626240/

Clutterbuck, E. A., Oh, S., Hamaluba, M., Westcar, S., Beverley, P. C. L., and Pollard, A. J. (2007). Serotype-specific and age-dependent generation of pneumococcal polysaccharide-specific memory B-cell and antibody responses to immunization with a pneumococcal conjugate vaccine. *Clin. Vaccine Immunol.* 15, 182–193. doi: 10.1128/CVI.00336-07

Cutts, F. T., Zaman, S. M., Enwere, G., Jaffar, S., Levine, O. S., Okoko, J. B., et al. (2005). Efficacy of nine-valent pneumococcal conjugate vaccine against pneumonia and invasive pneumococcal disease in The Gambia: randomised, double-blind, placebo-controlled trial. *Lancet* 365, 1139–1146. doi: 10.1016/S0140-6736(05)71876-6

Darton, T. C., Baker, S., Randall, A., Dongol, S., Karkey, A., Voysey, M., et al. (2017a). Identification of novel serodiagnostic signatures of typhoid fever using a Salmonella proteome array. *Front. Microbiol.* 8:1794. doi: 10.3389/fmicb.2017.01794

Darton, T. C., Jones, C., Dongol, S., Voysey, M., Blohmke, C. J., Shrestha, R., et al. (2017b). Assessment and translation of the antibody-in-lymphocyte supernatant (ALS) assay to improve the diagnosis of enteric fever in two controlled human infection models and an endemic area of Nepal. *Front. Microbiol.* 8:2031. doi: 10.3389/fmicb.2017.02031

Deen, J., von Seidlein, L., Andersen, F., Elle, N., White, N. J., and Lubell, Y. (2012). Community-acquired bacterial bloodstream infections in developing countries in south and southeast Asia: a systematic review. *Lancet Infect. Dis.* 12, 480–487. doi: 10.1016/S1473-3099(12)70028-2

Deloria Knoll, M., Morpeth, S. C., Scott, J. A. G., Watson, N. L., Park, D. E., Baggett, H. C., et al. (2017). Evaluation of pneumococcal load in blood by polymerase chain reaction for the diagnosis of pneumococcal pneumonia in young children in the PERCH study. *Clin. Infect. Dis.* 64, S357–S367. doi: 10.1093/cid/cix101

Driscoll, A. J., Deloria Knoll, M., Hammitt, L. L., Baggett, H. C., Brooks, W. A., Feikin, D. R., et al. (2017). The effect of antibiotic exposure and specimen volume on the detection of bacterial pathogens in children with pneumonia. *Clin. Infect. Dis.* 64, S368–S377. doi: 10.1093/cid/cix149

Feikin, D. R., Fu, W., Park, D. E., Shi, Q., Higdon, M. M., Baggett, H. C., et al. (2017a). Is higher viral load in the upper respiratory tract associated with severe pneumonia? Findings from the PERCH study. *Clin. Infect. Dis.* 64, S337–S346. doi: 10.1093/cid/cix148

Feikin, D. R., Hammitt, L. L., Murdoch, D. R., O'Brien, K. L., and Scott, J. A. G. (2017b). The enduring challenge of determining pneumonia etiology in children: considerations for future research priorities. *Clin. Infect. Dis.* 64, S188–S196. doi: 10.1093/cid/cix143

Feikin, D. R., Scott, J. A. G., and Gessner, B. D. (2014). Use of vaccines as probes to define disease burden. *Lancet* 383, 1762–1770. doi: 10.1016/S0140-6736(13)61682-7

Greenberg, D., Givon-Lavi, N., Newman, N., Bar-Ziv, J., and Dagan, R. (2011). Nasopharyngeal carriage of individual *Streptococcus pneumoniae* serotypes during pediatric pneumonia as a means to estimate serotype disease potential. *Pediatr. Infect. Dis. J.* 30, 227–233. doi: 10.1097/INF.0b013e3181f87802

Hall, M. L., Lee, A. C., Cartwright, C., Marahatta, S., Karki, J., and Simkhada, P. (2017). The 2015 Nepal earthquake disaster: lessons learned one year on. *Public Health* 145, 39–44. doi: 10.1016/j.puhe.2016.12.031

Herberg, J. A., Kaforou, M., Wright, V. J., Shailes, H., Eleftherohorinou, H., Hoggart, C. J., et al. (2016). Diagnostic test accuracy of a 2-transcript host

RNA signature for discriminating bacterial vs viral infection in febrile children. *JAMA* 316, 835–845. doi: 10.1001/jama.2016.11236

Higdon, M. M., Hammitt, L. L., Deloria Knoll, M., Baggett, H. C., Brooks, W. A., Howie, S. R. C., et al. (2017a). Should controls with respiratory symptoms be excluded from case-control studies of pneumonia etiology? Reflections from the PERCH study. *Clin. Infect. Dis.* 64, S205–S212. doi: 10.1093/cid/cix076

Higdon, M. M., Le, T., O'Brien, K. L., Murdoch D. R., Prosperi C., Baggett H. C., et al. (2017b). Association of C-reactive protein with bacterial and respiratory syncytial virus-associated pneumonia among children aged <5 years in the PERCH study. *Clin. Infect. Dis.* 64, S378–S386. doi: 10.1093/cid/cix150

Howie, S. R., Morris, G. A., Tokarz, R., Ebruke, B. E., Machuka, E. M., Ideh, R. C., et al. (2014). Etiology of severe childhood pneumonia in the Gambia, West Africa, determined by conventional and molecular microbiological analyses of lung and pleural aspirate samples. *Clin. Infect. Dis.* 59, 682–685. doi: 10.1093/cid/ciu384

Ideh, R. C., Howie, S. R., Ebruke, B., Secka, O., Greenwood, B. M., Adegbola, R. A., et al. (2011). Transthoracic lung aspiration for the aetiological diagnosis of pneumonia: 25 years of experience from The Gambia. *Int. J. Tuberc. Lung Dis.* 15, 729–735. doi: 10.5588/ijtld.10.0468

Johnson, H. L., Deloria-Knoll, M., Levine, O. S., Stoszek, S. K., Freimanis Hance, L., Reithinger, R., et al. (2010). Systematic evaluation of serotypes causing invasive pneumococcal disease among children under five: the pneumococcal global serotype project. *PLoS Med.* 7:e1000348. doi: 10.1371/journal.pmed.1000348

Kaforou, M., Herberg, J. A., Wright, V. J., Coin, L. J., and Levin, M. (2017). Diagnosis of bacterial infection using a 2-transcript host RNA signature in febrile infants 60 days or younger. *JAMA* 317, 1577–1578. doi: 10.1001/jama.2017.1365

Liu, L., Oza, S., Hogan, D., Chu, Y., Perin, J., Zhu, J., et al. (2016). Global, regional, and national causes of under-5 mortality in 2000–15: an updated systematic analysis with implications for the sustainable development goals. *Lancet* 388, 3027–3035. doi: 10.1016/S0140-6736(16)31593-8

Lubell, Y., Blacksell, S. D., Dunachie, S., Tanganuchitcharnchai, A., Althaus, T., Watthanaworawit, W., et al. (2015). Performance of C-reactive protein and procalcitonin to distinguish viral from bacterial and malarial causes of fever in Southeast Asia. *BMC Infect. Dis.* 15:511. doi: 10.1186/s12879-015-1272-6

Manoharan, A., Manchanda, V., Balasubramanian, S., Lalwani, S., Modak, M., Bai, S., et al. (2017). Invasive pneumococcal disease in children aged younger than 5 years in India: a surveillance study. *Lancet Infect. Dis.* 17, 305–312. doi: 10.1016/S1473-3099(16)30466-2

Ministry of Health and Population (MOHP), New ERA, ICF International (2012). *Nepal Demographic and Health Survey 2011*. Kathmandu: Ministry of Health and Population, New ERA, and ICF International.

Mitchell, R., Kelly, D. F., Pollard, A. J., and Trück, J. (2014). Polysaccharide-specific B cell responses to vaccination in humans. *Hum. Vaccin. Immunother.* 10, 1661–1668. doi: 10.4161/hv.28350

O'Brien, K. L., Baggett, H. C., Brooks, W. A., Feikin, D. R., Hammitt, L. L., Higdon, M. M., et al. (2019). Causes of severe pneumonia requiring hospital admission in children without HIV infection from Africa and Asia: the PERCH multi-country case-control study. *Lancet* 394, 757–779. doi: 10.1016/S0140-6736(19)30721-4

O'Brien, K. L., Wolfson, L. J., Watt, J. P., Henkle, E., Deloria-Knoll, M., McCall, N., et al. (2009). Burden of disease caused by *Streptococcus pneumoniae* in children younger than 5 years: global estimates. *Lancet* 374, 893–902. doi: 10.1016/S0140-6736(09)61204-6

Palkola, N. V., Blomgren, K., Pakkanen, S. H., Puohiniemi, R., Kantele, J. M., and Kantele, A. (2016). Immune defense in upper airways: a single-cell study of pathogen-specific plasmablasts and their migratory potentials in acute sinusitis and tonsillitis. *PLoS ONE* 11:e0154594. doi: 10.1371/journal.pone.0154594

Palkola, N. V., Pakkanen, S. H., Kantele, J. M., Rossi, N., Puohiniemi, R., and Kantele, A. (2012). Pathogen-specific circulating plasmablasts in patients with pneumonia. *PLoS ONE* 7:e34334. doi: 10.1371/journal.pone.0034334

Ramos-Sevillano, E., Ercoli, G., and Brown, J. S. (2019). Mechanisms of naturally acquired immunity to *Streptococcus pneumoniae*. *Front. Immunol.* 10:358. doi: 10.3389/fimmu.2019.00358

Saha, S. K., Hossain, B., Islam, M., Hasanuzzaman, M., Saha, S., Hasan, M., et al. (2015). Epidemiology of invasive pneumococcal disease in Bangladeshi children before introduction of pneumococcal conjugate vaccine. *Pediatr. Infect. Dis. J.* 35, 655–661. doi: 10.1097/INF.0000000000001037

Sariko, M., Anderson, C., Mujaga, B. S., Gratz, J., Mpagama, S. G., Heysell, S., et al. (2017). Evaluation of the antibody in lymphocyte supernatant assay to detect active tuberculosis. *PLoS ONE* 12:e0169118. doi: 10.1371/journal.pone.0169118

Scott, J. A., Hall, A. J., Dagan, R., Dixon, J. M., Eykyn, S. J., Fenoll, A., et al. (1996). Serogroup-specific epidemiology of *Streptococcus pneumoniae*: associations with age, sex, and geography in 7000 episodes of invasive disease. *Clin. Infect. Dis.* 22, 973–981. doi: 10.1093/clinids/22.6.973

Sheikh, A., Bhuiyan, M. S., Khanam, F., Chowdhury, F., Saha, A., Ahmed, D., et al. (2009). Salmonella enterica serovar Typhi-specific immunoglobulin A antibody responses in plasma and antibody in lymphocyte supernatant specimens in Bangladeshi patients with suspected typhoid fever. *Clin. Vaccine Immunol.* 16, 1587–1594. doi: 10.1128/CVI.00311-09

Tang, Y. W., Gonsalves, S., Sun, J. Y., Stiles, J., Gilhuley, K. A., Mikhlina, A., et al. (2016). Clinical evaluation of the Luminex NxTAG respiratory pathogen panel. *J. Clin. Microbiol.* 54, 1912–1914. doi: 10.1128/JCM.00482-16

Tuerlinckx, D., Smet, J., De Schutter, I., Jamart, J., Vergison, A., Raes, M., et al. (2013). Evaluation of a WHO-validated serotype-specific serological assay for the diagnosis of pneumococcal etiology in children with community-acquired pneumonia. *Pediatr. Infect. Dis. J.* 32, e277–e84. doi: 10.1097/INF.0b013e31828c363f

Wahl, B., O'Brien, K. L., Greenbaum, A., Majumder, A., Liu, L., Chu, Y., et al. (2018). Burden of *Streptococcus pneumoniae* and *Haemophilus influenzae* type b disease in children in the era of conjugate vaccines: global, regional, and national estimates for 2000–15. *Lancet Glob. Health* 6, e744–e757. doi: 10.1016/S2214-109X(18)30247-X

Wu, Z., Deloria-Knoll, M., Hammitt, L. L., and Zeger, S. L. (2016). Partially latent class models for case-control studies of childhood pneumonia aetiology. *Appl. Stat.* 65, 97–114. doi: 10.1111/rssc.12101

Zhang, Q., Bernatoniene, J., Bagrade, L., Pollard, A. J., Mitchell, T. J., Paton, J. C., et al. (2006). Serum and mucosal antibody responses to pneumococcal protein antigens in children: relationships with carriage status. *Eur. J. Immunol.* 36, 46–57. doi: 10.1002/eji.200535101

Zhang, Q., Choo, S., and Finn, A. (2002). Immune responses to novel pneumococcal proteins pneumolysin, PspA, PsaA, and CbpA in adenoidal B cells from children. *Infect. Immun.* 70, 5363–5369. doi: 10.1128/IAI.70.10.5363-5369.2002

Zou, H., and Hastie, T. (2005). Regularization and variable selection via the elastic net. *J. R. Stat. Soc. B* 67, 301–320. doi: 10.1111/j.1467-9868.2005.00503.x

Conflict of Interest: The authors declare that the research was conducted in the absence of any commercial or financial relationships that could be construed as a potential conflict of interest.

frontiers in Cellular and Infection Microbiology

ORIGINAL RESEARCH
published: 24 January 2020
doi: 10.3389/fcimb.2020.00004

Determination of Causative Human Papillomavirus Type in Tissue Specimens of Common Warts Based on Estimated Viral Loads

*Vesna Breznik[1], Kristina Fujs Komloš[2], Lea Hošnjak[2], Boštjan Luzar[3], Rajko Kavalar[4], Jovan Miljković[5] and Mario Poljak[2]**

[1] Department of Dermatology and Venereal Diseases, University Medical Centre Maribor, Maribor, Slovenia, [2] Institute of Microbiology and Immunology, Faculty of Medicine, University of Ljubljana, Ljubljana, Slovenia, [3] Institute of Pathology, Faculty of Medicine, University of Ljubljana, Ljubljana, Slovenia, [4] Department of Pathology, University Medical Centre Maribor, Maribor, Slovenia, [5] Faculty of Medicine, University of Maribor, Maribor, Slovenia

Background: Assessment of human papillomavirus (HPV) type-specific viral load (VL) is a valid tool for determining the etiology of HPV-related skin tumors, especially when more than one HPV type is detected within one lesion.

Methods: The causative HPV type was determined in 185 fresh-frozen tissue specimens of histologically confirmed common warts (CWs) collected from 121 immunocompetent patients. All tissues were tested using the type-specific quantitative real-time polymerase chain reactions (PCR) for the most common wart-associated *Alpha*-PV (HPV2/27/57) and *Mu*-PV types (HPV1/63/204). The presence of 23 additional low-risk HPVs was evaluated using a conventional wide-spectrum PCR.

Results: HPV DNA was detected in 176/185 (95.1%) CWs and multiple HPV types in 71/185 (38.4%) lesions. Using the VL approach and a robust cutoff of one viral copy/cell established in this study, HPV2/27/57 were determined as causative agents in 41/53 (77.3%) and 53/71 (74.7%) CWs with single and multiple HPVs, respectively.

Conclusions: CWs are mostly etiologically associated with HPV2/27/57 and only rarely with HPV1. In the majority of CWs containing multiple HPVs, a single HPV type was present in high concentration, indicating etiological association. No significant differences in VLs of lesion-causing HPV types in CWs containing single or multiple HPVs were found.

Keywords: common warts, human papillomaviruses, prevalence, viral load, causality

OPEN ACCESS

Edited by:
Aleksandra Barac, Faculty of Medicine, University of Belgrade, Serbia

Reviewed by:
Snjezana Zidovec Lepej, University Hospital for Infectious Diseases "Dr Fran Mihaljevic", Croatia
Alberto Enrico Maraolo, University of Naples Federico II, Italy

****Correspondence:***
Mario Poljak
mario.poljak@mf.uni-lj.si

Specialty section:
This article was submitted to Clinical Microbiology, a section of the journal Frontiers in Cellular and Infection Microbiology

Received: *25 November 2019*
Accepted: *07 January 2020*
Published: *24 January 2020*

Citation:
Breznik V, Fujs Komloš K, Hošnjak L, Luzar B, Kavalar R, Miljković J and Poljak M (2020) Determination of Causative Human Papillomavirus Type in Tissue Specimens of Common Warts Based on Estimated Viral Loads. Front. Cell. Infect. Microbiol. 10:4. doi: 10.3389/fcimb.2020.00004

INTRODUCTION

Cutaneous warts are ubiquitous benign skin tumors (van Haalen et al., 2009; de Koning et al., 2015), clinically presented as single or multiple dome-shaped keratotic lesions with exophytic growth (common warts; CWs) or endophytic keratotic papules on pressure points of soles (plantar warts) or smooth-surfaced flat-topped papules on the face and dorsum of hands (plane warts) (Jablonska et al., 1985; Cardoso and Calonje, 2011; Hogendoorn et al., 2018). Because cutaneous warts can be clinically misdiagnosed as corn, callus, fibroma, seborrheic keratosis, lichen ruber planus, molluscum contagiosum, anogenital wart, or even squamous cell carcinoma and melanoma

(De Giorgi and Massi, 2006; Bae et al., 2009; Sondermann et al., 2016), skin biopsy followed by histological assessment is considered the diagnostic gold standard (Aldabagh et al., 2013).

Based on large population studies, which were mostly performed on swabs of warts' surfaces, cutaneous warts have been associated with various papillomavirus (PV) types belonging to genera *Alpha-, Gamma-, Mu-,* and *Nupapillomavirus (Alpha-, Gamma-, Mu-,* and *Nu*-PVs) (Schmitt et al., 2011; Bruggink et al., 2012; Al Bdour et al., 2013; de Koning et al., 2015) with the type spectrum varying across different anatomical regions. Whereas, CWs have usually been linked with infection with human PV (HPV) types HPV1, 2, 4, 7, 27, and 57, plantar warts are usually associated with HPV1, 4, 57, 60, 63, 65, and 66, and plane warts with HPV3, 10, 26–29, and 41 (Cardoso and Calonje, 2011). However, de Koning et al. recently showed the presence of wart-associated HPVs in up to 80% of swab samples of clinically normal skin (de Koning et al., 2015), thus raising the question of whether HPV types detected on warts' surfaces represent colonization, latent or productive HPV infection. In contrast to skin swabs, tissue specimens of cutaneous warts can provide information about HPVs present throughout the entire thickness of the epidermis (Aldabagh et al., 2013).

To the best of our knowledge, only seven small-scale HPV prevalence studies performed on a total of 129 histologically confirmed CW tissue samples have been published in peer-reviewed literature to date (**Supplementary Table 1**) (Gross et al., 1982; Chen et al., 1993; Egawa, 1994; Lei et al., 2009; Sun et al., 2010; de Koning et al., 2011; Šterbenc et al., 2017), with HPV2/27/57 and HPV1 being the most prevalent HPVs detected, but with extremely variable detection rates obtained in different studies (0–83.5 and 0–46.7% prevalence, respectively). Similarly, detection rates of multiple HPVs (the presence of more than one HPV type within one lesion) were tremendously variable (0–88.9%), prompting the development of tools for assessment of the most probable lesion-causative HPV among those detected within a particular CW (Šterbenc et al., 2017). Reliable information on causative HPV types vs. bystander HPVs in CWs is of great importance for informed decisions concerning targeted HPV types in future vaccines against cutaneous HPVs (Senger et al., 2009, 2010; Vinzón et al., 2014; Gaiser et al., 2015), which would be most beneficial for immunocompromised patients, including organ/tissue transplant recipients, often suffering from numerous and treatment-resistant cutaneous warts (Harwood et al., 1999; Bouwes Bavinck et al., 2007).

Köhler et al. (2009) suggested HPV type-specific viral load (VL) estimation as a surrogate marker for determining the etiology of CWs. Their study included eight dermoscopically but not histologically confirmed CW tissue samples of immunocompetent patients, and the VLs of HPV3, 27, and 57 were estimated at 5.1×10^1, 1.1×10^4, and 4.4×10^4 viral copies/cell, respectively, suggesting an etiological role of these HPVs in a subset of CWs.

The aim of this study was to accurately determine the prevalence of several HPV types in by far the largest collection of fresh-frozen tissue samples of histologically confirmed CWs and to reliably assess the causative HPV based on estimation of type-specific HPV VLs using the robust cutoff value established in this study, especially in the most challenging warts containing multiple HPV types within one lesion.

MATERIALS AND METHODS

Characteristics of Patients and Wart Samples

The study included 185 histologically confirmed fresh-frozen CW tissue samples prospectively collected from 121 immunocompetent patients, older than 5 years, referred to a single dermatology outpatient clinic in Slovenia between February 2014 and April 2016.

The majority of patients (108/121; 89.3%) were older than 12 years, with a mean age of 29.3 years (standard deviation (SD) 16.4, median 25 years, range 5–78 years); 66/121 (54.5%) patients were males.

A single wart was collected from 76/121 (62.8%) patients and multiple warts from 45/121 (37.2%) patients: two, three, and five warts were collected from 28/121 (23.2%), 16/121 (13.2%), and 1/121 (0.8%) patients, respectively. Warts were collected from hands including wrists ($n = 131$), lower extremities including dorsal sides of feet ($n = 26$), upper extremities ($n = 14$), and head and neck region ($n = 14$). Mean duration of warts was 16 months (*SD* 21.1, median 12 months, range 1–180 months), with a mean wart diameter of 8.4 mm (*SD* 7.2, median 7.0 mm, range 2–60 mm).

After obtaining patients' written informed consent, their CWs were photographed and 3–4 mm punch biopsies were performed under local anesthesia. Wart samples were then bisected, with half of the sample immediately frozen and stored in liquid nitrogen at −197°C until HPV testing and the other half fixed in 4% neutral buffered formalin and further prepared for routine histological hematoxylin and eosin staining (Kocjan et al., 2015). In cases in which a single patient had multiple warts, only warts that were more than 1 cm apart were sampled in order to reduce potential cross-contamination (de Koning et al., 2011; Tom et al., 2016).

The study was conducted in compliance with the Declaration of Helsinki and approved by the Medical Ethics Committee of the Republic of Slovenia (consent number 63/10/13).

Detection of HPV Infection and HPV Typing

Total DNA from fresh-frozen CW tissue samples was extracted using the QIAamp DNA Mini Kit (Qiagen, Hilden, Germany), following protocol for nucleic acid purification from mammalian tissues, and spectrophotometrically quantified using the NanoDrop 2000c spectrophotometer (Thermo Fisher Scientific, Wilmington, DE). The integrity of extracted DNA was verified by real-time polymerase chain reaction (RT-PCR) amplification of a 268-bp fragment of human beta-globin gene, as described previously (Jancar et al., 2009). In order to determine the presence of HPV, 100 ng of each DNA sample was first tested for the presence of HPV2, 27, and 57, using type-specific quantitative multiplex RT-PCR, allowing sensitive detection and differentiation of HPV2, 27, and 57 in a single PCR reaction (Hošnjak et al., 2016). HPV2/27/57 RT-PCR–negative samples were additionally tested using a consensus primer set (Odar et al.,

2014) in combination with Sanger sequencing, preferentially allowing detection of 23 low-risk *Alpha*-PVs (LR-HPVs): HPV2, 3, 6, 7, 10, 11, 13, 27, 28, 29, 32, 40, 42, 43, 44, 55, 57, 74, 77, 91, 94, 117, and 125 etiologically associated with various mucosal and cutaneous warts. Furthermore, in all samples, the determination of potential *Mu*-PV (HPV1, 63, and 204) infection was performed using three type-specific quantitative RT-PCRs, as described previously (Šterbenc et al., 2017). Type-specific VLs, expressed as ratios between the number of viral copies and human diploid cells, were estimated based on concentrations obtained with type-specific quantitative RT-PCRs and the quantitative 150-bp beta-globin RT-PCR, respectively (Šterbenc et al., 2017).

Statistical Analysis

Results were presented as frequencies and percentages of descriptive nominal variables. For numerical variables, the minimum, maximum, arithmetic mean, standard deviation, and median values were calculated.

RESULTS

The 268-bp fragment of human beta-globin gene was successfully amplified from all 185 CW tissue samples, indicating adequate sample quality for further HPV testing.

As shown in **Table 1**, HPV DNA was detected in 176/185 (95.1%) samples, with single and multiple HPV infections detected in 105/185 (56.8%) and 71/185 (38.4%) samples, respectively. Two HPV types within a single lesion (double HPV infection) were present in one-third of CWs (66/185; 35.7%), and 1 in 50 lesions contained three different HPVs (5/185; 2.7%; **Table 1**). Overall, 12 different HPVs were identified in CWs, with HPV57, 27, and 2 representing by far the most common individual HPVs detected. Moreover, in combination with HPV1, these three HPVs were also the most prevalent in CWs containing two HPV types (**Table 1**).

As shown in **Table 2**, overall, the most frequent HPVs in CWs were HPV57, 1, 27, and 2, which were present in 67.7/185 (36.6%), 39.2/185 (21.2%), 38.0/185 (20.5%), and 13.3/185 (7.2%) CWs, respectively. The overall detection rate of HPV2/27/57 was 64.3% (119/185). In CWs with multiple HPVs, based on proportional attribution estimate (Insinga et al., 2008) HPV1 was the most frequent HPV type, detected in 31.2/71 (43.9%) samples, followed by HPV57, 27, and 63, detected in 19.7/71 (27.7%), 10/71 (14.1%), and 2.7/71 (3.8%) samples tested, respectively.

In the first part of the type-specific HPV VL study, 53 CWs containing a single HPV type were randomly selected to establish a robust cutoff value for further study on more challenging lesions containing multiple HPVs. As shown in **Table 3**, in these 53 randomly selected CWs containing a single HPV, the median VLs of HPV2, 27, and 57 were estimated at 3.3×10^4, 3.2×10^4, and 1.2×10^4 viral copies/cell, respectively, and were significantly higher compared to the estimated VLs of HPV1 (8.2×10^{-3} viral copies/cell) and HPV63 (1.5×10^{-3} viral copies/cell). Based on the clear bimodal distribution of estimated HPV VLs in 53 randomly selected CWs containing a single HPV, ranging from 5.0×10^{-4} to 7.1×10^6 copies/cell (**Supplementary Table 2**), a cutoff value of one viral copy/cell was used to discriminate between causative and non-causative HPVs (HPV bystanders). Consequently, 10/53 (18.9%) CWs containing a single HPV type and VLs of <1 viral copy/cell were assigned as "warts without determined causative HPV" (**Table 4**). As shown in **Table 4**, the most frequent causative HPVs in CWs containing a single HPV type were HPV57, 27, and 2, with an overall prevalence rate of 77.3% (41/53), followed by HPV1 (2/53; 3.8%). HPV63 was not determined as a causative agent in any of the CWs tested containing single HPV infection.

As shown in **Table 4**, the most prevalent causative HPVs in CWs containing multiple HPV types were again HPV57, 27, and 2, with an overall prevalence rate of 53/71 (74.7%), followed by HPV1 (3/71; 4.2%). In addition, based on data from **Supplementary Table 3**, the median VLs of HPV2, 27, 57, 1, 63, and 204 in CWs containing multiple HPVs were estimated at 2.6×10^4, 2.0×10^4, 2.8×10^4, 1.6×10^{-2}, 7.2×10^{-3}, and 5.7×10^{-3} viral copies/cell, respectively. The VLs of HPV2/27/57 ranged from 6.0×10^{-4} to 3.6×10^5 viral copies/cell and in

TABLE 1 | Distribution of human papillomavirus (HPV) types in 185 common warts with single and multiple HPV infections.

HPV types detected within particular lesion, *n* (%)	HPV type(s)	Samples (*n*)
Single HPV type: 105 (56.8)	HPV1	8
	HPV2	11
	HPV3	1
	HPV7	3
	HPV10	2
	HPV27	28
	HPV57	48
	HPV63	3
	HPV117	1
Two HPV types: 66 (35.7)	HPV1 + HPV2	4
	HPV1 + HPV7	2
	HPV1 + HPV10	2
	HPV1 + HPV27	15
	HPV1 + HPV29	1
	HPV1 + HPV57	31
	HPV1 + HPV63	2
	HPV1 + HPV94	1
	HPV1 + HPV117	1
	HPV7 + HPV57	1
	HPV27 + HPV57	3
	HPV57 + HPV63	2
	HPV57 + HPV204	1
Three HPV types: 5 (2.7)	HPV1 + HPV2 + HPV27	1
	HPV1 + HPV10 + HPV63	1
	HPV1 + HPV27 + HPV57	1
	HPV1 + HPV27 + HPV63	1
	HPV1 + HPV57 + HPV204	1
Warts negative for all HPVs tested: 9 (4.8)		
Total warts: 185 (100.0)		

TABLE 2 | Prevalence of human papillomavirus (HPV) types in 185 common warts of immunocompetent patients.

	HPV type	Cumulative $n = 185$ (100%)	Single HPVs $n = 105$ (100%)	[a]Multiple HPVs $n = 71$ (100%)
Alphapapillomavirus 2	HPV3	1 (0.5)	1 (1.0)	0
	HPV10	3.3 (1.8)	2 (1.9)	1.3 (1.8)
	HPV29	0.5 (0.3)	0	0.5 (0.7)
	HPV94	0.5 (0.3)	0	0.5 (0.7)
	HPV117	1.5 (0.8)	1 (1.0)	0.5 (0.7)
Alphapapillomavirus 4	HPV2	13.3 (7.2)	11 (10.5)	2.3 (3.3)
	HPV27	38 (20.5)	28 (26.7)	10 (14.1)
	HPV57	67.7 (36.6)	48 (45.7)	19.7 (27.7)
Alphapapillomavirus 8	HPV7	4.5 (2.4)	3 (2.8)	1.5 (2.2)
Mupapillomavirus 1	HPV1	39.2 (21.2)	8 (7.6)	31.2 (43.9)
Mupapillomavirus 2	HPV63	5.7 (3.1)	3 (2.8)	2.7 (3.8)
Mupapillomavirus 3	HPV204	0.8 (0.4)	0	0.8 (1.1)

[a]*To estimate the HPV type-specific prevalence in 71 warts with multiple HPV infections, the proportional attribution estimate was used. It was calculated using the method of Insinga et al. (2008), in which fractional allocation for each distinct HPV type was made.*

TABLE 3 | Estimated viral loads in 53 randomly selected warts with single human papillomavirus (HPV) infections.

No. of warts ($N = 53$)		Viral load (copies/cell)				
		Minimum	Maximum	Median	Mean	*SD*
HPV2	8	2.5×10^{-3}	1.4×10^{5}	3.3×10^{4}	4.7×10^{4}	5.1×10^{4}
HPV27	15	6.3×10^{3}	2.5×10^{5}	3.2×10^{4}	6.6×10^{4}	7.1×10^{4}
HPV57	22	6.0×10^{-4}	1.7×10^{5}	1.2×10^{4}	2.8×10^{4}	3.9×10^{4}
HPV1	5	5.0×10^{-4}	7.1×10^{6}	8.2×10^{-3}	1.5×10^{6}	3.2×10^{6}
HPV63	3	1.1×10^{-3}	1.8×10^{-2}	1.5×10^{-3}	6.9×10^{-3}	9.6×10^{-3}

Because estimated viral loads were not normally distributed, the median is statistically more appropriate than the mean.

TABLE 4 | Determined causative HPV types in 53 randomly selected warts with single human papillomavirus (HPV) infections and 71 warts with multiple HPV infections based on estimated type-specific HPV viral loads and set cutoff value.

	Single HPVs, *n* (%) $N = 53$ (100%)	Multiple HPVs, *n* (%) $N = 71$ (100%)
HPV2	7 (13.2)	5 (7.1)
HPV27	15 (28.3)	13 (18.3)
HPV57	19 (35.8)	35 (49.3)
HPV1	2 (3.8)	3 (4.2)
Without determined causative HPV	10 (18.9)	15 (21.1)

the great majority of CWs were higher than 100 viral copies/cell, whereas the VLs of HPV1/63/204 ranged from 7.0×10^{-4} to 1.6×10^{2} viral copies/cell and were generally lower than one copy/cell, except in five HPV1-positive warts. Consequently, as shown in **Supplementary Table 3**, a single HPV with 10^{3}-10^{8}-fold higher VLs in comparison to VLs of other HPVs detected within the same wart was present in 52/71 (73.2%) CWs, and such an HPV was securely assigned as the causative HPV. In 4/71 (5.6%) warts, two HPVs present in the same lesion had high VLs and were both co-assigned as potentially causative HPVs (HPV1+27 and HPV1+57 in two CWs each). The causative HPV could not be reliably determined in 15/71 (21.1%) CWs containing multiple HPVs due to the fact that: (i) the VLs of all HPVs detected within the lesion were far <1 viral copy/cell (six samples), or (ii) in addition to targeted HPVs with minute VLs, the CW also contained additional HPVs (HPV7, 10, 29, 94, or 117), for which we were unable to measure VLs due to the lack of appropriate methods (nine samples; **Supplementary Table 3**). Similar to 10 CWs containing single HPVs with minute VLs, these 15 CWs containing multiple HPVs were labeled as "warts without determined causative HPV." Thus, even though HPV63 and HPV204 were indeed detected in 2.7/71 (3.8%) and 0.8/71 (1.1%) warts containing multiple HPVs, respectively, they were not assigned as causative HPVs in any of the CWs tested due to minute VLs.

The majority of CWs containing multiple HPVs were obtained from hands (49/71; 69.0%), and others were collected from legs (10/71; 14.1%), arms (8/71; 11.3%), and head (4/71; 5.6%). The most frequent causative HPV in all four anatomical regions was HPV57 and caused all four CWs collected from the head. Interestingly, all four CWs samples with co-assigned causative HPVs (HPV1+27 and HPV1+57 in two CWs each) were collected from hands.

Among 45 patients with multiple CWs sampled, complete concordance of HPVs detected was found in only 14 (31.1%). However, at least one common HPV was present across all warts obtained from the same individual in 40/45 (88.9%) patients. In addition, in all 21 patients in whom multiple warts were available and HPV VLs could be estimated in all CWs sampled, 100% agreement across assigned causative HPVs was found.

DISCUSSION

Although a broad range of HPV types and a relatively high frequency of multiple HPVs have previously been reported in CWs' tissue samples (Gross et al., 1982; Chen et al., 1993; Egawa, 1994; Lei et al., 2009; Sun et al., 2010; de Koning et al., 2011; Šterbenc et al., 2017), previous studies suffered from small size, use of suboptimal specimens (formalin-fixed paraffin-embedded tissues), and inability to reliably assign the causative HPV type, especially in CWs containing multiple HPVs.

In this study, performed on the largest sample collection of CWs unambiguously diagnosed by histopathological assessment, HPV DNA detection rate was 176/185 (95.1%), which is in line with similar studies, in which HPV positivity ranged from 64.3 to 100% (Gross et al., 1982; Chen et al., 1993; Egawa, 1994; Lei et al., 2009; Sun et al., 2010; de Koning et al., 2011; Šterbenc et al., 2017). High HPV DNA prevalence in this study was most probably due to the use of optimal quality samples (fresh-frozen tissue), highly sensitive HPV detection and genotyping methods (Hošnjak et al., 2016; Šterbenc et al., 2017), and a relatively wide spectrum of HPV types tested ($n = 26$). Multiple HPVs were detected in 71/185 (38.4%) CWs, which is substantially higher in comparison to the majority of similar studies (Gross et al., 1982; Chen et al., 1993; Egawa, 1994; Lei et al., 2009; Sun et al., 2010;

de Koning et al., 2011). In agreement with other studies (Chen et al., 1993; Lei et al., 2009; Šterbenc et al., 2017), the majority of CWs with multiple HPVs contained two HPVs. LR-HPVs and *Mu*-PVs were concomitantly detected in the vast majority of CWs containing multiple HPVs (65/71; 91.5%), with the most frequent combinations being HPV1+27 and HPV1+57, in line with the findings of some previous studies (Lei et al., 2009; Šterbenc et al., 2017).

Although two previous studies showed that, in cutaneous warts containing multiple HPVs, HPV type-specific VL measurement could be useful for differentiating between productive HPV infection and clinically latent infection, a relatively small number of CWs have previously been evaluated using the VL approach ($n = 8$ and $n = 9$, respectively) (Köhler et al., 2009; Šterbenc et al., 2017). This study explored HPV type-specific VLs measured on the largest collection of CWs ($n = 124$), and significantly higher median VLs of HPV2/27/57 were observed in comparison to HPV1/63/204 (10^4 copies/cell and 10^{-3} copies/cell, respectively), irrespective of single or multiple HPVs present in CWs. This phenomenon could be a consequence of different phylogenetic backgrounds of the species *Alphapapillomavirus 4* and the genus *Mu*-PV (Bernard et al., 2010). The estimated high median VLs of HPV27 and 57 in this study are in line with the results of Köhler et al. (2009) and might explain the high prevalence of HPV2/27/57 in CWs of this cohort (119/185; 64.3%) and in previous studies (Gross et al., 1982; Lei et al., 2009; Sun et al., 2010; de Koning et al., 2011) due to copious viral shedding in the environment with subsequent growth of new warts.

To the best of our knowledge, VL cutoff(s) that could be used to reliably differentiate between causative and bystander HPV types in CWs, especially in challenging cases such as CWs containing multiple HPVs, have not been established yet. Based on the VLs measured in 53 randomly selected CWs containing a single HPV type, and clear bimodal distribution of the VLs obtained, in this study the cutoff value for causal determination was set at one copy/cell. Using this approach, HPV57 has been identified as the most important CW-related HPV causing a significant proportion of CWs (35.8 and 50.7% CWs containing single and multiple HPVs, respectively). Three HPV types (HPV2/27/57) were determined to be causative HPVs in three-quarters of CWs irrespective of whether CWs contained single or multiple HPVs, whereas HPV1 was assigned as the causative HPV in ∼4% of CWs, again irrespective of single/multiple HPV status. Similarly, a previous study performed on nine samples determined HPV2/27/57 and HPV1 to be causative HPVs in 6/9 (66.6%) and 1/9 (11.1%) CWs, respectively (Šterbenc et al., 2017). Based on our findings, HPV1—a classic skin HPV type—seems to be rarely causally involved in the development of CWs, in contrast to its prominent etiological role in plantar warts in children (Rübben et al., 1993; Bruggink et al., 2012; de Koning et al., 2015) and its frequent presence in clinically normal skin (de Koning et al., 2015). Similarly, HPV63 and 204 were present in only a small fraction of CWs, and were not assigned as causative HPVs in any of the CWs in this study due to minute VLs. Our results are consistent with previous studies, reporting frequent etiological association of HPV63 with plantar warts (Egawa et al., 1993a, 2015; Bruggink et al., 2013; de Koning et al., 2015) and its frequent presence in normal skin (de Koning et al., 2015), but not in swabs of CW surfaces (de Koning et al., 2015). Furthermore, HPV204, the last officially recognized *Mu*-PV (Kocjan et al., 2015), could be etiologically more important in skin/mucosal lesions other than CWs, preferably in the anogenital region (Šterbenc et al., 2017). In conclusion, the frequent presence of *Mu*-PVs in minute concentrations suggests that they mostly cause clinically latent infections and are present in tissue specimens of CWs as bystanders, not causative HPVs.

In 4/185 (2.2%) CWs, we assigned two co-causative HPVs. In these CWs, we most probably had colliding wart lesions, each associated with an individual causative HPV, as recently demonstrated in cervical intraepithelial neoplasia lesions using laser capture micro-dissection and HPV genotyping, under the "one virus, one lesion" concept (Quint et al., 2012).

In line with previously reported findings (de Koning et al., 2015), in this study a remarkable 100% agreement across all assigned causative HPVs in individuals was found in all 21 patients who had multiple warts and in whom HPV VLs could be determined in all CWs sampled, suggesting that a single HPV type might be implicated in the development of multiple CWs in an individual patient.

In this study, *Mu*-PVs and LR-HPVs were not detected in 9/185 (4.9%) CWs, and, in one-fifth of CWs containing either single or multiple HPVs, the causative HPV remained undetermined, suggesting that these CWs might be etiologically attributed to HPV types from other species such as *Alphapapillomavirus* 2 or 8, *Gamma*-PVs, *Nu*-PVs, or other novel, still-unidentified HPV types. Although the cumulative prevalence of HPVs from species *Alphapapillomavirus* 2 and 8 (HPV7, 10, 29, 94, and 117) was relatively low (11.6/185; 6.3%) and their VLs were not estimated in this study, these HPV types could potentially be considered as the causative HPV of warts in question because HPV1 and 63, co-detected in these CWs, were present in minute quantities. In previous studies performed on histologically confirmed CWs, the reported detection rate of HPV4/60/65 (genus *Gamma*-PV) and HPV41 (genus *Nu*-PV) varied between 0 and 100% (Gross et al., 1982; Chen et al., 1993; Egawa, 1994; de Koning et al., 2011; Šterbenc et al., 2017). However, the highest (100%) prevalence of *Gamma*-PVs in the study by Egawa (1994) could be attributed to selection bias due to histologically discerned type-specific cytopathogenic effects (CPEs), which have assisted in the assignment of possible causative HPV type(s) in cutaneous warts in the past (Jablonska et al., 1985; Egawa et al., 1993a,b; Egawa, 1994). Nowadays, histopathological assessment is not considered a reliable diagnostic method for differentiation between HPV types/genus; for this purpose, we need HPV genotyping methods (Kalantari et al., 2009).

Because the distribution of HPV types and VLs of wart-associated HPVs were found to be independent of immunosuppression (Rübben et al., 1993; Köhler et al., 2009), the findings of this study could also be of importance for immunocompromised patient populations, for whom potential future vaccine(s) against cutaneous HPVs would be most beneficial. In particular, our results reinforce the need for obligatory inclusion of virus-like particles (VLPs) against

HPV2/27/57 in such vaccines, which are currently in the early phase of development (Senger et al., 2010; Gaiser et al., 2015; Huber et al., 2017).

The main limitation of this study is potential selection bias because our cohort might not be fully representative of the general population due to enrollment of patients referred to the tertiary level of dermatological care, possibly due to more treatment-resistant warts or clinically atypical lesions. In addition, considering the benign nature of CWs and potential adverse events of the biopsy, including pain, allergic reactions to local anesthetics, and scarring (Wahie and Lawrence, 2007), only patients who consented to skin biopsy were enrolled, which may have caused additional selection bias and, consequently, fewer warts from children and from facial location were obtained. Another important limitation of this study is that due to technical limitations we were able to reliably assign the causative HPV based on an estimation of type-specific HPV VLs only for the six of the most prevalent CW-associated HPVs: *Alpha*-PV types HPV2/27/57 and *Mu*-PV types HPV1/63/204. Although we identified another six *Alpha*-PV 2 and 8 types (HPV types 3, 7, 10, 29, 94, and 117) as potential causative HPVs of nine warts, due to the lack of appropriate methods we were unable to measure the VLs of these HPVs, and consequently these CWs remain without a reliably assigned causative HPV.

In conclusion, this study was performed on by far the largest collection of histologically confirmed fresh-frozen CWs and—based on assessment of the causative HPV using an estimation of type-specific HPV VLs and the robust cutoff value of one viral copy/cell established in this study—it reliably assigned the causative HPV type in almost 80% of the CWs tested, including challenging lesions containing multiple HPVs. HPV57 has been identified as the most important CW-related HPV, causing at least one-third of CWs and three HPV types (HPV2/27/57) as causative HPVs of three-quarters of CWs irrespective of whether CWs contained single or multiple HPVs. This study provides further evidence for informed decisions about selecting the most appropriate targets for future vaccine(s) against cutaneous HPV-related benign tumors.

DATA AVAILABILITY STATEMENT

All datasets generated for this study are included in the article/**Supplementary Material**.

ETHICS STATEMENT

The studies involving human participants were reviewed and approved by Medical Ethics Committee of the Republic of Slovenia (consent number 63/10/13). Written informed consent to participate in this study was provided by the participants' legal guardian/next of kin.

AUTHOR CONTRIBUTIONS

MP, KF, JM, and VB designed the study. VB and KF organized the database and performed the statistical analysis. LH and KF performed laboratory testing. RK and BL performed histological assessment. VB drafted the first version of the manuscript. LH, KF, and MP drafted individual sections of the manuscript. MP produced the final version of the manuscript. All authors revised manuscript, read it, and approved the submitted version.

FUNDING

This work was supported by the Institute of Microbiology and Immunology at the University of Ljubljana's Faculty of Medicine, University Medical Centre Maribor and the Slovenian Research Agency (Agreement No. P3-0083). The funders had no role in the study design, data collection and analysis, decision to publish, or preparation of the manuscript.

ACKNOWLEDGMENTS

The authors would like to thank all participating patients, the staff from the Department of Dermatology at the University Medical Centre Maribor for their assistance in sample collection, the staff from the Department of Pathology at the University Medical Centre Maribor, the Institute of Pathology at the University of Ljubljana's Faculty of Medicine, and the Institute of Microbiology and Immunology at the University of Ljubljana's Faculty of Medicine for sample transport management and laboratory assistance.

SUPPLEMENTARY MATERIAL

The Supplementary Material for this article can be found online at: https://www.frontiersin.org/articles/10.3389/fcimb.2020.00004/full#supplementary-material

Supplementary Table 1 | Summary of previously published HPV prevalence studies performed on histologically confirmed tissue samples of common warts obtained from immunocompetent individuals.

Supplementary Table 2 | Estimated viral loads (VLs) of human papillomavirus (HPV) types 1, 2, 27, 57, and 63 in 53 randomly selected common warts containing a single HPV type and assigned causative HPV type based on estimation of type-specific HPV VLs.

Supplementary Table 3 | Estimated viral loads (VLs) of human papillomavirus (HPV) types 1, 2, 27, 57, 63, and 204 in 71 common warts containing multiple HPVs and assigned causative HPV type based on estimation of type-specific HPV VLs.

REFERENCES

Al Bdour, S., Akkash, L., and Shehabi, A. A. (2013). Detection and typing of common human papillomaviruses among Jordanian patients. *J. Med. Virol.* 85, 1058–1062. doi: 10.1002/jmv.23519

Aldabagh, B., Angeles, J. G., Cardones, A. R., and Arron, S. T. (2013). Cutaneous squamous cell carcinoma and human papillomavirus: is there an association? *Dermatol. Surg.* 39, 1–23. doi: 10.1111/j.1524-4725.2012.02558.x

Bae, J. M., Kang, H., Kim, H. O., and Park, Y. M. (2009). Differential diagnosis of plantar wart from corn, callus and healed wart with the aid of

dermoscopy. *Br. J. Dermatol.* 160, 220–222. doi: 10.1111/j.1365-2133.2008.08937.x

Bernard, H. U., Burk, R. D., Chen, Z., van Doorslaer, K., zur Hausen, H., and de Villiers, E. M. (2010). Classification of papillomaviruses (PVs) based on 189 PV types and proposal of taxonomic amendments. *Virology* 401, 70–79. doi: 10.1016/j.virol.2010.02.002

Bouwes Bavinck, J. N., Euvrard, S., Naldi, L., Nindl, I., Proby, C. M., Neale, R., et al. (2007). Keratotic skin lesions and other risk factors are associated with skin cancer in organ-transplant recipients: a case-control study in The Netherlands, United Kingdom, Germany, France, and Italy. *J. Invest. Dermatol.* 127, 1647–1656. doi: 10.1038/sj.jid.5700776

Bruggink, S. C., de Koning, M. N., Gussekloo, J., Egberts, P. F., Ter Schegget, J., Feltkamp, M. C., et al. (2012). Cutaneous wart-associated HPV types: prevalence and relation with patient characteristics. *J. Clin. Virol.* 55, 250–255. doi: 10.1016/j.jcv.2012.07.014

Bruggink, S. C., Gussekloo, J., de Koning, M. N., Feltkamp, M. C., Bavinck, J. N., Quint, W. G., et al. (2013). HPV type in plantar warts influences natural course and treatment response: secondary analysis of a randomised controlled trial. *J. Clin. Virol.* 57, 227–232. doi: 10.1016/j.jcv.2013.02.021

Cardoso, J. C., and Calonje, E. (2011). Cutaneous manifestations of human papillomaviruses: a review. *Acta. Dermatovenerol Alp Pannonica Adriat.* 20, 145–154.

Chen, S. L., Tsao, Y. P., Lee, J. W., Sheu, W. C., and Liu, Y. T. (1993). Characterization and analysis of human papillomaviruses of skin warts. *Arch. Dermatol. Res.* 285, 460–465. doi: 10.1007/BF00376818

De Giorgi, V., and Massi, D. (2006). Images in clinical medicine. Plantar melanoma–a false vegetant wart. *N. Engl. J. Med.* 355:e13. doi: 10.1056/NEJMicm055674

de Koning, M. N., Khoe, L. V., Eekhof, J. A., Kamp, M., Gussekloo, J., Ter Schegget, J., et al. (2011). Lesional HPV types of cutaneous warts can be reliably identified by surface swabs. *J. Clin. Virol.* 52, 84–87. doi: 10.1016/j.jcv.2011.06.016

de Koning, M. N., Quint, K. D., Bruggink, S. C., Gussekloo, J., Bouwes Bavinck, J. N., Feltkamp, M. C., et al. (2015). High prevalence of cutaneous warts in elementary school children and the ubiquitous presence of wart-associated human papillomavirus on clinically normal skin. *Br. J. Dermatol.* 172, 196–201. doi: 10.1111/bjd.13216

Egawa, K. (1994). New types of human papillomaviruses and intracytoplasmic inclusion bodies: a classification of inclusion warts according to clinical features, histology and associated HPV types. *Br. J. Dermatol.* 130, 158–166. doi: 10.1111/j.1365-2133.1994.tb02894.x

Egawa, K., Delius, H., Matsukura, T., Kawashima, M., and de Villiers, E. M. (1993a). Two novel types of human papillomavirus, HPV 63 and HPV 65: comparisons of their clinical and histological features and DNA sequences to other HPV types. *Virology* 194, 789–799. doi: 10.1006/viro.1993.1320

Egawa, K., Shibasaki, Y., and de Villiers, E. M. (1993b). Double infection with human papillomavirus 1 and human papillomavirus 63 in single cells of a lesion displaying only an human papillomavirus 63-induced cytopathogenic effect. *Lab Invest.* 69, 583–588.

Egawa, N., Egawa, K., Griffin, H., and Doorbar, J. (2015). Human papillomaviruses; epithelial tropisms, and the development of neoplasia. *Viruses* 7, 3863–3890. doi: 10.3390/v7072802

Gaiser, M. R., Textor, S., Senger, T., Schädlich, L., Waterboer, T., Kaufmann, A. M., et al. (2015). Evaluation of specific humoral and cellular immune responses against the major capsid L1 protein of cutaneous wart-associated alpha-Papillomaviruses in solid organ transplant recipients. *J. Dermatol. Sci.* 77, 37–45. doi: 10.1016/j.jdermsci.2014.11.002

Gross, G., Pfister, H., Hagedorn, M., and Gissmann, L. (1982). Correlation between human papillomavirus (HPV) type and histology of warts. *J. Invest. Dermatol.* 78, 160–164. doi: 10.1111/1523-1747.ep12506324

Harwood, C. A., Spink, P. J., Surentheran, T., Leigh, I. M., de Villiers, E. M., McGregor, J. M., et al. (1999). Degenerate and nested PCR: a highly sensitive and specific method for detection of human papillomavirus infection in cutaneous warts. *J. Clin. Microbiol.* 37, 3545–3555. doi: 10.1128/JCM.37.11.3545-3555.1999

Hogendoorn, G. K., Bruggink, S. C., de Koning, M. N. C., Eekhof, J. A. H., Hermans, K. E., Rissmann, R., et al. (2018). Morphological characteristics and human papillomavirus genotype predict the treatment response in cutaneous warts. *Br. J. Dermatol.* 178, 253–260. doi: 10.1111/bjd.15758

Hošnjak, L., Fujs Komloš, K., Kocjan, B. J., Seme, K., and Poljak, M. (2016). Development of a novel multiplex type-specific quantitative real-time PCR for detection and differentiation of infections with human papillomavirus types HPV2, HPV27, and HPV57. *Acta Dermatovenerol. Alp. Pannonica Adriat.* 25, 65–71. doi: 10.15570/actaapa.2016.20

Huber, B., Schellenbacher, C., Shafti-Keramat, S., Jindra, C., Christensen, N., and Kirnbauer, R. (2017). Chimeric L2-based virus-like particle (VLP) vaccines targeting cutaneous human papillomaviruses (HPV). *PLoS ONE* 12:e0169533. doi: 10.1371/journal.pone.0169533

Insinga, R. P., Liaw, K. L., Johnson, L. G., and Madeleine, M. M. (2008). A systematic review of the prevalence and attribution of human papillomavirus types among cervical, vaginal, and vulvar precancers and cancers in the United States. *Cancer Epidemiol. Biomarkers Prev.* 17, 1611–1622. doi: 10.1158/1055-9965.EPI-07-2922

Jablonska, S., Orth, G., Obalek, S., and Croissant, O. (1985). Cutaneous warts. Clinical, histologic, and virologic correlations. *Clin. Dermatol.* 3, 71–82. doi: 10.1016/0738-081X(85)90051-3

Jancar, N., Kocjan, B. J., Poljak, M., and Bokal, E. V. (2009). Comparison of paired cervical scrape and tumor tissue samples for detection of human papillomaviruses in patients with cervical cancer. *Eur. J. Gynaecol. Oncol.* 30, 675–678.

Kalantari, M., Garcia-Carranca, A., Morales-Vazquez, C. D., Zuna, R., Montiel, D. P., Calleja-Macias, I. E., et al. (2009). Laser capture microdissection of cervical human papillomavirus infections: copy number of the virus in cancerous and normal tissue and heterogeneous DNA methylation. *Virology* 390, 261–267. doi: 10.1016/j.virol.2009.05.006

Kocjan, B. J., Šterbenc, A., Hošnjak, L., Chouhy, D., and Bolatti, E., Giri, A. A., et al. (2015). Genome announcement: complete genome sequence of a novel Mupapillomavirus, HPV204. *Acta Dermatovenerol Alp. Pannonica Adriat.* 24, 21–23. doi: 10.15570/actaapa.2015.7

Köhler, A., Meyer, T., Stockfleth, E., and Nindl, I. (2009). High viral load of human wart-associated papillomaviruses (PV) but not beta-PV in cutaneous warts independent of immunosuppression. *Br. J. Dermatol.* 161, 528–535. doi: 10.1111/j.1365-2133.2009.09297.x

Lei, Y. J., Gao, C., Wang, C., Han, J., Chen, J. M., Xiang, G. C., et al. (2009). Molecular epidemiological study on prevalence of human papillomaviruses in patients with common warts in Beijing area. *Biomed. Environ. Sci.* 22, 55–61. doi: 10.1016/S0895-3988(09)60023-4

Odar, K., Kocjan, B. J., Hošnjak, L., Gale, N., Poljak, M., and Zidar, N. (2014). Verrucous carcinoma of the head and neck - not a human papillomavirus-related tumour? *J. Cell. Mol. Med.* 18, 635–645. doi: 10.1111/jcmm.12211

Quint, W., Jenkins, D., Molijn, A., Struijk, L., van de Sandt, M., Doorbar, J., et al. (2012). One virus, one lesion–individual components of CIN lesions contain a specific HPV type. *J Pathol.* 227, 62–71. doi: 10.1002/path.3970

Rübben, A., Krones, R., Schwetschenau, B., and Grussendorf-Conen, E. I. (1993). Common warts from immunocompetent patients show the same distribution of human papillomavirus types as common warts from immunocompromised patients. *Br. J. Dermatol.* 128, 264–270. doi: 10.1111/j.1365-2133.1993.tb00169.x

Schmitt, M., de Koning, M. N., Eekhof, J. A., Quint, W. G., and Pawlita, M. (2011). Evaluation of a novel multiplex human papillomavirus (HPV) genotyping assay for HPV types in skin warts. *J. Clin. Microbiol.* 49, 3262–3267. doi: 10.1128/JCM.00634-11

Senger, T., Becker, M. R., Schädlich, L., Waterboer, T., and Gissmann, L. (2009). Identification of B-cell epitopes on virus-like particles of cutaneous alpha-human papillomaviruses. *J. Virol.* 83, 12692–12701. doi: 10.1128/JVI.01582-09

Senger, T., Schädlich, L., Textor, S., Klein, C., Michael, K. M., Buck, C. B., et al. (2010). Virus-like particles and capsomeres are potent vaccines against cutaneous alpha HPVs. *Vaccine* 28, 1583–1593. doi: 10.1016/j.vaccine.2009.11.048

Sondermann, W., Zimmer, L., Schadendorf, D., Roesch, A., Klode, J., and Dissemond, J. (2016). Initial misdiagnosis of melanoma located on the foot is associated with poorer prognosis. *Medicine* 95:e4332. doi: 10.1097/MD.0000000000004332

Šterbenc, A., Hošnjak, L., Chouhy, D., Bolatti, E. M., Oštrbenk, A., Seme, K., et al. (2017). Molecular characterization, tissue tropism, and genetic variability

of the novel Mupapillomavirus type HPV204 and phylogenetically related types HPV1 and HPV63. *PLoS ONE* 12:e0175892. doi: 10.1371/journal.pone.0175892

Sun, C., Chen, K., Gu, H., Chang, B., and Jiang, M. (2010). Association of human papillomavirus 7 with warts in toe webs. *Br. J. Dermatol.* 162, 579–586. doi: 10.1111/j.1365-2133.2009.09564.x

Tom, L. N., Dix, C. F., Hoang, V. L., Lin, L. L., Nufer, K. L., Tomihara, S., et al. (2016). Skin microbiopsy for HPV DNA detection in cutaneous warts. *J. Eur. Acad. Dermatol. Venereol.* 30, e216–e217. doi: 10.1111/jdv.13548

van Haalen, F. M., Bruggink, S. C., Gussekloo, J., Assendelft, W. J., and Eekhof, J. A. (2009). Warts in primary schoolchildren: prevalence and relation with environmental factors. *Br. J. Dermatol.* 161, 148–152. doi: 10.1111/j.1365-2133.2009.09160.x

Vinzón, S. E., Braspenning-Wesch, I., Müller, M., Geissler, E. K., Nindl, I., Gröne, H. J., et al. (2014). Protective vaccination against papillomavirus-induced skin tumors under immunocompetent and immunosuppressive conditions: a preclinical study using a natural outbred animal model. *PLoS Pathog.* 10:e1003924. doi: 10.1371/journal.ppat.1003924

Wahie, S., and Lawrence, C. M. (2007). Wound complications following diagnostic skin biopsies in dermatology inpatients. *Arch. Dermatol.* 143, 1267–1271. doi: 10.1001/archderm.143.10.1267

Disclaimer: Partial results of this study were presented at the 22nd European Society for Clinical Virology's Annual Meeting, ESCV 2019, in September 2019 in Copenhagen, Denmark in an abstract titled "Determination of potential causative etiological human papillomavirus types in histologically confirmed common warts, based on estimated viral loads."

Conflict of Interest: The authors declare that the research was conducted in the absence of any commercial or financial relationships that could be construed as a potential conflict of interest.

frontiers in Microbiology

ORIGINAL RESEARCH
published: 31 January 2020
doi: 10.3389/fmicb.2020.00084

Outbreak of *Saprochaete clavata* Sepsis in Hematology Patients: Combined Use of MALDI-TOF and Sequencing Strategy to Identify and Correlate the Episodes

Giuliana Lo Cascio[1], Marcello Vincenzi[2], Fabio Soldani[2], Elena De Carolis[3], Laura Maccacaro[1], Annarita Sorrentino[1], Gianpaolo Nadali[4], Simone Cesaro[5], Michele Sommavilla[6], Valentina Niero[7], Laura Naso[1], Anna Grancini[8], Anna Maria Azzini[2], Maurizio Sanguinetti[3], E. Tacconelli[2] and Giuseppe Cornaglia[1]*

[1] Microbiology and Virology Unit, Department of Pathology, Azienda Ospedaliera Universitaria Integrata di Verona, Verona, Italy, [2] Infectious Disease Unit, Department of Diagnostics and Public Health, University of Verona, Verona, Italy, [3] Dipartimento di Scienze di Laboratorio e Infettivologiche, Fondazione Policlinico Universitario Agostino Gemelli IRCCS, Rome, Italy, [4] Haematology Unit, Department of Medicine, Azienda Ospedaliera Universitaria Integrata di Verona, Verona, Italy, [5] Division of Pediatric Oncohaematology, Department of Pediatrics, Azienda Ospedaliera Universitaria Integrata di Verona, Verona, Italy, [6] Direzione Medica Ospedaliera, Azienda Ospedaliera Universitaria Integrata di Verona, Verona, Italy, [7] Sezione di Igiene e Medicina Preventiva, Ambientale e Occupazionale, Dipartimento Diagnostica e Sanità Pubblica, Università di Verona, Verona, Italy, [8] Laboratorio di Analisi Chimico – Cliniche e Microbiologia, Fondazione IRCCS Cà Granda O. Maggiore Policlinico, Milan, Italy

OPEN ACCESS

Edited by:
Aleksandra Barac, University of Belgrade, Serbia

Reviewed by:
Javier Pemán, University and Polytechnic Hospital of La Fe, Spain
Michael Pfaller, The University of Iowa, United States

***Correspondence:**
Giuliana Lo Cascio
giuliana.locascio@aovr.veneto.it

Specialty section:
This article was submitted to Fungi and Their Interactions, a section of the journal Frontiers in Microbiology

Received: *06 November 2019*
Accepted: *15 January 2020*
Published: *31 January 2020*

Citation:
Lo Cascio G, Vincenzi M, Soldani F, De Carolis E, Maccacaro L, Sorrentino A, Nadali G, Cesaro S, Sommavilla M, Niero V, Naso L, Grancini A, Azzini AM, Sanguinetti M, Tacconelli E and Cornaglia G (2020) Outbreak of Saprochaete clavata Sepsis in Hematology Patients: Combined Use of MALDI-TOF and Sequencing Strategy to Identify and Correlate the Episodes. Front. Microbiol. 11:84. doi: 10.3389/fmicb.2020.00084

Introduction: New fungal species are increasingly reported in immunocompromised patients. *Saprochaete clavata* (*S. clavata*), an ascomycetous fungus formerly called *Geotrichum clavatum*, is intrinsically resistant to echinocandins and is often misidentified.

Objective: We describe a cluster of seven *S. clavata* infections in hospitalized hematology patients who developed this rare fungemia within a span of 11 months. Three of the seven patients died. Identification of the isolates was determined only with the Saramis database of VitekMS system and sequencing of the internal transcribed spacer (ITS) region. Clonal relatedness of the isolates was determined by matrix-assisted laser desorption ionization–time of flight mass spectrometry (MALDI-TOF) analysis; clonal correlation between the strains was investigated by means of phylogenetic analysis, based on single-nucleotide variants (SNPs). Clinical presentation, 1–3 β-D-glucan (BG) and galactomannan (GM) antigen results and analysis of possible sources of contamination are also described with a prospective case–control study of the outbreak.

Results: MALDI-TOF MS-Vitek (bioMerieux, Marcy l'Etoile, France) failed to identify the six isolates, while SARAMIS (bioMerieux, Marcy l'Etoile, France) identified the isolates as *S. clavata*. Initially, Vitek 2 identified the strains as *Geotrichum capitatum* in two of the seven cases. Molecular identification gave 99% homology with *S. clavata*. BG was positive in three out of six patients (range 159 to >523 pg/ml), GM results were always negative. All the isolates were resistant to echinocandins (anidulafungin, micafungin, and caspofungin) and Fluconazole, but susceptible to Flucytosine and Voriconazole. One isolate showed acquired resistance to Flucytosine and Amphotericin

B during treatment. Both the correlation-based dendrograms obtained by MALDI-TOF MS (Bruker Daltonics) and MS-Vitek not only clustered six of the seven bloodstream infection (BSI) isolates in the same group, but also showed their strong relatedness. Phylogenetic analysis using SNPrelate showed that the seven samples recorded during the investigation period clustered together. We observed a split between one case and the remainder with a node supported by a *z*-score of 2.3 (*p*-value = 0.021) and 16 mutations unique to each branch.

Conclusion: The use of proteomics for identification and evaluation of strain clonality in outbreaks of rare pathogens is a promising alternative to laborious and time-consuming molecular methods, even if molecular whole-genome sequencing (WGS) typing will still remain the reference method for rare emergent pathogens.

Keywords: *Saprochaete*, MALDI-TOF, yeast sepsi, outbreak, whole-genome sequencing

INTRODUCTION

Invasive fungal infections (IFIs) represent a public health burden worldwide, especially in immunocompromised patients, and their incidence has risen over the last decades due to the increased use of immunosuppressive and cytotoxic therapies, improved diagnostic techniques, greater awareness, and clinical suspicion. They are still a major cause of morbidity and mortality in patients with hematology malignancies (Girmenia et al., 2005; Miceli et al., 2011; Garcia-Ruiz et al., 2013; Picard et al., 2014; Stanzani et al., 2019). *Candida* and *Aspergillus* spp. play a major role. However, as a result of new prevention strategies, changes in host features and treatment protocols, new species are increasingly reported as agents of blood stream infections (BSIs) or disseminated fungi such as *Trichosporon* and *Geotrichum* (Girmenia et al., 2005; Miceli et al., 2011; Litvintseva et al., 2014; Picard et al., 2014). Particularly, *Geotrichum*, an arthroconidial yeast-like filamentous fungus whose nomenclature has recently been modified, demands special attention owing to recent outbreaks in hematology patients. Because our knowledge of these new species is poor, although improving, it is still difficult to distinguish between one fungus and another. For example, *Magnusiomyces clavatus*, formerly known as *Saprochaete clavata* or *Geotrichum clavatum*, is phylogenetically and phenotypically closely related to *Magnusiomyces capitatus*, formerly called *Geotrichum capitatum*. Both species are often misidentified and have been implicated in sporadic cases and outbreaks of fungemia mostly, but not only, in Mediterranean countries (Garcia-Ruiz et al., 2013; Desnos-Ollivier et al., 2014; Del Principe et al., 2016). Because of this microbiological flaw, and their intrinsic resistance to echinocandins and fluconazole, these infections restrict therapeutic options and are associated with high mortality rates. Here we present a prospective case–control study about an outbreak of *S. clavata* BSIs in adult and pediatric hematology patients of the Azienda Ospedaliera Universitaria Integrata di Verona, Italy, which occurred between September 2016 and July 2017. In order to provide clues about the isolates' relatedness, typing by matrix-assisted laser desorption ionization–time of flight mass spectrometry (MALDI-TOF) analysis was performed. Finally, clonal correlation between the strains was investigated by means of phylogenetic analysis based on single-nucleotide variants (SNPs). Clinical presentation, 1–3 β-D-glucan (BG), and galactomannan (GM) antigen results and analysis of possible sources of contamination are also described.

MATERIALS AND METHODS

Epidemiology Study

In order to limit the spread and to look for a common source of the infection, the hospital infection control and epidemiology teams, by agreement with the Medical Direction, organized a case–control study. From September 2016 to July 2017 a matched density-based sampling case–control study was undertaken, in order to investigate risk factors for *Saprochaete* fungemia in hematology patients hospitalized in the Azienda Ospedaliera Universitaria Integrata di Verona, Italy. Included cases were patients whose blood cultures proved positive for *Saprochaete* and who were hospitalized in the hematology, bone marrow transplant, and pediatric onco-hematology wards. Controls were patients hospitalized within 2 months prior to the isolation of *Saprochaete* from blood cultures of each case and with a minimum of 10 days' hospitalization in the same wards. Each case was matched with five controls, based on hospital ward, during clinical presentation of fungal sepsis. Information about comorbidities, chemotherapy, antimicrobial therapy, presence of indwelling catheters, transfusions, and nutrition were collected by examining patient medical files, food database from the organization which provided patient meals, Hematology database, and the Hospital Pharmacy. Given this rare infection, it has not been possible to precisely estimate the sample size and the statistical power. Owing to scant literature on this topic, almost always limited to small cluster epidemics and case series, we chose to perform a conditioned regression logistic analysis, considering a p-value < 0.05 as statistically significant.

This retrospective observational study was based on anonymized patient data, and was carried out in accordance with the Declaration of Helsinki, under the terms of relevant local legislation, and was cleared by the Institutional Review Board.

The requirement for informed consent was waived due to the observational and retrospective nature of this study.

Microbiological Study

The Bact/Alert3D (bioMerieux, Marcy l'Etoile, France) system was used for blood cultures. A minimum of two culture vials per patient in 24 h, one fastidious antibiotic neutralization (FAN) aerobic bottle and one FAN anaerobic bottle (bioMerieux, Marcy l'Etoile, France), were filled directly with blood according to the manufacturer's instructions. Cultures were incubated for a maximum of 5 days. On positive bottles gram staining was performed to allow direct microscopy, cultures were inoculated and incubated on Blood agar, Chocolate agar, Columbia agar (supplemented with 5% sheep blood), Sabouraud dextrose agar, and Schaedler agar under aerobic, micro-aerobic, and anaerobic conditions, respectively.

Identification of the blood isolates was undertaken using various methods, namely MS Vitek MALDI-TOF, SARAMIS, and VITEK 2(System (bioMerieux, Marcy l'Etoile, France). Primers ITS1 and ITS4 were used to amplify rDNA ITS region (White et al., 1990), while primers NL1 and NL4 were used to amplify rDNA D1–D2 region (Kurtzman and Robnett, 1997). Amplified sequences were compared with the GenBank Nucleotide Database[1] using the algorithm Blast N (Altschul et al., 1997; de Hoog and Smith, 2004; Nilsson et al., 2006; Bader et al., 2011).

Serum BG levels were determined by the Food and Drug Administration-approved Fungitell Assay (Associates of Cape Cod, Falmouth, MA, United States) according to the manufacturer's instructions (Budhavari, 2009). BG values < 60 pg/mL were interpreted as being negative, >80 pg/mL as being positive, and 60–79 pg/mL as indeterminate.

Serum GM levels were determined by Platelia Aspergillus (Bio-Rad, Marnes-la-Coquette, France) according to the manufacturer's recommendations. As cleared by the US FDA the results were analyzed using an optical density (OD) index cut-off value of 0.5 on serum. The test was considered positive with an OD index value of $\geq$0.8 or more rather than with an OD index of 0.5 in two consecutive samples (Favre et al., 2016).

In vitro susceptibilities to amphotericin B, fluconazole, itraconazole, voriconazole, posaconazole, anidulafungin, caspofungin, micafungin, and flucytosine were determined by Sensititre YeastOne Y10 panel (Thermo Fisher Inc.). Readings were taken at 24 and 48 h of incubation.

In order to provide clues about the isolates' relatedness, MALDI-TOF analysis was performed after the acquisition of the mass spectrum profiles in positive linear mode by a Microflex LT mass spectrometer (MSP, Bruker Daltonics) in accordance with the manufacturers' recommendations. Strains of *M. capitatus* and *S. clavata* belonging to collected strain of UCSC-Rome were evaluated to show any correlation. Following MSP creation from the seven isolates, a score-oriented dendrogram was generated from hierarchical cluster analysis using the integrated statistical tool of the BioTyper 3.1 software. Hence, the same analysis was done with SARAMIS software connected to MS-Vitek in accordance with the manufacturers' instructions. To evaluate any aspecific correlation, strains of *S. clavata* and *Geotrichum candidum* were submitted for the same analysis.

An environmental study was conducted to investigate possible sources of infection. Medical devices, drugs, blood-derived products and foods, in particular dairy products, were cultured for enrichment in Brain hearth infusion (BHI) broth and subculture in Blood agar, Chocolate agar, Columbia agar (supplemented with 5% sheep blood), and Sabouraud dextrose agar.

Genotyping Methods

All the strains of *S. clavata* occurring in the Verona outbreak and three strains of *Saprochaete capitata*, which had been isolated in another Italian hospital (Milan), were used to compare clonal correlation. All yeasts were sequenced. PCR-free DNAseq libraries were generated with the KAPA Hyper prep. Library kit. The sequencing process was based on an Illumina NextSeq500 using 2 $\times$ 150 bp-reads, analyzing 19.3 million fragments per sample on average. **Figure 1** shows the workflow used in this study, which involved a number of steps from raw fastq files to the production of a phylogenetic tree. In the first step, adapters removal and quality trimming were performed using shyte v.0.991 and sickle v.1.33 software to obtain high quality reads. Then, reads were aligned to the *S. clavata* reference assembly produced by Vaux et al. (2014) (17.5 Mb, 339 scaffolds), using mem algorithm of burrows wheeler aligner v.0.7.17 with default options except when a threads argument was available. The BAM files obtained from reads alignment were used to call variants. This step in the pipeline was done using mpileup command from samtools v.1.4. The genotyping was performed using *call* command from bcftools v.1.4. All the variant calls were filtered following criteria set in Vaux et al. (2014): (i) all the variants were supported at least with four reads for each orientation; (ii) all the reads with a mapping quality above 30 were considered; (iii) variants at $<$100 bp from the margins of a scaffold were excluded; and (iv) the variable characters were parsimony informative (containing more than one type of nucleotide, occurring at least in two isolates) to support phylogenetic clustering. Phylogenetic correlation was inferred from high quality SNPs. R packages SNPrelate v.3.7 and Ape/Phangorn v.2.4.0 were used to compute a nucleotide distance matrix and then to perform the clustering step using a neighbor joining algorithm. To support the phylogenetic analysis with a different clustering technique, the principal component analysis was applied. Normalization of SNPs number per scaffold length was performed to check for hypervariable regions possibly connected to Fungi adaptations. The hypervariable scaffold sequences were aligned with "Basic Local Alignment Search Tool" to search for similarities with NCBI database.

RESULTS

During the study period, a total of seven cases of *S. clavata* BSIs occurred in different hematology wards of our hospital (**Figure 2**). Thirty-five controls were enrolled. **Table 1**

[1] http://www.ncbi.nlm.nih.gov

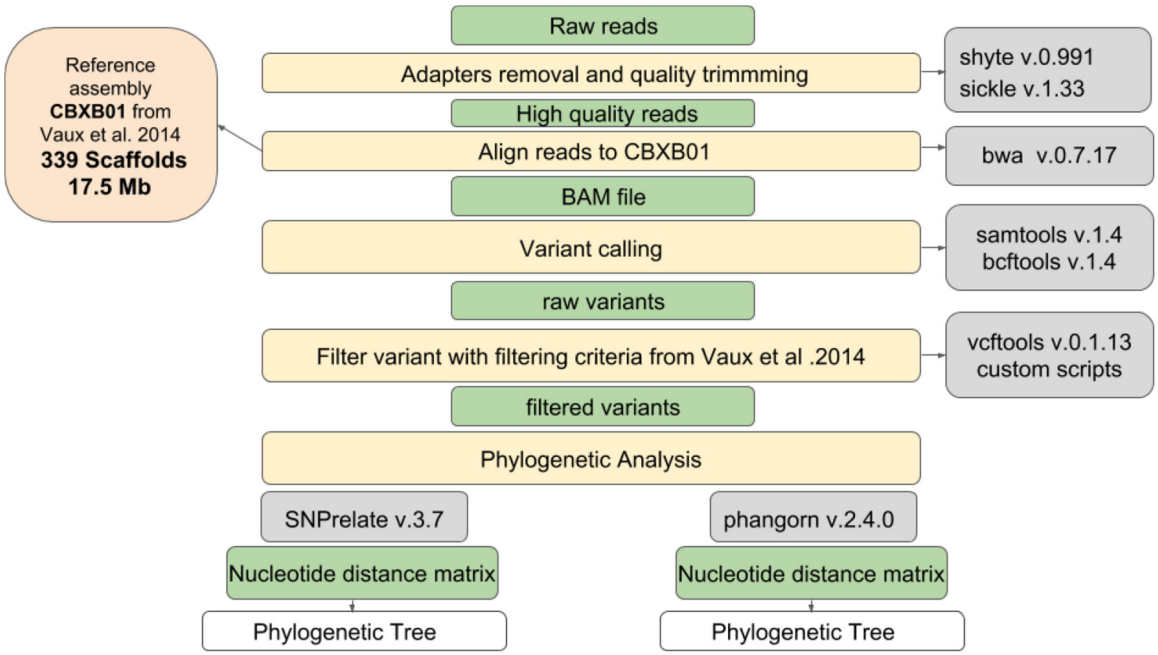

FIGURE 1 | Workflow used to produce the phylogenetic tree of isolated *Saprochaete*.

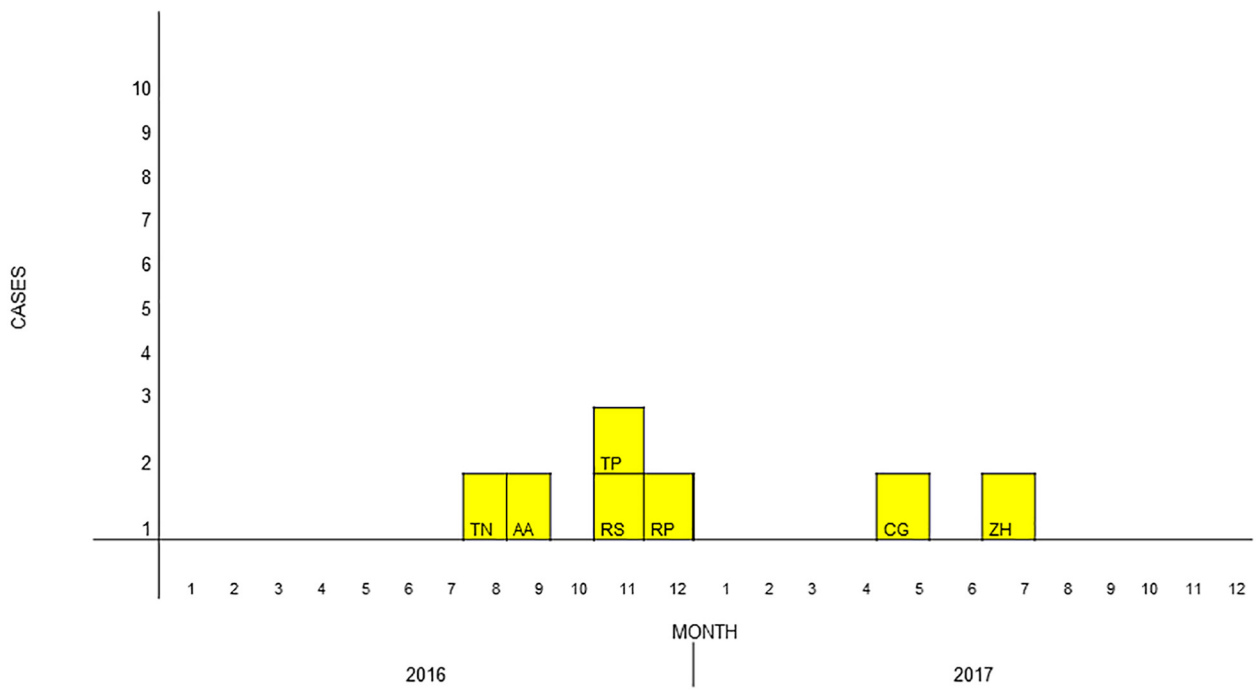

FIGURE 2 | Epidemiological curve of *Saprochaete clavata* infections. The cases are designated with letters which identify the isolate, with boxes corresponding to the date of the first positive blood culture.

summarizes the main characteristics of cases and controls. All but one of the patients were Italians. The mean ages of cases and controls were 41.1 and 51 years, respectively. Six (85.7%) cases and 18 (51.4%) controls were male. Underlying disease was acute myeloid leukemia (AML) in two of the seven cases, non-Hodgkin lymphoma in two, acute T-lymphoblastic leukemia in one, and other unspecified hematology diseases in the remaining two. It is noteworthy that all of the cases had a

TABLE 1 | Characteristics of the *Saprochaete* cases.

Characteristics	Cases *N* (%)	Controls *N* (%)
Sex female add a line with number of male patients and controls?	1 (14.3)	17 (48.6)
Mean age (SD)	41.1 (26.1)	51.0 (22.0)
Age in range		
0–40	3 (42.7)	8 (22.3)
41–50	1 (14.3)	4 (11.4)
51–60	1 (14.3)	9 (25.7)
61–70	2 (28.6)	10 (28.6)
>70	–	4 (11.4)
Transfer to other UO what is UO?	2 (28.6)	10 (28.6)
Underlying diseases or conditions		
Acute myeloid leukemia	2 (28.6)	10 (28.6)
Chronic myeloid leukemia	–	2 (5.7)
Lymphoma	2 (28.6)	14 (40.0)
Multiple myeloma	–	3 (8.6)
Other	3 (42.9)	6 (17.1)
Charlson co-morbidity score, media (DS)	3 (1.8)	4.3 (2.0)
Charlson score in range		
0–3	4 (57.1)	11 (31.4)
4–7	3 (42.9)	21 (60.0)
8–11	–	3 (8.6)
Barthel scale, mean (SD)	86.7 (21.8)	88.2 (19.6)
Dead, *N*(%)	3 (42.9)	2 (5.7)
Presence of CVC during recovery	7 (100)	32 (31.4)
Days with CVC		
0–20	2 (28.6)	18 (51.4)
21–40	–	10 (28.6)
>40	5 (71.4)	7 (20.0)
Days of CVC, mean (IQR)	64 (18–78)	20 (15–30)
Mechanical ventilation	1 (14.3)	2 (5.7)
Bladder catheter	3 (42.9)	9 (25.7)
Chemotherapy	7 (100)	29 (82.9)
Immunosuppression	7 (100)	24 (68.6)
Antibiotics	7 (100)	33 (94.3)
Aminoglycosides	6 (85.7)	11 (31.4)
Days with aminoglycosides, mean (SD)	11.4 (11.6)	0 (0.7)
Penicillin with beta-lactamases inhibitor	5 (71.4)	17 (48.6)
Days with penicillin with BL inhibitor, mean (SD)	5.5 (5.1)	4.0 (5.9)
Cephalosporins 3–4° gen.	3 (42.9)	13 (37.1)
Days with cephalosporins 3–4° gen., mean (SD)	7.1 (11.7)	3.9 (7.1)
Fluorochinolons	2 (28.2)	13 (37.1)
Days with fluorochinolons, mean (SD)	3.8 (9.4)	7.0 (11.1)
Glycopeptides, *N*(%)	4 (57.1)	9 (25.7)
Days with glycopeptides, mean(SD)	8.4 (12.0)	2.7(85.2)
Meropenem	5 (71.4)	5 (14.3)
Days with meropenem, mean (SD)	7.3 (10.0)	2.1 (8.6)
Co-trimoxazole	1 (14.3)	5 (14.3)
Days with co-trimoxazole, mean (SD)	0.3 (0.8)	0.6 (1.7)
Antifungals	4 (57.1)	26 (74.3)
Amphotericin	3	4
Days with amphotericin B, mean (SD)	2.9 (4.3)	2.6 (9.9)
Azols	2	25
Days with azols, mean (SD)	9.4 (19.5)	13.6 (11.5)
Echinocandins	2	2
Days with echinocandins, mean (SD)	3 (5.5)	0.4 (1.8)
HSCT	2 (28.6)	8 (22.9)
Days from the HSCT, mean (SD)	33 (22.6)	20.1 (9.0)
Proton pump inhibitors (PPI)	4 (57.1)	24 (68.6)
Neutropenia	7 (100)	30 (85.7)
Nadir of neutrophils, mean (DS)	11.4 (3.89)	121 (262.5)
Days with neutropenia, mean (DS)	23 (15.1)	9.9 (6.8)
Days with neutropenia in range		
0–10	3 (42.3)	18 (60.0)
11–20	–	10 (33.3)
>20	4 (57.1)	2 (6.7)
Growth factors	5 (71.4)	21 (60.0)
Mucositis	3 (42.9)	7 (20.0)
Diarrhea	6 (85.7)	17 (48.6)
Transfusion with RC	7 (100)	30 (85.7)
Number of red cell transfusion, mean (SD)	12.4 (9.7)	4.1 (3.3)
Plasma transfusion	4 (57.1)	4 (11.4)
Number of plasma transfusion, mean (SD)	3.1 (3.5)	0.3(1.0)
Platelet transfusion	7 (100)	26 (74.3)
Number of platelet transfusion, mean (SD)	14.4(11.7)	2.8(3.6)

central venous catheter (CVC) inserted at clinical presentation of sepsis, with a mean duration of 64 days, and positive blood cultures. All of them had undergone a course of chemotherapy before the infection occurred (three out of seven with cytarabine), they were neutropenic at the time of fungemia and were also given broad-spectrum antibiotics. On univariate analysis, risk factors strongly correlated to development of fungemia were the duration of neutropenia (p = 0.011; OR = 1.1; 95% CI, 1.0–1.18), the receipt of plasma transfusions (p = 0.022; OR = 13.7; 95% CI, 1.4–128.7), the number of transfusions of blood and platelets (p = 0.029; OR = 1.4; 95% CI, 1.0–1.8), the use of aminoglycosides (p = 0.025; OR = 12.5; 95% CI, 1.4–113.2) and meropenem (p = 0.011; OR = 8.8; 95% CI, 1.7–47.0) (**Table 2**).

Microscopy of positive blood cultures showed yeast-like cells (**Figure 3**), while cultures on Sabouraud agar showed farinose and

TABLE 2 | Conditioned univariate logistic regression analysis for *Saprochaete*-positive blood cultures risk factors.

Variable	OR (95% CI)	*P*-value
Aminoglycosides use	12.5 (1.4–113.2)	0.025
Meropenem use	8.8 (1.7–47.0)	0.011
Duration of neutropenia in days	1.1 (1.0–1.18)	0.011
Plasma transfusion	13.7 (1.4–128.7)	0.022
Number of transfused platelet unity	1.4 (1.0–1.8)	0.029
Duration of aminoglycosides therapy (days)	1.2 (1.0–1.4)	0.040

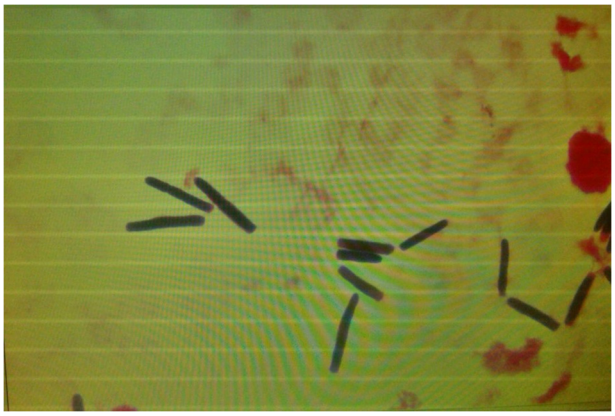

FIGURE 3 | Microscopic morphology of *Saprochaete clavat*a in positive blood cultures showing yeast-like cells.

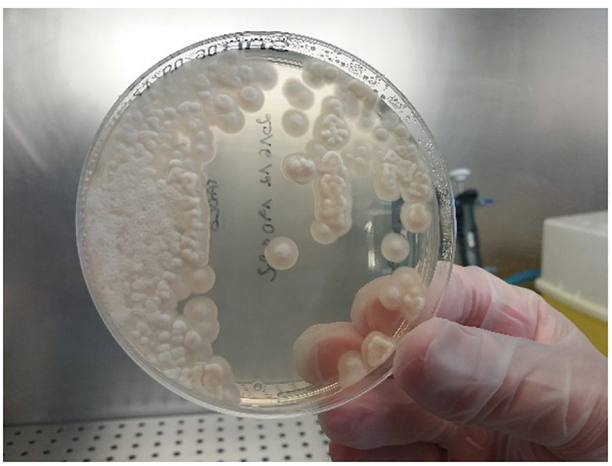

FIGURE 4 | Culture of *Saprochaete clavata* on Sabouraud dextrose agar.

dry yeast colonies (**Figure 4**). All the isolates were from blood and one patient also had an isolate from stool. Two of the seven BSI strains were identified as *G. capitatum* by Vitek-2, while MALDI-TOF MS-Vitek (bioMerieux, Marcy l'Etoile, France) did not give any precise identification. Use of RUO SARAMIS MALDI-TOF database (bioMerieux, Marcy l'Etoile, France) and gene sequencing of the D1D2 and ITS1-5.8S-ITS2 regions identified all the isolates as *S. clavata* subspecies *clavata* with 99% homology.

β-D-glucan test was positive in three out of seven cases (range 159 to >523 pg/mL), while serum GM antigen results (Platelia Aspergillus – Bio-Rad, France) were all negative.

All the seven isolates were resistant to echinocandins and fluconazole (MIC for anidulafungin, micafungin, caspofungin 2, 8, and 8 mg/L, respectively; MIC for fluconazole 16 mg/L). The strains were susceptible to flucytosine (MIC range 0.12–0.25 mg/L), voriconazole (MIC range 0.25–0.5 mg/L), and amphotericin B (MIC range 0.5–1 mg/L). One isolate showed acquired resistance to flucytosine and amphotericin B during treatment.

In the genotyping analysis, both the correlation-based dendrograms obtained by MALDI-TOF MS (Bruker Daltonics) and MS-Vitek not only clustered six of the seven BSI isolates in the same group, but also showed their strong relatedness (**Figure 5**). Bruker software correctly distinguished *M. capitatus* from *S. clavata*, and clustered the first six strains of our outbreak together. The second analysis with SARAMIS-MS Vitek software was carried out after the seventh case occurred. In the last patient (ZY075) *S. clavata* was isolated from blood and from stool and both isolates were analyzed. The SARAMIS analysis clustered these *S. clavata* strains together, except for the TN293 strain which appeared moderately far away from the others, and closest to the VR00018 strain, not involved in the outbreak. SARAMIS analysis well differentiated *S. clavata* from *G. candidum*.

The genotyping analysis was performed on *S. clavata* strains belonging to the Verona outbreak and from another hospital in Milan, during the same year.

After comparing our isolates with those from Milan, the mapping procedure gave 17.5 million mapped fragments on average, with a median coverage of 262×. The details per sample of the sequenced and mapped fragments are reported in **Table 3**.

The variant calling procedure produced a list of 1,529 variant sites that was reduced to 246 by filtering for SNVs. The set of 246 variant sites was then used to infer phylogeny. Phylogenetic analysis using SNPrelate (**Figure 6**) shows that of the 10 samples recorded during the investigation period, those from Milan MI409 MI691 and MI031 belonged to one clade while the samples from Verona (RS235, TP525, AA102, CG108, TN293, RO402, ZY075) accounted for another cluster, with a node supported by a z-score of 4.1 (p-value = 0.000041), with a final difference of 61 mutations between the two clusters. In particular, inside the second cluster, we observed a split between RS235 and the rest of the samples with a node supported by a z-score of 2.3 (p-value = 0.021) and 16 mutations unique to each branch. The phylogenetic analysis using Ape/Phangorn (**Figure 7**) shows the same tree topology as in **Figure 6**.

Such analysis provides a bootstrap value as a measure of statistical confidence: the higher the value, the larger the number of mutations supporting the branch. In this analysis, the same nodes in **Figure 7** are supported with a bootstrap value of 100 indicating full separation between the groups identified in the first analysis. The results for the first two principal components of the data set that explain together ∼80% of variation are shown in **Figure 8**.

The first component clearly divides the three samples MI409, MI691, and MI031 from the others. The sample RS235 is partially separated from the two main groups, consistent with results of our phylogenetic trees. Four contigs out of the 339 present in the genome assembly were identified as hypervariable; however, after alignment with blastn, none of them had significant similarities with sequences present in NCBI. Data set are available on request.

Environmental studies for possible sources of infection included microbiology investigation of different dairy products, and many medical devices and antibiotic formulations. In detail, microbiological investigation was conducted on 10 different yogurt products, 3 replicates of 3 different cheeses likely to have been eaten by patients in hospital meals, as suspected

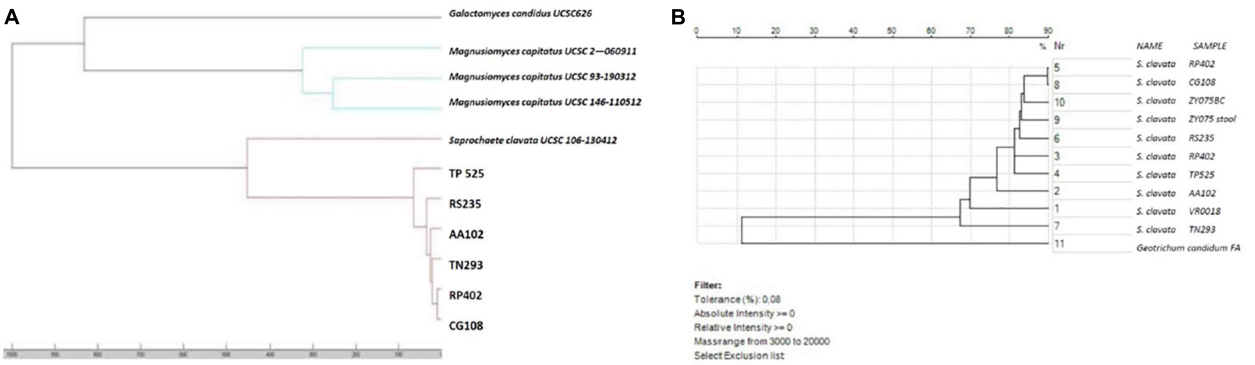

FIGURE 5 | Correlation-based dendrograms obtained by **(A)** MALDI-TOF MS (Bruker Daltonics) and **(B)** MS-Vitek Saramis (bioMerieux, Marcy l'Etoile, France).

during the epidemiological investigation. Additionally, medical devices, such as vascular catheters and platelet infusion kits, were cultured. Also cultured were apheresis platelet concentrates and plasma derivatives. Two different batches of amikacin, gentamicin, and meropenem were cultured after enrichment in BHI. The results of investigations of fungal contamination of food, medical devices, blood derivatives, and antibiotics were always negative.

Clinical Cases

Of the seven cases which occurred in Verona, clinical information are available for only four.

The first case was a 20-year-old Italian girl with a T-ALL diagnosis, admitted to our hematology ward for follow-up chemotherapy. A few days after the first infusion she became febrile with chills and broad spectrum antibiotics were given. Blood cultures turned positive for yeast-like fungi, so Caspofungin was added to therapy (Arendrup et al., 2014). The patient developed progressive arterial hypotension and was admitted to the ICU ward where she died of septic shock. The fungus, which was first isolated from blood cultures, was then identified as *G. clavatum* by means of Vitek-2. Drug susceptibility test showed a high-level resistance to fluconazole and all echinocandins.

TABLE 3 | Details of sequenced fragments for each strain of *Saprochaete* isolated from Verona and Milan.

Sample	Sequenced fragments	Mapped fragments	Average coverage
RS235	16,282,394	14,335,384	216.59
RP402	24,467,857	22,739,883	331.26
AA102	16,692,742	14,796,911	218.73
CG108	13,899,852	12,314,272	187.31
TP525	14,058,887	12,582,330	186.30
TN293	24,179,648	18,491,452	278.89
ZY075	22,790,265	21,525,722	330.71
MI409	19,684,314	18,707,031	287.14
MI691	19,061,001	18,077,681	280.81
MI031	21,889,597	20,360,099	311.55

The second case was a 65–70-year-old Italian patient with a cytotoxic NHL who was hospitalized in October 2016 in the hematology ward for follow-up chemotherapy. Before completing the cycle, he presented a high-grade fever, nausea with vomiting, and diarrhea. As well as antibiotics for CVC bacteremia due to *Pseudomonas aeruginosa*, he was given liposomal amphotericin-B for *G. clavatum* fungemia for a total of 7 days, then switched to voriconazole for a further 10 days on the basis of a drug susceptibility test. On CT scan, no disseminated disease was reported and the patient was finally discharged home.

The third case was a 4-year-old Italian child with AML, which was diagnosed when he was 1 year old. He started chemotherapy soon after diagnosis with good initial response. In October 2016 he was hospitalized because of a high-grade fever, anemia, low platelets, and leukocytosis. On blood examination, a recrudescence of his disease was evident, so new chemotherapy

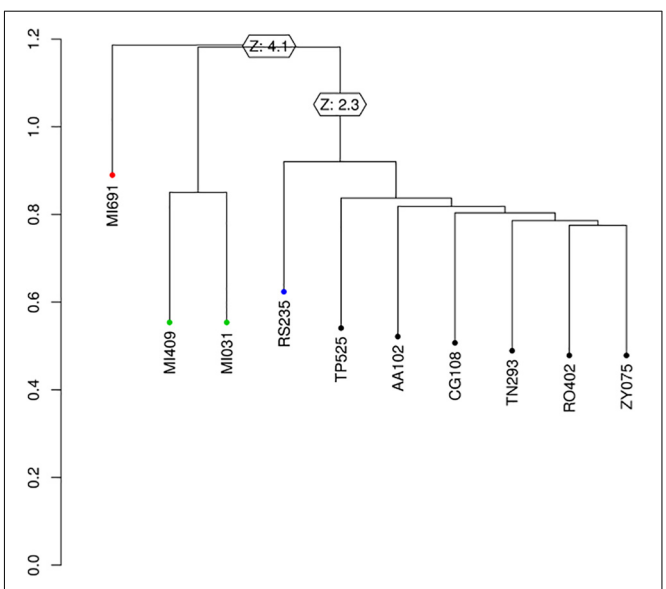

FIGURE 6 | Phylogenetic tree produced by SNprelate, *z*-score at supported nodes.

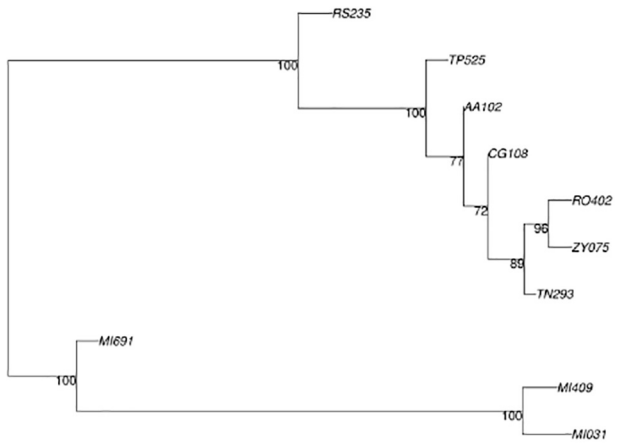

FIGURE 7 | Phylogenetic tree produced by Ape/Phangorn, bootstrap value at nodes.

was infused. After a few doses, he presented with a high-grade fever, cough, and diarrhea. Broad spectrum antibiotics and antifungals were given, after collection of blood cultures (Camus et al., 2014). *G. clavatum* and *St. epidermidis* were isolated, so targeted therapy with vancomycin and desoxycholate amphotericin B was used for up to 15 days. He was then discharged home and is still under hematology follow-up.

The fourth case was a 50–60-year-old Italian patient, admitted in November 2016 to the hematology ward for relapsing AML. During hospitalization, thanks to a good HLA match, he underwent hematopoietic stem cell transplant (HSCT) after induction chemotherapy. Five days after HSCT, he began to complain of fever with chills, vomiting, and diarrhea. Despite being on antifungal prophylaxis with Posaconazole, he developed *S. clavata* fungemia. On PET-CT scan no disseminated disease was reported. He received liposomal amphotericin B for 21 days with no relapse and was discharged home 1 month later.

The three cases in Milan were comparable for age and clinical history. They were Caucasian adult patients, admitted to the hematology ward to start chemotherapy for AML. Because of fever, blood was drawn for cultures. After being misidentified as *S. clavata*, the strains were then recognized as *S. capitata*. AMB-L and 5-FC therapy was started with resolution of symptoms.

DISCUSSION

While the general population is aging and experiencing multiple chronic comorbidities, together with new and increasingly complex therapies which strongly impact immune status, clinical suspicion of infectious diseases caused by rare pathogens must arise. Among these, fungi are playing an important role because they are difficult-to-treat, slow progressing infections with high morbidity and mortality. Unlike *Aspergillus* and *Candida*, little is known about *Saprochaete* spp., formerly known as *Geotrichum*, in immunosuppressed patients in terms of epidemiology, source of outbreaks, risk factors, treatment, and outcomes.

The taxonomic classification of *Geotrichum* is currently changing. It was originally known as *Trichosporon* spp. and classified among the basidiomycetes (Gurgui et al., 2011). Subsequently, due to its cell wall structure, septal pores, and its tendency to produce numerous arthroconidia and few blastoconidia, from a microbiological point of view it was considered to be an ascomycete (Kurtzman and Robnett, 1997). Further reclassification has been made recently, thanks to novel and finer microbiological techniques which rely on proteome and genome sequencing. *Geotrichum* species is now defined as *Saprochaete* even though some experts name it *Magnusiomyces* (Desnos-Ollivier et al., 2014; Vaux et al., 2014). Misidentification is frequent due to their similar phenotypes and limited information collected in the databases. As a consequence, differentiation may be very difficult when based on macroscopic and microscopic analysis. Colonies present white, farinose, dry with frosted glass appearance, and microscopic features consist of true hyphae organized in acute branches often disarticulated into arthroconidia with rectangular or rounded ends (Desnos-Ollivier et al., 2014).

The first case of *Geotrichum* infection was reported in 1965, and to date other cases or small outbreaks have been described, predominantly in Italy and France (Gadea et al., 2004; Girmenia et al., 2005; Del Principe et al., 2016; Esposto et al., 2018; Stanzani et al., 2019). Clinical presentations were sepsis, pulmonary hepatic and splenic lesions, brain abscesses, and were characterized by a high mortality rate, due to peculiar antifungal resistance patterns, difficult identification and, consequently, delay in diagnosis and correct treatment (Gadea et al., 2004; Cuenca-Estrella et al., 2011; Esposto et al., 2018). A 20-year observational multicenter Italian study reported 35 cases of *G. capitatum* infection, with a mortality rate of 57.1% (Girmenia et al., 2005; Esposto et al., 2018). Most of those cases occurred in patients with hematology malignancies, especially during profound neutropenia due to chemotherapy.

The optimal therapy has yet to be established and remains a challenge (White et al., 1990; Kurtzman and Robnett, 1997; Arendrup et al., 2014), because they are rare, subtle, and difficult-to-diagnose infections, with no current available breakpoints from EUCAST nor CLSI and intrinsic resistance to echinocandins and fluconazole.

Here we report a small cluster of seven *S. clavata* infections occurring between September 2016 and July 2017 in the Azienda Ospedaliera Universitaria Integrata di Verona, Italy. All infections developed in adult and pediatric hematology patients. Each case was matched with five controls on the basis of the ward of hospitalization during fungal sepsis. Of note, all clinical cases had experienced severe neutropenia following chemotherapy; had a CVC or other central vascular device; were given broad-spectrum antibiotics and transfusions; and had high-grade fever with chills, diarrhea, and vomiting. Significant associations with transfusions and antibiotics may be explained by the fact that almost all cases were septic and needed stronger supportive therapies than the controls. As seen in other reports, all of our patients who had experienced *S. clavata* fungemia were severely immunocompromised, underscoring that the most important epidemiological risk factor for this kind of infection

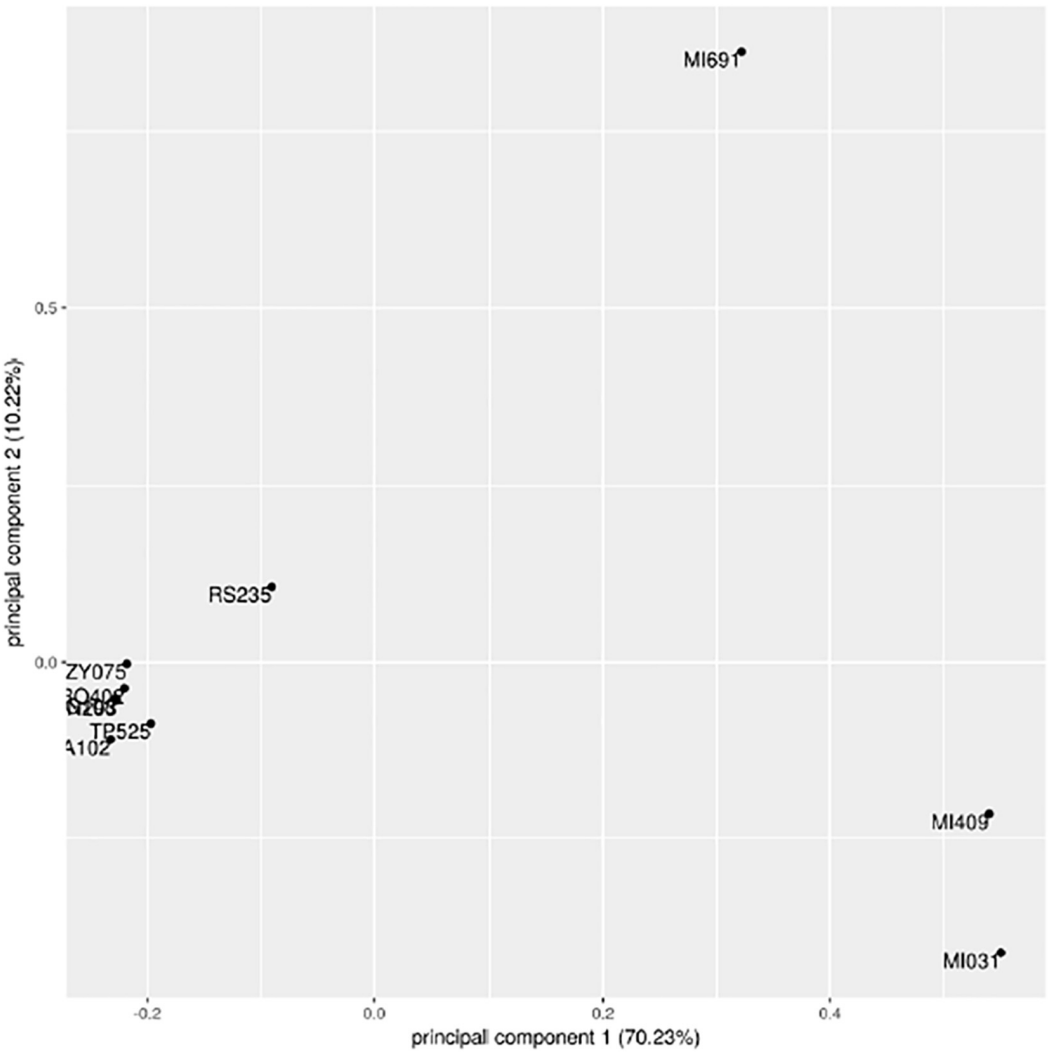

FIGURE 8 | Principal component analysis of 199 informative SNPs.

is immunosuppression and in particular neutropenia. It is noteworthy that, among patients of our hospital whose blood cultures turned positive for *S. clavata*, one tested positive also for stool, strengthening the hypothesis that this fungus can colonize the gut mucosa and migrate into the circulation or vice versa, as *Candida* spp. does. Probably, gut colonization and translocation, caused by chemotherapy-induced intestinal tract damage or mucositis, may have played an important role (Camera et al., 2003; Lee et al., 2014). In addition, we cannot exclude that *Saprochaete* could colonize the skin from the environment and invade the blood system through portals of entry such as catheters or wounds. As a retrospective study, the gut colonization of all the patients was not investigated, except for the last one.

Unlike previous historical outbreaks, mortality was not very high, thanks to rapid molecular identification and start of amphotericin B formulations, which is the recommended therapy for now, given intrinsic resistance to echinocandins and fluconazole.

Saprochaete clavata grew from all blood cultures and identification was made with SARAMIS-MS Vitek (bioMerieux, Marcy l'Etoile, France) and nucleotide sequencing. Actually, whole-genome sequence (WGS) typing is the best available molecular method to evaluate the clonality of a suspected outbreak caused by uncommon fungal species (Alanio et al., 2017; Bougnoux et al., 2018). It is based on the analysis of whole single-nucleotide polymorphisms (SNPs) within each genome, which enables comparison between strains. The number of different SNPs and their distances allow for inference of strains relatedness. Phylogenetic analysis using SNPrelate (**Figure 6**) showed that the seven samples from the Verona outbreak belonged to one clade. We observed a split between RS235 and the rest of the samples caused by 16 mutations, but further and more robust studies are needed to explain their significance. Vaux et al. (2014) described a nationwide outbreak which occurred in the spring of 2012 involving 10 health-care facilities in France, due to one clade of *S. clavata*. Even though they made a nationwide microbiological

and epidemiological investigation, they did not find the source of infection; however, food, especially dairy products, or apheresis platelet concentrates were strongly suspected. In our outbreak we observed seven cases in a very short period of time and we deemed that a common, easily diffusible source of infection could have been present in our hospital. We checked for diverse potential vehicles of infection although microbiology results were always negative. Because, during neutropenia and chemotherapy-induced mucositis the risk of gut translocation is high, we thought that food could have been one of the most likely sources. We then tested and cultured some dairy products (yogurt, creamy cheese), as our French colleagues had done before. Unfortunately, the retrospective nature of food investigation precluded collection of all potential sources of contamination, and microbiology gave negative results. Aside from foods, medical devices, and drugs, we did not perform culture investigation on healthcare providers as potential vectors of infection. As such, we cannot make conclusions on how the epidemic began; microbiology was always negative, so we could neither find a source of infection nor implement a plan to control or avoid it.

This is the largest outbreak by a rare fungus ever observed in our hospital, worthy to be described, and evaluated from a microbiological point of view. One strength of our work is that the clonal relatedness of our isolates relied on a proteomic approach, using two of the most diffuse mass spectrometry machines available in microbiology clinical laboratories, the Bruker and the Biomerieux MS Vitek. The clonality of the strains was evidenced by the clustering during proteomic evaluation. Both Bruker MALDI Biotyper system and bioMerieux MS-VITEK showed high similarity of the isolates. Interestingly, both systems highlighted that one different isolate did not strictly correlate with the other six. Few other reports have tried to discuss the usefulness of proteomic fungal typing by means of MALDI-TOF, which was able to describe and confirm strains' relatedness in an outbreak (Stanzani et al., 2019).

To date many papers have shown the ability of MALDI-TOF in accurately distinguishing different clusters of *Candida* strains, geographically grouped as in the case of *Candida auris* (Pracash et al., 2016) or in the case of multidrug resistant *Candida glabrata* (Dhieb et al., 2015) and *Candida parapsilosis* complex (De Carolis et al., 2014). MALDI-TOF mass spectra for genotyping would represent a rapid, first-level, easy, and cost-effective way to support clinicians, during uncommon fungal outbreaks, in treatment decision-making and in a clinical microbiology lab, although only WGS can confirm it. Of course, further studies are needed to strengthen the accuracy and efficacy of MALDI-TOF as a fungal typing tool even in rare infections. Although rare, *S. clavata* should be considered as a potential cause of IFI, particularly in cases of severe neutropenia. Last, but not least, its intrinsic resistance to echinocandins and fluconazole must be considered when selecting an empirical antifungal therapy as this infection may be rapidly lethal. National surveillance is desirable to successfully investigate multicenter outbreaks of infection due to rare pathogens.

DATA AVAILABILITY STATEMENT

The raw data supporting the conclusions of this article will be made available by the authors, without undue reservation, to any qualified researcher.

ETHICS STATEMENT

The studies involving human participants were reviewed and approved by the Institutional Review Board of Azienda Ospedaliera Universitaria Integrata di Verona. The requirement for written informed consent was waived due to the observational, retrospective nature of this study. The patients/participants provided their written informed consent to participate in this study.

AUTHOR CONTRIBUTIONS

GL, MS, ET, and GC contributed to the conception and design of the study. ED, LM, and AS performed the MALDI-TOF analysis. GN, SC, MS, AG, VN, and AA performed the microbiological and clinical analysis. LN performed the molecular analysis. MV and FS performed the case-control study.

ACKNOWLEDGMENTS

We thank Mr. Rodney Seddon for reviewing the American English style of the manuscript and Mrs. Cristina Caldana and Mrs. Maria Luisa Castellini for the epidemic investigation.

REFERENCES

Alanio, A., Desnos-Ollivier, M., Garcia-Hermoso, D., and Bretagne, S. (2017). Investigating clinical issues by genotyping of medically important Fungi: why and how? *Clin. Microbiol. Rev.* 30, 671–707. doi: 10.1128/CMR.00043-16

Altschul, S. F., Madden, T. L., Schäffer, A. A., Zhang, J., Zhang, Z., Miller, W., et al. (1997). Gapped BLAST and PSI-BLAST: a new generation of protein database search programs. *Nucleic Acids Res.* 25, 3389–3402. doi: 10.1093/nar/25.17.3389

Arendrup, M. C., Boekhout, T., Akova, M., Meis, J. F., Cornely, O. A., Lortholary, O., et al. (2014). ESCMID and ECMM joint clinical guidelines for the diagnosis and management of rare invasive yeast infections. *Clin. Microbiol. Infect.* 20(Suppl. 3), 76–98. doi: 10.1111/1469-0691.12360

Bader, O., Weig, M., Taverne-Ghadwal, L., Lugert, R., Gross, U., and Kuhns, M. (2011). Improved clinical laboratory identification of human pathogenic yeasts by matrix-assisted laser desorption ionization time-of-flight mass spectrometry. *Clin. Microbiol. Infect.* 17, 1359–1365. doi: 10.1111/j.1469-0691.2010.03398.x

Bougnoux, M., Brun, S., and Zahar, J. (2018). Healthcare-associated fungal outbreaks: new and uncommon species, New molecular tools for investigation and prevention. *Antimicrob. Resist. Infect. Control* 7:45. doi: 10.1186/s13756-018-0338-9

Budhavari, S. (2009). What's new in diagnostics? Fungitell: 1-3 beta-D glucan assay. *South. Afr. J. Epidemiol. Infect.* 24, 37–38. doi: 10.1080/10158782.2009.11441337

Camera, A., Andretta, C., Villa, M. R., Volpicelli, M., Picardi, M., Rossi, M., et al. (2003). Intestinal toxicity during induction chemotherapy with cytarabine-based regimens in adult acute myeloid leukemia. *Hematol. J.* 4, 346–350. doi: 10.1038/sj.thj.6200304

Camus, V., Thibault, M. L., David, M., Gargala, G., Compagnon, P., Lamoureux, F., et al. (2014). Invasive *Geotrichum clavatum* fungal infection in an acute myeloid leukaemia: a case report and review. *Mycopathologia* 177, 319–324. doi: 10.1007/s11046-014-9746-4

Cuenca-Estrella, M., Bassetti, M., Lass-Flörl, C., Rácil, Z., Richardson, M., and Rogers, T. R. (2011). Detection and investigation of invasive mould disease. *J. Antimicrob. Chemother.* 66, i15–i24. doi: 10.1093/jac/dkq438

De Carolis, E., Hensgens, L. A., Vella, A., Posteraro, B., Sanguinetti, M., Senesi, S., et al. (2014). Identification and typing of the *Candida parapsilosis* complex: MALDI-TOF MS vs. AFLP. *Med. Mycol.* 52, 123–130. doi: 10.1093/mmy/myt009

de Hoog, G. S., and Smith, M. T. (2004). Ribosomal gene phylogeny and species delimitation in *Geotrichum* and its teleomorphs. *Stud. Mycol.* 50, 489–516.

Del Principe, M. I., Sarmati, L., Cefalo, M., Fontana, C., De Santis, G., Buccisano, F., et al. (2016). A cluster of *Geotrichum clavatum* (Saprochaete clavata) infection in haematological patients: a first Italian report and review of the literature. *Mycoses* 59, 594–601. doi: 10.1111/myc.12508

Desnos-Ollivier, M., Blanc, C., Garcia-Hermoso, D., Hoinard, D., Alanio, A., and Dromer, F. (2014). Misidentification of *Saprochaete clavata* as *Magnusiomyces capitatus* in clinical isolates: utility of internal transcribed spacer sequencing and matrix-assisted laser desorption ionization-time of flight mass spectrometry and importance of reliable databases. *J. Clin. Microbiol.* 52, 2196–2198. doi: 10.1128/JCM.00039-14

Dhieb, C., Normand, A. C., Al-Yasiri, M., Chaker, E., El Euch, D., Vranckx, K., et al. (2015). MALDI-TOF typing highlights geographical and fluconazole resistance clusters in *Candida glabrata*. *Med. Mycol.* 53, 462–469. doi: 10.1093/mmy/myv013

Esposto, M. C., Prigitano, A., Lo Cascio, G., Ossi, C., Grancini, A., Cavanna, C., et al. (2018). Yeast-like filamentous fungi: molecular identification and *in vitro* susceptibility study. *Med. Mycol.* 0, 1–5. doi: 10.1093/mmy/myy133

Favre, S., Rougeron, A., Levoir, L., Pérard, B., Milpied, N., Accoceberry, I., et al. (2016). Saprochaete clavata invasive infection in a patient with severe aplastic anemia: efficacy of voriconazole and liposomal amphotericin B with adjuvant granulocyte transfusions before neutrophil recovery following allogenic bone marrow transplantation. *Med. Micol. Case Rep.* 11, 21–23. doi: 10.1016/j.mmcr.2016.03.001

Gadea, I., Cuenca-Estrella, M., Prieto, E., Diaz-Guerra, T. M., Garcia-Cia, J. I., Mellado, E., et al. (2004). Genotyping and antifungal susceptibility profile of *Dipodascus capitatus* isolates causing disseminated infection in seven hematological patients of a tertiary hospital. *J. Clin. Microbiol.* 42, 1832–1836. doi: 10.1128/jcm.42.4.1832-1836.2004

Garcia-Ruiz, J. C., Lopes-Soria, L., Olazabal, I., Amutio, E., Arrieta-Aguirre, I., Velasco-Benito, V., et al. (2013). Invasive infections caused by *Saprochaete capitata* in patients with haematological malignancies: report of five cases and review of the antifungal therapy. *Rev. Iberoam. Micol.* 30, 248–255. doi: 10.1016/j.riam.2013.02.004

Girmenia, C., Pagano, L., Martino, B., D'Antonio, D., Fanci, R., Specchia, G., et al. (2005). Invasive infections caused by trichosporon species and *Geotrichum capitatum* in patients with hematological malignancies: a retrospective multicenter study from Italy and review of the literature. *J. Clin. Microbiol.* 43, 1818–1828. doi: 10.1128/jcm.43.4.1818-1828.2005

Gurgui, M., Sanchez, F., March, F., Lopez-Contreras, J., Martino, R., Cotura, A., et al. (2011). Nosocomial outbreak of *Blastoschizomyces capitatus* associated with contaminated milk in haematological unit. *J. Hosp. Infect.* 78, 274–278. doi: 10.1016/j.jhin.2011.01.027

Kurtzman, C. P., and Robnett, C. J. (1997). Identification of clinically important ascomycetous yeasts based on nucleotide divergence in the 5_ end of the large-subunit (26S) ribosomal DNA gene. *J. Clin. Microbiol.* 35, 1216–1223. doi: 10.1128/jcm.35.5.1216-1223.1997

Lee, S. C., Billmyre, R. B., Li, A., Carson, S., Sykes, S. M., Huh, E. Y., et al. (2014). Analysis of a food-borne fungal pathogen outbreak: virulence and genome of a *Mucor circinelloides* isolate from yogurt. *mBio* 5:e1390-14. doi: 10.1128/mBio.01390-14

Litvintseva, A. P., Hurst, S., Gade, L., Frace, M. A., Hilsbeck, R., Schupp, J. M., et al. (2014). Whole-genome analysis of *Exserohilum rostratum* from an outbreak of fungal meningitis and other infections. *J. Clin. Microbiol.* 52, 3216–3222. doi: 10.1128/jcm.00936-14

Miceli, M. H., Dìaz, J. A., and Lee, S. A. (2011). Emerging opportunistic yeast infections. *Lancet Infect. Dis.* 11, 142–151. doi: 10.1128/JCM.43.4.1818-1828

Nilsson, R. H., Ryberg, M., Kristiansson, E., Abarenkiv, K., Larsson, K. H., and Köljalg, U. (2006). Taxonomic reliability of DNA sequences in public sequence databases: a fungal perspective. *PLoS One* 1:e59. doi: 10.1371/journal.pone.0000059

Picard, M., Cassaing, S., and Letocart, P. (2014). Concomitant cases of disseminated *Geotrichum clavatum* infections in patients with acute myeloid leukemia. *Leuk. Lymphoma* 55, 1186–1188. doi: 10.3109/10428194.2013.820290

Pracash, A., Sharma, C., Singh, A., Kumar Sing, P., Kumar, A., Hagen, F., et al. (2016). Evidence of genotypic diversity among *Candida auris* isolates by multilocus sequence typing, matrix-assisted laser desorption ionization time-of-flight mass spectrometry and amplified fragment length polymorphism. *Clin. Microbiol. Infect.* 22, 277.e1–277.e9. doi: 10.1016/j.cmi.2015.10.022

Stanzani, M., Cricca, M., Sassi, C., Sutto, E., De Cicco, G., Bonifazi, F., et al. (2019). *Saprochaete clavata* infections in patients undergoing treatment for hematological malignancies: a report of a monocentric outbreak and review of the literature. *Mycoses* 62, 1100–1107. doi: 10.1111/myc.12978

Vaux, S., Criscuolo, A., Desnos-Ollivier, M., Diancourt, L., Tarnaud, C., Vandenbogaert, M., et al. (2014). Multicenter outbreak of infections by *Saprochaete clavata*, an unrecognized opportunistic fungal pathogen. *mBio* 5, e2309–e2314. doi: 10.1128/mBio.02309-14

White, T. J., Bruns, T., Lee, S., and Taylor, J. (1990). "Amplification and direct sequencing of fungal ribosomal RNA genes for phylogenetics," in *PCR Protocols-A Guide to Methods and Applications*, eds M. A. Innis, D. H. Gelfand, J. J. Sninsky, and T. J. White (San Diego: Academic Press), 315–322. doi: 10.1016/b978-0-12-372180-8.50042-1

Conflict of Interest: The authors declare that the research was conducted in the absence of any commercial or financial relationships that could be construed as a potential conflict of interest.

frontiers in Cellular and Infection Microbiology

BRIEF RESEARCH REPORT
published: 18 February 2020
doi: 10.3389/fcimb.2020.00013

Rapid Detection of *Nocardia* by Next-Generation Sequencing

*Shan-Shan Weng†, Han-Yue Zhang†, Jing-Wen Ai†, Yan Gao, Yuan-Yuan Liu, Bin Xu and Wen-Hong Zhang**

Department of Infectious Diseases, Huashan Hospital of Fudan University, Shanghai, China

In this original study, we retrospectively reviewed the cases of nocardiosis diagnosed through culture and next-generation sequencing (NGS) methods between 2014 and 2018 in Huashan Hospital and found out that the latter way can not only improve the detection rate of *Nocardia* spp. but also greatly reduce the turnaround time. In addition, by comparing nocardiosis and non-nocardiosis patients both of whose samples had *Nocardia* spp. detected by NGS, we found that *Nocardia*'s specific reads ranking among top two might be a satisfactory cutoff value for clinical diagnosis of the disease. Our study introduced the promising value of the NGS method in the rapid diagnosis of nocardiosis.

Keywords: nocardiosis, next-generation sequencing, culture, diagnose, rapid detection

OPEN ACCESS

Edited by:
David Ong,
Sint Franciscus Gasthuis, Netherlands

Reviewed by:
Dalia Denapaite,
University of Trento, Italy
Daniel Angel Ortiz,
Beaumont Health, United States

****Correspondence:***
Wen-Hong Zhang
wenhongzhang_hs@126.com

†These authors have contributed equally to this work and share first authorship

Specialty section:
This article was submitted to Clinical Microbiology, a section of the journal Frontiers in Cellular and Infection Microbiology

Received: *04 October 2019*
Accepted: *13 January 2020*
Published: *18 February 2020*

Citation:
Weng S-S, Zhang H-Y, Ai J-W, Gao Y, Liu Y-Y, Xu B and Zhang W-H (2020) Rapid Detection of Nocardia by Next-Generation Sequencing. Front. Cell. Infect. Microbiol. 10:13. doi: 10.3389/fcimb.2020.00013

INTRODUCTION

Nocardiosis, caused by gram-positive aerobic actinomycetes in the genus *Nocardia*, is typically regarded as an opportunistic infection (Sorrell et al., 2010). *Nocardia* species are found worldwide in environments, and at least 33 of the total 80 more species have the ability to cause localized or systemic suppurative disease in human beings (Brown-Elliott et al., 2006). However, management of this rare infection is challenging, with mortality rates ranging from 20 o 30% in patients with disseminated infection, and up to 50% if there is central nervous system (CNS) involvement (Rouzaud et al., 2018).

Up to now, a definitive diagnosis of nocardiosis still relies on the isolation and identification of the organism from an infected site, which can take days to weeks. Molecular techniques such as 16S rRNA–based polymerase chain reaction (PCR) have also been used for rapid detection of *Nocardia* with high specificity and sensitivity (Couble et al., 2005), but such a technique requires the pre-considerations of nocardiosis by clinicians.

A previous study has reported that the next-generation sequencing (NGS) method could assist clinical decision making with minimized turnaround time as well as satisfying diagnostic performance, and also has the ability to identify nocardiosis in addition to traditional culture (Miao et al., 2018). Since January 2017, Huashan Hospital has gradually introduced NGS into the clinical approach to suspected infectious diseases with the aim of further increasing the chance of detecting pathogenic microorganisms. Here we retrospectively studied reported cases of nocardiosis identified through either NGS or conventional methods.

METHODS

Study Design

We conducted a retrospective review of patients diagnosed with nocardiosis in Huashan Hospital (a tertiary hospital in Shanghai, China) from September 1st, 2014, to September 1st, 2018. During the time period, a total of 30 patients were diagnosed. Four outpatients and one patient referred

TABLE 1 | Main characteristics of the nocardiosis population.

Characteristics	Total (21)
Age at diagnosis	49.5 ± 16.2
Male sex	10 (47.6%)
Immunocompromised state	14 (66.7%)
Suspicion for nocardiosis	4 (19.0%)
Antibiotic treatment before sampling	19 (90.5%)
SXT prophylaxis	1 (4.8%)
Culture positive	16 (76.2%)
Site of infection	
Systemic	9 (42.9%)
Pulmonary	7 (33.3%)
Central nervous system	4 (19.0%)
Cutaneous	1 (4.8%)

from another hospital were excluded because of deficient evidence for definite diagnosis. Four other patients were diagnosed with pulmonary nocardiosis based on histopathology or 16S rRNA–based PCR results and were therefore excluded in our study. Ultimately, 21 cases of nocardiosis were enrolled in this retrospective study. The samples collected from these patients were separated into the following groups:

1. NGS-positive group (NG): *Nocardia* spp. detected in clinical samples by NGS between January 2017 and August 2018, with clinical and/or radiological signs indicating a diagnosis of nocardiosis regardless of the culture results of the same sample site.
2. Culture-positive group (CG): Samples reported culture positive for *Nocardia* spp. between 2014 and 2018, regardless of the synchronous NGS results.

The demographic data and clinical data of the patients were recorded (**Table 1**, **Table S1**). The NGS data including the specific species of *Nocardia*, number of detected reads, proportion, and ranking of the species were also recorded (**Table S4**). The turnaround time of each sample in the NG group (**Table S6**) and CG group (**Table S7**) were noted separately.

Besides, to evaluate the possibility of false positive detection of *Nocardia* by NGS, we further reviewed samples that underwent NGS testing during the same time period and defined those with *Nocardia* spp. that were detected but contradicted with the patient's final diagnosis as being in the non-nocardiosis group (NN). The NGS data as well as the clinical data of the NN group were also recorded (**Table S5**).

Next-Generation Sequencing

Sample Processing and Library Construction

A 300 μl sample of cerebrospinal fluid (CSF), bronchoalveolar lavage fluid (BALF), tissue, sputum, etc. were collected in DNase/RNase tubes for the identification of potential pathogens. A common issue in metagenomic sequencing is the introduction of contaminating microbial nucleic acid during sample preparation. The potential contaminating source includes PCR reagents, nucleic acid extraction kits, human skin, as well as environment. In order to control the effect of contamination, a negative control was prepared in parallel and sequenced in the same run. Before nucleic acid extraction, the sputum was liquefied.

DNA and total RNA were extracted with a TIANamp Micro DNA Kit (DP316, TIANGEN BIOTECH, Beijing, China) and a QIAamp Viral RNA Mini Kit (52906, Qiagen, China) following the manufacturers' respective operational manuals. The RNA was reverse-transcribed and synthesized to double-stranded complementary DNA (ds cDNA) with a SuperScript II Reverse Transcription Kit (18064-014, Invitrogen, China). The DNA/cDNA from other samples was fragmented using a Bioruptor Pico instrument to generate 200–300 bp fragments (Bioruptor Pico protocols). Then, the libraries were constructed as follows: first, the DNA fragments were subjected to end-repair and added A-tailing in one tube; subsequently, the resulting DNA was ligated with bubble-adapters which contained a barcode sequence and then amplified by PCR method. Quality control was carried out using a bioanalyzer (Agilent 2100, Agilent Technologies, Santa Clara, CA, USA) to assess the DNA concentration and fragment size. Qualified libraries were pooled together to make a single-strand DNA circle (ssDNA circle) and then generate DNA nanoballs (DNBs) by rolling circle replication (RCA). The final DNBs were loaded into a sequence chip and sequenced on a BGISEQ platform using 50/100 bp single-end sequencing.

Bioinformatics Analysis

All raw reads were quality-filtered using a made-in-house program, including filtering adapter contamination and low-quality and low-complexity reads. Next, the clean reads after quality filtering were mapped to a human reference database including hg38 and Yanhuang genome sequence using Burrows–Wheeler Alignment (Version: 0.7.10). The remaining reads were aligned to the non-redundant bacterial, virus, fungal, and parasite databases using Burrows–Wheeler Alignment (Version: 0.7.10). The mapped data were processed for advanced data analysis.

We downloaded all the reference genomes from public databases, such as NCBI (https://www.ncbi.nlm.nih.gov/genome). Currently, our databases contain 4,152 whole genome sequences of viral taxa, 3,446 bacterial genomes or scaffolds, 206 fungi related to human infection, and 140 parasites associated with human diseases. The depth and coverage of each species were calculated with the SoapCoverage software from the SOAP website (https://github.com/sunhappy2019/soap.coverage).

The parameter values were normalized according the data size, which is 8 million reads for sputum and BALF and 20 million reads for other samples. The detected species that existed in the suspected background database or/and was also detected in the negative control sample was filtered, if reaching the threshold.

RESULTS

Ultimately, 21 cases of nocardiosis were enrolled in this retrospective study (**Table 1**). Of the 21 patients, 9 (42.9%) had disseminated infection, 7 (33.3%) had pulmonary infection, 4 (19.0%) had CNS infection, and 1 (4.8%) had cutaneous infection. Fourteen (66.7%) were immunocompromised (undergoing

glucocorticoid therapy or were organ transplant recipients) or had other underlying diseases such as tuberculosis.

Among 21 patients, 25 samples were collected (multiple specimens were collected from 3 patients). Fourteen NGS-positive samples were classified into the NG group, and 11 culture-positive-only samples and 5 culture- and NGS-positive samples were classified into the CG group (**Table 2**). Besides, 55 samples were included in the NN group (**Table S5**). The NG group consisted of five CSF, four BALF, two sputum, two lung tissue, and one cutaneous pus, while the CG group consisted of three blood, three CSF, three BALF, three cutaneous pus, two sputum, one urine, and one pleural effusion (**Figure 1**, **Table S3**).

All 14 samples in the NG group underwent culture simultaneously, and five reported positive results. Two of the samples had positive results on the first culture. Two other samples had positive results on the second culture. Another one had undergone a total of 10 cultures before finally obtaining a positive-culture result for *Nocardia* spp. (**Table S6**). The NGS data showed that all 14 samples' *Nocardia* spp. specific reads had ranked in the top two among all microbes, and 13 (92.9%) of the samples ranked at the top. In the NN group, however, the *Nocardia* spp. specific read ranking of the 55 samples ranged from 15 to 341, with an average of 163 (**Figure 1**, **Table S5**).

TABLE 2 | Group of 25 samples from 21 nocardiosis patients according to NGS and culture results.

	NGS not performed	NGS performed		Total
		NGS positive	NGS negative	
Culture positive	11	5	0	16 (CG)
Culture negative	Unknown	9	Unknown	/
Total	/	14 (NG)	/	/

NGS, next-generation sequencing; CG, culture-positive group; NG, NGS-positive group.

In addition, the proportions of *Nocardia* specific reads in all identified microbe sequences ranged from 18.2 to 90.2% in the NG group compared to an average of 0.06% in the NN group. Classified by specimen types, the average proportion of *Nocardia* specific reads in BALF (83.3%) and lung tissue (69.4%) was higher than that of sputum (54.4%) and CSF samples (52.7%). Six different species of *Nocardia* were identified through NGS—*Nocardia terpenica*, *Nocardia otitidiscaviarum*, *Nocardia farcinica*, *Nocardia cyriacigeorgica*, *Nocardia brasiliensis*, and *Nocardia africana* (**Table S4**). Strains identified through the culture method, however, were not classified into specific species.

As for the CG group, the turnaround time of culture ranged from 2 to 32 days with an average time of 7.5 ± 1.92 days, which is significantly higher than the 48 h per sample of the NG group ($P = 0.0054$) (**Figure 2**).

DISCUSSION

Up to now, culture is still the most commonly used diagnostic method for nocardiosis in clinical practice. According to a previous report, it usually takes about 2 to 7 days for the cultures of *Nocardia* to be positive, sometimes prolonged to at least 2 weeks for slow-growing species (Patricia et al., 2012). Thus, in clinical settings, delay in establishing the diagnosis is common due to the non-specific and diverse clinical presentation of the disease and the time consumption in cultivating *Nocardia*. In fact, the recorded mean time from the development of symptoms to diagnosis has, in different studies, ranged from 42 days to 12 months (Georghiou and Blacklock, 1992; Martínez Tomás et al., 2007), which may lead to poor clinical outcomes in some patient groups (Simpson et al., 1981; Uttamchandani et al., 1994).

Due to the continuous development of sequencing technology, we have been able to conduct rapid detection of clinical specimens for patients and thus diagnosed some of the patients with nocardiosis, most of which were unexpected.

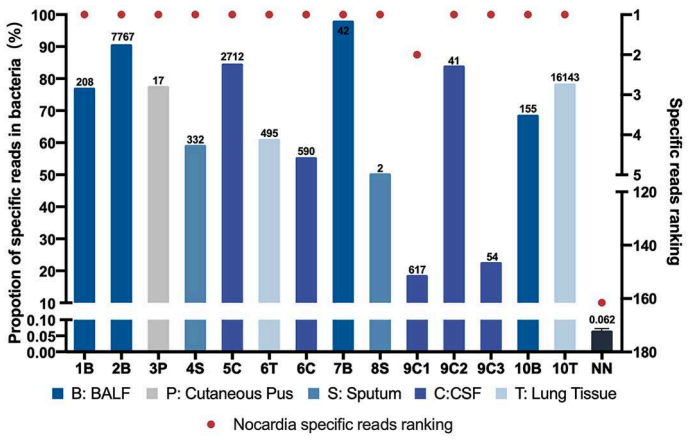

FIGURE 1 | *Nocardia* specific reads and their ranking in next-generation sequencing (NGS)–positive (NG) and non-nocardiosis (NN) group patients. Data of 14 samples from 10 patients in the NG group are presented respectively. The data of the NN group are presented as medians. Each red point indicates the ranking of the *Nocardia* spp. detected, each length of the bar indicates the proportion rate, and the numbers on the bars indicate the specific reads. Different colors represent different sample types. B, BALF; P, cutaneous pus; S, sputum; C, CSF.

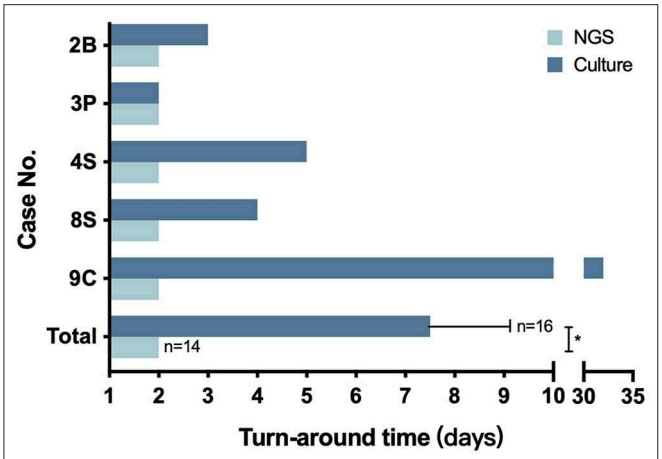

FIGURE 2 | The turnaround time of NGS and culture. The number in the Y axis represents the patient number in the NG group. The bottom pair is presented as means with standard deviation. *$P = 0.0054$.

Therefore, we retrospectively analyzed these cases of nocardiosis and tried to analyze the application value of the NGS testing method in diagnosing this easily missed disease.

In our study, 14 samples underwent both culture and NGS testing. All 14 samples were reported to be NGS-positive for *Nocardia* spp., while only 5 obtained culture-positive results. Nine samples failed the cultivation, and repeated cultures during hospitalization did not yield positive results either (**Table S6**). As previously reported, the difficulty of cultivating may be due to the strict requirements of some *Nocardia* spp. on the culture conditions and its slow growth ability. On the other hand, most patients in our study had been treated with antibiotics before sampling (**Table 1**, **Table S2**), which might also reduce the detection rate. This result suggested that compared with conventional methods, NGS was more efficient and sensitive in detecting *Nocardia* spp. Besides, the turnaround time had also been significantly reduced to 2 days by NGS, compared with an average of 7.5 days by culture (**Figure 2**). Although the sensitivity and specificity of NGS need to be further tested by well-designed studies with larger sample sizes, we believe that this method could be a promising tool in clinical practice.

As for the antibiotic susceptibility, only 3 of the 16 CG samples had related records, while the rest had nothing recorded, which may be due to incomplete records. These three strains were collected from patients 8, 18, and 19, respectively, and the drug susceptibility results were, in order, sensitive to all commonly used drugs, sensitive to sulfamethoxazole (STX) and linezolid, and sensitive to linezolid and levofloxacin while resistant to STX. The treatment of these three patients was based on the results of drug susceptibility (**Table S2**). For patients diagnosed with NGS alone, there were no strains for the antibiotic susceptibility test, and thus, medications could not be chosen accordingly. However, since *Nocardia* could be identified to species through NGS, this information may lead to an accurate antibiotic treatment based on the reported common susceptibility patterns of each individual species (Brown-Elliott et al., 2006).

In the meanwhile, through further analysis of the cases in the NG group, we found that NGS testing might compensate for the low detection ability of conventional culture methods in certain sample types. In our study, NGS was conducted in samples of different kinds such as CSF, BALF, sputum, cutaneous pus, and lung tissue. The only cutaneous pus sample and two sputum samples were reported to be both culture- and NGS-positive. Of the four BALF samples, one was reported to be culture positive. For the two lung tissue samples, NGS detected numerous reads and a high proportion of *Nocardia* spp., while repeated cultures reported negative results. Similarly, for five CSF samples, only one was reported positive after 32 days of culture, while the other four failed to get culture-positive results. This result suggested that NGS might have good detection potential for *Nocardia* in lung tissue and CSF samples.

By comparing the NGS data of the NN group and the NG group, we further explored the possible cutoff values of nocardiosis. With the specific reads ranging from 2 to 16,143, all detected *Nocardia* species ranked among the top two in the overall specific read ranking of each sample in the NG group. However, in the NN group, the specific reads ranged from 0 to 8 with the rankings from 15 to 341. In the NG group, the proportions of *Nocardia* specific reads in all detected microbial sequences ranged from 18.2 to 90.2% among different types of samples, compared with an average of 0.062% in the NN group. Therefore, our study suggested that *Nocardia*'s specific reads ranking among the top two might be a satisfactory cutoff value for clinical diagnosis of the disease. Due to the limitations of this study, we may regard the value not as an absolute diagnostic threshold but as a reference for clinical diagnosis.

In conclusion, our study originally illustrated the application of NGS in diagnosing nocardiosis and found that it had a satisfactory diagnostic value compared to conventional methods. NGS could not only identify different *Nocardia* species but also greatly reduce the detection turnaround time and thus contribute to a timely clinical diagnosis and treatment. Besides, by comparing nocardiosis and non-nocardiosis patients both of whose samples had *Nocardia* spp. detected by NGS, we suggested that *Nocardia*'s specific reads ranking among the top two might be a satisfactory cutoff value for clinical diagnosis of the disease. However, with the limit of sample size, further investigations and evaluation are necessary. Up to now, the high cost and low accessibility of NGS still limit its utility in general practice. We hope that in the near future, this technology will serve the clinic more appropriately and benefit more patients.

DATA AVAILABILITY STATEMENT

The datasets generated for this article can be found in European Nucleotide Archive (ENA) using the accession number PRJEB34974 (https://www.ebi.ac.uk/ena/browser/view/PRJEB34974).

ETHICS STATEMENT

The studies involving human participants were reviewed and approved by the ethics committee of Huashan Hospital

(Shanghai, China). The patients/participants provided their written informed consent to participate in this study.

AUTHOR CONTRIBUTIONS

S-SW designed the study, collected and analyzed the data, wrote, and edited the manuscript. H-YZ collected and analyzed the data and wrote the manuscript. J-WA designed the study, collected the data, and edited the manuscript. YG, BX, and Y-YL collected the samples and diagnosed and treated all the patients. W-HZ designed the study and was in charge of the overall cohort management.

FUNDING

This work was supported by the New and Advanced Technology Project of Shanghai Municipal Hospital: Application of next generation sequencing technique in precise diagnosis of infectious diseases under Grant SHDC12017104 and the Key Technologies Research and Development Program for Infectious Diseases of China under Grant 2018ZX10305-409-001-003.

ACKNOWLEDGMENTS

We acknowledge the professionalism and compassion demonstrated by all the healthcare workers involved in the care of patients.

SUPPLEMENTARY MATERIAL

The Supplementary Material for this article can be found online at: https://www.frontiersin.org/articles/10.3389/fcimb.2020.00013/full#supplementary-material

REFERENCES

Brown-Elliott, B. A., Brown, J. M., Conville, P. S., and Wallace, R. J. Jr. (2006). Clinical and laboratory features of the *Nocardia* spp. based on current molecular taxonomy. *Clin. Microbiol. Rev.* 19, 259–282. doi: 10.1128/CMR.19.2.259-282.2006

Couble, A., Rodriguez-Nava, V., De Montclos, M. P., Boiron, P., and Laurent, F. (2005). Direct detection of *Nocardia* spp. in clinical samples by a rapid molecular method. *J. Clin. Microbiol.* 43, 1921–1924. doi: 10.1128/JCM.43.4.1921-1924.2005

Georghiou, P. R., and Blacklock, Z. M. (1992). Infection with Nocardia species in Queensland. A review of 102 clinical isolates. *Med. J. Aust.* 156, 692–697.

Martínez Tomás, R., Menéndez Villanueva, R., Reyes Calzada, S., et al. (2007). Pulmonary nocardiosis: risk factors and outcomes. *Respirology* 12, 394–400. doi: 10.1111/j.1440-1843.2007.01078.x

Miao, Q., Ma, Y., Wang, Q., Pan, J., Zhang, Y., Jin, W., et al. (2018). Microbiological diagnostic performance of metagenomic next-generation sequencing when applied to clinical practice. *Clin. Infect. Dis.* 67(Suppl_2), S231–S240. doi: 10.1093/cid/ciy693

Patricia, S., Conville, P. S., and Witebsky, F. G. (2012). "Nocardia, Rhodococcus, Gordonia, Actinomadura, Streptomyces, and other aerobic actinomycetes," in *Manual of Clinical Microbiology, 10th Edn*, Vol. 1, eds J. Versalovic, K. C. Carroll, G. Funke, J. H. Jorgensen, M. L. Landry, and D. W. Warnock (Washington, DC: ASM Press), 443e71.

Rouzaud, C., Véronica, R. N., and Catherinot, E. (2018). Clinical assessment of a *Nocardia* spp. polymerase chain reaction (PCR)-based assay for the diagnosis of nocardiosis. *J. Clin. Microbiol.* 56:e00002-18. doi: 10.1128/JCM.00002-18

Simpson, G. L., Stinson, E. B., Egger, M. J., and Remington, J. S. (1981). Nocardial infections in the immunocompromised host: A detailed study in a defined population. *Rev. Infect. Dis.* 3, 492–507.

Sorrell, T. C., Mitchell, D. H., Iredell, J. R., and Chen, S. C.-A. (2010). "Nocardia Species," in *Principles and Practice of Infectious Diseases, 7*, eds G. L. Mandell, J. E. Bennett, and R. Dolin (Philadelphia, PA: Churchill Livingstone Elsevier), 3199.

Uttamchandani, R. B., Daikos, G. L., Reyes, R. R., Fischl, M. A., Dickinson, G. M., Yamaguchi, E., et al. (1994). Nocardiosis in 30 patients with advanced human immunodeficiency virus infection: clinical features and outcome. *Clin. Infect. Dis.* 18, 348–353. doi: 10.1093/clinids/18.3.348

Conflict of Interest: The authors declare that the research was conducted in the absence of any commercial or financial relationships that could be construed as a potential conflict of interest.

frontiers in Microbiology

MINI REVIEW
published: 26 February 2020
doi: 10.3389/fmicb.2020.00278

Lyme Endocarditis as an Emerging Infectious Disease: A Review of the Literature

Aleksandra Nikolić[1,2], Darko Boljević[2], Milovan Bojić[1,2], Stefan Veljković[2], Dragana Vuković[3], Bianca Paglietti[4], Jelena Micić[5] and Salvatore Rubino[4]*

[1] Faculty of Medicine, University of Belgrade, Belgrade, Serbia, [2] "Dedinje" Cardiovascular Institute, Belgrade, Serbia, [3] Institute of Microbiology and Immunology, Faculty of Medicine, University of Belgrade, Belgrade, Serbia, [4] Department of Biomedical Sciences, University of Sassari, Sassari, Italy, [5] Clinic for Gynecology and Obstetrics, Clinical Center of Serbia, Belgrade, Serbia

OPEN ACCESS

Edited by:
David Ong,
Franciscus Gasthuis & Vlietland, Netherlands

Reviewed by:
Marina Pekmezovic,
Leibniz Institute for Natural Product Research and Infection Biology, Germany
Muge Cevik,
University of St Andrews, United Kingdom

***Correspondence:**
Darko Boljević
darkoboljevic@gmail.com

Specialty section:
This article was submitted to Infectious Diseases, a section of the journal Frontiers in Microbiology

Received: 27 October 2019
Accepted: 06 February 2020
Published: 26 February 2020

Citation:
Nikolić A, Boljević D, Bojić M, Veljković S, Vuković D, Paglietti B, Micić J and Rubino S (2020) Lyme Endocarditis as an Emerging Infectious Disease: A Review of the Literature. Front. Microbiol. 11:278. doi: 10.3389/fmicb.2020.00278

Lyme endocarditis is extremely rare manifestation of Lyme disease. The clinical manifestations of Lyme endocarditis are non-specific and can be very challenging diagnosis to make when it is the only manifestation of the disease. Until now, only a few cases where reported. Physicians should keep in mind the possibility of borrelial etiology of endocarditis in endemic areas. Appropriate valve tissue sample should be sent for histopathology, culture, and PCR especially in case of endocarditis of unknown origin PCR on heart valve samples is recommended. With more frequent PCR, *Borrelia* spp. may be increasingly found as a cause of infective endocarditis. Prompt diagnosis and treatment of Lyme carditis may prevent surgical treatment and pacemaker implantations. Due to climate change and global warming Lyme disease is a growing problem. Rising number of Lyme disease cases we can expect and rising number of Lyme endocarditis.

Keywords: Lyme disease, Lyme endocarditis, PCR, *Borrelia* spp., valve involvement

LYME ENDOCARDITIS HIGHLIGHTS

- Lyme endocarditis is a rare manifestation of Lyme disease
- Manifestations of Lyme endocarditis are non-specific, and diagnosis can be challenging
- In case of endocarditis of unknown origin, Polymerase Chain Reaction (PCR) of heart valve samples is recommended
- If routine analyses do not reveal a pathogen agent, the physician should think about Lyme endocarditis
- When a cardiac surgeon, during surgery, suspects infective endocarditis, a tissue sample should be taken for histopathology, culture, and PCR
- Prompt diagnosis and treatment of Lyme carditis may avoid surgical treatment and pacemaker implantation
- Due to climate change, we can expect more cases of Lyme carditis with involvement of heart valve

INTRODUCTION

Almost 45 years after its first recognition, Lyme disease (LD) has recently become a huge and growing problem, both in Europe and the United States (Lindgren and Jaenson, 2006). Due to global climate changes, LD is emerging as a threat to public health, easy spreading rapidly into new territories with a lack of a prevention method. The vector that carries the infective agent can be found in places where it has never been found before (Estrada-Peña et al., 2018), and these tick distribution and density changes have been shown to be related to changes in climate (Liang and Gong, 2017). If it is not immediately recognized and treated, it can be a life-threatening disease with multiple cardiac and neurological manifestations (Kannangara et al., 2019).

Lyme carditis (LC) is a rare manifestation of LD that includes: heart conduction abnormalities, myocarditis, pericarditis, endocarditis, pancarditis, arrhythmias, dilatative cardiomyopathy and congestive heart failure, myocardial infarction, and coronary aneurysms (Hidri et al., 2012; Kostić et al., 2017). Lyme endocarditis (LE), one possible manifestation of LC, is rare and has been the subject of case reports. Due to climate change, an increased incidence rate of LC with involvement of heart valve can be expected (Lindgren and Jaenson, 2006; Liang and Gong, 2017; Estrada-Peña et al., 2018; Kannangara et al., 2019).

EPIDEMIOLOGY

Lyme disease is endemic and the most common vector-borne bacterial disease transmitted to humans in North America, Europe, and Asia. In the United States, around 60,000 cases were reported in 2017, according to the Centers for Disease Control and Prevention (CDC), an increase of more than 20% over 2016 (Centers for Disease Control and Prevention [CDC], 2018). In 2015, LD was the sixth most common nationally notifiable disease in the United States. In the states where LD is most common, the average incidence is 39.5 cases per 100,000 persons (Northeast, mid-Atlantic, and upper Midwest of the United States) (Bacon et al., 2008). It seems that this number is underestimated and that the actual incidence of LD could be as much as 10 times higher than the CDC data indicate. This is a result of inadequate reporting, misdiagnosis, and the fact that physicians tend to underreport reportable diseases (Adams et al., 2015).

Estimation from available national data suggests that there are about 85,000 cases per year in Europe where most LD is reported by Scandinavian countries, Germany, Austria, and Slovenia (Lindgren and Jaenson, 2006). Smith and Takkinen (2006) showed that the estimated incidence of LD was as high as 206 cases per 100,000 population in Slovenia and 135 cases per 100,000 population in Austria, which are among the highest reported rates in Europe. Increases in prevalence have also been observed in Sweden, Germany, Czechia, Norway, and Finland (Jaenson and Lindgren, 2011; Heinz et al., 2015; Semenza and Suk, 2017). In Asia, *Borrelia burgdorferi* infection has been reported in countries including China, Korea, Japan, Indonesia, and Nepal and in eastern Turkey (Jaenson and Lindgren, 2011; Heinz et al., 2015). Beside the above-mentioned areas, cases were reported in more tropical locales, and LD may exist in Australia (Dehhaghi et al., 2019).

CARDIAC MANIFESTATION OF LYME DISEASE AND VALVE INVOLVEMENT

Lyme carditis is rare, representing only 0.3–4% of cases in Europe (Hidri et al., 2012). In the United States, between 4 and 10% of patients who do not undergo treatment of LD develop carditis (Paim et al., 2018). LC is associated with acute-onset atrioventricular blocks (I–III), which are the most common feature of LC, arrhythmias and myocarditis or pericarditis, and pericardial effusion, while the chronic stage includes dilated cardiomyopathy (Palecek et al., 2010; Hidri et al., 2012). In a review of 84 patients who had LC, 69% reported palpitations, 19% had conduction abnormalities, 10% had myocarditis, and 5% had left ventricular systolic dysfunction (Paim et al., 2018).

Valvular involvement, as a manifestation of LC, is extremely rare and is the subject of case reports (Hidri et al., 2012; Paim et al., 2018). To date, seven cases in the adult population have been reported and one in the pediatric population. It is important to know that complete conduction recovery with antibiotic treatment occurs in more than 90% of LC cases (Kostić et al., 2017). In areas where LD is endemic, the evaluation of acute-onset cardiac symptoms, with evidence of conduction disease or valvular pathology, should lead to a work-up for LC (Palecek et al., 2010; Kostić et al., 2017; Paim et al., 2018). Prompt diagnosis and treatment of LC may prevent unnecessary surgical treatment, pacemaker implantation, or treatment of heart failure (Palecek et al., 2010; Hidri et al., 2012; Paim et al., 2018).

PATHOIMMUNOLOGY

Borrelia burgdorferi is a highly invasive spirochete that produces adhesions. Via these proteins, *B. burgdorferi* adheres to endothelial cells and to components of the extracellular matrix. By changing of its surface, *B. burgdorferi* modifies immunological response and decreases the phogocytosis of the infected organism (Zajkowska et al., 2000; Zajkowska and Hermanowska–Szpakowicz, 2002; Raveche et al., 2005). Wasiluk et al., in their paper, stated that, in resistant chronic LD, autoimmune mechanisms play a role in persistent disease (Wasiluk et al., 2011). *B. burgdorferi* displays tropism to heart connective tissue, synovial membrane, ligaments, tendon attachments, and vascular endothelium, where it makes molecular changes (dominantly in Lyme arthritis and LD) (Froude et al., 1989; Grzesik et al., 2004; Raveche et al., 2005; Petzke and Schwartz, 2015). There is a belief that autoimmunity and genetic predisposition may play important roles in the inflammation process. One of the mechanisms of autoimmunity is molecular mimicry. By aggregation with fibroblasts and tissue proteins, *B. burgdorferi* disturbs the secretion of cytokines and antibodies, but it can directly attack and destroy T and B lymphocytes as well (Zajkowska et al., 2000; Raveche et al., 2005). This spirochete

activates chemotactic factors by induction of interleukins (IL) IL1, IL6, IL8, and IL10, mediators of inflammation, and immunological complexes and activates the complement system (Steere et al., 2001; Tuchocka, 2002; Raveche et al., 2005; Wasiluk et al., 2011).

LYME ENDOCARDITIS: A REVIEW OF THE LITERATURE

A computerized literature search was conducted using the PubMed databases for relevant articles on LE published in English from 1977 to July of 2019. A possible connection between LD and valve involvement in a 56-year-old male was described in 1993 by Anish. The diagnosis was based on clinical findings: aortic valvular vegetation revealed by transesophageal echocardiography, positive *Borrelia* spp. serology, and prompt improvement after ceftriaxone therapy. However, neither histopathologic nor molecular screening of valvular tissue was performed in order to confirm the suspicions of LE (Anish, 1993). Canver et al. described a case of fulminant LE with involvement of mitral valve in a *B. burgdorferi* seropositive patient, but again, without valve tissue analysis for confirmation (Canver et al., 2000). *Borrelia bissettii was* detected in the aortic valve tissue of a patient with endocarditis and aortic stenosis in the Czechia. Molecular analysis of a valve sample confirmed the presence of *B. bissettii* DNA (Rudenko et al., 2008).

Hidri et al. (2012) described the first case of *Borrelia afzelii* LE, in a 61-year-old man living in an endemic area of France. They reported a case of endocarditis of mitral valve. The diagnosis was confirmed by detection of *B. afzelii* DNA by specific real-time Polymerase Chain Reaction (PCR). The patient was scheduled for mitral valve replacement due to mitral regurgitation caused by mitral valve prolapse and rope rupture. During surgery, the macroscopic analysis of the mitral valve, showing prolapse of the posterior and perforation of the anterior valve, suggested endocarditis. All routinely performed microbiological analysis was negative, but microscopic analysis revealed intracellular microorganisms that were ultimately confirmed as *B. afzelii*. This case emphasized the need to perform PCR on heart valve samples in the case of endocarditis of unknown origin and to have in mind the possibility of borrelial etiology in endemic areas.

The first case of LE confirmed by molecular diagnostics in the United States was reported by Paim et al. (2018) in a 68-year-old male who presented with heart failure with suspected community-acquired pneumonia. Transesophageal echocardiogram revealed severe mitral regurgitation due to aneurismal dilatation of the anterior mitral leaflet with a perforation. These findings suggested infectious etiology. The patient reported LD 8 years previously, which was treated with two sequential courses of doxycycline. The results of serological testing were negative, including four blood cultures as well as virus testing and PCR of *Tropheryma whippelii* and *Borrelia* spp. Results of the 16S rRNA PCR and sequencing performed on resected mitral valve tissue were positive for *B. burgdorferi*. Diagnosis of LE can be very challenging due to an inability to grow the organism in culture, and serologic testing cannot distinguish current from prior infection, especially when it is the only manifestation of the disease (Paim et al., 2018).

Authors from Cleveland reported a case of LE confirmed by PCR without prior clinical manifestations of LD. They described a case of a 65-year-old female with mitral regurgitation due to myxomatous mitral valve degeneration and valve prolapse who underwent mitral valve repair. She denied tick bites or annular rash. During the operation, the surgeon suspected an infective rather than degenerative etiology due to anterior leaflet scarring and destruction over the A2 area, with thickened chords. All tissue cultures were negative. DNA of *B. burgdorferi* was identified by 16S ribosomal ribonucleic acid sequencing. This case suggests that when the cardiac surgeon suspects on infective pathology, tissue samples should be sent for culture, histopathology, and PCR analysis (Haddad et al., 2019).

Cardiac manifestations of LD typically include the atrioventricular conduction system, rarely heart valves. Patel and Schachne (2017) reported a case of a 59-year-old male with involvement of both the electrical conduction system and the mitral valve. LD was diagnosed on the basis of elevated immunoglobulins IgA, IgM, and IgG to *B. burgdorferi*. The authors revealed that mitral regurgitation was likely to be chronic rather than acute due to the echo parameters. Complete recovery of the conduction system after antibiotic treatment was noticed in this case, and stress echocardiography showed reduced mitral regurgitation. Their conclusion was that local invasion of pathogen and macrophage caused leaflet edema. Histopathology was not done, and they speculated whether it was possible that local myocardial inflammation had worsened the regurgitation of a chronically diseased valve. Finally, in areas endemic for LD, the evaluation of acute-onset cardiac symptoms, especially with evidence of conduction disease or valvular pathology, physicians should think of LC and LE. Prompt diagnosis and treatment of LD and LE may prevent surgical treatment and pacemaker implantation (Patel and Schachne, 2017).

The only LD case in children with suspected involvement of mitral valve was reported by Kameda et al. (2012) They described an unusual manifestation of LD in a 7-year-old girl with Lyme neuroborreliosis with meningoradiculitis and involvement of mitral valve that was discovered due to a heart murmur. She was treated by cefotaxime for 4 weeks. After one year, echo showed a normal mitral valve with trivial mitral regurgitation. In children, LE is extremely rare, and this is the only case in the literature with suspected valve involvement in a child. Despite improvement after therapy, there was no evidence from histopathology or PCR of the valve tissue and no definitive diagnosis of LE (Kameda et al., 2012). A summary of the case reports is given in **Table 1**.

Lyme endocarditis is a rare condition, but new cases can be expected due to climate change. Global warming, as one of the components of climate change, has increased significantly in recent years, and it has had a huge impact on human health (Watts et al., 2015). The effect of global warming on human health is divided into two categories: a direct effect on disease, such as heat shock and increased mortality in the population with other diseases, and an indirect effect on diseases such as infectious diseases and allergies. Heatwaves, storms, drought, and floods result in a shift in the distribution of pathogens and vectors,

TABLE 1 | Summary of Case Reports of Lyme Endocarditis.

References	Valve type	Serologic test (blood)	Valve histopathology	Valve culture	Molecular testing	Treatment
Anish, 1993	Aortic	EIA 1.10 and repeat 1 week later 1.22 Western blot IgG P-41 band positive	Not performed	Not performed	Not performed	Ceftriaxone 2 g IV daily for 2 weeks, then doxycycline 100 mg po b.i.d for 30 days
Canver et al., 2000	Mitral	ELISA reactive (IgG and IgM). Immunoblot: 6 antigenic bands in IgG probe	Myxoid degeneration with infiltration of lymphocytes No evidence of fibrinoid exudate or Aschoff bodies	Not performed	Not performed	Not specified
Rudenko et al., 2008	Aortic	ELISA reactive (IgG) Western blot positive	Highly calcified dissected cardiac valve	Negative for aerobic and anaerobic microorganisms. Negative for spirochetes	PCR amplification: 99% identity to the *flagellin* gene of *Borrelia bissettii* strain	Antimicrobial therapy, not specified
Hidri et al., 2012	Mitral	ELISA reactive (IgG) Immunoblot: 6 antigenic bands in IgG probe	Endocarditis with foamy macrophages suggestive of intracellular microorganisms; Gram, PAS, and Giemsa stains were negative. Wharton-Starry stain showed only scarce curved rods, which had a morphology that was not specific to spirochetes.	Not specified	Universal PCR targeting 16S RNA-encoding DNA identified the genus *Borrelia.* Real time DNA amplification identified *B. afzelii*	Valve replacement (IV gentamicin and amoxicillin for 2 weeks, followed by 4 weeks of oral amoxicillin
Kameda et al., 2012	Mitral	ELISA reactive (IgG and IgM) Immunoblot: positive (data not shown)	Not performed	Not performed	Not performed	Cefotaxime (200 mg/kg/day) for 14 days
Patel and Schachne, 2017	Mitral	EIA) detected significant levels of IgG (24.3; ref range <1), IgM (9.6; ref range <1), and IgA (>9.9; ref range <1) to B. burgdorferi.	Not performed	Not performed	Not performed	Ceftriaxone IV in hospital followed by oral doxycycline at home
Paim et al., 2018.	Mitral	Results of serologic blood testing for *Bartonella* spp., *Coxiella burnetii*, *Chlamydia* spp., *Legionella pneumophila*, *Blastomyces dermatitidis*, *Coccidioides* spp., *Histoplasma capsulatum*, and HIV infection were negative. Serum cryptococcal and urinary *Histoplasma* antigens were both negative.	Not performed	Histopathology showed active native valve endocarditis with no microorganisms identified by Gram, Gomori methenamine silver, and periodic acid–Schiff-diastase (PAS-D), and Steiner stains.	PCR testing from the blood for *Tropheryma whippelii* and *Borrelia* spp. were negative. Results of the 16S rRNA PCR and sequencing on resected mitral valve tissue were positive for *B. burgdorferi*.	Ceftriaxone for 6 weeks (not specified)
Haddad et al., 2019	Mitral	Blood cultures, serology for *Bartonella* and *Coxiella* were unrevealing. IgM and IgG were positive by enzyme immunoassay as well as Western blot (2 IgM bands and 10 IgG bands)	Negative	Cultures were negative and histopathological evaluation of the submitted limited valve tissue was non-diagnostic.	16S Ribosomal ribonucleic acid (rRNA) sequencing identified DNA of *Borrelia burgdorferi*	The patient was treated with ceftriaxone 2 g IV q 24 h for 6 weeks

which consequently results in a shift in the distribution of human infectious disease (Kuhn et al., 2005; Tian et al., 2015).

Tick-born disease and the transmission of disease-causing agents are significantly influenced by weather and climate as well, which has an indirect effect on humans (IPCC, 2013). Milder winters and warmer falls and springs may enable the extension of Lyme borreliosis to higher altitudes and latitudes, predominantly in the north of Europe (Semenza and Menne, 2009). Thus, the level of influence depends on the kind of vector (Confalonieri et al., 2007; Kurane, 2010).

DIAGNOSIS

Lyme disease, and especially LE, can be very challenging to diagnose. The most specific (100%) examination is culture of *Borrelia* spp. This test provides information on active infection, enables the investigation of the structural, molecular, antigenic, and pathogenic properties of the antigen, and can distinguish live from dead organisms (Reed, 2002; Aguero-Rosenfeld et al., 2005; Murray and Shapiro, 2010). But, there are limitations to this exam. The main limitation is the time needed for the culture to reveal its results (up to 12 weeks for it to be considered negative). Other issues are the low sensitivity of the method in all other than the cutaneous manifestation of the disease, its inapplicability for diagnosis in antibiotic-treated patients, the need for special media, and its expense (Karlsson et al., 1990; Nadelman et al., 1990).

Serological examination is widely used and is available in the clinical setting. Frequently used assays are enzyme-linked immunosorbent assay (ELISA), immunofluorescence assays, and Western blotting (Tugwell, 1997; Schutzer et al., 2018), but false-negative and false-positive results may occur (Schutzer et al., 2018). ELISA is recommended as the initial serological examination. Tests are objective, fast, and easy to perform and are suitable for the diagnosis of other forms of LD beside cutaneous. This is the reason why, in the United States, a two-step protocol for the evaluation of *B. burgdorferi* antibodies in sera has been recommended (Miller et al., 2018). In both ELISA and Immunoblot assays, the antigens used should detect both IgM and IgG antibodies. Immunoblot should have a high specificity of at least 95% (Miller et al., 2018; Schutzer et al., 2018). In the early stages of the disease, serological tests may reveal false-negative results in a high percentage. False-positive results can be seen in mononucleosis, autoimmune states and *Treponema pallidum* infection. Western blot is more sensitive and specific than ELISA, and it is recommended as a second step in diagnosis and for confirmation of ELISA findings (Miller et al., 2018).

Polymerase Chain Reaction can be very helpful, since it detects the genetic material of *Borreliae* sp. directly in multiple tissues and provides molecular identification and antimicrobial therapy does not affect the results (Rijpkema et al., 1997). Transvenous endomyocardial biopsy can be indicative of LD. The band-like infiltrate is strongly suggestive, and it can be seen even if the quality of the specimen is limited (Marques, 2015). Its intrinsic limitations, which include sampling error, the necessity that the patient undergo an invasive procedure to obtain appropriate tissue, and the variability of interpretation, restrain its use in clinical practice (Reed, 2002; Aguero-Rosenfeld et al., 2005).

TREATMENT

Antibiotic therapy in the early stages of LD prevents or attenuates later complications of the disease (Sangha et al., 1998). Antibiotic regimens for the treatment of LD include amoxicillin 500 mg orally three or four times daily for 30 days, doxycycline 100 mg orally twice daily for 30 days, and ceftriaxone 2 g intravenously daily for 2 to 4 weeks (Fish et al., 2008). Cefotaxime 3 g intravenously twice daily for 2 to 4 weeks is reportedly as effective as ceftriaxone in patients who have other late manifestations of LD (50, 51). Patients who have minor cardiac involvement (e.g., prolongation of the PR interval of no more than 0.30 s) and no other symptoms should receive oral antibiotic therapy with amoxicillin or doxycycline as for early disease. Patients who have more severe LC, should be admitted to hospital and administered intravenous ceftriaxone or high-dose penicillin G. As has been mentioned, complete heart block generally resolves within 1 week, with resolution of lesser conduction disturbances within 6 weeks (Olson et al., 1986; McAlister et al., 1989; Fish et al., 2008). A summary of LE treatment from limited cases in the literature is given in **Table 1**.

SUMMARY AND CONCLUSION

Lyme endocarditis is an extremely rare manifestation of LD. The clinical manifestations of LE are non-specific, and it can be a very challenging diagnosis to make when it is the only manifestation of the disease. Until now, only a few cases have been reported. In case of endocarditis of unknown origin, PCR on heart valve samples is recommended. Physicians should keep in mind the possibility of a borrelial etiology of endocarditis in endemic areas. An appropriate valve tissue sample should be sent for histopathology, culture, and PCR when a cardiac surgeon suspects infective endocarditis during an operation. The use of PCR is crucial to detect and identify the causative organism in infective endocarditis, especially in those with negative blood and tissue cultures. With more frequent PCR, *Borrelia* sp. may be increasingly found to be the cause of infective endocarditis. Prompt diagnosis and treatment of LE and LC may allow surgical treatment and pacemaker implantation to be avoided. Due to climate change and global warming, LD is a growing problem, and, due to the rising number of LD cases, we can expect a rising number of LE cases as well.

AUTHOR CONTRIBUTIONS

AN, DB, and MB conceptualized this manuscript, collected the data, and drafted the first manuscript. BP and SR revised final revision of the manuscript. All authors provided critical feedback and contributed to the manuscript.

REFERENCES

Adams, D., Fullerton, K., Jajosky, R., Sharp, P., Onweh, D., Schley, A., et al. (2015). Summary of notifiable infectious diseases and conditions – United States, 2013. *MMWR Morb. Mortal. Wkly. Rep.* 62, 1–122. doi: 10.15585/mmwr.mm6253a1

Aguero-Rosenfeld, M., Wang, G., Schwartz, I., and Wormser, G. (2005). Diagnosis of Lyme borreliosis. *Clin. Microbiol. Rev.* 18, 484–509. doi: 10.1128/cmr.18.3.484-509.2005

Anish, S. A. (1993). Case report: possible Lyme endocarditis. *N. J. Med.* 90, 599–601.

Bacon, R. M., Kugeler, K. J., and Mead, P. S. (2008). Surveillance for Lyme disease-United States, 1992-2006. *MMWR Surveill. Summ.* 57, 1–9.

Canver, C. C., Chanda, J., DeBellis, D. M., and Kelley, J. M. (2000). Possible relationship between degenerative cardiac valvular pathology and Lyme disease. *Ann. Thorac. Surg.* 70, 283–285. doi: 10.1016/s0003-4975(00)01452-1

Centers for Disease Control and Prevention [CDC] (2018). *Lyme Disease: Data and Surveillance*. Available online at: http://www.cdc.gov/lyme/stats/index.html?s_cid=cs_281 (accessed October, 2019).

Confalonieri, U., Menne, B., and Akhtar, P. (2007). "Human health. Climate change: impacts, adaptation and vulnerability," in *Contribution of Working Group II to the Fourth Assessment Report of the Intergovernmental Panel on Climate Change*, eds M. L. Parry, O. F. Canziani, and J. P. Palutikof (Cambridge: Cambridge University Press), 391–431.

Dehhaghi, M., Kazemi Shariat, Panahi, H., Holmes, E., Hudson, B., Schloeffel, R., and Guillemin, G. (2019). Human tick-borne diseases in Australia. *Front. Cell. Infect. Microbiol.* 9:3. doi: 10.3389/fcimb.2019.00003

Estrada-Peña, A., Cutler, S., Potkonjak, A., Vassier-Tussaut, M., Van Bortel, W., Zeller, H., et al. (2018). An updated meta-analysis of the distribution and prevalence of *Borrelia burgdorferi* s.l. in ticks in Europe. *Int. J. Health Geogr.* 17:41. doi: 10.1186/s12942-018-0163-7

Fish, A., Pride, Y., and Pinto, D. (2008). Lyme carditis. *Infect. Dis. Clin. North Am.* 22, 275–288. doi: 10.1016/j.idc.2007.12.008

Froude, J., Gibofsky, A., Buskirk, D. R., Khanna, A., and Zabriskie, J. B. (1989). Cross-reactivity between streptococcus and human tissue: a model of molecular mimicry and autoimmunity. *Curr. Top. Microbiol. Immunol.* 145, 5–26. doi: 10.1007/978-3-642-74594-2_2

Grzesik, P., Oczko-Grzesik, B., and Kepa, L. (2004). *Borrelia burgdorferi* pathogenesis and the immune response. *Przegl. Epidemiol.* 58, 589–596.

Haddad, O., Gillinov, M., Fraser, T., Shrestha, N., and Pettersson, G. (2019). Mitral valve endocarditis: a rare manifestation of Lyme disease. *Ann. Thorac. Surg.* 108, e85-e86. doi: 10.1016/j.athoracsur.2018.12.046

Heinz, F., Stiasny, K., Holzmann, H., Kundi, M., Sixl, W., Wenk, M., et al. (2015). Emergence of tick-borne encephalitis in new endemic areas in Austria: 42 years of surveillance. *Euro Surveill.* 20, 9–16. doi: 10.2807/1560-7917.es2015.20.13.21077

Hidri, N., Barraud, O., de Martino, S., Garnier, F., Paraf, F., Martin, C., et al. (2012). Lyme endocarditis. *Clin. Microbiol. Infect.* 18, E531-E532. doi: 10.1111/1469-0691.12016

IPCC, (2013)."Summary for policymakers," in *Climate Change 2013: The Physical Science Basis. Contribution of Working Group I to the Fifth Assessment Report of the Intergovernmental Panel on Climate Change*, eds T. F. Stocker, D. Qin, G.-K. Plattner, M. Tignor, S. K. Allen, J. Boschung, et al. (Cambridge: Cambridge University Press).

Jaenson, T. G. T., and Lindgren, E. (2011). The range of *Ixodes ricinus* and therisk of contracting Lyme borreliosis will increase northwards when the vegetation period becomes longer. *Ticks Tick Borne Dis.* 2, 44–49. doi: 10.1016/j.ttbdis.2010.10.006

Kameda, G., Vieker, S., Hartmann, J., Niehues, T., and Längler, A. (2012). Diastolic heart murmur, nocturnal back pain, and lumbar rigidity in a 7-year girl: an unusual manifestation of Lyme disease in childhood. *Case Rep.* 2012:976961. doi: 10.1155/2012/976961

Kannangara, D., Sidra, S., and Pritiben, P. (2019). First case report of inducible heart block in Lyme disease and an update of Lyme carditis. *BMC Infect. Dis.* 19:428. doi: 10.1186/s12879-019-4025-0

Karlsson, M., Hovind-Hougen, K., Svenungsson, B., and Stiernstedt, G. (1990). Cultivation and characterization of spirochetes from cerebrospinal fluid of patients with Lyme borreliosis. *J. Clin. Microbiol.* 28, 473–479. doi: 10.1128/jcm.28.3.473-479.1990

Kostić, T., Momèilović, S., Perišić, Z., Apostolović, S., Cvetković, J., Jovanović, A., et al. (2017). Manifestations of Lyme carditis. *Int. J. Cardiol.* 232, 24–32. doi: 10.1016/j.ijcard.2016.12.169

Kuhn, K., Campbell-Lendrum, D., Haines, A., and Cox, J. (2005). *Using Climate to Predict Infectious Disease Epidemics*. Geneva: World Health Organization.

Kurane, I. (2010). The effect of global warming on infectious diseases. *Osong Public Health Res. Perspect.* 1, 4–9. doi: 10.1016/j.phrp.2010.12.004

Liang, L., and Gong, P. (2017). Climate change and human infectious diseases: a synthesis of research findings from global and spatio-temporal perspectives. *Environ. Int.* 103, 99–108. doi: 10.1016/j.envint.2017.03.011

Lindgren, E., and Jaenson, T. G. T. (2006). *Lyme Borreliosis in Europe: Influences of Climate and Climate Change, Epidemiology, Ecology and Adaptation Measures*. Copenhagen: WHO Regional Office for Europe.

Marques, A. (2015). Laboratory diagnosis of Lyme disease. *Infect. Dis. Clin. North Am.* 29, 295–307. doi: 10.1016/j.idc.2015.02.005

McAlister, H. F., Klementowicz, P. T., Andrews, C., Fisher, J. D., Feld, M., Furman, S., et al. (1989). Lyme carditis: an important cause of reversible heart block. *Ann. Intern. Med.* 110, 339–345.

Miller, J., Binnicker, M., Campbell, S., Carroll, K., Chapin, K., Gilligan, P., et al. (2018). A guide to utilization of the microbiology laboratory for diagnosis of infectious diseases: 2018 update by the infectious diseases society of America and the American Society for Microbiologya. *Clin. Infect. Dis.* 67, e1-e94. doi: 10.1093/cid/ciy381

Murray, T., and Shapiro, E. (2010). Lyme disease. *Clin. Lab. Med.* 30, 311–328. doi: 10.1016/j.cll.2010.01.003

Nadelman, R., Pavia, C., Magnarelli, L., and Wormser, G. (1990). Isolation of *Borrelia burgdorferi* from the blood of seven patients with Lyme disease. *Am. J. Med.* 88, 21–26. doi: 10.1016/0002-9343(90)90122-t

Olson, L. J., Okafor, E. C., and Clements, I. P. (1986). Cardiac involvement in Lyme disease: manifestations and management. *Mayo Clin. Proc.* 61, 745–749. doi: 10.1016/s0025-6196(12)62775-x

Paim, A., Baddour, L., Pritt, B., Schuetz, A., and Wilson, J. (2018). Lyme endocarditis. *Am. J. Med.* 131, 1126–1129. doi: 10.1016/j.amjmed.2018.02.032

Palecek, T., Kuchynka, P., Hulinska, D., Schramlova, J., Hrbackova, H., Vitkova, I., et al. (2010). Presence of *Borrelia burgdorferi* in endomyocardial biopsies in patients with new-onset unexplained dilated cardiomyopathy. *Med. Microbiol. Immunol.* 199, 139–143. doi: 10.1007/s00430-009-0141-146

Patel, L., and Schachne, J. (2017). Lyme carditis: a case involving the conduction system and mitral valve. *R. I. Med. J. (2013)* 100, 17–20.

Petzke, M., and Schwartz, I. (2015). *Borrelia burgdorferi* pathogenesis and the immune response. *Clin. Lab. Med.* 35, 745–764. doi: 10.1016/j.cll.2015.07.004

Raveche, E., Schutzer, S., Fernandes, H., Bateman, H., McCarthy, B., Nickell, S., et al. (2005). Evidence of *Borrelia* autoimmunity-induced component of Lyme carditis and arthritis. *J. Clin. Microbiol.* 43, 850–856. doi: 10.1128/jcm.43.2.850-856.2005

Reed, K. (2002). Laboratory testing for Lyme disease: possibilities and practicalities. *J. Clin. Microbiol.* 40, 319–324. doi: 10.1128/jcm.40.2.319-324.2002

Rijpkema, S., Tazelaar, D., Molkenboer, M., Noordhoek, G., Plantinga, G., Schouls, L., et al. (1997). Detection of *Borrelia afzelii*, *Borrelia burgdorferi* sensu stricto, *Borrelia garinii* and group VS116 by PCR in skin biopsies of patients with erythema migrans and acrodermatitis chronica atrophicans. *Clin. Microbiol. Infect.* 3, 109–116. doi: 10.1111/j.1469-0691.1997.tb00259

Rudenko, N., Golovchenko, M., Mokracek, A., Piskunova, N., Ruzek, D., Mallatova, N., et al. (2008). Detection of *Borrelia bissettii* in cardiac valve tissue of a patient with endocarditis and aortic valve stenosis in the Czech Republic. *J. Clin. Microbiol.* 46, 3540–3543. doi: 10.1128/jcm.01032-08

Sangha, O., Phillips, C. B., and Fleischmann, K. E. (1998). Lack of cardiac manifestations among patients with previously treated Lyme disease. *Ann. Intern. Med.* 128, 346–353.

Schutzer, S., Body, B., Boyle, J., Branson, B., Dattwyler, R., Fikrig, E., et al. (2018). Direct diagnostic tests for Lyme disease. *Clin. Infect. Dis.* 68, 1052–1057. doi: 10.1093/cid/ciy614

Semenza, J., and Suk, J. (2017). Vector-borne diseases and climate change: a European perspective. *FEMS Microbiol. Lett.* 365:fnx244. doi: 10.1093/femsle/fnx244

Semenza, J. C., and Menne, B. (2009). Climate change and infectious diseases in Europe. *Lancet Infect. Dis.* 9, 365–375. doi: 10.1016/S1473-3099(09)70104-5

Smith, R., and Takkinen, J. (2006). Lyme borreliosis: Europe-wide coordinated surveillance and action needed? *Euro Surveill.* 11:E060622.1. doi: 10.2807/esw.11.25.02977-en

Steere, A. C., Gross, D., Meyer, A. L., and Huber, B. T. (2001). Autoimmune mechanisms in antibiotic treatment-resistant Lyme arthritis. *J. Autoimmun.* 16, 263–268. doi: 10.1006/jaut.2000.0495

Tian, H. Y., Zhou, S., Dong, L., Van Boeckel, T. P., Cui, Y. J., Wu, Y., et al. (2015). Avian influenza H5N1 viral and bird migration networks in Asia. *Proc. Natl. Acad. Sci. U.S.A.* 112, 172–177. doi: 10.1073/pnas.1405216112

Tuchocka, A. (2002). Arthritis in the course of Lyme disease. *Nowa Klin.* 9, 1222–1227.

Tugwell, P. (1997). Laboratory evaluation in the diagnosis of Lyme disease. *Ann. Intern. Med.* 127, 1109–1123. doi: 10.7326/0003-4819-127-12-199712150-00011

Wasiluk, A., Zalewska-Szajda, B., Waszkiewicz, N., Kępka, A., Szajda, D. S., Wojewódzka-Żeleźniakowicz, M., et al. (2011). Lyme disease: etiology, pathogenesis, clinical courses, diagnostics and treatment. *Prog. Health Sci.* 1, 179–186.

Watts, N., Adger, W. N., Agnolucci, P., and Costello, A. (2015). Health and climate change: policy responses to protect public health. *Lancet* 386, 1861–1914.

Zajkowska, J., and Hermanowska–Szpakowicz, T. (2002). New aspects of the pathogenesis of Lyme disease. *Przegl. Epidemiol.* 56(Suppl. 1), 57–67.

Zajkowska, J. M., Hermanowska–Szpakowicz, T., Pancewicz, S. A., and Kondrusik, M. (2000). Selected aspects of immuno-patho-genesis in Lyme disease. *Pol. Merkur. Lekarski.* 9, 579–583.

Conflict of Interest: The authors declare that the research was conducted in the absence of any commercial or financial relationships that could be construed as a potential conflict of interest.

frontiers in Microbiology

MINI REVIEW
published: 09 March 2020
doi: 10.3389/fmicb.2020.00373

Dried Blood Spot Tests for the Diagnosis and Therapeutic Monitoring of HIV and Viral Hepatitis B and C

Edouard Tuaillon[1], Dramane Kania[2], Amandine Pisoni[1], Karine Bollore[1], Fabien Taieb[3], Esther Nina Ontsira Ngoyi[1], Roxane Schaub[4], Jean-Christophe Plantier[5], Alain Makinson[6] and Philippe Van de Perre[1]*

[1] Pathogenèse et Contrôle des Infections Chroniques, INSERM U1058, Centre Hospitalier Universitaire de Montpellier, Montpellier, France, [2] Centre Muraz, Bobo Dioulasso, Burkina Faso, [3] Emerging Diseases Epidemiology Unit, Center for Translational Science, Institut Pasteur, Paris, France, [4] CIC AG/INSERM 1424, Centre Hospitalier de Cayenne, Cayenne, France, [5] Laboratoire de Virologie, Normandie Université, CHU de Rouen, Rouen, France, [6] INSERM U1175/IRD UMI 233, IRD, CHU de Montpellier, Montpellier, France

OPEN ACCESS

Edited by:
David Ong,
Franciscus Gasthuis & Vlietland, Netherlands

Reviewed by:
Juan Carlos Hurtado,
Hospital Clínic de Barcelona, Spain
Lorenzo Zammarchi,
University of Florence, Italy

***Correspondence:**
Edouard Tuaillon
e-tuaillon@chu-montpellier.fr

Specialty section:
This article was submitted to Infectious Diseases, a section of the journal Frontiers in Microbiology

Received: 17 October 2019
Accepted: 19 February 2020
Published: 09 March 2020

Citation:
Tuaillon E, Kania D, Pisoni A, Bollore K, Taieb F, Ontsira Ngoyi EN, Schaub R, Plantier J-C, Makinson A and Van de Perre P (2020) Dried Blood Spot Tests for the Diagnosis and Therapeutic Monitoring of HIV and Viral Hepatitis B and C. Front. Microbiol. 11:373. doi: 10.3389/fmicb.2020.00373

Blood collected and dried on a paper card – dried blood spot (DBS) – knows a growing interest as a sampling method that can be performed outside care facilities by capillary puncture, and transported in a simple and safe manner by mail. The benefits of this method for blood collection and transport has recently led the World Health Organization to recommend DBS for HIV and hepatitis B and C diagnosis. The clinical utility of DBS sampling to improve diagnostics and care of HIV and hepatitis B and C infection in hard to reach populations, key populations and people living in low-income settings was highlighted. Literature about usefulness of DBS specimens in the therapeutic cascade of care – screening, confirmation, quantification of nucleic acids, and resistance genotyping -, was reviewed. DBS samples are suitable for testing antibodies, antigens, or nucleic acids using most laboratory methods. Good sensibility and specificity have been reported for infant HIV diagnosis and diagnosis of hepatitis B and C. The performance of HIV RNA testing on DBS to identified virological failure on antiretroviral therapy is also high but not optimal because of the dilution of dried blood in the elution buffer, reducing the analytical sensitivity, and because of the contamination by intracellular HIV DNA. Standardized protocols are needed for inter-laboratory comparisons, and manufacturers should pursue regulatory approval for *in vitro* diagnostics using DBS specimens. Despite these limitations, DBS sampling is a clinically relevant tool to improve access to infectious disease diagnosis worldwide.

Keywords: dried blood spot, hepatitis B, hepatitis C, HIV, diagnosis, hard-to-reach population

INTRODUCTION

The use of dried blood collected on blotting paper, – "Dried Blood Spot" (DBS) -, was developed gradually after the Second World War. The beginning of diagnosis on DBS is associated with Robert Guthrie who implemented large-scale neonatal screening for phenylketonuria in the 1960s. In the field of infectious disease diagnosis, the first references to DBS relate to syphilis, with studies

published as early as the 1950s (Blaurock et al., 1950). The DBS sample was also used for serological surveillance or diagnosis of trypanosomiasis, hepatic amebiasis, congenital rubella, or hepatitis B (Ashkar and Ochilo, 1972; Ambroise-Thomas and Meyer, 1975; Farzadegan et al., 1978; Sander and Niehaus, 1980). After these modest and historic beginnings, a progressively increasing interest for DBS was observed in the early 2000's, mainly due to the needs of therapeutic monitoring of HIV infection.

The blood can be directly deposited on the filter paper when a capillary blood collection is done with a retractable incision device, or using a pipette when peripheral venous blood is collected. The procedure for DBS collection has been detailed (Ostler et al., 2014). The capillary sampling on DBS is performed at the heel of the infant and at the level of the digital pulp in children and adults. Self-sampling is possible after a minimum training. For digital samples, the fingers innervated by the ulnar nerve (half of the 3rd finger and 4th or 5th finger) are generally preferred because less sensitive than fingers innervated by the median nerve. The size of the skin penetration depends on the size and type of lancet, and determines the amount of blood that can be collected. Standard DBS cards use pre-printed circles 12 mm in diameter to receive between 50 and 70 µl of blood. The massage of the finger before puncture and warming of the hands in warm water, can facilitate the sampling. After puncture it is important to exert a strong intermittent pressure to maintain the bleeding and complete the blotting paper card.

INDICATIONS OF DBS IN INFECTIOUS DISEASES

Dried blood spot sampling offers an alternative to the reference samples – plasma and serum – in situations where there are no facilities or expertise to take venous whole blood specimens; or where transport of body fluids is difficult. Hence, DBS specimens collected outside of healthcare facilities can be viewed as an alternative to rapid diagnostic tests (RDT). Compared to RDT, DBS sampling has advantages and limits summarized in **Table 1**. By comparison with RDT one of the main limit is that diagnostic approach using DBS request a post-test visit after the sampling which is associated with a risk of loss to follow up. On the other hand, it is useful to test a large number of persons by using DBS testing in a centralized laboratory, and it is possible to confirm the infections with Western blot and molecular tests. Hence, in countries with high economic resources, DBS can be used to promote access to screening in key populations having little use of care facilities. Screening programs using DBS have been running for several years in Great Britain, targeting in particular intravenous drug users. Up to 20% of new HCV diagnoses were made using DBS in 2013 in Scottish addiction treatment centers (McLeod et al., 2014). A program of this type has been implemented by the Montpellier teaching hospital since 2013 in all addiction treatment centers located in the Languedoc Roussillon Region (Accueillir, 2014). Sex workers (Shokoohi et al., 2016), homeless people (Foroughi et al., 2017), migrants and some men who have sex with men (MSM) (Bogowicz et al., 2016), as well as populations living in hard to reach areas such as French Guiana (Schaub, 2017) are also key populations that can have difficult access to laboratory infectious diseases testing for which the use of DBS should be considered.

TABLE 1 | Comparison of the characteristics of DBS tests and rapid diagnostic tests.

	DBS	Rapid Tests
Capillary blood	Yes	Yes
Hard to reach populations	Yes	Yes
Immediate result (<15 min)	No	Yes
Return visit request	Yes	No
CE-IVD, FDA, WHO prequalification	No*	Yes
Based on laboratory expertise	Yes	No
Useful for all diagnosis steps	Yes	No

**Except for HIV RNA nucleic acid tests. CE-IVD, CE-marked In Vitro Diagnostic Medical Device; FDA, Food and Drug Administration. Advantages of DBS tests are indicated in green and limits in red.*

In resource-limited settings the high rates of infectious disease mortality and morbidity are, to a large extent, due to a lack of diagnostic means (Global Health Workforce Alliance and World Health Organization [WHO], 2013). Insufficient access to nearby laboratory facilities is a major concern. The lack of adequate human and financial resources – health professionals and biologists – are also noteworthy. It is estimated that three-quarters of Africa's population have access to minimal health care structures in Africa, and more than 90% in Asia. By contrast, less than one-third of Africans would have access to advanced health facilities and just over 50% in Asia (RAND Corporation, 2007. Estimating the global health impact of improved diagnostic tools for the developing world; Abou Tayoun et al., 2014).

Point of care (POC) tests – usable outside healthcare facilities – and technologies requiring minimal infrastructure (near-POC tests), constitute a major progress but will require significant investments to expand the limited range of analyzable parameters. Necessity of machines maintenance, reagents supply and quality control assurance need also to be considered in a medium and long term approach for decentralized laboratories. Good acceptability of capillary blood sampling is another advantage of DBS when compared with venepuncture (Pell et al., 2014; Almond et al., 2016). In this context, sampling on DBS considers decentralized sampling as possible, whilst carrying out the test in a well-equipped centralized clinical laboratory, without waiting for the uncertain availability of new technologies and without necessity of maintaining a cold chain for transportation (**Figure 1A**). Transportation and storage in field situations can have a significant effect, as shown for HIV and HCV nucleic amplifications (Monleau et al., 2010; Tuaillon et al., 2010; Manak et al., 2018), and HCV antibodies testing (Marques et al., 2012). The filter papers used can also impact on the performances of *in vitro* diagnosis tests. Among the DBS collection cards available Whatman 903, Munktell TNF or Ahlstrom Grade 226 have been recommended but other cards have also demonstrated good performances (Waters et al., 2007; Rottinghaus et al., 2013; Smit et al., 2014; World Health Organization [WHO], 2014; Taieb et al., 2016). DBS specimens should be considered from a

public health perspective, for which the clinical performance of the *in vitro* laboratory assays is crucial. The clinical performance of a test can be analyzed as a trade-off between the intrinsic performances of the assay and its accessibility in the field. The best clinical performances are obtained in populations in whom the highest proportion of infected persons are tested and detected positive. High clinical performances may be achieved using DBS based strategies (**Figure 1B**). Implementation of DBS for HIV viral load is considered as one of the most medically effective immediate measures to reduce AIDS-related mortality in Africa (Phillips et al., 2015).

In addition to individual diagnosis, sampling, transport and storage simplification makes the DBS a particularly suitable tool for population studies. In France the mandatory reporting system for HIV is associated with virological surveillance by the HIV National Reference Center using dried serum spot (Lot et al., 2004). The HIV National Reference Center identifies HIV types, groups, and subtypes, and estimates incidence using a recent infection test. This surveillance system provides robust and comprehensive data on the HIV epidemic in France. Other countries, such as Germany, have also integrated DBS into their HIV surveillance system thanks to the DBS ease

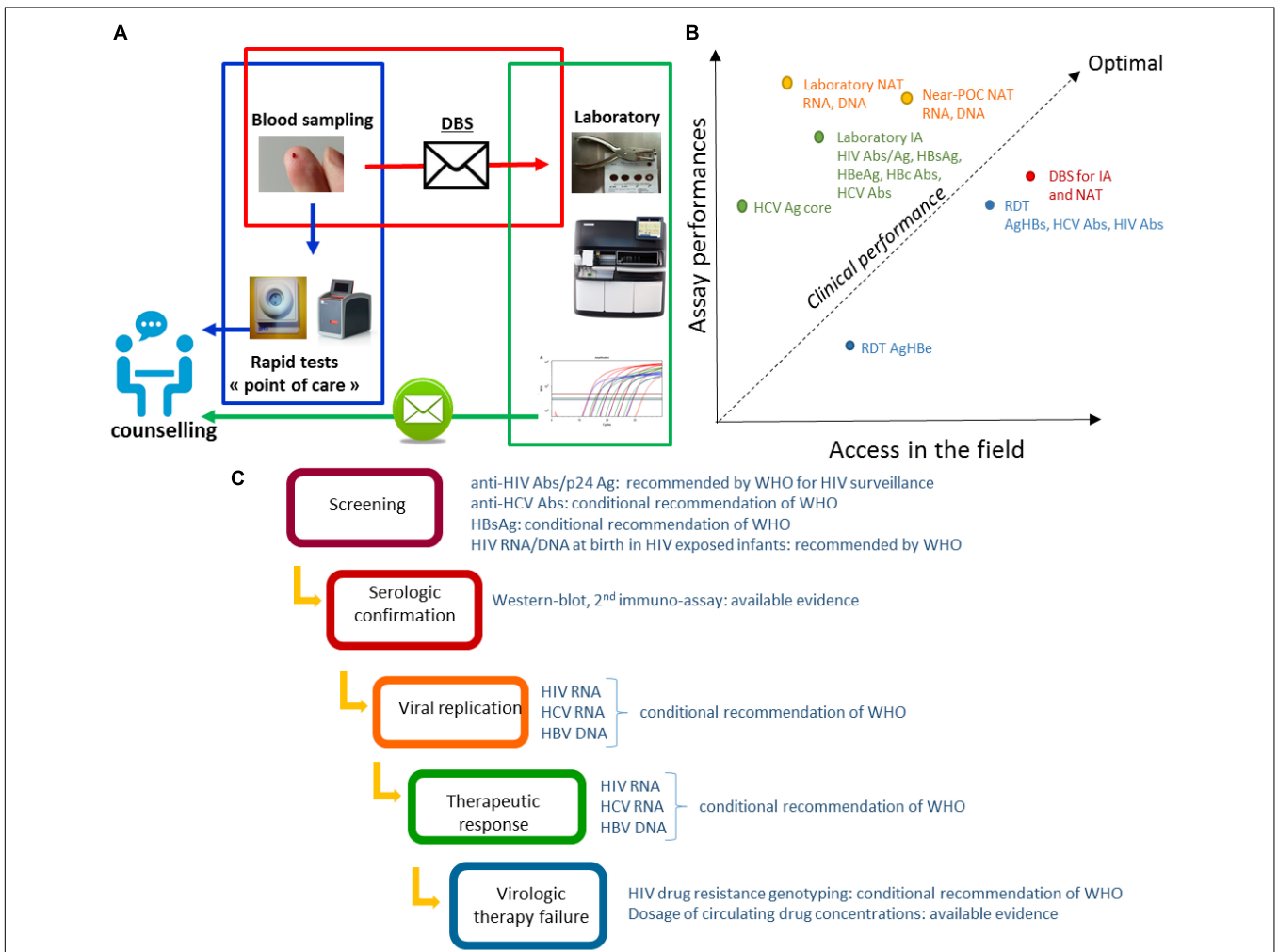

FIGURE 1 | (A) Possible organization of the diagnosis and management of infections combining rapid diagnostic tests and DBS. The sampling is carried out closer to the person detected or supported. Non-laboratory RDT are carried out in the peripheral structures in parallel with the sending of the DBS to the central laboratory carrying out complementary or confirmation analyses. Results are reported as part of the post-test counseling. **(B)** Clinical performance of *in vitro* assays dedicated to HBV, HCV, and HIV infections. The figure is a schematic representation of the clinical performances considered as a trade-off between assay performances and implementation coverage. Diagnosis and monitoring strategies based on different formats of tests have different clinical performances. Each format of test is characterized by its analytical performances mainly estimated by lower limit of detection (LOD), sensibility (Se) and specificity (Sp) based on previously published studies, and its global accessibility depending on parameters such as price, infrastructure requirements, distribution network, and acceptability as evaluated based on our own experience. The clinical performance in a population can be estimate by the proportion of infected persons tested and detected positive. Abs, antibodies; Ag, antigen; HIV Abs, anti-HIV antibodies; HCV Abs, anti-HCV antibodies; IA, immuno-assay; NAT, Nucleic acid tests; Near-POC NAT, Near point of care NAT; RDT, rapid diagnostic test. **(C)** DBS analyses during the therapeutic cascade for HIV, HBV, and HCV infections. The sampling on DBS allows the realization of the *in vitro* assays which are necessary at each steps of the therapeutic cascade: screening, confirmation, measurement of the replication, analysis of the therapeutic failures. Recommendations of WHO to the usage of DBS are indicated for each step of the cascade.

(Hofmann et al., 2017). In southern countries and areas with difficult access the DBS allows large-scale surveys to plan and monitor health programs. DBS specimens collected during Demographic and Health Surveys (DHS) are useful for estimating the prevalence of diseases, allowing reliable countrywide and regional distribution of HIV estimates (Bellan et al., 2013), but also of hepatitis B, C, and delta, as recently reported (Meda et al., 2018; Njouom et al., 2018; Tuaillon et al., 2018).

DBS IN THE THERAPEUTIC CASCADE OF CARE

Reaching and testing persons at risk of HBV, HCV, and HIV is a main challenge as part of the global effort to eliminate these infections as public health threats by 2030 (World Health Organization [WHO], 2016). Diagnosis of viral hepatitis and HIV follows a sequential strategy initiated by serological screening based on the detection of antibodies or antigens, to which succeeds a confirmation step and the therapeutic monitoring (**Figure 1C**). DBS analyses can be integrated into each steps of the diagnosis cascade.

DBS for Screening and Serologic Confirmation of HIV and Viral Hepatitis

Dried blood spot can be used in the initial serological screening step as an alternative to conventional assays based on venipuncture and RDT. DBS can be decentralized such as RDT, but requires a return visit for post-counseling. This second visit leads to a risk of loss to follow up (Bottero et al., 2015). The lower rate of retention in care using DBS is one of the limitations of DBS testing compared to RDT. Nevertheless, questioning health care workers about their perception of DBS testing highlights some advantages related to a diagnostic strategy requiring a second visit: (i) unlike for RDT, the person who performed the DBS does not bear the responsibility of performing the assay and of immediately notifying the diagnosis to the screened subject; (ii) in the event of a positive test, the medical team can anticipate and better organize the post-test counseling; (iii) in an approach of risk-reduction, the time between screening and the result announcement may be perceived as beneficial to raising awareness.

Dried blood spot samples can be used with standard HIV and viral hepatitis immunoassays. Automated immunoassays performed on DBS can be more efficient than RDT based on immuno-concentration, immunochromatography or agglutination methods. We reported that acute HIV infection was detected earlier on DBS using a fourth-generation HIV test (combining detection of total antibody and p24 Ag) compared to RDT (Kania et al., 2015). Suboptimal analytical sensitivity was also reported for HBsAg RDT (Scheiblauer et al., 2010). This analytical sensibility is generally insufficient to meet the minimum requirements of European regulatory authorities and WHO (Lower limit of detection (LOD) < 4 IU/mL) (Chevaliez et al., 2014; World Health Organization [WHO], 2019). HBsAg laboratory tests have a sensitivity <0.1 IU/mL (Tuaillon et al., 2012), suggesting that even with a dilution factor of 10 or 20 times related to the elution step, the DBS testing may have a better sensitivity than HBsAg RDT. Systematic reviews have reported 98% sensitivity and 100% specificity for HBsAg screening on DBS compared to 88.9% sensitivity and 98.4% specificity using HBsAg RDT (Amini et al., 2017; Lange et al., 2017a). By contrast, the overall performances of RDT and DBS test dedicated to anti-HCV detection appeared very close, with 98% sensitivity, and 99% specificity using DBS, and 98% sensitivity and 100% sensitivity using RDT (Lange et al., 2017a; Tang et al., 2017).

The confirmation of a positive screening test is a second and often crucial step in the cascade of care. DBS can be used for confirmation of anti-HIV and anti-HCV detection on Western blot. Results in band patterns are similar to those observed in blood and comparable performances in term of sensitivity and specificity (Tuaillon et al., 2010; Kania et al., 2013; Manak et al., 2018). However, these assays are rarely available in low incomes countries, and were generally expensive. Confirmation by genomic detection on DBS is also an effective means of confirming infections with HCV, HBV, and HIV (Tuaillon et al., 2010; Nhan et al., 2014). Nucleic acid tests on DBS are able to confirm and HIV and HCV replication since the RNA level is generally higher than the LOD in treatment naïve subjects (Smit et al., 2014; Nguyen et al., 2018), and to detect chronic active HBV infections (HBV DNA $>$ 2000 IU/ml). Access to a more efficient diagnostic tool in case of high clinical suspicion despite a negative result of TDR could be considered as another way of DBS use (Kania et al., 2015).

DBS for HIV and Viral Hepatitis Molecular Testing to Detect Viral Replication, Therapeutic Response and Virologic Theray Failure

One of the most obvious indications of the DBS concerns HIV, HBV, and HCV molecular tests. Testing HIV, HBV, and HCV nucleic acids is necessary for therapeutic initiation or monitoring of the therapeutic response. However, access to nucleic acid tests remains very limited in low income countries. The performances of most commercial HIV-1 RNA assays have been evaluated on DBS: Abbott RealTime, Roche Cobas, Siemens Versant, bioMérieux Nuclisens, Biocentric Generic, Cepheid GeneXpert. The Abbott test has been the most largely used assay, and can be considered as the reference for HIV viral load on DBS. The authors conclude quite consensually on the satisfactory performance of viral load on DBS (Smit et al., 2014). Nevertheless, the variability of the results must be underlined. Sensitivities ranged from less than 80% to almost 100% at the threshold of 1000 HIV RNA/mL recommended by WHO for virological failure, and specificity from less than 60% to nearly 95% for a given test (Smit et al., 2014; World Health Organization [WHO], 2014; Taieb et al., 2016). The viral reservoir of HIV DNA induces a quantification bias when whole blood is used. The HIV DNA contained in infected cells is released into the DBS eluate. We have shown that the risk of over-quantification becomes greater over 10^6 HIV DNA copies per million of peripheral blood mononuclear cells (Zida et al., 2016). The use of a

specific extraction of RNA or DNAse significantly improves the specificity (Rollins et al., 2002). At a threshold of 5000 HIV RNA copies/mL, the techniques on DBS show better performances, but this high threshold implies a deterioration of the negative predictive value for a test of therapeutic failure (World Health Organization [WHO], 2014).

The detection of nucleic acids on DBS also finds a strong clinical indication in the diagnosis of infections transmitted from mother to child. Regarding HIV diagnosis, the presence of maternal antibodies in infants makes serological tests ineffective until at least 1 year of age. Molecular diagnosis of HIV infection on DBS has been shown to be effective (Rollins et al., 2002) and is routinely used in clinical practice for this indication. DBS sampling is finally useful for specialized tests such as HIV resistance genotyping, and antiretroviral dosages (D'Avolio et al., 2010; Monleau et al., 2014). It should be noted that although the clinical relevance of HIV resistance genotyping on DBS is indisputable, it nevertheless faces the difficulty of molecular genotyping on DBS, at the threshold defining the therapeutic failure (Monleau et al., 2014).

For viral hepatitis, there are fewer data on molecular tests, but they show better clinical performance than those published for HIV. For HBV, sensitivities and specificities are estimated at 95% on average (D'Avolio et al., 2010), and the threshold for inactive hepatitis is easily reached in DBS (<2000 IU/mL, approximately equivalent to <10,000 DNA copies/mL). For HCV, mean sensitivities and specificities are also high and estimated >98% (Lange et al., 2017b), which can be explained by the paucity of low HCV viremia during the natural history of this infection. Confirmation of HCV viremia by testing HCV core antigen (HCVcAg) on DBS has also recently been reported in intravenous drug users living in Africa and Asia (Mohamed et al., 2017; Nguyen et al., 2018). This method appeared highly specific and may benefit from substantial stability under prolonged storage conditions but with a lower analytical sensitivity compared to DBS HCV RNA testing (Soulier et al., 2016; Nguyen et al., 2018).

SEROLOGICAL AND MOLECULAR TESTING USING DBS IN THE FIELD

Heterogeneity in the pre-analytical procedures used for DBS specimens between laboratories influence the result and make comparisons difficult. The size of the spot, the nature of the elution buffer, the elution volume – and therefore the dilution factor -, the extraction technique, impact the performance of the tests. WHO guidelines for the implementation of HIV viral load and viral hepatitis tests stress the need for the manufacturers to provide application notes for the use of DBS, and at best to pursue regulatory approval for *in vitro* diagnostics using DBS specimens (World Health Organization [WHO], 2014, 2017). The bioMerieux Nuclisens and Abbott RealTime HIV-1 viral load kits have obtained regulatory approval for use on DBS. On this matrix, the detection threshold (95% detection) is 802 copies/ml for the bioMerieux test (CE-IVD) and 839 copies/ml for the Abbott test (CE-IVD and WHO prequalification). However, a study has shown that the detection rate does not reach 95% for viral loads between 1000 and 5000 RNA copies/mL (Viljoen et al., 2010). WHO pre-qualification of the Abbott HIV test on DBS, report a sensitivity of 76.0% and a specificity of 89.7% at the threshold of 1000 RNA copies/mL (World Health Organization [WHO], 2018). Several qualitative RNA/DNA tests have regulatory approval for the perinatal diagnosis of HIV infection on DBS: the Cepheid XPERT HIV-1 QUAL test that detects HIV-1 DNA and RNA, the Abbott RealTime Qualitative test, as well as the Roche COBAS qualitative test.

For viral hepatitis B and C, no viral load test performed from DBS is currently IVD approved. The same scarcity situation must be noted for viral serology techniques, for which there is neither regulatory approval for use on DBS nor official application note from manufacturers. Despite these important limitations, DBS collection is recommended by WHO for diagnosis of HIV and viral hepatitis B and C in field settings to improve access to screening and management of populations with poor access to serum tests (Soulier et al., 2016; Taieb et al., 2018).

CONCLUSION

Capillary blood collected on blotting paper is an alternative method of sampling with many advantages compared to serum or plasma specimens. The lower analytical sensitivity of assays performed on DBS compared to serum/plasma is one of the limits of DBS, since biomarkers can be present at very low concentration during infection. However, data suggest that the analytical sensitivity of DBS is generally higher than RDT. Another limitation is the lack of commitment by manufacturers to use serological and molecular tests on DBS specimens. The pre-analytical steps of laboratory analyses performed on DBS keep a manual character, including the following steps: to punch out of the spot from each blood-soaked circle, to transfer to the elution tube or plate, to put the tube on a laboratory shaker and let the punched DBSs gently elute for a minimum of 2 h, to transfer the tubes to microcentrifuge to eliminate debris from the supernatants. Diagnostic tests on DBS are consequently difficult to integrate into the laboratory workflow. Hence, the tests on DBS require rigorous validation in clinical laboratories to guarantee the quality of the results. Despite these limitations, DBS is a clinically relevant tool for decentralized sampling. DBS can contribute more broadly to improve access to *in vitro* diagnosis in order to reach the treatment target to help end the AIDS epidemic and to eliminate viral hepatitis as a public health threat by 2030.

AUTHOR CONTRIBUTIONS

ET, DK, AP, KB, and PV contributed to the conception and wrote the manuscript. FT, EO, RS, J-CP, and AM participated to wrote and analysis. All authors read and approved the final manuscript.

REFERENCES

Abou Tayoun, A. N., Burchard, P. R., Malik, I., Scherer, A., and Tsongalis, G. J. (2014). Democratizing molecular diagnostics for the developing world. *Am. J. Clin. Pathol.* 141, 17–24. doi: 10.1309/AJCPA1L4KPXBJNPG

Accueillir (2014). *accompagner, dépister les personnes à risque d'hépatites B ou C en Languedoc-Roussillon**. Available at: http://www1.chu-montpellier.fr/fr/cohep/actualites/le-depistage-dontformations-trod/ (accessed Febuary 27, 2020).

Almond, D., Madanitsa, M., Mwapasa, V., Kalilani-Phiri, L., Webster, J., Ter Kuile, F., et al. (2016). Provider and user acceptability of intermittent screening and treatment for the control of malaria in pregnancy in Malawi. *Malar. J.* 15, 574. doi: 10.1186/s12936-016-1627-5

Ambroise-Thomas, P., and Meyer, H. A. (1975). Hepatic amebiasis in the Kilimanjaro region. Serodiagnosis on micro-specimens of dried blood and attempts at treatment with tinidazole (fasigyn). *Acta Trop.* 32, 359–364.

Amini, A., Varsaneux, O., Kelly, H., Tang, W., Chen, W., Boeras, D. I., et al. (2017). Diagnostic accuracy of tests to detect hepatitis B surface antigen: a systematic review of the literature and meta-analysis. *BMC Infectious Diseases* 17:698. doi: 10.1186/s12879-017-2772-3

Ashkar, T., and Ochilo, M. (1972). The application of the indirect fluorescent antibody test to samples of sera and dried blood from cattle in the Lambwe Valley, South Nyanza, Kenya. *Bull. World Health Organ.* 47, 769–772.

Bellan, S. E., Fiorella, K. J., Melesse, D. Y., Getz, W. M., Williams, B. G., and Dushoff, J. (2013). Extra-couple HIV transmission in sub-Saharan Africa: a mathematical modelling study of survey data. *The Lancet* 381, 1561–1569. doi: 10.1016/S0140-6736(12)61960-6

Blaurock, G., Rische, H., and Rohne, K. (1950). [Development of the blotting paper method in the dried blood reaction for syphilis]. *Dtsch Gesundheitsw* 5, 462–464.

Bogowicz, P., Moore, D., Kanters, S., Michelow, W., Robert, W., Hogg, R., et al. (2016). HIV testing behaviour and use of risk reduction strategies by HIV risk category among MSM in Vancouver. *Int J STD AIDS* 27, 281–287. doi: 10.1177/0956462415575424

Bottero, J., Boyd, A., Gozlan, J., Carrat, F., Nau, J., Pauti, M.-D., et al. (2015). Simultaneous Human Immunodeficiency Virus-Hepatitis B-Hepatitis C Point-of-Care Tests Improve Outcomes in Linkage-to-Care: Results of a Randomized Control Trial in Persons Without Healthcare Coverage. *Open Forum Infect Dis* 2, ofv162. doi: 10.1093/ofid/ofv162

Chevaliez, S., Challine, D., Naija, H., Luu, T. C., Laperche, S., Nadala, L., et al. (2014). Performance of a new rapid test for the detection of hepatitis B surface antigen in various patient populations. *Journal of Clinical Virology* 59, 89–93. doi: 10.1016/j.jcv.2013.11.010

D'Avolio, A., Simiele, M., Siccardi, M., Baietto, L., Sciandra, M., Bonora, S., et al. (2010). HPLC-MS method for the quantification of nine anti-HIV drugs from dry plasma spot on glass filter and their long term stability in different conditions. *J Pharm Biomed Anal* 52, 774–780. doi: 10.1016/j.jpba.2010.02.026

Farzadegan, H., Noori, K. H., and Ala, F. (1978). Detection of hepatitis-B surface antigen in blood and blood products dried on filter paper. *Lancet* 1, 362–363. doi: 10.1016/s0140-6736(78)91085-1

Foroughi, M., Moayedi-Nia, S., Shoghli, A., Bayanolhagh, S., Sedaghat, A., Mohajeri, M., et al. (2017). Prevalence of HIV, HBV and HCV among street and labour children in Tehran, Iran. *Sex Transm Infect* 93, 421–423. doi: 10.1136/sextrans-2016-052557

Global Health Workforce Alliance, and World Health Organization [WHO] (2013). *A Universal Truth: No Health Without a Workforce. Third Global Forum on Human Resources for Health Report**. Available at: http://www.who.int/workforcealliance/knowledge/resources/hrhreport2013/en/ (accessed Febuary 27, 2020).

Hofmann, A., Hauser, A., Zimmermann, R., Santos-Hövener, C., Bätzing-Feigenbaum, J., Wildner, S., et al. (2017). Surveillance of recent HIV infections among newly diagnosed HIV cases in Germany between 2008 and 2014. *BMC Infect. Dis.* 17:484. doi: 10.1186/s12879-017-2585-4

Kania, D., Bekalé, A. M., Nagot, N., Mondain, A.-M., Ottomani, L., Meda, N., et al. (2013). Combining rapid diagnostic tests and dried blood spot assays for point-of-care testing of human immunodeficiency virus, hepatitis B and hepatitis C infections in Burkina Faso, West Africa. *Clinical Microbiology and Infection* 19, E533–E541. doi: 10.1111/1469-0691.12292

Kania, D., Truong, T. N., Montoya, A., Nagot, N., Van de Perre, P., and Tuaillon, E. (2015). Performances of fourth generation HIV antigen/antibody assays on filter paper for detection of early HIV infections. *J. Clin. Virol.* 62, 92–97. doi: 10.1016/j.jcv.2014.11.005

Lange, B., Cohn, J., Roberts, T., Camp, J., Chauffour, J., Gummadi, N., et al. (2017a). Diagnostic accuracy of serological diagnosis of hepatitis C and B using dried blood spot samples (DBS): two systematic reviews and meta-analyses. *BMC Infectious Diseases* 17:700. doi: 10.1186/s12879-017-2777-y

Lange, B., Roberts, T., Cohn, J., Greenman, J., Camp, J., Ishizaki, A., et al. (2017b). Diagnostic accuracy of detection and quantification of HBV-DNA and HCV-RNA using dried blood spot (DBS) samples – a systematic review and meta-analysis. *BMC Infectious Diseases* 17:693. doi: 10.1186/s12879-017-2776-z

Lot, F., Semaille, C., Cazein, F., Barin, F., Pinget, R., Pillonel, J., et al. (2004). Preliminary results from the new HIV surveillance system in France. *Euro Surveill.* 9, 34–37.

Manak, M. M., Hack, H. R., Shutt, A. L., Danboise, B. A., Jagodzinski, L. L., and Peel, S. A. (2018). Stability of Human Immunodeficiency Virus Serological Markers in Samples Collected as HemaSpot and Whatman 903 Dried Blood Spots. *J. Clin. Microbiol.* 56, e933–e918. doi: 10.1128/JCM.00933-18

Marques, B. L. C., Brandão, C. U., Silva, E. F., Marques, V. A., Villela-Nogueira, C. A., Do Ó, K. M. R., et al. (2012). Dried blood spot samples: optimization of commercial EIAs for hepatitis C antibody detection and stability under different storage conditions. *J. Med. Virol.* 84, 1600–1607. doi: 10.1002/jmv.23379

McLeod, A., Weir, A., Aitken, C., Gunson, R., Templeton, K., Molyneaux, P., et al. (2014). Rise in testing and diagnosis associated with Scotland's Action Plan on Hepatitis C and introduction of dried blood spot testing. *J Epidemiol Community Health* 68, 1182–1188. doi: 10.1136/jech-2014-204451

Meda, N., Tuaillon, E., Kania, D., Tiendrebeogo, A., Pisoni, A., Zida, S., et al. (2018). Hepatitis B and C virus seroprevalence, Burkina Faso: a cross-sectional study. *Bulletin of the World Health Organization* 96, 750–759. doi: 10.2471/BLT.18.208603

Mohamed, Z., Mbwambo, J., Shimakawa, Y., Poiteau, L., Chevaliez, S., Pawlotsky, J.-M., et al. (2017). Clinical utility of HCV core antigen detection and quantification using serum samples and dried blood spots in people who inject drugs in Dar-es-Salaam, Tanzania. *Journal of the International AIDS Society* 20, 21856. doi: 10.7448/IAS.20.1.21856

Monleau, M., Aghokeng, A. F., Eymard-Duvernay, S., Dagnra, A., Kania, D., Ngo-Giang-Huong, N., et al. (2014). Field evaluation of dried blood spots for routine HIV-1 viral load and drug resistance monitoring in patients receiving antiretroviral therapy in Africa and Asia. *J. Clin. Microbiol.* 52, 578–586. doi: 10.1128/JCM.02860-13

Monleau, M., Butel, C., Delaporte, E., Boillot, F., and Peeters, M. (2010). Effect of storage conditions of dried plasma and blood spots on HIV-1 RNA quantification and PCR amplification for drug resistance genotyping. *J. Antimicrob. Chemother.* 65, 1562–1566. doi: 10.1093/jac/dkq205

Nguyen, T. T., Lemee, V., Bollore, K., Vu, H. V., Lacombe, K., Thi, X. L. T., et al. (2018). Confirmation of HCV viremia using HCV RNA and core antigen testing on dried blood spot in HIV infected peoples who inject drugs in Vietnam. *BMC Infect. Dis.* 18:622. doi: 10.1186/s12879-018-3529-3

Nhan, T. X., Teissier, A., Roche, C., and Musso, D. (2014). Sensitivity of Real-Time PCR Performed on Dried Sera Spotted on Filter Paper for Diagnosis of Leptospirosis. *Journal of Clinical Microbiology* 52, 3075–3077. doi: 10.1128/JCM.00503-14

Njouom, R., Siffert, I., Texier, G., Lachenal, G., Tejiokem, M. C., Pépin, J., et al. (2018). The burden of hepatitis C virus in Cameroon: Spatial epidemiology and historical perspective. *Journal of Viral Hepatitis* 25, 959–968. doi: 10.1111/jvh.12894

Ostler, M. W., Porter, J. H., and Buxton, O. M. (2014). Dried blood spot collection of health biomarkers to maximize participation in population studies. *J Vis Exp* 83, e50973. doi: 10.3791/50973

Pell, C., Meñaca, A., Chatio, S., Hodgson, A., Tagbor, H., and Pool, R. (2014). The acceptability of intermittent screening and treatment versus intermittent preventive treatment during pregnancy: results from a qualitative study in Northern Ghana. *Malar. J.* 13, 432. doi: 10.1186/1475-2875-13-432

Phillips, A., Shroufi, A., Vojnov, L., Cohn, J., Roberts, T., Ellman, T., et al. (2015). Sustainable HIV treatment in Africa through viral-load-informed differentiated care. *Nature* 528, S68–S76. doi: 10.1038/nature16046

RAND Corporation (2007). *Estimating the global health impact of improved diagnostic tools for the developing world*. Santa Monica, CA: RAND Corporation.

Rollins, N. C., Dedicoat, M., Danaviah, S., Page, T., Bishop, K., Kleinschmidt, I., et al. (2002). Prevalence, incidence, and mother-to-child transmission of HIV-1 in rural South Africa. *Lancet* 360, 389. doi: 10.1016/s0140-6736(02)09599-5

Rottinghaus, E., Bile, E., Modukanele, M., Maruping, M., Mine, M., Nkengasong, J., et al. (2013). Comparison of Ahlstrom grade 226, Munktell TFN, and Whatman 903 filter papers for dried blood spot specimen collection and subsequent HIV-1 load and drug resistance genotyping analysis. *J. Clin. Microbiol.* 51, 55–60. doi: 10.1128/JCM.02002-12

Sander, J., and Niehaus, C. (1980). [Rubella screening using the haemolysis-in-gel test from dried newborn blood on filter paper (author's transl)]. *Dtsch. Med. Wochenschr.* 105, 827–829. doi: 10.1055/s-2008-1070762

Schaub, R. (2017). Hepatitis Band C in the migrant and transboundary communities of the Maroni River: the MaHevi research project*.

Scheiblauer, H., El-Nageh, M., Diaz, S., Nick, S., Zeichhardt, H., Grunert, H.-P., et al. (2010). Performance evaluation of 70 hepatitis B virus (HBV) surface antigen (HBsAg) assays from around the world by a geographically diverse panel with an array of HBV genotypes and HBsAg subtypes. *Vox Sang.* 98, 403–414. doi: 10.1111/j.1423-0410.2009.01272.x

Shokoohi, M., Karamouzian, M., Khajekazemi, R., Osooli, M., Sharifi, H., Haghdoost, A. A., et al. (2016). Correlates of HIV Testing among Female Sex Workers in Iran: Findings of a National Bio-Behavioural Surveillance Survey. *PLoS ONE* 11:e0147587. doi: 10.1371/journal.pone.0147587

Smit, P. W., Sollis, K. A., Fiscus, S., Ford, N., Vitoria, M., Essajee, S., et al. (2014). Systematic review of the use of dried blood spots for monitoring HIV viral load and for early infant diagnosis. *PLoS ONE* 9:e86461. doi: 10.1371/journal.pone.0086461

Soulier, A., Poiteau, L., Rosa, I., Hézode, C., Roudot-Thoraval, F., Pawlotsky, J.-M., et al. (2016). Dried Blood Spots: A Tool to Ensure Broad Access to Hepatitis C Screening, Diagnosis, and Treatment Monitoring. *J Infect Dis.* 213, 1087–1095. doi: 10.1093/infdis/jiv423

Taieb, F., Tram, T. H., Ho, H. T., Pham, V. A., Nguyen, L., Pham, B. H., et al. (2016). Evaluation of Two Techniques for Viral Load Monitoring Using Dried Blood Spot in Routine Practice in Vietnam (French National Agency for AIDS and Hepatitis Research 12338). *Open Forum Infect Dis* 3, ofw142. doi: 10.1093/ofid/ofw142

Taieb, F., Tran Hong, T., Ho, H. T., Nguyen Thanh, B., Pham Phuong, T., Viet Ta, D., et al. (2018). First field evaluation of the optimized CE marked Abbott protocol for HIV RNA testing on dried blood spot in a routine clinical setting in Vietnam. *PLoS ONE* 13:e0191920. doi: 10.1371/journal.pone.0191920

Tang, W., Chen, W., Amini, A., Boeras, D., Falconer, J., Kelly, H., et al. (2017). Diagnostic accuracy of tests to detect Hepatitis C antibody: a meta-analysis and review of the literature. *BMC Infectious Diseases* 17:695. doi: 10.1186/s12879-017-2773-2

Tuaillon, E., Kania, D., Gordien, E., Van de Perre, P., and Dujols, P. (2018). Epidemiological data for hepatitis D in Africa. *Lancet Glob Health* 6, e33. doi: 10.1016/S2214-109X(17)30463-1

Tuaillon, E., Mondain, A.-M., Meroueh, F., Ottomani, L., Picot, M.-C., Nagot, N., et al. (2010). Dried blood spot for hepatitis C virus serology and molecular testing. *Hepatology* 51, 752–758. doi: 10.1002/hep.23407

Tuaillon, E., Mondain, A.-M., Nagot, N., Ottomani, L., Kania, D., Nogue, E., et al. (2012). Comparison of serum HBsAg quantitation by four immunoassays, and relationships of HBsAg level with HBV replication and HBV genotypes. *PLoS ONE* 7:e32143. doi: 10.1371/journal.pone.0032143

Viljoen, J., Gampini, S., Danaviah, S., Valéa, D., Pillay, S., Kania, D., et al. (2010). Dried blood spot HIV-1 RNA quantification using open real-time systems in South Africa and Burkina Faso. *J. Acquir. Immune Defic. Syndr.* 55, 290–298. doi: 10.1097/QAI.0b013e3181edaaf5

Waters, L., Kambugu, A., Tibenderana, H., Meya, D., John, L., Mandalia, S., et al. (2007). Evaluation of filter paper transfer of whole-blood and plasma samples for quantifying HIV RNA in subjects on antiretroviral therapy in Uganda. *J. Acquir. Immune Defic. Syndr.* 46, 590–593. doi: 10.1097/qai.0b013e318159d7f4

World Health Organization [WHO] (2014). *Technical and operational considerations for implementing HIV viral load testing: interim technical update*. Geneva: WHO.

World Health Organization [WHO] (2016). *Combating hepatitis B and C to reach elimination by 2030*. Geneva: World Health Organization.

World Health Organization [WHO] (2017). *Guidelines on hepatitis B and C testing*. Geneva: WHO.

World Health Organization [WHO] (2018). *Public reports of World Health Organization prequalified IVDs: Abbott RealTime HIV-1 (m2000sp). PQDx* 0145-027-00. 2018, version 8.0. Geneva: WHO.

World Health Organization [WHO] (2019). *Performance evaluation acceptance criteria for HBsAg In vitro diagnostics in the context of WHO prequalification**. Available at: http://www.who.int/diagnostics_laboratory/evaluations/hepb/161125_who_performance_criteria_hbsag_ivd.pdf (accessed Febuary 27, 2020).

Zida, S., Tuaillon, E., Barro, M., Kwimatouo Lekpa Franchard, A., Kagoné, T., Nacro, B., et al. (2016). Estimation of HIV-1 DNA Level Interfering with Reliability of HIV-1 RNA Quantification Performed on Dried Blood Spots Collected from Successfully Treated Patients. *J. Clin. Microbiol.* 54, 1641–1643. doi: 10.1128/JCM.03372-15

Conflict of Interest: The authors declare that the research was conducted in the absence of any commercial or financial relationships that could be construed as a potential conflict of interest.

frontiers in Microbiology

METHODS
published: 20 March 2020
doi: 10.3389/fmicb.2020.00440

Rapid and Low-Cost Culture-Based Method for Diagnosis of Mucormycosis Using a Mouse Model

*Afsane Vaezi[1,2], Hamed Fakhim[3,4], Macit Ilkit[5], Leila Faeli[2,6], Mahdi Fakhar[7], Vahid Alinejad[8], Nathan P. Wiederhold[9] and Hamid Badali[1,2,9]**

[1] Invasive Fungi Research Center, School of Medicine, Mazandaran University of Medical Sciences, Sari, Iran, [2] Department of Medical Mycology, School of Medicine, Mazandaran University of Medical Sciences, Sari, Iran, [3] Department of Medical Parasitology and Mycology, Faculty of Medicine, Urmia University of Medical Sciences, Urmia, Iran, [4] Infectious Diseases and Tropical Medicine Research Center, Isfahan University of Medical Sciences, Isfahan, Iran, [5] Division of Mycology, Department of Microbiology, Faculty of Medicine, University of Çukurova, Adana, Turkey, [6] Student Research Committee, Mazandaran University of Medical Sciences, Sari, Iran, [7] Toxoplasmosis Research Center, Department of Parasitology, Mazandaran University of Medical Sciences, Sari, Iran, [8] Patient Safety Research Center, Urmia University of Medical Sciences, Urmia, Iran, [9] Fungus Testing Laboratory, Department of Pathology and Laboratory Medicine, University of Texas Health Science Center at San Antonio, San Antonio, TX, United States

Prompt and targeted antifungal treatment has a positive impact on the clinical outcome of mucormycosis; however, current diagnostic tools used in histopathology laboratories often fail to provide rapid results. Rapid culture-based strategies for early diagnosis of *Mucorales* infections, which may influence treatment decisions, are urgently needed. Herein, we evaluated a microculture assay for the early diagnosis of mucormycosis in an immunocompetent murine model of disseminated infection, by comparing it with traditional diagnostic methods. The assay specificity was assessed using blood (n = 90) and tissue (n = 90) specimens obtained from mice infected with *Rhizopus arrhizus* using different inoculum sizes [1×10^4, 1×10^5, and 1×10^6 colony forming units (CFUs)/mouse] and blood (n = 15) and tissue specimens (n = 15) from uninfected mice. Surprisingly, 26 of 90 (28.9%) blood samples revealed positive results by microculture, whereas all blood samples were negative when assayed by conventional culture. The overall positive conventional culture rate for the mouse tissue (kidney) samples was 31.1% (28/90). The calculated sensitivity for kidney microculture was 98.8% [95% confidence interval (CI) 96.6–100], with an assay specificity of 100%. Hence, the microculture assay may be useful for rapid culturing and diagnosis of mucormycosis caused by *R. arrhizus* directly in blood and tissue samples. Hence, this method may allow for the timely administration of an appropriate treatment.

Keywords: microculture, rapid diagnosis, *Rhizopus arrhizus*, mucormycosis, murine model

OPEN ACCESS

Edited by:
David Ong, Franciscus Gasthuis & Vlietland, Netherlands

Reviewed by:
Alexandre Alanio, Paris Diderot University, France
Abdullah M. S. Al-Hatmi, Ministry of Health, Oman

***Correspondence:**
Hamid Badali
badalii@yahoo.com; badali@uthscsa.edu

Specialty section:
This article was submitted to Fungi and Their Interactions, a section of the journal Frontiers in Microbiology

Received: *21 November 2019*
Accepted: *02 March 2020*
Published: *20 March 2020*

Citation:
Vaezi A, Fakhim H, Ilkit M, Faeli L, Fakhar M, Alinejad V, Wiederhold NP and Badali H (2020) Rapid and Low-Cost Culture-Based Method for Diagnosis of Mucormycosis Using a Mouse Model. Front. Microbiol. 11:440. doi: 10.3389/fmicb.2020.00440

INTRODUCTION

Mucormycosis (previously called zygomycosis), an aggressive infection caused by mucoralean fungi, is the third most prevalent fungal disease after candidiasis and aspergillosis, among populations at high risk, including those with uncontrolled diabetes, solid organ or allogeneic stem cell transplant recipients, and patients undergoing immunosuppressive therapies (Petrikkos et al., 2012; Danion et al., 2015; Farmakiotis and Kontoyiannis, 2016; Hoenigl et al., 2018; Cornely et al., 2019). The reported incidence of mucormycosis is 0.2–95 cases per 1,000,000 individuals in

Europe; 3.0 cases per 1,000,000 individuals in the United States; 1.2 cases per 1,000,000 individuals in Canada; and 0.6 cases per 1,000,000 individuals in Australia (Skiada et al., 2012). Although few studies in Asia have reported the prevalence of *Mucorales* infections (Yamazaki et al., 1999; Chakrabarti and Singh, 2014; Vaezi et al., 2016), a national investigation of medical autopsies revealed that the incidence of these infections in Japan increased by 16% in a 20-year span (Prakash and Chakrabarti, 2019). Early diagnosis and application of multimodal treatment, including appropriate antifungal therapy, may have a positive impact on clinical outcomes in patients with mucormycosis, including improved survival rates (Spellberg et al., 2005; Skiada et al., 2018).

The current gold standard for diagnosing mucormycosis is based on histopathological and mycological findings, followed by unspecific radiological criteria. However, these procedures require specialized expertise and the results are often not available in a timely fashion (Hammond et al., 2011; Cornely et al., 2019). To enhance outcomes, patients suspected to have mucormycosis should be immediately treated. Despite our improved understanding of the disease and the availability of various medico-surgical treatments, the survival rate in mucormycosis patients remains poor (Kontoyiannis and Lewis, 2011; Katragkou et al., 2014; Pilmis et al., 2018; Skiada et al., 2018). Therefore, there is a need for novel diagnostic assays. Several new molecular methods for the diagnosis of mucormycosis have been reported (Hammond et al., 2011; Dadwal and Kontoyiannis, 2018); however, these techniques may lack sensitivity, can be time-consuming and expensive to perform, and are not universally available (Katragkou et al., 2014).

The choice of an effective treatment regimen against mucormycosis requires early diagnosis and identification of the causative pathogen and its antifungal susceptibility profile, for which a positive culture is needed (Walsh et al., 2014; Hoenigl et al., 2018; Cornely et al., 2019). However, due to the unique physiology of these etiological agents (e.g., fragile and non-septate hyphae), cultures are frequently negative, and the processing of clinical specimens requires a suspicion of *Mucorales* as the causative agent and experienced laboratory personnel than may be required for fungi with septate hyphae (Ben-Ami et al., 2009; Hammond et al., 2011; Lewis et al., 2013; Cornely et al., 2019).

Here, we report the first study to evaluate a microculture assay as a putative, rapid, and low-cost culture-based method for the early diagnosis of mucormycosis. An established murine model was utilized to compare the performance of this microculture assay with those of traditional diagnostic methods.

MATERIALS AND METHODS

Isolate and Inocula

Rhizopus arrhizus var. *arrhizus* clinical isolate (CBS 112.07), obtained from the reference culture collection of the Westerdijk Fungal Biodiversity Institute (Utrecht, Netherlands), was used in this study. Species identity was confirmed by DNA sequence analysis of the internal transcribed spacer (ITS) region of ribosomal DNA (rDNA), as previously described (Nagao et al., 2005). For inoculum preparation, the strain was sub-cultured onto potato dextrose agar (PDA) at 37°C (Difco, Leeuwarden, Netherlands) 10 days before the inoculation in mice to ensure viability and purity. On the day of inoculation, sterile phosphate-buffered saline (PBS) containing 0.1% (v/v) Tween 20 was added to the plate, and the surface of colonies was gently scraped. After centrifugation at 15,000 rpm for 15 min, the supernatant was removed, and the cells were washed twice in PBS. The spore count was enumerated with a hemocytometer for preparing the final inocula. The cell concentrations were adjusted to three different inoculum sizes, 1×10^4, 1×10^5, and 1×10^6 spores/ml. To confirm each inoculum size, dilutions were prepared and streaked onto PDA, and the fungal colonies were enumerated after 24 h of incubation at 30°C.

Animal Model

Female immunocompetent ICR mice (weighing 22–25 g, 6-week old, $n = 105$) were purchased from the Royan Institute (Tehran, Iran). The animals were housed in groups of 30 mice each at the Animal Experimentation Facility under standard conditions. All mice were provided food and water *ad libitum* and were monitored daily, based on the recommendations of the guide for the Care and Use of Laboratory Animals of the National Research Council (2011). All animal experiments were approved by the Institutional Animal Ethical Committee (IAEC) of Mazandaran University of Medical Sciences, Sari, Iran (IR.MAZUMS.REC.1397.9).

Experimental Model of Disseminated Infection

In total, 90 mice were randomly divided into three groups ($n = 30$ per group), and a 0.2 ml solution containing one of the three inocula [1×10^4, 1×10^5, and 1×10^6 colony forming units (CFUs)/mouse] was injected into the lateral tail vein of each mouse. Pilot experiments demonstrated that the inoculum sizes of 1×10^4, 1×10^5, and 1×10^6 CFU/mouse proved to be the optimal doses leading to a severe infection; all animals died within 10 days of infection. In the fungal burden arm, mice were sacrificed by cervical dislocation on experimental day 4 post-infection. After sacrifice, kidneys were removed, homogenized, serially diluted (1:10), and plated on Sabouraud dextrose agar (SDA) for CFU/g calculation. The control group ($n = 15$) received intravenous injections of cell-free PBS using the same method. Mice were assessed at least twice daily, and moribund mice were euthanized by exsanguination (intracardiac puncture under general anesthesia) (Conti et al., 2014) after detecting symptoms of disseminated infection. Moribund animals were identified by the following criteria: decreased activity, inability to eat or drink, hypothermia, hunched posture, and torticollis or barrel rolling.

Histopathological and Mycological Characterization

Blood and tissue (kidney) samples were recovered under aseptic conditions. Blood samples were collected by cardiac puncture

(approximately 200 μl into heparin-coated tubes) and were stored at −20°C until further analysis. The kidneys were minced and used for histopathology, microculture assay, traditional culture analysis. Kidney samples were first fixed in 10% (w/v) buffered formalin, dehydrated, paraffin-embedded (FFPE), sectioned (5-μm-thick sections), and stained with Periodic acid–Schiff (PAS) for direct microscopic examination, as previously described (Rickerts, 2016). Minced kidney and blood samples were also cultured on SDA and brain heart infusion (BHI) agar at 35°C. Moreover, the blood samples were inoculated into diphasic blood-culture bottles containing BHI broth and agar (Kusha Faravar Giti, Karaj, Iran). The samples were incubated at 37°C for at least 2 weeks. The remainder of the kidney samples and additional blood samples were used for microculture assay. Furthermore, control kidney and blood samples were also collected from uninfected mice for analysis.

Microculture Assay

For the assay, 50 μl of blood was sampled using a sterile non-heparinized 1 × 75 mm glass capillary tube. Blood sampling was performed by extracting the blood directly into the capillary tubes. For tissue samples, 20–50 mg of minced kidney was inserted into a sterile glass Pasteur pipette (146 × 6.5 mm). The capillary tubes and Pasteur pipette were then loaded with 50–70 μl and approximately 200 μl of RPMI 1640 medium (Sigma, St. Louis, MO, United States), respectively. The tubes were sealed with wax and incubated at 35°C. One capillary tube sample and one Pasteur pipette sample were prepared for each animal. All samples were examined daily using an inverted microscope (Motic AE31 Elite Inverted Phase Contrast Microscope, magnification 100×). Culture-negative samples were monitored for up to 30 days. Capillary tubes were examined under a light microscope (Nikon YS100 Biological Microscope, magnification 400×). For the light microscopy analysis, two capillary tubes were placed horizontally on a microscope slide, and another slide was placed over them. The gap between the slides was filled with sterile water.

Statistical Analysis

Median survival time was estimated by the Kaplan–Meier method, compared among groups by the log-rank test. Tissue burden data of tested organ in the different experimental groups were analyzed by using the Kruskal–Wallis test in SPSS (version 17.0 for Windows; Chicago, IL, United States) and plotted using GraphPad Prism version 6.01 (Graph Prism Software Inc., United States). Categorical differences between positive and negative results for samples between the traditional culture (SDA) and microculture techniques were also determined by the equality of mean differences using a Chi-square 2 × 2 contingency table at a 95% confidence interval. p-values < 0.05 were considered as statistically significant.

RESULTS

An overall schematic of this study of the evaluation of microculture for the early diagnosis of mucormycosis in an immunocompetent murine model of disseminated infection compared with routinely performed methods is shown in **Figure 1**.

Preliminary experiments using three different inocula demonstrated that median survival time was 8, 7, and 5 days for mouse inoculation with 1×10^4, 1×10^5, and 1×10^6 CFU/mouse, respectively (**Figure 2**). The fungal tissue burden results are summarized in **Figure 3**. Fungal burden was significantly higher in mice infected with 1×10^6 CFUs compared to the other inocula levels in the 1×10^4 and 1×10^5 CFU/mouse groups ($p < 0.001$).

Histopathological examination of kidney sections stained with PAS revealed irregular, broad, and non-septate hyphae, hallmarks of *Mucorales*, with several foreign bodies and langhans giant cells surrounded by a dense inflammatory response (**Figure 4A**). Subsequently, the performance of the microculture assay was evaluated by comparing it with culturing on media plates.

Diagnostic Performance of the Microculture Assay

Blood Samples

The animals were euthanized on days 3–7 post-infection. Of the 90 blood samples, 26 (28.9%) were positive using the microculture assay (**Figures 4B,C**). This included 6 in the lower inoculum group, 11 in the medium inoculum group, and 9 in the high inoculum group. Microculture samples in each group were positive between days 3 and 7 post-inoculations. In contrast, all blood samples were negative by culture (on SDA and BHI).

Kidney Samples

Microculture results were positive in 89 of 90 kidney samples (98.9%). The overall positive conventional culture rate for the mouse kidney samples was 31.1% (28/90). Therefore, 89 samples presented a positive result for kidney microculture assay, of which 28 were in accordance with the results of the SDA culture. There was significant difference in the positive microculture compared with SDA plates ($p < 0.0001$). All the samples collected from the 15 uninfected mice were negative by each assay. The concordance of detection (calculated sensitivity) for kidney microculture was 98.8% (95% CI 96.6–100), with a calculated assay specificity of 100%. For kidney samples, the SDA culture presented the lower sensitivity (33.7%; 95% CI 23.9–43.5). These data demonstrate that the microculture assay (98.9% positivity) is superior to conventional culture (31.1% positivity) in this murine model in detecting *R. arrhizus* directly from the primary blood and kidney samples within 18–24 h of sampling.

DISCUSSION

In this study, we present the results of a microculture assay for timely culture of *R. arrhizus*. This is the first study to demonstrate that a microculture approach can be used for fungal culture within 24 h of sampling. Early diagnosis via multiple approaches is an important aspect of care in patients with mucormycosis (Blyth et al., 2011; Walsh et al., 2014; Hoenigl et al., 2018). A timely and efficient diagnosis, as well as an

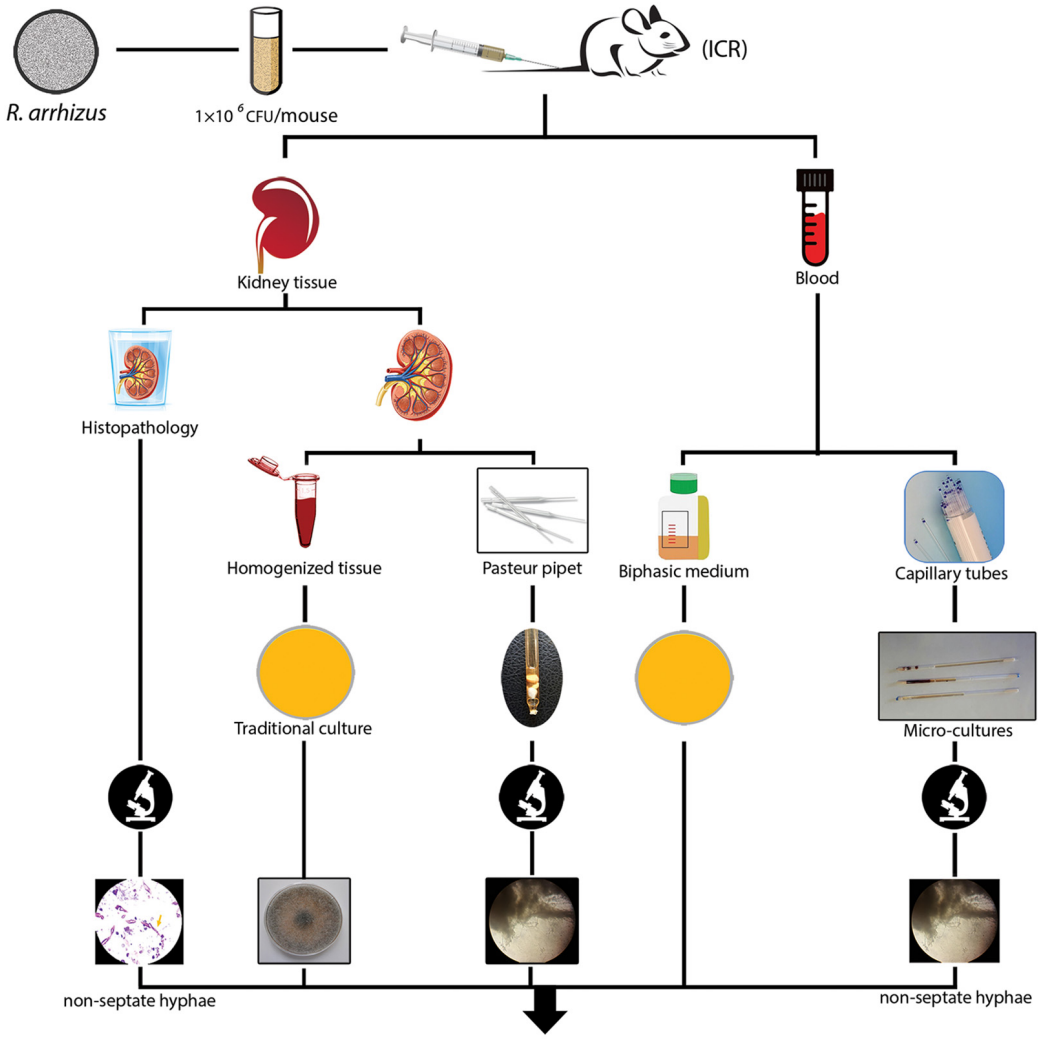

Samples	Assay	No. of positive (%)	No. of negative (%)
Blood (n = 90)	Microculture	26 (28.8)	64 (71.1)
	Traditional Culture (SDA)	0	90 (100)
Tissue (n = 90)	Microculture	89 (98.8)	1 (1.1)
	Traditional Culture (SDA)	28 (31.1)	62 (68.8)

FIGURE 1 | Schematic of this study evaluating microculture compared with the traditional diagnostic methods.

aggressive multimodal treatment approach, is critical in the management of this fulminant progressive and invasive disease, as delays may result in an increased mortality risk (Walsh et al., 2014; Jeong et al., 2016). Indeed, a delay of more than 5 days of an effective antifungal therapy in patients with hematological malignancies leads to approximately twofold increase in 12-week mortality (Spellberg et al., 2005; Chamilos et al., 2008; Palejwala et al., 2016). Rapid mycological diagnostic methods may assist with timely initiation of appropriate antifungal therapy, which may prevent progressive tissue invasion, lead to decreased mortality, and overall improvement in healthcare utilization (i.e., shorter hospitalization duration and reduced costs). Histological analysis is an important diagnostic tool in the early management of this devastating disease (Skiada et al., 2018); however, the 24-h turnaround time of the microculture approach is considerably shorter than that of histological analysis (48–72 h) (Dekio et al., 2015) or conventional culturing (3–7 days) (Skiada et al., 2018).

Conventional tissue fungal cultures are typically positive in only 50% of mucormycosis cases (Skiada et al., 2018). Positive

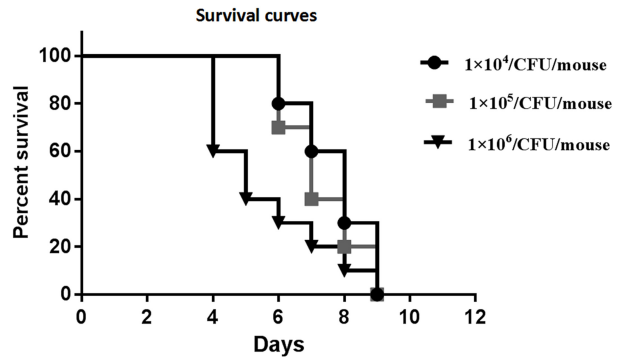

FIGURE 2 | Survival curves of preliminary experiments carried out using three different inoculum sizes [1×10^4, 1×10^5, and 1×10^6 colony forming units (CFUs)/mouse] for each group, which consisted of 10 mice intravenously (IV) infected with the inocula of the *Rhizopus arrhizus* clinical isolate.

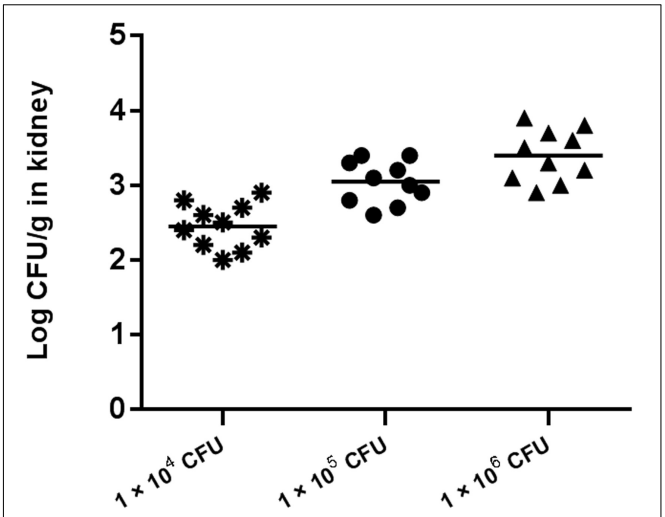

FIGURE 3 | Fungal tissue burden results in ICR mice infected with inocula of 1×10^4, 1×10^5, and 1×10^6 CFU/mouse on day 4.

cultures and fungal identification, even at the genus level only, allow for the appropriate choice of antifungal regimens and further assessment of antifungal resistance patterns and emerging resistance (Cornely et al., 2014; Beardsley et al., 2018). Although some molecular identification methods may be able to provide results within a few hours, the microculture assay described in this study does not require specialized training or equipment. Surprisingly, in the present study, 26 of 90 blood samples were positive by microculture, while all blood samples were negative with traditional culture. Increased CO_2 levels during incubation, leading to a lower pH, may facilitate the growth of *R. arrhizus* in microculture tubes.

Culture-based methods for fungal identification are generally practical, economical, and accessible. The microculture method presented in this study is relatively rapid and easy to perform. Hence, this approach could also be considered for the diagnosis of other fungal infections, which may be challenging using traditional culture methods.

The promising results of the present study require confirmation through further studies. Microculture methods should be further assessed for the detection of other members of the order *Mucorales* as well as in other fungi. In addition, the performance of this assay in other murine models (e.g., pulmonary mucormycosis and in immunosuppressed hosts) should be evaluated. These additional studies are warranted given the relative ease of use of this method and the impact it may have within the clinical microbiology laboratory.

AUTHOR'S NOTE

A part of this work was presented as a poster presentation at the 20th Congress of the International Society for Human and Animal Mycology (ISHAM), Amsterdam, 30 June to 4 July 2018.

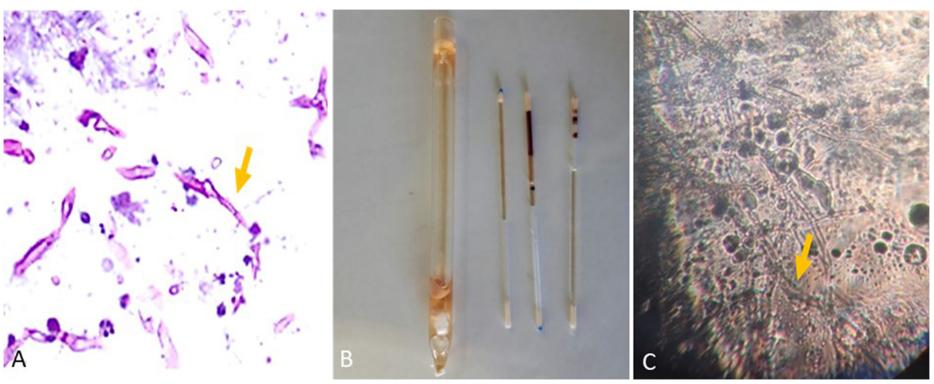

FIGURE 4 | (A) Representative histopathological periodic acid-Schiff (PAS) section of kidney from Institute of Cancer Research (ICR) female mice intravenously infected with *R. arrhizus* (1×10^6 CFU/mouse) tested on day 7 post-challenge. **(B)** Blood and tissue sampling for the microculture assay using a sterile non-heparinized glass capillary tube. **(C)** Images captured 18 h after commencing the experiment (*Mucorales hyphae*).

DATA AVAILABILITY STATEMENT

The raw data supporting the conclusions of this article will be made available by the authors, without undue reservation, to any qualified researcher.

ETHICS STATEMENT

This study was carried out in accordance with the recommendations of Guide for the Care and Use of Laboratory Animals, Committee for the Update of the Guide for the Care and Use of Laboratory Animals. The protocol was approved by the Ethics and Research Committee of Mazandaran University of Medical Sciences, Sari, Iran (IR.MAZUMS.REC.1397.9).

AUTHOR CONTRIBUTIONS

AV and HB contributed to the design and implementation of the research, and drafted the manuscript. AV, HB, and HF curated the data. AV, HB, and VA performed the formal analysis of the study and contributed to funding acquisition and project administration. AV, MF, HF, and LF provided the methodology for this study. MI and NW validated the data and revised the manuscript. All authors contributed to approve the final version of the manuscript.

FUNDING

The work of HB partially was supported by a grant (Nr. 9) from the School of Medicine, Mazandaran University of Medical Sciences, Sari, Iran, which we gratefully acknowledge.

ACKNOWLEDGMENTS

The authors are indebted to Dr. Sarvi and his colleagues for their excellent technical assistance with the animal experiments at the Mazandaran University of Medical Sciences, Sari, Iran. In addition, they would like to acknowledge Hossein Chehre for providing the photographic plates.

REFERENCES

Beardsley, J., Halliday, C. L., Chen, S. C., and Sorrell, T. C. (2018). Responding to the emergence of antifungal drug resistance: perspectives from the bench and the bedside. *Future Microbiol.* 13, 1175–1191. doi: 10.2217/fmb-2018-0059

Ben-Ami, R., Luna, M., Lewis, R. E., Walsh, T. J., and Kontoyiannis, D. P. (2009). A clinicopathological study of pulmonary mucormycosis in cancer patients: extensive angioinvasion but limited inflammatory response. *J. Infect.* 59, 134–138. doi: 10.1016/j.jinf.2009.06.002

Blyth, C. C., Gomes, L., Sorrell, T. C., da Cruz, M., Sud, A., and Chen, S. C. (2011). Skull-base osteomyelitis: fungal vs. bacterial infection. *Clin. Microbiol. Infect.* 17, 306–311. doi: 10.1111/j.1469-0691.2010.03231.x

Chakrabarti, A., and Singh, R. (2014). Mucormycosis in India: unique features. *Mycoses* 57(Suppl. 3), 85–90. doi: 10.1111/myc.12243

Chamilos, G., Lewis, R. E., and Kontoyiannis, D. P. (2008). Delaying amphotericin B-based frontline therapy significantly increases mortality among patients with hematologic malignancy who have zygomycosis. *Clin. Infect. Dis.* 47, 503–509. doi: 10.1086/590004

Conti, H. R., Huppler, A. R., Whibley, N., and Gaffen, S. L. (2014). Animal models for candidiasis. *Curr. Protoc. Immunol.* 105, 11–17. doi: 10.1002/0471142735.im1906s105

Cornely, O. A., Alastruey-Izquierdo, A., Arenz, D., Chen, S. C. A., Dannaoui, E., Hochhegger, B., et al. (2019). Global guideline for the diagnosis and management of mucormycosis: an initiative of the European confederation of medical mycology in cooperation with the mycoses study group education and research consortium. *Lancet Infect. Dis.* 19, e405–e421. doi: 10.1016/S1473-3099(19)30312-3

Cornely, O. A., Arikan-Akdagli, S., Dannaoui, E., Groll, A. H., Lagrou, K., Chakrabarti, A., et al. (2014). European society of clinical microbiology and infectious diseases fungal infection study group; European confederation of medical mycology. ESCMID and ECMM joint clinical guidelines for the diagnosis and management of mucormycosis 2013. *Clin. Microbiol. Infect.* 20(Suppl. 3), 5–26. doi: 10.1111/1469-0691.12371

Dadwal, S. S., and Kontoyiannis, D. P. (2018). Recent advances in the molecular diagnosis of mucormycosis. *Expert Rev. Mol. Diagn.* 18, 845–854. doi: 10.1080/14737159.2018.1522250

Danion, F., Aguilar, C., Catherinot, E., Alanio, A., DeWolf, S., Lortholary, O., et al. (2015). Mucormycosis: new developments into a persistently devastating infection. *Semin. Respir. Crit. Care Med.* 36, 692–705. doi: 10.1055/s-0035-1562896

Dekio, F., Bhatti, T. R., Zhang, S. X., and Sullivan, K. V. (2015). Positive impact of fungal histopathology on immunocompromised pediatric patients with histology-proven invasive fungal infection. *Am. J. Clin. Pathol.* 144, 61–67. doi: 10.1309/AJCPEMVYT88AVFKG

Farmakiotis, D., and Kontoyiannis, D. P. (2016). Mucormycoses. *Infect. Dis. Clin. North Am.* 30, 143–163. doi: 10.1016/j.idc.2015.10.011

Hammond, S. P., Bialek, R., Milner, D. A., Petschnigg, E. M., Baden, L. R., and Marty, F. M. (2011). Molecular methods to improve diagnosis and identification of mucormycosis. *J. Clin. Microbiol.* 49, 2151–2153. doi: 10.1128/JCM.00256-11

Hoenigl, M., Gangneuxm, J. P., Segal, E., Alanio, A., Chakrabarti, A., Chen, S. C., et al. (2018). Global guidelines and initiatives from the European confederation of medical mycology to improve patient care and research worldwide: new leadership is about working together. *Mycoses* 61, 885–894. doi: 10.1111/myc.12836

Jeong, S. J., Lee, J. U., Song, Y. G., Lee, K. H., and Lee, M. J. (2016). Delaying diagnostic procedure significantly increases mortality in patients with invasive mucormycosis. *Mycoses* 58, 746–752. doi: 10.1111/myc.12428

Katragkou, A., Walsh, T. J., and Roilides, E. (2014). Why is mucormycosis more difficult to cure than more common mycoses? *Clin. Microbiol. Infect.* 20(Suppl. 6), 74–81. doi: 10.1111/1469-0691.12466

Kontoyiannis, D. P., and Lewis, R. E. (2011). How I treat mucormycosis. *Blood* 118, 1216–1224. doi: 10.1182/blood-2011-03-316430

Lewis, R. E., Cahyame-Zuniga, L., Leventakos, K., Chamilos, G., Ben-Ami, R., Tamboli, P., et al. (2013). Epidemiology and sites of involvement of invasive fungal infections in patients with haematological malignancies: a 20-year autopsy study. *Mycoses* 56, 638–645. doi: 10.1111/myc.12081

Nagao, K., Ota, T., Tanikawa, A., Takae, Y., Mori, T., Udagawa, S., et al. (2005). Genetic identification and detection of human pathogenic *Rhizopus* species, a major mucormycosis agent, by multiplex PCR based on internal transcribed spacer region of rRNA gene. *J. Dermatol. Sci.* 39, 23–31. doi: 10.1016/j.jdermsci.2005.01.010

National Research Council (2011). *Guide for the Care and Use of Laboratory Animals*, 8th Edn. Washington, DC: National Academies Press.

Palejwala, S. K., Zangeneh, T. T., Goldstein, S. A., and Lemole, G. M. (2016). An aggressive multidisciplinary approach reduces mortality in rhinocerebral mucormycosis. *Surg. Neurol. Int.* 7:61. doi: 10.4103/2152-7806.182964

Petrikkos, G., Skiada, A., Lortholary, O., Roilides, E., Walsh, T. J., and Kontoyiannis, D. P. (2012). Epidemiology and clinical manifestations of mucormycosis. *Clin. Infect. Dis.* 54(Suppl. 1), S23–S34. doi: 10.1093/cid/cir866

Pilmis, B., Alanio, A., Lortholary, O., and Lanternier, F. (2018). Recent advances in the understanding and management of mucormycosis. *F1000Res* 7:F1000FacultyRev-1429. doi: 10.12688/f1000research.15081.1

Prakash, H., and Chakrabarti, A. (2019). Global epidemiology of mucormycosis. *J. Fungi.* 5:26. doi: 10.3390/jof5010026

Rickerts, V. (2016). Identification of fungal pathogens in Formalin-fixed, Paraffin-embedded tissue samples by molecular methods. *Fungal Biol.* 120, 279–287. doi: 10.1016/j.funbio.2015.07.002

Skiada, A., Lass-Floerl, C., Klimko, N., Ibrahim, A., Roilides, E., and Petrikkos, G. (2018). Challenges in the diagnosis and treatment of mucormycosis. *Med. Mycol.* 56(Suppl. 1), 93–101. doi: 10.1093/mmy/myx101

Skiada, A., Rigopoulos, D., Larios, G., Petrikkos, G., and Katsambas, A. (2012). Global epidemiology of cutaneous zygomycosis. *Clin. Dermatol.* 30, 628–632. doi: 10.1016/j.clindermatol.2012.01.010

Spellberg, B., Edwards, J. Jr., and Ibrahim, A. (2005). Novel perspectives on mucormycosis: pathophysiology, presentation, and management. *Clin. Microbiol. Rev.* 18, 556–569. doi: 10.1128/CMR.18.3.556-569.2005

Vaezi, A., Moazeni, M., Rahimi, M. T., de Hoog, S., and Badali, H. (2016). Mucormycosis in Iran: a systematic review. *Mycoses* 59, 402–415. doi: 10.1111/myc.12474

Walsh, T. J., Skiada, A., Cornely, O. A., Roilides, E., Ibrahim, A., Zaoutis, T., et al. (2014). Development of new strategies for early diagnosis of mucormycosis from bench to bedside. *Mycoses* 57(Suppl. 3), 2–7. doi: 10.1111/myc.12249

Yamazaki, T., Kume, H., Murase, S., Yamashita, E., and Arisawa, M. (1999). Epidemiology of visceral mycoses: analysis of data in annual of the pathological autopsy cases in Japan. *J. Clin. Microbiol.* 37, 1732–1738.

Conflict of Interest: The authors declare that the research was conducted in the absence of any commercial or financial relationships that could be construed as a potential conflict of interest.

The reviewer AA-H declared past co-authorship with several of the authors, AV, HF, MI, and HB, to the handling Editor.

frontiers in Microbiology

MINI REVIEW
published: 24 March 2020
doi: 10.3389/fmicb.2020.00467

Timely Diagnosis of Histoplasmosis in Non-endemic Countries: A Laboratory Challenge

*María José Buitrago[1] and M. Teresa Martín-Gómez[2]**

[1] Mycology Reference Laboratory, National Centre of Microbiology, Instituto de Salud Carlos III, Madrid, Spain, [2] Microbiology Department, Vall d'Hebron University Hospital, Barcelona, Spain

Human histoplasmosis is a fungal infection caused by the inhalation of microconidia of the thermally dimorphic fungi *Histoplasma capsulatum*. Autochthonous cases of histoplasmosis have been diagnosed in almost every country, but it is considered an endemic infection in specific areas of the world. Many of them are popular travel destinations or the source of migratory movements. Thus, the vast majority of the registered cases in non-endemic countries are imported. They correspond to people having been exposed to the fungus in endemic locations as immigrants, expatriates, transient workers or tourists, with reported cases also associated to organ donation. Misdiagnosis and delays in initiation of treatment are not uncommon in cases of imported histoplasmosis. They are associated to high fatality-rates specially in patients with compromised cellular immunity in which progressive disseminated forms develop. The diagnosis of this infection in non-endemic countries is hampered by the lack of clinical suspicion and a dearth of available diagnostic tools adequate to offer rapid and accurate results. Non-culture-based assays such as nucleic-acid amplification tests present as a suitable alternative in this situation, offering improved sensitivity and specificity, shortened turnaround time, and increased biosafety by avoiding culture manipulation. In non-endemic regions, molecular techniques are being used mainly in laboratories from countries that have registered an increase in the incidence of imported cases. However, the number of published techniques is limited and lack consensus. Efforts are currently under way to standardize nucleic acid amplification-based techniques for its implementation in areas registering a rising number of imported cases.

Keywords: histoplasmosis, laboratory, diagnosis, non-endemic areas, PCR

OPEN ACCESS

Edited by:
David Ong, Franciscus Gasthuis & Vlietland, Netherlands

Reviewed by:
Guillaume Desoubeaux, Université de Tours, France
Diego Hernando Caceres, Centers for Disease Control and Prevention (CDC), United States
Antoine Adenis, Centre Hospitalier de Cayenne, French Guiana

****Correspondence:***
M. Teresa Martín-Gómez
mtmartin@vhebron.net

Specialty section:
This article was submitted to Fungi and Their Interactions, a section of the journal Frontiers in Microbiology

Received: *15 November 2019*
Accepted: *04 March 2020*
Published: *24 March 2020*

Citation:
Buitrago MJ and Martín-Gómez MT (2020) Timely Diagnosis of Histoplasmosis in Non-endemic Countries: A Laboratory Challenge. Front. Microbiol. 11:467. doi: 10.3389/fmicb.2020.00467

We are living an era of massive population movements due to immigration, volunteering, and affordable adventure travels to areas not previously accessible to the general public. This opens the door to the emergence of exotic infections in countries where such illnesses are infrequent (Barboza and Ouatresous, 2007; Schlagenhauf et al., 2015). That is the case of histoplasmosis (Manfredi et al., 1994; Bahr et al., 2015).

Human histoplasmosis is a fungal infection caused by inhalation of microconidia of the thermally dimorphic fungi *Histoplasma capsulatum* v. *capsulatum* and *H. capsulatum* v. *duboisii*. In immunocompetent individuals, exposure to this fungus usually remains unnoticed or manifests as a flu-like respiratory episode, whereas immunocompromised patients are exposed to life-threatening disseminated infections (Wheat et al., 2016).

The distribution of *H. capsulatum* v. *duboisii* seem to be restricted to Sub-Saharian Africa. *H. capsulatum* v. *capsulatum,* in contrast, can be found irregularly distributed worldwide. The latter is more prevalent in the Eastern Coast of United States, Central-America, Northern countries of South-America, South-Eastern Asia, and territories crossed by the Yangtze River and the Brahmaputra River, and is rarely found in more temperate regions of the world (Antinori, 2014; Baker et al., 2019). Thus, although autochthonous cases of histoplasmosis have been described in many countries, it is commonly considered an "endemic infection" only in specific areas, many of which are popular travel destinations (UNWTO, 2019) or the source of migratory movements (International Organization for Migration, 2018).

HISTOPLASMOSIS IN NON-ENDEMIC COUNTRIES: THE EXTENT OF THE PROBLEM

Histoplasmosis is not a notifiable disease, and it is not included in most Public Health surveillance systems, making difficult to quantify its real burden (Nacher et al., 2018). Incomplete data exist on the incidence and prevalence of this infection in non-endemic countries. In Spain, a prevalence of 0.31 cases (SD 0.1) per 100,000 population-year has been reported, but this may be an underestimation, as only patients seeking for medical advice upon arrival from a presumed endemic region were included (Molina-Morant et al., 2018). Similar studies are lacking in other non-endemic regions. Available figures indicate that histoplasmosis is the most frequent imported mycosis (Salzer et al., 2018): cases correspond to immigrants, expatriates, transient workers or tourists having had *Histoplasma* exposure in endemic areas (Molina-Morant et al., 2018; Salzer et al., 2018; Staffolani et al., 2018). Transmission related to solid organ donation has been sporadically described (Kamei et al., 2003; Ashbee et al., 2008; Berger, 2018).

On the basis of histoplasmin skin test studies, it has been estimated that up to 20% of travelers returning from Latin America may have had contact with *Histoplasma* (Norman et al., 2009). Activities related to cave exploration, or exposure to soils enriched in nitrogen from bats and birds droppings are the common denominator of up to 29.4% cases of imported histoplasmosis (Kamei et al., 2003; Ashbee et al., 2008). Clusters of cases are associated to groups undergoing leisure or professional activities in high risk locations (Alonso et al., 2007; Cottle et al., 2013), and sum up to 56.2% of well-documented published cases in European travelers (Staffolani et al., 2018).

Spain along with France and Italy have reported the largest numbers of sporadic cases involving travelers and immigrants (Loulergue et al., 2007; Peigne et al., 2011; Buitrago and Cuenca-Estrella, 2012; Nacher et al., 2018; Staffolani et al., 2018). They accumulate up to 64.1% of the cases diagnosed in immunocompetent European travelers (Staffolani et al., 2018), and concentrate 66.4% of travel-related cases belonging to a cluster. Isolated cases have been communicated in several other European countries (Ashbee et al., 2008; Doleschal et al., 2016; Lindner et al., 2018) as well as in Asia (Cho et al., 2018) and the MiddleEast (Segel et al., 2015).

CLINICAL PRESENTATION

Most histoplasmosis cases detected in areas of low-endemicity occur following three main patterns. The most difficult to detect corresponds to immunocompetent individuals exposed to a low infectious inoculum that experience an asymptomatic seroconversion or a mild flu-like respiratory episode. This is presumedly the most frequent form of imported histoplasmosis (Norman et al., 2009). After return to their country of origin, these cases usually remain unnoticed unless patients are investigated in the setting of an outbreak (Staffolani et al., 2018). Some patients fail to clear the infection and evolve inadvertently to a chronic form with pulmonary nodules. They may be incidentally found later in life, being commonly misdiagnosed as lung cancer or tuberculosis (Ashbee et al., 2008; Norman et al., 2009; Wheat et al., 2016; Azar et al., 2018; Oladele et al., 2018). Because of the wide time gap between primary exposure and diagnosis, it is hard to establish an epidemiological link, of help to guide medical interventions.

The second pattern is seen in cases of massive *Histoplasma* exposure (i.e., high-risk activities in heavily contaminated areas), after which immunocompetent patients may develop an acute pneumonia days to a few weeks later. This presentation was reported in 90.7% of the cases included in the Staffolani's review (Staffolani et al., 2018).

The third pattern corresponds to progressive disseminated histoplasmosis, usually seen in patients with compromised cellular immunity, mainly related to HIV infection, but also to organ transplant and biological therapies, in particular anti-TNF-α drugs (Baddley et al., 2018). This scenario is frequently associated to individuals that have resided for long periods of time in endemic areas before moving to receptor countries, but and manifests in the setting of an acquired immunologic incompetence (Ashbee et al., 2008; Norman et al., 2009).

Risk of reactivation exists even decades after the initial infection (Loulergue et al., 2007; Richaud et al., 2014). Up to 25% of cases registered in European travelers developed 5 years after exposure, and 41% of disseminated forms were reactivations of infections occurring at least 5 years before (Ashbee et al., 2008). This event is usually related to an acquired immunocompromise.

The mortality rate of cases diagnosed in non-endemic areas depends on the clinical form, and the immune status of the host, but also on the diagnostic and therapeutic promptness. For immunocompetent individuals it ranges between 2 and 17.4% (Kamei et al., 2003; Molina-Morant et al., 2018; Salzer et al., 2018). A 10% attributable mortality is reported for histoplasmosis in solid organ transplant recipients (Gajurel et al., 2017). The highest fatality rates are associated to misdiagnosed forms of progressive disseminated histoplasmosis: 42% mortality if treatment is delayed, and 100% if antifungal therapy is not prescribed (Ashbee et al., 2008; Scheel et al., 2014). Some cases are only revealed at autopsy (Kamei et al., 2003; Antinori et al., 2006; Denning, 2016).

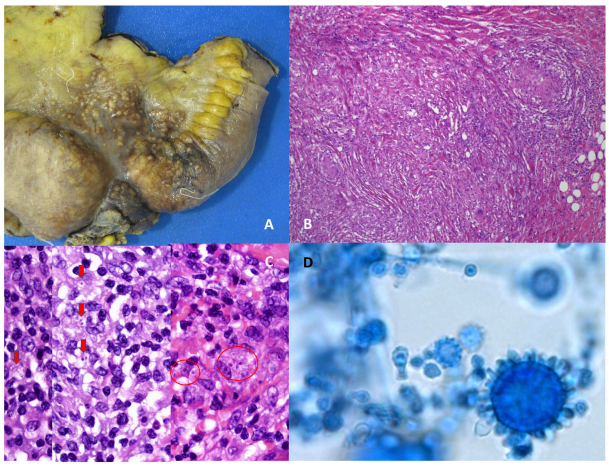

FIGURE 1 | Morphological appearance of *Histoplasma capsulatum* var. *capsulatum* in culture and in affected tissues. Images **(A–C)** are courtesy of Dr. Steffania Landolfi. **(A)** Surgically excised ileum showing stenosis and multiple macroscopic nodules from a case of disseminated histoplasmosis with intestinal involvement. **(B)** Tipical appearance of granulomas in tissue, hematoxilin-Eosin. **(C)** Intracellular yeasts surrounded by a clear area resembling a pseudocapsula (Hematoxilin-Eosin staining). **(D)** Tuberculate macroconidia of *Histoplasma capsulatum* var. *capsulatum* in culture.

HANDICAPS OF LABORATORY DIAGNOSIS IN NON-ENDEMIC AREAS

The two main diagnostic handicaps in non-endemic areas are the usually low index of suspicion, and the scarceness of tools for a fast and accurate identification of the infection.

Conventional laboratory tests for the diagnosis of histoplasmosis include mycological cultures and histopathology of affected organs and tissues (**Figure 1**). Isolation of the fungus in culture is considered the gold standard for diagnosis. *H. capsulatum* can grow in mycological media of common use in routine laboratories, and current MALDI-TOF systems can provide a presumptive identification (Panda et al., 2015; Rizzato et al., 2015; Rychert et al., 2018; Valero et al., 2018). Cultures, however, have well-known limitations, i.e., slowness, suboptimal sensitivity, and requirement of BSL3 facilities to manipulate them (Kauffman, 2009). Typical tuberculate macroconidia closely resemble the saprophyte *Sepedonium*, and microconidia can be misidentified as *Chrysosporium*. The histopathological observation also requires skilled personnel. A plethora of findings complicates the microscopic diagnosis to pathologists non-familiar with this infection: images range from localized granulomas to extensive aggregates of macrophages fulfilled with small yeasts surrounded by pseudocapsules (Woods and Schnadig, 2003). Intracellular yeasts are often confused with *Leishmania* spp., *Cryptococcus* or *C. glabrata* by non-expert observers (Wheat, 2003; Wheat et al., 2016).

Complement fixation (CF) or Immunodiffusion (ID) are common techniques used for *Histoplasma* antibody detection. Their sensitivity greatly varies depending on the clinical form and the immune status of the host. Antibody detection is of limited usefulness in severely immunocompromised individuals, and to diagnose acute infections in early phases (Azar and Hage, 2017). In non-endemic areas serology is usually performed in reference centers as a complementary tool, meaning that results are not readily available. Despite this, antibody detection was used in the diagnostic workup of 74.7% cases reported in immunocompetent European travelers (Staffolani et al., 2018). Novel FDA cleared tests seem to be of help in the differential diagnosis of pulmonary nodules, but currently they are not available overseas (Deppen et al., 2019).

Histoplasma antigen detection in body fluids is currently considered the most sensitive and quickest technique to diagnose this infection (Azar and Hage, 2017). It is particularly useful in progressive disseminated forms, and it has proven its applicability to infected animals that may act as potential reservoirs for humans (Cunningham et al., 2015; Rothenburg et al., 2019). Combined detection in serum and urine seem to provide the best diagnostic performance, with some differences in the diagnostic yield between FDA cleared tests (Theel et al., 2013; Fandiño-Devia et al., 2016; Azar and Hage, 2017; Torres-González et al., 2018). Antigen detection provides a clear improvement for the management of histoplasmosis, especially in highly endemic areas where this infection frequently coexists with tuberculosis (Bansal et al., 2019), and recently it has been included in the WHO list of essential diagnostic test[1]. Despite FDA-approved commercial tests are available, their use is mostly restricted to developed endemic areas (Bongomin et al., 2019a). There is little data regarding its performance in non-endemic areas. The reported use of antigen detection in non-United States cases of imported histoplasmosis is very limited: performance of an antigen test (in urine and/or serum) was declared only in 9 out of 319 cases of histoplasmosis in immunocompetent travelers diagnosed out of the United States (Staffolani et al., 2018). Even in non-endemic areas of the United States, the use of the EIA antigen detection has been seldom reported (Benedict et al., 2015). The underlying reason may be at least partially related to the overall scarcity of imported cases, making the test non-cost-effective in settings of no endemicity.

MOLECULAR ALTERNATIVES TO DIAGNOSE HISTOPLASMOSIS

Historically, antigen detection tests use to be not available in non-endemic regions, so molecular techniques may represent a suitable alternative for a rapid diagnosis. They offer the opportunity to shorten turnaround times, and to diminish the risk of laboratory-acquired infection where laboratory personnel is not used to handle *Histoplasma* positive cultures. In non-endemic regions, the use of molecular techniques has been described mainly in countries that have registered an increase in the incidence of imported cases, such as Spain (Buitrago et al., 2011). Staffolani reflected the sporadic use of PCR techniques in travelers (Staffolani et al., 2018) and, more recently, a case

[1]https://www.who.int/medical_devices/publications/Standalone_document_v8.pdf

TABLE 1 | Characteristics of published nucleic acid amplification assays based on conventional and Real Time PCR for the diagnosis of histoplasmosis.

References	Country	PCR assay	Target	Clinical samples	Sensitivity (samples tested)	Specificity
Bialek et al., 2001*	Germany/United States	Conventional (nested)	18S rDNA	Blood, spleen, lung (mice)	83.1%	ND
Rickerts et al., 2002	Germany/United States	Conventional (nested)	100-kDa-like protein Gene	Biopsy	70%	100%
Guedes et al., 2003[1]	Brazil	Conventional	M antigen gene	NO[1]	100%	100%
Bracca et al., 2003	Argentina	Conventional (semi-nested)	M antigen gene	Biopsy, blood, mucose	ND (30)	ND
Martagon-Villamil et al., 2003[2]	United States	Real time	ITS rDNA	BAL, lung biopsy, bone marrow	100% (3)	100%
Maubon et al., 2007	French Guiana	Bialek et al., 2002	100-kDa-like protein Gene	Blood, serum, BAL, BAS, biopsy, CSF, others	100% (40)	100%
Buitrago et al., 2011	Spain	Real time	ITS rDNA	Blood, serum, bone marrow, sputum, BAS, BAL, biopsy, CSF, others	89% Proven H (54); 60% probable H (13)	100%
Simon et al., 2010	French Guiana	Real time	ITS rDNA	BAL, biopsy, bone marrow, CSF	95,4% (348)	96%
Gago et al., 2014	Spain	Multiplex real time	ITS rDNA	BAL, biopsy, serum, bone marrow	92.5% (72)	100%
López et al., 2017[3]*	Colombia	Real time PCR	M antigen gene H antigen gene ITS rDNA	Lung biopsy (mice)	ND	ND[3]

**Murine model; (1) tested on DNA from strains; (2) tested mainly on DNA from strains; (3) comparative analysis of three techniques; BAL, bronchoalveolar lavage; BAS, broncho aspirate; Proven H, proven histoplamosis by EORTC/MSG criteria; Probable H, probable histoplasmosis by EORTC/MSG criteria; ND, no data.*

was diagnosed with the use of a panfungal assay in Germany (Lindner et al., 2018). Beside this, PCR-based techniques have been claimed to be of help in the detection of environmental reservoirs, and in the design of strategies of intervention to prevent exposure risk (Gómez et al., 2018, 2019).

No commercial PCR-based test has been approved for *in vitro* diagnosis yet, but published techniques show promising results. In a recent meta-analysis Caceres and coworkers reported an overall sensitivity and specificity (95% CI) of 95.4 (88.8–101.9) and 98.7 (95.7–101.7) respectively in cases of progressive disseminated histoplasmosis of HIV + patients (Caceres et al., 2019). To date, the reported assays target different regions in the genome, being the most successful the ITS multicopy region of the ribosomal DNA, and genes encoding the M antigen or the 100-kDa-like protein. Techniques encompass conventional and nested PCR, as well as the more user-friendly and less cumbersome real-time PCR (**table 1**). A Reference Laboratory in Spain has developed various real time PCR-based assays, showing an excellent performance for the diagnosis of 39 cases of histoplasmosis (Buitrago et al., 2006, 2011; Gago et al., 2014). Samples were obtained from cases of probable infection in immunocompetent travelers (23%), and of proven histoplasmosis diagnosed in immigrants (77%), 97% of them having AIDS as underlying disease. The sensitivity of the PCR for disseminated disease was 89% showing superiority over mycological culture (73%) and antibody detection (40%) (Buitrago et al., 2011). An interesting multiplex approach developed by the same group targets mixed infections with *Pneumocystis jirovecii* and *Cryptococcus neoformans*, common opportunistic fungal pathogens of HIV-infected patients. This design showed an overall sensitivity of 93 and 100% specificity.

Regarding the best samples to test, different types of specimens have been studied, including respiratory secretions, biopsies, bone marrow, blood, or sera. Good performance of respiratory samples and biopsies has been reported (Buitrago et al., 2011). The sensitivity for blood and bone marrow specimens reached 100% in immunocompromised patients with disseminated disease (Maubon et al., 2007), but was more modest in immunocompetent patients (Buitrago et al., 2011) reflecting the lower amount of circulating DNA circulating in these patients. An important point was the increased sensitivity obtained by testing more than one sample per patient in cases with extra-pulmonary involvement (Gago et al., 2014). Overall, although the diagnostic yield seem variable depending on the disease stage, clinical form, and type of specimen, PCR based techniques may be the answer to provide the much desired rapid results, particularly to diagnose severe cases in non-endemic locations (Vasconcellos et al., 2019).

As compared to other PCR modalities, isothermal nucleic acid amplification techniques are considered cheaper and more user-friendly. No sophisticated equipment is required, and handling can be done by personnel lacking expertise in molecular test (Lee, 2017). However, limited attempts have been made to design isothermal assays. All of them dealt with progressive disseminated histoplasmosis samples of HIV + patients from endemic countries, with reasonably good results (Scheel et al., 2014; Zatti et al., 2019). Their diagnostic yield varied greatly depending on the type of sample tested: an 83% sensitivity was

reported for blood and bone marrow as compared to a nested PCR targeting the *Hcp100* gene (Zatti et al., 2019), whereas a more modest 67% sensitivity was achieved in antigen positive urine samples. Altogether, isothermal assays could become suitable for use as a complementary diagnostic test in low-income countries, and potentially useful techniques for implementation in non-endemic areas.

Major drawbacks of in-house molecular tests are the lack standardization and consensus among laboratories. These aspects have been addressed by the only inter-laboratory study focused on molecular techniques for the diagnosis of histoplasmosis published to date (Buitrago et al., 2013). Seven PCR protocols (conventional and real time) were compared, with an overall sensitivity and specificity of 86 and 100% respectively. The results of this work led the authors to conclude that multicopy targets were the best option when designing an assay as they provide and increase in sensitivity without decreasing specificity; real time PCR proved to be more advantageous than conventional PCR. In contrast, one study limited to a small number of samples from a single laboratory showed a better sensitivity of nested PCR assays as compared to designs based on cycling-probe real-time PCR (Muraosa et al., 2016). Such differences highlight the need of collaborative networks to assess the diagnostic yield of different molecular assay designs for the diagnosis of histoplasmosis, particularly in areas of low prevalence.

FUTURE DIRECTIONS AND CONCLUSION

Education has proven to be an essential tool to increase the recognition of cases in endemic resource-constrained settings (Caceres et al., 2015), and also, it may be a future strategy to implement in non-endemic areas. Other pillars of utmost importance to effectively fight against histoplasmosis should be to consider it a notifiable infection, to quantify the real extent of the problem (Bongomin et al., 2019b; Staffolani et al., 2020), and to put into practice the use of rapid and reliable tools to detect and control potential environmental and animal sources of human infection (Cunningham et al., 2015; Gómez et al., 2018, 2019; Rothenburg et al., 2019).

Sadly, histoplasmosis is not classified as a neglected disease by organizations involved in Public Health, and published cases are thought to be just the tip of the iceberg. This hampers the development of affordable and accurate diagnostic tools. Efforts, however, are under way. A Colombian group is working on the development of an IGRA-based assay with promising preliminary results, and a huge potential for the diagnosis of subclinical infections regardless of the immune status of the host (Rubio-Carrasquilla et al., 2019); more results are awaited. A lateral flow device (LFD) for the detection of *Histoplasma* antigen in serum has been developed recently showing an excellent sensitivity, and extensive validation in non-progressive disseminated cases is expected (Cáceres et al., 2019). Molecular test might be part of the diagnostic armamentarium in settings where clinicians and laboratory personnel are not familiar with this pathogen. Reference laboratories from non-endemic regions with growing number of histoplasmosis cases are accumulating experience, and they are developing new assays that could also be of great help in areas of high endemicity.

Much remains to be done to improve the laboratory diagnosis of imported histoplasmosis. Efforts include extensive standardization and validation of already developed PCR-based techniques, and definition of the diagnostic yield in different types of samples and clinical settings. Initiatives to perform multicenter studies in non-endemic regions are being launched (Buitrago MJ, personal communication) to achieve a consensus on technical issues such as the best DNA extraction method or the most suitable targets, among others.

In conclusion, histoplasmosis is a primary fungal infection increasingly seen in non-endemic countries as a result of recreational travels and migratory movements. In receptor areas timely diagnosis is hampered by the lack of clinical awareness, and the scarcity of laboratory techniques able to provide accurate results with a short turn-around time regardless of the immune status of the host and the extent of the disease. Molecular techniques are seen as a suitable alternative for this purpose in areas of low prevalence. Much needed efforts to standardize such assays and to define their diagnostic yield are in progress. Molecular test promise to be of great help non-endemic areas, and as adjunctive tests for the laboratory diagnosis of histoplasmosis in areas of high endemicity.

AUTHOR CONTRIBUTIONS

MB and MM-G contributed equally to the design, elaboration, and review of this manuscript.

ACKNOWLEDGMENTS

The authors are thankful to Dr. Steffania Landolfi for kindly providing the histopathology images that illustrate this manuscript.

REFERENCES

Alonso, D., Muñoz, J., Letang, E., Salvadó, E., Cuenca-Estrella, M., Maria José Buitrago, M. J., et al. (2007). Imported acute histoplasmosis with rheumatologic manifestations in spanish travelers. *J. Travel. Med.* 14, 338–342. doi: 10.1111/j.1708-8305.2007.00138.x

Antinori, S. (2014). Histoplasma capsulatum: more widespread than previously thought. *Am. J. Trop. Med. Hyg.* 90, 982–983. doi: 10.4269/ajtmh.14-0175

Antinori, S., Magni, C., Nebuloni, M., Parravicini, C., Corbellino, M., Sollima, S., et al. (2006). Histoplasmosis among human immunodeficiency virus-infected people in europe. *Medicine* 85, 22–36. doi: 10.1097/01.md.0000199934.38120.d4

Ashbee, H. R., Evans, E. G. V., Viviani, M. A., Dupont, B., Chryssanthou, E., Surmont, I., et al. (2008). Histoplasmosis in Europe: report on an epidemiological survey from the European confederation of medical mycology working group. *Med. Mycol.* 46, 57–65. doi: 10.1080/13693780701591481

Azar, M. M., and Hage, C. A. (2017). Laboratory diagnostics for histoplasmosis. *J. Clin. Microbiol.* 55, 1612–1620. doi: 10.1128/JCM.02430-16

Azar, M. M., Zhang, X., Assi, R., Hage, C., Wheat, L. J., and Malinis, M. F. (2018). Clinical and epidemiological characterization of histoplasmosis cases in a nonendemic area. Connecticut, United States. *Med. Mycol.* 56, 896–899. doi: 10.1093/mmy/myx120

Baddley, J. W., Cantini, F., Goletti, D., Gómez-Reino, J. J., Mylonakis, E., San-Juan, R., et al. (2018). ESCMID study group for infections in compromised hosts (ESGICH) consensus document on the safety of targeted and biological therapies: an infectious diseases perspective (soluble immune effector molecules [I]: anti-tumor necrosis factor-α agents). *Clin. Microbiol. Infect.* 24, S10–S20. doi: 10.1016/j.cmi.2017.12.025

Bahr, N. C., Antinori, S., Wheat, L. J., and Sarosi, G. A. (2015). Histoplasmosis infections worldwide: thinking outside of the Ohio River Valley. *Curr. Trop. Med. Rep.* 2, 70–80. doi: 10.1007/s40475-015-0044-0

Baker, J., Setianingrum, F., Wahyuningsih, R., and Denning, D. W. (2019). Mapping histoplasmosis in South East Asia – implications for diagnosis in AIDS. *Emerg. Microbes Infect.* 8, 1139–1145. doi: 10.1080/22221751.2019.1644539

Bansal, N., Sethuraman, N., Gopalakrishnan, R., Ramasubramanian, V., Kumar, D. S., Nambi, P. S., et al. (2019). Can urinary *Histoplasma* antigen test improve the diagnosis of histoplasmosis in a tuberculosis endemic region? *Mycoses* 62, 502–507. doi: 10.1111/myc.12902

Barboza, P., and Ouatresous, I. (2007). Globalization, emergence and importation of infectious diseases. *Rev. Prat.* 57, 867–873.

Benedict, K., Thompson, G. R., Stan Deresinski, S., and Chiller, T. (2015). Mycotic infections acquired outside areas of known endemicity. United States. *Emerg. Infect. Dis.* 21, 1935–1941. doi: 10.3201/eid2111.141950

Berger, S. (2018). *GIDEON Guide to Outbreaks*. Available online at https://www.gideononline.com/ebooks/outbreaks/

Bialek, R., Feucht, A., Aepinus, C., Just-Nübling, G., Robertson, V. J., Knobloch, J., et al. (2002). Evaluation of two nested PCR assays for detection of *Histoplasma capsulatum* DNA in human tissue. *J. Clin. Microbiol.* 40, 1644–1647. doi: 10.1128/jcm.40.5.1644-1647.2002

Bialek, R., Fischer, J., Feucht, A., Najvar, L. K., Dietz, K., Knobloch, J., et al. (2001). Diagnosis and monitoring of murine histoplasmosis by a nested PCR assay. *J. Clin. Microbiol.* 39, 1506–1509. doi: 10.1128/JCM.39.4.1506-1509.2001

Bongomin, F., Govender, N. P., Chakrabarti, A., Robert-Gangneux, F., Boulware, D. R., Zafar, A., et al. (2019a). Essential *in vitro* diagnostics for advanced HIV and serious fungal siseases: international experts' consensus recommendations. *Eur. J. Clin. Microbiol. Infect. Dis.* 38, 1581–1584. doi: 10.1007/s10096-019-03600-4

Bongomin, F., Kwizera, R., and Denning, D. W. (2019b). Getting histoplasmosis on the map of international recommendations for patients with advanced HIV disease. *J. Fungi.* 5:E80. doi: 10.3390/jof5030080

Bracca, A., Tosello, M. E., Girardini, J. E., Amigot, S. L., Gomez, C., and Serra, E. (2003). Molecular detection of *Histoplasma capsulatum* var. *capsulatum* in human clinical samples. *J. Clin. Microbiol.* 41, 1753–1755. doi: 10.1128/jcm.41.4.1753-1755.2003

Buitrago, M. J., Berenguer, J., Mellado, E., Rodríguez-Tudela, J. L., and Cuenca-Estrella, M. (2006). Detection of imported histoplasmosis in serum of HIV-infected patients using a real-time PCR-based assay. *Eur. J. Clin. Microbiol. Infect. Dis.* 25, 665–668. doi: 10.1007/s10096-006-0207-y

Buitrago, M. J., Bernal-Martínez, L., Castelli, M. V., Rodríguez-Tudela, J. L., and Cuenca-Estrella, M. (2011). Histoplasmosis and paracoccidioidomycosis in a non-endemic area: a review of cases and diagnosis. *J. Trav. Med.* 18, 26–33. doi: 10.1111/j.1708-8305.2010.00477.x

Buitrago, M. J., Canteros, C. E., Frías De León, G., González, A., Marques-Evangelista, De Oliveira, M., et al. (2013). Comparison of PCR protocols for detecting *Histoplasma capsulatum* DNA through a multicenter study. *Rev. Iberoam. Micol.* 30, 256–260. doi: 10.1016/j.riam.2013.03.004

Buitrago, M. J., and Cuenca-Estrella, M. (2012). Current epidemiology and laboratory diagnosis of endemic mycoses in Spain. *Enferm. Infec. Microbiol. Clin.* 30, 407–413. doi: 10.1016/j.eimc.2011.09.014

Cáceres, D. H., Gómez, B. L., Tobón, A. M., Chiller, T. M., and Lindsley, M. D. (2019). Evaluation of a *Histoplasma* antigen lateral flow assay for the rapid diagnosis of progressive disseminated histoplasmosis in Colombian patients with AIDS.". *Mycoses* 63, 139–144. doi: 10.1111/myc.13023

Caceres, D. H., Knuth, M., Derado, G., and Lindsley, M. D. (2019). Diagnosis of progressive disseminated histoplasmosis in advanced HIV: a meta-analysis of assay analytical performance. *J. Fungi.* 5:E76. doi: 10.3390/jof5030076

Caceres, D. H., Zuluaga, A., Arango-Bustamante, K., de Bedout, C., Tobón, A. M., Restrepo, A., et al., (2015). Implementation of a training course increased the diagnosis of histoplasmosis in Colombia. *Am. J. Trop. Med. Hyg.* 93, 662–667. doi: 10.4269/ajtmh.15-0108

Cho, S.-H., Yu, Y.-B., Jark, J.-S., Yook, K.-D., and Kim, Y.-K. (2018). Epidemiological characterization of imported systemic mycoses occurred in Korea. *Osong. Public Health Res. Perspect.* 9, 255–260. doi: 10.24171/j.phrp.2018.9.5.07

Cottle, L. E., Gkrania−Klotsas, E., Williams, H. J., Brindle, H. E., Carmichael, A. J., Fry, G., et al. (2013). A multinational outbreak of histoplasmosis following a biology field trip in the Ugandan rainforest. *J. Trav. Med.* 20, 83–87. doi: 10.1111/jtm.12012

Cunningham, L., Cook, A., Hanzlicek, A., Harkin, K., Wheat, J., Goad, C., et al. (2015). Sensitivity and specificity of *Histoplasma* antigen detection by enzyme immunoassay. *J. Am. An. Hosp. Assoc.* 51, 306–310. doi: 10.5326/JAAHA-MS-6202

Denning, D. W. (2016). Minimizing fungal disease deaths will allow the UNAIDS target of reducing annual AIDS deaths below 500 000 by 2020 to be realized. *Philos. Trans. R. Soc. Lond. B Biol. Sci.* 371:20150468. doi: 10.1098/rstb.2015.0468

Deppen, S. A., Massion, P. P., Blume, J., Walker, R. C., Antic, S., Chen, H., et al. (2019). Accuracy of a novel histoplasmosis enzyme immunoassay to evaluate suspicious lung nodules. *Cancer Epidemiol. Biomarkers Prev.* 28, 321–326. doi: 10.1158/1055-9965.EPI-18-0169

Doleschal, B., Rödhammer, T., Tsybrovskyy, O., Aichberger, K. J., and Lang, F. (2016). Disseminated histoplasmosis: a challenging differential diagnostic consideration for suspected malignant lesions in the digestive Ttact. *Case Rep. Gastroenterol.* 10, 653–660. doi: 10.1159/000452203

Fandiño-Devia, E., Rodríguez-Echeverri, C., Cardona-Arias, J., and Gonzalez, A. (2016). Antigen detection in the diagnosis of histoplasmosis: a meta-analysis of diagnostic performance. *Mycopathologia* 181, 197–205. doi: 10.1007/s11046-015-9965-3

Gago, S., Esteban, C., Valero, C., Zaragoza, O., Puig De La Bellacasa, J., and Buitrago, M. J. (2014). A multiplex real-time PCR assay for identification of *Pneumocystis jirovecii, Histoplasma capsulatum,* and *Cryptococcus neoformans/Cryptococcus gattii* in samples from AIDS patients with opportunistic pneumonia. *J. Clin. Microbiol.* 52, 1168–1176. doi: 10.1128/JCM.02895-13

Gajurel, K., Dhakal, R., and Deresinski, S. (2017). Histoplasmosis in transplant recipients. *Clin. Transplant.* 31:e13087. doi: 10.1111/ctr.13087

Gómez, L. F., Arango, M., McEwen, J. G., Gómez, O. M., Zuluaga, A., Peláez, C. A., et al. (2019). Molecular epidemiology of Colombian *Histoplasma capsulatum* isolates obtained from human and chicken manure samples. *Heliyon* 5:e02084. doi: 10.1016/j.heliyon.2019.e02084

Gómez, L. F., Torres, I. P., Jiménez-A, M. P., McEwen, J. G., de Bedout, C., Peláez, C. A., et al. (2018). Detection of *Histoplasma capsulatum* in organic fertilizers by Hc100 nested polymerase chain reaction and Its correlation with the physicochemical and microbiological characteristics of the samples. *Am. J. Trop. Med. Hyg.* 98, 1303–1312. doi: 10.4269/ajtmh.17-0214

Guedes, H. L. M., Guimarães, A. J., Muniz, M. M., Pizzini, C. V., Hamilton, A. J., and Peralta, J. M. (2003). PCR assay for identification of *Histoplasma capsulatum* based on the nucleotide sequence of the M antigen. *J. Clin. Microbiol.* 41, 535–539. doi: 10.1128/jcm.41.2.535-539.2003

International Organization for Migration (2018). *Migration and Migrants: A Global Overview. World Migration Report 2018*. Geneva: International Organization for Migration.

Kamei, K., Sano, A., Kikuchi, K., Makimura, K., Niimi, M., Kazuo Suzuki, K., et al. (2003). The trend of imported mycoses in Japan. *J. Infect. Chemother.* 9, 16–20. doi: 10.1007/s10156-002-0217-3

Kauffman, C. A. (2009). Histoplasmosis. *Clin. Chest. Med.* 30, 217–225. doi: 10.1016/j.ccm.2009.02.002

Lee, P. L. M. (2017). DNA amplification in the field: move over PCR, here comes LAMP. *Mol. Ecol. Resour.* 17, 138–141. doi: 10.1111/1755-0998.12548

Lindner, A. K., Rickerts, V., Kurth, F., Wilmes, D., and Richter, J. (2018). Chronic oral ulceration and lip swelling after a long term stay in Guatemala: a diagnostic challenge. *Trav. Med. Infect. Dis.* 23, 103–104. doi: 10.1016/j.tmaid.2018.04.009

López, L. F., Muñoz, C. O., Cáceres, D. H., Tobón, A. M., Loparev, V., Clay, O., et al. (2017). Standardization and validation of real time PCR assays for the diagnosis of histoplasmosis using three molecular targets in an animal model. *PloS One* 12:e0190311. doi: 10.1371/journal.pone.0190311

Loulergue, P., Bastides, F., Baudouin, V., Chandenier, J., Mariani-Kurkdjian, P., Dupont, B., et al. (2007). Literature review and case histories of *Histoplasma capsulatum* var. *duboisii* infections in HIV-infected patients. *Emerg. Infect. Dis.* 13, 1647–1652. doi: 10.3201/eid1311.070665

Manfredi, R., Mazzoni, A., Nanetti, A., and Chiodo, F. (1994). *Histoplasmosis capsulati* and *duboisii* in Europe: the Impact of the HIV pandemic, travel and immigration. *Eur. J. Epidemiol.* 10, 675–681. doi: 10.1007/BF01719280

Martagon-Villamil, J., Shrestha, N., Sholtis, M., Isada, C. M., Hall, G. S., Bryne, T., et al. (2003). Identification of *Histoplasma capsulatum* from culture extracts by real-time PCR. *J. Clin. Microbiol.* 41, 1295–1298. doi: 10.1128/jcm.41.3.1295-1298.2003

Maubon, D., Simon, S., and Aznar, C. (2007). Histoplasmosis diagnosis using a polymerase chain reaction method. application on human samples in French Guiana, South America. *Diagn. Microbiol. Infect. Dis.* 58, 441–444. doi: 10.1016/j.diagmicrobio.2007.03.008

Molina-Morant, D., Sánchez-Montalvá, A., Salvador, F., Sao-Avilés, A., and Molina, I. (2018). Imported endemic mycoses in Spain: evolution of hospitalized cases, clinical characteristics and correlation with migratory movements, 1997-2014. *PLoS Negl. Trop. Dis.* 12:e0006245. doi: 10.1371/journal.pntd.0006245

Muraosa, Y., Toyotome, T., Yahiro, M., Watanabe, A., Shikanai-Yasuda, M. A., and Kamei, K. (2016). Detection of *Histoplasma capsulatum* from clinical specimens by cycling probe-based real-time PCR and nested real-time PCR. *Med. Mycol.* 54, 433–438. doi: 10.1093/mmy/myv106

Nacher, M., Blanchet, D., Bongomin, F., Chakrabarti, A., Couppié, P., Demar, M., et al. (2018). *Histoplasma capsulatum* antigen detection tests as an essential diagnostic tool for patients with advanced HIV disease in low and middle income countries: a systematic review of diagnostic accuracy studies. *PLoS Negl. Trop. Dis.* 12:e0006802. doi: 10.1371/journal.pntd.0006802

Norman, F. F., Martín-Dávila, P., Fortún, J., Dronda, F., Quereda, C., Sánchez-Sousa, A., et al. (2009). Imported histoplasmosis: two distinct profiles in travelers and immigrants. *J. Trav. Med.* 16, 258–262. doi: 10.1111/j.1708-8305.2009.00311.x

Oladele, R. O., Ayanlowo, O. O., Richardson, M. D., and Denning, D. W. (2018). Histoplasmosis in Africa: an emerging or a neglected disease? *PLoS Negl. Trop. Dis.* 12:e0006046. doi: 10.1371/journal.pntd.0006046

Panda, A., Ghosh, A. K., Mirdha, B. R., Xess, I., Paul, S., Samantaray, J. C., et al. (2015). MALDI-TOF mass spectrometry for rapid identification of clinical fungal isolates based on ribosomal protein biomarkers. *J. Microbiol. Methods* 109, 93–105. doi: 10.1016/j.mimet.2014.12.014

Peigne, V., Dromer, F., Elie, C., Lidove, O., Lortholary, O., and French Mycosis Study Group. (2011). imported acquired immunodeficiency syndrome-related histoplasmosis in metropolitan France: a comparison of pre-highly active anti-retroviral therapy and highly active anti-retroviral therapy eras. *Am. J. Trop. Med. Hyg.* 85, 934–941. doi: 10.4269/ajtmh.2011.11-0224

Richaud, C., Chandesris, M. O., Lanternier, F., Benzaquen-Forner, H., Garcia-Hermoso, D., Picard, C., et al. (2014). Case report: imported african histoplasmosis in an immunocompetent patient 40 years after staying in a disease-endemic area. *Am. J. Trop. Med. Hyg.* 91, 1011–1014. doi: 10.4269/ajtmh.13-0731

Rickerts, V., Bialek, R., Tintelnot, K., Jacobi, V., and Just-Nübling, G. (2002). Rapid PCR-based diagnosis of disseminated histoplasmosis in an AIDS patient. *Eur. J. Clin. Microbiol. Infect. Dis.* 21, 821–823. doi: 10.1007/s10096-002-0833-y

Rizzato, C., Lombardi, L., Zoppo, M., Lupetti, A., and Tavanti, A. (2015). Pushing the limits of MALDI-TOF mass spectrometry: beyond fungal species identification. *J. Fungi.* 1, 367–383. doi: 10.3390/jof1030367

Rothenburg, L., Hanzlicek, A. S., and Payton, M. E. (2019). A monoclonal antibody−based urine *Histoplasma* antigen enzyme immunoassay (IMMY§) for the diagnosis of histoplasmosis in cats. *J. Vet. Intern. Med.* 33, 603–610. doi: 10.1111/jvim.15379

Rubio-Carrasquilla, M., Santa, C. D., Rendón, J. P., Botero-Garcés, J., Guimarães, A. J., Moreno, E., et al. (2019). An interferon gamma release assay specific for *Histoplasma capsulatum* to detect asymptomatic infected individuals: a proof of concept study. *Med. Mycol.* 57, 724–732. doi: 10.1093/mmy/myy131

Rychert, J., Slechta, E. S., Barker, A. P., Miranda, E., Babady, N. E., Tang, Y. W., et al. (2018). Multicenter evaluation of the Vitek MS v3.0 System for the identification of filamentous fungi. *J. Clin. Microbiol.* 56, e1353–e1317. doi: 10.1128/JCM.01353-17

Salzer, H. J. F., Stoney, R. J., Angelo, K. M., Rolling, T., Grobusch, M. P., Michael Libman, M., et al. (2018). Epidemiological aspects of travel-related systemic endemic mycoses: a GeoSentinel analysis, 1997-2017. *J. Trav. Med.* 25:tay055. doi: 10.1093/jtm/tay055

Scheel, C. M., Zhou, Y., Theodoro, R. C., Abrams, B., Balajee, S. A., and Litvintseva, A. P. (2014). Development of a loop-mediated isothermal amplification method for detection of *Histoplasma capsulatum* DNA in clinical samples. *J. Clin. Microbiol.* 52, 483–488. doi: 10.1128/JCM.02739-13

Schlagenhauf, P., Weld, L., Goorhuis, A., Gautret, P., Weber, R., von Sonnenburg, F., et al. (2015). Travel-associated infection presenting in Europe (2008–12): an analysis of EuroTravNet longitudinal, surveillance data, and evaluation of the effect of the pre-travel consultation. *Lancet Infect. Dis.* 15, 55–64. doi: 10.1016/S1473-3099(14)71000-X

Segel, M. J., Lindsley, M. D., Rozenman, J., Schwartz, E., Berkman, N., Neuberger, A., et al. (2015). Histoplasmosis in Israeli travelers. *Am. J. Trop. Med. Hyg.* 92, 1168–1172. doi: 10.4269/ajtmh.14-0509

Simon, S., Veron, V., Boukhari, R., Denis Blanchet, D., and Aznar, C. (2010). Detection of *Histoplasma capsulatum* DNA in human samples by real-time polymerase chain reaction. *Diagn. Microbiol. Infect. Dis.* 66, 268–273. doi: 10.1016/j.diagmicrobio.2009.10.010

Staffolani, S., Buonfrate, D., Angheben, A., Gobbi, F., Giorli, G., Guerriero, M., et al. (2018). Acute histoplasmosis in immunocompetent travelers: a systematic review of literature. *BMC Infect. Dis.* 18:673. doi: 10.1186/s12879-018-3476-z

Staffolani, S., Riccardi, N., Farina, C., Lo Cascio, G., Gulletta, M., and Federico Gobbi, F. (2020). Acute histoplasmosis in travelers: a retrospective study in an Italian referral center for tropical diseases. *Pathog. Global Health* doi: 10.1080/20477724.2020.1716517 [Epub ahead of print].

Theel, E. S., Jespersen, D. J., Harring, J., Mandrekar, J., and Binnicker, M. J. (2013). Evaluation of an enzyme immunoassay for detection of *Histoplasma capsulatum* antigen from urine specimens. *J. Clin. Microbiol.* 51, 3555–3559. doi: 10.1128/JCM.01868-13

Torres-González, P., Niembro-Ortega, M. D., Martínez-Gamboa, A., Ahumada-Topete, V. H., Andrade-Villanueva, J., Javier Araujo-Meléndez, J., et al. (2018). Diagnostic accuracy cohort study and clinical value of the *Histoplasma* urine antigen (ALPHA Histoplasma EIA) for disseminated histoplasmosis among HIV infected patients: a multicenter study. *PLoS Negl. Trop. Dis.* 12:e0006872. doi: 10.1371/journal.pntd.0006872

UNWTO (2019). International Tourism Highlights. International Tourism Continues to Outpace the Global Economy. Available online at: https://www.e-unwto.org/doi/pdf/10.18111/9789284421152?download=true (accessed November 10, 2019).

Valero, C., Buitrago, M. J., Gago, S., Quiles-Melero, I., and García-Rodríguez, J. (2018). A matrix-assisted laser desorption/ionization time of flight mass spectrometry reference database for the identification of *Histoplasma capsulatum*. *Med. Mycol.* 56, 307–314. doi: 10.1093/mmy/myx047

Vasconcellos, I. C. S., Dalla Lana, D. F., and Pasqualotto, A. C. (2019). The role of molecular tests in the diagnosis of disseminated histoplasmosis. *J. Fungi.* 6:E1. doi: 10.3390/jof6010001

Wheat, L. J. (2003). Current diagnosis of histoplasmosis. *Trends Microbiol.* 11, 488–494. doi: 10.1016/j.tim.2003.08.007

Wheat, L. J., Azar, M. M., Bahr, N. C., and Spec, A. (2016). Histoplasmosis. *Infect. Dis. Clin. North Am.* 30, 207–227. doi: 10.1016/j.idc.2015.10.009

Woods, G. L., and Schnadig, V. J. (2003). "Histopathology of fungal infections, in *Clinical Mycology*, eds E. J. Anaissie, M. R. McGinnis, and M. A. Pfaller 1st Edn, Philadelphia: Churchill Livigston, 80–95.

Zatti, M. S., Arantes, T. D., Fernandes, J. A. L., Bay, M. B., Milan, E. P., Naliato, G. F. S., et al. (2019). Loop-mediated isothermal amplification and nested PCR of the internal transcribed spacer (ITS) for *Histoplasma capsulatum* detection. *PLoS Negl. Trop. Dis.* 13:e0007692. doi: 10.1371/journal.pntd.0007692

Conflict of Interest: The authors declare that the research was conducted in the absence of any commercial or financial relationships that could be construed as a potential conflict of interest.

frontiers in Cellular and Infection Microbiology

ORIGINAL RESEARCH
published: 09 April 2020
doi: 10.3389/fcimb.2020.00140

Autoinducer-2 May Be a New Biomarker for Monitoring Neonatal Necrotizing Enterocolitis

Chun-Yan Fu[1,2,3,4,5,6], *Lu-Quan Li*[1,2,3,4,5,6]*, *Ting Yang*[1,2,3,4,5,6], *Xiang She*[1,2,3,4,5,6], *Qing Ai*[1,2,3,4,5,6] *and Zheng-Li Wang*[1,2,3,4,5,6]*

[1] Department of Neonatal Diagnosis and Treatment Center, Children's Hospital of Chongqing Medical University, Chongqing, China, [2] Ministry of Education Key Laboratory of Child Development and Disorders, Chongqing, China, [3] National Clinical Research Center for Child Health and Disorders, Chongqing, China, [4] China International Science and Technology Cooperation Base of Child Development and Critical Disorders, Chongqing, China, [5] Children's Hospital of Chongqing Medical University, Chongqing, China, [6] Chongqing Key Laboratory of Child Infection and Immunity, Chongqing, China

OPEN ACCESS

Edited by:
David Ong,
Franciscus Gasthuis & Vlietland, Netherlands

Reviewed by:
Travis K. Price,
University of California, Los Angeles, United States
Karina Kersbergen,
Amsterdam University Medical Center (UMC), Netherlands

***Correspondence:**
Lu-Quan Li
liluquan123@163.com
Zheng-Li Wang
zhengli_wang@126.com

Specialty section:
This article was submitted to Clinical Microbiology, a section of the journal Frontiers in Cellular and Infection Microbiology

Received: 22 October 2019
Accepted: 18 March 2020
Published: 09 April 2020

Citation:
Fu C-Y, Li L-Q, Yang T, She X, Ai Q and Wang Z-L (2020) Autoinducer-2 May Be a New Biomarker for Monitoring Neonatal Necrotizing Enterocolitis. Front. Cell. Infect. Microbiol. 10:140. doi: 10.3389/fcimb.2020.00140

Autoinducer-2 (AI-2) has a widely accepted role in bacterial intra- and interspecies communication. Little is known about the relationships between AI-2 and NEC. This study found that AI-2 levels in patients and in a NEC mouse model were detected using the *Vibrio harveyi* BB170 assay system. Bacterial communities of the newborns' stool microbiota (NEC acute group, NEC recovery group, control group, and antibiotics-free group) and of the NEC mouse model (NEC group and control group) were detected by high-throughput sequencing. Intestinal histopathological changes were observed after HE staining. The AI-2 level in the NEC acute group (44.75 [40.17∼65.52]) was significantly lower than that in the control group, NEC recovery group and antibiotics-free group. The overall microbiota compositions of each group at the phylum level were not significantly different. The proportions of Enterococcus, Clostridium_sensu_stricto_1, Peptoclostridium, and Veillonella had significant differences among the 4 groups at the genus level. In animal experiments, the AI-2 level in feces of NEC mice (56.89 ± 11.87) was significantly lower than that in the feces of control group mice (102.70 ± 22.97). The microbiota compositions of NEC and control group mice at the phylum level were not significantly different. At the genus level, Klebsiella, Clostridium_sensu_stricto_1, and Peptoclostridium abundances in the NEC group increased significantly compared with those in the control group ($P < 0.05$). In addition, Lactobacillus, Pasteurella, and Parabacteroides abundances in the NEC group decreased significantly compared with those in the normal control group ($P < 0.05$), while Lactobacillus, Pasteurella, and Parabacteroides abundances had the opposite trend. The AI-2 concentration decreased significantly in the acute phase of NEC and increased gradually in the convalescent phase. We conclude that the concentration of AI-2 was correlated with intestinal flora disorder and different stages of disease. AI-2 may be a new biomarker for the diagnosis and monitoring of NEC.

Trial Registry: ClinicalTrials.gov; ChiCTR-ROC-17013746; URL: www.clinicaltrials.gov

Keywords: autoinducer-2 (AI-2), necrotizing enterocolitis (NEC), biomarker, intestinal flora, newborn—intensive care units

INTRODUCTION

Necrotizing enterocolitis (NEC) is a serious neonatal intestinal disease that most frequently affects preterm infants. NEC reportedly affects ∼10% of all premature infants (Hackam et al., 2018). Neonatal care has evolved greatly over time, but despite improvements in ventilation, nutrition, and temperature regulation, NEC remains a leading cause of death from gastrointestinal disease (Warner et al., 2016). Prematurity, feeding patterns, incremental milk-feeding rates, antibiotics, intestinal ischemia, genetic factors, and intestinal bacterial colonization have been considered to be risk factors for NEC (Morrow et al., 2013). Although neonates often present with obvious clinical signs, the diagnosis of NEC can also be subtle and insidious. NEC in newborns often develops rapidly and is difficult to detect early due to a lack of specific biomarkers. Furthermore, the diagnostic modalities are always invasive or radioactive. Therefore, identifying a new biomarker for the diagnosis and monitoring of NEC that is non-invasive, non-radiative, inexpensive, and rapid is an important endeavor.

NEC does not occur in sterile animals, which proves the importance of intestinal bacterial colonization for NEC. NEC and gut bacteria are generally accepted to be causally associated (Rusconi et al., 2017). The use of antibiotics can lead to intestinal flora disorders, and many studies have reported an increased risk of NEC due to antibiotic use (Morrow et al., 2013). As Mihatsch et al. (2011) also reported, several randomized controlled trials in preterm infants have shown that probiotics can reduce the risk of NEC. Increasing evidence indicates that direct microbe-microbe interactions play a critical role in this process (Grigg and Sonnenberg, 2017), which involves density-dependent recognition of autoinducer-2 (AI-2). AI-2 is a well-known bacterial Quorum-sensing (QS) system signaling molecule that plays an important role in bacterial communication (Sun et al., 2015).

AI-2 synthase is encoded by *LuxS*, which has been shown to be able to regulate bacterial virulence, biofilm formation, and the production and release of virulence factors in numerous species (Buck et al., 2009). Many different gram-positive and gram-negative species have been reported to be able to detect the *LuxS* gene, and this phenomenon likely contributes to the interactions between bacteria inhabiting the mammalian gut (Sun et al., 2015; Thompson et al., 2015; Ismail et al., 2016). Artificially increasing the levels of AI-2 can partially counterbalance antibiotic-induced intestinal dysbiosis (Sun et al., 2015). AI-2 not only has important effects on gut colonization and probiotic functionality (Christiaen et al., 2014) but is also usually related to virulence and pathogenicity (Rees et al., 2017). Apart from these initial findings, no report on the relationship between NEC and AI-2 is available. As AI-2 is closely related to enteropathogenic bacteria and the colonization of probiotics, we speculate that AI-2 can be used as a biomarker to reflect the process of NEC.

Thus, we analyzed the bacterial composition of intestinal flora and the levels of AI-2 in infants with NEC and in control infants. The aim of the present study was to investigate whether the levels of AI-2 can help to monitor intestinal flora disorders and the intestinal inflammation of NEC.

MATERIALS AND METHODS

Patient Selection and Sample Collection

NEC and non-NEC newborns in the Department of Neonatology at the Children's Hospital of Chongqing Medical University were enrolled in this study. NEC diagnosis was performed according to the Bell NEC standard (Hoytema van Konijnenburg et al., 2017); stage II and above cases were selected to be included in the NEC group and divided into the NEC acute group (NEC acute phase group); and NEC recovery group (NEC recovery phase). Meanwhile, non-NEC neonates that had pneumonia or hyperbilirubinemia and no clinical symptoms of the gastrointestinal tract (bloating, vomiting, bloody stool) were included in the control group. The gestational age, day age, delivery mode, feeding practices and medical conditions for each infant in the control group and antibiotic-free group (no use of antibiotics) were matched with those in the NEC group. In addition, antibiotic use in the control group was also matched with that in the NEC group.

Feces collection was performed within 24 h after the diagnosis of NEC and 3 days after initiation of feeding in the NEC acute group and in the NEC recovery group, respectively. Infants in the control group had fecal samples collected according to the matching principles mentioned before. All fecal samples were collected in sterile tubes and frozen at −80°C for subsequent measurements of AI-2 and the microbial community. Finally, 20 samples from each group were included in this study.

Sample Preparation and AI-2 Activity Measurement

The AI-2 activity of the fecal samples was determined using the *V. harveyi* reporter strain BB170, as described previously (Raut et al., 2013; Hsiao et al., 2014). The BB170 strain (obtained from Prof. Baolin Sun, University of Science and Technology of China) was grown for 18 h at 30°C in 2216E (QDRS BIOTEC, China) medium and diluted 1:5,000 into fresh 2216E medium. Previously, frozen fecal samples were weighed to 40 mg, mixed with 1.6 ml of 2216E broth, vortexed for 5 min, and centrifuged at 4°C and 5,000 rpm for 10 min; supernatants were filtered through a 0.22 μl filter membrane (MILLIPORE, American), and the filtrate was harvested and then added to *V. harveyi* BB170 strain diluent for the AI-2 bioassay. Additionally, 20 μl of fecal filtrate, 1 μM AI-2 (Omm Scientific, American) standard solution and 2216E broth (as negative control) were added in quintuplicate to a 96-well-assay plate (Corning, American) with 180 μl of BB170 diluent to produce a final volume of 200 μl. The 96-well-assay plate was shaken at 30°C and 120 rpm. After 2.5 h, the bioluminescence intensity was measured every 30 min by

a multifunction microplate reader (Thermo, USA) until the value of the negative control group was minimized. The ratio of the fluorescence of the supernatant of the fecal sample to the 1 μM AI-2 standard solution represents the relative luminescence intensity.

Analysis of Fecal Sample Microbial Communities

Fecal microbial DNA was extracted according to the QIAamp FAST DNA Stool Mini-Kit (Qiagen, Germany) kit instructions. The V3+V4 region of the 16S rDNA gene was amplified using the universal primers 338F (5′-barcode-ACTCCTACGGGAGGCAGCA-3′) and 806R (5′-GGACTACHVGGGTWTCTAAT-3′). The polymerase chain reaction (PCR) conditions were as follows: predenaturation at 95°C for 3 min; 95°C for 30 s, 55°C for 30 s, and 72°C for 45 s for a total of 27 cycles; and, finally, 72°C for 10 min. The PCR amplification product was separated by 2% agarose gel electrophoresis, and the PCR product was recovered using an AxyPrep DNA Gel Recovery Kit (AXYGEN) and then quantitatively detected by a QuantiFluor^{TM}-ST Blue Fluorescence System (Promega). The library was built and sequenced according to the Illumina MiSeq platform-related process. The obtained raw data were optimized to remove bases with a tail mass value of 20 or less, to filter reads with an overlap length >10 bp, to filter reads at a mismatch ratio >0.2 in the overlap region of the splicing sequence, and to remove reads with a mismatched barcode sequence. The optimized sequence was divided into operational taxonomic units (OTUs) by Usearch (version 7.0), and statistical analysis of the biological information was usually performed at the OTU of 97% of similarity.

Animal Experiments

Neonatal Necrotizing Enterocolitis Mouse Model

Newborn C57BL/6J mice were purchased from the Animal Experiment Center of Chongqing Medical University (Chongqing, China). The NEC mouse model was previously described by Garg et al. (2015), Li et al. (2017), and Xiao et al. (2018) and was adopted here with some modifications: 7-day-old C57BL/6 newborn mice were randomly separated into two groups. The control group was breast-fed with their mothers, and the experimental group was fed with formula milk (2 g of Similac Advance in 10 ml of 33% Esbilac puppy milk replacer) (Zeng et al., 2017) at 30 μl/1 g body weight every 4 h with a silicone tube (1.9 Fr) for 3 days. These pups were also stressed three times a day with hypoxia treatments (100% nitrogen gas for 1 min) and cold stimulation (4°C) for 10 min; the control group did not undergo these interventions.

Histology Examination

Both the control and NEC group animals were decapitated 3 days after NEC induction. After the intestine was removed from the body, a 1-cm section of the distal ileum was cut and fixed in a 4% paraformaldehyde solution. Next, the tissue sample was dehydrated, embedded in paraffin, and cut into 4 μm slices. Subsequently, 4 μm tissue slices were stained with hematoxylin and eosin (HE). Finally, we observed histopathological changes under an optical microscope. The scoring system was graded as follows: normal (0); epithelial cell lifting or separation (1); necrosis to the midvillous level (2); necrosis of the entire villus (3); and transmural necrosis (4). The intestinal tissue injury was graded by a blinded evaluator, and a score of ≥2 points was considered positive for NEC (Dvorak et al., 2008; Yu et al., 2009).

Mouse Intestinal Content Collection and AI-2 Activity Measurement

The ileum and colon of the mice were lavaged with 400 μl of 2216E broth, and the intestinal contents were collected in sterile tubes before vortex oscillating, centrifuging, and filtering as previously described. Then, the supernatant filtrate was collected for an AI-2 bioassay, and the sediment was stored at −80°C. The AI-2 standard solution was diluted to 1 μM, 100 nM, and 10 nM. Finally, the AI-2 activity assay was performed as described above.

Analysis of Intestinal Microbial Community

The sediment from the previous step was used for intestinal microbial community analysis, as described above.

Statistical Analysis

SPSS version 24.0 (SPSS Inc., USA) was used to perform statistical analyses. The measurement data were tested for normal distribution. The data showing a normal distribution were expressed as the mean ± standard deviation (SD) and analyzed by a paired *t*-test or independent-sample *t*-test. Skewed data were analyzed by the Mann-Whitney *U*-test or Kruskal-Wallis test and described by the median and interquartile range (IQR).

RESULTS

Clinical Characteristics

Clinical background information of the enrolled infants is shown in **Table 1**. The subjects in the three groups—the NEC group, antibiotic-free group and control group—were sufficiently case-matched, and the flowchart is shown in **Figure 1**. No significant differences in the mode of delivery, type of feeding, gestational age, and gender ratio were noted between the NEC group and the control group.

AI-2 Assays of Neonatal Feces

To determine whether the level of AI-2 varies with disease progression, the relative levels of AI-2 in the 4 groups were analyzed. As shown in **Figure 2**, the level of AI-2 in the NEC acute group (44.75 [40.17∼65.52]) was significantly lower than that in the control group (76.65 [55.85∼112.77], $P = 0.004$) and antibiotic-free group (123.33 [93.15∼167.21], $P < 0.0001$).

Furthermore, the level of AI-2 in the antibiotic-free group was significantly higher than that in the control group ($P < 0.001$). The level of AI-2 in the NEC recovery group (76.68 [50.99∼104.48]) was significantly higher than that in the NEC acute group (44.75 [40.17∼65.52], $P = 0.007$), but 3 NEC infants showed the opposite trend (lower or almost the same compared with their recovery phase). One of the 3 infants suffered NEC recurrence, and another one developed milking slowness and abdominal distension.

TABLE 1 | Patient characteristics.

Variables	Anti-free ($n = 20$)	Control ($n = 20$)	NEC ($n = 20$)	*P-value
Age, ($\bar{x} \pm s$) day	11.80 ± 6.60	12.35 ± 6.59	12.45 ± 6.72	0.265
GA, ($\bar{x} \pm s$) week	37.85 ± 2.35	37.65 ± 2.25	37.60 ± 2.62	0.17
Male, % (n)	55% (11)	55% (11)	11/9	1
Breast feeding, % (n)	20% (4)	15% (3)	10% (2)	0.38/0.63
Vaginal delivery, % (n)	40% (8)	40% (8)	40% (8)	1
Procalcitonin M (P_{25}, P_{75}) ng/ml	0.08 (0.06, 0.10)	0.34 (0.10, 3.34)	1.47 (0.09, 15.68)	0.00
CRP > 8 mg/L, % (n)*	0% (0)	45% (9)	50% (10)	0.00
Bloody stool, % (n)	0% (0)	0% (0)	80% (16)	0.00
Vomiting	0% (0)	0% (0)	30% (6)	0.00
Intrahepatic or portal venous gas, % (n)	0% (0)	0% (0)	100% (20)	0.00

**CRP, C-reactive protein.*

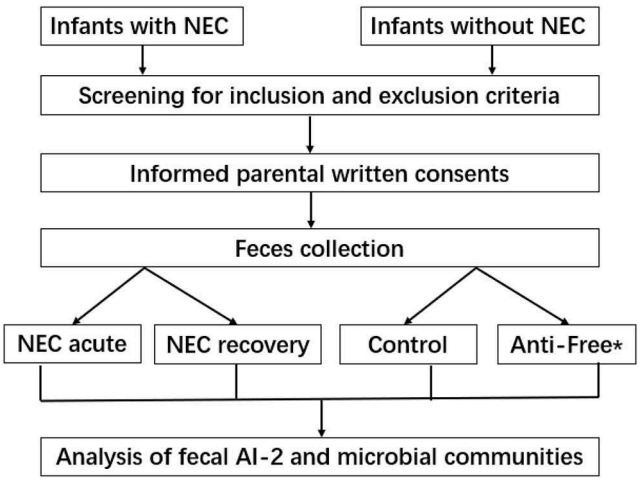

FIGURE 1 | Flow diagram of the study protocol. *Anti-free, the antibiotic-free group.

Diversity Analysis of the Microbiota

Fecal samples collected from the infants were amplified by the universal bacterial 16S rRNA primers. The positive PCR products were sequenced by the Illumina MiSeq high-throughput platform, and 7,15,040 effective sequences (through quality control) were generated, with an average of 8,938 sequences per sample.

The Shannon index values of the NEC acute and NEC recovery groups tended to be lower than those of the control group and antibiotic-free group. Nevertheless, no significant difference was found among the 4 groups (**Table 2**).

Composition Analysis of the Microbiota

The overall microbiota compositions of each group at the phylum and genus levels are shown in **Figures 3**, **4**. At the phylum level, the prevalence of *Firmicutes* was higher in the acute and recovery phases of NEC than that in the control group and antibiotic-free group, while *Bacteroides* tended to decrease in the acute and recovery phases of NEC, but no significant difference was observed ($P > 0.05$). As shown in **Figure 3**, *Enterococcus* increased in the acute and recovery NEC stage groups ($P = 0.0005$) compared with in the antibiotics-free group. *Clostridium_sensu_stricto_1* increased significantly in the acute stage of NEC ($P = 0.0002$); *Peptoclostridium* had the highest average proportion in the NEC recovery group and the lowest average proportion in the antibiotics-free group ($P = 0.02$); and *Veillonella* had the highest average proportion in the antibiotics-free group and the lowest average proportion in the NEC recovery group ($P = 0.003$).

General Situation of Model Mice

Neonatal mice in the control group grew well, reacted sensitively, moved normally, fed and defecated normally, and had plentiful subcutaneous fat. Neonatal mice in the NEC group gradually developed gastric retention, feeding difficulties, abdominal distention, diarrhea and even black stool, and hematochezia from the second day of modeling, accompanied by an obvious decrease in activity, poor reaction, and small size (**Figure 5**). As shown in **Figure 6**, the intestinal barrier was destroyed, and intestinal wall tissue necrosis occurred in the NEC group, while the intestinal wall barrier in the control group was intact without tissue necrosis. The pathological injury score results showed that the pathological injury score of intestinal tissue in the NEC group was significantly higher than that in the control group (**Figure 7**).

AI-2 Assays of Mouse Feces

As shown in **Figure 8**, the AI-2 level in the feces of NEC mice (56.89 ± 11.87) was significantly lower than that in the control group (102.70 ± 22.97), which was consistent with the clinical findings above.

Composition Analysis of the Microbiota in the NEC Mouse Model

At the phylum level (**Figure 9**), *Proteus* in the NEC mouse group was more abundant than that in the control group, while *Bacteroides* in the NEC group was less abundant than that in the normal control group, but no significant difference was noted ($P > 0.05$). At the genus level (**Figure 10**), *Klebsiella, Clostridium_sensu_stricto_1,* and *Peptoclostridium* abundance

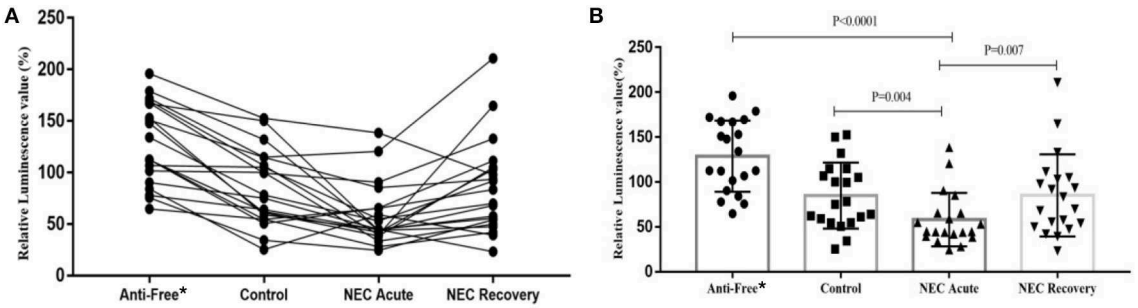

FIGURE 2 | The relative biofluorescence values of AI-2 in feces from each group. **(A)** Bar graph of the relative biofluorescence values of AI-2 in feces and **(B)** Line graph of the relative biofluorescence values of AI-2 in feces. *Anti-free, antibiotic-free group.

TABLE 2 | The Shannon index of each group at the phylum and genus levels, *M* (P_{25}∼P_{75}).

Shannon index	Anti-free*	Control	NEC acute	NEC recovery	*H*-value	*P*
Phylum level	0.67 (0.36∼0.84)	0.47 (0.35∼0.72)	0.51 (0.20∼0.62)	0.32 (0.08∼0.62)	3.94	0.27
Genus level	0.85 (0.61∼1.20)	0.93 (0.64∼1.09)	0.83 (0.71∼1.09)	0.68 (0.23∼1.04)	3.90	0.27

**Anti-free, antibiotic-free group.*

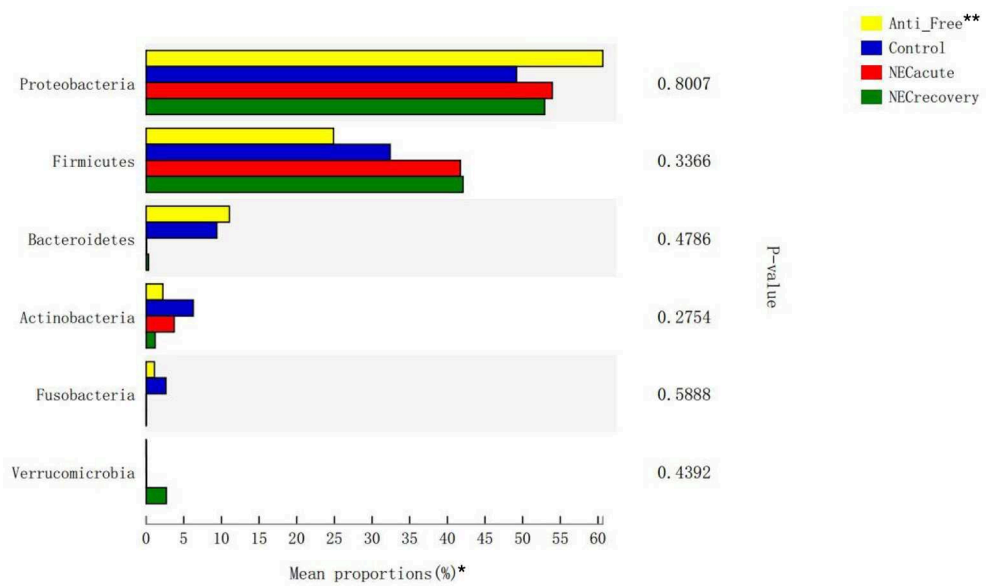

FIGURE 3 | Differences in flora composition in different groups at the phylum level. *The top six phyla are shown in the figure. **Anti-free, antibiotic-free group.

levels in the NEC mouse group increased significantly compared with those in the control group ($P < 0.05$). In addition, *Lactobacillus, Pasteurella,* and *Parabacteroides* abundances in the NEC group decreased significantly compared with those in the control group ($P < 0.05$).

DISCUSSION

NEC is a serious intestinal disorder of newborns, with high mortality and morbidity. In clinical practice, the main examinations for monitoring diseases include white blood cell count, procalcitonin levels, C-reactive protein levels, abdominal imaging and so on. Our study further revealed that AI-2 was significantly associated with the occurrence and recovery of NEC and that the level of AI-2 in NEC patients in the acute stage was lower than that in the controls and NEC patients in the recovery stage.

Although no single pathogen or pathogenic microbial community has been consistently identified to be associated with NEC, abnormal intestinal colonization has long been thought to contribute to NEC in newborns (Anatoly et al.,

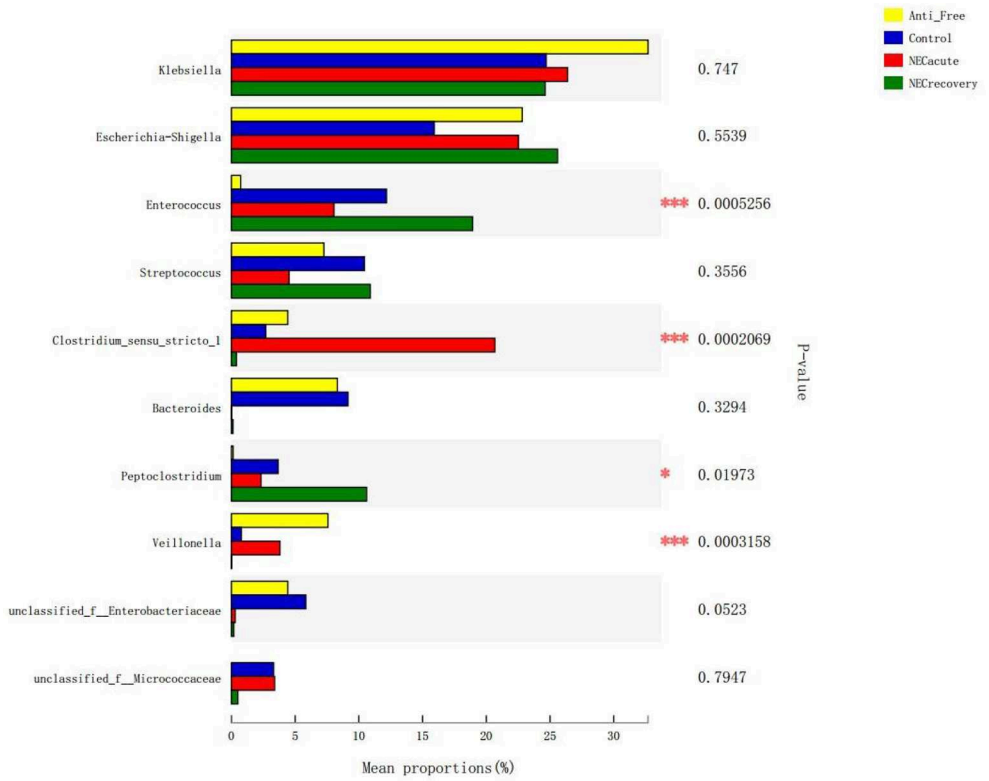

FIGURE 4 | Differences in flora composition in different groups at the genus level. Anti-free, antibiotic-free group (*$P < 0.05$; ***$P < 0.001$).

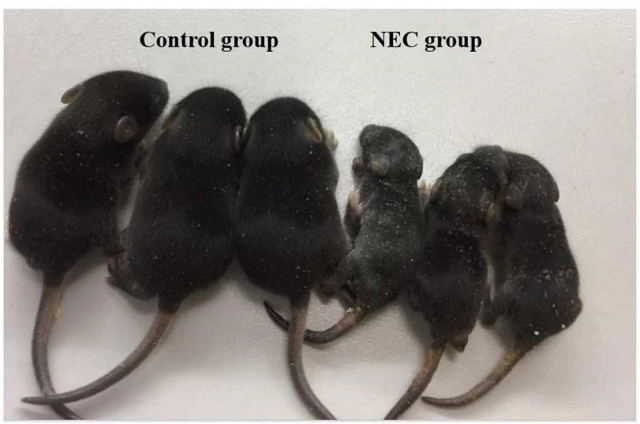

FIGURE 5 | The physical growth of mice in the NEC group and mice in the control group.

2013). Compared with previous studies that relied on culture or gel-based technology for microbial identification, the application of second-generation sequencing technology has improved our ability to evaluate this hypothesis (Morrow et al., 2013; Rusconi et al., 2017). When gut microbial diversity is examined in NEC, irrespective of the community composition, the results are mixed between studies. Many studies have reported a decrease in stool microbial diversity between NEC and control infants (McMurtry et al., 2015; Stewart et al., 2016; Ward et al., 2016; Warner et al., 2016), whereas some studies have found no difference (Mai et al., 2011; Morrow et al., 2013; Torrazza et al., 2013). As shown in **Table 2**, no difference was identified in the abundance of Proteobacteria at the phylum level (**Figure 3**) or in the Shannon index of each group at the phylum and genus levels. Furthermore, there was a significant difference in the abundance of *Enterococcus, Clostridium_sensu_stricto_1, Veillonella,* and *Peptoclostridium* at the genus level (**Figure 4**). The NEC recovery group had the lowest proportion of *Veillonella* and the highest proportion of *Peptoclostridium*. Gupta et al. (1994) also reported that *Enterococcus* spp., *Staphylococcus epidermidis,* and *Escherichia coli* were the most common aerobic bacterial species isolated, but no single pathogen was associated with the occurrence of NEC. A recent study reported that the proportion of *Clostridium_sensu_stricto_1* was increased in the pediatric diarrheic intestine (Wang et al., 2018). Wang Y. et al. (2017) also reported that, a high-grain diet dynamically increased the relative abundance of *Clostridium_sensu_stricto_1* and induced mucosal injuries in the colon of sheep. Quinoa consumption has been reported (Liu et al., 2018) to significantly alleviate DSS-induced dysbiosis as indicated by decreased abnormal expansion of the phylum Proteobacteria and decreased overgrowth of the genus *Peptoclostridium*. We also found that the abundances of *Enterococcus, Peptoclostridium,* and *Veillonella* were significantly

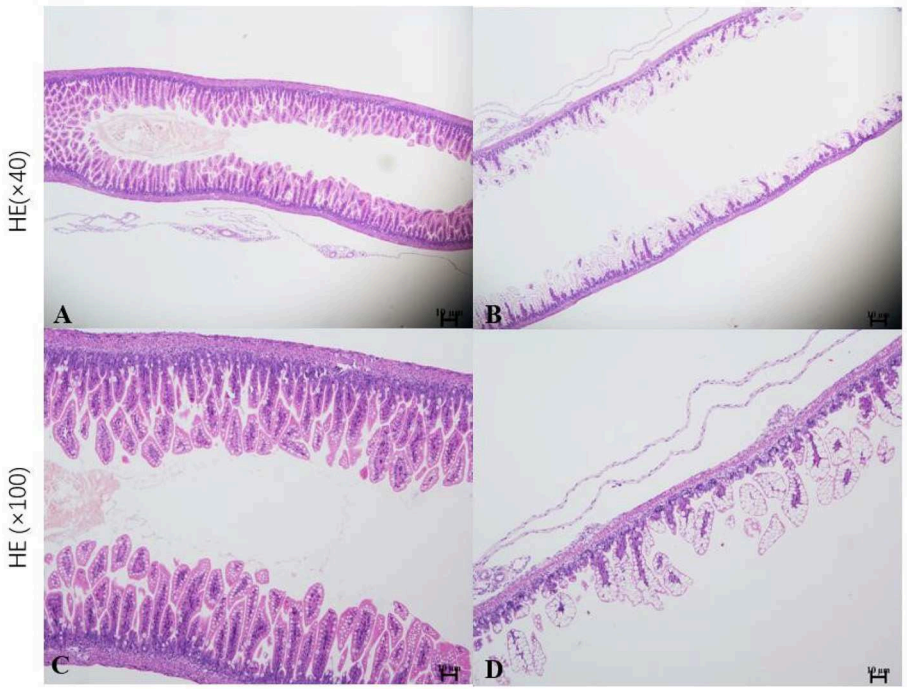

FIGURE 6 | Histopathological analysis of the intestinal tissue in mice. *Sections of intestinal tissue stained with hematoxylin and eosin are shown. **(A,C)** Control group and **(B,D)** NEC group.

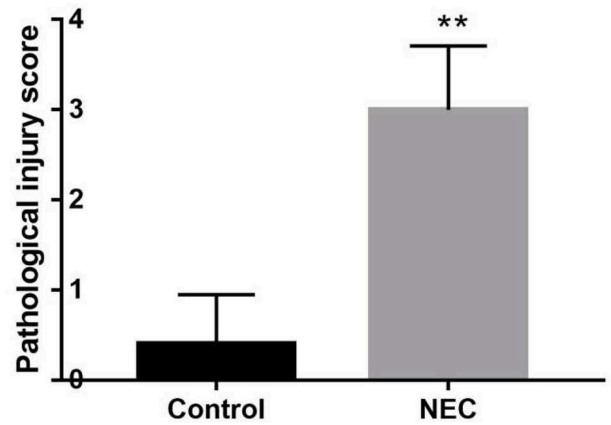

FIGURE 7 | Comparison of intestinal histopathological injury scores between NEC group mice and control group mice $^{**}P < 0.05$.

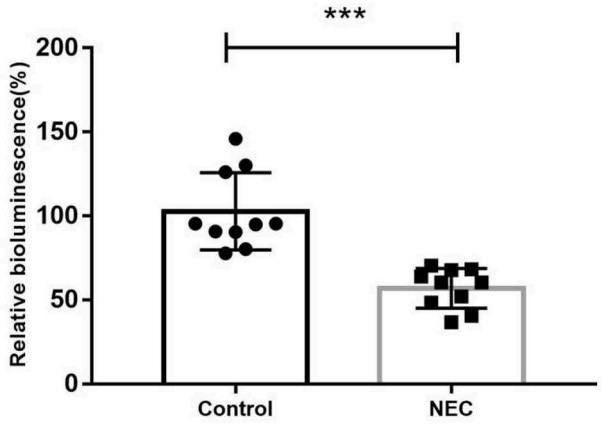

FIGURE 8 | The relative biofluorescence values of AI-2 in feces from two groups of newborn mice ($^{***}P < 0.0001$).

different between the antibiotics-free group and the control group, which indicated that antibiotics have a great influence on the intestinal flora of newborns.

AI-2 is a bacterial interspecies signaling molecule that plays an important role in the regulation of virulence factor production in pathogenic gram-negative and gram-positive bacteria (Pereira et al., 2013; Christiaen et al., 2014). AI-2 can be detected by bioluminescence method, only 50-100 mg feces are needed, a little bacterial culture medium and conventional bacterial culture equipment are used, and the detection can be completed in 3–4 h. It affects bacterial toxin production, biofilm formation, intestinal dysbiosis, motility, adherence to epithelial cells, and metabolism (Pereira et al., 2013; Sun et al., 2015; Thompson et al., 2015; Ismail et al., 2016; Wang et al., 2016). In the present study, there was a reduction in AI-2 levels in the NEC acute group, which were increased in the NEC recovery group. Furthermore, the AI-2 level of the control group was relatively lower than that of the antibiotics-free group, which indicated that antibiotic treatment had an effect on AI-2 levels.

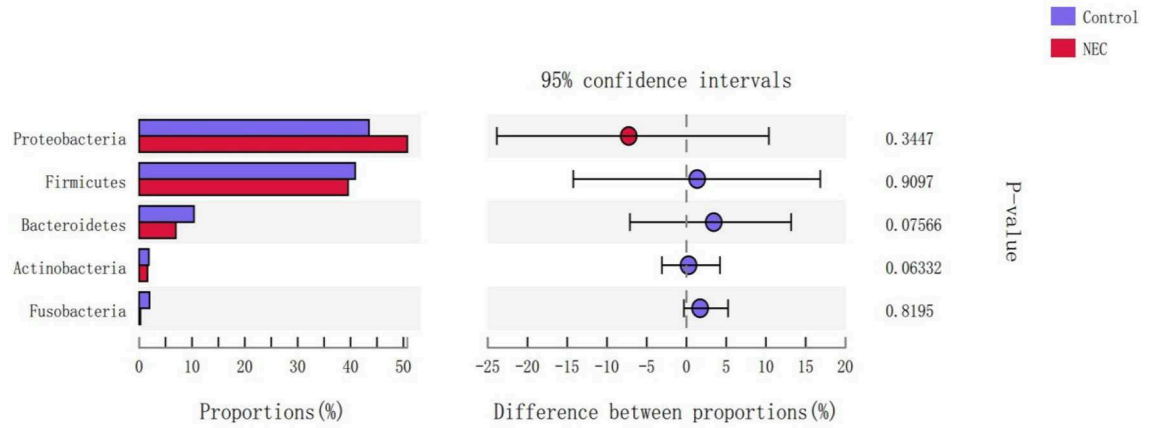

FIGURE 9 | Differences in the flora composition of mice at the phylum level.

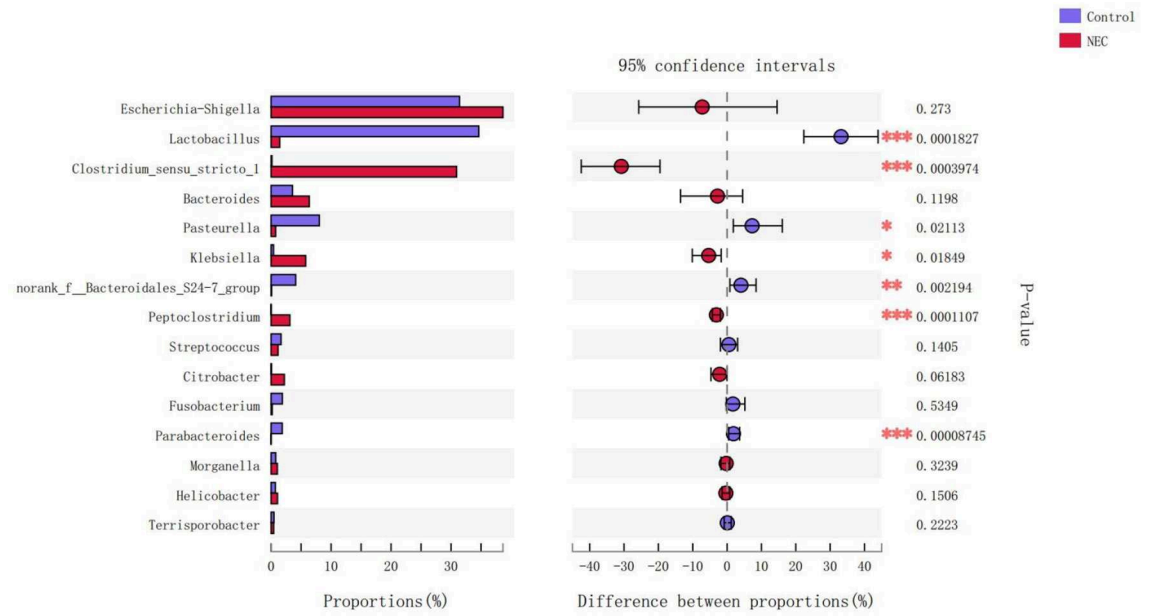

FIGURE 10 | Differences in the flora composition of mice at the genus level (*$P < 0.05$; **$P < 0.01$; ***$P < 0.001$).

Interestingly, the AI-2 levels of three NEC acute subjects were lower than those of the recovery phase subjects, one of whom had a recurrence of NEC and another of which had mild abdominal distension, poor digestion of milk, and a slow feeding rate. As Sun et al. (2015) also reported, antibiotic treatment leads to disruption of the normal composition of the microbiota and reductions in AI-2 levels and AI-2-producing bacteria, resulting in enhanced virulence gene expression by pathogens, while artificially increasing the levels of AI-2 partially reverses dysbiosis and reduces virulence gene expression (Sun et al., 2015). As Hsiao et al. (2014) also reported, *R. obeum* AI-2 reduces *Vibrio* colonization/pathogenicity and autoinducers and/or other mechanisms to limit colonization with *V. cholerae* or conceivably other enteropathogens. We speculate that when NEC occurs, the concentration of AI-2 decreases, the inhibitory effect of AI-2 on the virulence of pathogenic bacteria is reduced, and probiotic colonization is blocked. When NEC recovers, the AI-2 concentration increases, which may inhibit the virulence of pathogenic bacteria and promote the colonization of probiotics. These findings may indicate that AI-2 is related to intestinal flora disorders, which can also reflect bacterial pathogenicity and disease recovery in NEC to some extent.

Usually, we monitor NEC progress through WBC (white blood cell) counts, PCT (procalcitonin) levels, C-reactive protein levels, abdominal imaging, and so on. Recently, there have been many publications examining NEC biomarkers in the

past decades, such as cytokines (IL-8, TGF-β, IL-1RA, IL-1β), calprotectin, the non-protein amino acid citrulline, urine intestinal fatty acid-binding protein (IFABP), serum amyloid A (SAA), fecal calprotectin, the EpCAM/MMp7 ratio, a serum protein panel, volatile organic compounds, acylcarnitines, fibrinogen-g dimers, and so on (Rusconi et al., 2017; Hackam et al., 2018). However, no biomarkers have achieved widespread clinical application, and existing biomarkers cannot reflect intestinal flora disorder (Anatoly et al., 2013; Neu, 2014; Garg et al., 2018); furthermore, such examinations are usually invasive or radioactive (Stoll et al., 2015; Rusconi et al., 2017).

Methods such as direct-from-stool amplification and sequencing of the 16S ribosomal RNA subunit DNA or whole-genome shotgun (WGS) sequencing help us to identify microbial community members and distributions. However, these methods are very expensive and time-consuming (Rusconi et al., 2017). AI-2 has been proposed to promote interspecies bacterial communication in the mammalian gut (Ismail et al., 2016) and not only plays a crucial role in gut colonization and probiotic functionality (Christiaen et al., 2014) but is also related to intestinal dysbiosis (Bivar, 2018; Zhao et al., 2018). As in shown in **Figures 2**, **3**, we found that the level of AI-2 is affected by antibiotics, and that AI-2 can change before the proportion of bacteria changes significantly. In addition, the AI-2 examination was non-invasive, fast, inexpensive, and radiation free and may therefore play an important role in the diagnosis and monitoring of diseases.

Based on the current findings, the NEC mouse model showed similar changes in intestinal flora disorder and AI-2 concentrations, as shown in **Figures 6**–**8**. The changes in intestinal flora, AI-2 level, and pathology in the NEC mouse model were similar to those in infants with NEC. Interestingly, *Clostridium_sensu_stricto_1,* which was also much more abundant in NEC infants of the acute stage than in the other infants (**Figure 10**), was significantly more abundant in the NEC mouse group than in the control mouse group. *Clostridium* is one of the most common anaerobes identified from the common fecal microflora of preterm infants (Laurent et al., 2012), and *Clostridium_sensu_stricto_1* in particular was considered to be associated with NEC (Schonherr-Hellec and Aires, 2019). In studies of the intestinal flora of animals, *Clostridium_sensu_stricto_1* has been reported to have a detrimental effect on the colonic health of sheep (Wang J. et al., 2017; Wang Y. et al., 2017).

Our study suggested that AI-2 has obvious changes associated with the onset and progression of NEC in both animal experiments and clinical studies, so AI-2 may be a new marker for monitoring NEC.

In summary, the present results reveal that the AI-2 concentration decreased significantly in the acute phase of NEC and increased gradually in the convalescent phase of NEC. The concentration of AI-2 was correlated with intestinal flora disorder and different stages of disease and changed before the proportion of bacteria changed significantly. AI-2 may be a new biomarker for monitoring NEC.

DATA AVAILABILITY STATEMENT

The datasets generated for this study are available on request to the corresponding author.

ETHICS STATEMENT

The studies involving human participants were reviewed and approved by the Ethics Committee of the Children's Hospital of Chongqing Medical University. Written informed consent to participate in this study was provided by the participants' legal guardian/next of kin. The animal study was reviewed and approved by Institutional Animal Care and Use Committee (IACUC) at the University of Chongqing Medical University.

AUTHOR CONTRIBUTIONS

L-QL and Z-LW contributed to conceptualization, funding acquisition, and supervision. C-YF and TY helped with data curation. L-QL, C-YF, TY, and XS worked on the formal analysis. C-YF, L-QL, TY, XS, and Z-LW carried out the investigation. C-YF, XS, Z-LW, and QA contributed to the methodology. C-YF and Z-LW were responsible for project administration and writing the original draft. TY and QA contributed to resources. TY was responsible for the validation. Z-LW and L-QL reviewed and edited the manuscript.

FUNDING

This work was supported by the National Natural Science Foundation of China (Grant No. 81601323), the Scientific Research Foundation of the Science and Technology Commission of Chongqing (Grant Nos. cstc2019jcyj-msxmX0169 and cstc2018jscx-msybX0027), and Chongqing Municipal Administration of Human Resources and Social Security (Grant No. Cx2017107).

REFERENCES

Anatoly, G., Stephanie, P., Brandon, B., Jin, W., and Ford, H. R. (2013). The role of the intestinal microbiota in the pathogenesis of necrotizing enterocolitis. *Semin. Pediatr. Surg.* 22, 69–75. doi: 10.1053/j.sempedsurg.2013.01.002

Bivar, K. X. (2018). Bacterial interspecies quorum sensing in the mammalian gut microbiota. *C. R. Biol.* 341, 297–299. doi: 10.1016/j.crvi.2018.03.006

Buck, B. L., Azcarate-Peril, M. A., and Klaenhammer, T. R. (2009). Role of autoinducer-2 on the adhesion ability of *Lactobacillus acidophilus*. *J. Appl. Microbiol* 107, 269–279. doi: 10.1111/j.1365-2672.2009.04204.x

Christiaen, S. E. A., Motherway, M. O. C., Bottacini, F., Lanigan, N., Casey, P. G., Huys, G., et al. (2014). Autoinducer-2 plays a crucial role in gut colonization and probiotic functionality of *Bifidobacterium breve* UCC2003. *PLoS ONE* 9:e98111. doi: 10.1371/journal.pone.0098111

Dvorak, B., Khailova, L., Clark, J. A., Hosseini, D. M., Arganbright, K. M., Reynolds, C. A., et al. (2008). Comparison of epidermal growth factor and heparin-binding epidermal growth factor-like growth factor for prevention of experimental necrotizing enterocolitis. *J. Pediatr. Gastroenterol. Nutr.* 47, 11–18. doi: 10.1097/MPG.0b013e3181788618

Garg, B. D., Sharma, D., and Bansal, A. (2018). Biomarkers of necrotizing enterocolitis: a review of literature. *J. Matern. Fetal Neonatal Med.* 31, 3051–3064. doi: 10.1080/14767058.2017.1361925

Garg, P. M., Tatum, R., Ravisankar, S., Shekhawat, P. S., and Chen, Y. H. (2015). Necrotizing enterocolitis in a mouse model leads to widespread renal inflammation, acute kidney injury, and disruption of renal tight junction proteins. *Pediatr. Res.* 78, 527–532. doi: 10.1038/pr.2015.146

Grigg, J. B., and Sonnenberg, G. F. (2017). Host-microbiota interactions shape local and systemic inflammatory diseases. *J. Immunol.* 198, 564–571. doi: 10.4049/jimmunol.1601621

Gupta, S., Morris, J. G., Panigrahi, P., Nataro, J. P., Glass, R. I., and Gewolb, I. H. (1994). Endemic necrotizing enterocolitis: lack of association with a specific infectious agent. *Pediatr. Infect. Dis. J.* 13, 728–734. doi: 10.1097/00006454-199408000-00010

Hackam, D. J., Sodhi, C. P., and Good, M. (2018). New insights into necrotizing enterocolitis: from laboratory observation to personalized prevention and treatment *J. Pediatr. Surg.* 54, 398–404. doi: 10.1016/j.jpedsurg.2018.06.012

Hoytema van Konijnenburg, D. P., Reis, B. S., Pedicord, V. A., Farache, J., Victora, G. D., and Mucida, D. (2017). Intestinal epithelial and intraepithelial T cell crosstalk mediates a dynamic response to infection. *Cell.* 171, 783–794.e13. doi: 10.1101/154237

Hsiao, A., Ahmed, A. M., Subramanian, S., Griffin, N. W., Drewry, L. L., Petri, W. A. Jr., et al. (2014). Members of the human gut microbiota involved in recovery from *Vibrio cholerae* infection. *Nature* 515, 423–426. doi: 10.1038/nature13738

Ismail, A. S., Valastyan, J. S., and Bassler, B. L. (2016). A host-produced autoinducer-2 mimic activates bacterial quorum sensing. *Cell Host Microbe* 19, 470–480. doi: 10.1016/j.chom.2016.02.020

Laurent, F., Jos, B. M., Florence, C., Michel, V., Christophe, R. J., Julio, A., et al. (2012). Clostridia in premature neonates' gut: incidence, antibiotic susceptibility, and perinatal determinants influencing colonization. *PLoS ONE* 7:e30594. doi: 10.1371/journal.pone.0030594

Li, X., Li, X., Shang, Q., Gao, Z., Hao, F., Guo, H., et al. (2017). Fecal microbiota transplantation (FMT) could reverse the severity of experimental necrotizing enterocolitis (NEC) via oxidative stress modulation. *Free Radic. Biol. Med.* 108, 32–43. doi: 10.1016/j.freeradbiomed.2017.03.011

Liu, W., Zhang, Y., Qiu, B., Fan, S., Ding, H., and Liu, Z. (2018). Quinoa whole grain diet compromises the changes of gut microbiota and colonic colitis induced by dextran Sulfate sodium in C57BL/6 mice. *Sci. Rep.* 8:14916doi: 10.1038/s41598-018-33092-9

Mai, V., Young, C. M., Ukhanova, M., Wang, X., Sun, Y., Casella, G., et al. (2011). Fecal microbiota in premature infants prior to necrotizing enterocolitis. *PLoS ONE* 6:e20647doi: 10.1371/journal.pone.0020647

McMurtry, V. E., Gupta, R. W., Tran, L., Blanchard, E. E. T., Penn, D., Taylor, C. M., et al. (2015). Bacterial diversity and *Clostridia abundance* decrease with increasing severity of necrotizing enterocolitis. *Microbiome* 3:11. doi: 10.1186/s40168-015-0075-8

Mihatsch, W. A., Braegger, C. P., Decsi, T., Kolacek, S., Lanzinger, H., Mayer, B., et al. (2011). Critical systematic review of the level of evidence for routine use of probiotics for reduction of mortality and prevention of necrotizing enterocolitis and sepsis in preterm infants. *Clin. Nutr.* 31, 6–15. doi: 10.1016/j.clnu.2011.09.004

Morrow, A. L., Lagomarcino, A. J., Schibler, K. R., Taft, D. H., Yu, Z., Wang, B., et al. (2013). Early microbial and metabolomic signatures predict later onset of necrotizing enterocolitis in preterm infants. *Microbiome* 1:13. doi: 10.1186/2049-2618-1-13

Neu, J. (2014). Necrotizing enterocolitis: the mystery goes on. *Neonatology* 106, 289–295. doi: 10.1159/000365130

Pereira, C. S., Thompson, J. A., and Xavier, K. B. (2013). AI-2-mediated signalling in bacteria. *FEMS Microbiol. Rev.* 37, 156–181. doi: 10.1111/j.1574-6976.2012.00345.x

Raut, N., Pasini, P., and Daunert, S. (2013). Deciphering bacterial universal language by detecting the quorum sensing signal, autoinducer-2, with a whole-cell sensing system. *Anal. Chem.* 85, 9604–9609. doi: 10.1021/ac401776k

Rees, C. M., Hall, N. J., Fleming, P., and Eaton, S. (2017). Probiotics for the prevention of surgical necrotising enterocolitis: systematic review and meta-analysis. *BMJ Paediatr. Open* 1:e000066. doi: 10.1136/bmjpo-2017-000066

Rusconi, B., Good, M., and Warner, B. B. (2017). The microbiome and biomarkers for necrotizing enterocolitis: are we any closer to prediction? *J. Pediatr.* 189, 40–47.e2. doi: 10.1016/j.jpeds.2017.05.075

Schonherr-Hellec, S., and Aires, J. (2019). Clostridia and necrotizing enterocolitis in preterm neonates. *Anaerobe* 58, 6–12. doi: 10.1016/j.anaerobe.2019.04.005

Stewart, C. J., Embleton, N. D., Marrs, E. C., Smith, D. P., Nelson, A., Abdulkadir, B., et al. (2016). Temporal bacterial and metabolic development of the preterm gut reveals specific signatures in health and disease. *Microbiome* 4:67. doi: 10.1186/s40168-016-0216-8

Stoll, B. J., Hansen, N. I., Bell, E. F., Walsh, M. C., Carlo, W. A., Shankaran, S., et al. (2015). Trends in care practices, morbidity, and mortality of extremely preterm neonates, 1993-2012. *JAMA* 314, 1039–1051. doi: 10.1001/jama.2015.10244

Sun, Z., Grimm, V., and Riedel, C. U. (2015). AI-2 to the rescue against antibiotic-induced intestinal dysbiosis? *Trends Microbiol.* 23, 327–328. doi: 10.1016/j.tim.2015.04.002

Thompson, J. A., Oliveira, R. A., Djukovic, A., Ubeda, C., and Xavier, K. B. (2015). Manipulation of the quorum sensing signal AI-2 affects the antibiotic-treated gut microbiota. *Cell Rep.* 10, 1861–1871. doi: 10.1016/j.celrep.2015.02.049

Torrazza, R. M., Ukhanova, M., Wang, X., Sharma, R., Hudak, M. L., Neu, J., et al. (2013). Intestinal microbial ecology and environmental factors affecting necrotizing enterocolitis. *PLoS ONE* 8:e83304. doi: 10.1371/journal.pone.0083304

Wang, J., Li, C., Nesengani, L. T., Gong, Y., Zhang, S., and Lu, W. (2017). Characterization of vaginal microbiota of endometritis and healthy sows using high-throughput pyrosequencing of 16S rRNA gene. *Microb. Pathog.* 111, 325–330. doi: 10.1016/j.micpath.2017.08.030

Wang, Y., Xu, L., Liu, J., Zhu, W., and Mao, S. (2017). A high grain diet dynamically shifted the composition of mucosa-associated microbiota and induced mucosal injuries in the colon of sheep. *Front. Microbiol.* 8:2080. doi: 10.3389/fmicb.2017.02080

Wang, Y., Zhang, H., Zhu, L., Xu, Y., Liu, N., Sun, X., et al. (2018). Dynamic distribution of gut microbiota in goats at different ages and health states. *Front. Microbiol.* 9:2509. doi: 10.3389/fmicb.2018.02509

Wang, Z., Xiang, Q., Yang, T., Li, L., Yang, J., Li, H., et al. (2016). Autoinducer-2 of *Streptococcus mitis* as a target molecule to inhibit pathogenic multi-species biofilm formation *in vitro* and in an endotracheal intubation rat model. *Front. Microbiol.* 7:88. doi: 10.3389/fmicb.2016.00088

Ward, D. V., Scholz, M., Zolfo, M., Taft, D. H., Schibler, K. R., Tett, A., et al. (2016). Metagenomic sequencing with strain-level resolution implicates uropathogenic *E. coli* in necrotizing enterocolitis and mortality in preterm infants. *Cell Rep.* 14, 2912–2924. doi: 10.1016/j.celrep.2016.03.015

Warner, B. B., Deych, E., Zhou, Y., Hallmoore, C., Weinstock, G. M., Sodergren, E., et al. (2016). Gut bacteria dysbiosis and necrotising enterocolitis in very low birthweight infants: a prospective case-control study. *Lancet* 387, 1928–1936. doi: 10.1016/S0140-6736(16)00081-7

Xiao, S., Li, Q., Hu, K., He, Y., Ai, Q., Hu, L., et al. (2018). Vitamin A and retinoic acid exhibit protective effects on necrotizing enterocolitis by regulating intestinal flora and enhancing the intestinal epithelial barrier. *Arch. Med. Res.* 49, 1–9. doi: 10.1016/j.arcmed.2018.04.003

Yu, X., Radulescu, A., Zorko, N., and Besner, G. E. (2009). Heparin-binding EGF-like growth factor increases intestinal microvascular blood flow in necrotizing enterocolitis. *Gastroenterology* 137, 221–230. doi: 10.1053/j.gastro.2009.03.060

Zeng, Q., He, X., Puthiyakunnon, S., Xiao, H., Gong, Z., Boddu, S., et al. (2017). Probiotic mixture golden bifido prevents neonatal *Escherichia coli* K1 translocation via enhancing intestinal defense. *Front. Microbiol.* 8:1798. doi: 10.3389/fmicb.2017.01798

Zhao, J., Quan, C., Jin, L., and Chen, M. (2018). Production, detection and application perspectives of quorum sensing autoinducer-2 in bacteria. *J. Biotechnol.* 268, 53–60. doi: 10.1016/j.jbiotec.2018.01.009

Conflict of Interest: The authors declare that the research was conducted in the absence of any commercial or financial relationships that could be construed as a potential conflict of interest.

frontiers in Cellular and Infection Microbiology

MINI REVIEW
published: 29 April 2020
doi: 10.3389/fcimb.2020.00181

Current and Future Point-of-Care Tests for Emerging and New Respiratory Viruses and Future Perspectives

Philipp P. Nelson[1], Barbara A. Rath[2,3,4†], Paraskevi C. Fragkou[4,5†], Emmanouil Antalis[5], Sotirios Tsiodras[4,5] and Chrysanthi Skevaki[1,4] on behalf of the ESCMID Study Group for Respiratory Viruses (ESGREV)*

[1] Institute of Laboratory Medicine, Universities of Giessen and Marburg Lung Center (UGMLC), Philipps University Marburg, German Center for Lung Research (DZL) Marburg, Marburg, Germany, [2] Vienna Vaccine Safety Initiative - Pediatric Infectious Diseases and Vaccines, Berlin, Germany, [3] UMR Chrono-Environnement, Université Bourgogne Franche-Comté, Besançon, France, [4] ESCMID Study Group for Respiratory Viruses (ESGREV), Basel, Switzerland, [5] 4th Department of Internal Medicine, Attikon University Hospital, National and Kapodistrian University of Athens, Athens, Greece

The availability of pathogen-specific treatment options for respiratory tract infections (RTIs) increased the need for rapid diagnostic tests. Besides, retrospective studies, improved lab-based detection methods and the intensified search for new viruses since the beginning of the twenty-first century led to the discovery of several novel respiratory viruses. Among them are human bocavirus (HBoV), human coronaviruses (HCoV-HKU1, -NL63), human metapneumovirus (HMPV), rhinovirus type C (RV-C), and human polyomaviruses (KIPyV, WUPyV). Additionally, new viruses like SARS coronavirus (SARS-CoV), MERS coronavirus (MERS-CoV), novel strains of influenza virus A and B, and (most recently) SARS coronavirus 2 (SARS-CoV-2) have emerged. Although clinical presentation may be similar among different viruses, associated symptoms may range from a mild cold to a severe respiratory illness, and thus require a fast and reliable diagnosis. The increasing number of commercially available rapid point-of-care tests (POCTs) for respiratory viruses illustrates both the need for this kind of tests but also the problem, i.e., that the majority of such assays has significant limitations. In this review, we summarize recently published characteristics of POCTs and discuss their implications for the treatment of RTIs. The second key aspect of this work is a description of new and innovative diagnostic techniques, ranging from biosensors to novel portable and current lab-based nucleic acid amplification methods with the potential future use in point-of-care settings. While prototypes for some methods already exist, other ideas are still experimental, but all of them give an outlook of what can be expected as the next generation of POCTs.

Keywords: virus diagnostics, innovative approaches, biosensors, bedside testing, POCT, commercial point-of-care tests

OPEN ACCESS

Edited by:
David Ong,
Franciscus Gasthuis & Vlietland, Netherlands

Reviewed by:
Kai Huang,
The University of Texas Medical Branch at Galveston, United States
Valentijn Schweitzer,
University Medical Center Utrecht, Netherlands

***Correspondence:**
Chrysanthi Skevaki
chrysanthi.skevaki@uk-gm.de

†These authors have contributed equally to this work

Specialty section:
This article was submitted to Clinical Microbiology, a section of the journal Frontiers in Cellular and Infection Microbiology

Received: *22 November 2019*
Accepted: *06 April 2020*
Published: *29 April 2020*

Citation:
Nelson PP, Rath BA, Fragkou PC, Antalis E, Tsiodras S and Skevaki C (2020) Current and Future Point-of-Care Tests for Emerging and New Respiratory Viruses and Future Perspectives. Front. Cell. Infect. Microbiol. 10:181. doi: 10.3389/fcimb.2020.00181

INTRODUCTION

Respiratory viruses such as influenza A viruses (IAV) or human respiratory syncytial virus (RSV) are well-known, circulate worldwide, and are associated with significant morbidity and mortality (Iuliano et al., 2018; Shi et al., 2019). On the other hand, there are emerging infectious diseases which were, according to the definition by the WHO, hitherto unknown or rare but are now rapidly spreading either in number of cases or geographically (WHO, 2014a). In the last 20 years, in addition to the emergence of novel influenza and coronaviruses, advances in molecular detection methods have led to the discovery of new respiratory viruses already circulating worldwide (Jartti et al., 2012).

In 2001 human metapneumovirus (HMPV) was discovered (van den Hoogen et al., 2001). The outbreaks of severe acute respiratory syndrome coronavirus (SARS-CoV) in 2003, Middle East respiratory syndrome coronavirus (MERS-CoV) since April 2012, and SARS-CoV-2 since December 2019 highlight the danger of emerging (zoonotic) and highly pathogenic respiratory viruses (Fouchier et al., 2003; Zaki et al., 2012; WHO, 2020c). Two other coronaviruses, human coronaviruses (HCoV) NL63 and HKU1 were discovered in 2004 and 2005, respectively (Fouchier et al., 2004; van der Hoek et al., 2004; Woo et al., 2005). In 2005, Allander et al. described a new member of the family *Parvoviridae*, human bocavirus (HBoV) (Allander et al., 2005). The two new human polyomaviruses KI and WU (KIPyV, WUPyV) were first discovered in 2007 (Allander et al., 2007; Gaynor et al., 2007) and although often detected in samples, their role in causality of respiratory illness is still under discussion (reviewed in Jartti et al., 2012). In 2007, the human rhinovirus group C (RV-C) was introduced when newly sequenced strains differed significantly from the existing groups A and B (Lee et al., 2007). Finally, avian influenza viruses (AIV) such as IAV H5N1, H7N7, or H9N2 crossed the species barrier to infect humans several times in the last years (reviewed in Kim et al., 2016).

Lab-based techniques still dominate the field of virus diagnostics. Classical methods such as virus cultures, electron microscopy, and serology have been complemented by nucleic acid amplification tests (NAATs), sequencing (including next generation sequencing), and different antigen detection methods. Today, in most clinical settings, NAATs have replaced virus cultures as the gold standard, due to their high specificity, faster turnaround times, and absence of limitations posed by the need for susceptible cell lines (Fox, 2007).

In contrast to lab-based tests, point-of-care tests (POCTs) are performed at the site of sample collection (e.g., bedside, physician's office, or emergency department) and provide results usually in <2 h (Basile et al., 2018; Vos et al., 2019). Furthermore, they require only little hands-on time and no specific laboratory training as most critical steps are automated in a single device. The latter may range from handheld to benchtop size and is not designed for high-throughput sample processing. POCTs and other fast diagnostic tests performed in laboratories but provide results within 1–2 h may be called near-POCTs. Prompt identification of the causative pathogen may help the responsible healthcare professional choosing the appropriate treatment or take the right decisions in outbreak situations, regarding hospitalization and quarantine (Brendish et al., 2015).

In this review, we provide a brief overview of currently available POCTs for the diagnosis of emerging and new respiratory viruses along with their advantages and limitations and discuss recently published approaches and techniques with a potential use in future POCTs.

COMMERCIALLY AVAILABLE TEST SYSTEMS

For the diagnosis of commonly encountered respiratory viruses such as IAV, influenza B virus (IBV), and RSV many commercially available POCTs and near-POCTs with different sensitivities and specificities for each virus are available (**Supplementary Table 1**). However, a recent meta-analysis has demonstrated that three newer generation rapid multiplex polymerase chain reaction systems (mPCRs) (*bioMérieux*BioFire® FilmArray® RP, Nanosphere Verigene® RV+ test, and Hologic Gen-Probe Prodesse assays) are highly accurate, though usually more expensive, and may provide important diagnostic information for early identification of IAV, IBV, and RSV (Huang H. S. et al., 2018; Rabold and Waggoner, 2019).

Diagnosis of emerging and novel viruses, including HBoV, RV-C, coronaviruses (e.g., HCoV-HKU1, HCoV-NL63, SARS-CoV-2) as well as specific subtypes of AIV (H5N1, H7N9, H10N8) and reassortant IAV strains remains challenging (Schuster and Williams, 2018; WHO, 2020a). The diagnosis of most of these viruses is based on molecular techniques that can only be performed at specialized referral centers. Recently, there has been increased interest in using POCTs in other settings, such as emergency departments, although implementation might be hampered by the need for specific training (Bouzid et al., 2020). NAATs have higher sensitivity than immunochromatographic assays, but generally, they require a higher degree of technical skills and training (Drancourt et al., 2016). Polymerase chain reaction (PCR) remains the gold standard technique for the diagnosis of AIV subtypes while WHO recommends against the utilization of rapid tests in avian flu diagnosis (WHO, 2005; Monne et al., 2008; Schuster and Williams, 2018). RV-C, is typically detected from nasopharyngeal specimens using reverse transcriptase PCR (RT-PCR) and specific species and serotypes can be further identified by semi-nested PCRs or sequencing (Bochkov et al., 2011; Jartti et al., 2012; Schuster and Williams, 2018).

Diagnosis of HBoV was based on the detection of the specific IgM antibody along with a 4-fold increase of the IgG titer or low IgG avidity indicative of seroconversion, but adaptive immune response requires several hours or even days to develop, thus the utility of such tests in acute settings is limited (Soderlund-Venermo et al., 2009). As HBoV DNA persists in airway secretions for months after an acute infection, quantitative PCR along with serology are currently the preferred diagnostic methods (Christensen et al., 2019). Viral DNAemia, mRNA detection via RT-PCR, and antigen immunodetection assays have

shown some promising results but further studies to define their sensitivity, specificity, and applicability in clinical practice are needed (Soderlund-Venermo et al., 2009; Christensen et al., 2010, 2013, 2019; Proenca-Modena et al., 2011; Xu et al., 2017).

The detection of KIPyV and WUPyV, found in secretion from both symptomatic and asymptomatic patients, is based on PCR and serology testing (Neske et al., 2010; Touze et al., 2010; Jartti et al., 2012).

SARS-CoV-2, HCoV-NL63, and -HKU1 as well as HMPV diagnosis is based primarily on RT-PCR methods (van den Hoogen et al., 2004; Nichols et al., 2008; Jartti et al., 2012; WHO, 2020a). No data is available for fluorescent antibody, rapid cultures and enzyme immunoassay (EIA) diagnostic tests for coronaviruses NL63 and HKU1, whereas fluorescent antibody assays may be of some utility for HMPV (Nichols et al., 2008; Jartti et al., 2012). For HMPV specifically, multiplex ligation-dependent probe amplification (MLPA) on a nasopharyngeal swab has high sensitivity and specificity rates (100 and 96%, respectively) (Reijans et al., 2008; Panda et al., 2014; Hoppe et al., 2016).

Available tests for the now extinct SARS-CoV include antibody testing using an EIA and RT-PCR tests in respiratory, blood, and stool specimens (CDC, 2004). For the detection of MERS-CoV, that has its epicenter in the Arabian peninsula, the United States Centers for Disease Control and Prevention (CDC) and the WHO recommend sampling from the lower respiratory tract and real-time RT-PCR (rRT-PCR) testing with specific primers since this appears to be more sensitive than testing of upper respiratory tract specimens (WHO, 2014b,c; CDC, 2015).

NAATs have been proven to be highly accurate and easily scalable tests during large outbreaks of novel or emerging viruses, like the SARS-CoV-2 pandemic. Rapid genome sequencing analysis accommodates the fast development of reliable in-house and commercially available NAATs reagents shortly after an outbreak onset (CDC, 2020; WHO, 2020b).

INNOVATIVE APPROACHES FOR FUTURE POCTs

Biosensors

Biosensors can be a reliable and cost-effective way to detect specific pathogens in point-of-care settings. Different types of sensors for rapid identification of respiratory viruses have been developed recently. By using a gold-coated array of carbon electrodes, the authors were able to detect MERS-CoV spike protein in the picogram range within 20 min (Layqah and Eissa, 2019). This electrochemical assay is based on the competitive binding of a MERS-CoV antibody either to the virus in the sample or to the immobilized antigen on the electrode, which can be measured by a reduced peak current through the chip. In theory, this technique can be easily expanded to simultaneously detect multiple viruses, however, its diagnostic performance needs to be validated with the use of patient samples.

Different types of biosensors for AIV detection use nanobio hybrid materials (reviewed in Lee et al., 2018). In one of those approaches, a DNA probe coupled to a field-effect transistor enabled detection of target DNA down to 1 fM (Lin et al., 2009). Another sensitive technique is based on surface plasmon resonance (SPR), in which biomolecules bound to a metal surface lead to the reduction of the reflection of an incident light beam (Tang et al., 2010; Chang et al., 2018). With a new antibody against a recombinant AIV H7N9, the authors were able to reach a detection limit of a few hundred copies per mL nasal fluid within 10 min of processing time. Although still experimental, the characteristics of this approach render it a promising candidate for a future rapid POCT.

New Techniques and Prototypes

In a capillary convective PCR (CCPCR), the reagents circulate across a temperature gradient in a simple capillary tube, which allows run times shorter than 30 min (Chou et al., 2011). Together with a self-made dipstick detection method, this principle was already used to test for non-respiratory viruses like hepatitis C virus (Zhang et al., 2013, 2014). Zhou et al. integrated this method into a 1.5 kg device for the automation of the detection of different IAV strains (Zhuo et al., 2018). Although fast and sensitive, manual RNA extraction limits the use as POCT so far. Hardick et al. presented another portable NAAT device not only for the detection of IAV, but also for IBV, RSV, and MERS-CoV. It is based on a RT-PCR in microfluidic cards but likewise lacks automated nucleic acid extraction (Hardick et al., 2018).

Alternatively to nucleic acid-based techniques, giant magnetoresistive (GMR) biosensors function comparable to an enzyme-linked immunosorbent assay but use magnetic labels instead of enzymes or fluorophores coupled to detection antibodies (Hall et al., 2010). With such a sensor, Wu et al. constructed a handheld device which, in connection with a computer or smartphone, was able to detect IAV H3N2 in purified and disrupted virus solutions (Wu et al., 2017). Although H3N2 strains are circulating already since 1968 in the human population (Smith et al., 2004), this method is likely adaptable to emerging AIVs with the use of appropriate capture antibodies.

By designing a prototype for a lateral flow assay for approximately 5 US$, Huang et al. proved that the simultaneous detection of IAV and IBV in swab samples is possible at very low costs (Huang et al., 2017). However, the sensitivity of this prototype needs significant improvements before it can be used under clinical conditions. Instead of constructing a completely new apparatus, Cui et al. used commercially available glucose test strips together with specifically designed glucose-bearing substrates to test for the cleavage activity of IAV neuraminidase in spiked samples (Cui et al., 2017).

Although the majority of the presented approaches and prototypes focuses on the detection of influenza viruses, most of them can theoretically be applied to emerging or new viruses with only minor changes.

Lab-Based NAATs With Potential Use as Point-of-Care Applications

In comparison to PCRs, isothermal NAATs do not require complex devices when working with extracted nucleic acids. Reverse transcription strand invasion-based amplification (RT-SIBA) and reverse transcription loop-mediated isothermal amplification (RT-LAMP) are two examples which have been used to detect e.g., HMPV (Song et al., 2014), IAV (Eboigbodin

et al., 2016), and MERS-CoV (Huang P. et al., 2018). Wang et al. went on to integrate seven RT-LAMP assays into a microfluidic chip for the multiplex detection of different respiratory viruses in a device weighing <3 kg (Wang et al., 2018). Another chip-based system, named iROAD, uses reverse transcription-based recombinase polymerase amplification (RT-RPA) and was able to rapidly identify IAV, different HCoVs, and other respiratory viruses in extracted nucleic acids (Koo et al., 2017).

DISCUSSION

Clinical Performance of POCTs

The development of new laboratory and point-of-care diagnostic tests for influenza, RSV, and emerging respiratory viruses has taken up pace in recent years. Healthcare professionals, hospital managers, and laboratory directors will need to update and re-evaluate best practices regularly.

The advancement of diagnostic capabilities may change the way we identify, document, and communicate respiratory viral infections in the future. Along with these developments, the expectations of patients and healthcare professionals may change as well, i.e., patients will want to know the responsible pathogen and their clinical prognosis. With the development of specific antiviral therapies and vaccines, new diagnostic algorithms will be needed to ensure the highest quality of care while containing costs.

From a viewpoint of quality of care and clinical management, timely infection control, and the ability to act upon results, the future will likely belong to portable, CLIA-waived rapid diagnostic tests that take 10–20 min.

A key criterion for the evaluation of diagnostic tests will be their clinical utility, i.e., their ability to identify the current culprit for the patient's symptoms, and to distinguish relevant pathogen(s) from bystander pathogens. More research is needed to correlate clinical outcomes and laboratory data.

A second concern will be the correct timing of diagnostic testing with regards to a patient's course of illness. The sensitivity and positive predictive value of a diagnostic test depend on specimen quality and virus load (which is usually higher in children and early in the course of illness), duration of viral shedding, and patient's immune status. Future diagnostic algorithms will need to consider these factors in addition to the epidemiology of viruses in the respective season or region.

Advantages and Limitations of POCTs

The initial criticism of POCTs was directed toward a lack of sensitivity and a high degree of variability in test results. Early studies during the 2009/10 flu pandemic reported sensitivities for influenza POCTs ranging from 20 to 70% for the same test kit (Rath et al., 2012). In published evaluation studies, it was not entirely clear whether POCTs were performed at the bedside or whether samples were sent to the laboratory, which would constitute a near-POCT. These methodological inconsistencies also impaired the value of meta-analyses comparing the point-of-care performance of different commercial tests (Chartrand et al., 2015). The reported performance differences also hint to the fact that the training and experience of the staff performing the test have an impact. Procedural concerns were most pronounced with early-stage lateral flow ("strip") tests, where the result was read manually. Second-generation antigen POCTs and modern molecular POCTs achieve significantly higher reproducibility and sensitivity through automation of key steps in the process. In 2018, the FDA implemented new performance regulations setting new sensitivity thresholds required for POCTs to maintain approval (FDA, 2017). As a result, only several influenza POCTs were taken off the market. The role of regulators in setting quality standards for POCTs cannot be underestimated (Zhang et al., 2016; Azar and Landry, 2018).

In addition to the reliability of the POCT result itself, the hands-on time and the time-to-result are still critical for user-acceptance at the bedside. It is expected that future POCTs will be more robust and easier to use.

As the majority of acute respiratory infections (ARI) is of viral origin, these infections are common reasons for inappropriate antibiotic use (Harris et al., 2016; Tief et al., 2016). Studies have raised the expectation that expanded use of virus diagnostics at the point-of-care may help to limit the use of antibiotics (Bonner et al., 2003). The European Health Action Plan on AMR (European Parliament, 2018) and the O'Neill Report on "Tackling Drug-resistant infections globally" (O'Neill, 2016) both point to rapid diagnostics as a key instrument in tackling AMR. Including POCTs in antimicrobial stewardship programs might increase their acceptance by physicians.

The ability to direct "the right treatment to the right patient at the right time" facilitates precision medicine. In the future, advanced virus diagnostics may be combined with biomarker POCTs for the prediction of individual-level host responses to further target treatment to those who are most likely to benefit from it.

A major obstacle to expanding the use of POCTs is cost. In fact, POCTs would be most impactful in settings where the majority of early treatment decisions are made. The current pricing schemes, however, seem too high for broad-scale testing in the community and emergency departments. In addition to pricing, reimbursement strategies need to be reconsidered. Even in hospital emergency rooms, per-capita standard reimbursements disincentivize the use of virus diagnostics in patients with ARI. Up-to-date economic models are needed to clarify the cost-effectiveness of different types of POCTs.

The steepest increase in antimicrobial resistance is being observed in low-middle income countries (LMIC) (WHO-PAHO, 2018). For LMIC, portable POCTs with multi-modality for known and emerging pathogens, or simple lab-based instrumentation with no/minimal need for cold chain or refrigeration of reagents, may be the most likely to succeed.

Priorities for the Development of New POCTs

None of the currently commercially available POCTs covers all viruses discussed here (**Tables 1**, **2**, **Supplementary Table 1**). To date, the same holds true for new technologies as well. However, it is conceivable that these techniques may be adapted to other respiratory viruses after having shown their usefulness in practice. Especially biosensors have the potential for a wider spectrum of applications. They also do not encounter the major

TABLE 1 | Selected commercial nucleic acid-based point-of-care tests (ordered by time to result).

POCT commercial name	Method/Time to result (min)	Detection of new and emerging respiratory viruses: Sensitivity (%)/Specificity(%)									
		HBoV	SARS-CoV	SARS-CoV-2	MERS-CoV	HCoV-HKU1	HCoV-NL63	KIPyV, WUPyV	HMPV	RV-C	Emerging IAV
Cepheid Xpert® Xpress Flu/RSV[b,c1]	rRT-PCR/20-30	N/A	N/A	N/A	N/A	N/A	N/A	N/A	N/A	N/A	H1N1pdm09, H3N2, AIV (H5N2, H5N8) 97.8/100
Mesabiotech™ Accula™ Influenza A&B and RSV[a2]	RT-PCR/30	N/A	N/A	N/A	N/A	N/A	N/A	N/A	N/A	N/A	H1N1pdm09, H3N2 97/94
Sekisui Diagnostics Silaris™ Influenza A&B Test[3]	PCR/30	N/A	N/A	N/A	N/A	N/A	N/A	N/A	N/A	N/A	H1N1pdm09, H3N2 97/94
Cepheid Xpert® Flu/RSV XC[b,c]	rRT-PCR/40-63	N/A	N/A	N/A	N/A	N/A	N/A	N/A	N/A	N/A	H1N1pdm09, H3N2, AIV (H5N2, H5N8) •
(Cepheid Xpert® Xpress SARS-CoV-2, 2020)[e]	rRT-PCR/ 45	N/A	N/A	•	N/A	N/A	N/A	N/A	N/A	N/A	N/A
BioMérieuxBioFire® FilmArray® Respiratory Panel 2 *plus*[4]	Endpoint melt curve analysis/45	N/A	N/A	N/A	•	95.8/99.8	95.8/100	N/A	94.6/99.2	N/A	H1N1pdm09, H3N2 88.9-100/99.6-100
Quidel® Solana® Respiratory Viral Panel Influenza A&B and RSV & HMPV[a5]	RT-HDA/45	N/A	N/A	N/A	N/A	N/A	N/A	N/A	•	N/A	*Strains not specified* •
DiaSorin Simplexa™ Flu A/B & RSV Direct Kit[6]	RT-PCR/60	N/A	N/A	N/A	N/A	N/A	N/A	N/A	N/A	N/A	H1N1pdm09, H3N2, >20 AIVs, 2 swine influenza strains 97/97.9
Cepheid Xpert® Flu[b]	rRT-PCR/75	N/A	N/A	N/A	N/A	N/A	N/A	N/A	N/A	N/A	H1N1pdm09 97.1-100/99.6
Luminex Verigene® RP Flex Test[7]	RT-PCR/<120	N/A	N/A	N/A	N/A	N/A	N/A	N/A	•	N/A	H1, H3 •
GenMark Dx® ePlex® Respiratory Panel[d]	PCR/<120	N/A	N/A	N/A	N/A	•	•	N/A	N/A	N/A	H1N1pdm09, H3N2 •
(GenMark Dx ePlex® SARS-CoV-2 Test, 2020) Test[e]	rRT-PCR/<120	N/A	N/A	•	N/A	N/A	N/A	N/A	N/A	N/A	N/A
(QIAGEN, 2019) Panel v2	rRT-PCR/120	100/99.5	N/A	N/A	N/A	100/100	91.7/100	N/A	100/100	N/A	H1N1pdm09, H3N2 91.7-100/100

[1] *Cepheid Xpert Flu. Product Page. Available online at: https://www.cepheid.com/en/cepheid-solutions/clinical-ivd-tests/critical-infectious-diseases/xpert-flu (accessed September 13, 2019).*

[2] *Mesabiotech™ Accula™ Flu A/FluB Test Package Insert. Manual. Available online at: https://static1.squarespace.com/static/5ca44a0a7eb88c46af449a53/t/5cddacb3f9689300010d93c3/1558031549318/LBL-60010$+$Accula$+$Flu$+$A$+$Flu$+$B$+$Package$+$Insert$+$EU.pdf (accessed November 10, 2019).*

[3] *Sekisui Diagnostics Silaris™ Influenza A&B Test. Manual. 481. Available online at: https://sekisuidiagnostics.com/product-documents/60012-d_v1.5_silaris_ifu.pdf (accessed November 10, 2019).*

[4] *Biomerieux BIOFIRE® FILMARRAY® Panels. Product Page. Available online at: https://www.biomerieux-diagnostics.com/filmarrayr-respiratory-panel (accessed September 13, 2019).*

[5] *Quidel® Solana Respiratory Viral Panel. Product Page. Available online at: https://www.quidel.com/molecular-diagnostics/respiratory-viral-panel (accessed November 10, 2019).*

[6] *DiaSorin Simplexa® Flu A/B and RSV Direct Kit. Product Page. Available online at: https://molecular.diasorin.com/us/kit/simplexa-flu-ab-rsv-direct-kit/ (accessed November 10, 2019).*

[7] *Luminex Verigene® Respiratory Pathogens Flex Test. Product Page. Available online at: https://www.luminexcorp.com/respiratory-pathogens-flex-test/ (accessed September 13, 2019).*

N/A, Virus not included in this assay; • Virus included, but specificity/sensitivity not available; RT-HAD, Reverse transcriptase helicase-dependent amplification; RT-PCR, Reverse transcriptase polymerase chain reaction; rRT-PCR, real-time RT-PCR; HBoV, Human bocavirus; (H)CoV, (Human) coronavirus; KI/WUPyV, KI/WU polyomavirus; HMPV, Human metapneumovirus; RV-C, Human rhinovirus type C; IAV, Influenza A virus; IBV, Influenza B virus; H1N1pdm09, Influenza A H1N1 pandemic 2009; AIV, Avian influenza virus; RSV, Respiratory Syncytial virus.

Please refer to ***Supplementary Table 1*** *for detailed reliability parameters.*

[a] Two different kits for Influenza (A, B) and RSV; [b] Performance reviewed in Basile et al. (2018); [c] Described in Loeffelholz et al. (2019); [d] Performance tested by Babady et al. (2018); [e] For use under the Emergency Use Authorization (EUA) only.

TABLE 2 | Selected commercial antigen-based point-of-care tests (ordered by time to result).

POCT commercial name	Method/Time to result (min)	Detection of new and emerging respiratory viruses: Sensitivity (%)/Specificity(%)									
		HBoV	SARS-CoV	SARS-CoV-2	MERS-CoV	HCoV-HKU1	HCoV-NL63	KIPyV, WUPyV	HMPV	RV-C	Emerging IAV
BD Veritor™ System Influenza A+B and RSV[a,b8]	LFIC/Digital immunoassay/ 10-11	N/A	N/A	N/A	N/A	N/A	N/A	N/A	N/A	N/A	H1N1pdm09, H3N2, AIV (H5N1, H5N2, N7N9) 89.6-90.2/99.07
Abbott SD BIOLINE Influenza Ag A/B/A(H1N1) pandemic[b9]	CI/10-15	N/A	N/A	N/A	N/A	N/A	N/A	N/A	N/A	N/A	H1N1pdm09 54.5-91.8/96.8-100
Princeton BioMeditech BioSign® Rapid Flu A+B Antigen Panel Test[10]	ICMI/10-15	N/A	N/A	N/A	N/A	N/A	N/A	N/A	N/A	N/A	H1N1pdm09, H3N2v, AIV (H5N1, H7N9) 89.2/99.4
Quidel® QuickVue® Influenza A+B and RSV[a,b11]	LFIC/10-15	N/A	N/A	N/A	N/A	N/A	N/A	N/A	N/A	N/A	H3N2, variable performance against other strains 20-98/89-100
Abbott Alere BinaxNOW® Influenza A+B and RSV[a,b12]	LFIC/15	N/A	N/A	N/A	N/A	N/A	N/A	N/A	N/A	N/A	H3 44.8-83/93-100
Quidel® Sofia® Influenza A+B Fluorescent Immunoassay[13]	FIA/15	N/A	N/A	N/A	N/A	N/A	N/A	N/A	N/A	N/A	H1N1pdm09, H3N2, variable performance against other strains 90-99/95-96
Thermo Scientific™ Xpect™ Influenza A+B and RSV[a14]	LFIC/15	N/A	N/A	N/A	N/A	N/A	N/A	N/A	N/A	N/A	H1N1pdm09, H3N2, AIV (H5N1, H7N9, H9N2) 92.2/100
ArcDia mariPOC® Respi[b15]	PE/20-120	76.5/100	N/A	N/A	N/A	N/A	N/A	N/A	78/100	N/A	H1N1v, H2N2, H3N2, AIV (H5N1, H7N9, H9N2, H7N3) 92.3-100/99.8-100

[8]*BDVeritor™ Flu A+B. Product Page. Available online at: https://www.bd.com/en-us/offerings/capabilities/microbiology-solutions/point-of-care-testing/veritor-system (accessed September 13, 2019).*
[9]*Abbot SD BIOLINE Influenza Ag A/ B/ A(H1N1) Pandemic. Product Page. Available online at: https://www.alere.com/en/home/product-details/sd-bioline-influenza-ag-aba-pandemic.html (accessed September 13, 2019).*
[10]*Princeton BioMeditech BioSign® Flu A+B. Product Page. Available online at: http://pbm.pequod.com/pages/products/biosign_flu_ab (accessed November 10, 2019).*
[11]*Quidel® QuickVue® Influenza A+B Test. Manual. Available online at: https://www.quidel.com/sites/default/files/product/documents/EF1350313EN00_1.pdf (accessed September 13, 2019).*
[12]*Abbot Alere Binax NOW®. Product Page. Available online at: https://www.alere.com/en/home/products-services/brands/binaxnow.html (accessed September 13, 2019).*
[13]*Quidel® Sofia® Influenza A+B FIA. Manual. Available online at: https://www.quidel.com/sites/default/files/product/documents/EF1219109EN00.pdf (accessed September 13, 2019).*
[14]*Thermo Scientific™ Xpect™ Flu A and B, and RSV. Brochure. Available online at: https://assets.thermofisher.com/TFS-Assets/MBD/brochures/Xpect-Flu-RSV-Brochure-991-135-ENG.pdf (accessed November 10, 2019).*
[15]*ArcDia mariPOC® respi. Brochure. Available online at: https://www.arcdia.com/wp-content/uploads/2019/05/2019-03-mariPOC-Respi-brochure-EN.pdf (accessed September 13, 2019).*
N/A, Virus not included in this assay; FIA, Fluorescent immunoassay; LFIC, Lateral flow immunochromatography assay; CI, Chromatographic immunoassay; PE, Photofluorescent excitation; ICMI, Immunochromatographic membrane immunoassay; HBoV, Human bocavirus; (H)CoV, (Human) coronavirus; KI/WUPyV, KI/WU polyomavirus; HMPV, Human metapneumovirus; RV-C, Human rhinovirus type C; IAV, Influenza A virus; H1N1pdm09, Influenza A H1N1 pandemic 2009; AIV, Avian influenza virus; IBV, Influenza B virus; RSV, Respiratory Syncytial virus.
Please refer to ***Supplementary Table 1*** *for detailed reliability parameters.*
[a]*Two different kits for Influenza (A, B) and RSV;* [b]*Performance reviewed in Basile et al. (2018).*

limitation of NAATs as POCTs: the extraction of nucleic acids (Ali et al., 2017). For these tests, even less obvious complications, like the stability of the plastic materials against required chemicals, have to be overcome for future highly specific nucleic acid-based POCTs.

Any ideal POCT should fulfill the ASSURED criteria of the World Health Organization to be applicable in resource-limited settings (Mabey et al., 2004). Currently, this is most likely true for tests based on lateral flow immunochromatography but coming improvements e.g., in miniaturization and battery capacity may facilitate the use of other test principles (Basile et al., 2018).

While economic benefits of POCTs and better outcomes for the patients are still discussed, it is likely that these tests will gain further importance with decreasing processing costs and improved robustness.

AUTHOR CONTRIBUTIONS

CS and PN planned, structured, and edited the manuscript. PN searched the literature and integrated all contributions. PN, BR, PF, EA, and ST participated in the writing of the first draft of the manuscript and subsequent revisions. BR and PF contributed equally to this work. All authors critically read, reviewed, and approved the submitted final version of the manuscript.

FUNDING

CS was supported by Universities Giessen and Marburg Lung Center (UGMLC), the German Center for Lung Research (DZL), University Hospital Giessen and Marburg (UKGM) research funding according to article 2, section 3 cooperation agreement, and the Deutsche Forschungsgemeinschaft (DFG)-funded-SFB 1021 (C04), -KFO 309 (P10), and SK 317/1-1 (project number 428518790). PF was supported by Doctorate scholarship by the State Scholarships Foundation (IKY), Partnership Agreement (PA) 2014-2020, co-financed by Greece and the European Union (European Social Fund - ESF) through the Operational Programme Human Resources Development, Education and Lifelong Learning 2014-2020.

ACKNOWLEDGMENTS

Authors would like to thank the ESCMID Study Group on Respiratory Viruses (ESGREV) for providing a platform for interaction between authors.

SUPPLEMENTARY MATERIAL

The Supplementary Material for this article can be found online at: https://www.frontiersin.org/articles/10.3389/fcimb.2020.00181/full#supplementary-material

REFERENCES

Ali, N., Rampazzo, R. D. C. P., Costa, A. D. T., and Krieger, M. A. (2017). Current nucleic acid extraction methods and their implications to point-of-care diagnostics. *Biomed. Res. Int.* 2017:9306564. doi: 10.1155/2017/9306564

Allander, T., Andreasson, K., Gupta, S., Bjerkner, A., Bogdanovic, G., Persson, M. A. A., et al. (2007). Identification of a third human polyomavirus. *J. Virol.* 81, 4130–4136. doi: 10.1128/JVI.00028-07

Allander, T., Tammi, M. T., Eriksson, M., Bjerkner, A., Tiveljung-Lindell, A., and Andersson, B., (2005). Cloning of a human parvovirus by molecular screening of respiratory tract samples. *Proc. Natl. Acad. Sci. U.S.A.* 102, 12891–12896. doi: 10.1073/pnas.0504666102

Azar, M. M., and Landry, M. L. (2018). Detection of influenza A and B viruses and respiratory syncytial virus by use of clinical laboratory improvement amendments of 1988 (CLIA)-waived point-of-care assays: a paradigm shift to molecular tests. *J. Clin. Microbiol.* 56:e00367-18. doi: 10.1128/JCM.00367-18

Babady, N. E., England, M. R., Jurcic Smith, K. L., He, T., Wijetunge, D. S., Tang, Y.-W., et al. (2018). Multicenter evaluation of the eplex respiratory pathogen panel for the detection of viral and bacterial respiratory tract pathogens in nasopharyngeal swabs. *J. Clin. Microbiol.* 56:e01658-17. doi: 10.1128/JCM.01658-17

Basile, K., Kok, J., and Dwyer, D. E. (2018). Point-of-care diagnostics for respiratory viral infections. *Expert. Rev. Mol. Diagn.* 18, 75–83. doi: 10.1080/14737159.2018.1419065

Bochkov, Y. A., Palmenberg, A. C., Lee, W. M., Rathe, J. A., Amineva, S. P., Sun, X., et al. (2011). Molecular modeling, organ culture and reverse genetics for a newly identified human rhinovirus C. *Nat. Med.* 17, 627–632. doi: 10.1038/nm.2358

Bonner, A. B., Monroe, K. W., Talley, L. I., Klasner, A. E., and Kimberlin, D. W. (2003). Impact of the rapid diagnosis of influenza on physician decision-making and patient management in the pediatric emergency department: results of a randomized, prospective, controlled trial. *Pediatrics* 112, 363–367. doi: 10.1542/peds.112.2.363

Bouzid, D., Zanella, M.-C., Kerneis, S., Visseaux, B., May, L., Schrenzel, J., et al. (2020). Rapid diagnostic tests for infectious diseases in the emergency department. *Clin. Microbiol. Infect*. doi: 10.1016/j.cmi.2020.02.024. [Epub ahead of print].

Brendish, N. J., Schiff, H. F., and Clark, T. W. (2015). Point-of-care testing for respiratory viruses in adults: the current landscape and future potential. *J. Infect.* 71, 501–510. doi: 10.1016/j.jinf.2015.07.008

CDC (2004). *Severe Acute Respiratory Syndrome*. Available online at: https://www.cdc.gov/sars/surveillance/absence.pdf (accessed September 13, 2019).

CDC (2015). *Interim Guidelines for Collecting, Handling, and Testing Clinical Specimens from Patients Under Investigation (PUIs) for Middle East Respiratory Syndrome Coronavirus (MERS-CoV) – Version 2.1*. Available online at: https://www.cdc.gov/coronavirus/mers/downloads/Guidelines-Clinical-Specimens.pdf (accessed March 01, 2019).

CDC (2020). *Frequently Asked Questions on COVID-19 Testing at Laboratories*. Available online at: https://www.cdc.gov/coronavirus/2019-ncov/lab/testing-laboratories.html (accessed March 14, 2020).

Cepheid Xpert® Xpress SARS-CoV-2 (2020). *Assay Manual*. Available online at: https://www.fda.gov/media/136314/download (accessed March 25, 2020).

Chang, Y.-F., Wang, W.-H., Hong, Y.-W., Yuan, R.-Y., Chen, K.-H., Huang, Y.-W., et al. (2018). Simple strategy for rapid and sensitive detection of avian influenza a H7N9 virus based on intensity-modulated SPR biosensor and new generated antibody. *Anal. Chem.* 90, 1861–1869. doi: 10.1021/acs.analchem.7b03934

Chartrand, C., Tremblay, N., Renaud, C., and Papenburg, J., (2015). Diagnostic accuracy of rapid antigen detection tests for respiratory syncytial virus infection: systematic review and meta-analysis. *J. Clin. Microbiol.* 53, 3738–3749. doi: 10.1128/JCM.01816-15

Chou, W. P., Chen, P. H., Miao, M., Kuo, L. S., Yeh, S. H., and Chen, P. J. (2011). Rapid DNA amplification in a capillary tube by natural convection with a single isothermal heater. *BioTechniques* 50, 52–57. doi: 10.2144/000113589

Christensen, A., Dollner, H., Skanke, L. H., Krokstad, S., Moe, N., and Nordbo, S. A. (2013). Detection of spliced mRNA from human bocavirus 1 in clinical samples from children with respiratory tract infections. *Emerg. Infect. Dis.* 19, 574–580. doi: 10.3201/eid1904.121775

Christensen, A., Kesti, O., Elenius, V., Eskola, A. L., Døllner, H., Altunbulakli, C., et al. (2019). Human bocaviruses and paediatric infections. *Lancet* 3, 418–426. doi: 10.1016/S2352-4642(19)30057-4

Christensen, A., Nordbo, S. A., Krokstad, S., Rognlien, A. G., and Dollner, H. (2010). Human bocavirus in children: mono-detection, high viral load and viraemia are associated with respiratory tract infection. *J. Clin. Virol.* 49, 158–162. doi: 10.1016/j.jcv.2010.07.016

Cui, X., Das, A., Dhawane, A. N., Sweeney, J., Zhang, X., Chivukula, V., et al. (2017). Highly specific and rapid glycan based amperometric detection of influenza viruses. *Chem. Sci.* 8, 3628–3634. doi: 10.1039/C6SC03720H

Drancourt, M., Michel-Lepage, A., Boyer, S., and Raoult, D. (2016). The point-of-care laboratory in clinical microbiology. *Clin. Microbiol. Rev.* 29, 429–447. doi: 10.1128/CMR.00090-15

Eboigbodin, K., Filén, S., Ojalehto, T., Brummer, M., Elf, S., Pousi, K., et al. (2016). Reverse transcription strand invasion based amplification (RT-SIBA): a method for rapid detection of influenza A and B. *Appl. Microbiol. Biotechnol.* 100, 5559–5567. doi: 10.1007/s00253-016-7491-y

European Parliament (2018). *European One Health Action Plan Against Antimicrobial Resistance (AMR)*. Available online at: https://oeil.secure.europarl.europa.eu/oeil/popups/ficheprocedure.do?lang=en&reference=2017/2254(INI) (accessed April 02, 2019).

FDA (2017). *Microbiology Devices; Reclassification of Influenza Virus Antigen Detection Test Systems Intended for Use Directly With Clinical Specimens*. Docket No. FDA-2014-N-0440. Available online at: https://www.govinfo.gov/content/pkg/FR-2017-01-12/pdf/2017-00199.pdf (accessed November 14, 2019).

Fouchier, R. A. M., Hartwig, N. G., Bestebroer, T. M., Niemeyer, B., Jong, J. C., de Simon, J. H., et al. (2004). A previously undescribed coronavirus associated with respiratory disease in humans. *Proc. Natl. Acad. Sci. U.S.A.* 101, 6212–6216. doi: 10.1073/pnas.0400762101

Fouchier, R. A. M., Kuiken, T., Schutten, M., van Amerongen, G., van Doornum, G. J. J., van den Hoogen, B. G., et al. (2003). Aetiology: koch's postulates fulfilled for SARS virus. *Nature* 423:240. doi: 10.1038/423240a

Fox, J. D. (2007). Nucleic acid amplification tests for detection of respiratory viruses. *J. Clin. Virol.* 40, S15–S23. doi: 10.1016/S1386-6532(07)70005-7

Gaynor, A. M., Nissen, M. D., Whiley, D. M., Mackay, I. M., Lambert, S. B., Wu, G., et al. (2007). Identification of a novel polyomavirus from patients with acute respiratory tract infections. *PLoS Pathog.* 3:e64. doi: 10.1371/journal.ppat.0030064

GenMark Dx ePlex® SARS-CoV-2 Test (2020). *Assay Manual*. Available online at: https://www.fda.gov/media/136282/download (accessed March 25, 2019).

Hall, D. A., Gaster, R. S., Lin, T., Osterfeld, S. J., Han, S., Murmann, B., et al. (2010). GMR biosensor arrays: a system perspective. *Biosens. Bioelectron.* 25, 2051–2057. doi: 10.1016/j.bios.2010.01.038

Hardick, J., Metzgar, D., Risen, L., Myers, C., Balansay, M., Malcom, T., et al. (2018). Initial performance evaluation of a spotted array mobile analysis platform (MAP) for the detection of influenza A/B, RSV, and MERS coronavirus. *Diagn. Microbiol. Infect. Dis.* 91, 245–247. doi: 10.1016/j.diagmicrobio.2018.02.011

Harris, A. M., Hicks, L. A., and Qaseem, A. (2016). Appropriate antibiotic use for acute respiratory tract infection in adults: advice for high-value care from the american college of physicians and the centers for disease control and prevention. *Ann. Intern. Med.* 164, 425–434. doi: 10.7326/M15-1840

Hoppe, B. P. C., Jongh, E., de Griffioen-Keijzer, A., Zijlstra-Baalbergen, J. M., IJzerman, E. P. F., and Baboe, F. (2016). Human metapneumovirus in haematopoietic stem cell transplantation recipients: a case series and review of the diagnostic and therapeutic approach. *Neth. J. Med.* 74, 336–341. Available online at: http://www.njmonline.nl/article.php?a=1762&d=1172&i=199

Huang, H. S., Tsai, C. L., Chang, J., Hsu, T. C., Lin, S., and Lee, C. C. (2018). Multiplex PCR system for the rapid diagnosis of respiratory virus infection: systematic review and meta-analysis. *Clin. Microbiol. Infect.* 24, 1055–1063. doi: 10.1016/j.cmi.2017.11.018

Huang, P., Wang, H., Cao, Z., Jin, H., Chi, H., Zhao, J., et al. (2018). A rapid and specific assay for the detection of MERS-CoV. *Front. Microbiol.* 9:1101. doi: 10.3389/fmicb.2018.01101

Huang, S., Abe, K., Bennett, S., Liang, T., Ladd, P. D., Yokobe, L., et al. (2017). Disposable autonomous device for swab-to-result diagnosis of influenza. *Anal. Chem.* 89, 5776–5783. doi: 10.1021/acs.analchem.6b04801

Iuliano, A. D., Roguski, K. M., Chang, H. H., Muscatello, D. J., Palekar, R., Tempia, S., et al. (2018). Estimates of global seasonal influenza-associated respiratory mortality: a modelling study. *Lancet* 391, 1285–1300. doi: 10.1016/S0140-6736(17)33293-2

Jartti, T., Jartti, L., Ruuskanen, O., and Söderlund-Venermo, M. (2012). New respiratory viral infections. *Curr. Opin. Pulm. Med.* 18, 271–278. doi: 10.1097/MCP.0b013e328351f8d4

Kim, S. M., Kim, Y.-I., Pascua, P. N. Q., and Choi, Y. K. (2016). Avian influenza a viruses: evolution and zoonotic infection. *Semin. Respir. Crit. Care Med.* 37, 501–511. doi: 10.1055/s-0036-1584953

Koo, B., Jin, C. E., Lee, T. Y., Lee, J. H., Park, M. K., Sung, H., et al. (2017). An isothermal, label-free, and rapid one-step RNA amplification/detection assay for diagnosis of respiratory viral infections. *Biosens. Bioelectron.* 90, 187–194. doi: 10.1016/j.bios.2016.11.051

Layqah, L. A., and Eissa, S. (2019). An electrochemical immunosensor for the corona virus associated with the middle east respiratory syndrome using an array of gold nanoparticle-modified carbon electrodes. *Mikrochim. Acta* 186:224. doi: 10.1007/s00604-019-3345-5

Lee, T., Ahn, J.-H., Park, S. Y., Kim, G.-H., Kim, J., Kim, T.-H., et al. (2018). Recent advances in AIV biosensors composed of nanobio hybrid material. *Micromachines* 9:651. doi: 10.3390/mi9120651

Lee, W.-M., Kiesner, C., Pappas, T., Lee, I., Grindle, K., Jartti, T., et al. (2007). A diverse group of previously unrecognized human rhinoviruses are common causes of respiratory illnesses in infants. *PLoS ONE* 2:e966. doi: 10.1371/journal.pone.0000966

Lin, C.-H., Hung, C.-H., Hsiao, C.-Y., Lin, H.-C., Ko, F.-H., and Yang, Y.-S. (2009). Poly-silicon nanowire field-effect transistor for ultrasensitive and label-free detection of pathogenic avian influenza DNA. *Biosens. Bioelectron.* 24, 3019–3024. doi: 10.1016/j.bios.2009.03.014

Loeffelholz, M., Jones, R., Uy, C., Lo, D., Kele, A., and Baron, E. J. (2019). *Cepheid assays Detect a Broad Range of Contemporary Human and Avian Influenza strains*. Available online at: https://www.cepheid.com/administrator/components/com_productcatalog/library-files/13c07133b4e35667b67e9158de356e05-1353---Monograph-on-Human-Influenza-and-Avian-Strains-Final-08082019-08082021.pdf (accessed September 13, 2019).

Mabey, D., Peeling, R. W., Ustianowski, A., and Perkins, M. D. (2004). Diagnostics for the developing world. *Nat. Rev. Microbiol.* 2, 231–240. doi: 10.1038/nrmicro841

Monne, I., Ormelli, S., Salviato, A., Battisti, C., de Bettini, F., Salomoni, A., et al. (2008). Development and validation of a one-step real-time PCR assay for simultaneous detection of subtype H5, H7, and H9 avian influenza viruses. *J. Clin. Microbiol.* 46, 1769–1773. doi: 10.1128/JCM.02204-07

Neske, F., Prifert, C., Scheiner, B., Ewald, M., Schubert, J., Opitz, A., et al. (2010). High prevalence of antibodies against polyomavirus WU, polyomavirus KI, and human bocavirus in German blood donors. *BMC Infect. Dis.* 10:215. doi: 10.1186/1471-2334-10-215

Nichols, W. G., Peck Campbell, A. J., and Boeckh, M. (2008). Respiratory viruses other than influenza virus: impact and therapeutic advances. *Clin. Microbiol. Rev.* 21, 274–90. doi: 10.1128/CMR.00045-07

O'Neill, J. (2016). *Tackling Drug-Resistant Infections Globally, Final Report and Recommendations*. Available online at: https://amr-review.org/sites/default/files/160518_Final%20paper_with%20cover.pdf (accessed March 20, 2020).

Panda, S., Mohakud, N. K., Pena, L., and Kumar, S. (2014). Human metapneumovirus: review of an important respiratory pathogen. *Int. J. Infect. Dis.* 25, 45–52. doi: 10.1016/j.ijid.2014.03.1394

Proenca-Modena, J. L., Gagliardi, T. B., Paula, F. E., Iwamoto, M. A., Criado, M. F., Camara, A. A., et al. (2011). Detection of human bocavirus mRNA in respiratory secretions correlates with high viral load and concurrent diarrhea. *PLoS ONE* 6:e21083. doi: 10.1371/journal.pone.0021083

QIAGEN (2019). *QIAstat-Dx® Respiratory Panel Instructions for Use: Version 2. Manual*. Available online at: https://www.qiagen.com/ie/resources/resourcedetail?id=371ac902-c220-4e88-9d22-9012c33f268b&lang$=$en (accessed November 10, 2019).

Rabold, E., and Waggoner, J. (2019). *Rapid Diagnostic Tests for Infectious Diseases*. Available online at: https://wwwnc.cdc.gov/travel/yellowbook/2020/posttravel-evaluation/rapid-diagnostic-tests-for-infectious-diseases (accessed March 08, 2020).

Rath, B., Tief, F., Obermeier, P., Tuerk, E., Karsch, K., Muehlhans, S., et al. (2012). Early detection of influenza A and B infection in infants and children using conventional and fluorescence-based rapid testing. *J. Clin. Virol.* 55, 329–333. doi: 10.1016/j.jcv.2012.08.002

Reijans, M., Dingemans, G., Klaassen, C. H., Meis, J. F., Keijdener, J., Mulders, B., et al. (2008). RespiFinder: a new multiparameter test to differentially identify fifteen respiratory viruses. *J. Clin. Microbiol.* 46, 1232–1240. doi: 10.1128/JCM.02294-07

Schuster, J. E., and Williams, J. V. (2018). Emerging respiratory viruses in children. *Infect. Dis. Clin. North. Am.* 32, 65–74. doi: 10.1016/j.idc.2017.10.001

Shi, T., Denouel, A., Tietjen, A. K., Campbell, I., Moran, E., Li, X., et al. (2019). Global disease burden estimates of respiratory syncytial virus-associated acute respiratory infection in older adults in 2015: a systematic review and meta-analysis. *J. Infect. Dis.* jiz059. doi: 10.1093/infdis/jiz059

Smith, D. J., Lapedes, A. S., Jong, J. C., de Bestebroer, T. M., Rimmelzwaan, G. F., Osterhaus, A. D. M. E., et al. (2004). Mapping the antigenic and genetic evolution of influenza virus. *Science* 305, 371–376. doi: 10.1126/science.1097211

Soderlund-Venermo, M., Lahtinen, A., Jartti, T., Hedman, L., Kemppainen, K., Lehtinen, P., et al. (2009). Clinical assessment and improved diagnosis of bocavirus-induced wheezing in children, Finland. *Emerg. Infect. Dis.* 15, 1423–1430. doi: 10.3201/eid1509.090204

Song, Q., Zhu, R., Sun, Y., Zhao, L., Wang, F., Deng, J., et al. (2014). Identification of human metapneumovirus genotypes A and B from clinical specimens by reverse transcription loop-mediated isothermal amplification. *J. Virol. Methods* 196, 133–138. doi: 10.1016/j.jviromet.2013.10.037

Tang, Y., Zeng, X., and Liang, J. (2010). Surface plasmon resonance: an introduction to a surface spectroscopy technique. *J. Chem. Educ.* 87, 742–746. doi: 10.1021/ed100186y

Tief, F., Hoppe, C., Seeber, L., Obermeier, P., Chen, X., Karsch, K., et al. (2016). An inception cohort study assessing the role of pneumococcal and other bacterial pathogens in children with influenza and ILI and a clinical decision model for stringent antibiotic use. *Antivir. Ther.* 21, 413–424. doi: 10.3851/IMP3034

Touze, A., Gaitan, J., Arnold, F., Cazal, R., Fleury, M. J., Combelas, N., et al. (2010). Generation of merkel cell polyomavirus (MCV)-like particles and their application to detection of MCV antibodies. *J. Clin. Microbiol.* 48, 1767–1770. doi: 10.1128/JCM.01691-09

van den Hoogen, B. G., Jong, J. C., de Groen, J., Kuiken, T., Groot, R., de, Fouchier, R. A. M., et al. (2001). A newly discovered human pneumovirus isolated from young children with respiratory tract disease. *Nat. Med.* 7, 719–724. doi: 10.1038/89098

van den Hoogen, B. G., Osterhaus, D. M. E., and Fouchier, R. A. M. (2004). Clinical impact and diagnosis of human metapneumovirus infection. *Pediatr. Infect. Dis. J.* 23, S25–32. doi: 10.1097/01.inf.0000108190.09824.e8

van der Hoek, L., Pyrc, K., Jebbink, M. F., Vermeulen-Oost, W., Berkhout, R. J. M., Wolthers, K. C., et al. (2004). Identification of a new human coronavirus. *Nat. Med.* 10, 368–373. doi: 10.1038/nm1024

Vos, L. M., Bruning, A. H. L., Reitsma, J. B., Schuurman, R., Riezebos-Brilman, A., Hoepelman, A. I. M., et al. (2019). Rapid molecular tests for influenza, respiratory syncytial virus, and other respiratory viruses: a systematic review of diagnostic accuracy and clinical impact studies. *Clin. Infect. Dis.* 69, 1243–1253. doi: 10.1093/cid/ciz056

Wang, R., Zhao, R., Li, Y., Kong, W., Guo, X., Yang, Y., et al. (2018). Rapid detection of multiple respiratory viruses based on microfluidic isothermal amplification and a real-time colorimetric method. *Lab. Chip.* 18, 3507–3515. doi: 10.1039/C8LC00841H

WHO (2005). *Recommendations on the Use of Rapid Testing for Influenza Diagnosis*. Available online at: https://www.who.int/influenza/resources/documents/RapidTestInfluenza_WebVersion.pdf (accessed September 13, 2019).

WHO (2014a). *A Brief Guide to Emerging Infectious Diseases and Zoonoses*. World Health Organization, Regional Office for South-East Asia. Available online at: https://apps.who.int/iris/handle/10665/204722 (accessed March 27, 2020).

WHO (2014b). *Interim Surveillance Recommendations for Human Infection with Middle East Respiratory Syndrome Coronavirus*. Available online at: https://www.who.int/csr/disease/coronavirus_infections/InterimRevisedSurveillanceRecommendations_nCoVinfection_14July2014.pdf?ua=1 (accessed September 13, 2019).

WHO (2014c). *Laboratory Testing for Middle East Respiratory Syndrome Coronavirus: Interim Recommendations (revised)*. Available online at: https://www.who.int/csr/disease/coronavirus_infections/WHO_interim_recommendations_lab_detection_MERSCoV_092014.pdf?ua,$=$1 (accessed September, 13, 2019).

WHO (2020a). *Coronavirus Disease (COVID-19) Technical Guidance: Laboratory Testing For 2019-nCoV in Humans*. Available online at: https://www.who.int/emergencies/diseases/novel-coronavirus-2019/technical-guidance/laboratory-guidance (accessed March 08, 2020).

WHO (2020b). *Laboratory Testing For 2019 Novel Coronavirus (2019-nCoV) in Suspected Human Cases: Interim Guidance*. Available online at: https://www.who.int/publications-detail/laboratory-testing-for-2019-novel-coronavirus-in-suspected-human-cases-20200117 (accessed March 14, 2020).

WHO (2020c). *Report of the WHO-China Joint Mission on Coronavirus Disease 2019 (COVID-19)*. Available online at: https://www.who.int/docs/default-source/coronaviruse/who-china-joint-mission-on-covid-19-final-report.pdf (accessed March 01, 2020).

WHO-PAHO (2018). *Recommendations for Implementing Antimicrobial Stewardship Programs in Latin America and the Caribbean: Manual for Public Health Decision-Makers*. Available online at: http://iris.paho.org/xmlui/handle/123456789/49645 (accessed November 13, 2020).

Woo, P. C. Y., Lau, S. K. P., Chu, C.-M., Chan, K.-H., Tsoi, H.-W., Huang, Y., et al. (2005). Characterization and complete genome sequence of a novel coronavirus, coronavirus HKU1, from patients with pneumonia. *J. Virol.* 79, 884–895. doi: 10.1128/JVI.79.2.884-895.2005

Wu, K., Klein, T., Krishna, V. D., Su, D., Perez, A. M., and Wang, J.-P. (2017). Portable GMR handheld platform for the detection of influenza a virus. *ACS Sens.* 2, 1594–1601. doi: 10.1021/acssensors.7b00432

Xu, M., Arku, B., Jartti, T., Koskinen, J., Peltola, V., Hedman, K., et al. (2017). Comparative diagnosis of human bocavirus 1 respiratory infection with messenger RNA reverse-transcription polymerase chain reaction (PCR), DNA quantitative PCR, and serology. *J. Infect. Dis.* 215, 1551–1557. doi: 10.1093/infdis/jix169

Zaki, A. M., van Boheemen, S., Bestebroer, T. M., Osterhaus, A. D. M. E., and Fouchier, R. A. M. (2012). Isolation of a novel coronavirus from a man with pneumonia in Saudi Arabia. *N. Engl. J. Med.* 367, 1814–1820. doi: 10.1056/NEJMoa1211721

Zhang, L., Hao, M., Zhang, K., Zhang, R., Lin, G., Jia, T., et al. (2016). External quality assessment for the molecular detection of MERS-CoV in China. *J. Clin. Virol.* 75, 5–9. doi: 10.1016/j.jcv.2015.12.001

Zhang, S., Lin, Y., Wang, J., Wang, P., Chen, J., Xue, M., et al. (2014). A convenient nucleic acid test on the basis of the capillary convective PCR for the on-site detection of enterovirus 71. *J. Mol. Diagn.* 16, 452–458. doi: 10.1016/j.jmoldx.2014.04.002

Zhang, S., Xue, M., Zhang, J., Chen, Q., Chen, J., Wang, Z., et al. (2013). A one-step dipstick assay for the on-site detection of nucleic acid. *Clin. Biochem.* 46, 1852–1856. doi: 10.1016/j.clinbiochem.2013.10.013

Zhuo, Z., Wang, J., Chen, W., Su, X., Chen, M., Fang, M., et al. (2018). A rapid on-site assay for the detection of influenza a by capillary convective PCR. *Mol. Diagn. Ther.* 22, 225–234. doi: 10.1007/s40291-018-0320-5

Conflict of Interest: CS received consultancy fees and research funding from Hycor Biomedical and Thermo Fisher Scientific, research funding from Mead Johnson Nutrition (MJN), and consultancy fees from Bencard Allergie.

The remaining authors declare that the research was conducted in the absence of any commercial or financial relationships that could be construed as a potential conflict of interest.

frontiers in Cellular and Infection Microbiology

ORIGINAL RESEARCH
published: 05 May 2020
doi: 10.3389/fcimb.2020.00127

Development of a Rapid and Sensitive Colorimetric Loop-Mediated Isothermal Amplification Assay: A Novel Technology for the Detection of *Coxiella burnetii* From Minimally Processed Clinical Samples

Nazish Sheikh[1], *Sanjay Kumar*[1]*, *Harsh Kumar Sharma*[2], *Sameer S. Bhagyawant*[3] and *Duraipandian Thavaselvam*[1]

[1] Biodetector Development Test and Evaluation Division, Defence Research and Development Establishment, Gwalior, India, [2] Division of Veterinary Public Health and Epidemiology, Sher-e-Kashmir University of Agricultural Sciences and Technology (SKUAST), Jammu, India, [3] SOS in Biotechnology, Jiwaji University, Gwalior, India

OPEN ACCESS

Edited by:
Aleksandra Barac,
University of Belgrade, Serbia

Reviewed by:
Rachael Priestley,
Centers for Disease Control and Prevention (CDC), United States
Mohammad Khalili,
Shahid Bahonar University of Kerman, Iran
Fimme Jan van der Wal,
Wageningen Bioveterinary Research (WBVR), Netherlands

***Correspondence:**
Sanjay Kumar
drksanjay78@gmail.com

Specialty section:
This article was submitted to Clinical Microbiology, a section of the journal Frontiers in Cellular and Infection Microbiology

Received: 13 September 2019
Accepted: 06 March 2020
Published: 05 May 2020

Citation:
Sheikh N, Kumar S, Sharma HK, Bhagyawant SS and Thavaselvam D (2020) Development of a Rapid and Sensitive Colorimetric Loop-Mediated Isothermal Amplification Assay: A Novel Technology for the Detection of Coxiella burnetii From Minimally Processed Clinical Samples. Front. Cell. Infect. Microbiol. 10:127. doi: 10.3389/fcimb.2020.00127

Q fever is an important zoonotic disease caused by the bacterium *Coxiella burnetii*. The agent is considered as a potential agent for bioterrorism because of its low infectious dose, aerial route of transmission, resistance to drying, and many commonly used disinfectants. Humans are largely infected by the inhalation of aerosols that are contaminated with parturition products of infected animals as well as by the consumption of unpasteurized milk products. Thus, rapid and accurate detection of *C. burnetii* in shedders, especially those that are asymptomatic, is important for early warning, which allows controlling its spread among animals and animal-to-human transmission. In the present study, a colorimetric loop-mediated isothermal amplification (LAMP) assay was developed to confirm the presence of *IS*1111a gene of *C. burnetii* in sheep vaginal swabs. The sensitivity of this assay was found to be very comparable to the quantitative PCR (qPCR) assay, which could detect three copies of the gene, which corresponds to a single cell of *C. burnetii*. The applicability of the colorimetric LAMP assay in the disease diagnosis was assessed by evaluating 145 vaginal swab samples collected from the sheep breeding farms with a history of stillbirth and repeated abortions. Compared to qPCR, colorimetric LAMP had a sensitivity of 93.75% (CI, 69.77–99.84%) and specificity of 100% (CI, 97.20–100%), with a positive (PPV) and negative predictive value (NPV) of 100 and 99.24%, respectively. A very high level of agreement was observed between both colorimetric LAMP and reference qPCR assay. The colorimetric LAMP assay reported here is a rapid and simple test without extensive sample preparation and has a short turnaround time of <45 min. To the best of our understanding, it is the very first study describing the use of colorimetric LAMP assay that detects *C. burnetii* in vaginal swab samples with minimal sample processing for DNA extraction.

Keywords: colorimetric LAMP, qPCR, POC, sensitive detection, *Coxiella burnetii*, Q fever

INTRODUCTION

Q fever is an important worldwide zoonosis caused by *Coxiella burnetii*, an obligate intracellular bacterium that has a wide host range including humans, ruminants, companion animals, birds, reptiles, and ticks (Angelakis and Raoult, 2010). In human infection, 60% of cases are reported to be asymptomatic. In symptomatic patients, an acute onset is characterized by headache, fever, myalgia, muscle cramps, and frequently an atypical pneumonia or hepatitis. Chronic manifestations may include endocarditis (Maurin and Raoult, 1999). *C. burnetii*-infected animals usually go unnoticed, while certain complications such as abortions, infertility, stillbirth, and metritis are frequently reported. *C. burnetii* shedding is mainly observed during parturition; however, other shedding routes such as milk, vaginal mucus, urine, and feces have also been reported (Porter et al., 2011). Humans are largely infected by the inhalation of aerosols that are contaminated with parturition products of animals as well as by the consumption of unpasteurized milk products (Raoult, 1996; Bouvery et al., 2003). Hence, rapid and accurate detection of *C. burnetii* in shedders is important for early warning, which allows controlling its spread among animals and animal-to-human transmission to obviate devastating outbreaks, such as of Netherlands (2007–2010). The outbreak involved thousands of registered cases of humans along with high reporting of abortions due to Q fever in livestock and accompanied an estimated total cost of 307 million for controlling it, which resulted in huge economic losses to both veterinary industry and society at large (Roest et al., 2011; Van Asseldonk et al., 2013).

C. burnetii isolation is time consuming, hazardous, and restricted to BSL-3 laboratories. The serological diagnosis fails to diagnose early infection, as *C. burnetii*-specific antibodies appear only after 2–3 weeks of infection (Fournier et al., 1998). Moreover, these techniques do not demonstrate the current shedding animals (Maurin and Raoult, 1999). Since molecular techniques have been proven to provide rapid and early diagnosis, conventional PCR (Stein and Raoult, 1992; Willems et al., 1994; Ibrahim et al., 1997; Lorenz et al., 1998), nested PCR (Willems et al., 1993; Kato et al., 1998; Zhang et al., 1998a,b), and quantitative PCR (qPCR) (Klee et al., 2006; De Bruin et al., 2013) are used to diagnose *C. burnetii* DNA in different clinical matrices. However, these techniques limits its adoption in resource-poor regions due to the requirement of maintenance of cold chain transportation and need for expensive instrumentation and trained personnel, which preclude the use of PCR at point of care (POC).

Loop-mediated isothermal amplification (LAMP) is a relatively novel type of DNA amplification assay that offers very sensitive, simple, and less time-consuming diagnostic method occurring at temperatures between 55 and 65°C. This assay makes use of a strand displacement activity enabled DNA polymerase and a set of four to six specific primers that recognize six to eight specific target regions, which eliminates the chance of non-specific binding and hence increases the specificity of the assay (Notomi et al., 2000; Nagamine et al., 2002). LAMP is capable of amplifying up to 10^9 copies of a target in <1 h using simple incubators such as heating blocks or water baths, which makes the method suitable for field conditions and in resource-poor laboratories (Notomi et al., 2000). Moreover, it is reported that LAMP reagents are thermostable at a storage temperature of 25 or 37°C. This, together with resistance of the LAMP assay to inhibitors found in crude clinical samples, makes it amenable to use at POC (Thekisoe et al., 2009). The results of the LAMP assay can be analyzed by observing turbidity with expensive turbidimeter, which restricts its use in resource-poor region (Parida et al., 2005; Zhang et al., 2014). Moreover, results can also be analyzed by performing the agarose gel electrophoresis or addition of intercalating dyes such as SYBR green or propidium iodide postamplification, which increases the risk of amplicon carryover contamination (Parida et al., 2005; Goto et al., 2009). The use of hydroxy naphthol blue (HNB) allows observation of LAMP products with the naked eye, thereby reducing the requirement of instruments. Furthermore adding HNB before the reaction in reaction mix minimizes the risk of obtaining false positives through aerosol, thus enabling the assay to be used in field settings (Goto et al., 2009). Addition of HNB to the reaction produced a visual color change from violet to blue (as the Mg^{2+} ions in solution were chelated by pyrophosphate ions). A positive reaction is indicated by a color change from violet to sky blue (Goto et al., 2009).

The present study describes the development of a rapid, specific, and sensitive colorimetric LAMP assay for the detection of *C. burnetii*. The utility of the assay was applied to sheep vaginal swabs that had undergone a rapid DNA extraction protocol (boiling) and has a short turnaround time of <45 min.

MATERIALS AND METHODS

Design of Colorimetric LAMP Primers

The primers used for colorimetric LAMP assay were designed based on the transposase gene insertion element *IS*1111a (GenBank, accession no. AE016828.2) of *C. burnetii*. Five sets of primers were designed using Primer Explorer V5 software (**Table S1**). All primers were synthesized by Eurofins MWG Operon (Bangalore, India). The F3 and B3 primers used for the colorimetric LAMP were also made use of to determine the sensitivity of qPCR and conventional PCR.

*IS*1111a Recombinant Plasmid Construction

To determine the analytical sensitivity of the colorimetric LAMP assay, a plasmid construct was made with the target sequence of *IS*1111a gene (AE016828.2). The region between the F3 and B3 primer was amplified using primers F3 (5′- GACGGGTTAAGCGTGCTC-3′) and B3 (5′-CTGCGCATCGTTACGATCA-3′). The resultant amplicon (194 bp) was cloned into the pGEM-T easy Vector System I (Promega, WI, United States). The recombinant plasmid was quantified by a Nanodrop 1000 (Thermo Scientific, United States) and was diluted serially 10-fold to analyze the sensitivity of the colorimetric LAMP.

DNA Extraction for qPCR and Colorimetric LAMP

A total of 145 vaginal swab samples were collected from the sheep breeding farms with stillbirth and repeated abortion of Jammu province of Jammu and Kashmir state, India. These samples were initially analyzed by nested PCR as per the protocol of Fenollar et al. (2004), and out of 145 samples, 15 samples were found positive for *C. burnetii*. Crude DNA preparation was performed by firmly pressing the collected vaginal swab against the side of a microfuge tube containing 400 μl of sterile phosphate buffered saline (pH 7.8). A 200-μl saline suspension was heated at 95°C for 5 min and subsequently centrifuged at 10,000 rpm for 5 min to obtain clear liquid on the top (Berri et al., 2001). A 5-μl aliquot of lysis supernatant was used for colorimetric LAMP testing. Total DNA was extracted from the remaining 200-μl saline suspensions left from crude DNA preparation procedure by a DNeasy Blood and Tissue kit (Qiagen) as per the manufacturer's protocols. The resultant 200 μl eluted genomic extract was aliquoted and stored at −80°C until required for qPCR and colorimetric LAMP analysis.

Bacterial genomic DNA for specificity evaluation was extracted using the same DNA extraction kit mentioned above.

Colorimetric LAMP Reaction

The colorimetric LAMP reaction mixture consisted of 25 μl of total reaction volume, which contained 1× isothermal amplification buffer (New England BioLabs, MA, United States), 0.8 μM of each of the loop forward (LF) and loop backward (LB) primer, 0.2 μM each of the F3 and B3 primers, and 1.6 μM each of the forward inner primer (FIP) and backward inner primer (BIP), 1.4 mM of deoxyribonucleotide triphosphates (dNTPs) (10 mM each; New England BioLabs, MA, United States), 6 mM $MgSO_4$ (100 mM; New England BioLabs, MA, United States), 5 μl of extracted DNA (crude DNA preparation and commercial kit extracted), 8 U of *Bst* Warm Start DNA Polymerase (New England BioLabs, MA, United States), and 0.8 M Betaine (Sigma). The optimization of optimal reaction temperature was accessed by performing a temperature gradient from 55 to 65°C in dry bath for 30 min, and the reaction was terminated by heating at 80°C for 5 min. The results were analyzed by both electrophoresis (2% agarose gels) and by visual detection, which involved the inclusion of HNB dyes at a final concentration of 120 μM during the reaction setup. A positive reaction is indicated by a color change from violet to sky blue.

Each run contained a positive control with *C. burnetii* DNA and a negative control without DNA template. Three different rooms were used for template preparation, LAMP master mix preparation, and the amplification by LAMP to circumvent any carry-over contamination with amplified products.

Sensitivity and Specificity of Colorimetric LAMP

For the determination of the limit of detection (LOD) and to analyze the reproducibility of the colorimetric LAMP assay, three independent assays were performed employing 10-fold serial dilutions of *IS*1111a recombinant plasmid to concentrations of 3×10^7 to 3×10^{-1} copies/μl made in a suitable buffer (25 mM Tris, pH 8.0). One microliter of these dilutions was added as the template to the final reaction volume of 25 μl, and tubes were incubated as per the optimized conditions mentioned earlier.

Similarly, the limit of detection of conventional PCR assay was also performed thrice. The PCR assay was performed using F3 and B3 LAMP primers, which resulted in 194 bp amplicon of the targeted *IS*1111a gene of *C. burnetii*. The PCR mixture contained 0.2 mM of each dNTP, 1× PCR buffer, 500 nM each of F3 and B3 primers, 1.5 mM $MgCl_2$, 1 U of Taq DNA polymerase (MBI Fermentas, Germany), and 1 μl of template DNA. The reaction volume was adjusted to 20-μl by nuclease-free water. The amplification was carried out in the C1000 thermal cycler (BioRad, United States) with a reaction condition of 95°C for 30 s for initial denaturation, followed by 30 cycles of denaturation at 95°C for 30 s, annealing at 61°C for 60 s, extension at 72°C for 30 s, and final extension at 72°C for 5 min. The endpoint detection of amplified products was done on 2.0% agarose gel by electrophoresis.

The specificity of the colorimetric LAMP assay was confirmed employing the DNAs (10 ng/reaction) of closely related bacteria (*Legionella pneumophila* and *Francisella tularensis*). Based on the sequence of its 16S rRNA, *C. burnetii* is classified into the order Legionellales, with *Legionella* spp. and *Francisella* spp. as nearest phylogenetic neighbors (Drancourt and Raoult, 2005). Other bacteria of BW importance such as *Vibrio cholera* **(02)**, *Brucella abortus* **(06)**, *Brucella melitensis* **(06)**, *Burkholderia pseudomallei* **(02)** and *Burkholderia mallei* **(02)**, *Bacillus anthracis* **(02)**, *Salmonella typhi*, *Shigella dysenteriae*, and *Escherichia coli* were analyzed as described above. The *C. burnetii* NMI and NMII served as positive control. The DNAs used in the experiment were from clinical isolates and standard type cultures.

qPCR Detection

The qPCR was employed as the reference molecular detection method. For the comparative analysis of the sensitivities of the colorimetric LAMP assay and qPCR, triplicate assays of nine 10-fold serial dilutions (to concentrations of 3×10^7 to 3×10^{-1} copies/μl) of *IS*1111a recombinant plasmid mentioned above were used to obtain the standard curves. The qPCR reaction was performed on ABI StepOne Real-Time PCR system (Applied Biosystems, USA) using 2× FAST SYBR Green Mastermix (Applied Biosystems, United States), 500 nM of forward primer F3, 500 nM of reverse primer B3, and 1 μl of DNA template for sensitivity determination, whereas for screening of vaginal swab samples, 5 μl of extracted DNA (crude DNA preparation and commercial kit extracted) was used in a total of 20 μl volume. The qPCR amplification condition involved an initial activation at 95°C for 20 s, which was followed by 40 cycles of 95°C for 3 s and 60°C for 30 s. The uniqueness of the amplified product was confirmed by performing a melting curve analysis.

Appropriate positive and negative controls were included for each run. To avoid any carry-over contamination with amplified products, proper precautions were taken as discussed earlier as taken for the colorimetric LAMP assay. The results were interpreted according to the software guidelines from

the manufacturer (ABI StepOne apparatus, Applied Biosystems, United States).

Statistical Analysis

The specificity, clinical sensitivity, positive predictive values (PPV), and negative predictive values (NPV) of the colorimetric LAMP assay was compared to those of the qPCR using MedCalc Statistical Software (http://www.medcalc.org). A sample was considered a true positive if it was identified as qPCR positive. The level of agreement was analyzed between colorimetric LAMP and the reference qPCR assay using the kappa (*k*) coefficient with 95% confidence levels (Cohen, 1960).

RESULTS

The Best Primer Set

The colorimetric LAMP assay was carried out with all five primer sets in a range of 55–65°C for 30 min using genomic DNA of *C. burnetii*. The sets 2–5 resulted in inconsistent and non-specific target amplification on repeated runs. The primer set 1 described in **Table 1** was found best in amplifying the target consistently at 63°C, and this combination was used for subsequent experiments. The primer FIP, BIP, F3, and B3 has similar sequences to one of the primer set as reported by (Chen and Ching, 2014). The position of primer sequences in the transposase gene insertion element *IS*1111a is depicted in **Figure 1**.

TABLE 1 | List of primer sequences for colorimetric loop-mediated isothermal amplification (LAMP).

Primer type	Sequence (5′-3′)
Trans FIP (F1c-F2)	GCTCCTCCACACGCTTCCATTGTATCCACCGTAGCCAGTC
Trans BIP (B1c-B2)	ATCGGACGTTTATGGGGATGGGACATACGGTTTGACGTGCTG
Trans F3	GACGGGTTAAGCGTGCTC
Trans B3	CTGCGCATCGTTACGATCA
Trans LF	CCACGCAGCCCACCTTAA
Trans LB	TATCCCAACGCAGTTGATCAGT

Colorimetric LAMP Product Detection

The colorimetric LAMP products were analyzed by performing agarose gel electrophoresis, and the gel was visualized under UV light post ethidium bromide staining. For the visual detection of the colorimetric LAMP products, HNB dyes were added at a final concentration of 120 μM during the reaction setup. A positive reaction is indicated by a color change from violet to sky blue (**Figure 2A**).

Sensitivity of Colorimetric LAMP

The LOD of the colorimetric LAMP assay was determined using the 10-fold serial dilutions of the recombinant plasmid harboring 194 bp amplified fragment of *IS*1111a gene of the *C. burnetii*. The LOD of colorimetric LAMP and conventional PCR assay was found to be 3 and 30 copies/reaction, respectively (**Figures 2A–C**). Hence, the colorimetric LAMP assay was found to be 10 times more sensitive in detecting C. *burnetii* as compared to conventional PCR.

Specificity of Colorimetric LAMP

The specificity of the colorimetric LAMP assay was assessed employing the DNA (genomic) of closely related bacteria to *C. burnetii* and other bacteria mentioned in Materials and Methods. The colorimetric LAMP assay was found to be very specific, as no cross-reactivity was seen with any of the bacterial species tested.

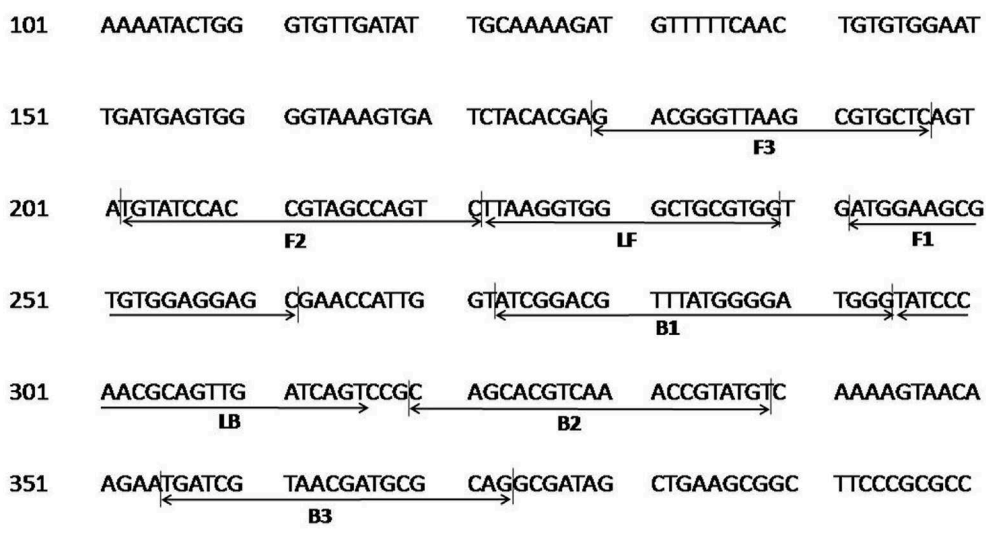

FIGURE 1 | Nucleotide sequence of the transposase gene insertion element *IS*1111a of *C. burnetii* used for designing the LAMP primers. Numbers on the left correspond to the positions in the transposase gene (GenBank, accession no. AE016828.2). The locations of the target sequences are underlined with an arrow. FIP consists of the F1c and F2 sequences, and BIP consists of B1c and B2 sequences.

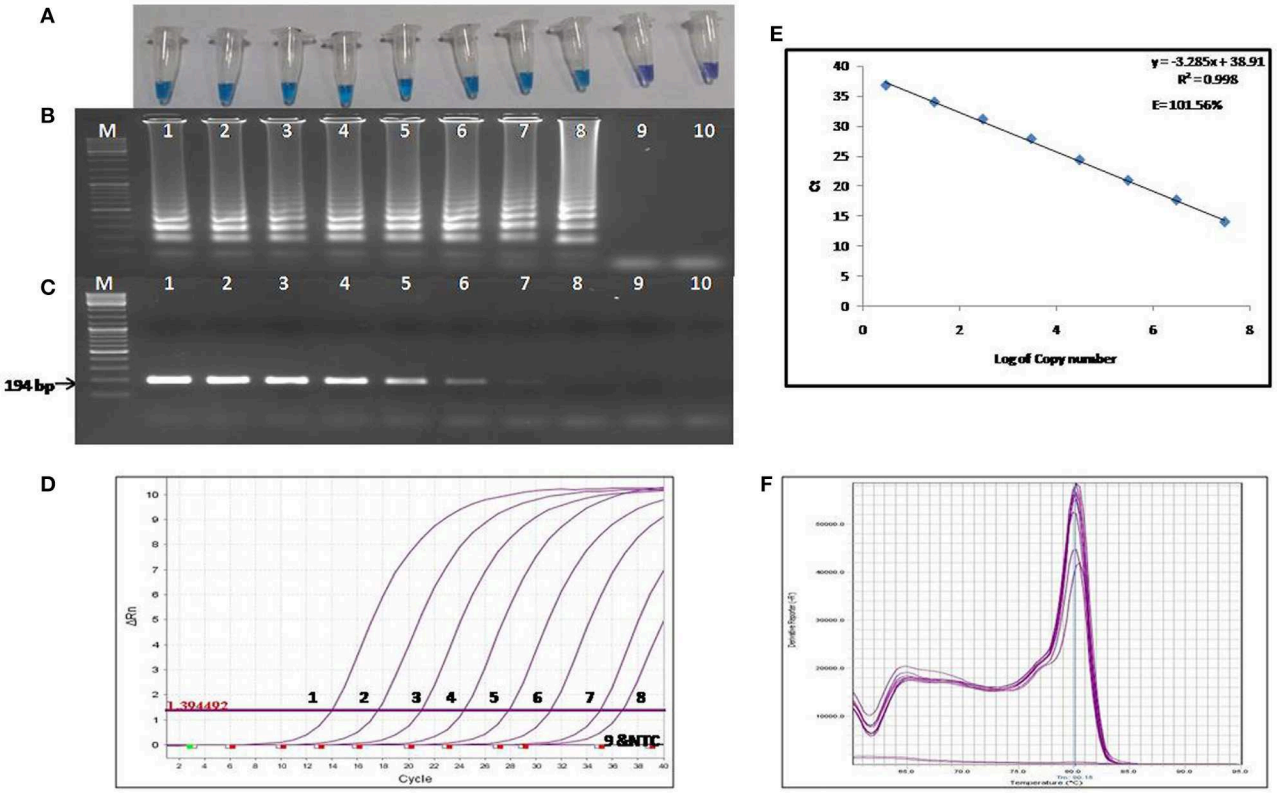

FIGURE 2 | Comparison of the sensitivity of colorimetric LAMP, conventional PCR and qPCR. **(A)** Results of colorimetric LAMP analysis, **(B)** Agarose gel electrophoresis of colorimetric LAMP products, **(C)** Agarose gel electrophoresis of conventional PCR products **(D)** Results of qPCR Analysis, **(E)** Standard curve and amplification efficiency, **(F)** Melting curve analysis. Lane, M: DNA marker; Lanes 1-9: Reaction results from a 10-fold serial dilution of plasmid containing the transposase gene from 3×10^7 to 3×10^{-1} copies per reaction; Lane 10: Negative control (nuclease free water).

Sensitivity and Specificity of qPCR

The LOD of the reference qPCR was determined by amplifying the 10-fold serial dilutions of the recombinant plasmid harboring the *IS*1111a gene fragment of the *C. burnetii*. The detection limit was found to be three copies per reaction (**Figure 2D**), which is equivalent to about one cell of *C. burnetii*. The sensitivity of the reference qPCR was found to be similar to that of colorimetric LAMP assay. The standard curve generated by qPCR was linear, generating a coefficient of correlation $R^2 = 0.998$, a slope of −3.28 with an efficiency of 101.56% (**Figure 2E**). Melting curve analysis revealed the specificity of primers for the target gene sequence, as all the amplified products showed a uniform melting temperature (T_m) of ∼80.15°C (**Figure 2F**).

TABLE 2 | Performance of colorimetric loop-mediated isothermal amplification (LAMP) for clinical sheep vaginal swabs ($n = 145$) compared to reference CB qPCR method.

CB qPCR	Colorimetric LAMP	
	Positive	**Negative**
Positive (15)	14	1
Negative (130)	0	130
Sensitivity	93.75%	
Specificity	100%	
PPV	100%	
NPV	99.24%	
Agreement (*k* value)	96.2% ($k = 0.962$, almost perfect agreement)	

Evaluation of the Colorimetric LAMP Assay With Sheep Vaginal Samples

The diagnostic applicability of the colorimetric LAMP assay was evaluated by testing 145 vaginal swab samples collected from the sheep breeding farms with stillbirth and repeated abortion. Results were compared with the results of the qPCR assay. Fourteen samples were found positive by both colorimetric LAMP and qPCR employing crude DNA preparation and DNA extracted with commercial kit. One sample that was found to be negative by the colorimetric LAMP assay was observed positive by qPCR, and this could be most likely due to a low target level (Ct, 38.12) in the sample. Compared to qPCR, colorimetric LAMP had a sensitivity of 93.75% (CI, 69.77–99.84%) and specificity of 100% (CI, 97.20–100%), with a PPV and NPV of 100 and 99.24%, respectively. A very high level of agreement was found between both colorimetric LAMP and reference qPCR assay. Compared to qPCR, the level of agreement was found to be of 96.2% for colorimetric LAMP ($k = 0.962$; strength of agreement, almost perfect). The outcome of the present study

is depicted in **Table 2**. The colorimetric LAMP assay required a total of 45 min (meantime) from the arrival of a swab in the laboratory to the final result dissemination (10 min crude DNA preparation, 5 min for assay setup, and 30 min for colorimetric LAMP), compared to 1 h, 45 min for conventional LAMP with DNA extraction protocol and 2 h, 30 min for the reference qPCR test.

DISCUSSION

The majority of human Q fever cases are related to exposure to domestic ruminants. Preventive measure in controlling Q fever includes a temporary breeding ban, antibiotic treatment, vaccination, safe disposal of placentas and fetuses by burning or burying, and isolation of infected animals from the herd (Van Asseldonk et al., 2013). Finally, when no preventive measures can be applied and if too many contaminated animals are involved, the culling of herds is the ultimate solution. All these control measures lead to a huge economic burden; thus, the diagnosis of animals is of paramount importance to prevent human outbreaks (Brom et al., 2015). The diagnosis of Q fever is very difficult because of its non-specific clinical manifestations (Angelakis and Raoult, 2010). The isolation of the agent is the most reliable diagnosis for Q fever, but it is not routinely practiced because of its poor sensitivity in both cell culture and animal inoculation. This procedure also requires skilled personnel and has to be performed in a containment facility of BSL III level (Maurin and Raoult, 1999). Currently, indirect immunofluorescent antibody assay (IFA) and ELISA are the methods of choice for the serological diagnosis of Q fever (Angelakis and Raoult, 2010). However, these methods are not suitable for early disease reporting because *C. burnetii*-specific antibody appear late as disease progress (Maurin and Raoult, 1999). Moreover, these techniques do not provide the status of current shedding animals (Magouras et al., 2017). The molecular-based techniques such as conventional or quantitative PCRs offer a suitable substitute to culture in demonstrating the presence of *C. burnetii* in clinical samples. Several nested PCR or seminested PCR were developed to detect Q fever with a higher level of specificity and sensitivity (Fournier and Raoult, 2003; Turra et al., 2006). qPCR has several advantages with specific reference to sensitivity, quantification, and control of contamination, but at the same time, it also requires a high-end PCR machine (Panning et al., 2008; Schneeberger et al., 2010). However, these assays limit its use in resource-poor regions due to the requirement of maintenance of cold chain transportation and need for expensive instrumentation and trained personnel, which avert the use of PCR at POC. The LAMP assay is an alternative nucleic acid detection method that has many advantages, such as ease of operation, rapidity, low cost, and modest equipment requirements, making it convenient for use in field conditions (Lucchi et al., 2010; Njiru et al., 2012; Pan et al., 2013).

In the present study, a sensitive and specific colorimetric LAMP assay was developed based on the transposase gene insertion element *IS*1111a of *C. burnetii*. The *IS*1111a gene target was selected because it is a highly conserved gene sequence among the different strains of *C. burnetii*, and the presence of multiple copies in the bacteria leads to a higher sensitivity (Chen and Ching, 2014). The assay could detect as low as three copies per reaction supporting the applicability for the detection of infections with low bacteremia. The colorimetric LAMP assay was further tested for its specificity, employing the genomic DNA of closely related bacteria to *C. burnetii* and other bacteria mentioned in Materials and Methods, and the results indicate no cross-reaction among tested bacteria, confirming that the colorimetric LAMP assay is also highly specific.

The applicability of the colorimetric LAMP assay for the disease diagnosis was assessed by evaluating 145 vaginal swab samples collected from the sheep breeding farms with a history of stillbirth and repeated abortions. The screening of vaginal swabs was executed because the shedding of the agent in the vaginal mucus is higher within 14 days of abortion, and also the handling of swab sample is easy in the field settings (Hansen et al., 2011; Guatteo et al., 2012). The vaginal swab samples were collected after disinfection of the vulva with chlorhexidine solution by authorized veterinarians following standard biosafety procedures. The triple-packed samples were transported from the field to the laboratory in a cool box (4–12°C). The samples were processed for DNA extraction in Biosafety Level 3 laboratory, following which swabs were disposed off postautoclaving (Crews and Gaunt, 2008). To the best of our understanding, it is the very first study describing the use of colorimetric LAMP assay that detects *C. burnetii* in vaginal swab samples with minimal sample processing for DNA extraction. Compared to qPCR, colorimetric LAMP had a sensitivity of 93.75% (CI, 69.77–99.84%) and specificity of 100% (CI, 97.20–100%), with a PPV and NPV of 100 and 99.24%, respectively. A very high level of agreement was observed between both colorimetric LAMP and reference qPCR assay. Only two reports are describing the utility of LAMP assay for the *C. burnetii* detection directly from clinical matrices, namely, abortive products and serum samples of humans and animal origin (Pan et al., 2013; Raele et al., 2015). In their study, DNA extraction was done using commercial kits, which is not only time consuming and tedious but also ill-suited in field conditions. Moreover, in these studies, the LAMP results were analyzed by performing 2% agarose gel electrophoresis followed by its staining with ethidium bromide or by SYBR Green I dye aided visual inspection. In the present study, the colorimetric LAMP was shown to be compatible with a simple heating block and the minimal sample processing (direct detection—no extraction protocol) with sensitivity very comparable to the reference method, qPCR capable of detecting a single cell of *C. burnetii*. The present finding implies that it can be well-suited in areas with limited resources, obviating the dependence on expensive high-end instrumentation and tedious nucleic acid extraction procedures. Additionally, HNB used for the analysis of LAMP products is added before amplification, hence minimizing the risk of aerosol contamination, which results in false positives (Goto et al., 2009). Based on the above attributes, the present colorimetric LAMP technique appears to be a promising substitute to qPCR for detecting *C. burnetii*.

In conclusion, we developed a rapid, simple, and sensitive colorimetric LAMP assay for the detection of *C. burnetii*.

The present study enables early detection of the infection in shedding animals, which will allow controlling its spread among animals and animal-to-human transmission. Our present method has not only a short turnaround time but also avoided cross-contamination problem and dependence on expensive equipment, which are desirable characteristics amenable to POC use in resource-limited settings.

DATA AVAILABILITY STATEMENT

All datasets generated for this study are included in the article/**Supplementary Material**.

AUTHOR CONTRIBUTIONS

SK conceived and designed the experiments. NS and SK performed the experiments. SK, HS, SB, and DT analyzed the data. SK and NS wrote the paper. All authors read and approved the final manuscript.

FUNDING

This work was supported by Defense Research and Development Organization (DRDO) research funds and NS is a recipient of DRDO-SRF fellowship.

ACKNOWLEDGMENTS

The authors would like to express their gratitude to the Director, Defense Research and Development Establishment (DRDE), Ministry of Defense, Government of India for his keen interest and constant support in this study (DRDE Accession No. DRDE/BDTE/11/2019).

SUPPLEMENTARY MATERIAL

The Supplementary Material for this article can be found online at: https://www.frontiersin.org/articles/10.3389/fcimb.2020.00127/full#supplementary-material

REFERENCES

Angelakis, E., and Raoult, D. (2010). Q fever. *Vet. Microbial.* 140, 297–309. doi: 10.1016/j.vetmic.2009.07.016

Berri, M., Souriau, A., Crosby, M., Crochet, D., Lechopier, P., and Rodolakis, A. (2001). Relationships between the shedding of *Coxiella burnetii*, clinical signs and serological responses of 34 sheep. *Vet. Rec.* 148, 502–505. doi: 10.1136/vr.148.16.502

Bouvery, N. A., Souriau, A., Lechopier, P., and Rodolakis, A. (2003). Experimental *Coxiella burnetii* infection in pregnant goats: excretion routes. *Vet. Res.* 34, 423–433. doi: 10.1051/vetres:2003017

Brom, R. V. D., Engelen, E. V., Roest, H. I. J., Hoek, W. V. D., and Vellema, P. (2015). *Coxiella burnetii* infections in sheep or goats: an opinionated review. *Vet. Microbiol.* 181, 119–129. doi: 10.1016/j.vetmic.2015.07.011

Chen, H.W., and Ching, W.M. (2014). Development of loop-mediated isothermal amplification assays for rapid and easy detection of Coxiella burnetii. *J. Microbiol. Methods.* 107, 176–181. doi: 10.1016/j.mimet.2014.07.039

Cohen, J. (1960). A coefficient of agreement for nominal scales. *Educ. Psychol. Meas.* 20, 37–46. doi: 10.1177/001316446002000104

Crews, C. J., and Gaunt, E. E. (2008). Comparative analysis of the fourth and fifth editions of biosafety in microbiological and biomedical laboratories, section IV (BSL2–4). *Appl. Biosaf.* 13, 6–15. doi: 10.1177/153567600801300102

De Bruin, A., Janse, I., Koning, M., De Heer, L., Van der Plaats, R. Q., Van Leuken, J. P., et al. (2013). Detection of *Coxiella burnetii* DNA in the environment during and after a large Q fever epidemic in the Netherlands. *J. Appl. Microbiol.* 114, 1395–1404. doi: 10.1111/jam.12163

Drancourt M, Raoult D. (2005). "Family coxiellaceae," in *Bergey's Manual of Systematic Bacteriology 2nd ed., Part B: The Gammaproteobacteria*, ed G. M. Garrity (New York, NY: Springer), 237–247.

Fenollar, F., Fournier, P. E., and Raoult, D. (2004). Molecular detection of *Coxiella burnetii* in the sera of patients with Q fever endocarditis or vascular infection. *J. Clin. Microbiol.* 42, 4919–4924. doi: 10.1128/JCM.42.11.4919-4924.2004

Fournier, P. E., Marrie, T. J., and Raoult, D. (1998). Diagnosis of Q fever. *J. Clin. Microbiol.* 36, 1823–1834. doi: 10.1128/JCM.36.7.1823-1834.1998

Fournier, P. E., and Raoult, D. (2003). Comparison of PCR and serology assays for early diagnosis of acute Q fever. *J. Clin. Microbiol.* 41, 5094–5098. doi: 10.1128/JCM.41.11.5094-5098.2003

Goto, M., Honda, E., Ogura, A., Nomoto, A., and Hanaki, K. I. (2009). Colorimetric detection of loop-mediated isothermal amplification reaction by using hydroxy naphthol blue. *BioTechniques* 46, 167–172. doi: 10.2144/000113072

Guatteo, R., Joly, A., and Beaudeau, F. (2012). Shedding and serological patterns of dairy cows following abortions associated with *Coxiella burnetii* DNA detection. *Vet. Microbiol.* 155, 430–433. doi: 10.1016/j.vetmic.2011.09.026

Hansen, M. S., Rodolakis, A., Cochonneau, D., Agger, J. F., Christoffersen, A. B., and Jensen, T. K. (2011). Coxiella burnetii associated placental lesions and infection level in parturient cows. *Vet. J.* 190, 135–139. doi: 10.1016/j.tvjl.2010.12.021

Ibrahim, A., Norlander, L., Macellaro, A., and Sjöstedt, A. (1997). Specific detection of *Coxiella burnetii* through partial amplification of 23S rDNA. *Eur. J. Epidemiol.* 13, 329–334. doi: 10.1023/A:1007385104687

Kato, K., Arashima, Y., Asai, S., Furuya, Y., Yoshida, Y., Murakami, M., et al. (1998). Detection of *Coxiella burnetii* specific DNA in blood samples from Japanese patients with chronic nonspecific symptoms by nested polymerase chain reaction. *FEMS Immunol. Med. Microbiol.* 21, 139–144. doi: 10.1111/j.1574-695X.1998.tb01159.x

Klee, S. R., Tyczka, J., Ellerbrok, H., Franz, T., Linke, S., Baljer, G., et al. (2006). Highly sensitive real-time PCR for specific detection and quantification of *Coxiella burnetii*. *BMC Microbiol.* 6:2. doi: 10.1186/1471-2180-6-2

Lorenz, H., Jäger, C., Willems, H., and Baljer, G. (1998). PCR detection of *Coxiella burnetii* from different clinical specimens, especially bovine milk, on the basis of DNA preparation with a silica matrix. *Appl. Environ. Microbiol.* 64, 4234–4237. doi: 10.1128/AEM.64.11.4234-4237.1998

Lucchi, N. W., Demas, A., Narayanan, J., Sumari, D., Kabanywanyi, A., Kachur, S. P., et al. (2010). Real-time fluorescence loop mediated isothermal amplification for the diagnosis of malaria. *PLoS ONE* 5:e13733. doi: 10.1371/journal.pone.0013733

Magouras, I., Hunninghaus, J., Scherrer, S., Wittenbrink, M. M., Hamburger, A., Stark, K. D. C., et al. (2017). *Coxiella burnetii* infections in small ruminants and humans in Switzerland. *Transbound. Emerg. Dis.* 64, 204–212. doi: 10.1111/tbed.12362

Maurin M and Raoult D. (1999) Q fever. *Clin. Microbiol. Rev.* 12, 518–553. doi: 10.1128/CMR.12.4.518

Nagamine, K., Hase, T., and Notomi, T. (2002). Accelerated reaction by loop-mediated isothermal amplification using loop primers. *Mol. Cell. Probes.* 16, 223–229. doi: 10.1006/mcpr.2002.0415

Njiru, Z. K., Yeboah-Manu, D., Stinear, T. P., and Fyfe, J. A. (2012). Rapid and sensitive detection of *Mycobacterium ulcerans* using a loop-mediated isothermal amplification test. *J. Clin. Microbiol.* 50, 1737–1741. doi: 10.1128/JCM.06460-11

Notomi, T., Okayama, H., Masubuchi, H., Yonekawa, T., Watanabe, K., Amino, N., et al. (2000). Loop-mediated isothermal amplification of DNA. *Nucleic Acids Res.* 28, e63–e63. doi: 10.1093/nar/28.12.e63

Pan, L., Zhang, L., Fan, D., Zhang, X., Liu, H., Lu, Q., et al. (2013). Rapid, simple and sensitive detection of Q fever by loop-mediated isothermal amplification of the htpAB gene. *PLoS Negl. Trop. Dis.* 7:e2231. doi: 10.1371/journal.pntd.0002231

Panning, M., Kilwinski, J., Greiner-Fischer, S., Peters, M., Kramme, S., Frangoulidis, D., et al. (2008). High throughput detection of *Coxiella burnetii* by real-time PCR with internal control system and automated DNA preparation. *BMC Microbiol.* 8:77. doi: 10.1186/1471-2180-8-77

Parida, M., Horioke, K., Ishida, H., Dash, P. K., Saxena, P., Jana, A. M., et al. (2005). Rapid detection and differentiation of dengue virus serotypes by a real-time reverse transcription-loop-mediated isothermal amplification assay. *J. Clin. Microbiol.* 43, 2895–2903. doi: 10.1128/JCM.43.6.2895-2903.2005

Porter, S. R., Czaplicki, G., Mainil, J., Horii, Y., Misawa, N., and Saegerman, C. (2011). Q fever in Japan: an update review. *Vet. Microbiol.* 149, 298–306. doi: 10.1016/j.vetmic.2010.11.017

Raele, D. A., Garofolo, G., Galante, D., and Cafiero, M. A. (2015). Molecular detection of *Coxiella burnetii* using an alternative loop-mediated isothermal amplification assay (LAMP). *Vet. Ital.* 51, 73–8. doi: 10.12834/VetIt.304.1168.4

Raoult, D. (1996). Q fever: still a query after all these years. *J. Med. Microbiol.* 44, 77–78. doi: 10.1099/00222615-44-2-77

Roest, H. I., Ruuls, R. C., Tilburg, J. J., Nabuurs-Franssen, M. H., Klaassen, C. H., Vellema, P., et al. (2011). Molecular epidemiology of *Coxiella burnetii* from ruminants in Q fever outbreak, the Netherlands. *Emerging Infect. Dis.* 17:668. doi: 10.3201/eid1704.101562

Schneeberger, P. M., Hermans, M. H., van Hannen, E. J., Schellekens, J. J., Leenders, A. C., and Wever, P. C. (2010). Real-time PCR with serum samples is indispensable for early diagnosis of acute Q fever. *Clin. Vaccine Immunol.* 17, 286–290. doi: 10.1128/CVI.00454-09

Stein, A., and Raoult, D. (1992). Detection of *Coxiella burnetti* by DNA amplification using polymerase chain reaction. *J. Clin. Microbiol.* 30, 2462–2466. doi: 10.1128/JCM.30.9.2462-2466.1992

Thekisoe, O. M., Bazie, R. S., Coronel-Servian, A. M., Sugimoto, C., Kawazu, S. I., and Inoue, N. (2009). Stability of loop-mediated isothermal amplification (LAMP) reagents and its amplification efficiency on crude trypanosome DNA templates. *J. Vet. Med. Sci.* 71, 471–475. doi: 10.1292/jvms.71.471

Turra, M., Chang, G., Whybrow, D., Higgins, G., and Qiao, M. (2006). Diagnosis of acute Q fever by PCR on sera during a recent outbreak in rural South Australia. *Ann. N. Y. Acad. Sci.* 1078, 566–569. doi: 10.1196/annals.1374.112

Van Asseldonk, M. A. P. M., Prins, J., and Bergevoet, R. H. M. (2013). Economic assessment of Q fever in the Netherlands. *Prev. Vet. Med.* 112, 27–34. doi: 10.1016/j.prevetmed.2013.06.002

Willems, H., Thiele, D., Frolich-Ritter, R., and Krauss, H. (1994). Detection of *Coxiella burnetii* in cow's milk using the polymerase chain reaction (PCR). *J. Vet. Med. Series B.* 41, 580–587. doi: 10.1111/j.1439-0450.1994.tb00267.x

Willems, H., Thiele, D., and Krauss, H. (1993). Plasmid based differentiation and detection of *Coxiella burnetii* in clinical samples. *Eur. J. Epidemiol.* 9, 411–418. doi: 10.1007/BF00157399

Zhang, G. Q., Hotta, A., Mizutani, M., Ho, T., Yamaguchi, T., Fukushi, H., et al. (1998a). Direct identification of *Coxiella burnetii* plasmids in human sera by nested PCR. *J. Clin. Microbiol.* 36, 2210–2213. doi: 10.1128/JCM.36.8.2210-2213.1998

Zhang, G. Q., Nguyen, S. V., To, H., Ogawa, M., Hotta, A., Yamaguchi, T., et al. (1998b). Clinical evaluation of a new PCR assay for detection of *Coxiella burnetii* in human serum samples. *J. Clin. Microbiol.* 36, 77–80. doi: 10.1128/JCM.36.1.77-80.1998

Zhang, X., Lowe, S. B., and Gooding, J. J. (2014). Brief review of monitoring methods for loop-mediated isothermal amplification (LAMP). *Biosens Bioelectron.* 61, 491–499. doi: 10.1016/j.bios.2014.05.039

Conflict of Interest: The authors declare that the research was conducted in the absence of any commercial or financial relationships that could be construed as a potential conflict of interest.

Advantages of publishing in Frontiers

OPEN ACCESS
Articles are free to read for greatest visibility and readership

FAST PUBLICATION
Around 90 days from submission to decision

HIGH QUALITY PEER-REVIEW
Rigorous, collaborative, and constructive peer-review

TRANSPARENT PEER-REVIEW
Editors and reviewers acknowledged by name on published articles

Frontiers
Avenue du Tribunal-Fédéral 34
1005 Lausanne | Switzerland

Visit us: www.frontiersin.org
Contact us: info@frontiersin.org | +41 21 510 17 00

REPRODUCIBILITY OF RESEARCH
Support open data and methods to enhance research reproducibility

DIGITAL PUBLISHING
Articles designed for optimal readership across devices

FOLLOW US
@frontiersin

IMPACT METRICS
Advanced article metrics track visibility across digital media

EXTENSIVE PROMOTION
Marketing and promotion of impactful research

LOOP RESEARCH NETWORK
Our network increases your article's readership